COLUMBIA
ACCIDENT INVESTIGATION BOARD

REPORT
VOLUME IV

COLUMBIA ACCIDENT INVESTIGATION BOARD

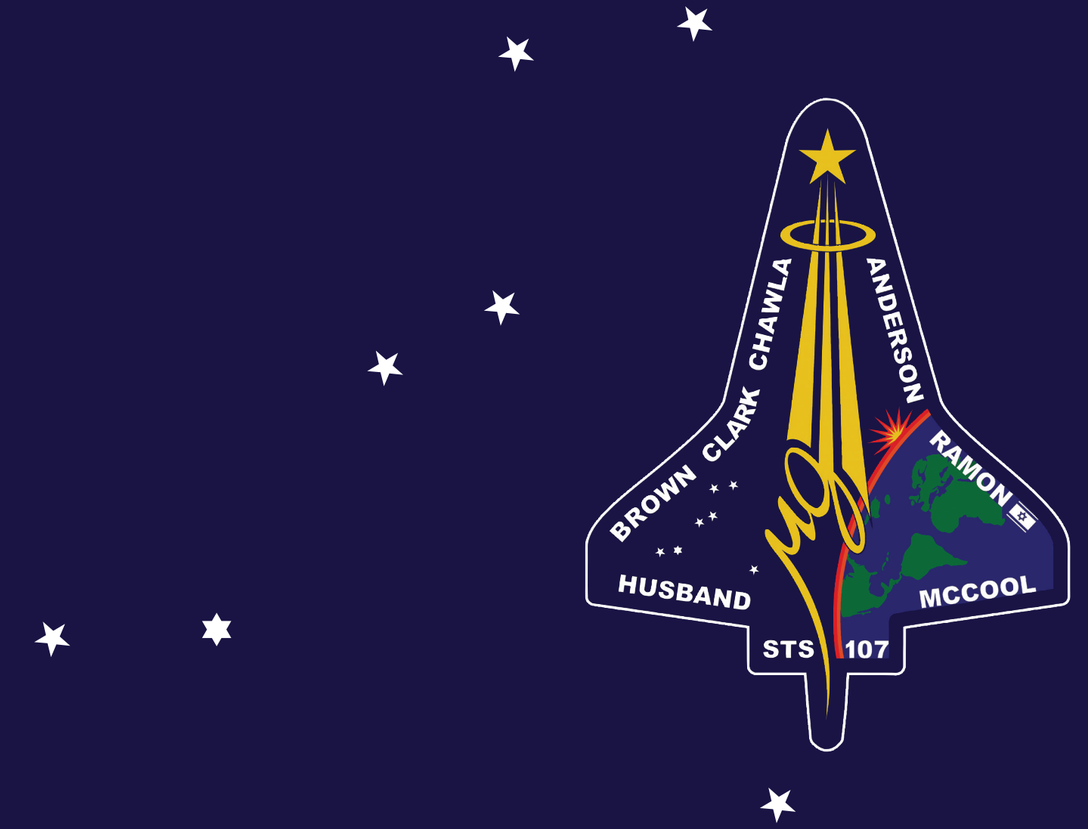

OCTOBER
2003

REPORT VOLUME IV
OCTOBER 2003

COLUMBIA

ACCIDENT INVESTIGATION BOARD

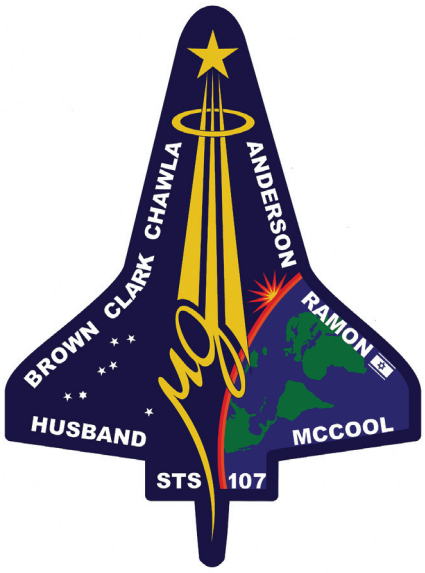

Note: Volumes II – VI contain a number of conclusions and recommendations, several of which were adopted by the Board in Volume I. The other conclusions and recommendations drawn in Volumes II – VI do not necessarily reflect the opinion of the Board, but are included for the record. When there is conflict, Volume I takes precedence.

REPORT VOLUME IV
OCTOBER 2003

On the Front Cover

This was the crew patch for STS-107. The central element of the patch was the microgravity symbol, μg, flowing into the rays of the Astronaut symbol. The orbital inclination was portrayed by the 39-degree angle of the Earth's horizon to the Astronaut symbol. The sunrise was representative of the numerous science experiments that were the dawn of a new era for continued microgravity research on the International Space Station and beyond. The breadth of science conducted on this mission had widespread benefits to life on Earth and the continued exploration of space, illustrated by the Earth and stars. The constellation Columba (the dove) was chosen to symbolize peace on Earth and the Space Shuttle Columbia. In addition, the seven stars represent the STS-107 crew members, as well as honoring the original Mercury 7 astronauts who paved the way to make research in space possible. The Israeli flag represented the first person from that country to fly on the Space Shuttle.

On the Back Cover

This emblem memorializes the three U.S. human space flight accidents – Apollo 1, Challenger, and Columbia. The words across the top translate to: "To The Stars, Despite Adversity – Always Explore"

The Board would like to acknowledge the hard work and effort of the following individuals in the production of Volumes II – VI.

Maj. Gen. John L. Barry	Executive Director to the Chairman
Dennis R. Jenkins	Investigator and Liaison to the Board
Lt. Col. Donald J. White	Technical Editor
Lt. Col. Patrick A. Goodman	Technical Editor
Joshua M. Limbaugh	Layout Artist
Joseph A. Reid	Graphic Designer
Christine F. Cole	Administrative Assistant
Jana T. Schultz	Administrative Assistant
Lester A. Reingold	Lead Editor
Christopher M. Kirchhoff	Editor
Ariel H. Simon	Assistant Editor
Jennifer L. Bukvics	Lead Project Manager
Donna J. Fudge	Senior Paralegal, Group II Coordinator
Susan M. Plott	Project Supervisor, Group III Coordinator
Ellen M. Tanner	Project Supervisor
Matthew J. Martin	Government Relations Consultant
Frances C. Fisher	ANSER Liaison

Limited First Printing, October 2003, by the
Columbia Accident Investigation Board

Subsequent Printing and Distribution by the
National Aeronautics and Space Administration
and the
Government Printing Office
Washington, D.C.

VOLUME I

PART ONE	THE ACCIDENT
Chapter 1	The Evolution of the Space Shuttle Program
Chapter 2	*Columbia*'s Final Flight
Chapter 3	Accident Analysis
Chapter 4	Other Factors Considered
PART TWO	WHY THE ACCIDENT OCCURRED
Chapter 5	From *Challenger* to *Columbia*
Chapter 6	Decision Making at NASA
Chapter 7	The Accident's Organizational Causes
Chapter 8	History as Cause: *Columbia* and *Challenger*
PART THREE	A LOOK AHEAD
Chapter 9	Implications for the Future of Human Space Flight
Chapter 10	Other Significant Observations
Chapter 11	Recommendations
PART FOUR	APPENDICES
Appendix A	The Investigation
Appendix B	Board Member Biographies
Appendix C	Board Staff

VOLUME II

CAIB TECHNICAL DOCUMENTS CITED IN THE REPORT

	Reader's Guide to Volume II
Appendix D.a	Supplement to the Report
Appendix D.b	Corrections to Volume I of the Report
Appendix D.1	STS-107 Training Investigation
Appendix D.2	Payload Operations Checklist 3
Appendix D.3	Fault Tree Closure Summary
Appendix D.4	Fault Tree Elements – Not Closed
Appendix D.5	Space Weather Conditions
Appendix D.6	Payload and Payload Integration
Appendix D.7	Working Scenario
Appendix D.8	Debris Transport Analysis
Appendix D.9	Data Review and Timeline Reconstruction Report
Appendix D.10	Debris Recovery
Appendix D.11	STS-107 Columbia Reconstruction Report
Appendix D.12	Impact Modeling
Appendix D.13	STS-107 In-Flight Options Assessment
Appendix D.14	Orbiter Major Modification (OMM) Review
Appendix D.15	Maintenance, Material, and Management Inputs
Appendix D.16	Public Safety Analysis
Appendix D.17	MER Manager's Tiger Team Checklist
Appendix D.18	Past Reports Review
Appendix D.19	Qualification and Interpretation of Sensor Data from STS-107
Appendix D.20	Bolt Catcher Debris Analysis

VOLUME III — OTHER TECHNICAL DOCUMENTS

Reader's Guide to Volume III
Appendix E.1 CoFR Endorsements
Appendix E.2 STS-107 Image Analysis Team Final Report
Appendix E.3 An Assessment of Potential Material Candidates for the "Flight Day 2" Radar Object Observed during the NASA Mission STS-107
Appendix E.4 *Columbia* Early Sighting Assessment Team Final Report

VOLUME IV — OTHER TECHNICAL DOCUMENTS

Reader's Guide to Volume IV 5
Appendix F.1 Water Absorption by Foam 7
Appendix F.2 Follow the TPS 19
Appendix F.3 MADS Sensor Data 53
Appendix F.4 ET Cryoinsulation 179
Appendix F.5 Space Shuttle STS-107 Columbia Accident Investigation, External Tank Working Group Final Report – Volume 1 239

VOLUME V — OTHER SIGNIFICANT DOCUMENTS

Reader's Guide to Volume V
Appendix G.1 Requirements and Procedures for Certification of Flight Readiness
Appendix G.2 Appendix R, Space Shuttle Program Contingency Action Plan
Appendix G.3 CAIB Charter, with Revisions
Appendix G.4 Group 1 Matrix Brief on Maintenance, Material, and Management
Appendix G.5 Vehicle Data Mapping (VDM) Team Final Report, Jun 13, 2003
Appendix G.6 SRB Working Group Presentation to CAIB
Appendix G.7 Starfire Team Final Report, Jun 3, 2003
Appendix G.8 Using the Data and Observations from Flight STS-107... Exec Summary
Appendix G.9 Contracts, Incentives, and Safety/Technical Excellence
Appendix G.10 Detailed Summaries: Rogers Commission Report, ASAP Report, SIAT Report
Appendix G.11 Foam Application and Production Chart
Appendix G.12 Crew Survivability Report
Appendix G.13 Aero/Aerothermal/Thermal/Structures Team Final Report, Aug 6, 2003

VOLUME VI — TRANSCRIPTS OF BOARD PUBLIC HEARINGS

Reader's Guide to Volume VI
Appendix H.1 March 6, 2003 Houston, Texas
Appendix H.2 March 17, 2003 Houston, Texas
Appendix H.3 March 18, 2003 Houston, Texas
Appendix H.4 March 25, 2003 Cape Canaveral, Florida
Appendix H.5 March 26, 2003 Cape Canaveral, Florida
Appendix H.6 April 7, 2003 Houston, Texas
Appendix H.7 April 8, 2003 Houston, Texas
Appendix H.8 April 23, 2003 Houston, Texas
Appendix H.9 May 6, 2003 Houston, Texas
Appendix H.10 June 12, 2003 Washington, DC

Reader's Guide to Volume IV

Volume III of the Report contains appendices that were not cited in Volume I. These consist of documents produced by NASA and other organizations, which were provided to the Columbia Accident Investigation Board in support of its inquiry into the February 1, 2003 destruction of the Space Shuttle *Columbia*. The documents are compiled in this volume in the interest of establishing a complete record, but they do not necessarily represent the views of the Board. Volume I contains the Board's findings, analysis, and recommendations. The documents in Volume III through V are also contained in their original color format on the DVD disc in the back of Volume II.

THIS PAGE INTENTIONALLY LEFT BLANK

Volume IV
Appendix F.1
Water Absorption by Foam

The CAIB requested these data be included in this Appendix. This Appendix is a summary of present and past efforts that were initiated to characterize the moisture absorption capability of sprayed-on-foam-insulation (SOFI) and specifically, BX-250.

THIS PAGE INTENTIONALLY LEFT BLANK

Preliminary Evaluation of Water vapor transmission and Liquid Water Absorption in ET Foam Samples

Leon R. Glicksman
June 1, 2003

I have examined the report of May 15 on water vapor transmission testing of BX 250 foam by Jeff Kolodziejczak and the report by Palmer Peters on water absorption by external tank foam. Although I have corresponded with both of them, because of my academic schedule I have been unable to visit the Marshall Center. I hope to do that in the next few weeks so that I can gain further insight into the details of their work and allow me to submit a final report.

The tests described in the reports appear to yield the property data that was initially requested by the Board. The test results of both water vapor permeability and liquid water absorption of polyurethane foams agree with previous tests reported in the literature as well as personal communications I have with people in industry and government labs knowledgeable about foams.

The test results by Palmer Peters raises some intriguing questions about the possibility of liquid water penetrating through wormholes or in knit lines that extend from the surface to the interior of the foam. If this is substantiated, it could represent a mechanism by which liquid water is trapped near the surface and is subsequently vaporized to initiate a crack in the foam. I would suggest further tests to investigate this possibility. Other means of detecting water within the foam sample should be explored.

The role of long voids within the foam needs to be examined in terms of permeability enhancement and possible sites for water accumulation.
Tests should also be undertaken to determine water vapor permeation and liquid or solid water accumulation within the foam when a substantial temperature gradient exists through the foam.

Although the test results raise the possibility of water ingress into the foam and subsequent vaporization and possible crack formation, the amount of water would not cause a substantial increase in the foam density by water or ice formation.

The test results need to be integrated into a mechanistic, quantitative model of possible failure modes to determine if any are possible.

Leon R. Glicksman
Consultant

Summary of Water Absorption Data of BX-250 to Address CAIB Action B1-00194

Scotty Sparks/NASA/MSFC/ED34
27 May 2003

The following is a summary of present and past efforts that were initiated to characterize the moisture absorption capability of sprayed-on-foam-insulation (SOFI) and, specifically, BX-250. Recent efforts to characterize moisture absorption were conducted by Drs. Palmer Peters/NASA-MSFC and Jeff Kolodziejczak/NASA-MSFC. Peters investigated the ability of foam to absorb liquid water and Kolodziejczak characterized the water vapor transmissibility of foam. Their work enjoyed the oversight of Dr. Leon Glicksman/MIT who helped coordinate test plans, review data, and offer expert analysis of the data. Other efforts, which include accelerated moisture absorption and on-pad rainfall significance, are two different sets of data that lend understanding to the moisture-to-foam relationship.

The Columbia Accident Investigation Board (CAIB) initiated the following request (CAIB Action B1-00194) to compile data to support their investigation:

> *"Request that MSFC: 1) plan and conduct moisture absorption testing on foam exposed to low (less than 100 °F) ambient temperatures, 2) use Prof. Leon Glicksman of MIT as an outside expert for planning tests and analyzing the results, and 3) report results obtained from these tests and from previous moisture absorption tests to the CAIB."*

Moisture Absorption (Peters, Kolodziejczak, Sharpe)

- Liquid Phase Absorption
  - Date: May 2003
  - Test Conductor: Dr. Palmer Peters/MSFC
  - Scope: To characterize the moisture absorption of BX-250 via submersion in dyed liquid water
  - Procedure:
    - NCFI 24-124 and BX-250 as two small, 1-inch-cube specimens referred to as Foam1 (NCFI 24-124) and Foam 2 (BX-250). Water-mass gain was measured when these specimens were submerged 2 ½ inches below distilled, de-aired water surfaces for 3,765 minutes. See Figure 1.
  - Conclusions:
    - "Water absorbed by submersion can be accounted for primarily by liquid in open surface cells resulting from machining or removing the outer skin, or rind."
    - "… indicate limited penetration of water into submerged foam surfaces. This agrees with prior reported studies and expert opinions, which indicate most absorption occurs through water vapor permeating foam having a temperature gradient"
      - Sectioning of foam after submersion indicated only absorption in thin layer around the machined foam. This layer characterized to be less than or equivalent to broken cells on surface. See Figure 2.
    - "The amount of increased mass from submersion is equivalent to a thickness of water comparable to the cell dimensions, as shown in Table 1, suggesting that damaged (open) cells at the surface and surface connected voids absorb most, if not all, of the water."
  - Reference:
    - Investigation of Water Absorption by External-Tank-Types of Foam, Palmer N. Peters, SD46, Marshall Space Flight Center, May 2003.
- Vapor Phase Transmission
  - Date: May 2003
  - Test Conductor: Dr. Jeff Kolodziejczak/MSFC

- Scope: These tests are specifically designed to study the transmission of water vapor through BX-250 foam in the context of evaluation of the probability of external tank foam loss scenarios and determination of foam debris properties as they relate to the Columbia Accident Investigation.
- Conclusions:
  - All specimens exhibited water vapor transmission at a level consistent published polyurethane foam values, for example a web summary of BASF Walltite foam quotes values from 30 to 125 ng/Pa-s-m^2 as typical for tests of 25mm thick commercial foam samples. See Figure 3.
    - This level of transmission deemed to be insignificant in terms of producing detrimental effects *(still pending concurrence from additional experts-ss)*
      - Low level of moisture absorption
      - Limited time (from tanking to launch) with imposed thermal gradient
  - All of the permeability values are within ±25% of the mean. Local effects in the test chamber, differences among the test specimens and differences among the test dishes may contribute uncertainty to the values at the 25% level.
- Reference: Procedure for Testing Water Vapor Transmission of BX-250 Foam Under Thermal and Pressure Gradient Conditions, Jeff Kolodziejczak, Marshall Space Flight Center, May 2003.

- Accelerated Moisture Conditioning
  - Date: April 2003
  - Test Conductor: Jon Sharpe/LMC
  - Scope: Observe accelerated moisture absorption characteristics of BX-250 that was soon to undergo testing to support the investigation and corrective action for IFA-87.

    Variables such as conditions (120 °F/93% RH and 32 °F/76% RH), cure state (freshly sprayed vs. two-week cured), and surface preparation (rind vs. machined) were included in the testing.
  - Conclusions:
    - Data confounded by the measurement of combined mass of aluminum substrate and foam
    - Approximately no absorption observed in 32 °F/76% RH conditioning for both just-sprayed and two-week cured materials. See Figure 4.
    - Just-sprayed material arrived to maximum moisture absorption in 48 hours in 120 °F/93% RH conditioning. See Figure 5.
    - Two-week cured material absorbed very little moisture at 120 °F/93% RH conditioning
  - Reference: Lockheed-Martin Job Order 9266 – BX-250 Moisture Absorption

On-Pad Rainfall Significance (Bourgeois)

- Date: April 1999
- Test Conductor: Chris Bourgeois/LMC
- Scope: Analyze the correlation of on-pad rainfall to orbiter hit count to support investigation and corrective action of IFA-87.
- Conclusions:
  - Limited positive correlation between KSC Prelaunch Dew Point and Bipod foam loss from STS-108 to STS-107 (7 flights spanning 12/01 to 1/03). See Table 2.
  - Limited absence of correlation between on-pad rainfall and orbiter lower-surface tile damage (>1") from STS-86 to STS-96 (8 flights spanning 9/97 to 5/99). See Figure 6.
- Reference:
  - "ET Weather Report 11", Jeff Kolodziejczak, February 2003.
  - "KSC ET Exposure Environments", Chris Bourgeois, April 1999.

- "KSC Environments vs. Orbiter Damage", Chris Bourgeois, April 1999.
- "KSC Rainfall Data vs. Orbiter Damage", Chris Bourgeois, April 1999.

Peters sums up well in his report data compiled to the present, "Water absorbed by submersion can be accounted for primarily by liquid in open surface cells resulting from machining or removing the outer skin, or rind….This agrees with prior reported studies and expert opinions, which indicate most absorption occurs through water vapor permeating foam having a temperature gradient". Furthermore, moisture absorption per vapor transmission under a temperature gradient was shown not to be significant due to the low permeability of the SOFI.

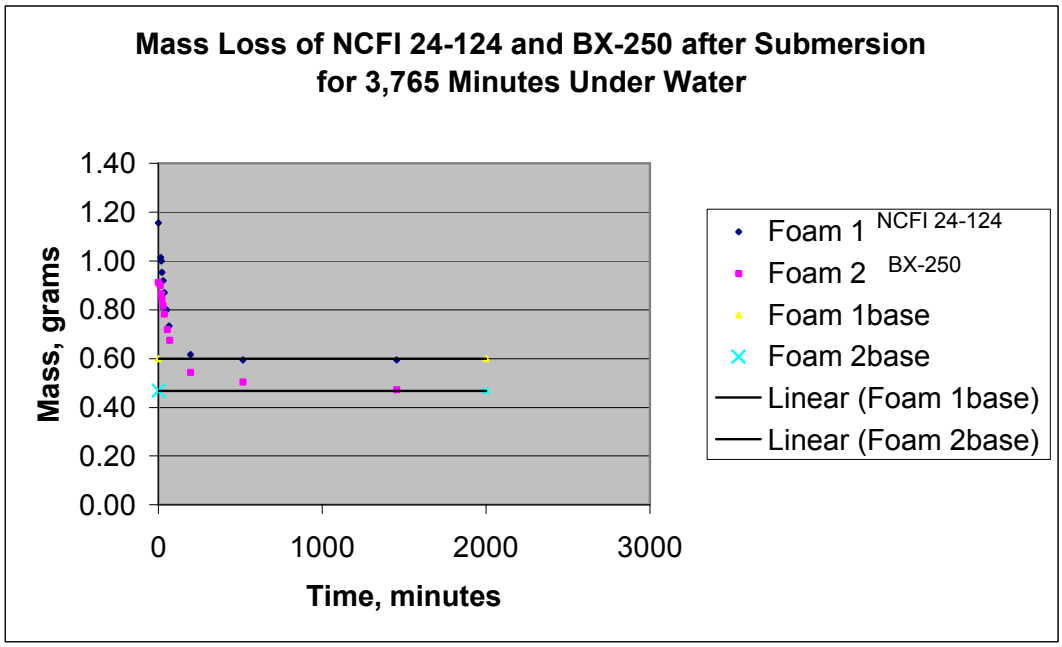

Figure 1. Plot of mass changes for NCFI 24-124 and BX-250 following submersion under 2.5 inches of distilled water for 3,765 minutes and blotting excess surface water before starting measurements.

Figure 2. (a) Shows blue dye decorating the surface of a BX-250 foam cube that was submerged 26.5 hours then sectioned, revealing the interior. (b) Shows a magnified image at the sectioned surface.

Table 1: Measured Water Absorption/De-Sorption Characteristics by Submersion.

Specimen	Size, cm	Initial Mass, g	*Submersion Data	+Mass After Submersion, g	++H_2O Liquid thickness, µm	Initial Evaporation Rate, mg/min	Comments
Foam 1, the only NSFI 24-124	2.54 cube	0.5990 ambient	6 cm; 21° C 62.8 hrs.	1.1560 increase=93%	143 (cell=80)	Not established	Lacking rapid, initial data
Foam 2, BX-250	2.54 cube	0.4673 ambient	6cm; 21° C 62.8 hrs.	0.9110 increase=95%	115 (cell~150)	Inaccurate; late aver. ~2.7	Late start
04/30/03 BX-250	2.86 aver, cube	0.8655 ambient	5 cm, 21° C 26.5 hrs. in blue dye	Shook instead of blotted, est. = 1.80	191 with dye error (cell ~150)	>3	Shaking left little excess puddle
05/07/03-1 BX-250	2.51 aver, cube	0.5204 ambient	5 cm; 21° C 21 hrs.	Not measured to speed up first IR image	Not determined	Not determined	IR image priority
05/07/03-2 BX-250	2.78 x2.54 x2.94	0.7710 ambient	5 cm; 21° C 20.8 hrs	Not measured to speed up IR image	Not determined	Not determined	IR image priority
05/08/03-1 BX-250	2.64 x2.7 x2.74	0.6412 baked @ 50° C	5 cm; 0.1° C 113 hrs. in blue dye	1.1516 increase=80%	117 with dye error (cell~150)	3.85 aver, 1st 10 min.	Blotted, weighed, IR imaged
05/08/03-2 BX-250	2.6 x2.65 x2.7	0.5985 baked @ 50° C	5 cm; 0.1° C 113 hrs	1.0937 increase=83%	118 (cell~150)	6.4 aver, 1st 26 min.	Blotted, weighed, repeatedly imaged, weighed
05/10/03-1 BX-250	2.60 x2.48 x2.60	0.5631 baked @ 50° C	5 cm; 52° C 148.8 hrs.	1.2258 increase=118%	168 (cell~150)	6.0	Blotted, Interior rind dark in image
05/10/03-2 BX-250	2.57 x2.70 x2.39	0.5855 baked @ 50° C	5 cm; 52° C 148.6 hrs. in blue dye	1.1543 increase=97%	146 (cell~150)	6.0	Blotted, Interior rind dark in image

Summary of Results

Specimen	Dimensions	Specific Gravity	ΔT	ΔP H20	Transmission g/hr-m^2	Permeance ng/s-Pa-m^2	Permeability ng/s-Pa-m
#1 (rind)	4"x4"x0.9"	0.03687	38°C	9 kPa	3.32	102.82	2.35
#2 (knit line)	4"x4"x1.0"	0.02975	38°C	9 kPa	2.44	75.51	1.92
#3 (bulk)	4"x4"x0.6"	0.0286	38°C	9 kPa	3.07	95.04	1.45

Discussion

- All specimens exhibited water vapor transmission at a level consistent published polyurethane foam values, for example a web summary of BASF Walltite foam quotes values from 30 to 125 ng/Pa-s-m^2 as typical for tests of 25mm thick commercial foam samples.

- The relative values did not exhibit expected behavior. The sample with rind exhibited the highest rate of transmission, while the purely bulk sample (no knit-line, no rind) exhibited the lowest permeability. The results do not correlate with density either.

- The specimens vary in the number of large elongated voids in the bulk material. These voids have diameters from 10 to 40 mil and extend in depth along the direction of rise as much as 0.5 inches.

- An unmodeled parameter such as the number and depth of large elongated voids may be a dominate permeability factor. So far, no attempt to characterize these voids has been made in this test set.

- All of the permeability values are within ±25% of the mean. Local effects in the test chamber, differences among the test specimens and differences among the test dishes may contribute uncertainty to the values at the 25% level.

Figure 3. Summary for "Procedure for Testing Water Vapor Transmission of BX-250 Foam Under Thermal and Pressure Gradient Conditions"

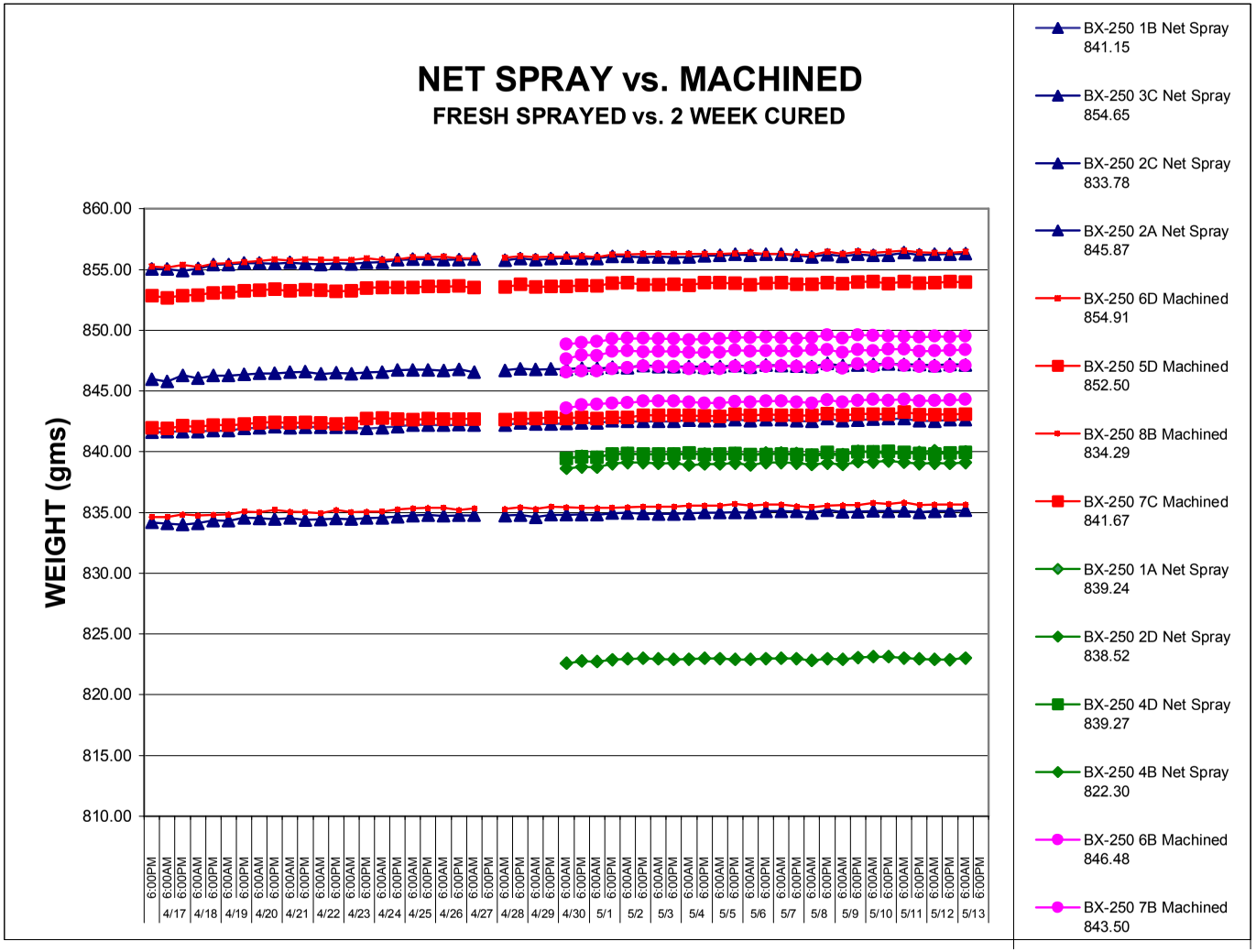

Figure 4. Accelerated Moisture Conditioning (32 °F/76% RH)

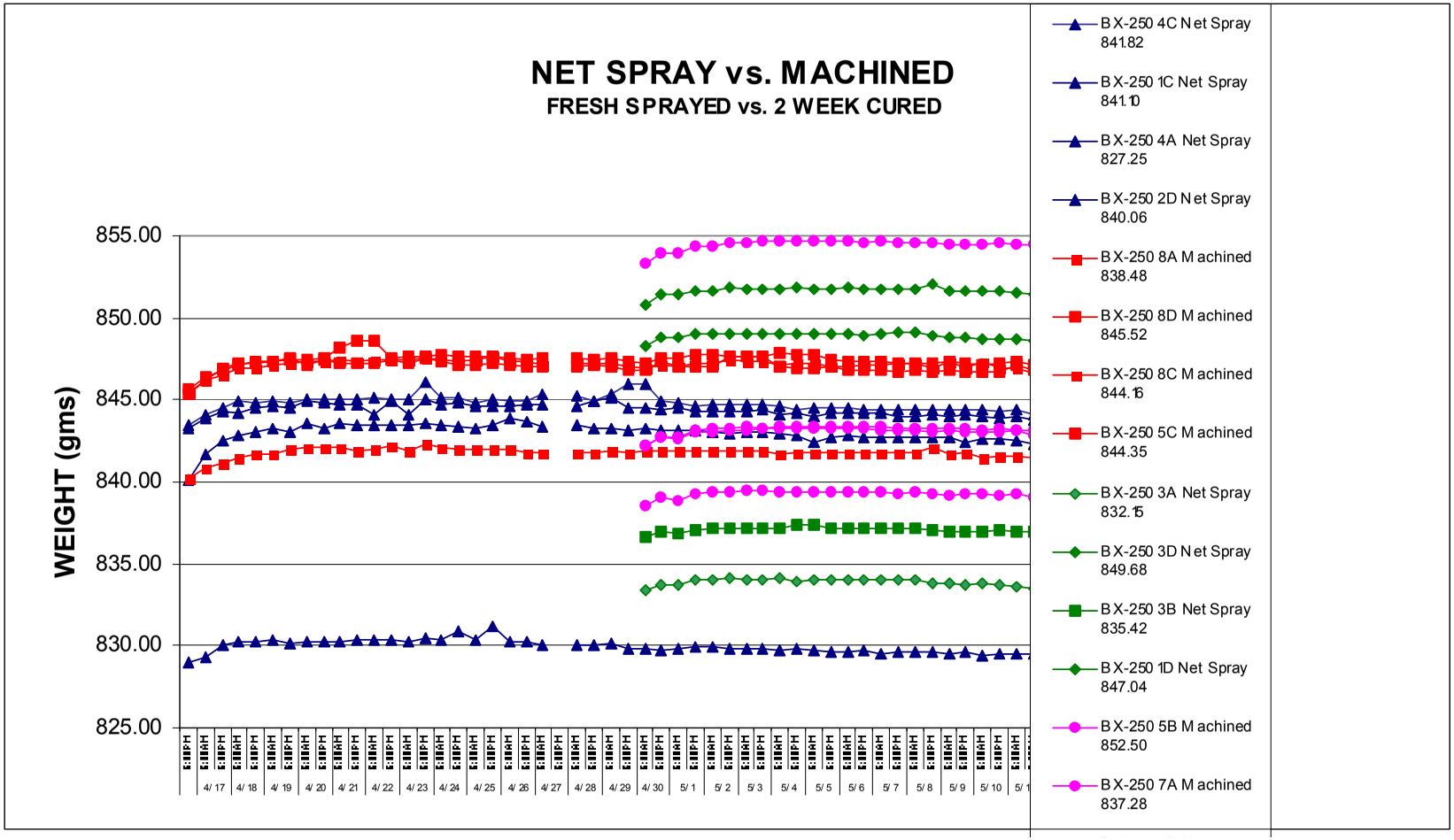

Figure 5. Accelerated Moisture Conditioning (120 °F/98% RH)

Date/EST	STS	Bipod Foam Loss?	Melbourne: (Temperature-Dew Point Temperature) @L-8hrs
01/16/03:10:39	107	Yes	1°F
11/23/02:19:49	113	No	22°F
10/07/02:15:45	112	Yes	0°F
06/05/02:17:22	111	No	10°F
04/08/02:16:44	110	No	16°F
03/01/02:06:22	109	No	14°F
12/05/01:17:19	108	No	11°F

Table 2. Preliminary analysis of environmental moisture conditions for launches with bipod foam loss vs. those without observed loss. (Melbourne, FL)

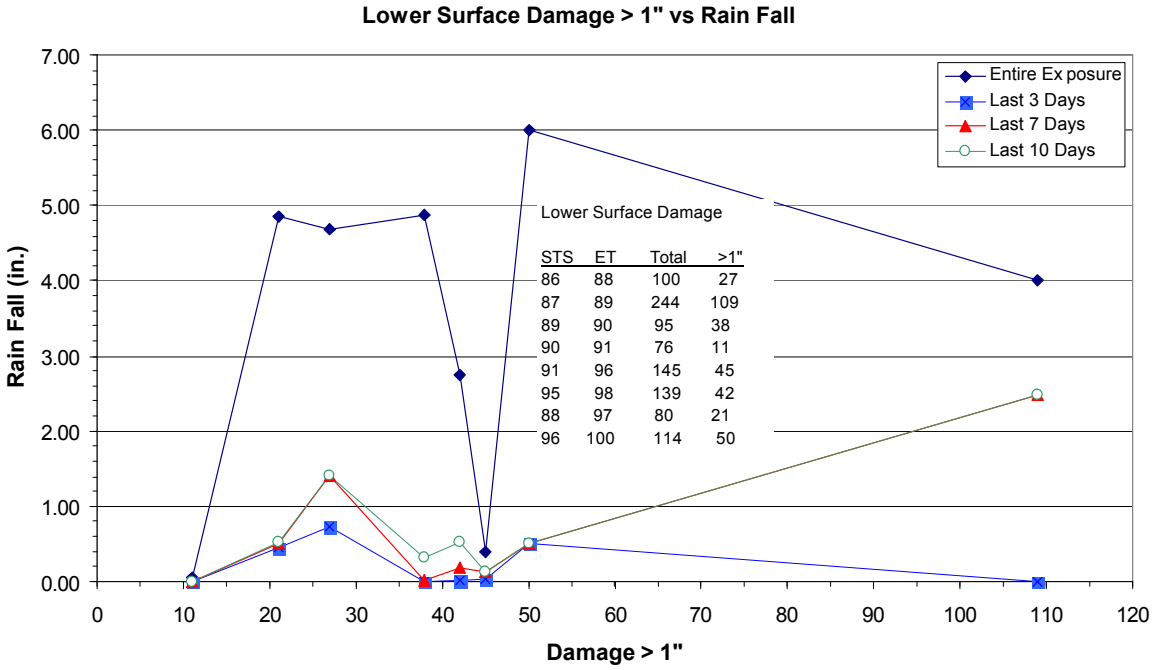

Figure 6. Correlation of On-Pad Rainfall to Orbiter Lower Surface Tile Damage.

Volume IV
Appendix F.4
ET Cryoinsulation

ET cryoinsulation Power Point Slides presented 7 April 2003 at the CAIB Public Hearing: ET cryoinsulation, by Lee Foster and Scotty Sparks, MSFC.

THIS PAGE INTENTIONALLY LEFT BLANK

CAIB Public Hearing: ET Cryoinsulation
Lee Foster / MSFC
Scotty Sparks / MSFC
April 7, 2003

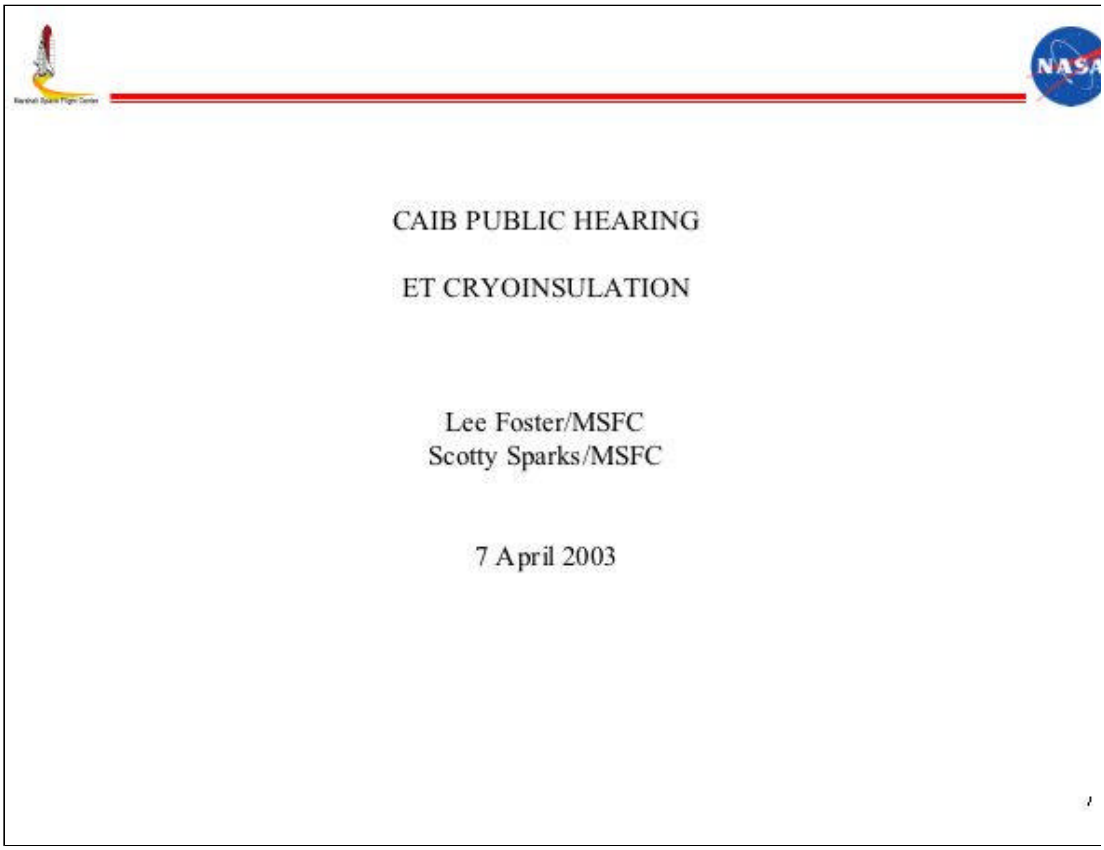

CAIB PUBLIC HEARING

ET CRYOINSULATION

Lee Foster/MSFC
Scotty Sparks/MSFC

7 April 2003

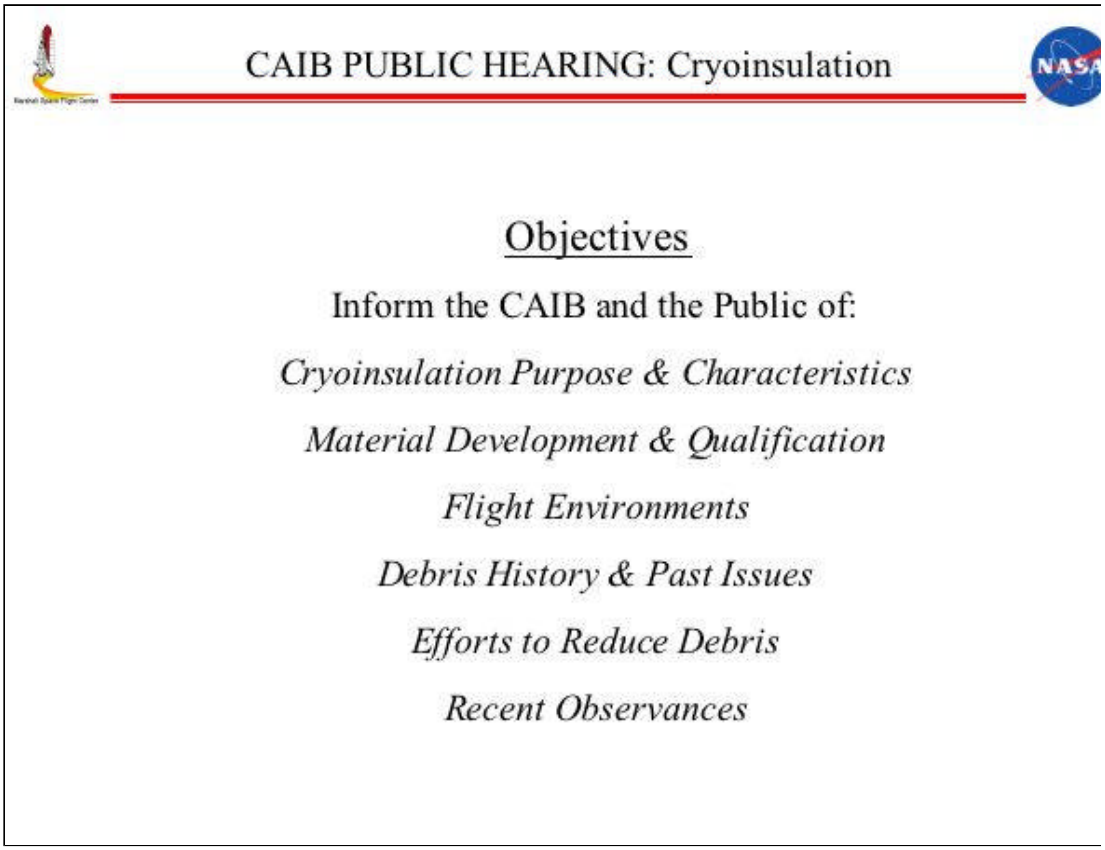
CAIB PUBLIC HEARING: Cryoinsulation
NASA
Objectives
Inform the CAIB and the Public of:
Cryoinsulation Purpose & Characteristics
Material Development & Qualification
Flight Environments
Debris History & Past Issues
Efforts to Reduce Debris
Recent Observances

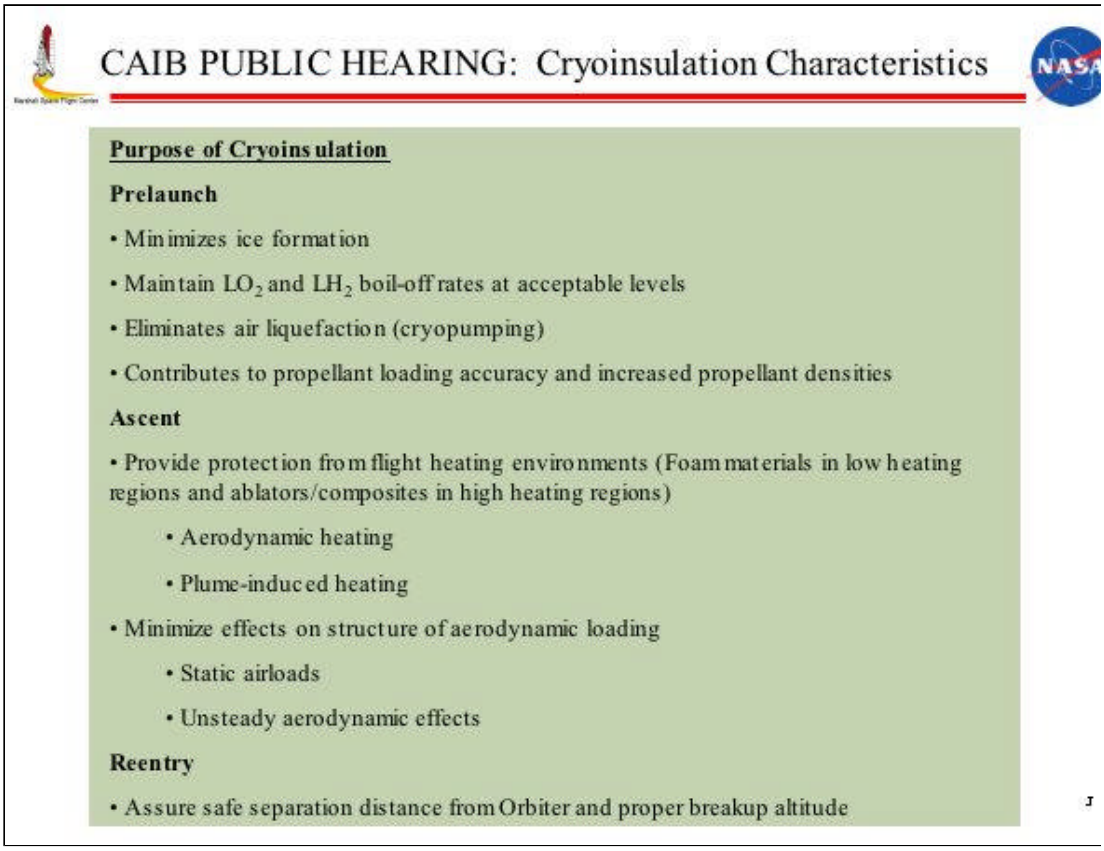
CAIB PUBLIC HEARING: Cryoinsulation Characteristics
NASA
Purpose of Cryoinsulation
Prelaunch
• Minimizes ice formation
• Maintain LO_2 and LH_2 boil-off rates at acceptable levels
• Eliminates air liquefaction (cryopumping)
• Contributes to propellant loading accuracy and increased propellant densities
Ascent
• Provide protection from flight heating environments (Foam materials in low heating regions and ablators/composites in high heating regions)
• Aerodynamic heating
• Plume-induced heating
• Minimize effects on structure of aerodynamic loading
• Static airloads
• Unsteady aerodynamic effects
Reentry
• Assure safe separation distance from Orbiter and proper breakup altitude

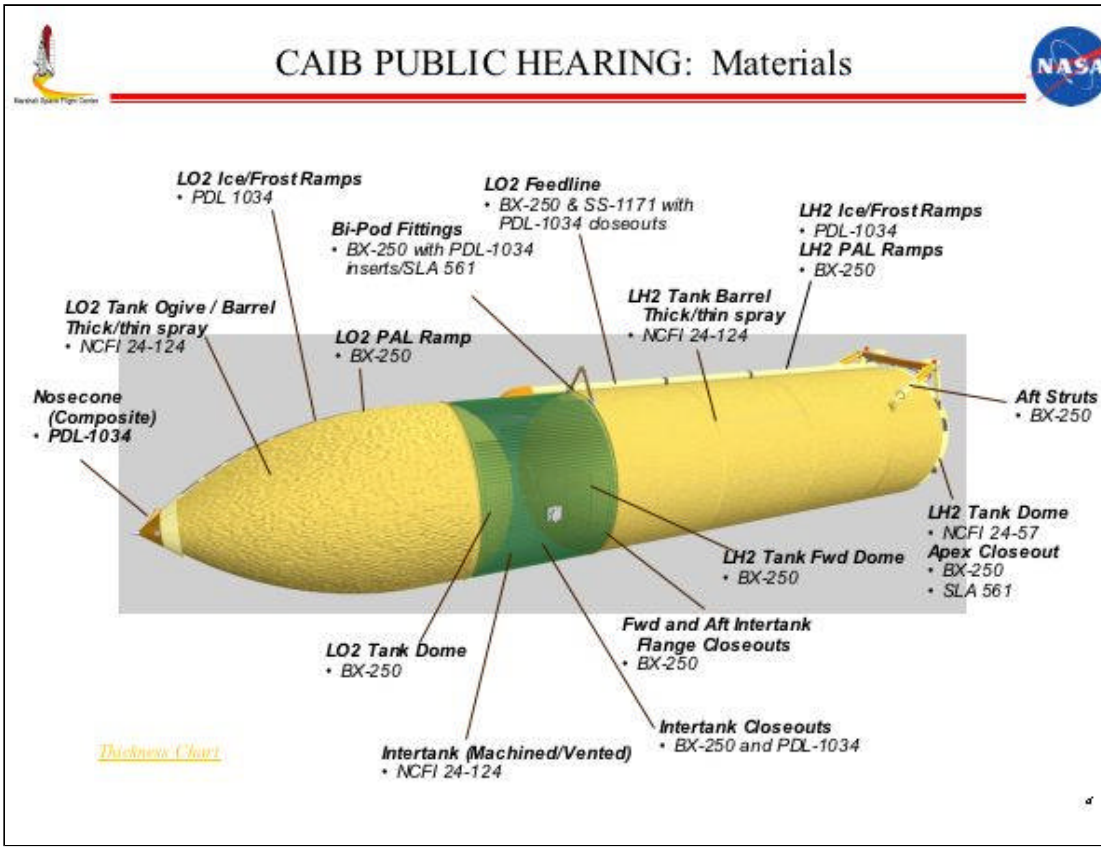
CAIB PUBLIC HEARING: Materials
LO2 Ice/Frost Ramps
• PDL 1034
LO2 Feedline
• BX-250 & SS-1171 with PDL-1034 closeouts
Bi-Pod Fittings
• BX-250 with PDL-1034 inserts/SLA 561
LH2 Ice/Frost Ramps
• PDL-1034
LH2 PAL Ramps
• BX-250
LO2 Tank Ogive / Barrel Thick/thin spray
• NCFI 24-124
LO2 PAL Ramp
• BX-250
LH2 Tank Barrel Thick/thin spray
• NCFI 24-124
Nosecone (Composite)
• PDL-1034
Aft Struts
• BX-250
LH2 Tank Dome
• NCFI 24-57
Apex Closeout
• BX-250
• SLA 561
LH2 Tank Fwd Dome
• BX-250
Fwd and Aft Intertank Flange Closeouts
• BX-250
LO2 Tank Dome
• BX-250
Intertank Closeouts
• BX-250 and PDL-1034
Intertank (Machined/Vented)
• NCFI 24-124
Thickness Chart

CAIB PUBLIC HEARING: Cryoinsulation Characteristics

Levels of Structure

1. Polymeric Structure

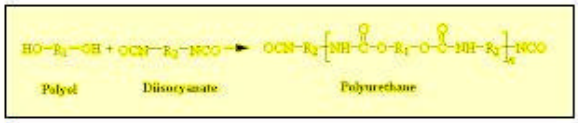

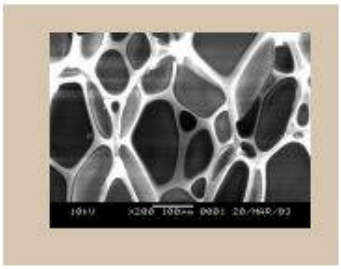

2. Cellular Structure

3. Knitline Geometry
4. Substrate Geometry

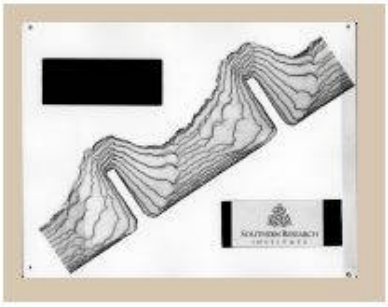

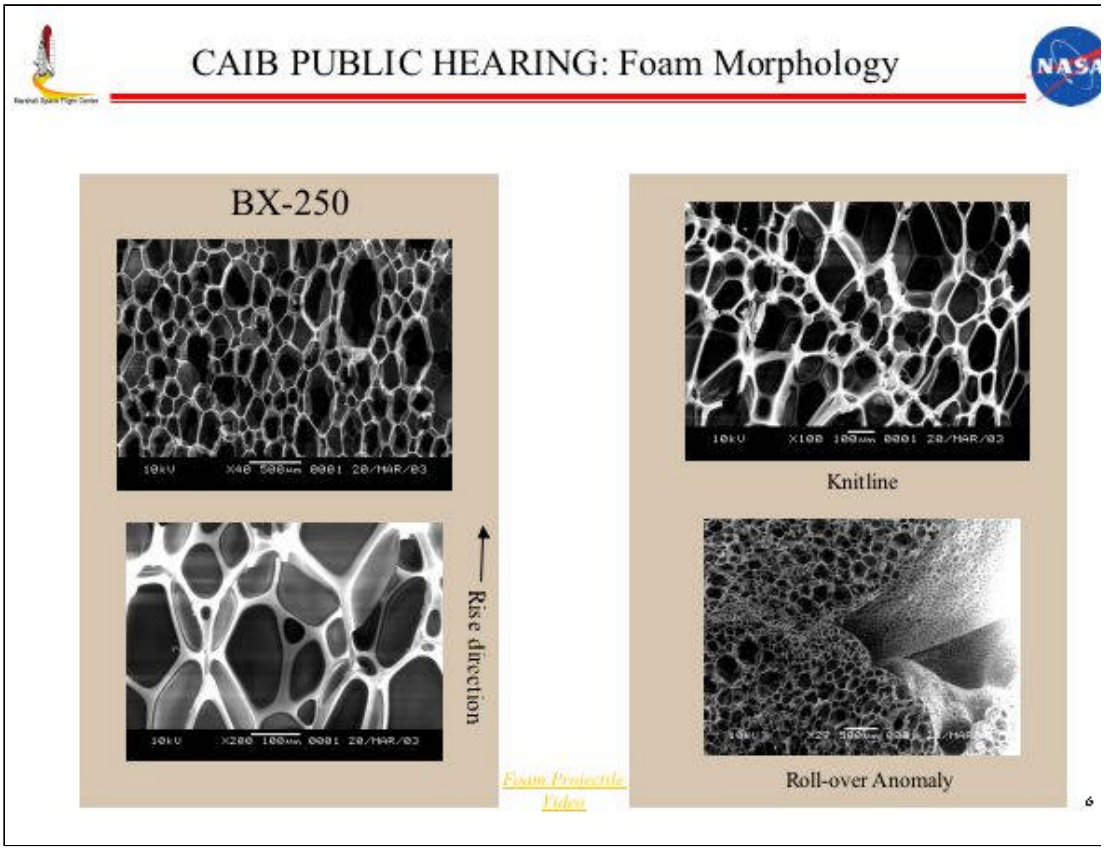
CAIB PUBLIC HEARING: Foam Morphology
BX-250
Rise direction
Foam Projectile Video
Knitline
Roll-over Anomaly
6

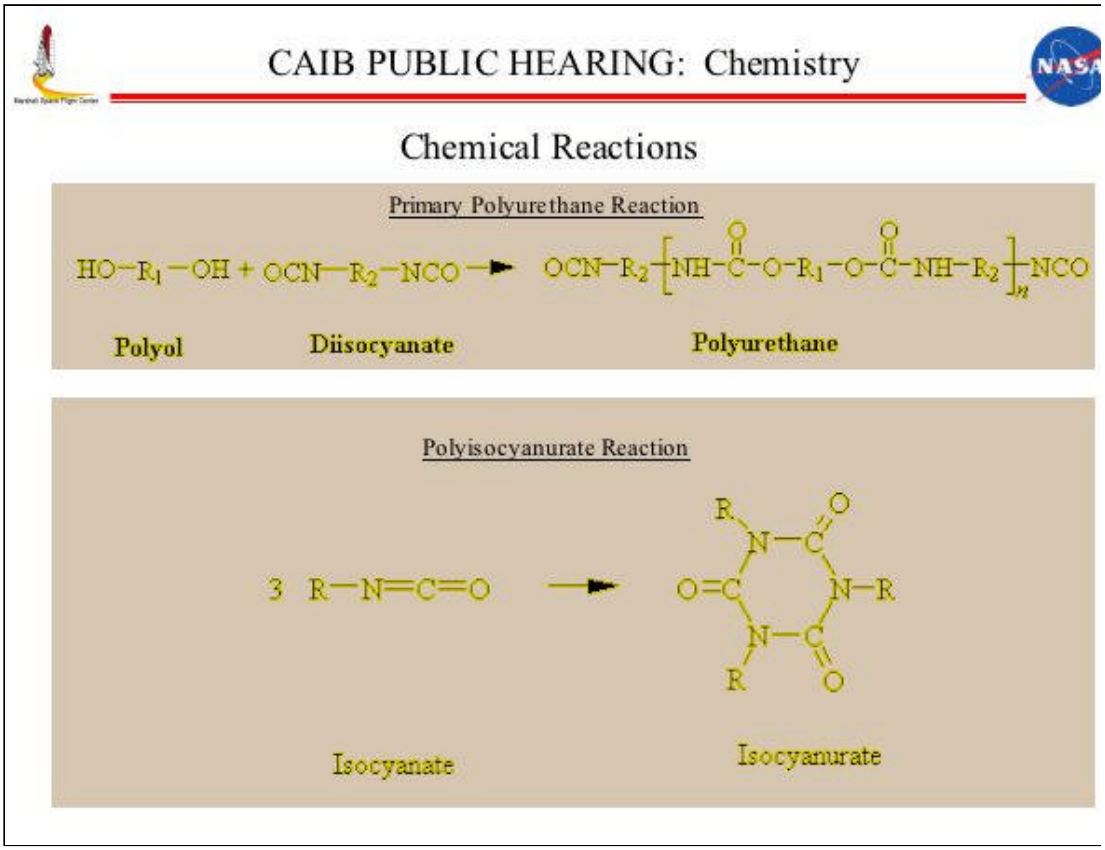
CAIB PUBLIC HEARING: Chemistry
Chemical Reactions
Primary Polyurethane Reaction
HO–R1–OH + OCN–R2–NCO
OCN–R2–[NH–C(=O)–O–R1–O–C(=O)–NH–R2]n–NCO
Polyol
Diisocyanate
Polyurethane
Polyisocyanurate Reaction
3 R–N=C=O
Isocyanate
Isocyanurate

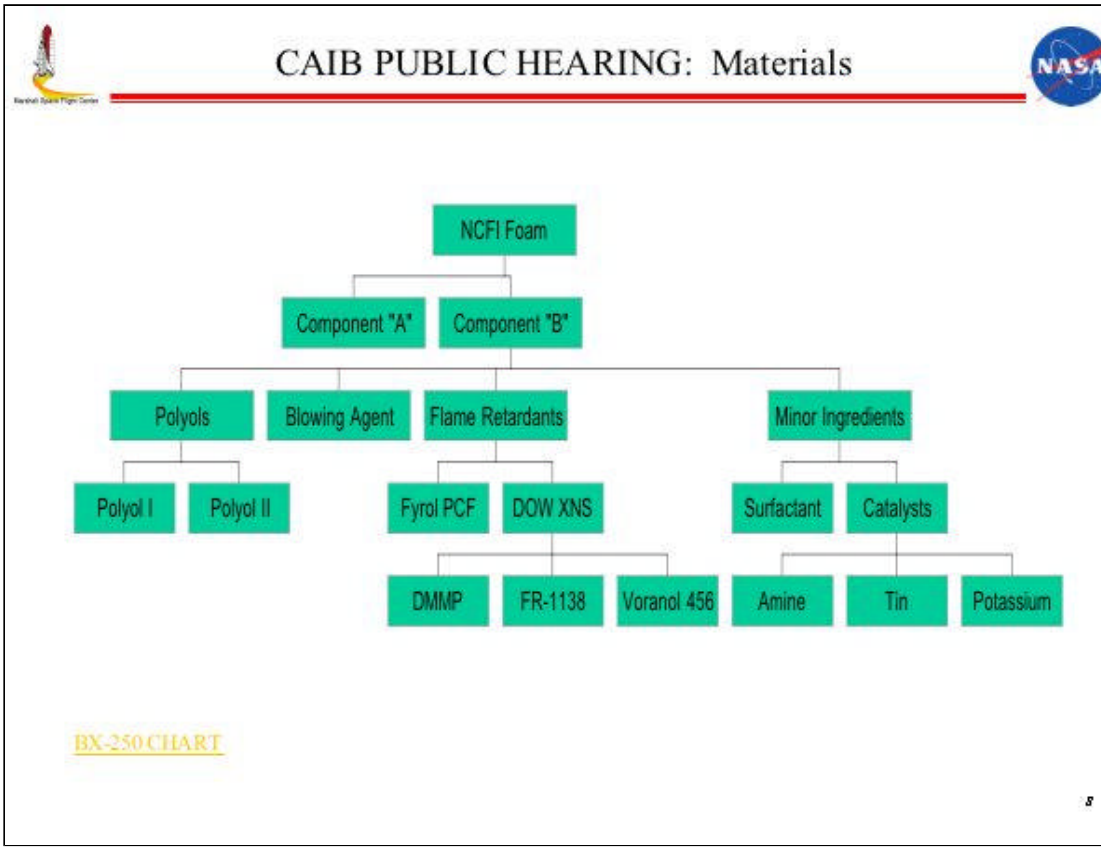
CAIB PUBLIC HEARING: Materials
NCFI Foam
Component "A"
Component "B"
Polyols
Blowing Agent
Flame Retardants
Minor Ingredients
Polyol I
Polyol II
Fyrol PCF
DOW XNS
Surfactant
Catalysts
DMMP
FR-1138
Voranol 456
Amine
Tin
Potassium
BX-250 CHART

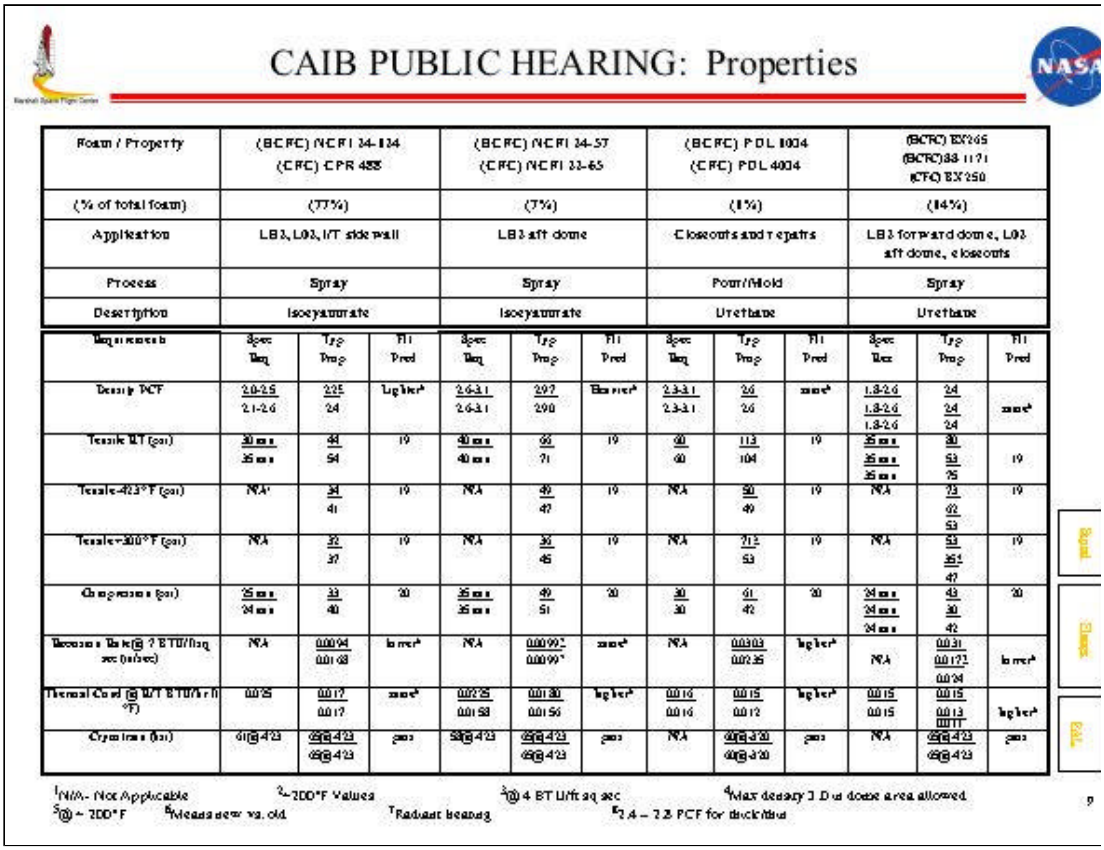

CAIB PUBLIC HEARING: Properties

Foam / Property	(BCFC) NCFI 24-124 (CFC) CPR 488			(BCFC) NCFI 24-57 (CFC) NCFI 22-65			(BCFC) PDL 1004 (CFC) PDL 4004			(BCFC) EX265 (BCFC)SS 1171 (CFC) EX250		
(% of total foam)	(77%)			(7%)			(1%)			(14%)		
Application	LB2, L02, I/T side wall			LB2 aft dome			Closeouts and repairs			LB2 forward dome, L02 aft dome, closeouts		
Process	Spray			Spray			Pour/Mold			Spray		
Description	Isocyanurate			Isocyanurate			Urethane			Urethane		
Requirements	Spec Req	Typ Prop	Fit Pred	Spec Req	Typ Prop	Fit Pred	Spec Req	Typ Prop	Fit Pred	Spec Req	Typ Prop	Fit Pred
Density PCF	2.0-2.5 2.1-2.6	2.25 2.4	Lighter[6]	2.6-3.1 2.6-3.1	2.97 2.90	Heavier[6]	2.3-3.1 2.3-3.1	2.6 2.6	same[6]	1.8-2.6 1.8-2.6 1.8-2.6	2.4 2.4 2.4	same[6]
Tensile RT (psi)	30 min 35 min	44 54	19	40 min 40 min	66 71	19	60 60	113 104	19	35 min 35 min 35 min	80 53 75	19
Tensile -423°F (psi)	N/A[1]	34 41	19	N/A	49 47	19	N/A	50 49	19	N/A	73 62 53	19
Tensile +300°F (psi)	N/A	32 37	19	N/A	36 45	19	N/A	71[2] 53	19	N/A	53 35[2] 47	19
Compression (psi)	25 min 24 min	33 40	20	35 min 35 min	49 51	20	30 30	61 42	20	24 min 24 min 24 min	43 30 42	20
Recession Rate @ 7 BTU/ft sq sec (in/sec)	N/A	0.0094 0.0168	lower[6]	N/A	0.00992 0.0099[7]	same[6]	N/A	0.0303 0.0235	higher[6]	N/A	0.031 0.0172 0.024	lower[6]
Thermal Cond @ R/T BTU/hr ft °F)	0.025	0.017 0.017	same[6]	0.0225 0.0158	0.0180 0.0156	higher[6]	0.016 0.016	0.015 0.012	higher[6]	0.015 0.015	0.015 0.013 0.011	higher[6]
Cryostrain (ksi)	61@-423	65@-423 65@-423	pass	58@-423	65@-423 65@-423	pass	N/A	60@-320 60@-320	pass	N/A	65@-423 65@-423	pass

[1]N/A- Not Applicable [2]~200°F Values [3]@ 4 BTU/ft sq sec [4]Max density 3 D in dome area allowed
[5]@ ~ 200°F [6]Means new vs. old [7]Radiant heating [8]2.4 – 2.8 PCF for thick/thin

9

Signal
Elements
Exit

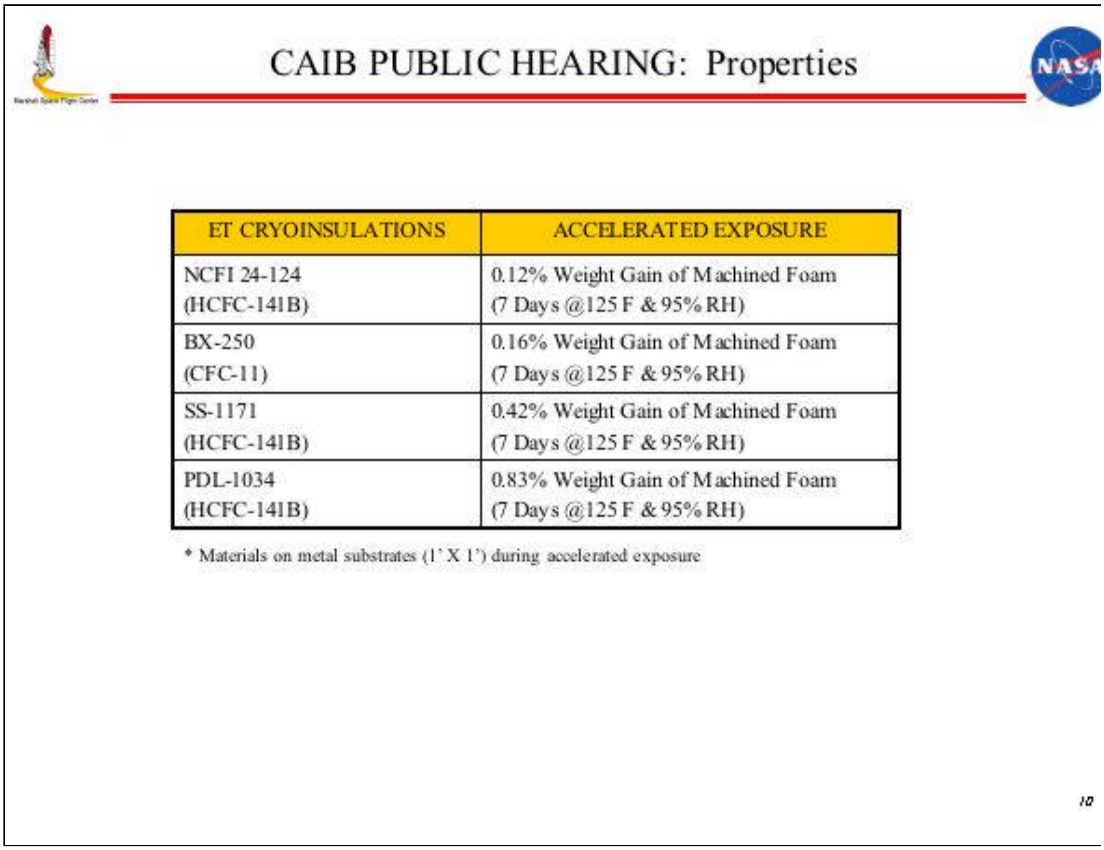

ET CRYOINSULATIONS	ACCELERATED EXPOSURE
NCFI 24-124 (HCFC-141B)	0.12% Weight Gain of Machined Foam (7 Days @125 F & 95% RH)
BX-250 (CFC-11)	0.16% Weight Gain of Machined Foam (7 Days @125 F & 95% RH)
SS-1171 (HCFC-141B)	0.42% Weight Gain of Machined Foam (7 Days @125 F & 95% RH)
PDL-1034 (HCFC-141B)	0.83% Weight Gain of Machined Foam (7 Days @125 F & 95% RH)

* Materials on metal substrates (1' X 1') during accelerated exposure

CAIB PUBLIC HEARING: Qualification Activities
NASA
Testing Performed Throughout Qualification Activities
Several lots of material were tested to characterize the material variability and process repeatability.
Physical Properties
Bond Tension (-423 to 300 °F)
Flatwise Tension (-423 to 300 °F)
Plug Pulls
Density
Compression
Mechanical Properties
Cryoflex (-423 & -320 °F)
Monostrain (-423 to 400 °F)
Torsion Shear
Poisson Ratio
Thermal Properties
Thermal Conductivity (-423 to 200 °F)
Oxygen Index
Flammability
Specific Heat & TGA
Aero-recession (Hot Gas)
Thermal-Vac
Major Flight Acceptance Tests:
Wind Tunnel (aero-recession for ascent)
Plasma Arc (Entry recession)
PAL Ramps
Aft Dome Test (Stop Sign)
Combined Environments (combined lift-off environments)

CAIB PUBLIC HEARING: Process Control

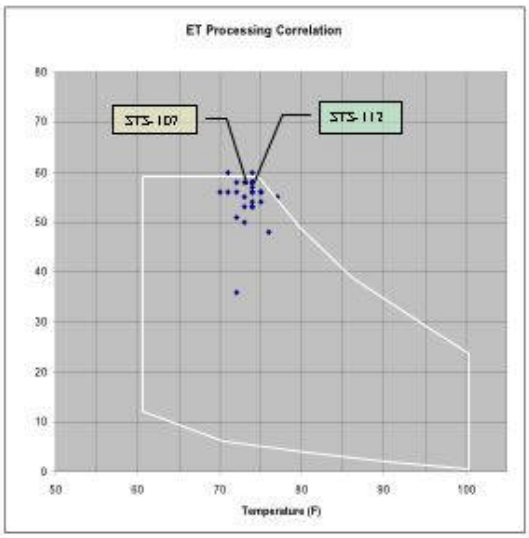

BX-250 Bipod Application	Work Area Temperature (F)	Work Area Relative Humidity (%)
ET-106 -Y	72	56
ET-106 +Y	72	58
ET-107 -Y	75	56
ET-107 +Y	74	57
ET-108 -Y	73	50
ET-108 +Y	75	54
ET-109 -Y	74	54
ET-109 +Y	76	48
ET-110 -Y	74	56
ET-110 +Y	77	55
ET-111 -Y	74	58
ET-111 +Y	74	60
ET-93 -Y	73	58
ET-93 +Y	74	58
ET-94 -Y	74	56
ET-94 +Y	72	51
ET-112 -Y	72	36
ET-112 +Y	71	56
ET-113 -Y	70	56
ET-113 +Y	75	56
ET-114 -Y	73	53
ET-114 +Y	74	53
ET-115 -Y	74	58
ET-115 +Y	74	53
ET-116 -Y	73	55
ET-116 +Y	71	60

STS-112 STS-107

12

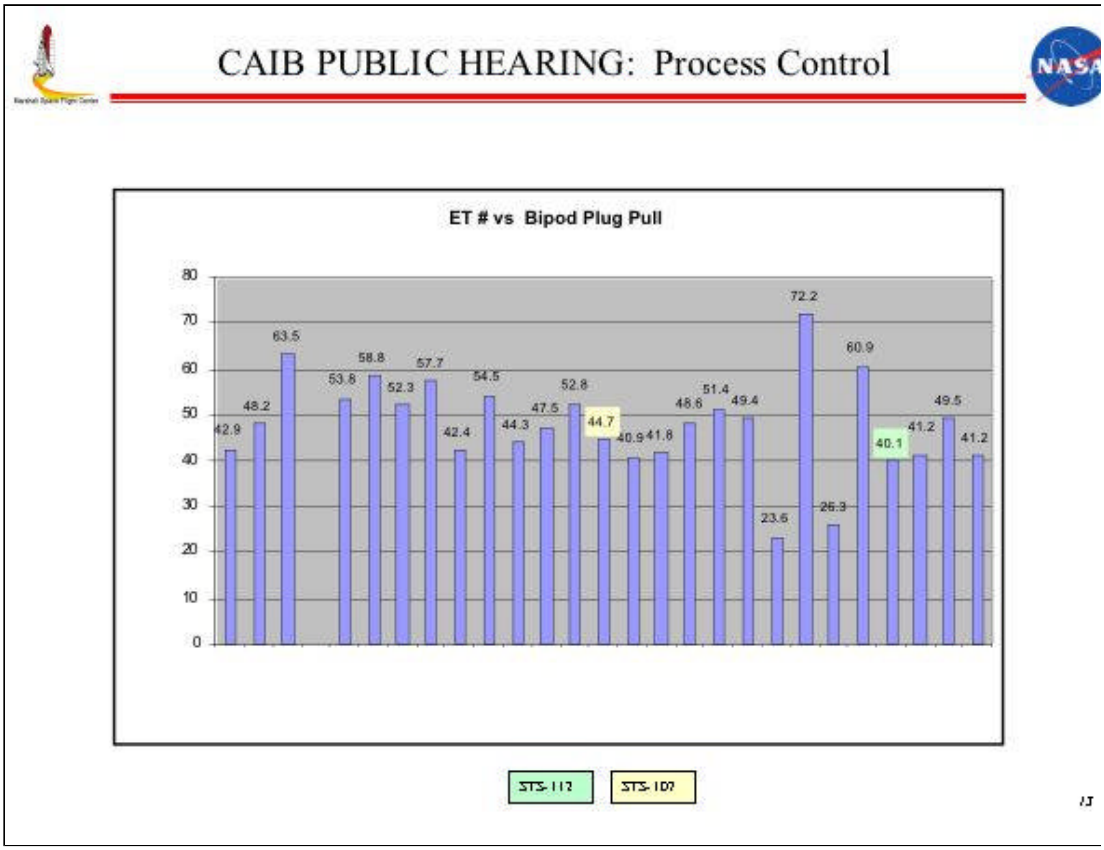
CAIB PUBLIC HEARING: Process Control
ET # vs Bipod Plug Pull
80
70
60
50
40
30
20
10
0
42.9
48.2
63.5
53.8
58.8
52.3
57.7
42.4
54.5
44.3
47.5
52.8
44.7
40.9
41.8
48.6
51.4
49.4
23.6
72.2
26.3
60.9
40.1
41.2
49.5
41.2
STS-112
STS-107

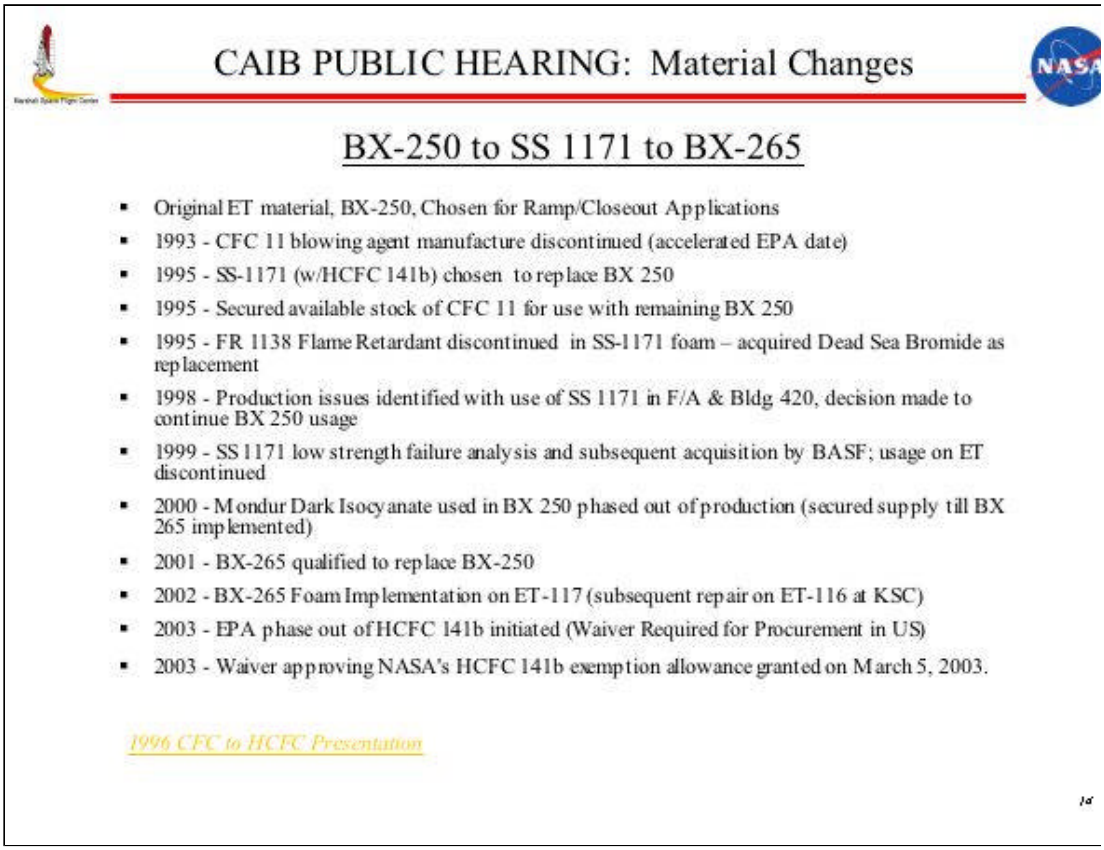
CAIB PUBLIC HEARING: Material Changes
BX-250 to SS 1171 to BX-265
Original ET material, BX-250, Chosen for Ramp/Closeout Applications
1993 - CFC 11 blowing agent manufacture discontinued (accelerated EPA date)
1995 - SS-1171 (w/HCFC 141b) chosen to replace BX 250
1995 - Secured available stock of CFC 11 for use with remaining BX 250
1995 - FR 1138 Flame Retardant discontinued in SS-1171 foam – acquired Dead Sea Bromide as replacement
1998 - Production issues identified with use of SS 1171 in F/A & Bldg 420, decision made to continue BX 250 usage
1999 - SS 1171 low strength failure analysis and subsequent acquisition by BASF; usage on ET discontinued
2000 - Mondur Dark Isocyanate used in BX 250 phased out of production (secured supply till BX 265 implemented)
2001 - BX-265 qualified to replace BX-250
2002 - BX-265 Foam Implementation on ET-117 (subsequent repair on ET-116 at KSC)
2003 - EPA phase out of HCFC 141b initiated (Waiver Required for Procurement in US)
2003 - Waiver approving NASA's HCFC 141b exemption allowance granted on March 5, 2003.
1996 CFC to HCFC Presentation

CAIB PUBLIC HEARING: Flight Environments
SUBSONIC, TRANSONIC & SUPERSONIC AERODYNAMICS
FORCES
MOMENTS
LOADS
PRESSURES
VENTING
JET EFFECTS
PARACHUTE AERODYNAMICS
HEAT TRANSFER
AERODYNAMIC HEATING
CONVECTIVE HEATING FROM JETS
RADIATIVE HEATING FROM JETS
LAUNCH PAD EFFECTS
DETERMINATION OF INDUCED ENVIRONMENTS FOR LAUNCH VEHICLES
SSME ENGINE PLUMES
SHOCK WAVE SYSTEM
SEPARATED FLOW & RECIRCULATION
BOUNDARY LAYER BUILDUP
FLOW
PROTUBERANCE
SRB PLUME
HOT GAS RECIRCULATION
RADIATION
BASE AREAS AFFECTED BY HEAT & PRESSURE
HOT SPOTS
MSFC 3/60 SA4100 53
Synchronized Flight Environments

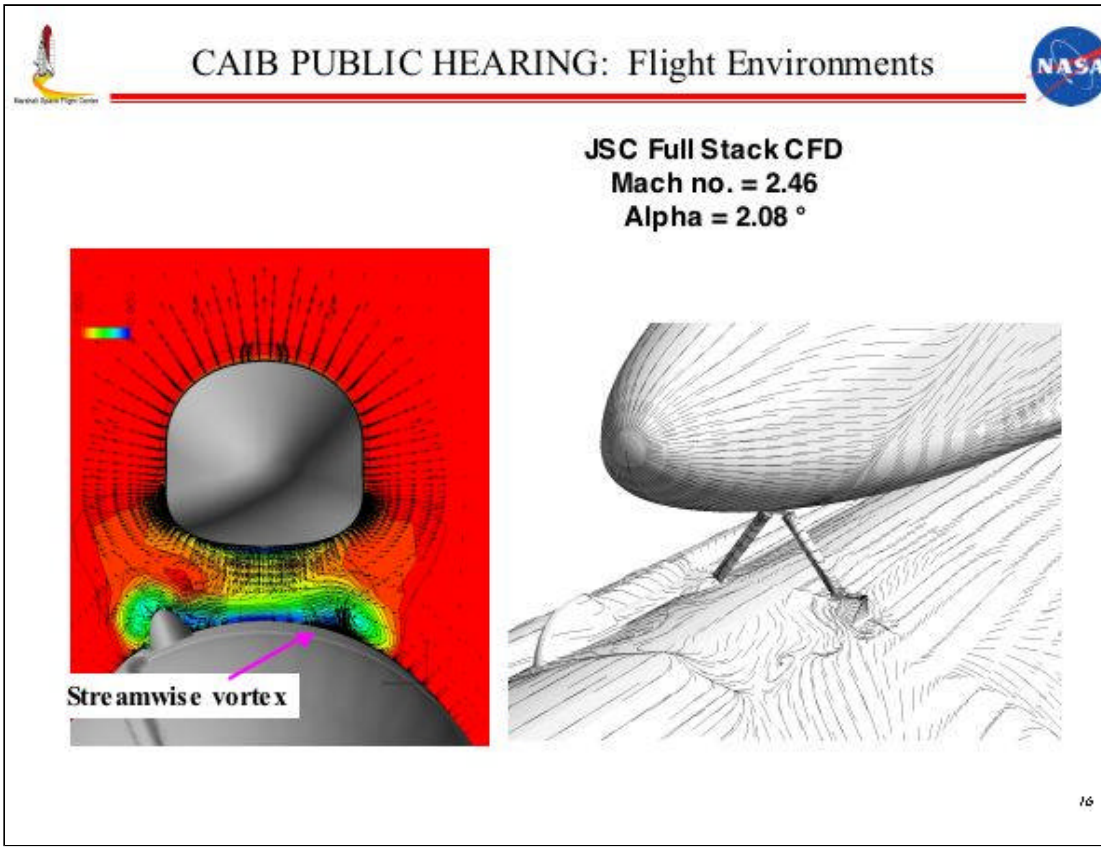
CAIB PUBLIC HEARING: Flight Environments
JSC Full Stack CFD
Mach no. = 2.46
Alpha = 2.08 °
Streamwise vortex
16

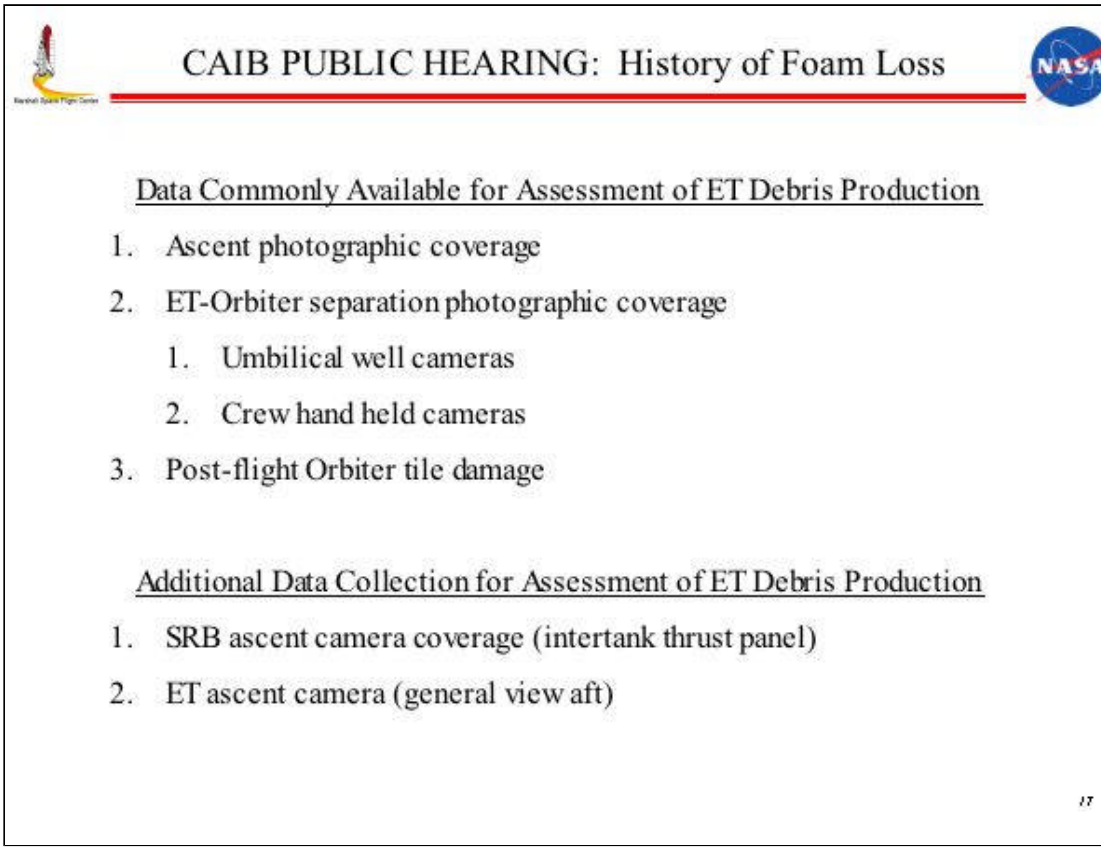
CAIB PUBLIC HEARING: History of Foam Loss
NASA
Data Commonly Available for Assessment of ET Debris Production
1. Ascent photographic coverage
2. ET-Orbiter separation photographic coverage
1. Umbilical well cameras
2. Crew hand held cameras
3. Post-flight Orbiter tile damage
Additional Data Collection for Assessment of ET Debris Production
1. SRB ascent camera coverage (intertank thrust panel)
2. ET ascent camera (general view aft)

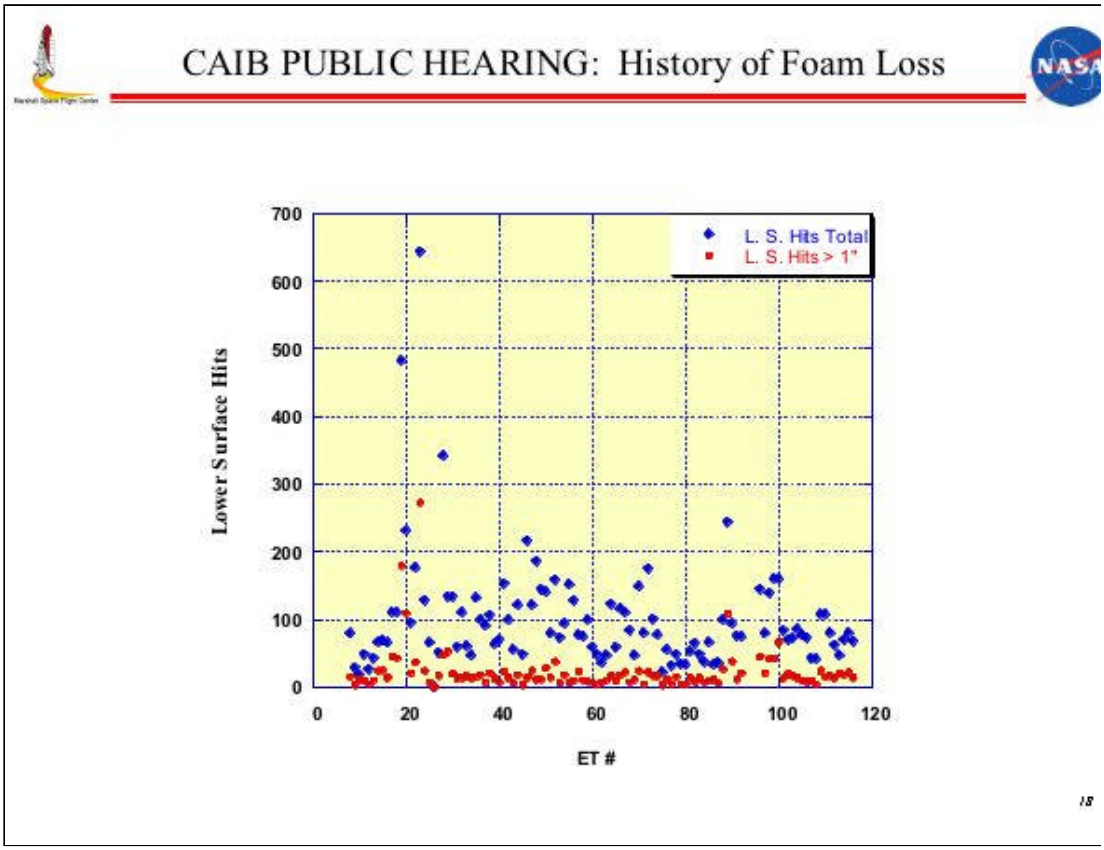
CAIB PUBLIC HEARING: History of Foam Loss
NASA
L. S. Hits Total
L. S. Hits > 1"
Lower Surface Hits
700
600
500
400
300
200
100
0
0
20
40
60
80
100
120
ET #
18

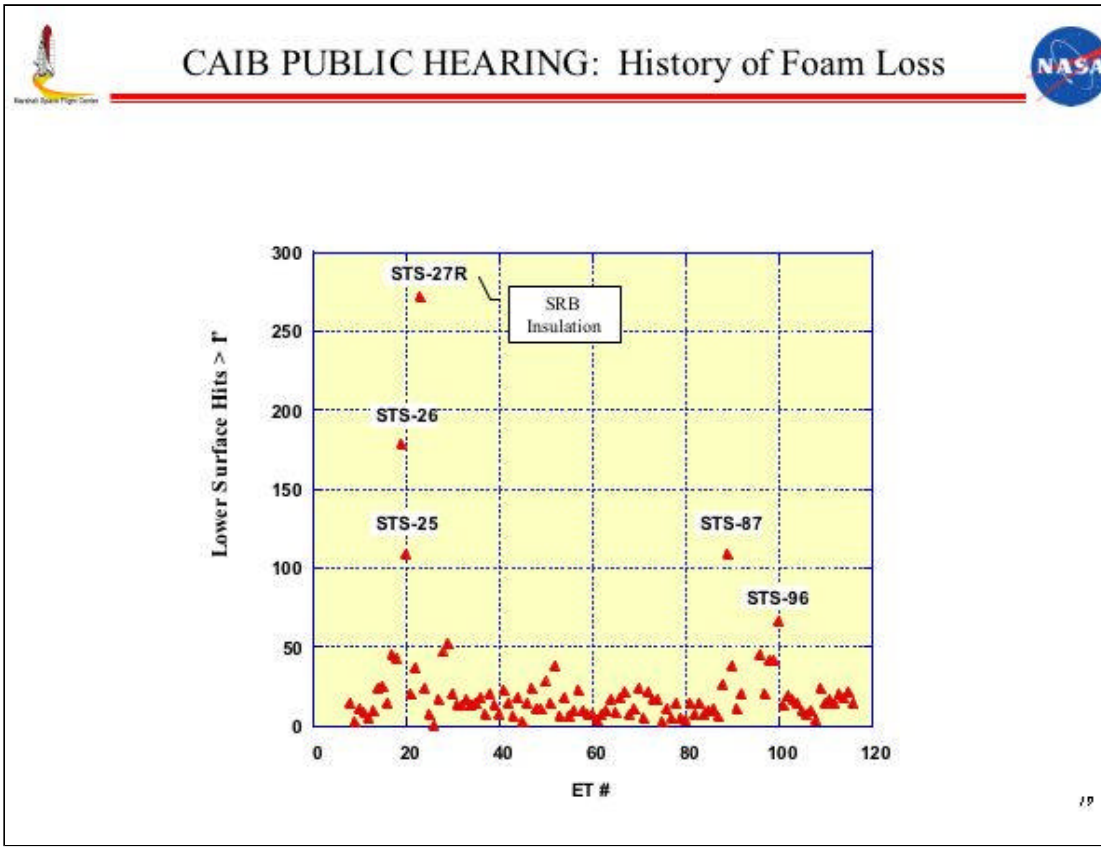
CAIB PUBLIC HEARING: History of Foam Loss
Lower Surface Hits > 1"
ET #
STS-27R
SRB Insulation
STS-26
STS-25
STS-87
STS-96
0
50
100
150
200
250
300
0
20
40
60
80
100
120

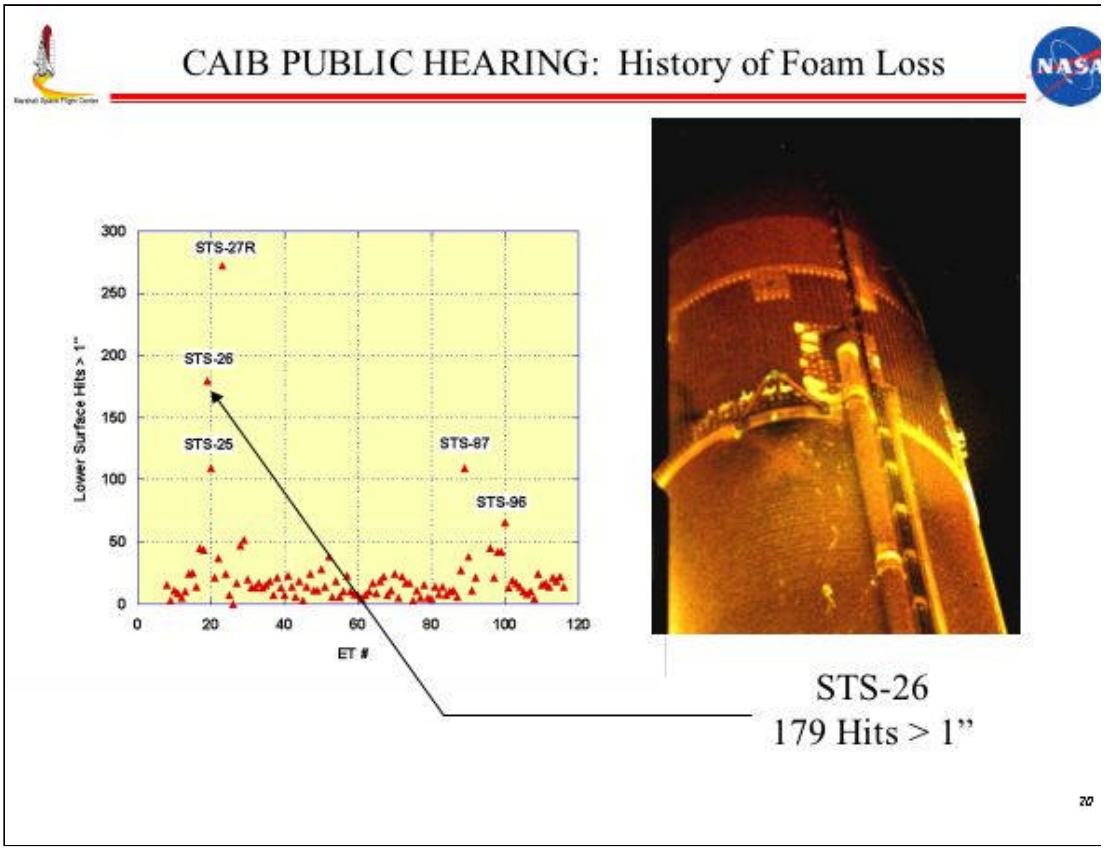
CAIB PUBLIC HEARING: History of Foam Loss
NASA
Lower Surface Hits > 1"
ET #
STS-27R
STS-26
STS-25
STS-87
STS-95
0
50
100
150
200
250
300
0
20
40
60
80
100
120
STS-26
179 Hits > 1"
20

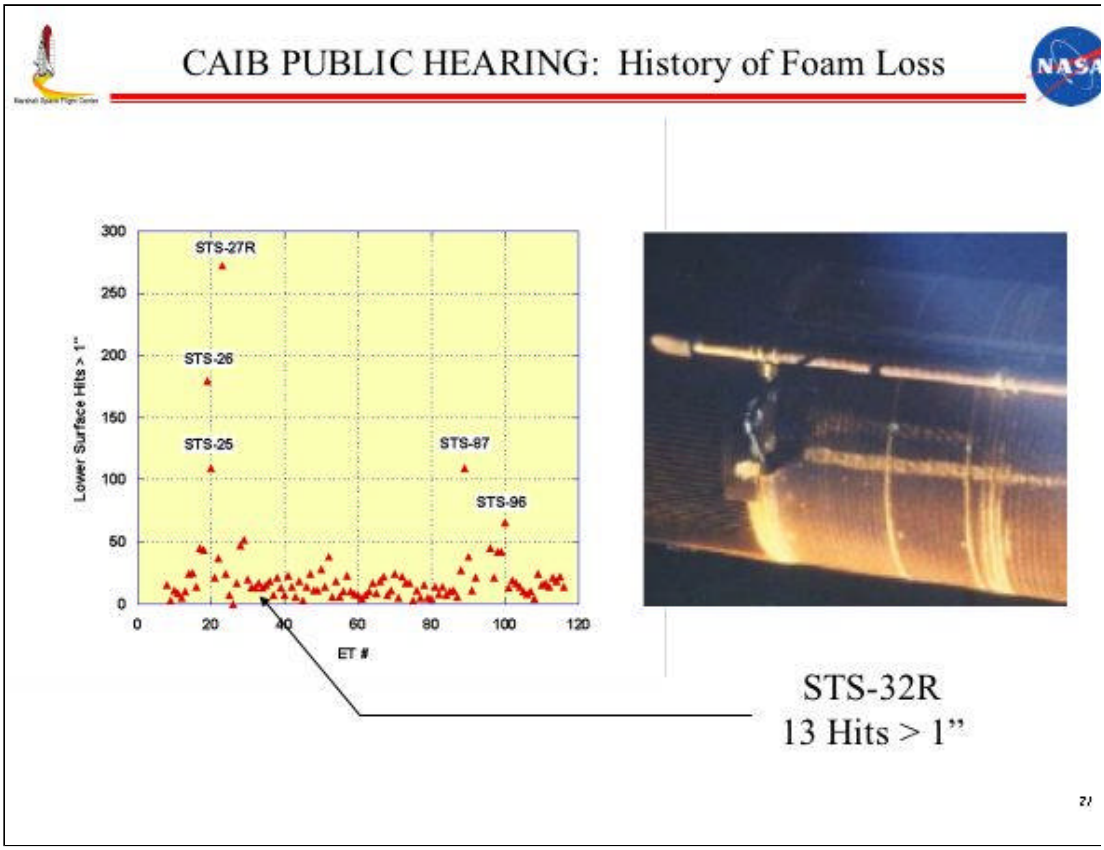
CAIB PUBLIC HEARING: History of Foam Loss
NASA
Lower Surface Hits > 1"
300
250
200
150
100
50
0
STS-27R
STS-26
STS-25
STS-87
STS-95
0
20
40
60
80
100
120
ET #
STS-32R
13 Hits > 1"
21

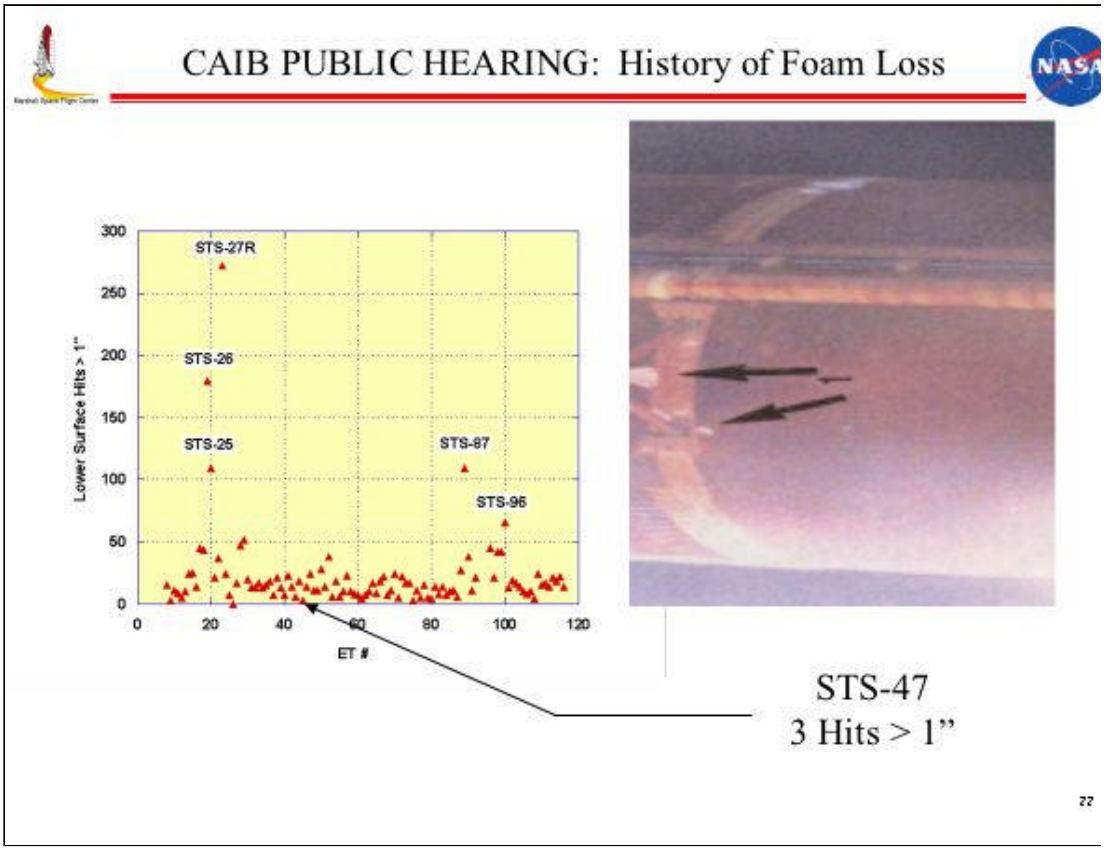
CAIB PUBLIC HEARING: History of Foam Loss
NASA
Lower Surface Hits > 1"
300
250
200
150
100
50
0
STS-27R
STS-26
STS-25
STS-87
STS-95
0
20
40
60
80
100
120
ET #
STS-47
3 Hits > 1"
22

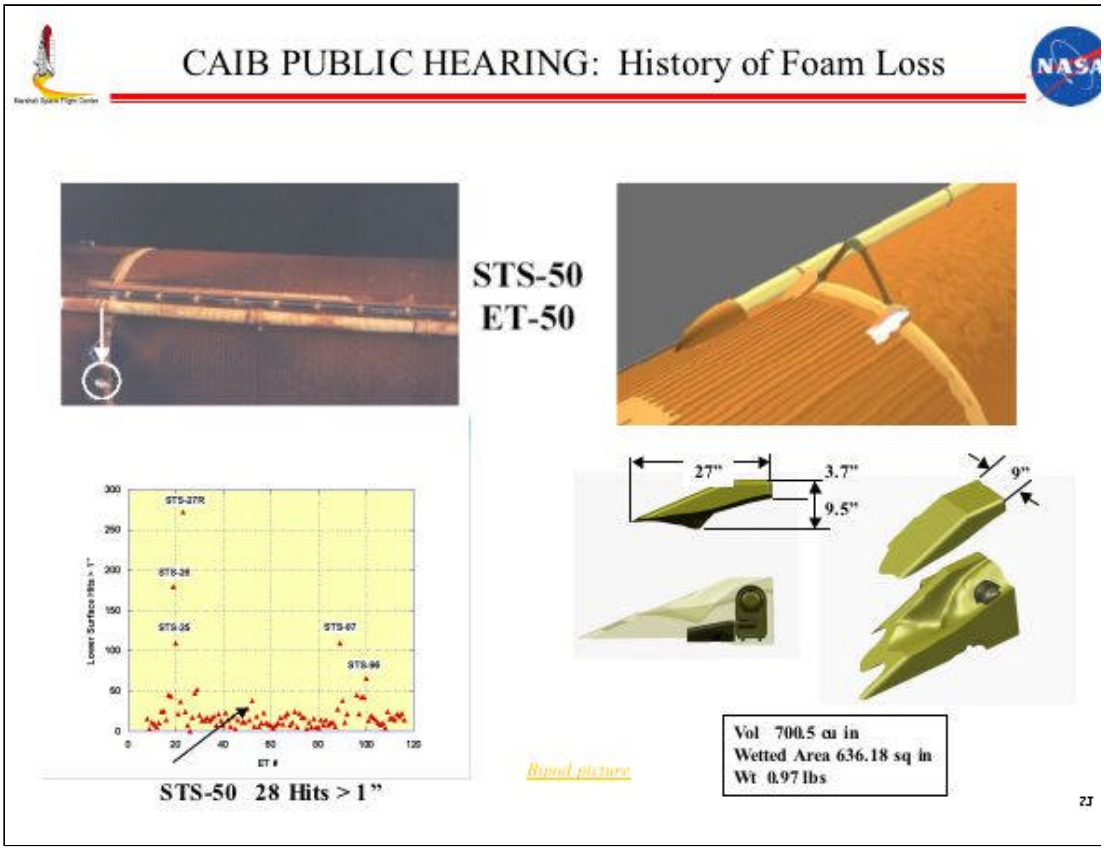
CAIB PUBLIC HEARING: History of Foam Loss
STS-50
ET-50
27"
3.7"
9.5"
9"
Vol 700.5 cu in
Wetted Area 636.18 sq in
Wt 0.97 lbs
STS-50 28 Hits > 1"

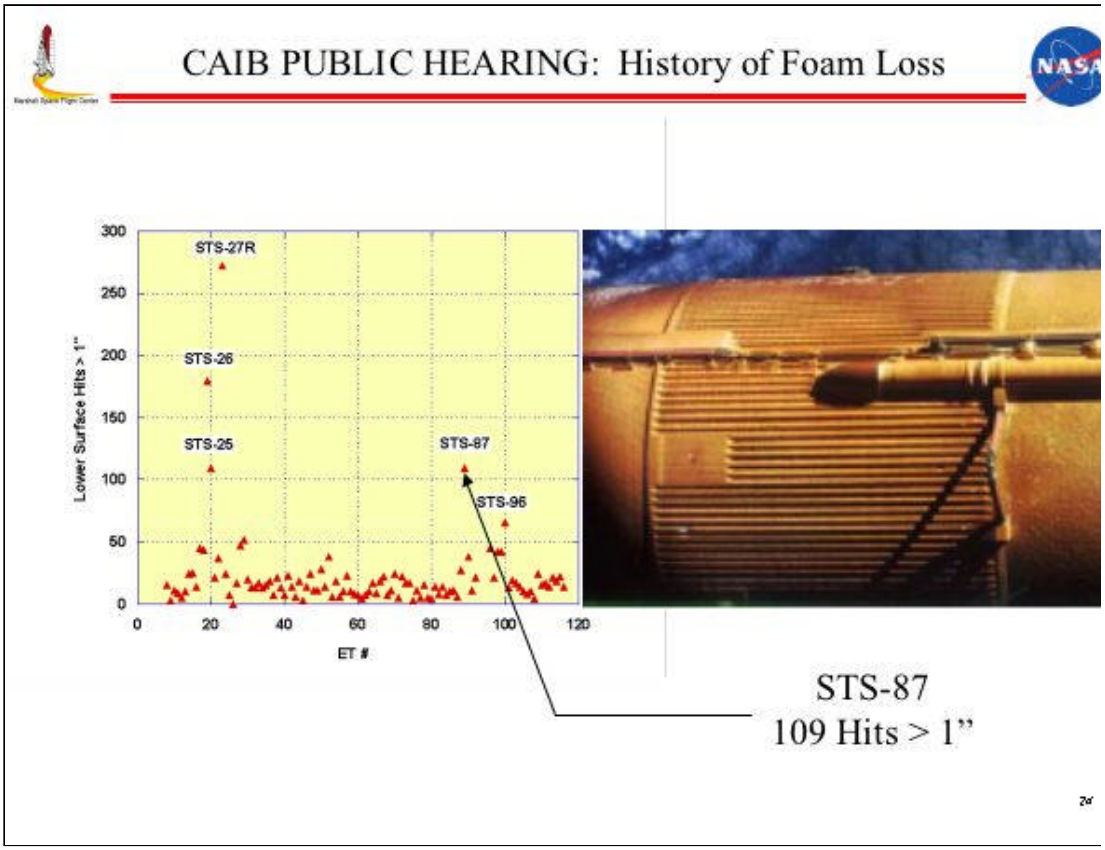
CAIB PUBLIC HEARING: History of Foam Loss
NASA
Lower Surface Hits > 1"
ET #
STS-27R
STS-26
STS-25
STS-87
STS-95
0
50
100
150
200
250
300
0
20
40
60
80
100
120
STS-87
109 Hits > 1"

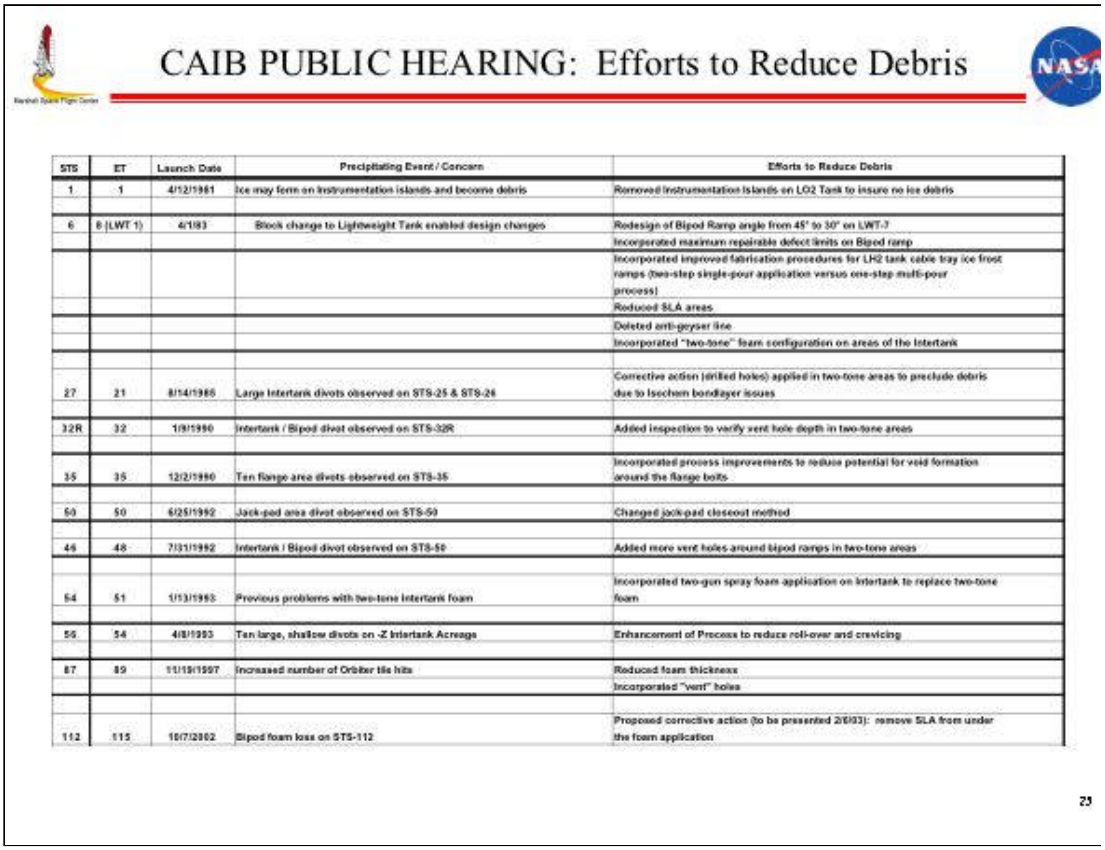

CAIB PUBLIC HEARING: Efforts to Reduce Debris

STS	ET	Launch Date	Precipitating Event / Concern	Efforts to Reduce Debris
1	1	4/12/1981	Ice may form on instrumentation islands and become debris	Removed instrumentation islands on LO2 Tank to insure no ice debris
6	6 (LWT 1)	4/1/83	Block change to Lightweight Tank enabled design changes	Redesign of Bipod Ramp angle from 45° to 30° on LWT-7
				Incorporated maximum repairable defect limits on Bipod ramp
				Incorporated improved fabrication procedures for LH2 tank cable tray ice frost ramps (two-step single-pour application versus one-step multi-pour process)
				Reduced SLA areas
				Deleted anti-geyser line
				Incorporated "two-tone" foam configuration on areas of the Intertank
27	21	8/14/1985	Large Intertank divots observed on STS-25 & STS-26	Corrective action (drilled holes) applied in two-tone areas to preclude debris due to Isochem bondlayer issues
32R	32	1/9/1990	Intertank / Bipod divot observed on STS-32R	Added inspection to verify vent hole depth in two-tone areas
35	35	12/2/1990	Ten flange area divots observed on STS-35	Incorporated process improvements to reduce potential for void formation around the flange bolts
50	50	6/25/1992	Jack-pad area divot observed on STS-50	Changed jack-pad closeout method
46	48	7/31/1992	Intertank / Bipod divot observed on STS-50	Added more vent holes around bipod ramps in two-tone areas
54	51	1/13/1993	Previous problems with two-tone Intertank foam	Incorporated two-gun spray foam application on Intertank to replace two-tone foam
56	54	4/8/1993	Ten large, shallow divots on -Z Intertank Acreage	Enhancement of Process to reduce roll-over and crevicing
87	89	11/19/1997	Increased number of Orbiter tile hits	Reduced foam thickness
				Incorporated "vent" holes
112	115	10/7/2002	Bipod foam loss on STS-112	Proposed corrective action (to be presented 2/Ei03): remove SLA from under the foam application

25

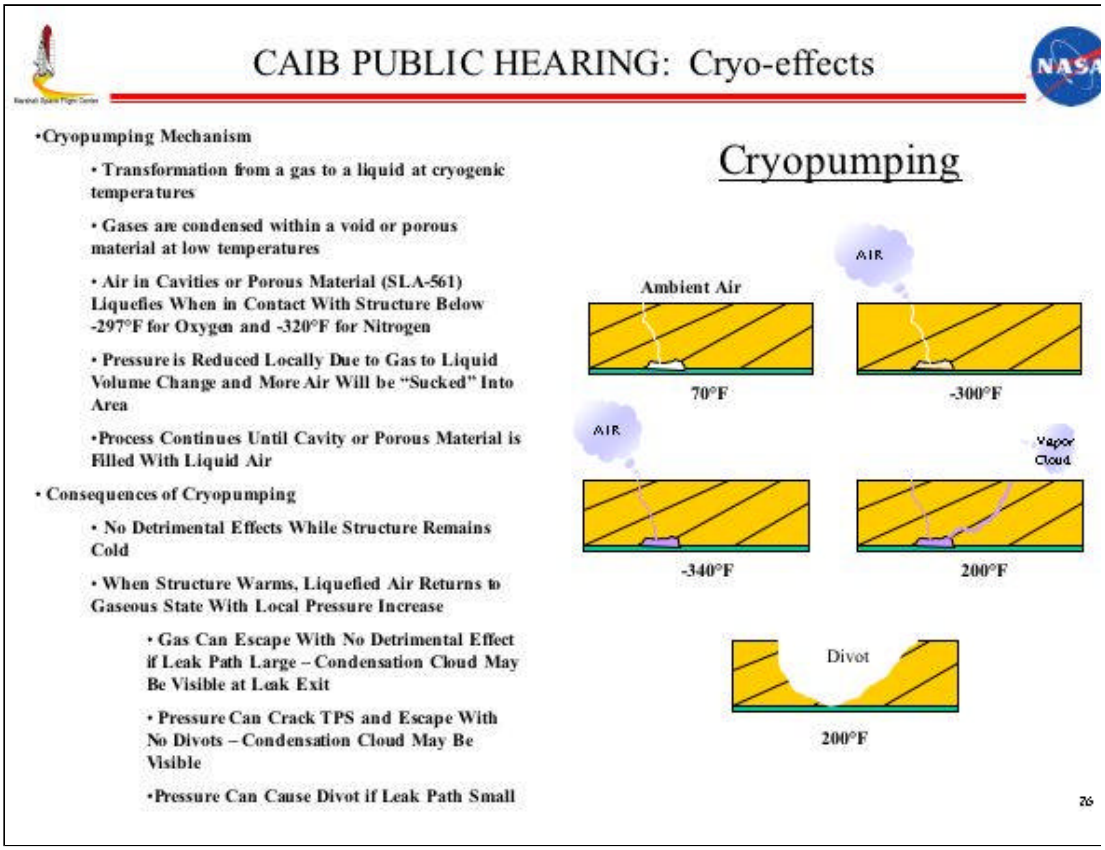
CAIB PUBLIC HEARING: Cryo-effects
NASA
•Cryopumping Mechanism
• Transformation from a gas to a liquid at cryogenic temperatures
• Gases are condensed within a void or porous material at low temperatures
• Air in Cavities or Porous Material (SLA-561) Liquefies When in Contact With Structure Below -297°F for Oxygen and -320°F for Nitrogen
• Pressure is Reduced Locally Due to Gas to Liquid Volume Change and More Air Will be "Sucked" Into Area
•Process Continues Until Cavity or Porous Material is Filled With Liquid Air
• Consequences of Cryopumping
• No Detrimental Effects While Structure Remains Cold
• When Structure Warms, Liquefied Air Returns to Gaseous State With Local Pressure Increase
• Gas Can Escape With No Detrimental Effect if Leak Path Large – Condensation Cloud May Be Visible at Leak Exit
• Pressure Can Crack TPS and Escape With No Divots – Condensation Cloud May Be Visible
•Pressure Can Cause Divot if Leak Path Small
Cryopumping
AIR
Ambient Air
70°F
AIR
-300°F
AIR
-340°F
Vapor Cloud
200°F
Divot
200°F
26

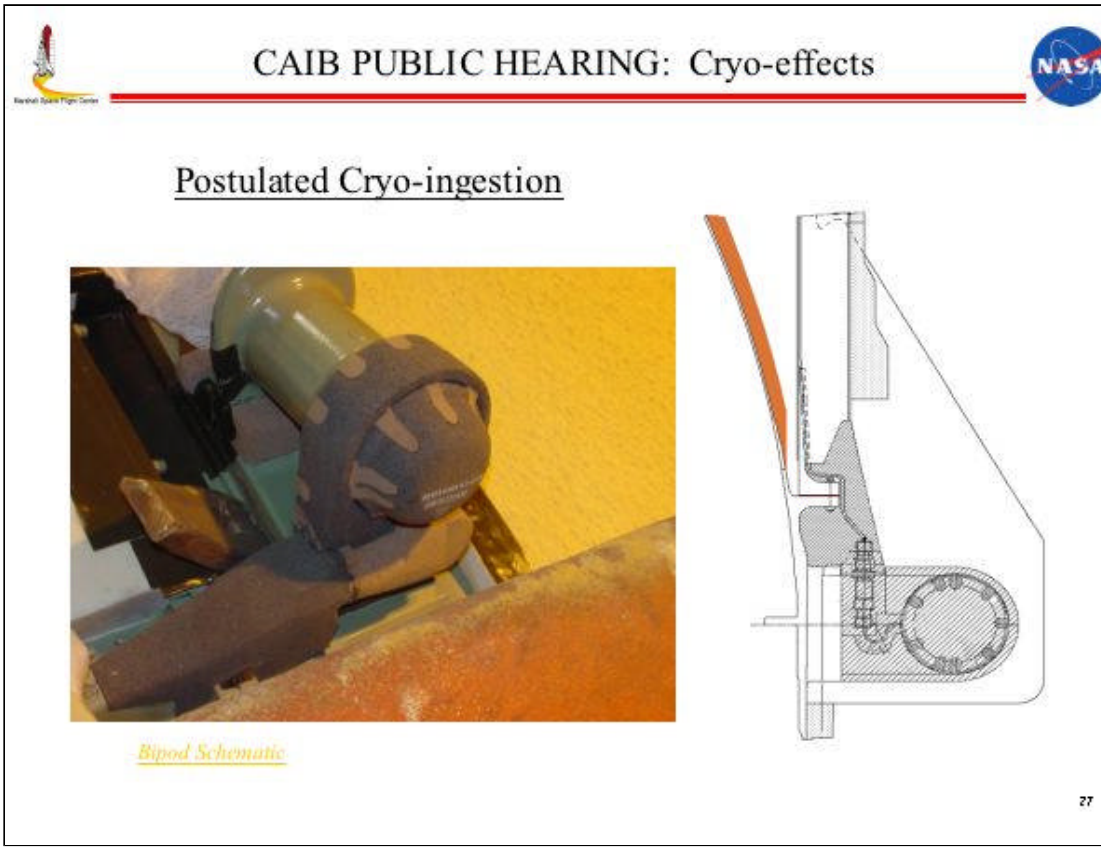
CAIB PUBLIC HEARING: Cryo-effects
Postulated Cryo-ingestion
Bipod Schematic
27

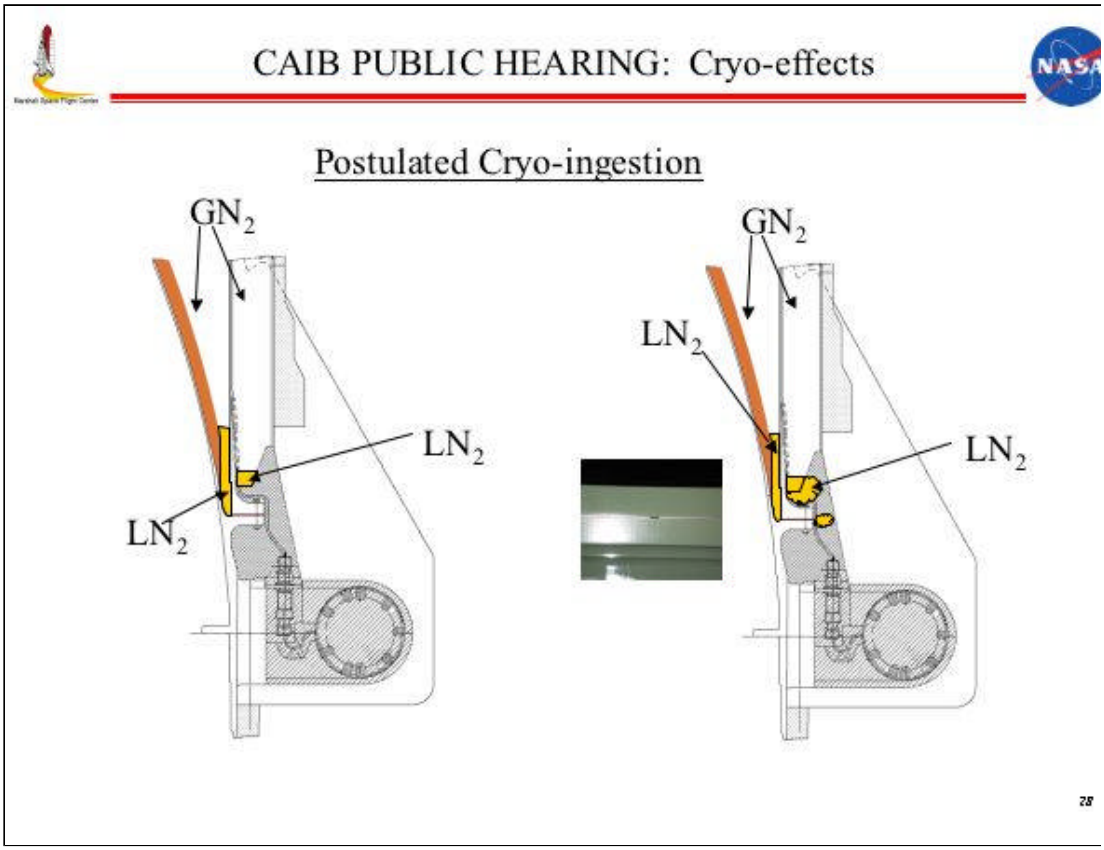
CAIB PUBLIC HEARING: Cryo-effects
Postulated Cryo-ingestion
GN2
LN2
LN2
GN2
LN2
LN2
28

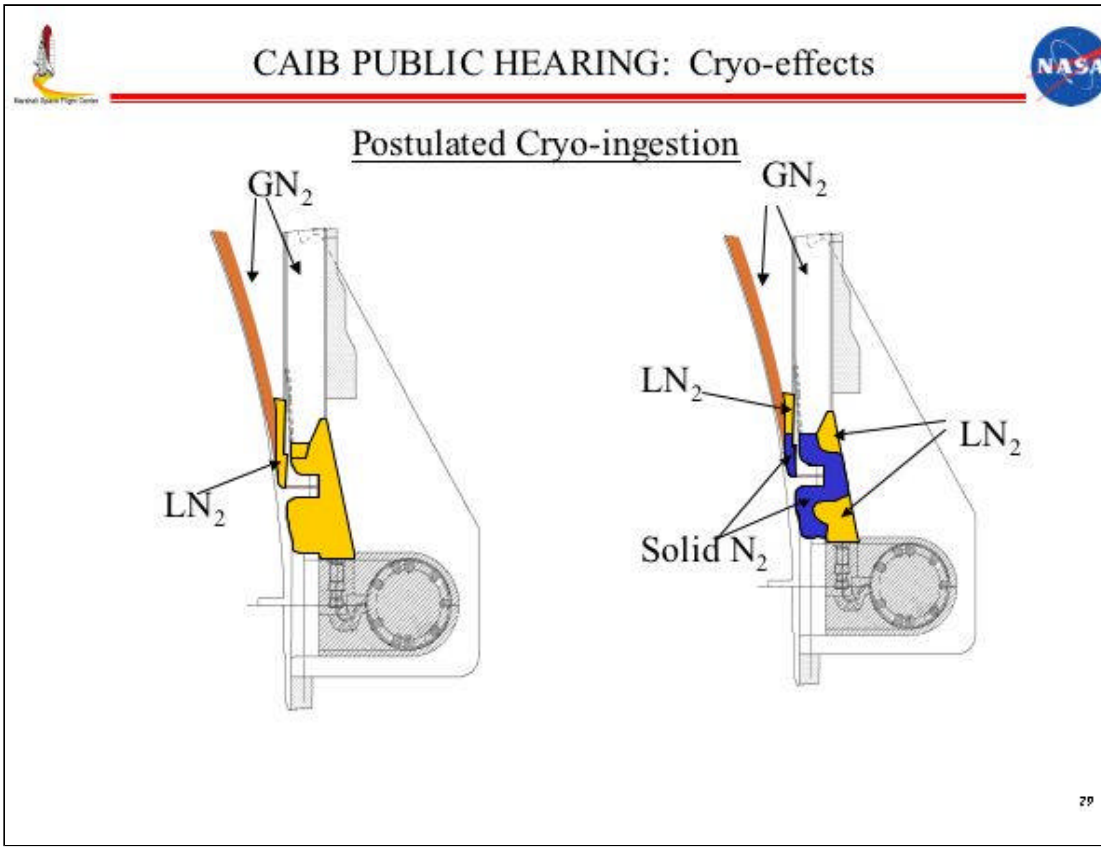
CAIB PUBLIC HEARING: Cryo-effects
Postulated Cryo-ingestion
GN2
LN2
GN2
LN2
LN2
Solid N2
29

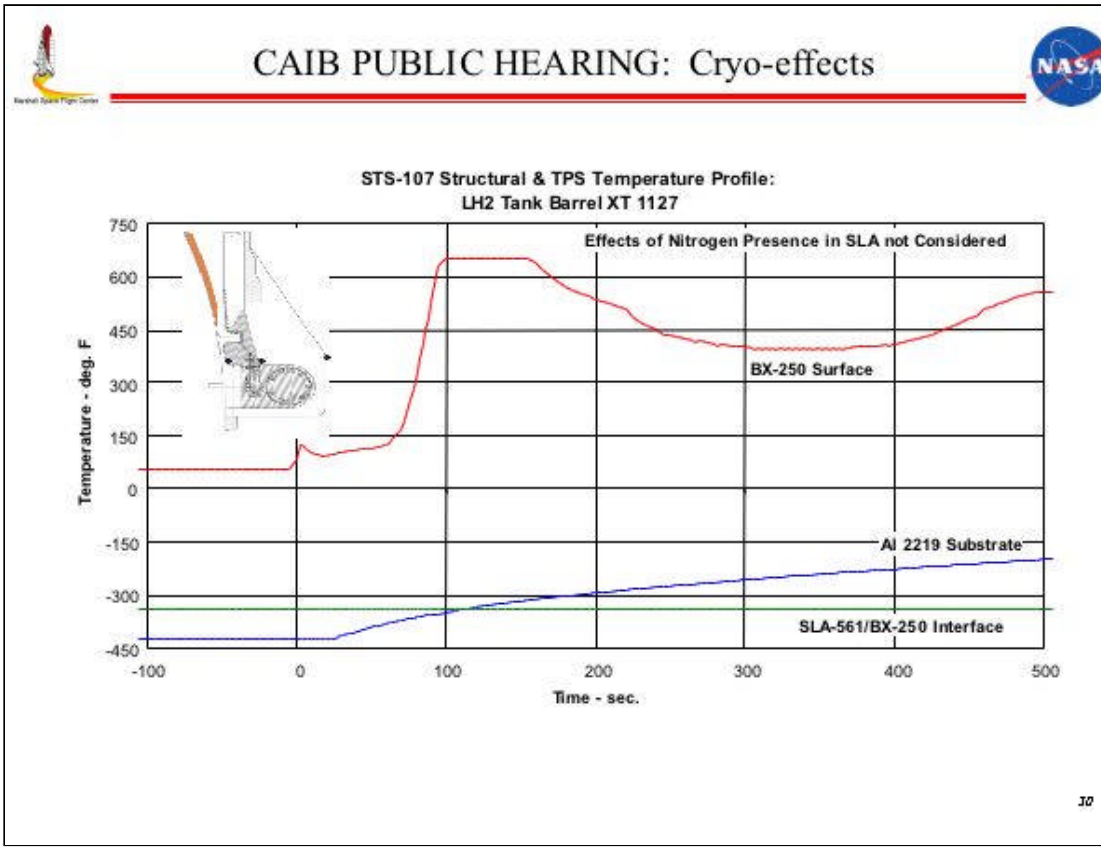
CAIB PUBLIC HEARING: Cryo-effects
STS-107 Structural & TPS Temperature Profile:
LH2 Tank Barrel XT 1127
Effects of Nitrogen Presence in SLA not Considered
BX-250 Surface
Al 2219 Substrate
SLA-561/BX-250 Interface
Temperature - deg. F
Time - sec.
750
600
450
300
150
0
-150
-300
-450
-100
0
100
200
300
400
500

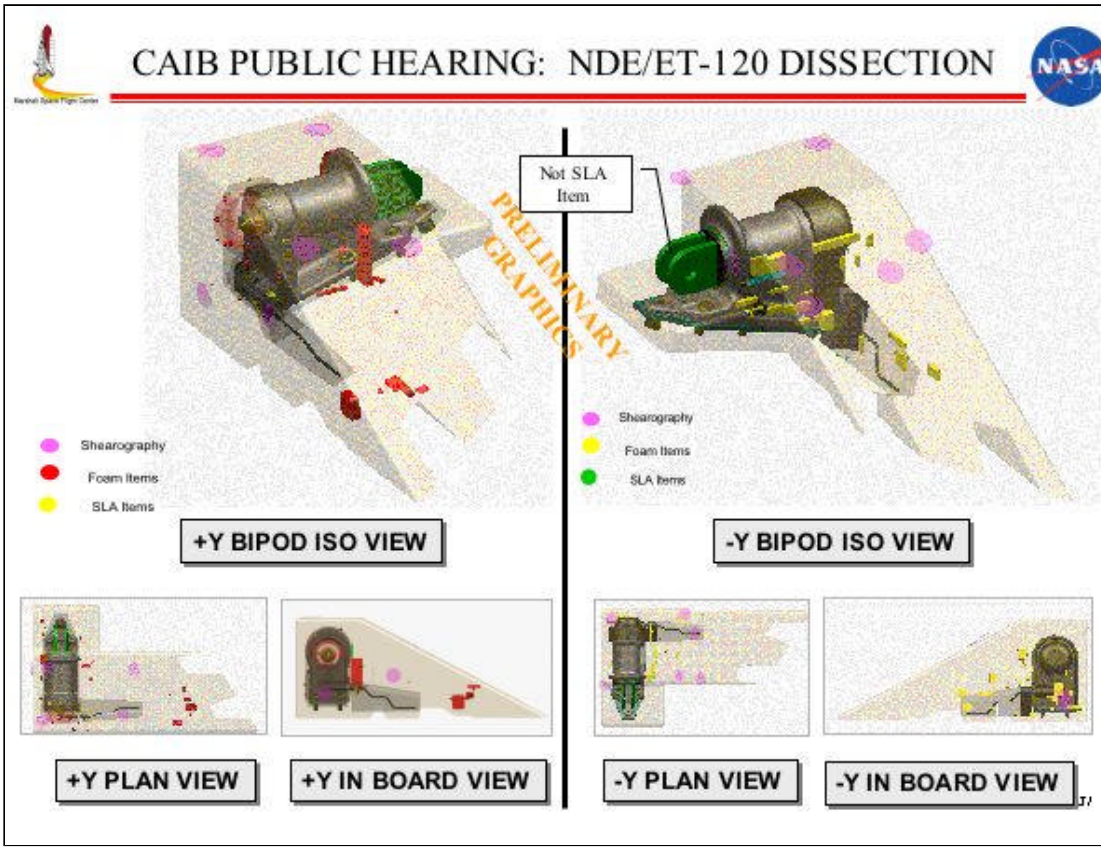
CAIB PUBLIC HEARING: NDE/ET-120 DISSECTION
NASA
Not SLA Item
PRELIMINARY GRAPHICS
Shearography
Foam Items
SLA Items
+Y BIPOD ISO VIEW
Shearography
Foam Items
SLA Items
-Y BIPOD ISO VIEW
+Y PLAN VIEW
+Y IN BOARD VIEW
-Y PLAN VIEW
-Y IN BOARD VIEW

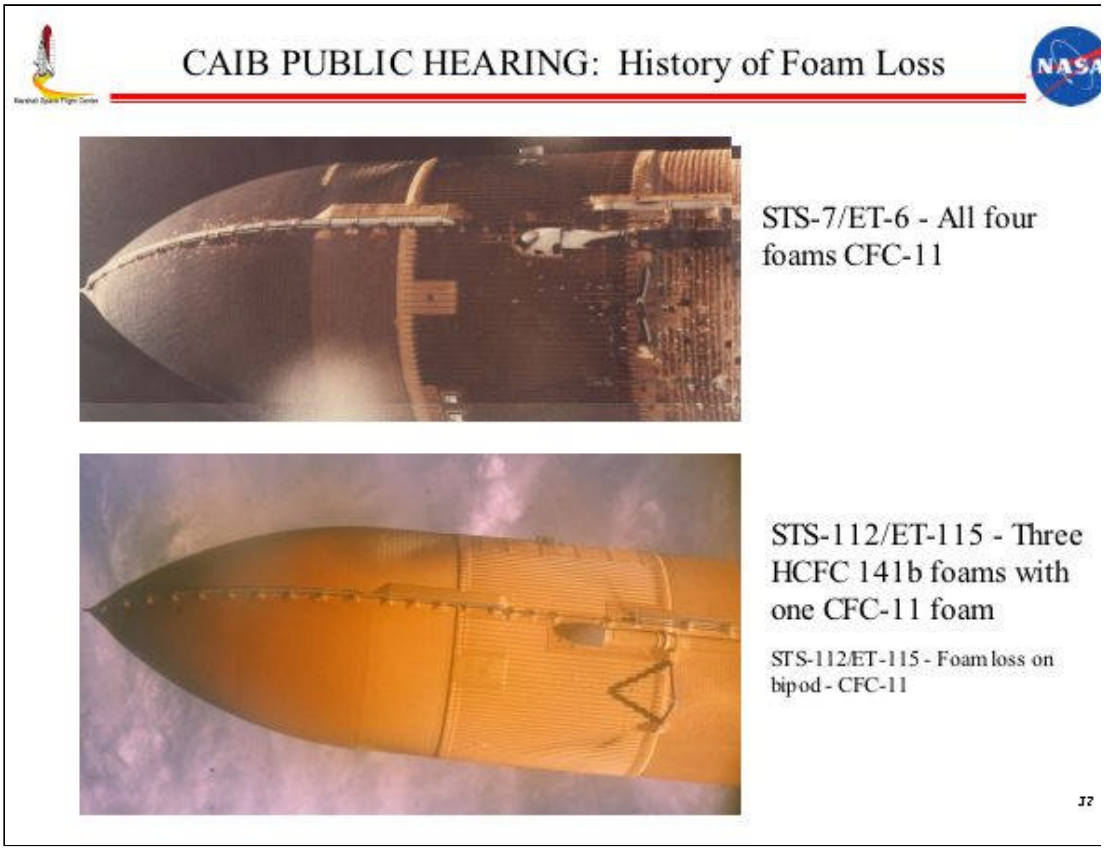
CAIB PUBLIC HEARING: History of Foam Loss
NASA
STS-7/ET-6 - All four foams CFC-11
STS-112/ET-115 - Three HCFC 141b foams with one CFC-11 foam
STS-112/ET-115 - Foam loss on bipod - CFC-11
37

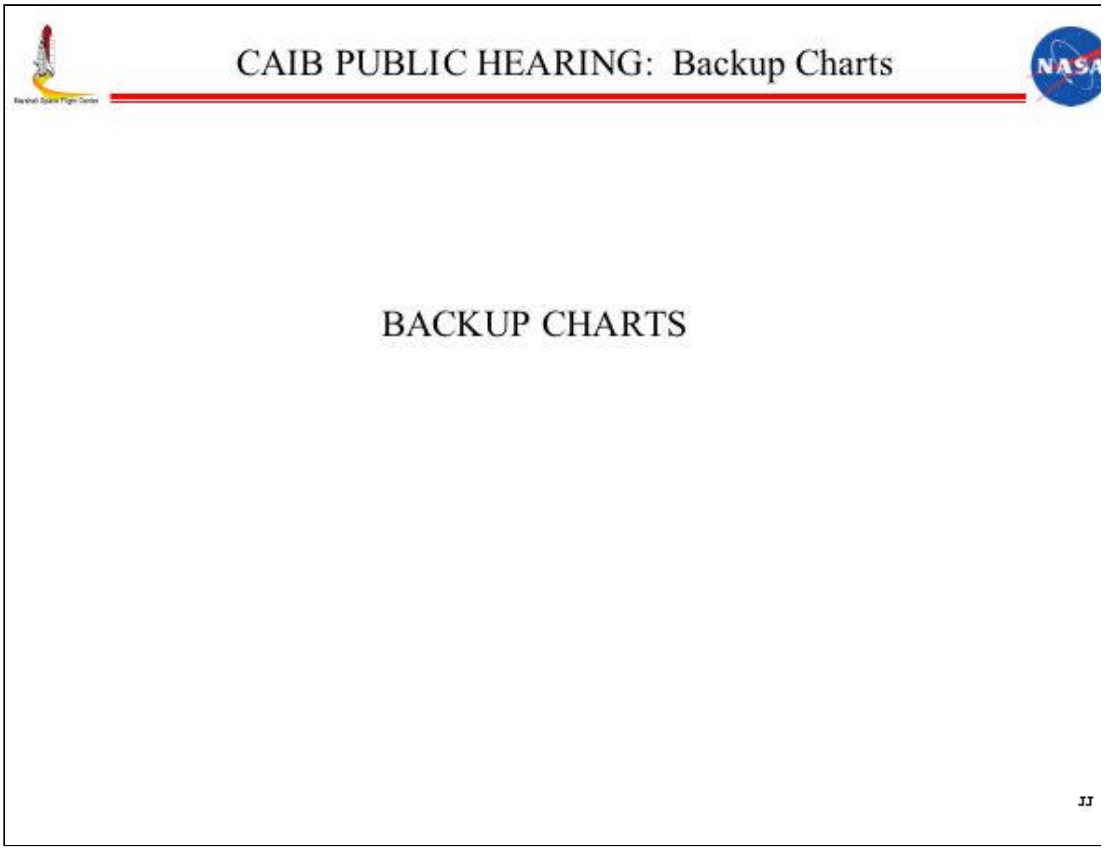
CAIB PUBLIC HEARING: Backup Charts
NASA
BACKUP CHARTS
JJ

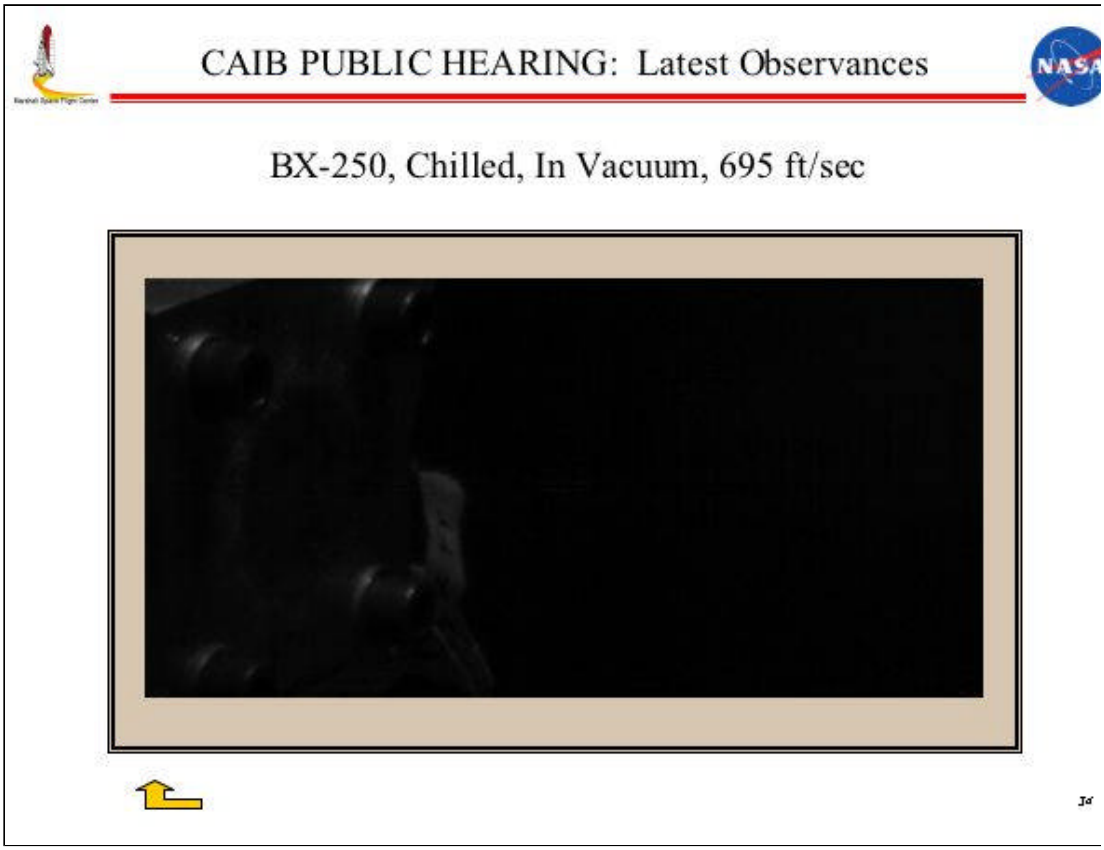
CAIB PUBLIC HEARING: Latest Observances
NASA
BX-250, Chilled, In Vacuum, 695 ft/sec

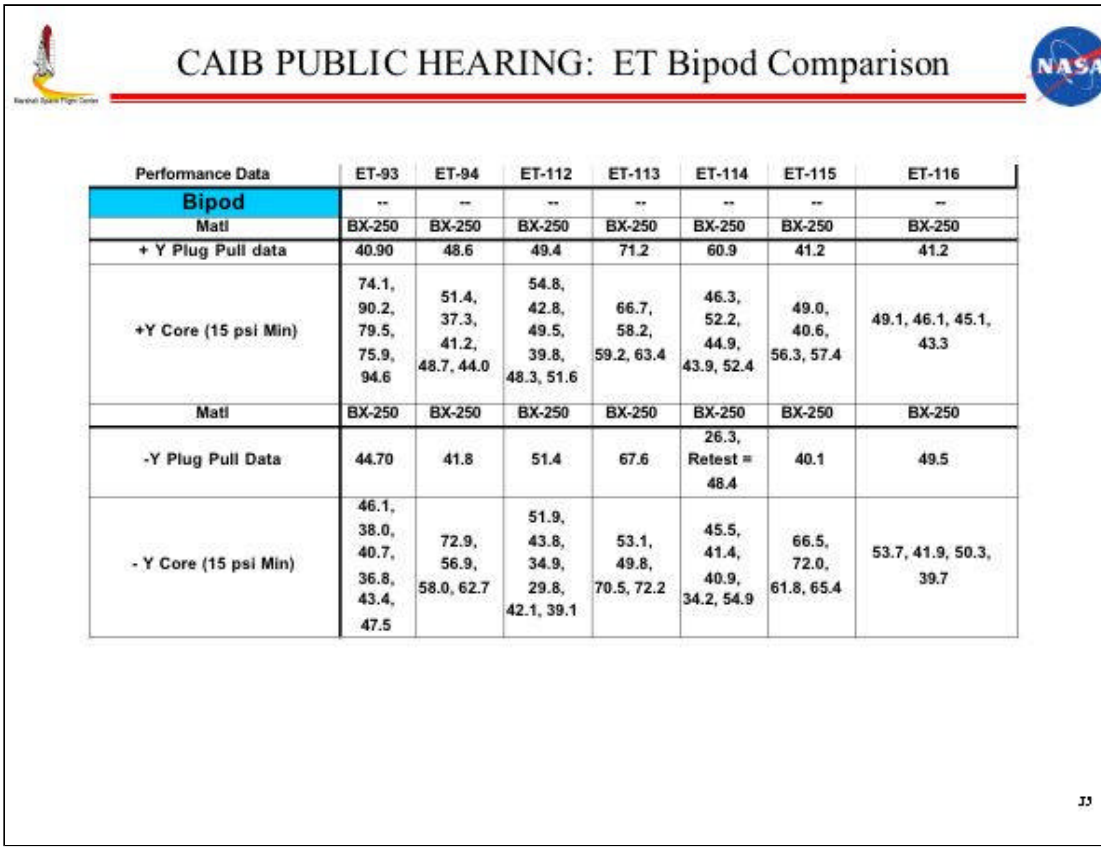

CAIB PUBLIC HEARING: ET Bipod Comparison

Performance Data	ET-93	ET-94	ET-112	ET-113	ET-114	ET-115	ET-116
Bipod	--	--	--	--	--	--	--
Matl	BX-250	BX-250	BX-250	BX-250	BX-250	BX-250	BX-250
+ Y Plug Pull data	40.90	48.6	49.4	71.2	60.9	41.2	41.2
+Y Core (15 psi Min)	74.1, 90.2, 79.5, 75.9, 94.6	51.4, 37.3, 41.2, 48.7, 44.0	54.8, 42.8, 49.5, 39.8, 48.3, 51.6	66.7, 58.2, 59.2, 63.4	46.3, 52.2, 44.9, 43.9, 52.4	49.0, 40.6, 56.3, 57.4	49.1, 46.1, 45.1, 43.3
Matl	BX-250	BX-250	BX-250	BX-250	BX-250	BX-250	BX-250
-Y Plug Pull Data	44.70	41.8	51.4	67.6	26.3, Retest = 48.4	40.1	49.5
- Y Core (15 psi Min)	46.1, 38.0, 40.7, 36.8, 43.4, 47.5	72.9, 56.9, 58.0, 62.7	51.9, 43.8, 34.9, 29.8, 42.1, 39.1	53.1, 49.8, 70.5, 72.2	45.5, 41.4, 40.9, 34.2, 54.9	66.5, 72.0, 61.8, 65.4	53.7, 41.9, 50.3, 39.7

33

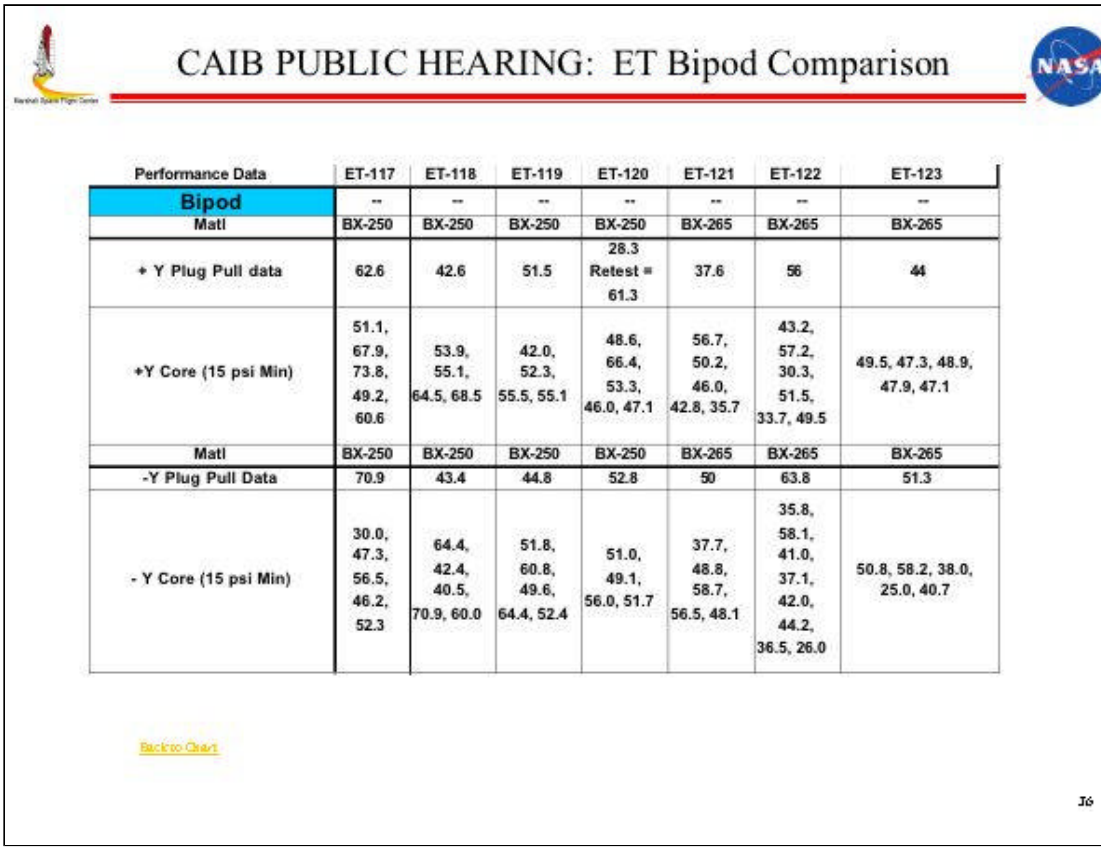

CAIB PUBLIC HEARING: ET Bipod Comparison

Performance Data	ET-117	ET-118	ET-119	ET-120	ET-121	ET-122	ET-123
Bipod	--	--	--	--	--	--	--
Matl	BX-250	BX-250	BX-250	BX-250	BX-265	BX-265	BX-265
+ Y Plug Pull data	62.6	42.6	51.5	28.3 Retest = 61.3	37.6	56	44
+Y Core (15 psi Min)	51.1, 67.9, 73.8, 49.2, 60.6	53.9, 55.1, 64.5, 68.5	42.0, 52.3, 55.5, 55.1	48.6, 66.4, 53.3, 46.0, 47.1	56.7, 50.2, 46.0, 42.8, 35.7	43.2, 57.2, 30.3, 51.5, 33.7, 49.5	49.5, 47.3, 48.9, 47.9, 47.1
Matl	BX-250	BX-250	BX-250	BX-250	BX-265	BX-265	BX-265
-Y Plug Pull Data	70.9	43.4	44.8	52.8	50	63.8	51.3
- Y Core (15 psi Min)	30.0, 47.3, 56.5, 46.2, 52.3	64.4, 42.4, 40.5, 70.9, 60.0	51.8, 60.8, 49.6, 64.4, 52.4	51.0, 49.1, 56.0, 51.7	37.7, 48.8, 58.7, 56.5, 48.1	35.8, 58.1, 41.0, 37.1, 42.0, 44.2, 36.5, 26.0	50.8, 58.2, 38.0, 25.0, 40.7

Backup Chart

J6

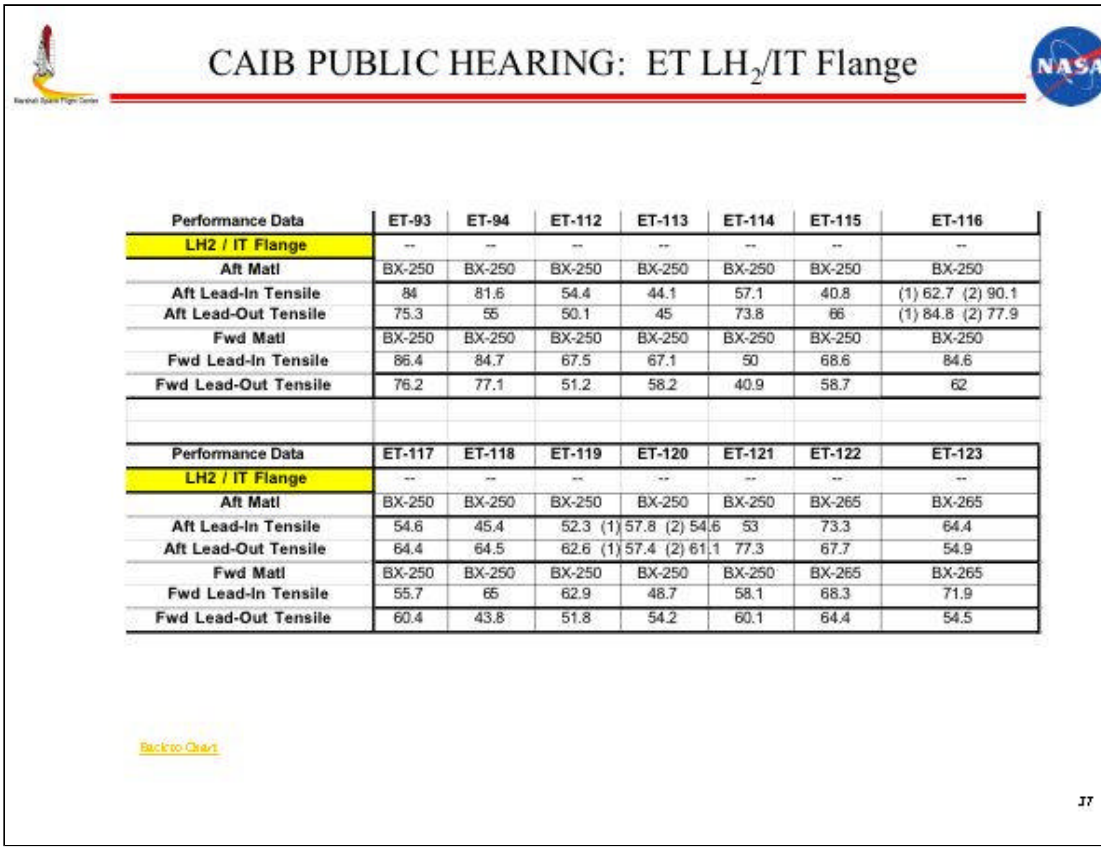

CAIB PUBLIC HEARING: ET LH_2/IT Flange

Performance Data	ET-93	ET-94	ET-112	ET-113	ET-114	ET-115	ET-116
LH2 / IT Flange	--	--	--	--	--	--	--
Aft Matl	BX-250	BX-250	BX-250	BX-250	BX-250	BX-250	BX-250
Aft Lead-In Tensile	84	81.6	54.4	44.1	57.1	40.8	(1) 62.7 (2) 90.1
Aft Lead-Out Tensile	75.3	55	50.1	45	73.8	66	(1) 84.8 (2) 77.9
Fwd Matl	BX-250	BX-250	BX-250	BX-250	BX-250	BX-250	BX-250
Fwd Lead-In Tensile	86.4	84.7	67.5	67.1	50	68.6	84.6
Fwd Lead-Out Tensile	76.2	77.1	51.2	58.2	40.9	58.7	62

Performance Data	ET-117	ET-118	ET-119	ET-120	ET-121	ET-122	ET-123
LH2 / IT Flange	--	--	--	--	--	--	--
Aft Matl	BX-250	BX-250	BX-250	BX-250	BX-250	BX-265	BX-265
Aft Lead-In Tensile	54.6	45.4	52.3 (1)	57.8 (2) 54.6	53	73.3	64.4
Aft Lead-Out Tensile	64.4	64.5	62.6 (1)	57.4 (2) 61.1	77.3	67.7	54.9
Fwd Matl	BX-250	BX-250	BX-250	BX-250	BX-250	BX-265	BX-265
Fwd Lead-In Tensile	55.7	65	62.9	48.7	58.1	68.3	71.9
Fwd Lead-Out Tensile	60.4	43.8	51.8	54.2	60.1	64.4	54.5

Backup Chart

37

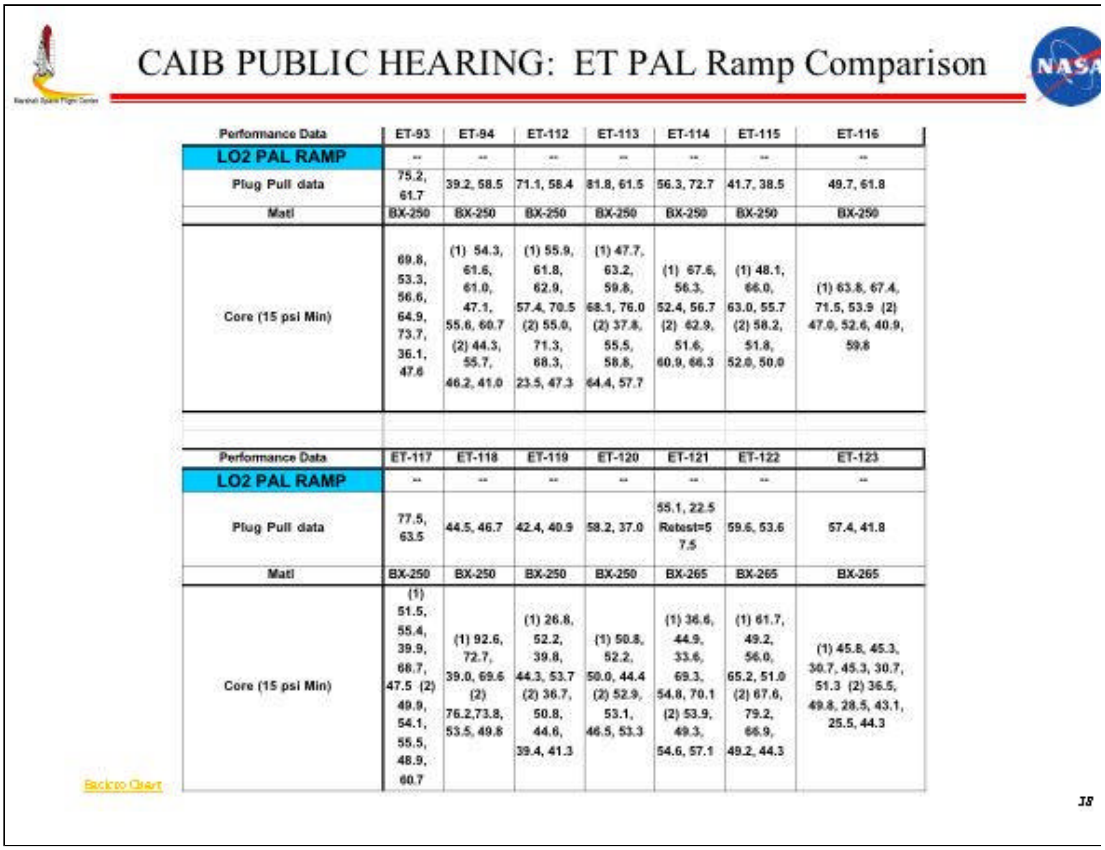

CAIB PUBLIC HEARING: ET PAL Ramp Comparison

Performance Data	ET-93	ET-94	ET-112	ET-113	ET-114	ET-115	ET-116
LO2 PAL RAMP	--	--	--	--	--	--	--
Plug Pull data	75.2, 61.7	39.2, 58.5	71.1, 58.4	81.8, 61.5	56.3, 72.7	41.7, 38.5	49.7, 61.8
Matl	BX-250	BX-250	BX-250	BX-250	BX-250	BX-250	BX-250
Core (15 psi Min)	69.8, 53.3, 56.6, 64.9, 73.7, 36.1, 47.6	(1) 54.3, 61.6, 61.0, 47.1, 55.6, 60.7 (2) 44.3, 55.7, 46.2, 41.0	(1) 55.9, 61.8, 62.9, 57.4, 70.5 (2) 55.0, 71.3, 68.3, 23.5, 47.3	(1) 47.7, 63.2, 59.8, 68.1, 76.0 (2) 37.8, 55.5, 58.8, 64.4, 57.7	(1) 67.6, 56.3, 52.4, 56.7 (2) 62.9, 51.6, 60.9, 66.3	(1) 48.1, 66.0, 63.0, 55.7 (2) 58.2, 51.8, 52.0, 50.0	(1) 63.8, 67.4, 71.5, 53.9 (2) 47.0, 52.6, 40.9, 59.8

Performance Data	ET-117	ET-118	ET-119	ET-120	ET-121	ET-122	ET-123
LO2 PAL RAMP	--	--	--	--	--	--	--
Plug Pull data	77.5, 63.5	44.5, 46.7	42.4, 40.9	58.2, 37.0	55.1, 22.5 Retest=5 7.5	59.6, 53.6	57.4, 41.8
Matl	BX-250	BX-250	BX-250	BX-250	BX-265	BX-265	BX-265
Core (15 psi Min)	(1) 51.5, 55.4, 39.9, 68.7, 47.5 (2) 49.9, 54.1, 55.5, 48.9, 60.7	(1) 92.6, 72.7, 39.0, 69.6 (2) 76.2,73.8, 53.5, 49.8	(1) 26.8, 52.2, 39.8, 44.3, 53.7 (2) 36.7, 50.8, 44.6, 39.4, 41.3	(1) 50.8, 52.2, 50.0, 44.4 (2) 52.9, 53.1, 46.5, 53.3	(1) 36.6, 44.9, 33.6, 69.3, 54.8, 70.1 (2) 53.9, 49.3, 54.6, 57.1	(1) 61.7, 49.2, 56.0, 65.2, 51.0 (2) 67.6, 79.2, 66.9, 49.2, 44.3	(1) 45.8, 45.3, 30.7, 45.3, 30.7, 51.3 (2) 36.5, 49.8, 28.5, 43.1, 25.5, 44.3

Backup Chart

18

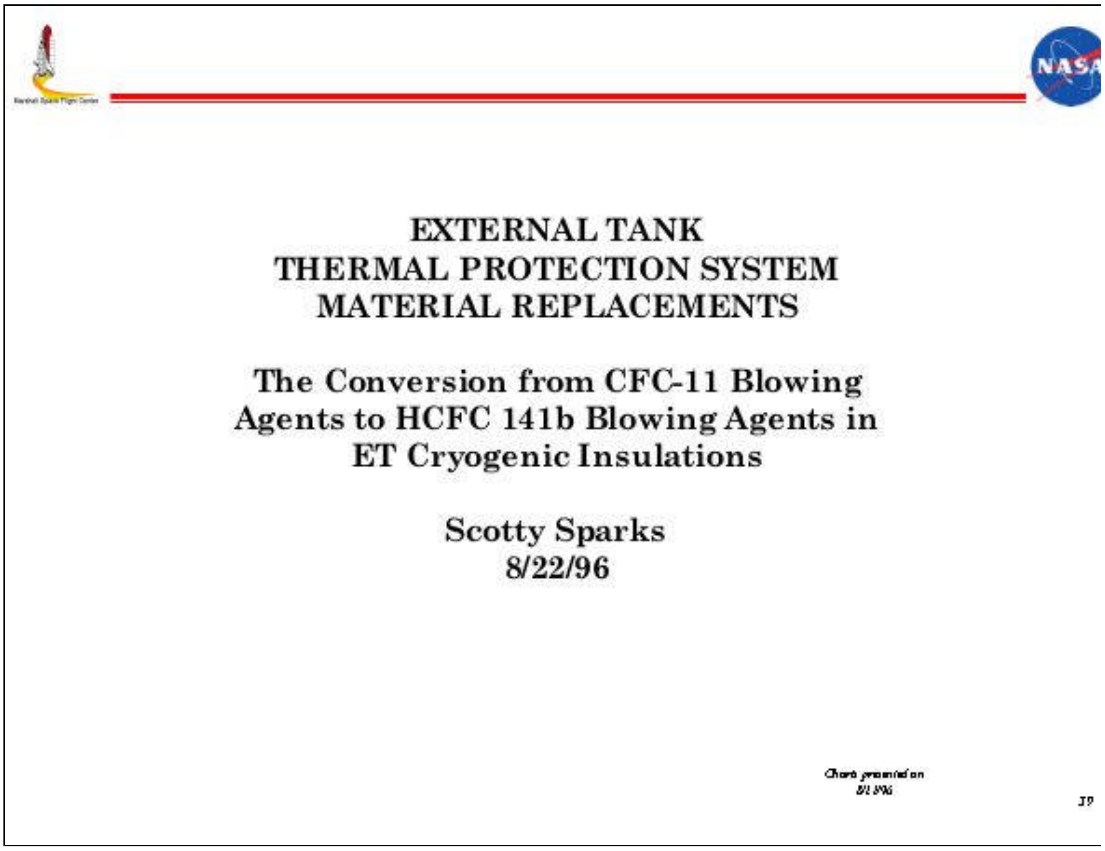

EXTERNAL TANK
THERMAL PROTECTION SYSTEM
MATERIAL REPLACEMENTS

The Conversion from CFC-11 Blowing Agents to HCFC 141b Blowing Agents in ET Cryogenic Insulations

Scotty Sparks
8/22/96

Chart presented on
8/ /96

19

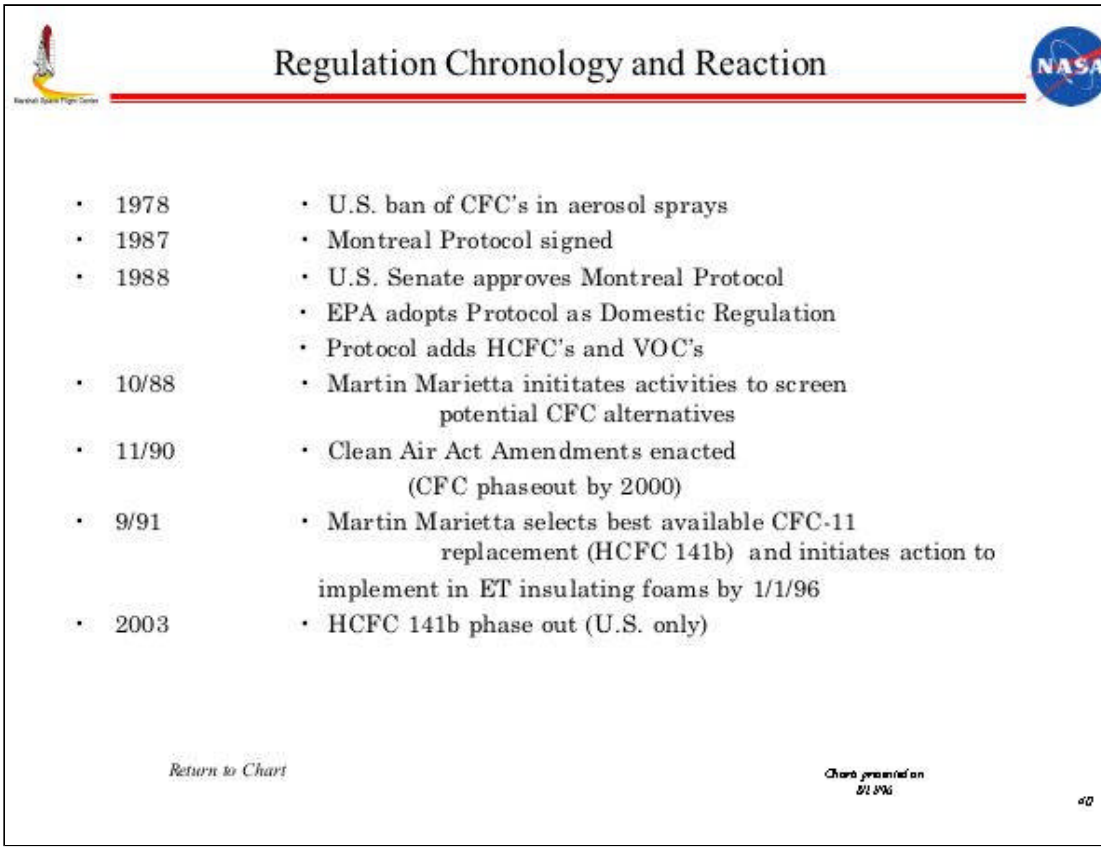
Regulation Chronology and Reaction
NASA
• 1978 • U.S. ban of CFC's in aerosol sprays
• 1987 • Montreal Protocol signed
• 1988 • U.S. Senate approves Montreal Protocol
• EPA adopts Protocol as Domestic Regulation
• Protocol adds HCFC's and VOC's
• 10/88 • Martin Marietta inititates activities to screen potential CFC alternatives
• 11/90 • Clean Air Act Amendments enacted (CFC phaseout by 2000)
• 9/91 • Martin Marietta selects best available CFC-11 replacement (HCFC 141b) and initiates action to implement in ET insulating foams by 1/1/96
• 2003 • HCFC 141b phase out (U.S. only)
Return to Chart

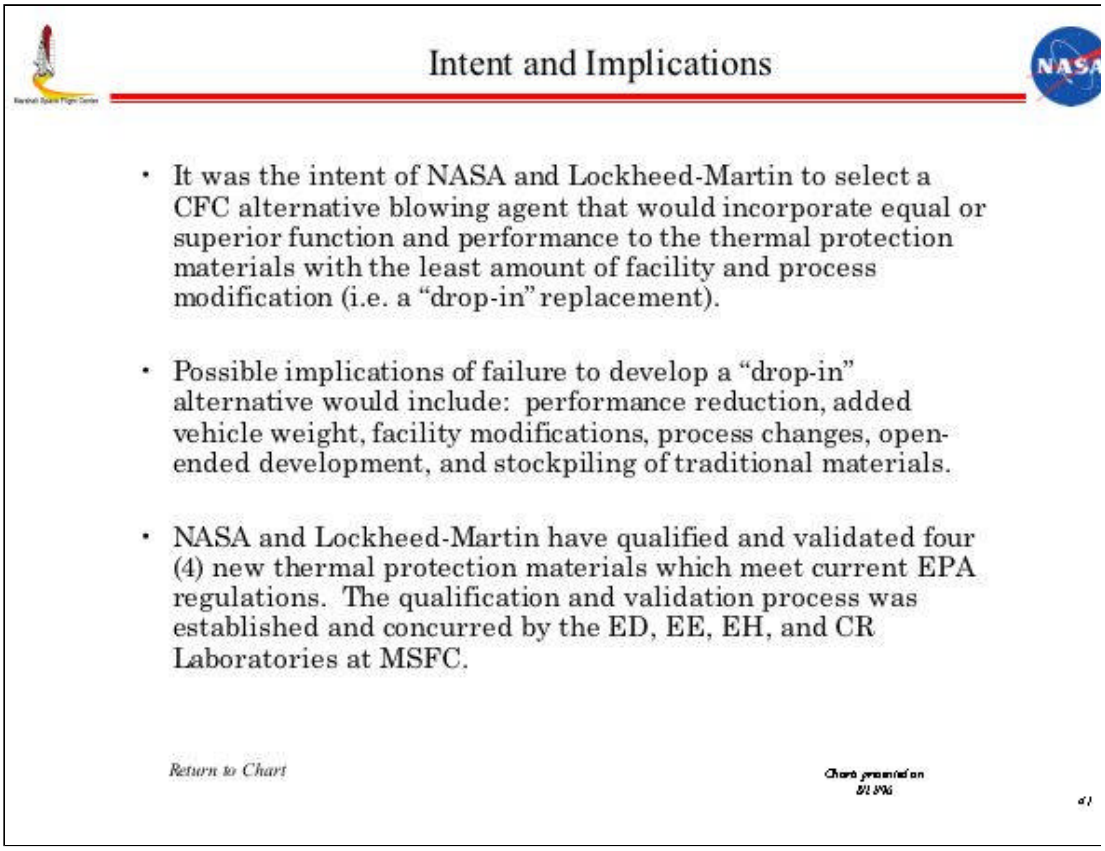
Intent and Implications
NASA
• It was the intent of NASA and Lockheed-Martin to select a CFC alternative blowing agent that would incorporate equal or superior function and performance to the thermal protection materials with the least amount of facility and process modification (i.e. a "drop-in" replacement).
• Possible implications of failure to develop a "drop-in" alternative would include: performance reduction, added vehicle weight, facility modifications, process changes, open-ended development, and stockpiling of traditional materials.
• NASA and Lockheed-Martin have qualified and validated four (4) new thermal protection materials which meet current EPA regulations. The qualification and validation process was established and concurred by the ED, EE, EH, and CR Laboratories at MSFC.
Return to Chart

Qualification Activities
Testing Performed Throughout Qualification Activities
Several lots of material were tested to characterize the material variability and process repeatability.
Physical Properties
Bond Tension (-423 to 300 °F)
Flatwise Tension (-423 to 300 °F)
Plug Pulls
Density
Compression
Mechanical Properties
Cryoflex (-423 & -320 °F)
Monostrain (-423 to 400 °F)
Torsion Shear
Poisson Ratio
Thermal Properties
Thermal Conductivity (-423 to 200 °F)
Oxygen Index
Flammability
Specific Heat & TGA
Aero-recession (Hot Gas)
Thermal-Vac
Major Flight Acceptance Tests:
Wind Tunnel (aero-recession for ascent)
Plasma Arc (Entry recession)
PAL Ramps
Aft Dome Test (Stop Sign)
Combined Environments (combined lift-off environments)
Return to Chart

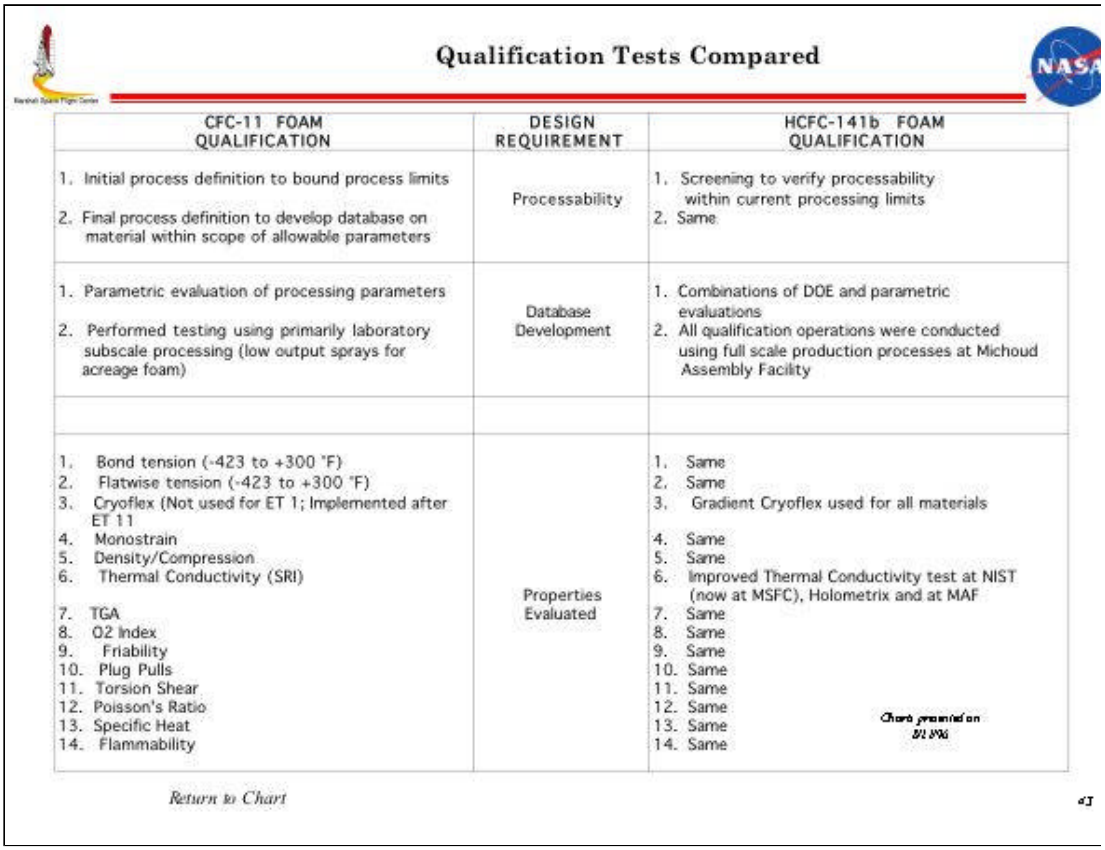

Qualification Tests Compared

CFC-11 FOAM QUALIFICATION	DESIGN REQUIREMENT	HCFC-141b FOAM QUALIFICATION
1. Initial process definition to bound process limits 2. Final process definition to develop database on material within scope of allowable parameters	Processability	1. Screening to verify processability within current processing limits 2. Same
1. Parametric evaluation of processing parameters 2. Performed testing using primarily laboratory subscale processing (low output sprays for acreage foam)	Database Development	1. Combinations of DOE and parametric evaluations 2. All qualification operations were conducted using full scale production processes at Michoud Assembly Facility
1. Bond tension (-423 to +300 °F) 2. Flatwise tension (-423 to +300 °F) 3. Cryoflex (Not used for ET 1; Implemented after ET 11 4. Monostrain 5. Density/Compression 6. Thermal Conductivity (SRI) 7. TGA 8. O2 Index 9. Friability 10. Plug Pulls 11. Torsion Shear 12. Poisson's Ratio 13. Specific Heat 14. Flammability	Properties Evaluated	1. Same 2. Same 3. Gradient Cryoflex used for all materials 4. Same 5. Same 6. Improved Thermal Conductivity test at NIST (now at MSFC), Holometrix and at MAF 7. Same 8. Same 9. Same 10. Same 11. Same 12. Same 13. Same 14. Same

Return to Chart

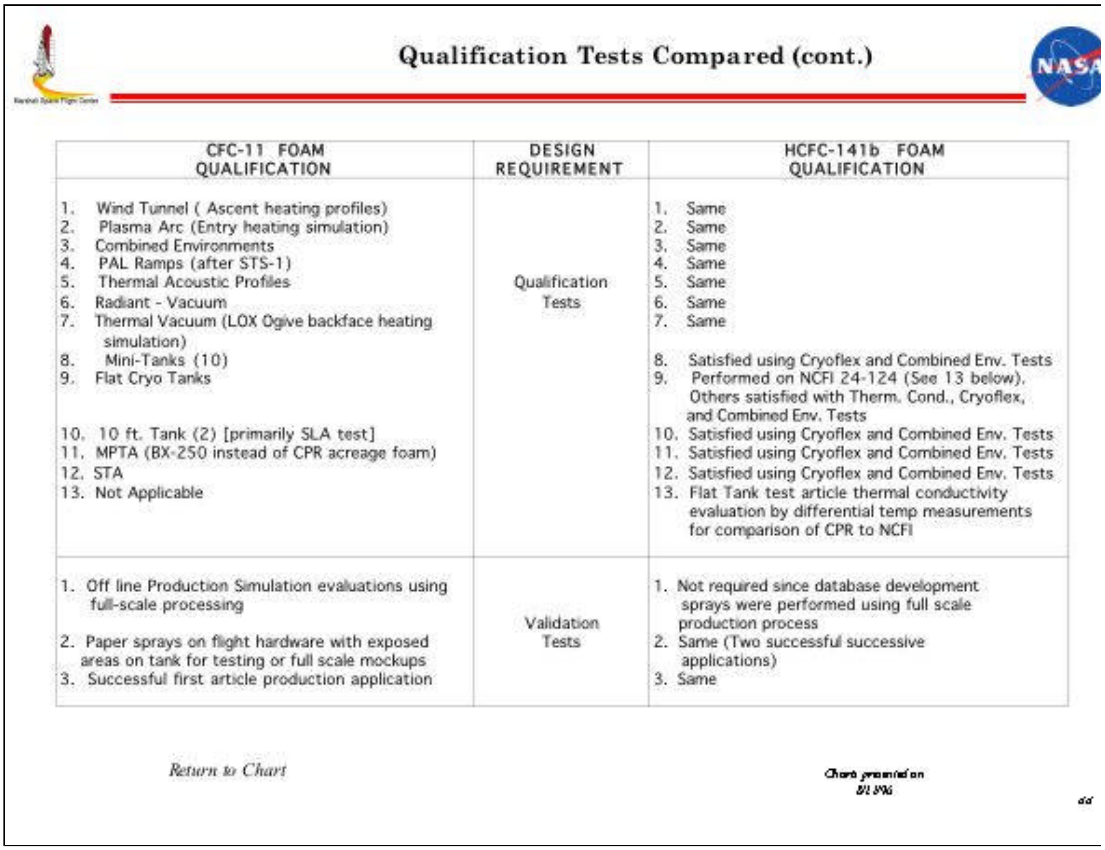

Qualification Tests Compared (cont.)

CFC-11 FOAM QUALIFICATION	DESIGN REQUIREMENT	HCFC-141b FOAM QUALIFICATION
1. Wind Tunnel (Ascent heating profiles) 2. Plasma Arc (Entry heating simulation) 3. Combined Environments 4. PAL Ramps (after STS-1) 5. Thermal Acoustic Profiles 6. Radiant - Vacuum 7. Thermal Vacuum (LOX Ogive backface heating simulation) 8. Mini-Tanks (10) 9. Flat Cryo Tanks 10. 10 ft. Tank (2) [primarily SLA test] 11. MPTA (BX-250 instead of CPR acreage foam) 12. STA 13. Not Applicable	Qualification Tests	1. Same 2. Same 3. Same 4. Same 5. Same 6. Same 7. Same 8. Satisfied using Cryoflex and Combined Env. Tests 9. Performed on NCFI 24-124 (See 13 below). Others satisfied with Therm. Cond., Cryoflex, and Combined Env. Tests 10. Satisfied using Cryoflex and Combined Env. Tests 11. Satisfied using Cryoflex and Combined Env. Tests 12. Satisfied using Cryoflex and Combined Env. Tests 13. Flat Tank test article thermal conductivity evaluation by differential temp measurements for comparison of CPR to NCFI
1. Off line Production Simulation evaluations using full-scale processing 2. Paper sprays on flight hardware with exposed areas on tank for testing or full scale mockups 3. Successful first article production application	Validation Tests	1. Not required since database development sprays were performed using full scale production process 2. Same (Two successful successive applications) 3. Same

Return to Chart

Chart presented on 8/1/96

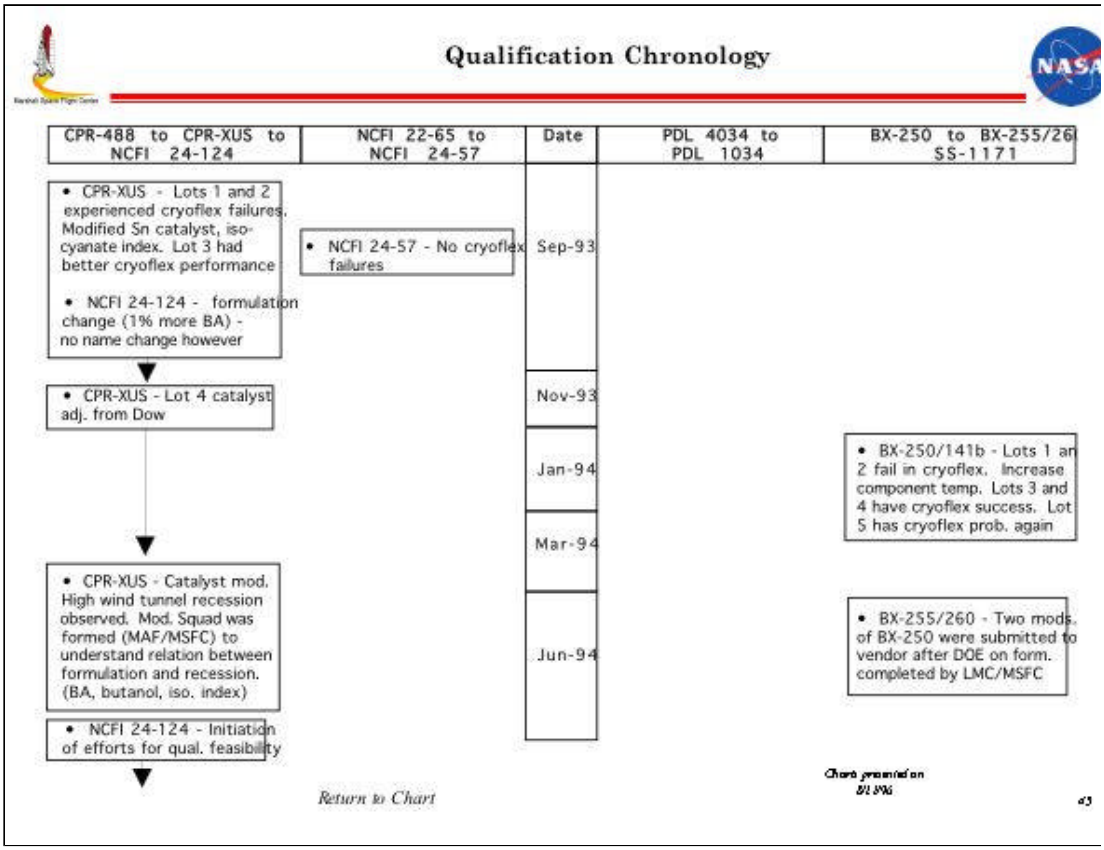
Qualification Chronology
CPR-488 to CPR-XUS to NCFI 24-124
NCFI 22-65 to NCFI 24-57
Date
PDL 4034 to PDL 1034
BX-250 to BX-255/26
SS-1171
• CPR-XUS - Lots 1 and 2 experienced cryoflex failures. Modified Sn catalyst, iso-cyanate index. Lot 3 had better cryoflex performance
• NCFI 24-124 - formulation change (1% more BA) - no name change however
• NCFI 24-57 - No cryoflex failures
Sep-93
• CPR-XUS - Lot 4 catalyst adj. from Dow
Nov-93
Jan-94
• BX-250/141b - Lots 1 an 2 fail in cryoflex. Increase component temp. Lots 3 and 4 have cryoflex success. Lot 5 has cryoflex prob. again
Mar-94
• CPR-XUS - Catalyst mod. High wind tunnel recession observed. Mod. Squad was formed (MAF/MSFC) to understand relation between formulation and recession. (BA, butanol, iso. index)
Jun-94
• BX-255/260 - Two mods. of BX-250 were submitted to vendor after DOE on form. completed by LMC/MSFC
• NCFI 24-124 - Initiation of efforts for qual. feasibility
Return to Chart

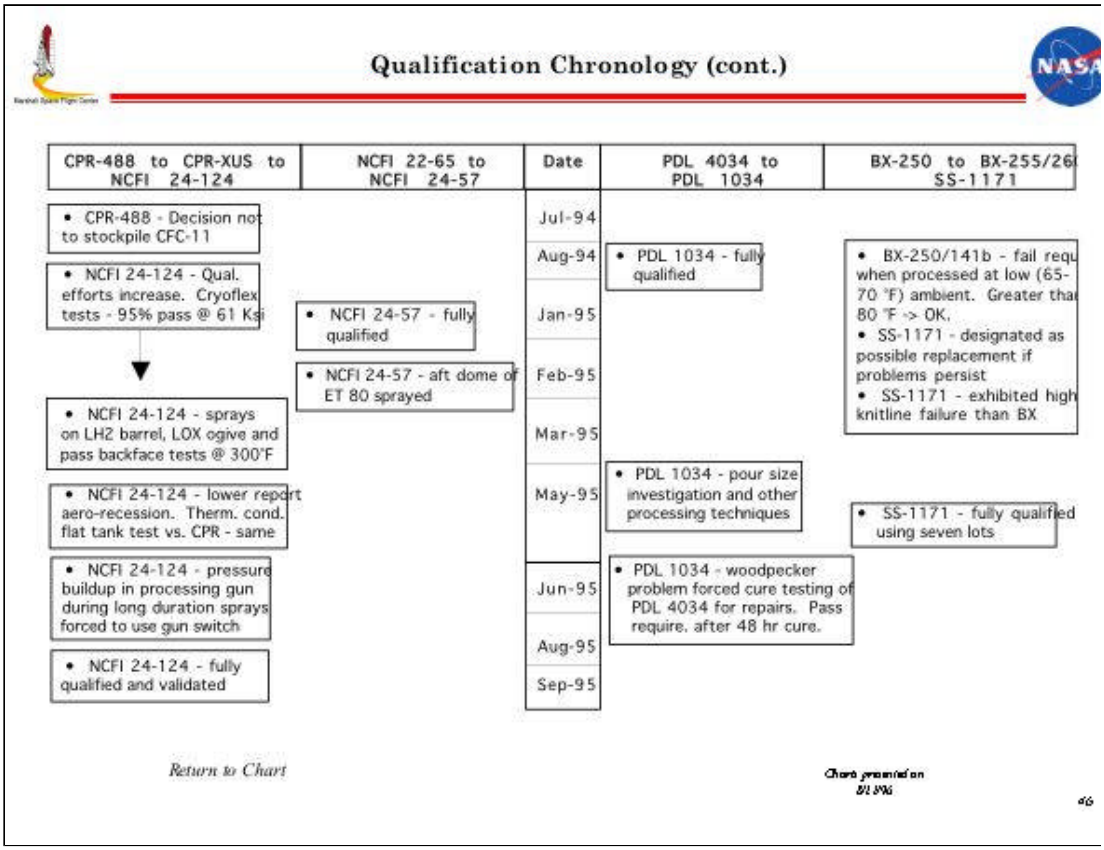
Qualification Chronology (cont.)
CPR-488 to CPR-XUS to NCFI 24-124
NCFI 22-65 to NCFI 24-57
Date
PDL 4034 to PDL 1034
BX-250 to BX-255/26 SS-1171
• CPR-488 - Decision not to stockpile CFC-11
• NCFI 24-124 - Qual. efforts increase. Cryoflex tests - 95% pass @ 61 Ksi
• NCFI 24-124 - sprays on LH2 barrel, LOX ogive and pass backface tests @ 300°F
• NCFI 24-124 - lower report aero-recession. Therm. cond. flat tank test vs. CPR - same
• NCFI 24-124 - pressure buildup in processing gun during long duration sprays forced to use gun switch
• NCFI 24-124 - fully qualified and validated
• NCFI 24-57 - fully qualified
• NCFI 24-57 - aft dome of ET 80 sprayed
Jul-94
Aug-94
Jan-95
Feb-95
Mar-95
May-95
Jun-95
Aug-95
Sep-95
• PDL 1034 - fully qualified
• PDL 1034 - pour size investigation and other processing techniques
• PDL 1034 - woodpecker problem forced cure testing of PDL 4034 for repairs. Pass require. after 48 hr cure.
• BX-250/141b - fail requ when processed at low (65-70 °F) ambient. Greater tha 80 °F -> OK.
• SS-1171 - designated as possible replacement if problems persist
• SS-1171 - exhibited high knitline failure than BX
• SS-1171 - fully qualified using seven lots
Return to Chart

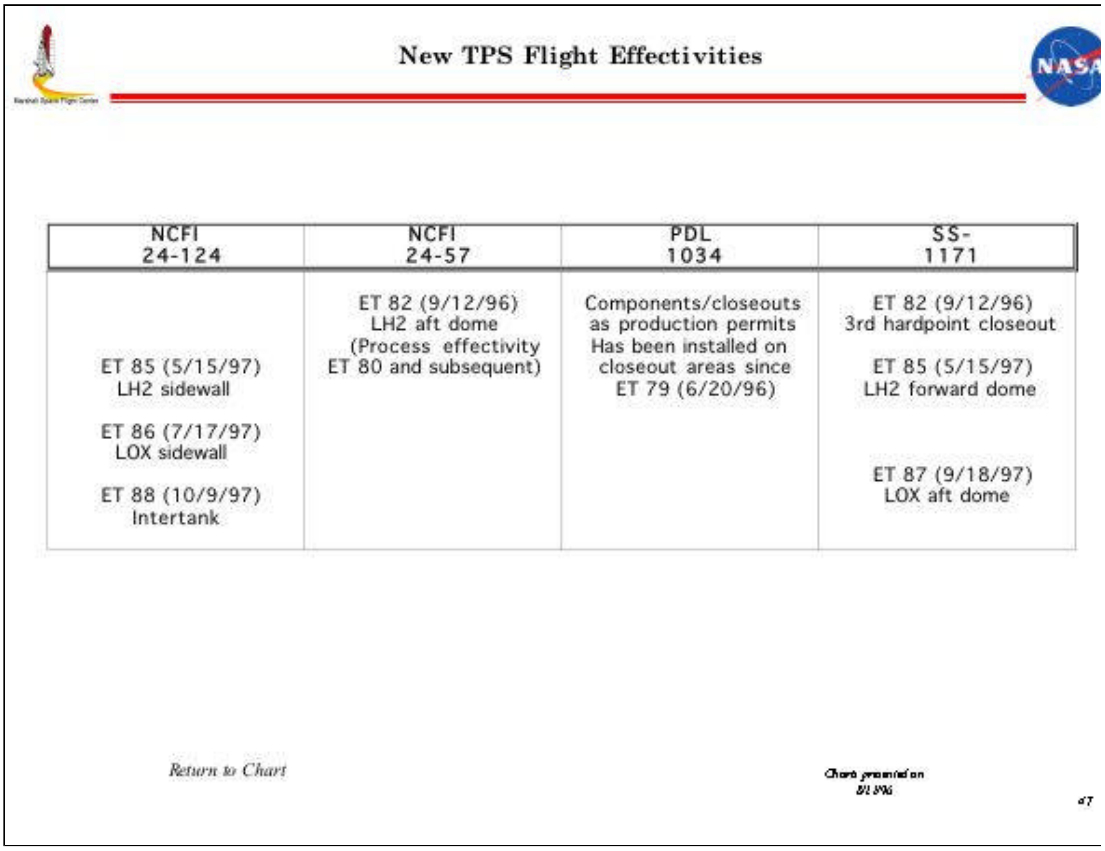

New TPS Flight Effectivities

NCFI 24-124	NCFI 24-57	PDL 1034	SS-1171
ET 85 (5/15/97) LH2 sidewall ET 86 (7/17/97) LOX sidewall ET 88 (10/9/97) Intertank	ET 82 (9/12/96) LH2 aft dome (Process effectivity ET 80 and subsequent)	Components/closeouts as production permits Has been installed on closeout areas since ET 79 (6/20/96)	ET 82 (9/12/96) 3rd hardpoint closeout ET 85 (5/15/97) LH2 forward dome ET 87 (9/18/97) LOX aft dome

Return to Chart

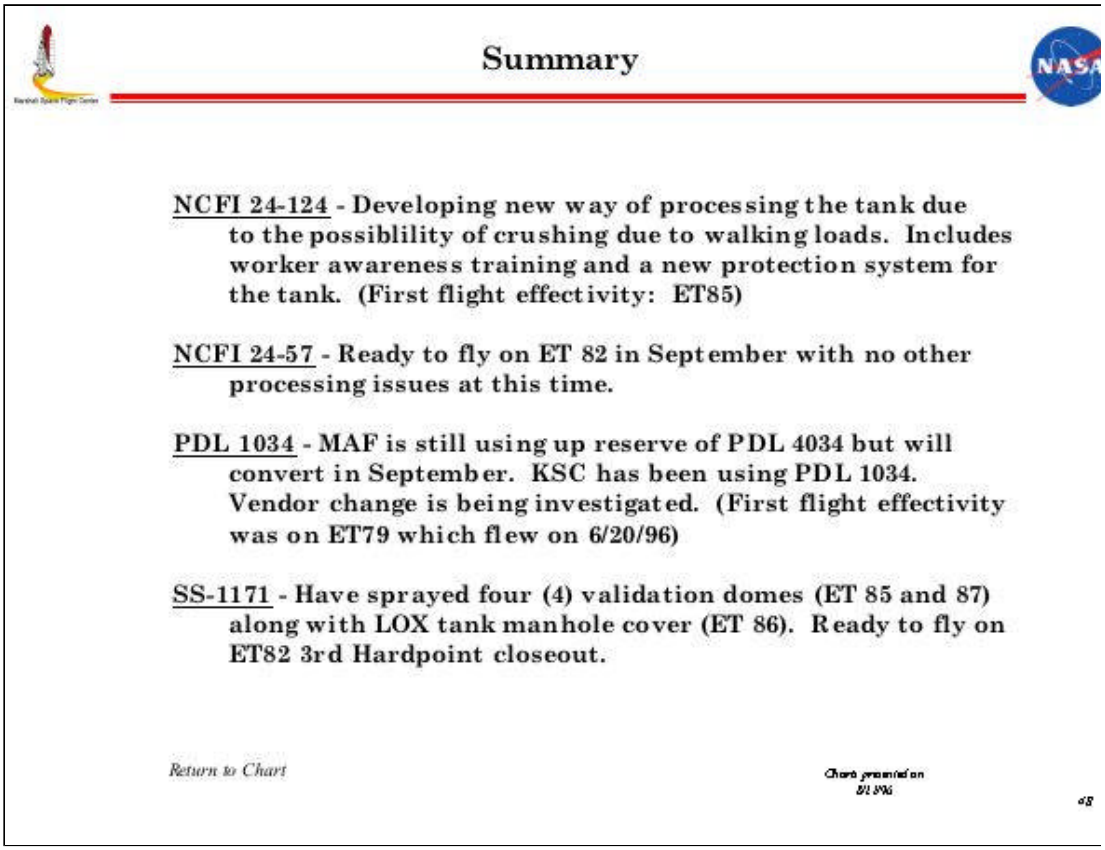
Summary
NCFI 24-124 - Developing new way of processing the tank due to the possiblility of crushing due to walking loads. Includes worker awareness training and a new protection system for the tank. (First flight effectivity: ET85)
NCFI 24-57 - Ready to fly on ET 82 in September with no other processing issues at this time.
PDL 1034 - MAF is still using up reserve of PDL 4034 but will convert in September. KSC has been using PDL 1034. Vendor change is being investigated. (First flight effectivity was on ET79 which flew on 6/20/96)
SS-1171 - Have sprayed four (4) validation domes (ET 85 and 87) along with LOX tank manhole cover (ET 86). Ready to fly on ET82 3rd Hardpoint closeout.
Return to Chart

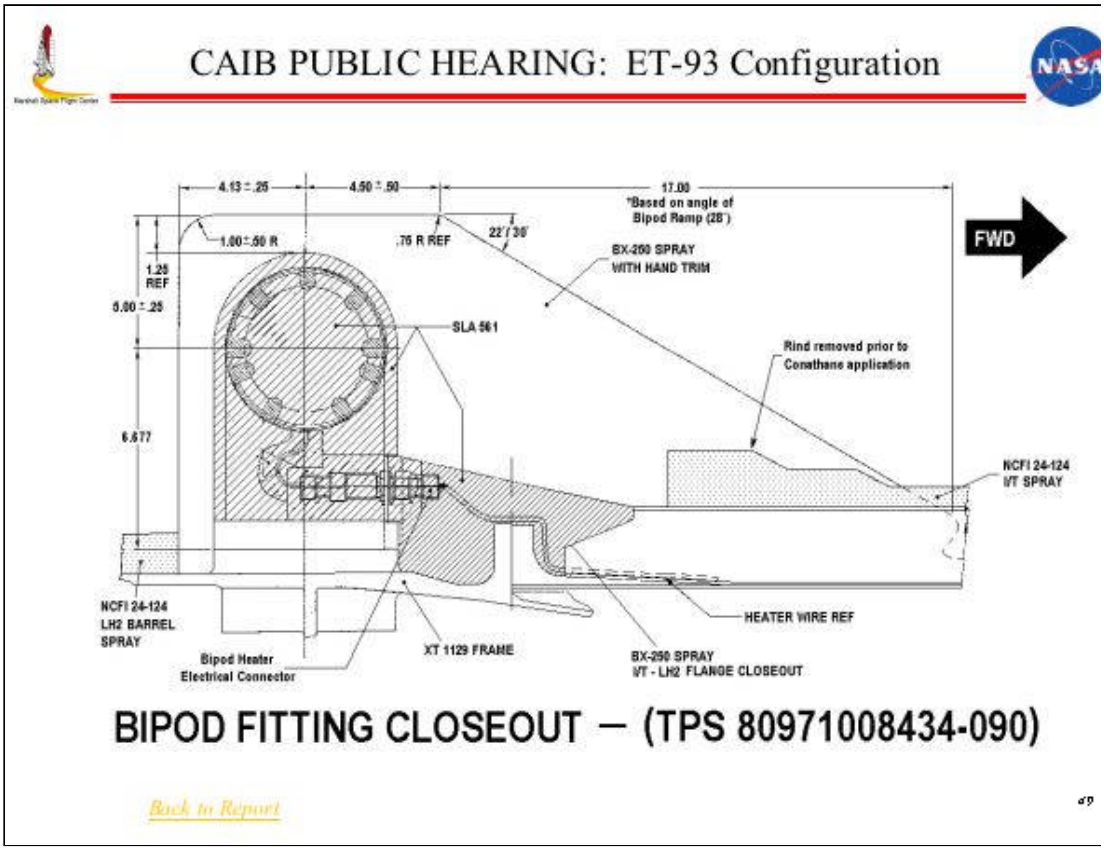
CAIB PUBLIC HEARING: ET-93 Configuration
4.13 ± .25
4.50 ± .50
17.00
*Based on angle of Bipod Ramp (28°)
1.00 ± .50 R
.75 R REF
22° / 30°
BX-250 SPRAY WITH HAND TRIM
FWD
1.25 REF
5.80 ± .25
SLA 561
Rind removed prior to Conathane application
6.677
NCFI 24-124 I/T SPRAY
NCFI 24-124 LH2 BARREL SPRAY
HEATER WIRE REF
Bipod Heater Electrical Connector
XT 1129 FRAME
BX-250 SPRAY I/T - LH2 FLANGE CLOSEOUT
BIPOD FITTING CLOSEOUT – (TPS 80971008434-090)
Back to Report

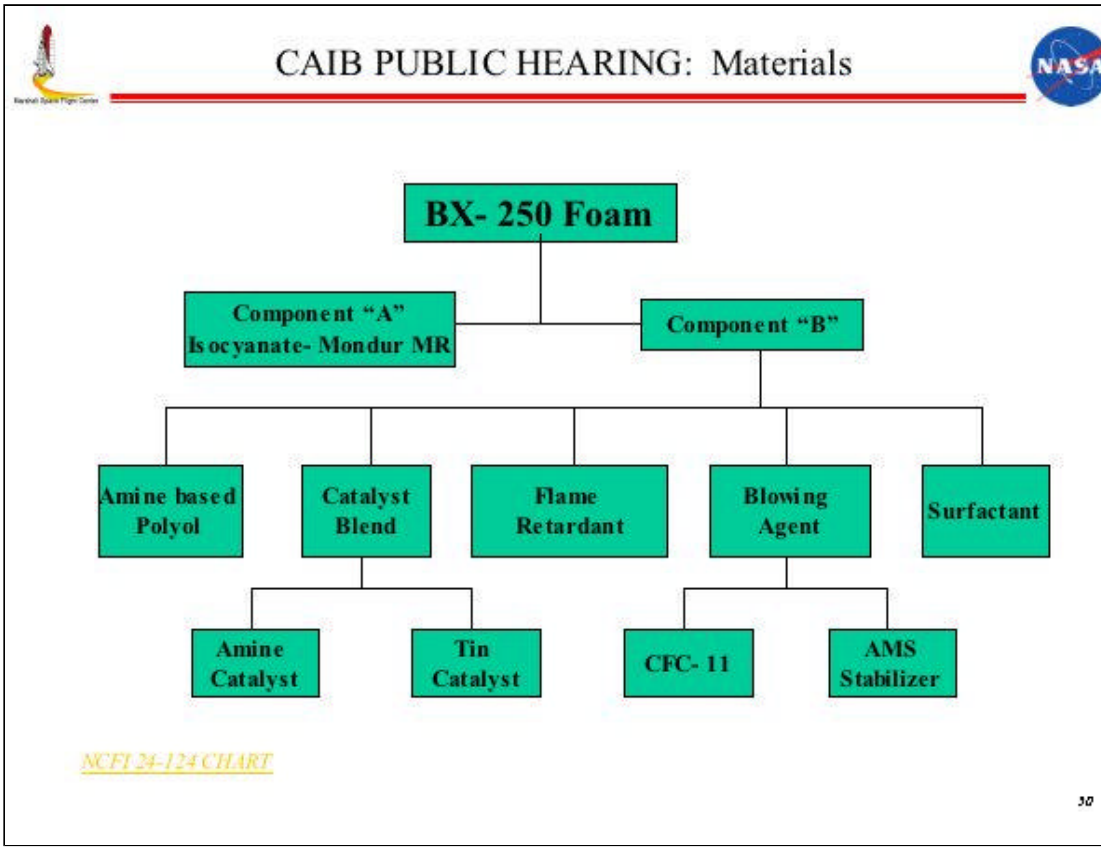
CAIB PUBLIC HEARING: Materials
BX- 250 Foam
Component "A"
Isocyanate- Mondur MR
Component "B"
Amine based Polyol
Catalyst Blend
Flame Retardant
Blowing Agent
Surfactant
Amine Catalyst
Tin Catalyst
CFC- 11
AMS Stabilizer
NCFI 24-124 CHART
30

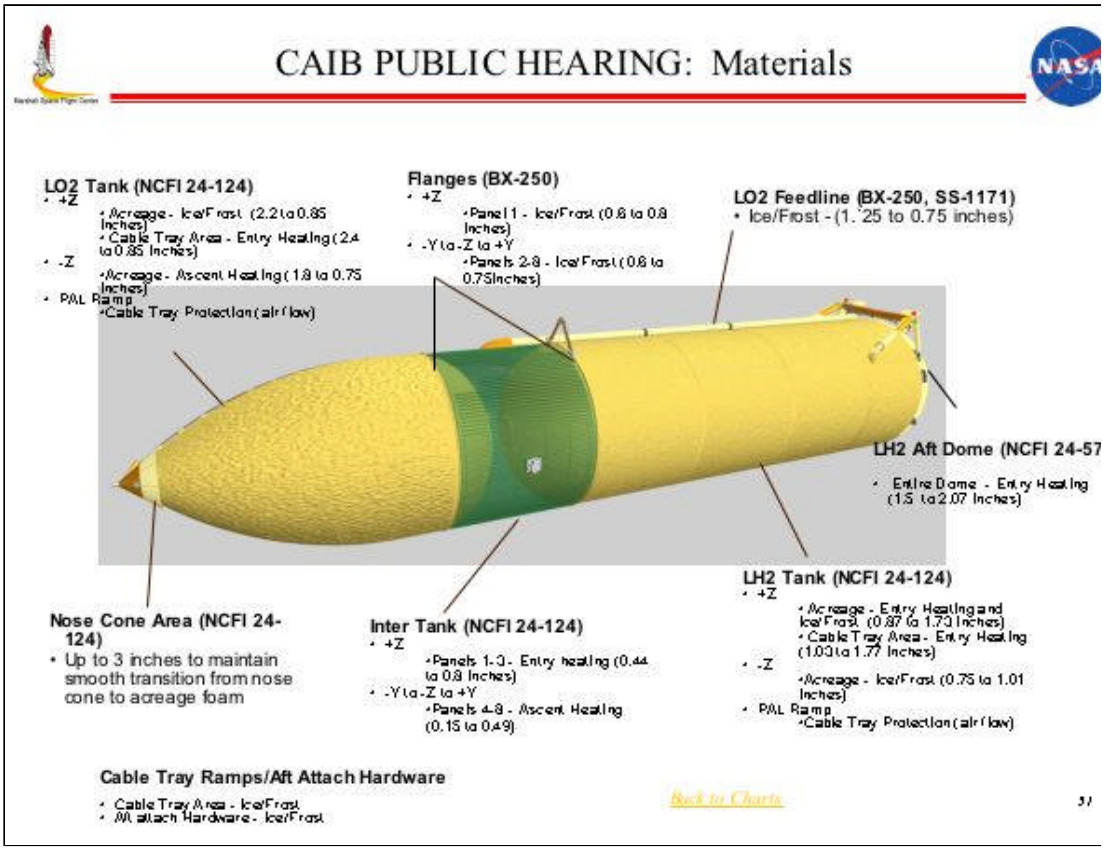
CAIB PUBLIC HEARING: Materials
LO2 Tank (NCFI 24-124)
+Z
Acreage - Ice/Frost (2.2 to 0.85 Inches)
Cable Tray Area - Entry Heating (2.4 to 0.85 Inches)
-Z
Acreage - Ascent Heating (1.8 to 0.75 Inches)
PAL Ramp
Cable Tray Protection (air flow)
Flanges (BX-250)
+Z
Panel 1 - Ice/Frost (0.8 to 0.8 Inches)
-Y to -Z to +Y
Panels 2-8 - Ice/Frost (0.8 to 0.75Inches)
LO2 Feedline (BX-250, SS-1171)
Ice/Frost - (1.25 to 0.75 inches)
LH2 Aft Dome (NCFI 24-57
Entire Dome - Entry Heating (1.5 to 2.07 Inches)
LH2 Tank (NCFI 24-124)
+Z
Acreage - Entry Heating and Ice/Frost (0.87 to 1.73 Inches)
Cable Tray Area - Entry Heating (1.03 to 1.77 Inches)
-Z
Acreage - Ice/Frost (0.75 to 1.01 Inches)
PAL Ramp
Cable Tray Protection (air flow)
Nose Cone Area (NCFI 24-124)
Up to 3 inches to maintain smooth transition from nose cone to acreage foam
Inter Tank (NCFI 24-124)
+Z
Panels 1-3 - Entry heating (0.44 to 0.8 Inches)
-Y to -Z to +Y
Panels 4-8 - Ascent Heating (0.15 to 0.49)
Cable Tray Ramps/Aft Attach Hardware
Cable Tray Area - Ice/Frost
Attach Hardware - Ice/Frost
Back to Charts
37

CAIB PUBLIC HEARING: Bipod Area Configuration

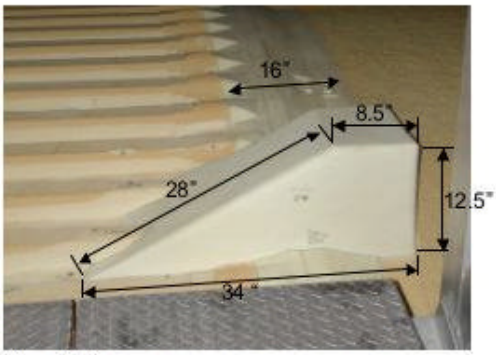

Bipod Ramp

Note: Dimensions from ET-121

- Estimated volume -1.1 cu. Ft.
- Estimated weight - 1.98 to 2.86 Lbs (1.8 to 2.6 lbs./cu.ft)

Flange Closeout

- Estimated volume/foot of length
  - Between bipod ramps (16" width) - 0.235 cu/ft per foot
  - Outboard of bipod ramps (12" width) - 0.177 cu/ft per foot
- Estimated volume
  - Between ramps - 0.42 to 0.61 lbs/ft (1.8 to 2.6 lbs./cu.ft)
  - Outboard of ramps - 0.32 to 0.46 lbs/ft (1.8 to 2.6 lbs./cu.ft)

Back to Chart

32

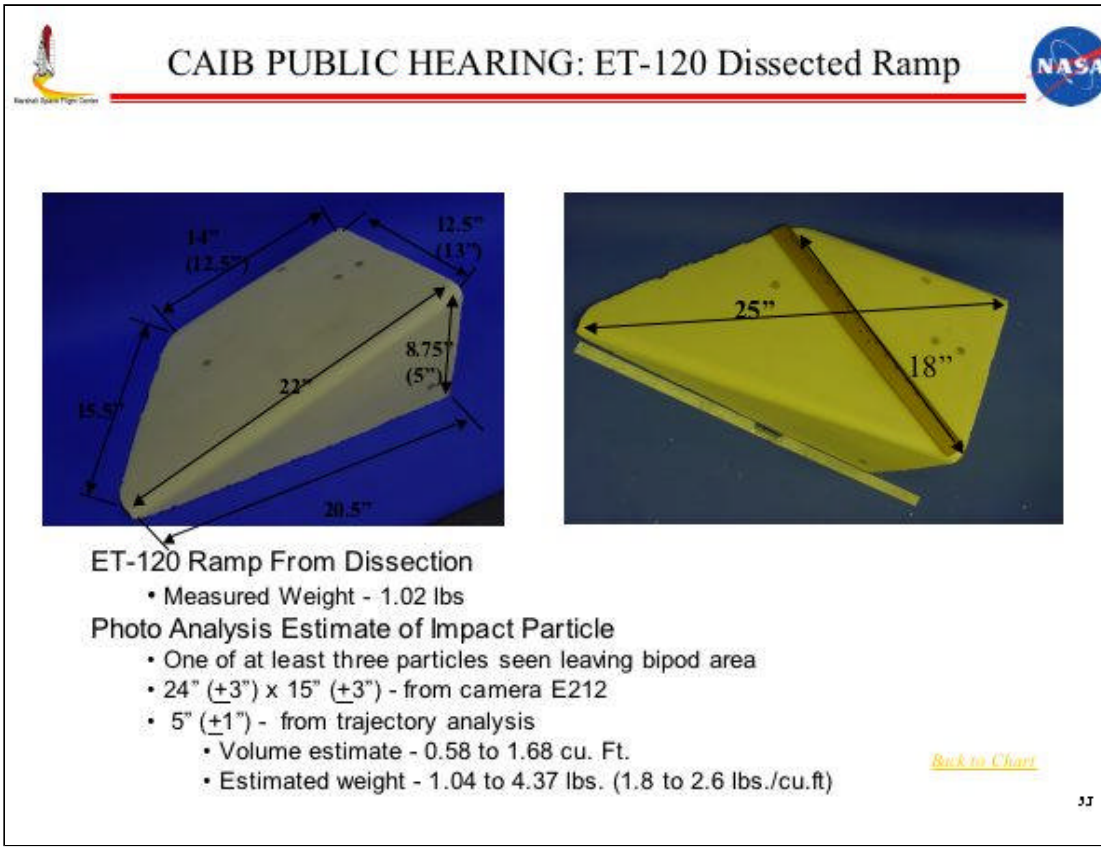
CAIB PUBLIC HEARING: ET-120 Dissected Ramp
NASA
14"
(12.5")
12.5"
(13")
8.75"
(5")
22"
15.5"
20.5"
25"
18"
ET-120 Ramp From Dissection
• Measured Weight - 1.02 lbs
Photo Analysis Estimate of Impact Particle
• One of at least three particles seen leaving bipod area
• 24" (±3") x 15" (±3") - from camera E212
• 5" (±1") - from trajectory analysis
• Volume estimate - 0.58 to 1.68 cu. Ft.
• Estimated weight - 1.04 to 4.37 lbs. (1.8 to 2.6 lbs./cu.ft)
Back to Chart
33

CAIB PUBLIC HEARING: History of Foam Loss

STS-7/ET-6 (launched 06/18/83)

- Post separation film showed a large portion of the –Y (LH) bipod ramp missing
- Lower surface Orbiter tile damage locations = 151 with 40 >1"

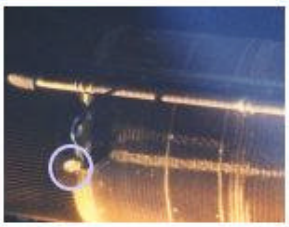

STS-32/ET-32 (launched 01/09/90)

- Post separation film showed two divots measuring 12 to 14 inches between bipod and just above the flange and a third divot 14" in diameter centered between between ramps and extending into the flange area measuring 28" wide. The third divot surrounded the forward part of the –Y (LH) bipod ramp
- Lower surface Orbiter tile damage locations = 111 with 13 >1"
  - Largest damage: 2.0" x 3.0" x 0. 5"D (Right side of Orbiter, aft of the forward Main Landing Gear)

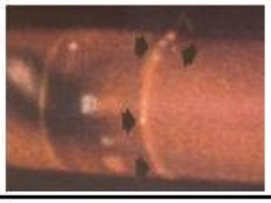

STS-35/ET-35 (launched 12/02/90)

- Ten circular TPS divots in the Intertank to Hydrogen tank flange closeout (ranging 8 to 10")
- Lower surface Orbiter tile damage locations = 132 with 15 >1"
  - Largest damage: 5.75" x 3.75" x 0.25"D (Right side of Orbiter, aft of forward Main Landing Gear)

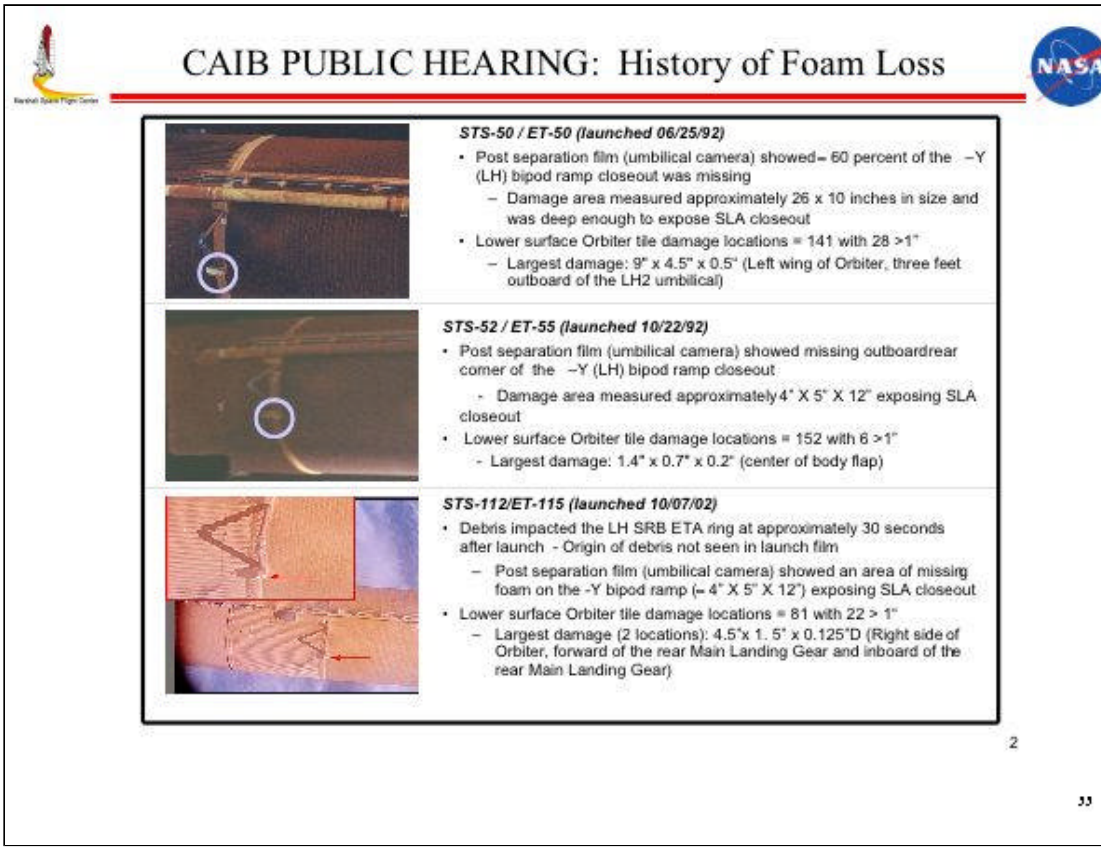
CAIB PUBLIC HEARING: History of Foam Loss
STS-50 / ET-50 (launched 06/25/92)
• Post separation film (umbilical camera) showed ~ 60 percent of the –Y (LH) bipod ramp closeout was missing
– Damage area measured approximately 26 x 10 inches in size and was deep enough to expose SLA closeout
• Lower surface Orbiter tile damage locations = 141 with 28 >1"
– Largest damage: 9" x 4.5" x 0.5" (Left wing of Orbiter, three feet outboard of the LH2 umbilical)
STS-52 / ET-55 (launched 10/22/92)
• Post separation film (umbilical camera) showed missing outboard rear corner of the –Y (LH) bipod ramp closeout
- Damage area measured approximately 4" X 5" X 12" exposing SLA closeout
• Lower surface Orbiter tile damage locations = 152 with 6 >1"
- Largest damage: 1.4" x 0.7" x 0.2" (center of body flap)
STS-112/ET-115 (launched 10/07/02)
• Debris impacted the LH SRB ETA ring at approximately 30 seconds after launch - Origin of debris not seen in launch film
– Post separation film (umbilical camera) showed an area of missing foam on the -Y bipod ramp (~ 4" X 5" X 12") exposing SLA closeout
• Lower surface Orbiter tile damage locations = 81 with 22 > 1"
– Largest damage (2 locations): 4.5"x 1. 5" x 0.125"D (Right side of Orbiter, forward of the rear Main Landing Gear and inboard of the rear Main Landing Gear)
2

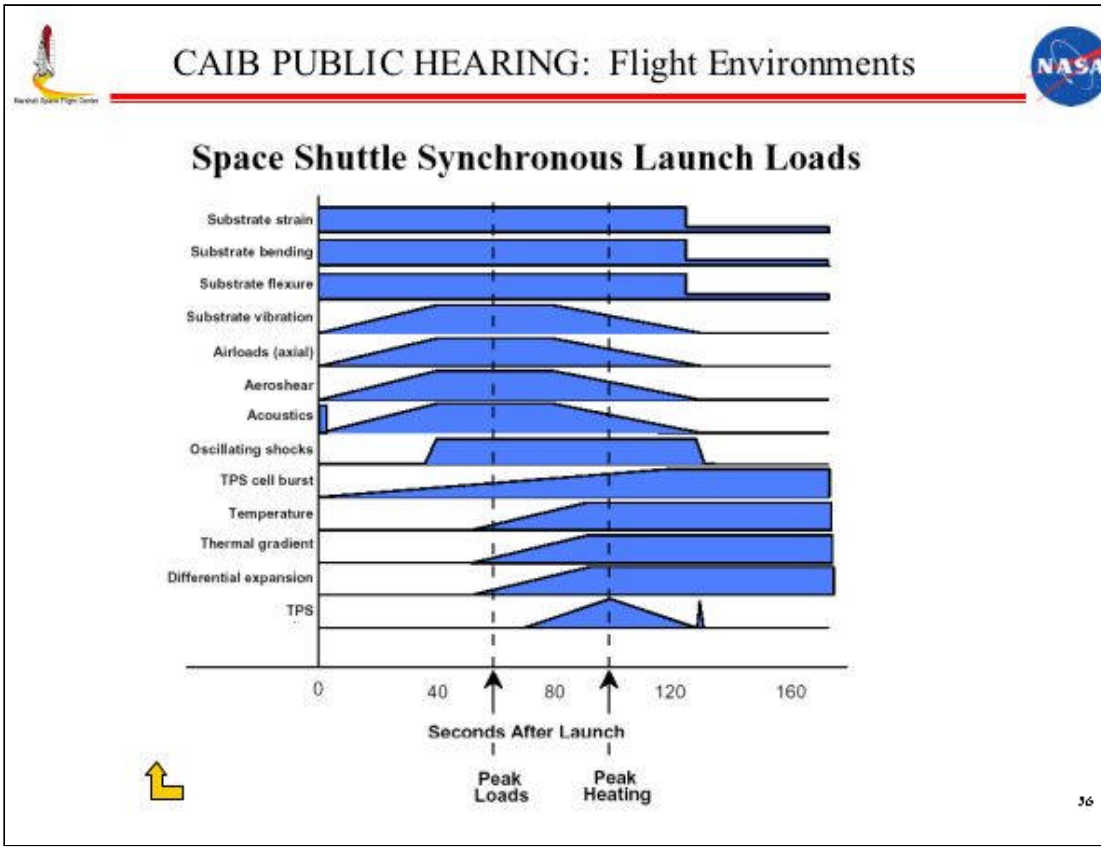
CAIB PUBLIC HEARING: Flight Environments
Space Shuttle Synchronous Launch Loads
Substrate strain
Substrate bending
Substrate flexure
Substrate vibration
Airloads (axial)
Aeroshear
Acoustics
Oscillating shocks
TPS cell burst
Temperature
Thermal gradient
Differential expansion
TPS
0
40
80
120
160
Seconds After Launch
Peak Loads
Peak Heating
36

CAIB PUBLIC HEARING: NDE Correlation +Y Bipod

- ET120 +Y Bipod Results
  - Several indications noted post wedge removal which may be attributable to complex part geometry, density gradients, or defects
  - Dissection revealed no significant correlation between indicated regions and subsurface defects

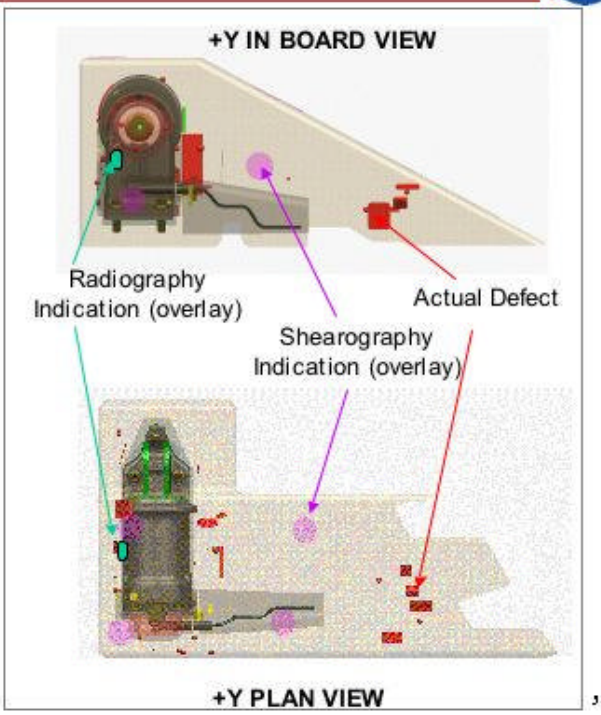

37

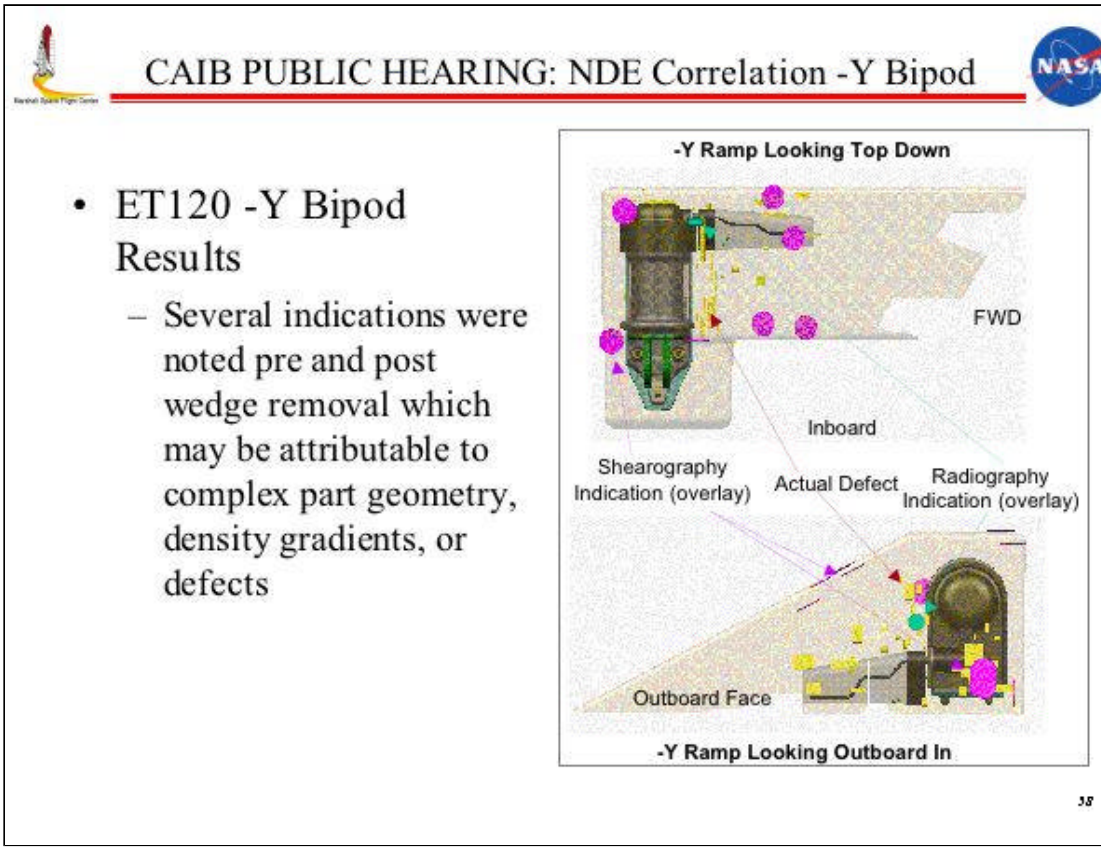

April 7, 2003 Presentations

Privacy Policy | DISCLAIMER | Accessibility

Volume IV
Appendix F.3
MADS Sensor Data

This Appendix presents three different Boeing analyses: MADS Instrumentation Evaluation, STS-107X1040 Spar Cap Strain Gage Assessment and Induced Thermal Strain Scenario. These presentations were identified as preliminary information at the time they were presented to the CAIB. The documents are now available to the public.

THIS PAGE INTENTIONALLY LEFT BLANK

MADS Instrumentation Evaluation

Doug White

4/24/03

This material is PRELIMINARY information only. It is for limited distribution. DO NOT FORWARD.

Instrumentation Subsystem Is Continuing to Assess the Reliability of the MADS Data

- Large Quantities of Measurements Develop Erratic Responses in the Vicinity of EI + 480 to 600 Seconds
  - Equivalent GMT is 1352 to 1354 GMT (EI: 1344:09 GMT)
- The Instrumentation Team Is Responsible for Determining Data Validity Based on Assessment of the MADS Avionics Telemetry Behavior
  - The goal is to establish a range or a point beyond which data validity is unreliable and convey that information to the MADS user community
- Where Possible, Failure Modes Were Developed to Explain the Invalid Data Observed
  - Sensor type segregation approach was utilized, that is
    - Pressures—Pulse Code Modulation (PCM) and Strain Gauge Signal Conditioner (SGSC)
    - Strains
    - Temperatures—Resistance Temperature Device (RTD) and Thermocouple
- General Statements Regarding the MADS System Performance Can Be Made Based on Assessments of the Telemetry

This material is PRELIMINARY information only. It is for limited distribution. DO NOT FORWARD.

MADS Instrumentation Types

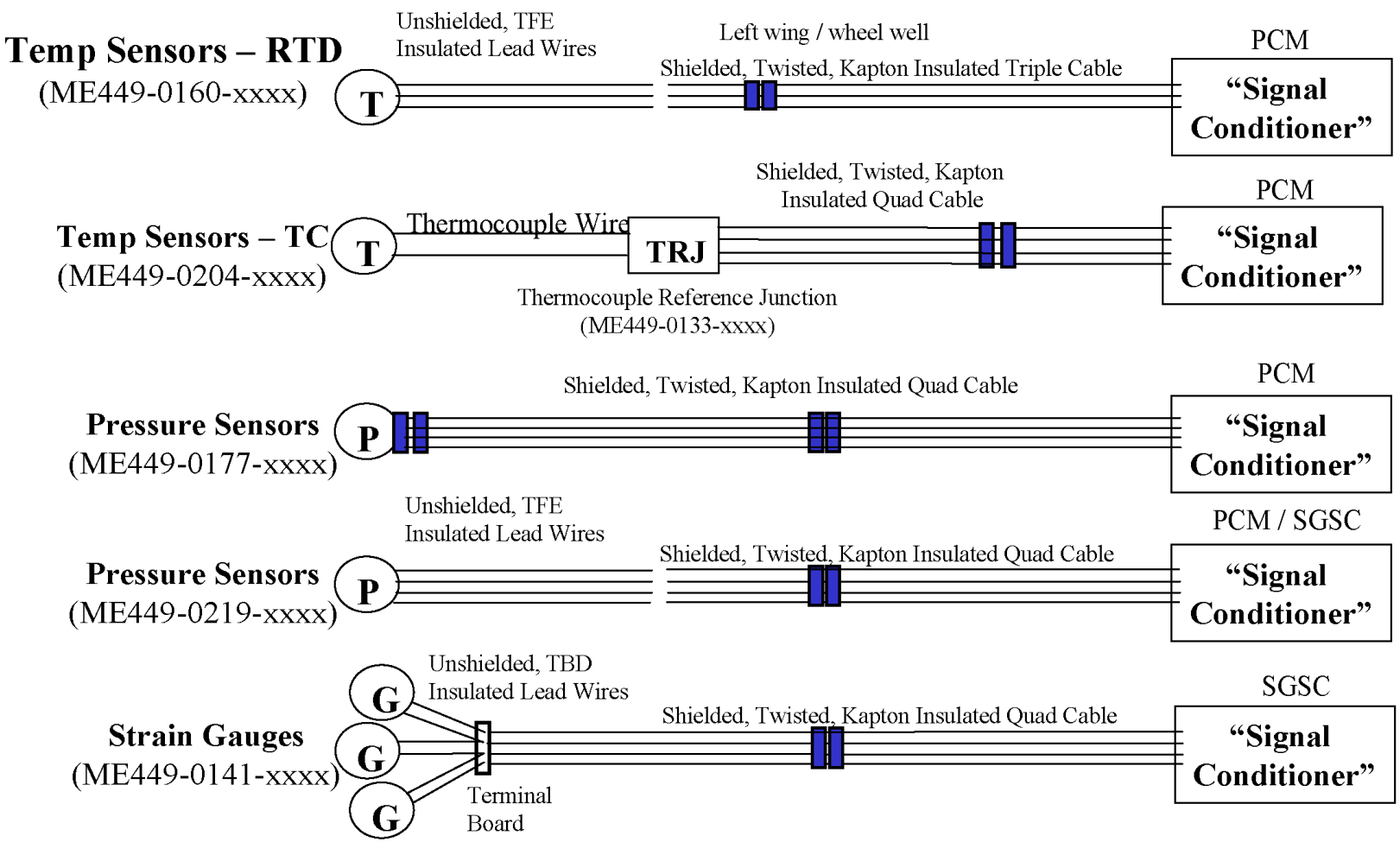

This material is PRELIMINARY information only. It is for limited distribution. DO NOT FORWARD.

MADS Transducer and Avionics Failure Susceptibilities

- Excitation Voltage Commonality Within the MADS Avionics Can Provide for Perturbations in the MADS Data From Varying and Seemingly Unrelated Sensor Locations
  - For example, wiring anomalies in the left wing could result in erratic data from right wing sensors
- Specific Observations—SGSC Pressures
  - 24 left and right wing pressure measurements are biased in the PCM by Strain Gauge Signal Conditioners (SGSCs)
  - In the absence of the nominal excitation voltage, the PCM would detect the 500mV bias voltage (0 psi) which would be detectable in the MADS data
  - At ~1352:10 GMT, the voltage was 0 volts indicating that the excitation leads were shorted to signal minus
  - This would cause left and right wing pressure sensors to read 0 psi
  - The data from these sensors is invalid following ~1352:10 GMT

This material is PRELIMINARY information only. It is for limited distribution. DO NOT FORWARD.

MADS Transducer and Avionics Failure Susceptibilities

- Specific Observations—Strain Gauges
  - Following installation, strain gauges are biased balanced in place to achieve 0 micro strains due to variations in the gauge and the effects of gauge installation
    - Biasing is achieved via potentiometer adjustment at the SGSC resulting in a non-zero voltage presented to the PCM
  - Typical signature observed in erratic strain data was characterized by off-scale excursions followed by a near zero response
  - Analysis of the data indicates that upper and lower range excursions are due to alterations in the resistance presented to the sensing bridge circuit
  - The subsequent non-zero response is believed to be the result of the bias voltage being reflected following gauge lead burn through
  - Strain gauge responses are to be considered invalid following the initial upper or lower range excursions

This material is PRELIMINARY information only. It is for limited distribution. DO NOT FORWARD.

MADS Transducer and Avionics Failure Susceptibilities

- Specific Observations—Pressures
  - The pressure transducers use five volt excitation from the PCMs
    - Two transducer types are used—Kulite (ME449-0219-xxxx) and Statham (ME449-0177-xxxx)
  - Complete loss of the five volt excitation from the MADS PCM will cause the measurement to fail off scale low
  - Various shorting combinations could cause the sensors to read either off-scale high or off-scale low
  - Insulation degradation also provides for intermittent conductor-to-conductor shorts which could explain the upper to lower range excursions
  - Ultimately, the vast majority of pressures fail off-scale low which is attributed to sensor leads burned through and shorted and / or open circuited
  - Pressure measurements are considered invalid following excursions to upper or lower ranges

This material is PRELIMINARY information only. It is for limited distribution. DO NOT FORWARD.

MADS Transducer and Avionics Failure Susceptibilities

- Specific Observations—Temperatures RTDs
  - The Resistance Temperature Device (RTD) is used to complete a wheatstone bridge internal to the MADS PCM
  - The bridge output is determined by the resistance between different leads on the RTD
  - Various shorting combinations could cause the sensors to read either off-scale high or off-scale low
  - Insulation degradation also provides for intermittent conductor-to-conductor shorts which would cause increases or decreases in the measurement value
  - RTD measurements are considered invalid following excursions to upper or lower ranges

This material is PRELIMINARY information only. It is for limited distribution. DO NOT FORWARD.

MADS Transducer and Avionics Failure Susceptibilities

- Specific Observations—Temperatures Thermocouples
  - Thermocouple measurements use compensating reference junctions which are powered by 5 volt excitation from the PCMs
  - Loss of the 5 volt excitation will cause the measurement to fail off scale low
  - Various shorting combinations could cause the sensors to read either off-scale high or off-scale low
  - Insulation degradation also provides for intermittent conductor-to-conductor shorts which would cause increases or decreases in the measurement value
  - The majority of thermocouple temperatures fail off-scale low which is attributed to sensor leads burned through and shorted and / or open circuited
  - Thermocouple measurements are considered invalid following excursions to upper or lower ranges
  - Temperatures preceding the inflection point toward off-scale high are considered valid up to the point of rapid slope change

This material is PRELIMINARY information only. It is for limited distribution. DO NOT FORWARD.

MADS Transducer and Avionics Failure Susceptibilities

- Specific Observations—Specific Temperature Set
  - A specific set of temperature measurements observed to display anomalous behavior during the STS-107 entry is similar to a previous unexplained anomaly on MADS PCM 1
  - Measurements V07T9636A, V07T9480A, V07T9489A, V07T9492A, V07T9522A which use MADS PCM 1 excitation output PPS089 all show a step in their signal level at approximately 13:52:20 GMT
  - Measurements V07T9253A, V07T9270A, V07T9468A, V07T9470A, V07T9478A which use MADS PCM 1 excitation output PPS087 showed a similar failure signature during STS-73, STS-75 and STS-78 on MADS PCM s/n 304
  - After STS-78, the PCM unit was removed from the vehicle and shipped to the vendor, B.F. Goodrich, for TT&E and test
    - The unit was tested at ambient, hot and cold temperatures without repetition of the failure condition
  - The failures repeated on STS-80, STS-94 and STS-87.
  - The cause and mechanism of this failure signature is unknown, however it is independent of the MADS PCM

This material is PRELIMINARY information only. It is for limited distribution. DO NOT FORWARD.

STS-107 MADS Temperature Data
RCC Panel 9 Ascent Data

This material is PRELIMINARY information only. It is for limited distribution. DO NOT FORWARD.

Ascent Response on RCC Panel 9 Spar

- Compared STS-107 Data Against Previous OV-102 Mission Data: 50, 73, 94, 87, 90, 93, and 109
  - Mission: launch date, GMT time, inclination, beta angle
  - STS-107: 01/16/03, 15:38: 59, 39°, -55.7°
  - STS-109: 03/01/02, 11:22:01, 28.45°, -7.0°
    - Flight preceding STS-107
  - STS-93: 07/23/99, 04:30:59, 28.45°, +47.8°
  - STS-90: 04/17/98, 18:18:59, 39°, -7.6°
  - STS-87: 11/19/97, 19:46:00, 28.45°, -38.4°
  - STS-94: 07/01/97, 18:02:00, 28.45, -4.7°
  - STS-73: 10/20/95, 13:53:00, 39°, -49.3°
  - STS-50: 06/25/92, 16:12:23, 28.5°, -4.4°

This material is PRELIMINARY information only. It is for limited distribution. DO NOT FORWARD.

RCC Panel 9 Spar Temperature Data - Ascent

- Reviewed Previous OV-102 Ascent Data
  - STS-107 has earliest warming indication at 310 seconds
  - STS-107 has only occurrence of a 3 bit (7.5°F) warming during ascent, 67°F initial temp.
    - STS-94, a summer launch with 82°F initial temp, had less than a 2 bit rise
  - No spar temperature sensor on other vehicles

This material is PRELIMINARY information only. It is for limited distribution. DO NOT FORWARD.

RCC Panel 9 Sensor Locations

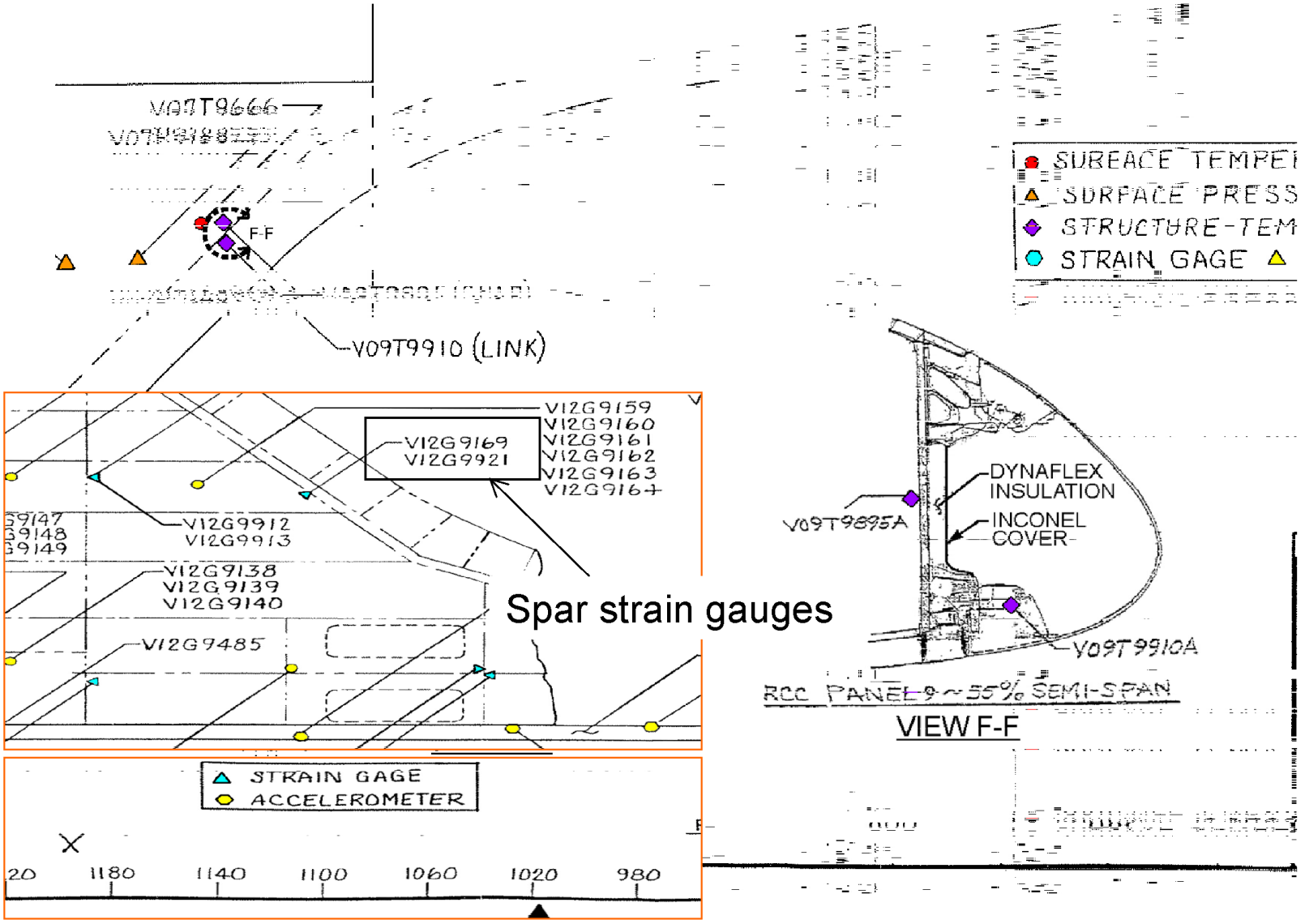

This material is PRELIMINARY information only. It is for limited distribution. DO NOT FORWARD.

RCC Panel 9 Spar Response - Ascent

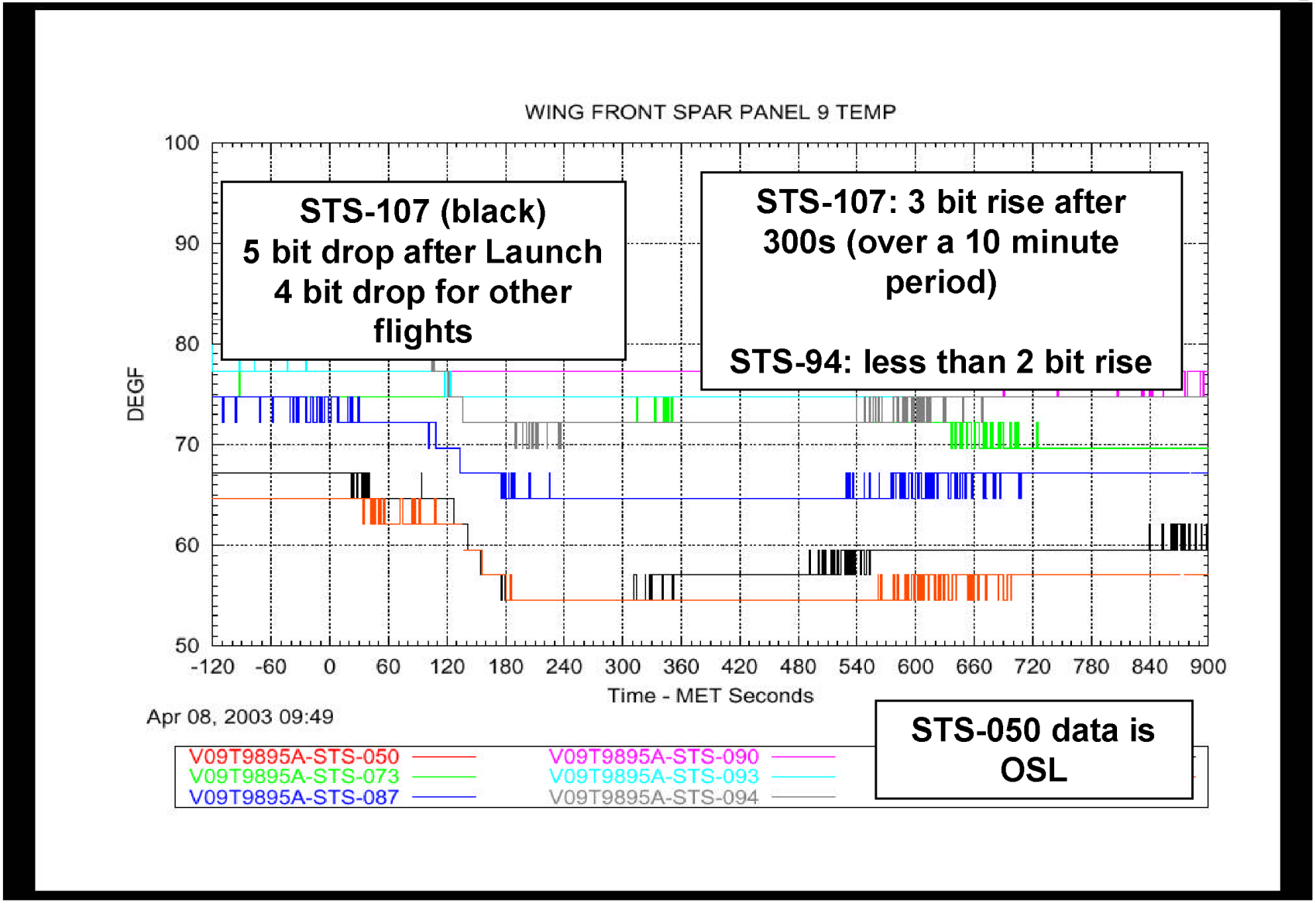

This material is PRELIMINARY information only. It is for limited distribution. DO NOT FORWARD.

RCC Panel 9 Spar Data Bit Summary

OV-102 Columbia	Ascent Bits Down/Up in 900 seconds RCC Panel 9 Spar Temp V09T9895a
STS-73 10/20/95	2/0
STS-75 02/22/96	3/0
STS-78 06/20/96	3/0
STS-80 11/19/96	1/0
STS-83 04/04/97	2/0
STS-94 07/01/97	5/2 (82 degF initial temp)
STS-87 11/19/97	4/1
STS-90 04/17/98	1/0
STS-93 07/22/99	1/0
STS-109 03/01/02	4/1
STS-107 01/16/03	5/3 (67 degF initial temp)

This material is PRELIMINARY information only. It is for limited distribution. DO NOT FORWARD.

STS-107 MADS Temperature Data Entry

This material is PRELIMINARY information only. It is for limited distribution. DO NOT FORWARD.

MADS Entry Data Review Process

- Compared STS-107 Data Against Previous OV-102 Mission Data: STS-50, 73, 94, 87, 90, 93, and 109
  - Mission: weight, inclination, transition from laminar to turbulent flow, altitude, center of gravity xo at EI
  - STS-107: ~233,995 lbs, 39°, Mach NA, 148 nm, 1078.27
  - STS-109: ~222,500 lbs, 28.45°, Mach ~8.7, 290 nm, 1083.8
    - Flight preceding STS-107
  - STS-93: ~203,300 lbs, 28.45°, Mach ~8.1, 148 nm, 1098.9
  - STS-90: ~233,500 lbs, 39°, Mach ~8.1, 142 nm, 1081.4
  - STS-87: ~233,400 lbs, 28.45°; Mach ~8.9, 153 nm, 1082.2
  - STS-94: ~231,750 lbs, 28.45°, Mach ~16.5, 164 nm ,1079.9
  - STS-73: ~231,300 lbs, 39°, Mach ~19.2, 142 nm, 1082.4
  - STS-50: ~227,000 lbs, 28.45°, Mach ~9.4, 146 nm, 1080.7

This material is PRELIMINARY information only. It is for limited distribution. DO NOT FORWARD.

Temperature Observations

- Observations on 49 Temperature Measurements
  - All nominal response to MADS data loss EI+965 (14:00:14.490 GMT) – 2 sensors in RCC chin panel structure
  - All bad data – 2 sensors (pre-existing condition, door insulation and chin panel surface)
  - Trend to off-scale low at ~EI+490 seconds (13:52:24 GMT) – 15 sensors, all left wing
  - Sharp 300 to 350°F temp increase at ~EI+490 - 3 sensors,
    - LWR Xo 1004.1, Yo –99.8; Xo 1391.5, Yo 0.0; Xo 1511.1, Yo 1.3
  - Off-nominal trend (cooling) at ~EI+344 (13:49:53 GMT) seconds followed by off-nominal heating at ~EI+520 seconds until erratic temp trend at ~EI+933 seconds (13:59:42.49 GMT) – 14 sensors, left side and left pod
  - Off-nominal temperature increase start ~EI+290 sec - RCC Panel 9 spar and clevis

This material is PRELIMINARY information only. It is for limited distribution. DO NOT FORWARD.

Lower Surface Temperatures and Pressures

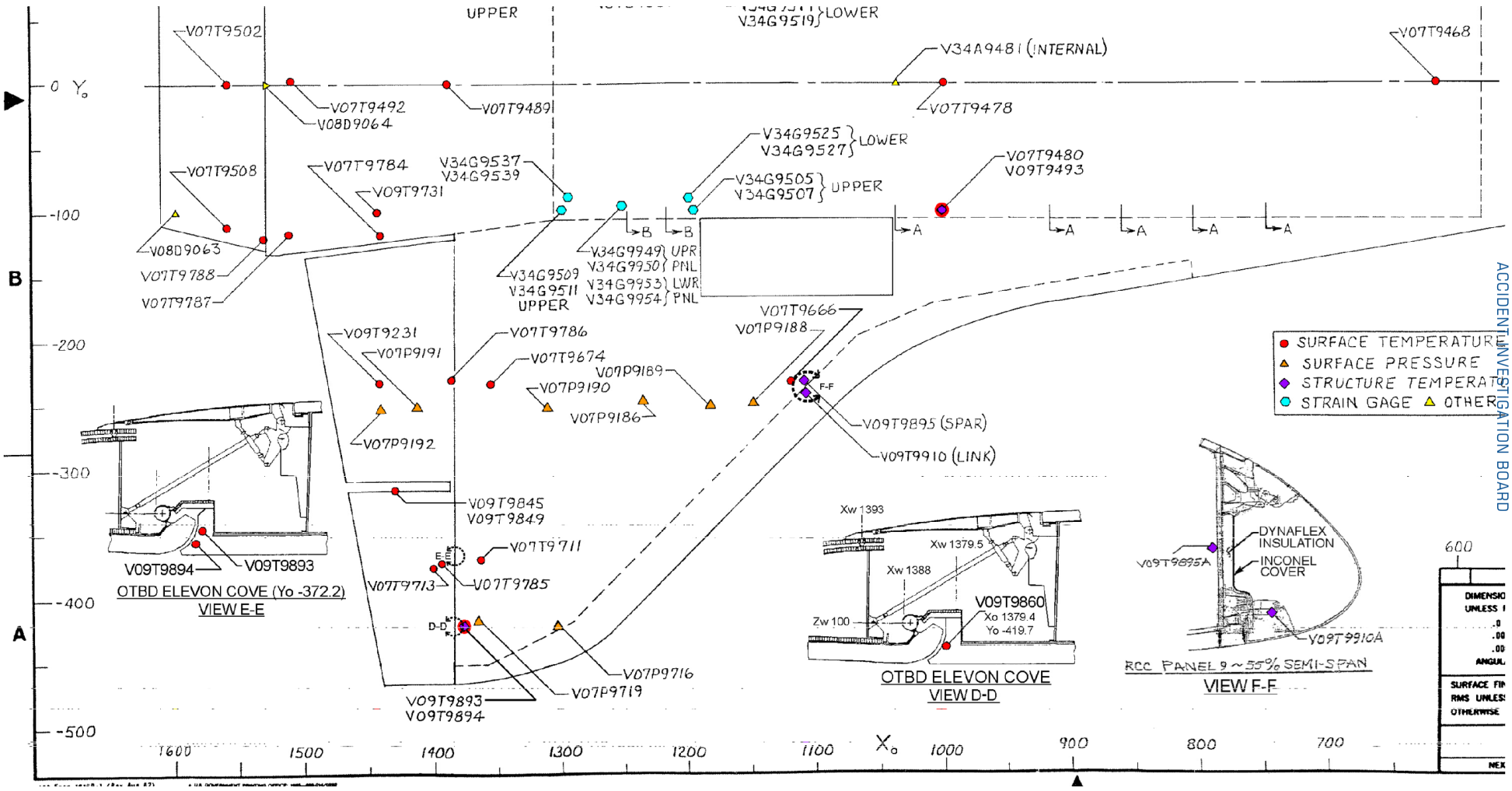

This material is PRELIMINARY information only. It is for limited distribution. DO NOT FORWARD.

Lower Wing Surface Temperatures STS-107

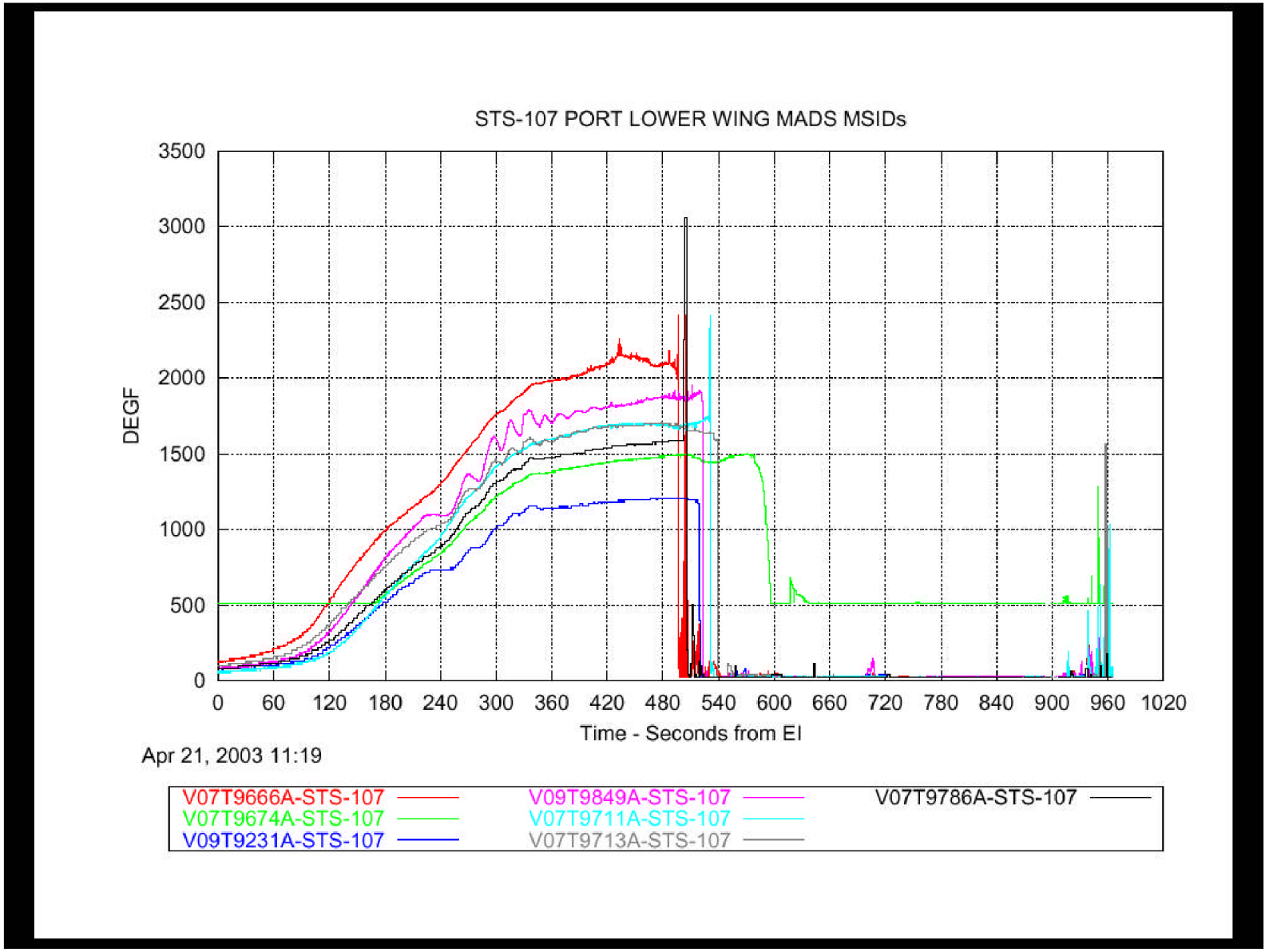

Lower Surface Sharp Temp Rise and Bondline OI

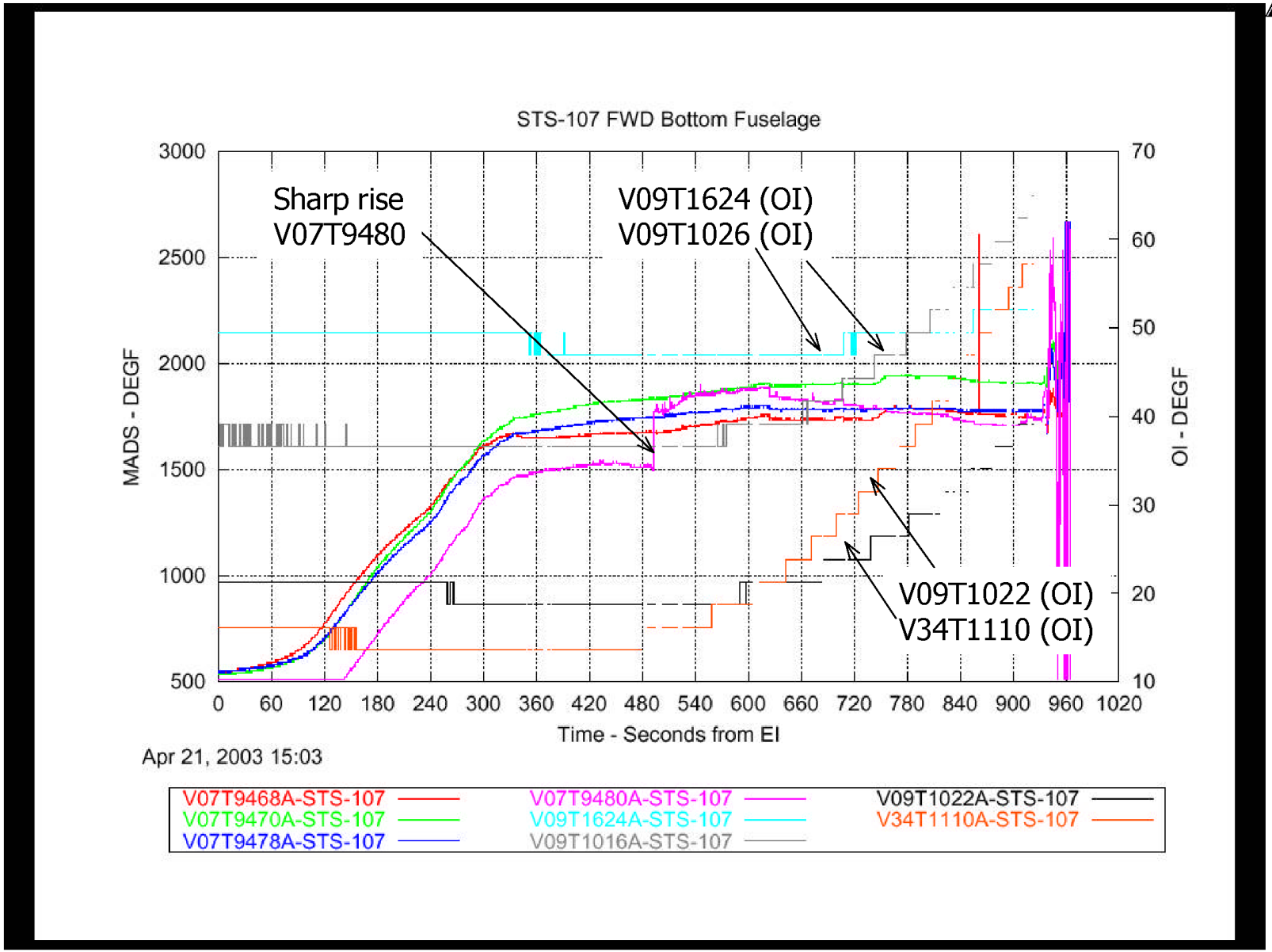

This material is PRELIMINARY information only. It is for limited distribution. DO NOT FORWARD.

Trend to OSL & Early Warming Trend

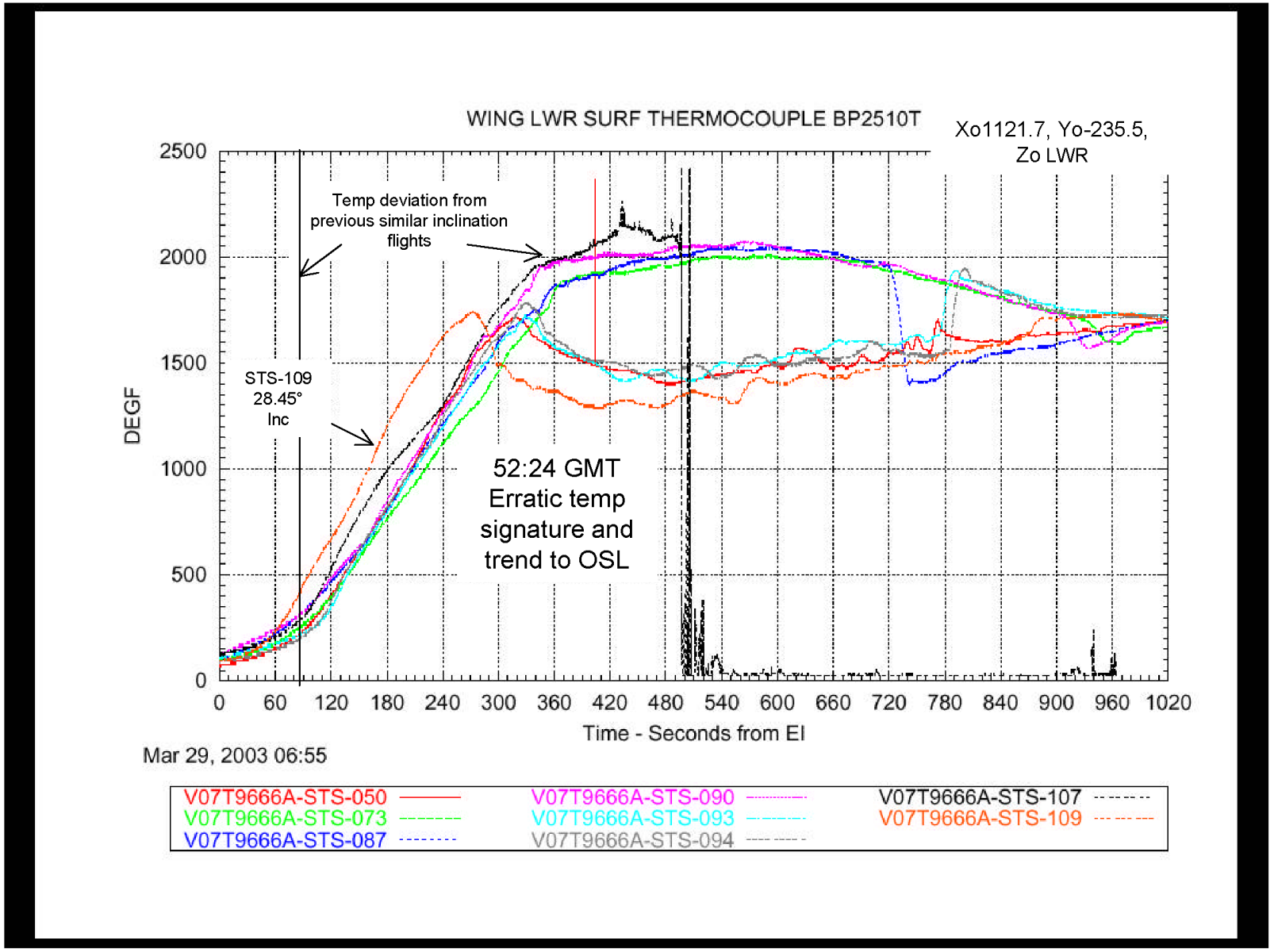

Sharp Temp Rise

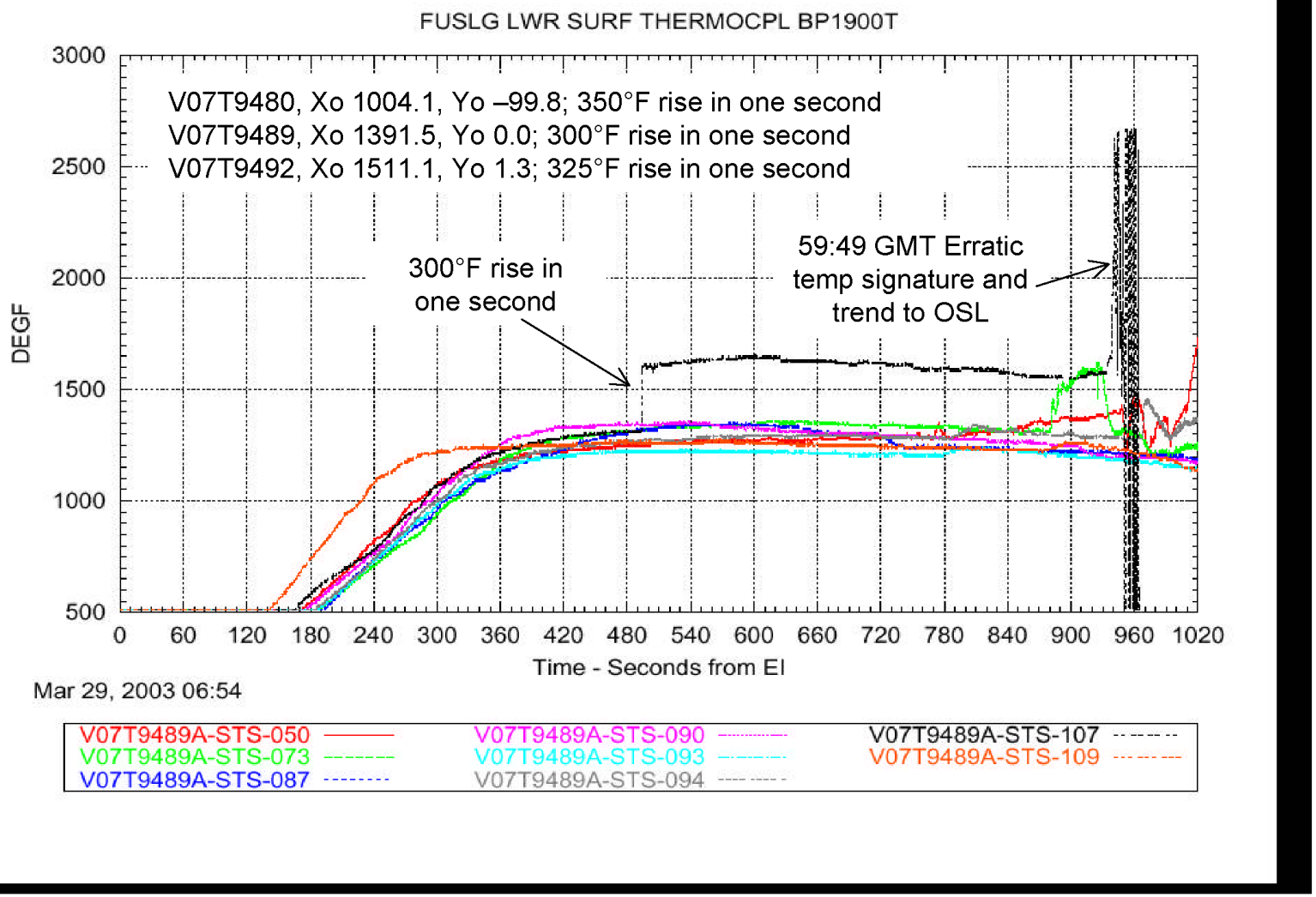

This material is PRELIMINARY information only. It is for limited distribution. DO NOT FORWARD.

Left Side Temperature Sensor Locations

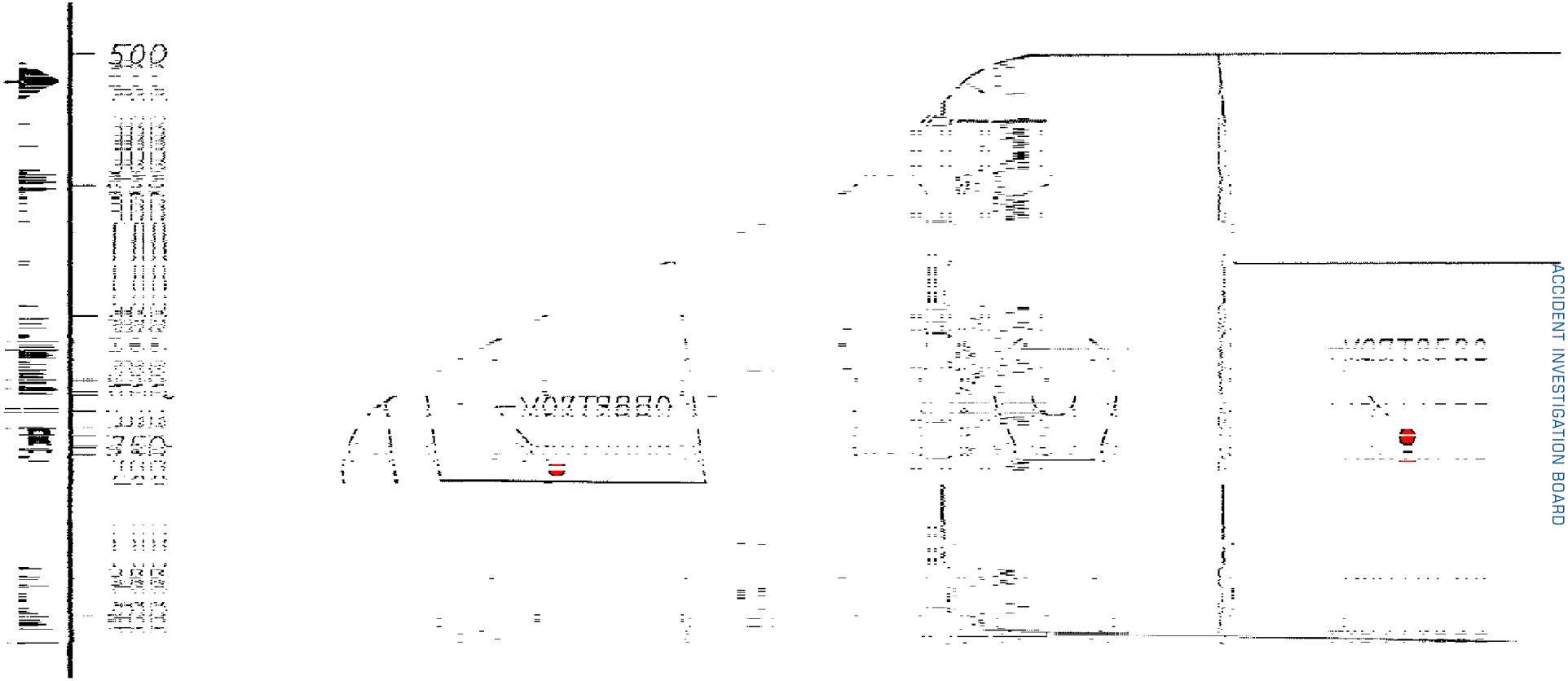

This material is PRELIMINARY information only. It is for limited distribution. DO NOT FORWARD.

Left Side Surface Temperature Locations

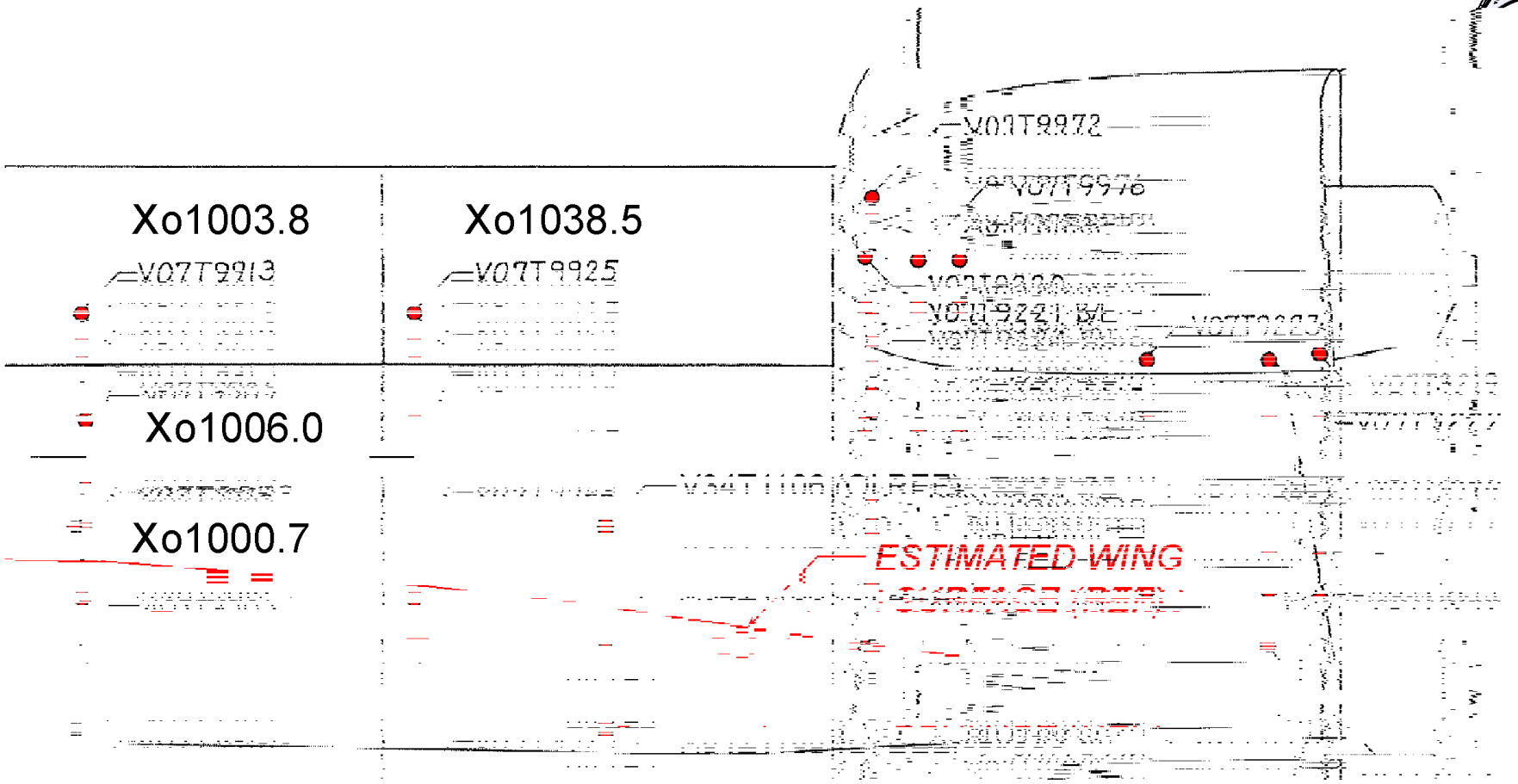

This material is PRELIMINARY information only. It is for limited distribution. DO NOT FORWARD.

Left Side Surface and OI Temperatures

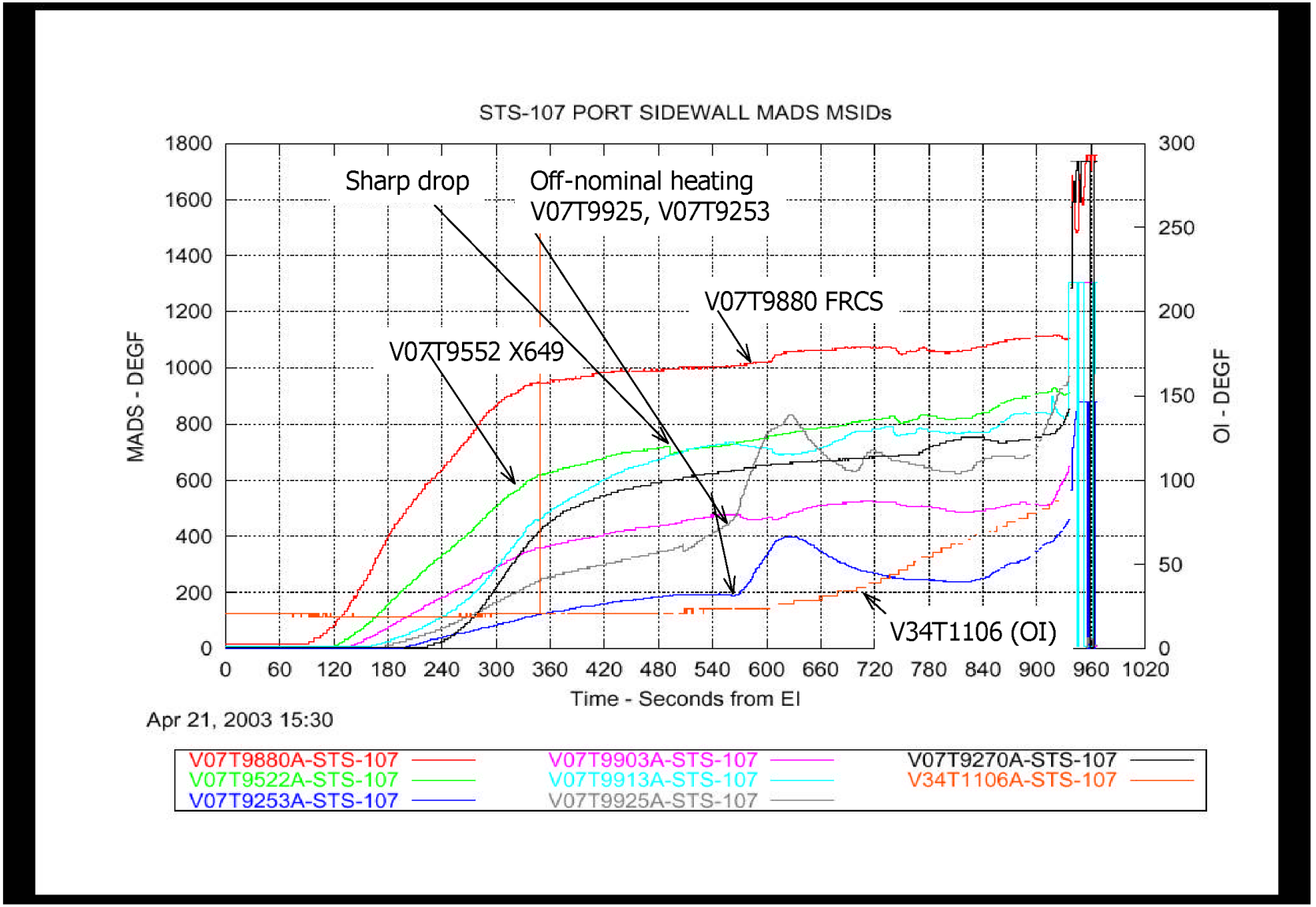

This material is PRELIMINARY information only. It is for limited distribution. DO NOT FORWARD.

Left Pod Surface Temperatures - Entry

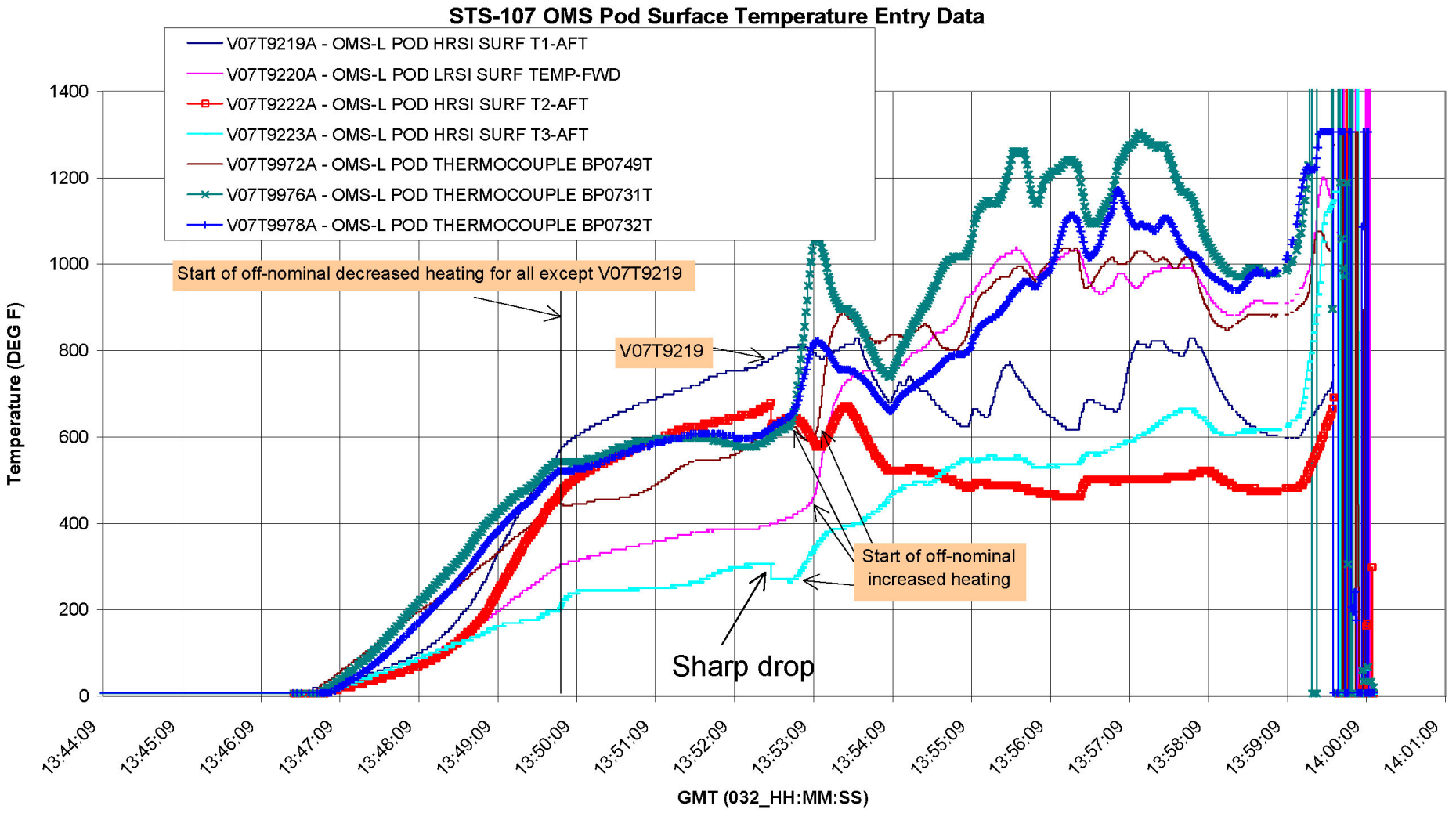

This material is PRELIMINARY information only. It is for limited distribution. DO NOT FORWARD.

RCC Panel 9 Sensor Locations

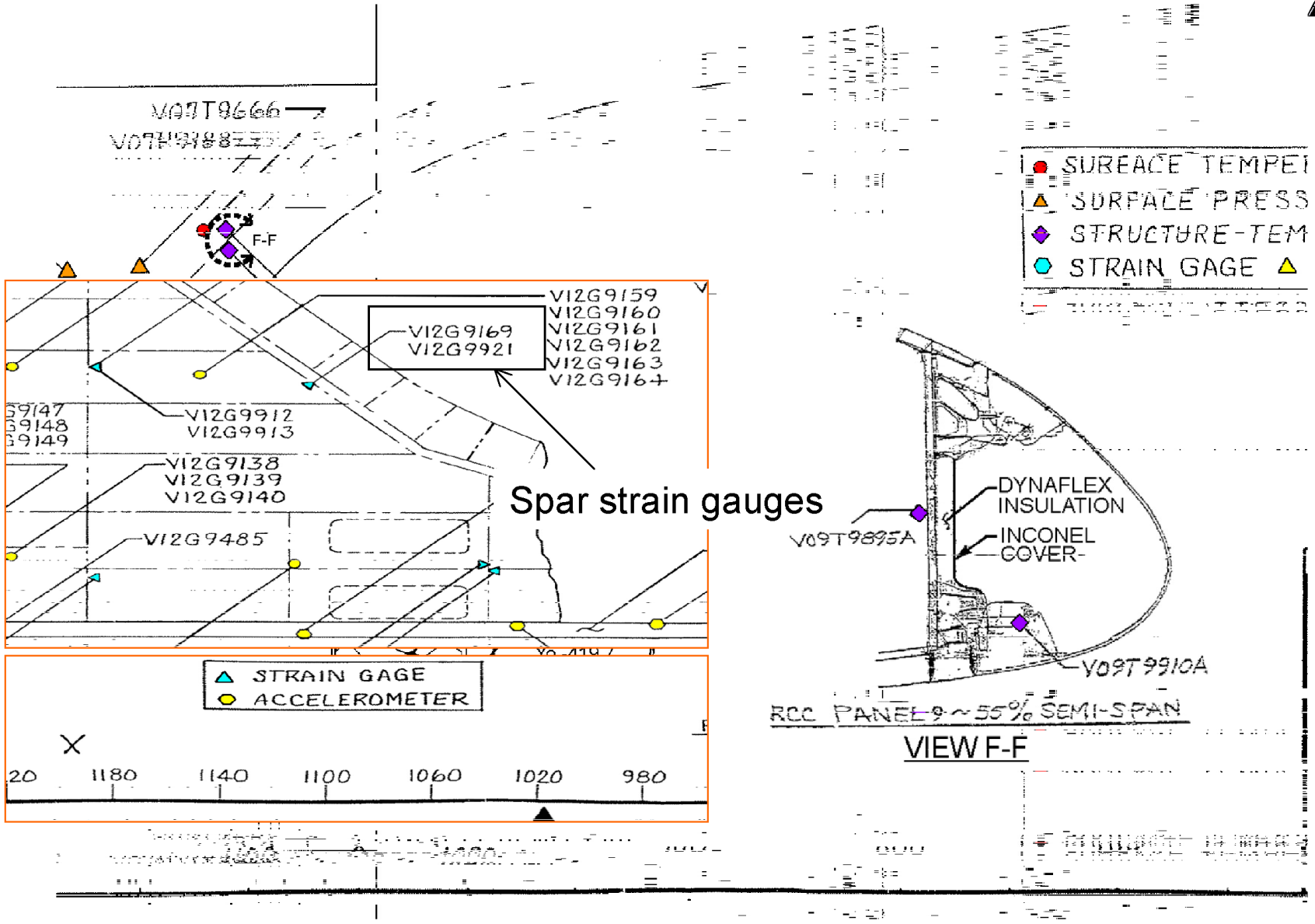

This material is PRELIMINARY information only. It is for limited distribution. DO NOT FORWARD.

RCC Panel 9 Area Temp & Strain

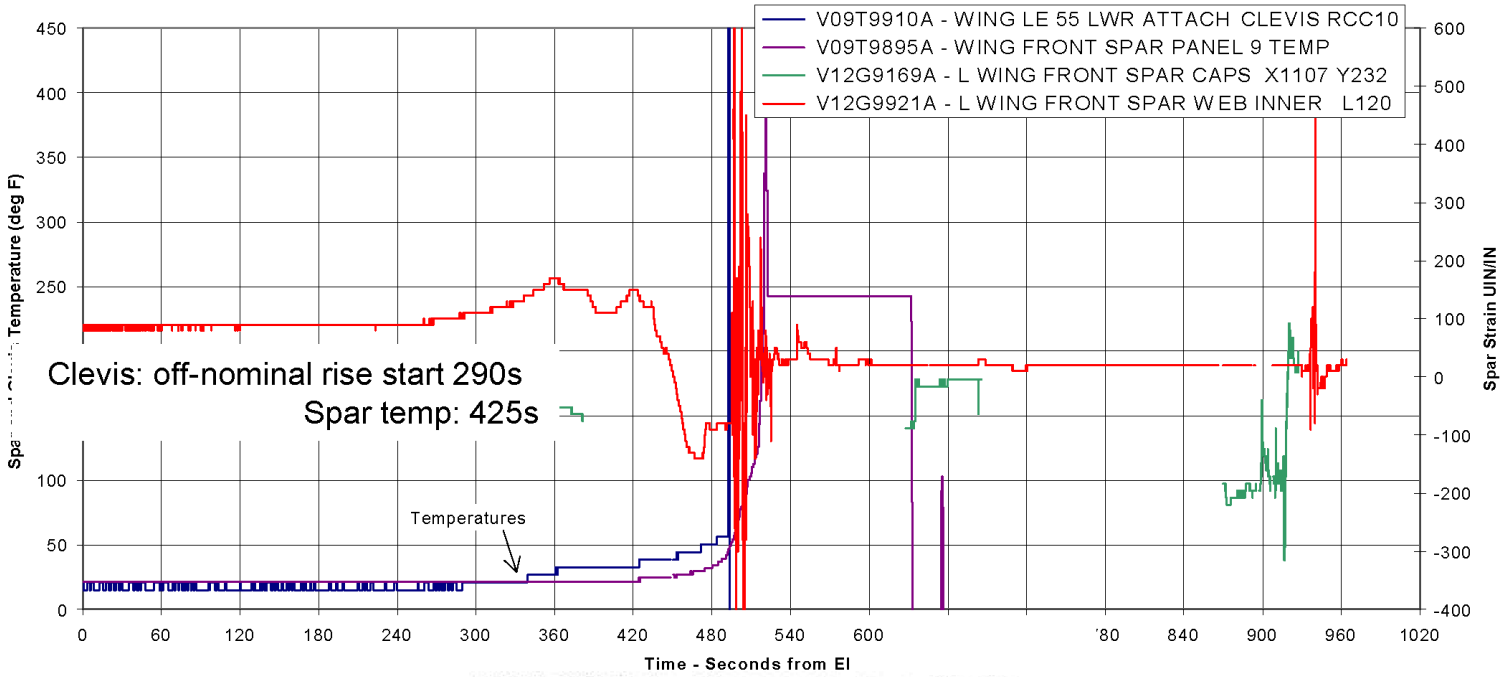

STS-107 Entry Temperature vs Strain

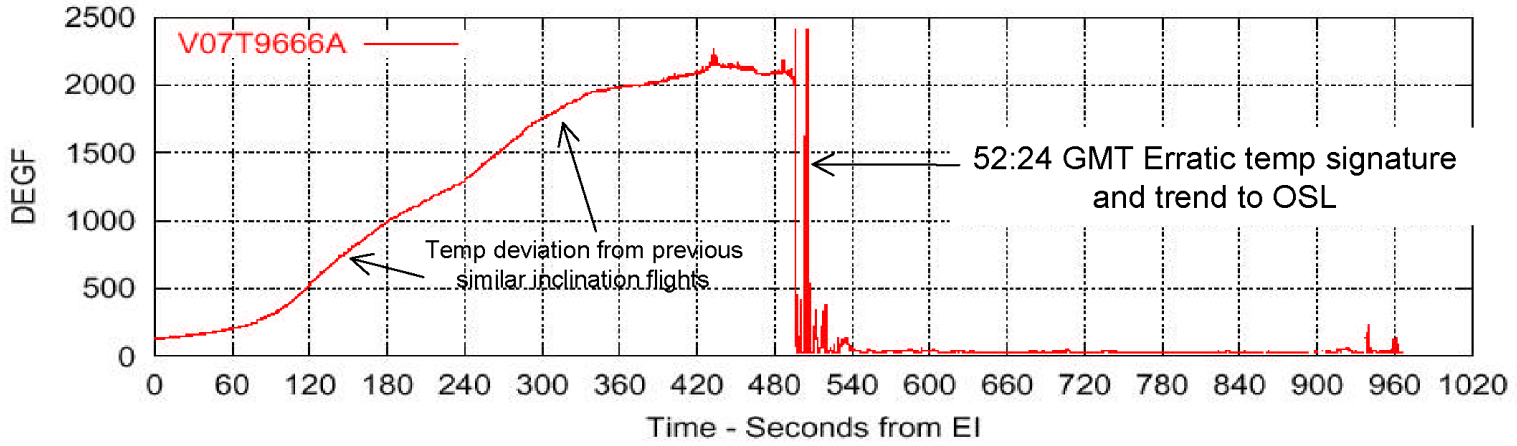

This material is PRELIMINARY information only. It is for limited distribution. DO NOT FORWARD.

STS-107 MADS Strain Gauge Data Entry

This material is PRELIMINARY information only. It is for limited distribution. DO NOT FORWARD.

Summary

- A Number of MADS Strain Gauges Were Identified As Showing Abnormal Data Trends Versus Typical Strain Gauge Responses Observed on STS-107 entry
- Abnormal Gauges Were Grouped and Plotted Together According to Location on the Vehicle
- An Examination Was Performed for Strain and Temperature Gauges Near Left Wing RCC Panel #9
- Several Immediate Observations May Be Made from the Data
  - A number of other studies are currently in work

This material is PRELIMINARY information only. It is for limited distribution. DO NOT FORWARD.

Abnormal Gauge Groupings

- Left Wing, x1040 Spar Gauges
- Mid Fuselage Gauges
- Right Wing Spar Cap Gauges
- Right Wing Skin Gauges @ x1334
- Right Wing Skin Gauges @ x1217.9
- Right Wing Skin Gauges @ x1276

This material is PRELIMINARY information only. It is for limited distribution. DO NOT FORWARD.

Data Observations/Future Work

- Left Wing x1040 Spar Cap Gauges Show an Anomalous Trend Initiating Between EI +500 and EI +600 Seconds. Web Gauges Have "Snapshot Mode" Data Which Suggest Off-nominal Trending After EI +500 Seconds
  - The spar cap gauges are two of only three left wing gauges which did not fail prior to vehicle breakup
  - Further analysis is in work to assess potential explanations for these anomalous signatures
- Some Mid Fuselage and Right Wing Spar Cap Gauges Show Mild Discrepancies Versus Previous Flights
  - Discrepancies are more subtle
- A Number of Right Wing Skin Gauges Show off Nominal Trending Initiating Near EI +500 Seconds
  - Currently under further investigation

This material is PRELIMINARY information only. It is for limited distribution. DO NOT FORWARD.

Left Wing X1040 Spar Cap Gauges Show an Anomalous Trend Initiating Between EI +500 and EI +600 Seconds

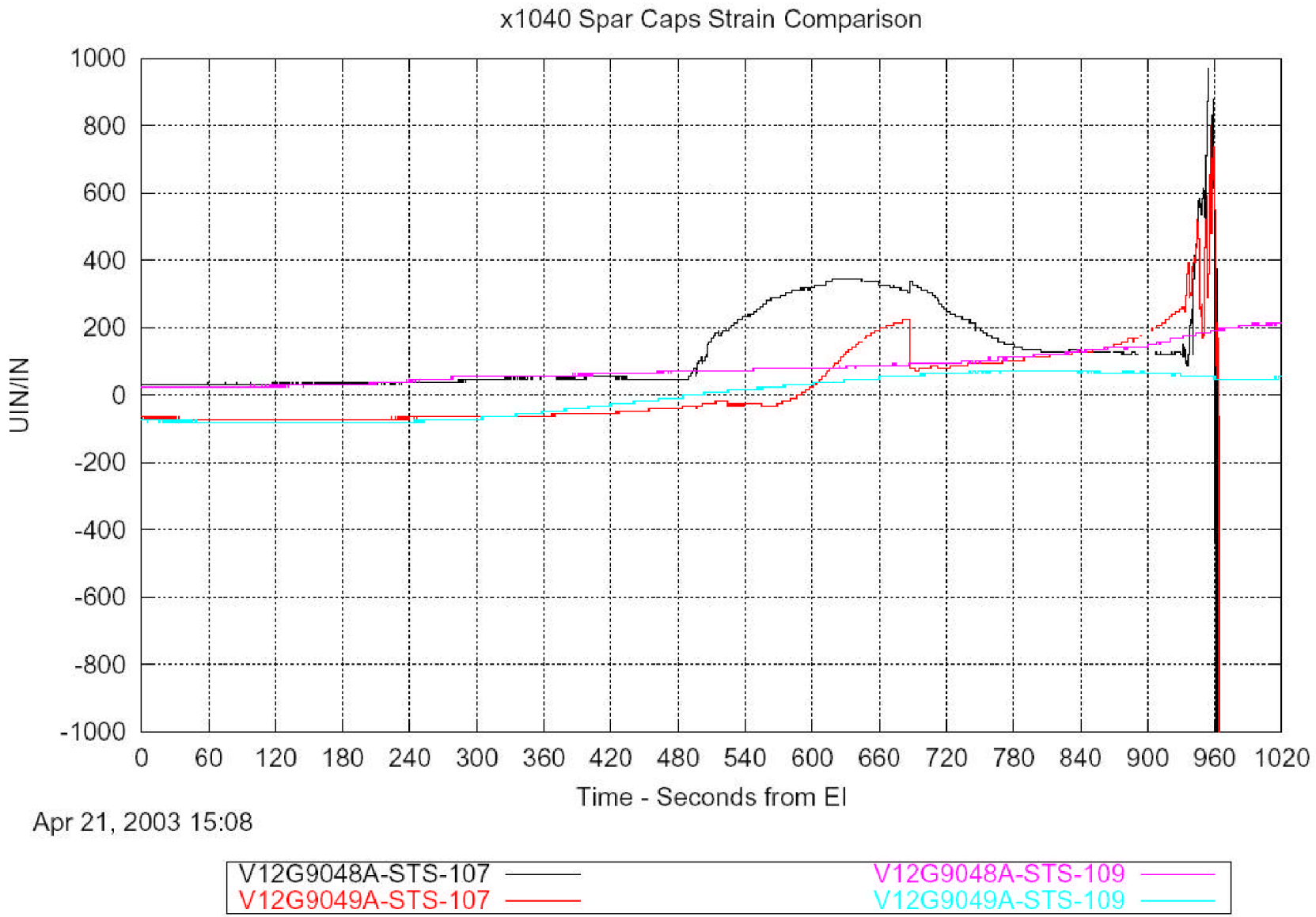

This material is PRELIMINARY information only. It is for limited distribution. DO NOT FORWARD.

Left Wing X1040 Spar Cap Gauges Show an Anomalous Trend Initiating Between EI +500 and EI +600 Seconds

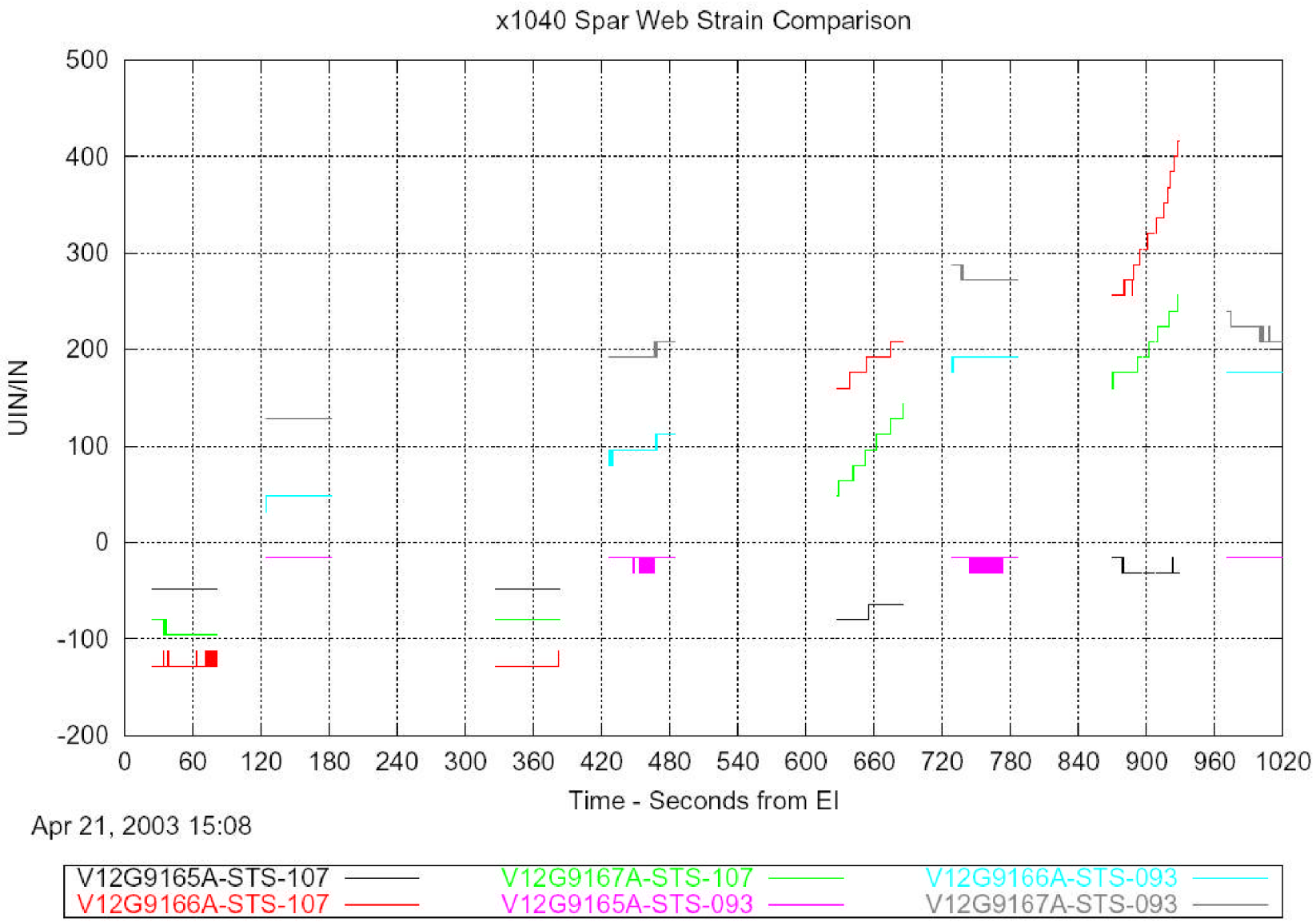

This material is PRELIMINARY information only. It is for limited distribution. DO NOT FORWARD.

Some Mid Fuselage Gauges Show Mild Discrepancies Versus Previous Flights

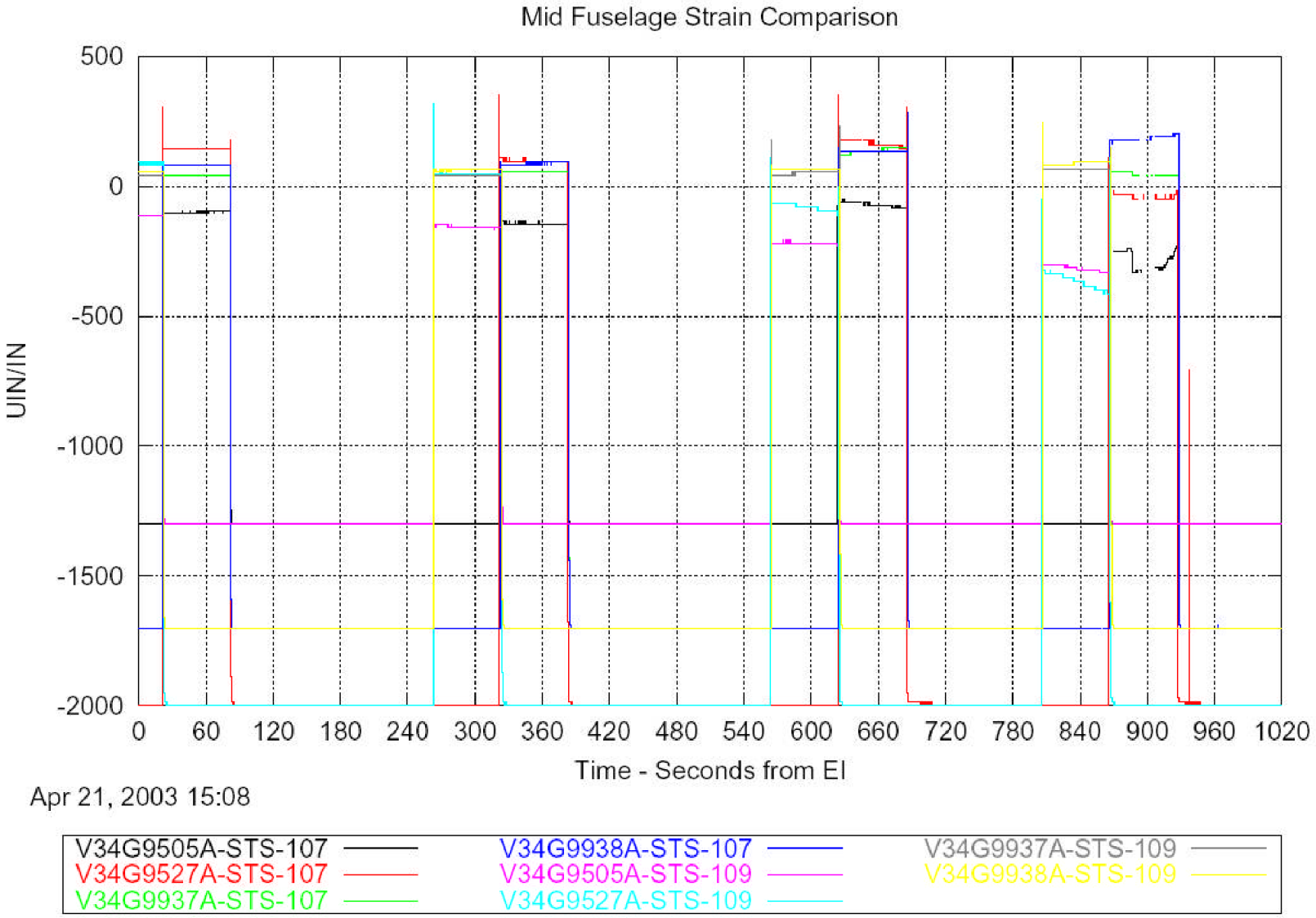

This material is PRELIMINARY information only. It is for limited distribution. DO NOT FORWARD.

Some Right Wing Spar Cap Gauges Show Mild Discrepancies Versus Previous Flights

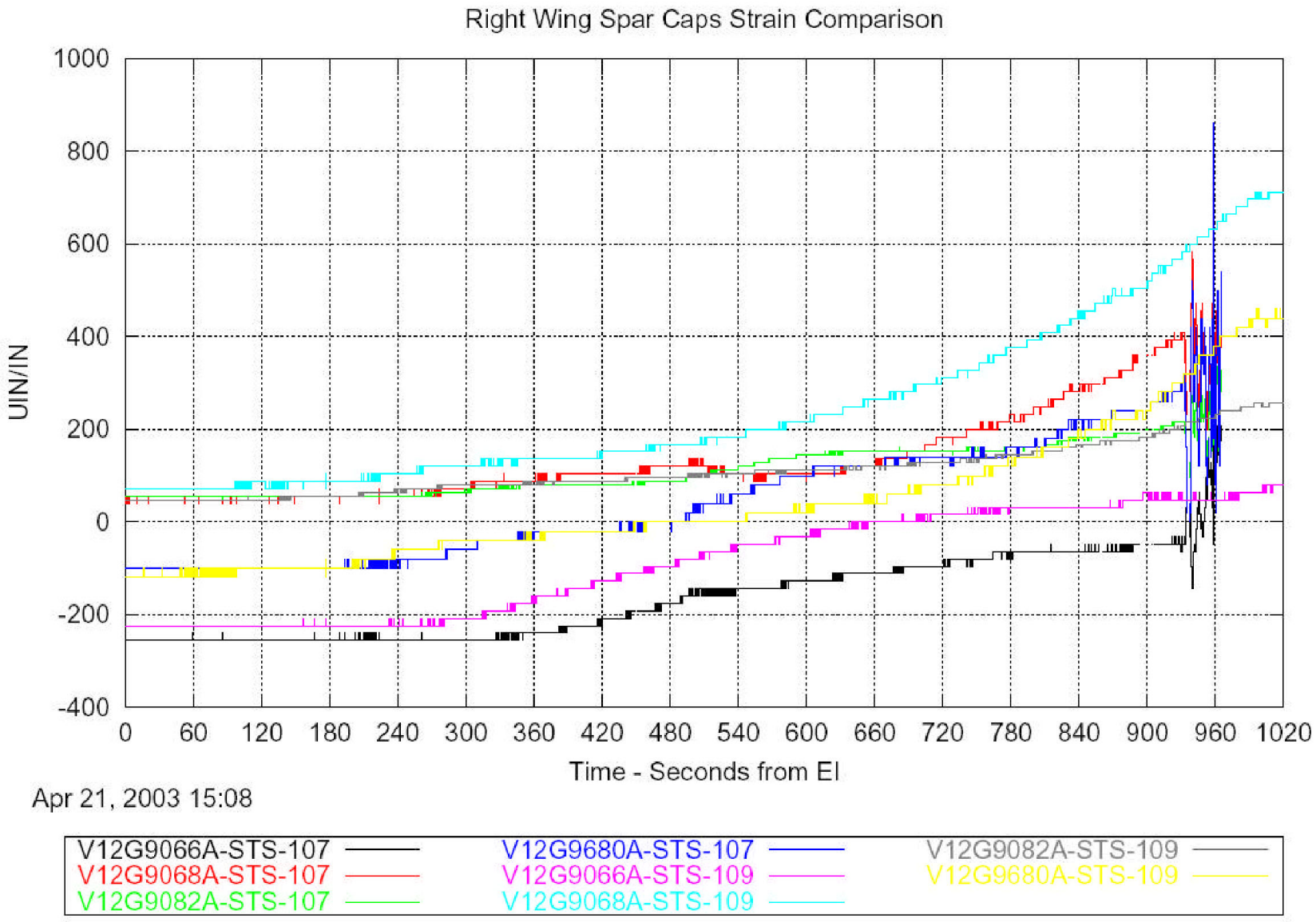

This material is PRELIMINARY information only. It is for limited distribution. DO NOT FORWARD.

A Number of Right Wing Skin Gauges Show Off-Nominal Trending Initiating Near EI +500 Seconds

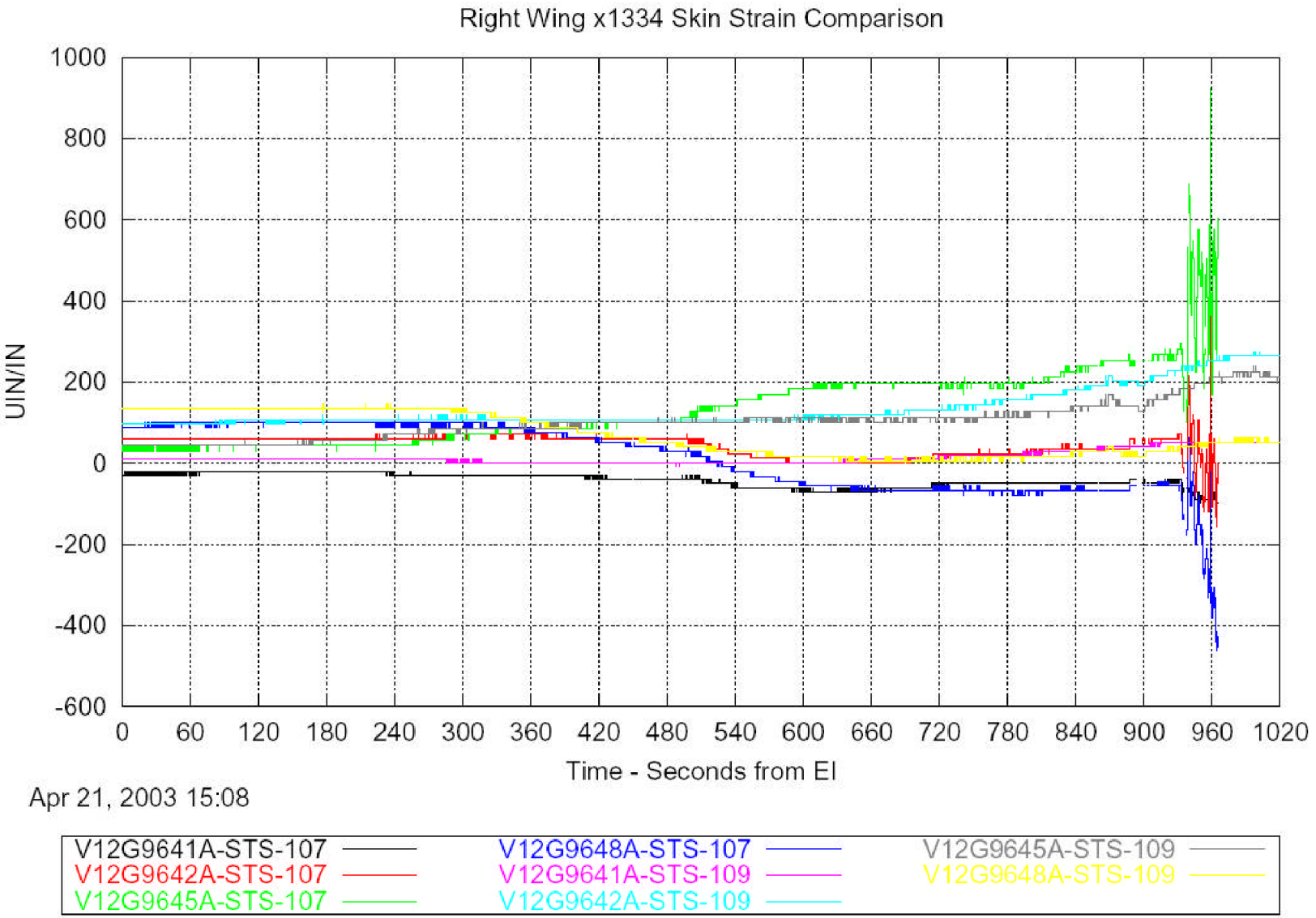

This material is PRELIMINARY information only. It is for limited distribution. DO NOT FORWARD.

A Number of Right Wing Skin Gauges Show Off-Nominal Trending Initiating Near EI +500 Seconds

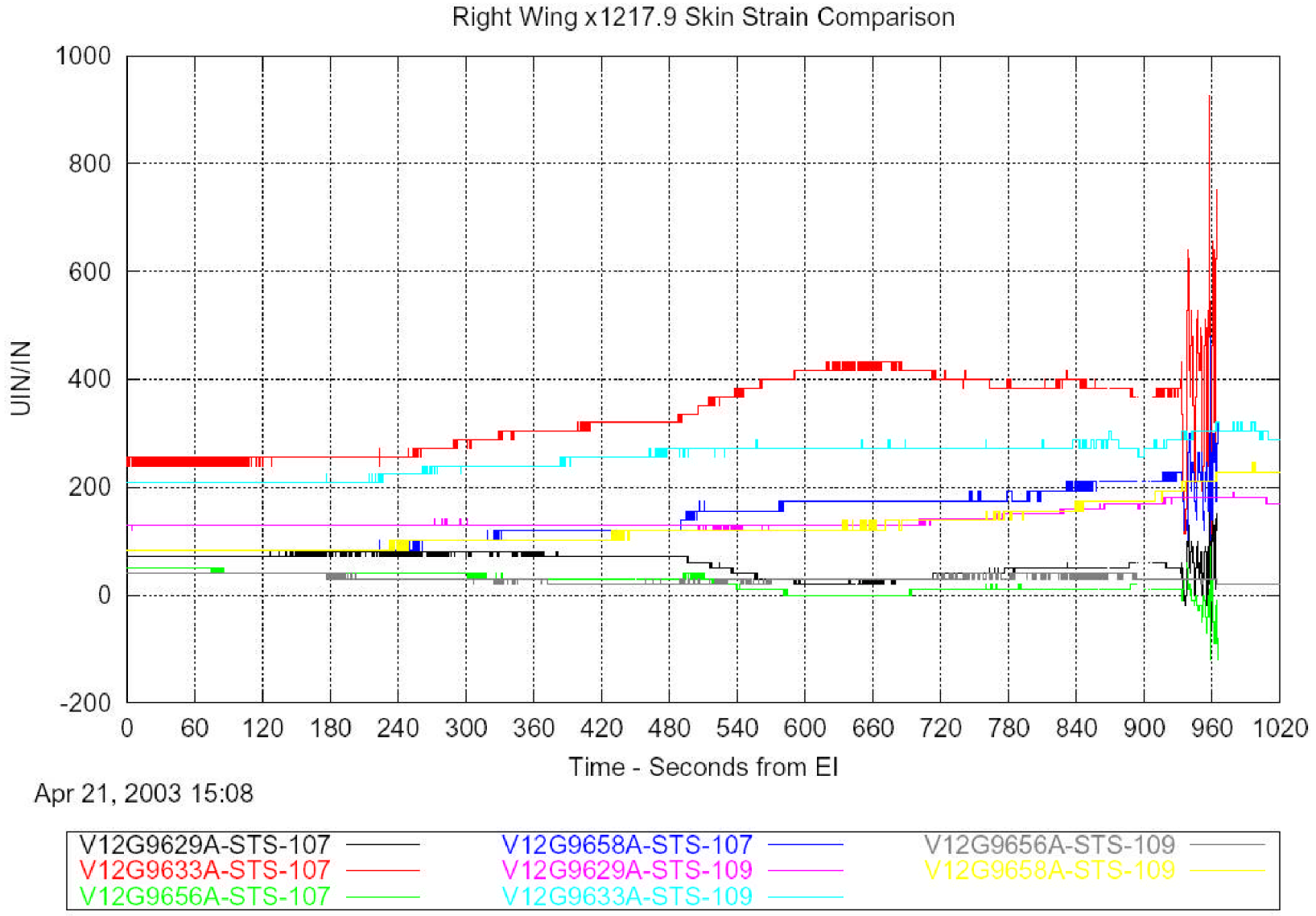

This material is PRELIMINARY information only. It is for limited distribution. DO NOT FORWARD.

A Number of Right Wing Skin Gauges Show Off-Nominal Trending Initiating Near EI +500 Seconds

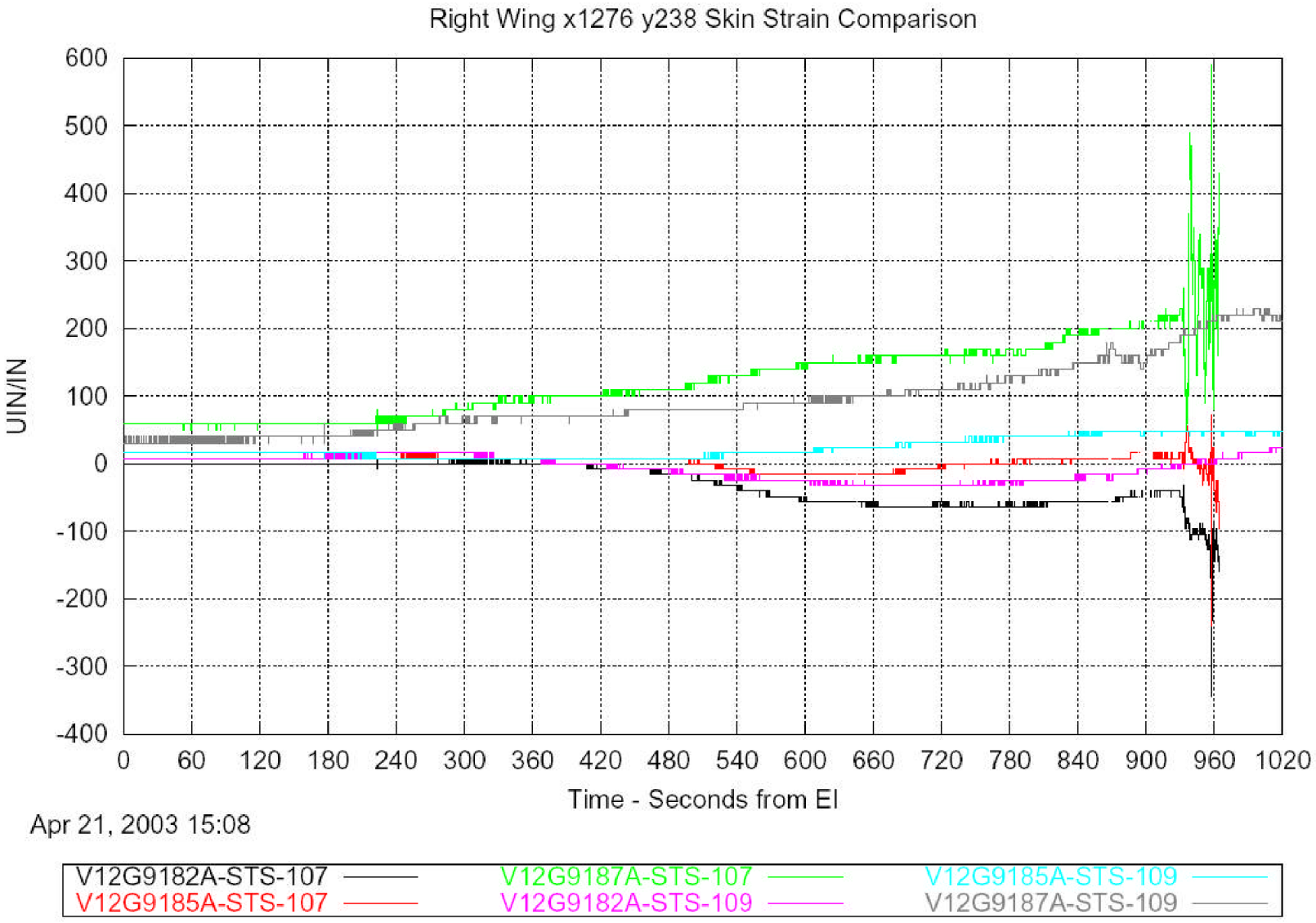

This material is PRELIMINARY information only. It is for limited distribution. DO NOT FORWARD.

A Number of Right Wing Skin Gauges Show Off-Nominal Trending Initiating Near EI +500 Seconds

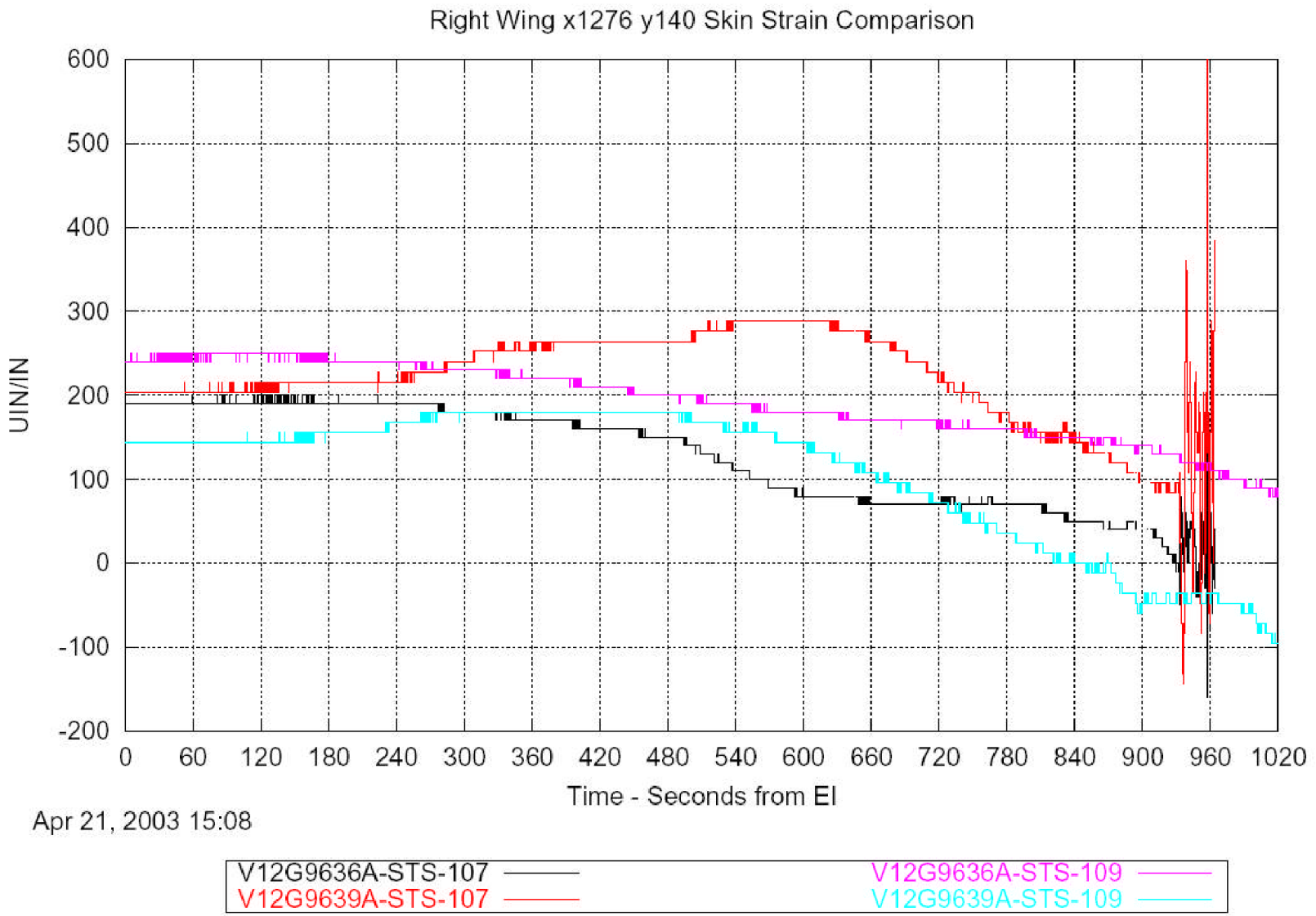

This material is PRELIMINARY information only. It is for limited distribution. DO NOT FORWARD.

RCC Panel 9

- Three MADS gauges of particular interest near RCC Panel 9 on the Left Wing
  - One Strain gauge, Two Temperature gauges
    - V12G9921A, V09T9910A, & V09T9895A
  - Data for these three gauges was plotted together
    - Indicates failure at approximately the same time for V12G9921A and V09T9910A (~EI +495sec)
    - Later failure for V09T9895A (~EI +515sec)
  - Continued analysis is underway for this data.

This material is PRELIMINARY information only. It is for limited distribution. DO NOT FORWARD.

RCC Panel 9 Strain and Temperature Gauges

RCC Panel 9 OEX Gages, STS-107

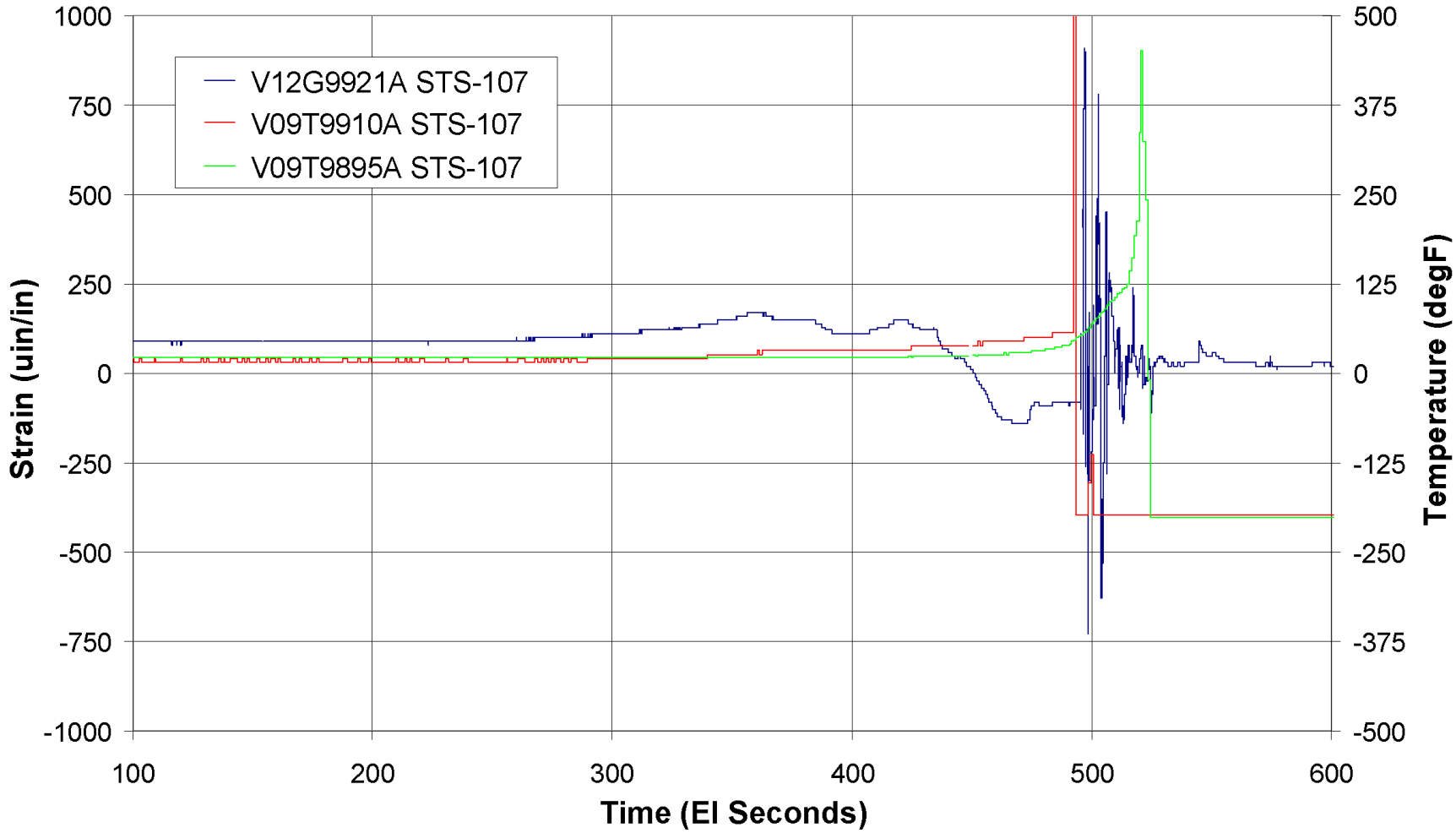

This material is PRELIMINARY information only. It is for limited distribution. DO NOT FORWARD.

STS-107 MADS Pressure Data

This material is PRELIMINARY information only. It is for limited distribution. DO NOT FORWARD.

Summary

- Ascent
  - Pressure transducers are sized for ascent load environments
  - Pressures were compared within Y-station family and with past flights
  - Pressure tap V07P8073 appears to have been hit at 84.4 seconds
  - Pressure tap V07P8074 is “out-of-family” after 82 seconds as compared to past flights
  - Pressure taps V07P8070, V07P8075 and V07P9189 have similar strange behavior around 102-104 seconds
  - Remaining pressure taps show no significant events
- Entry
  - Pressures also compared within Y-station and past flights
  - Data review typically made in the Mach 3.5 to 0.6 range for instrument functionality and “signature” comparison
  - Pressures generally show intermittent data spikes/dropouts in the 480-660 sec and 930-970 sec timeframe

This material is PRELIMINARY information only. It is for limited distribution. DO NOT FORWARD.

Lower Left Wing Y-Station Taps

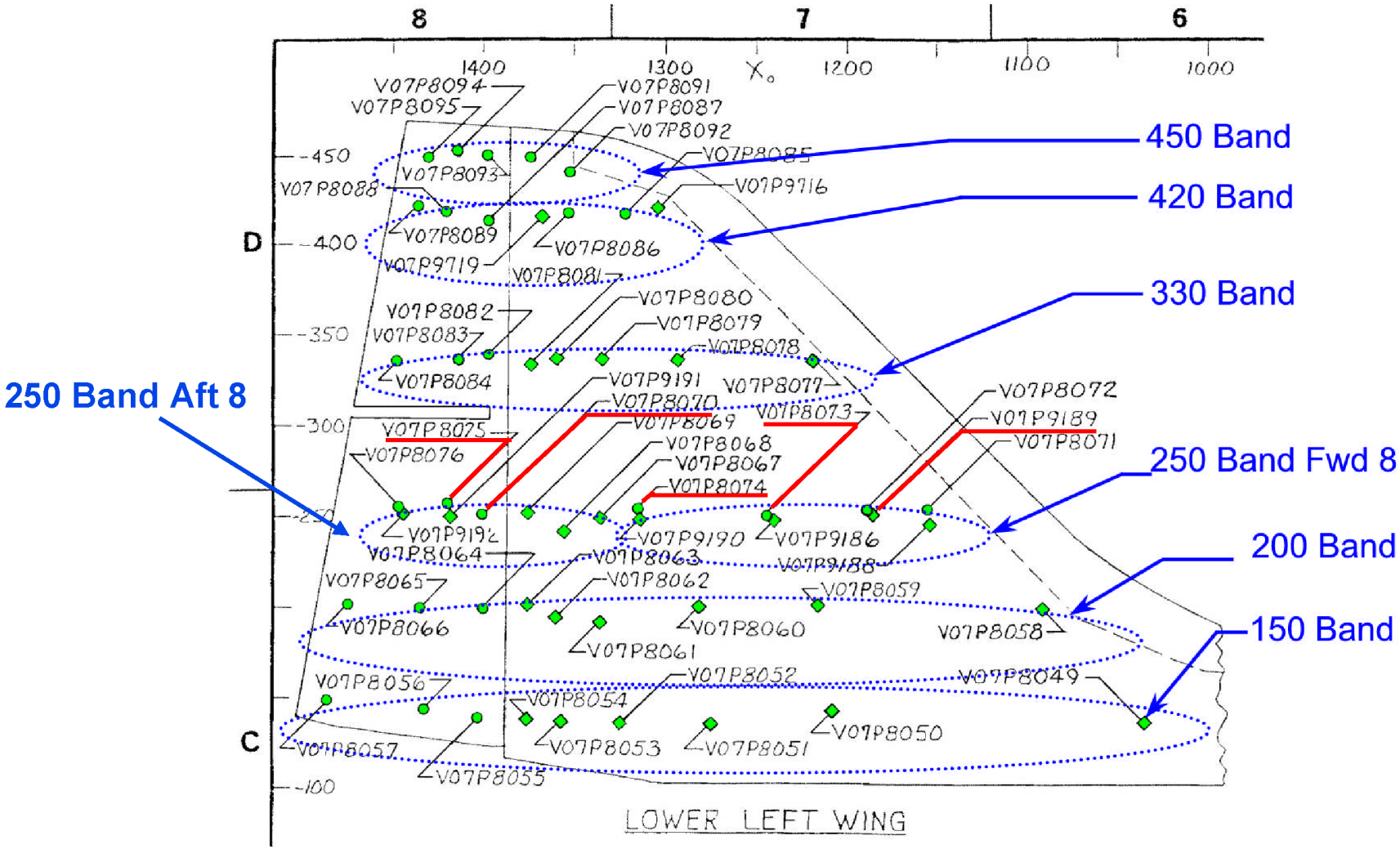

This material is PRELIMINARY information only. It is for limited distribution. DO NOT FORWARD.

Upper Left Wing Y-Station Taps

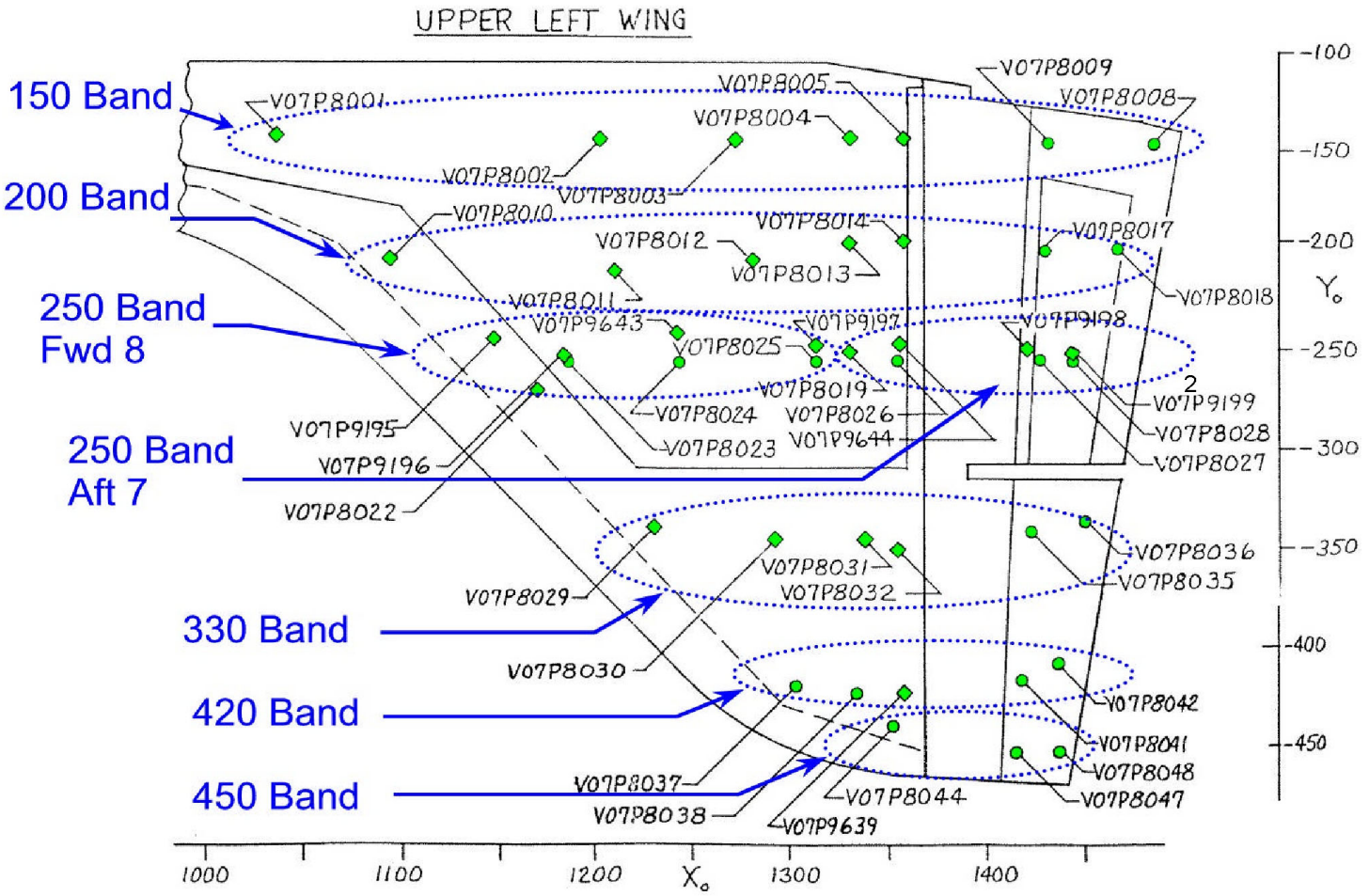

STS-107 MADS Pressure Data Ascent

This material is PRELIMINARY information only. It is for limited distribution. DO NOT FORWARD.

Lower Left Wing Y=200 Taps

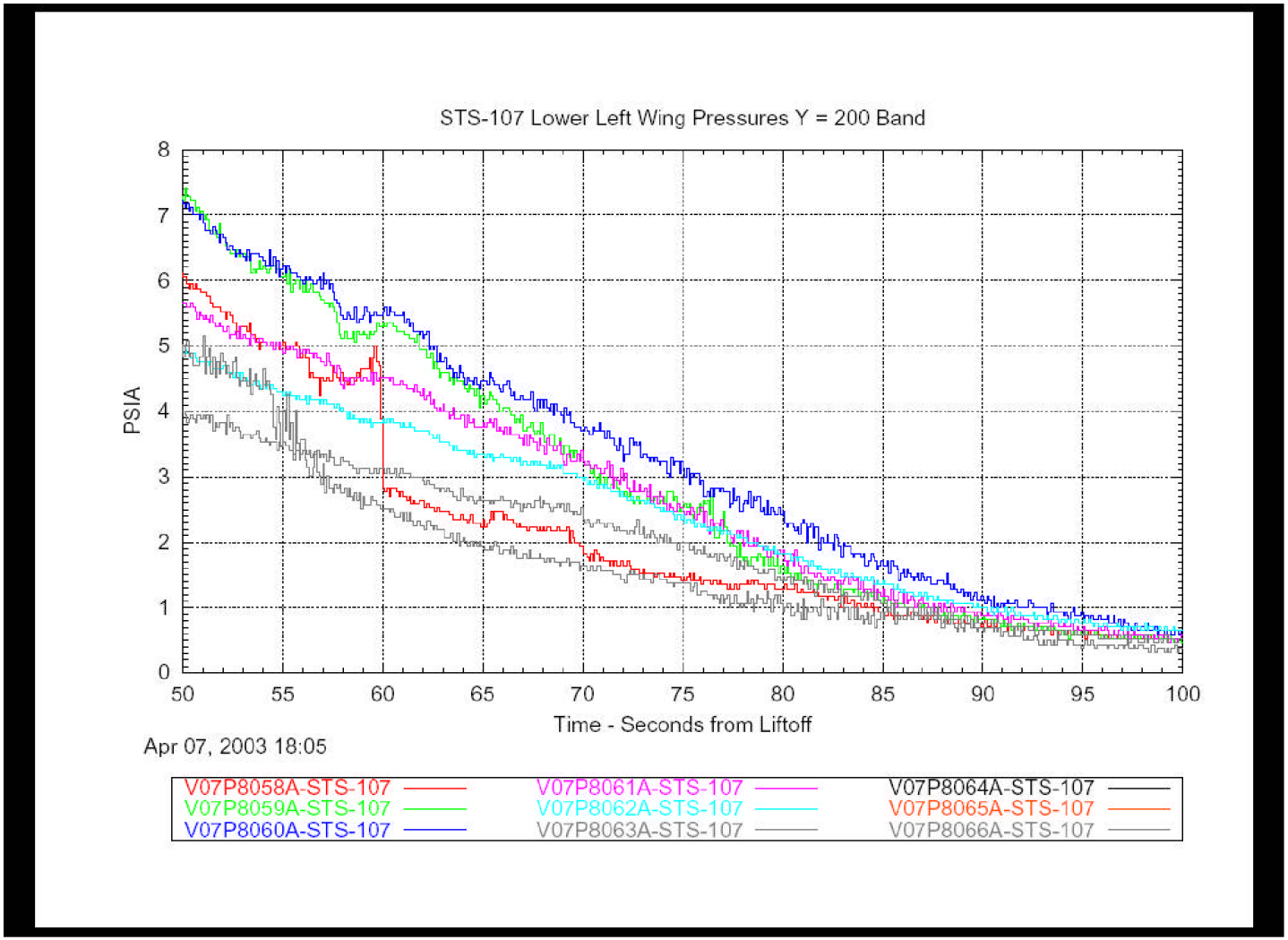

This material is PRELIMINARY information only. It is for limited distribution. DO NOT FORWARD.

Lower Left Wing Y=250 Taps (Fwd 8)

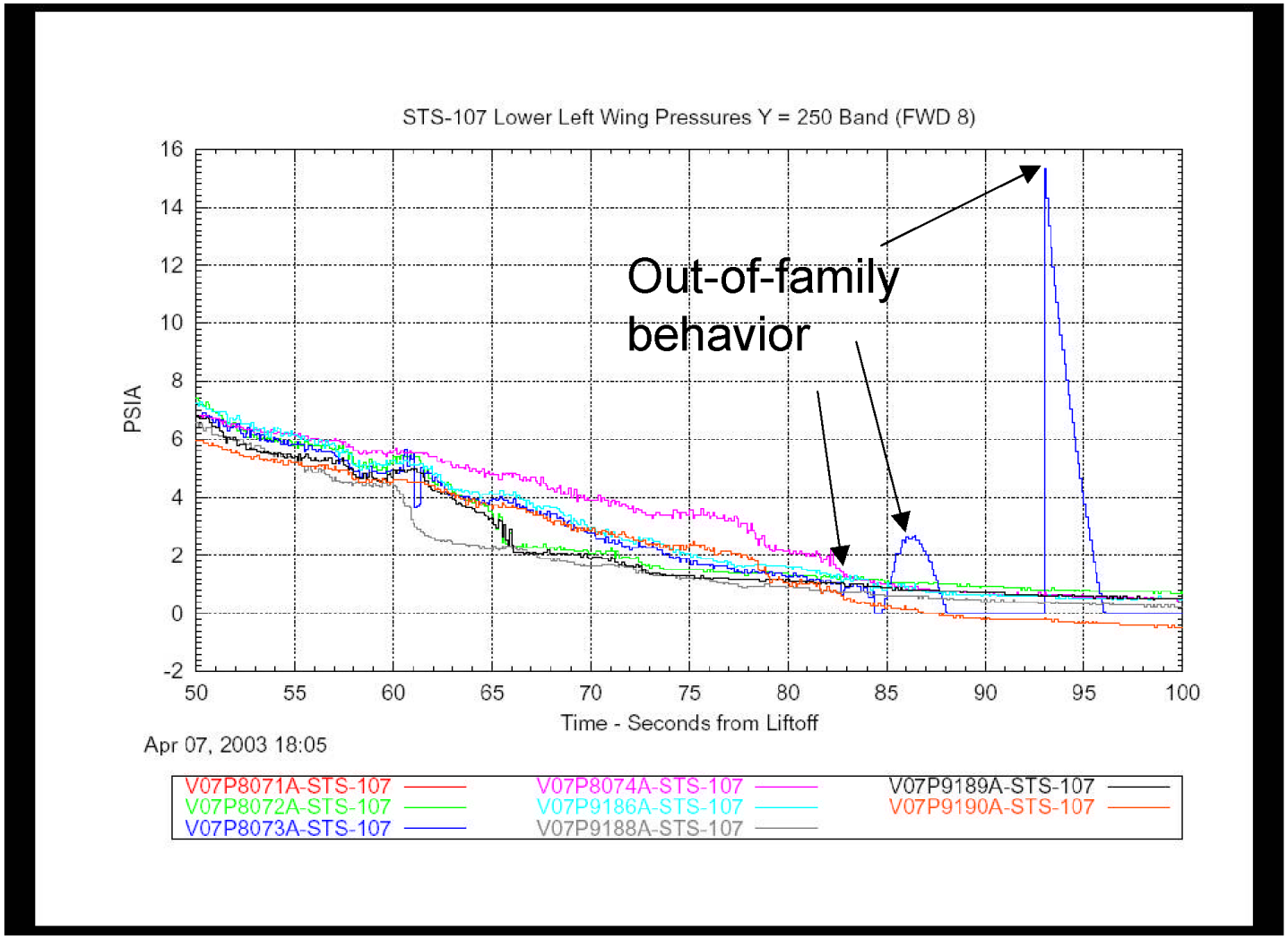

This material is PRELIMINARY information only. It is for limited distribution. DO NOT FORWARD.

Lower Left Wing Y=250 Tap V07P8074A (Fwd 8)

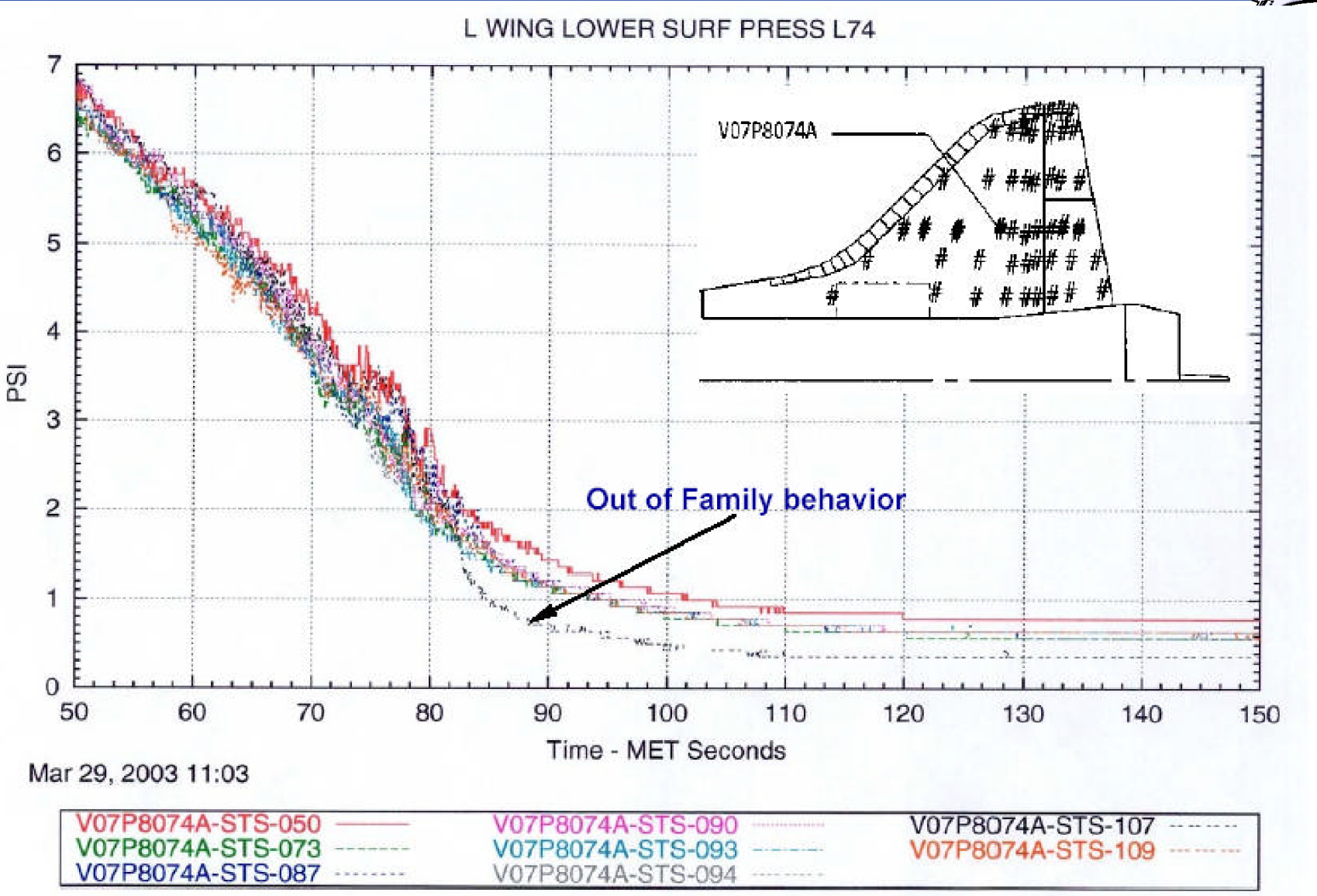

This material is PRELIMINARY information only. It is for limited distribution. DO NOT FORWARD.

Lower Left Wing Y=250 Taps (Aft 8)

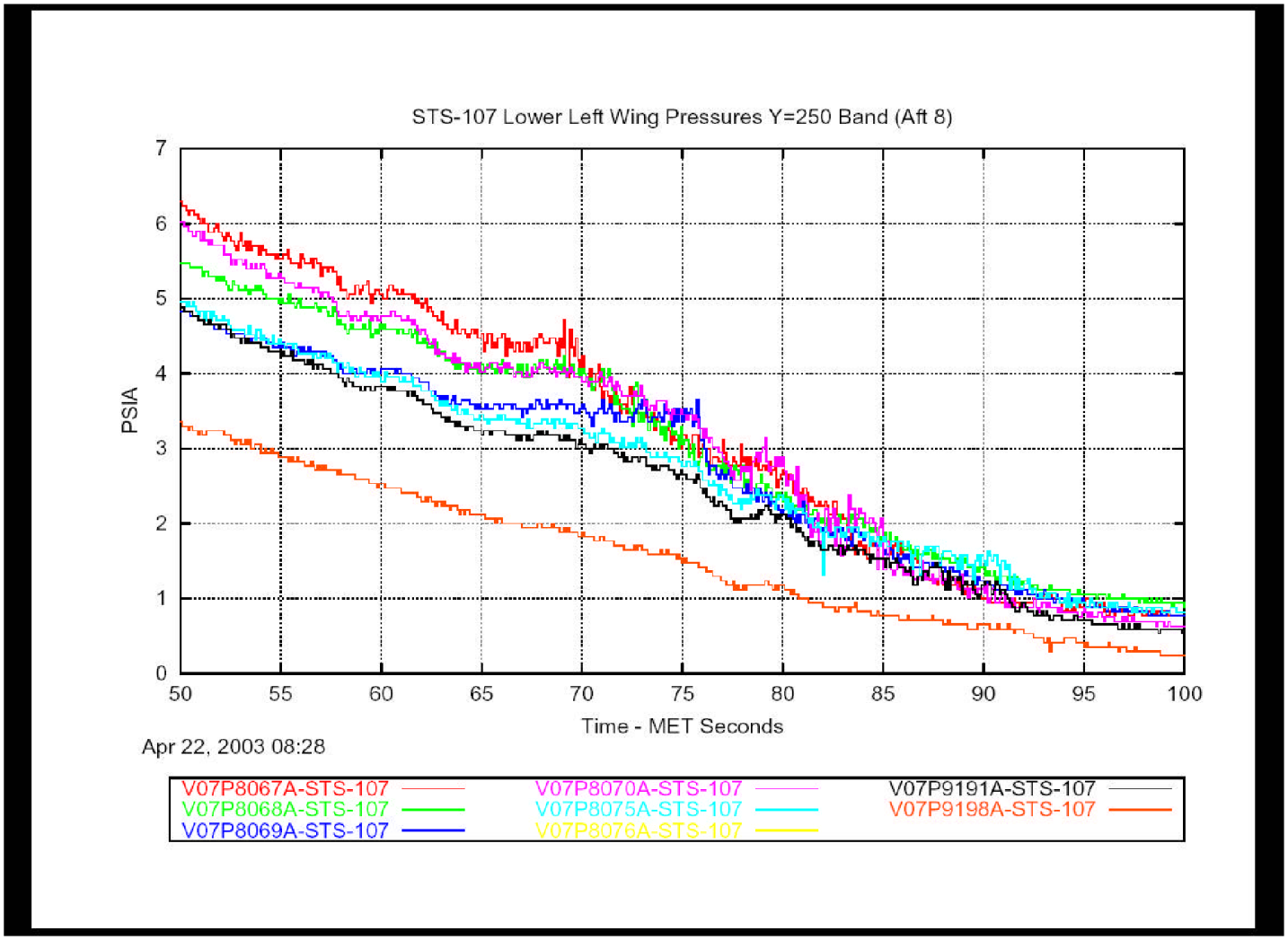

This material is PRELIMINARY information only. It is for limited distribution. DO NOT FORWARD.

Three Lower Left Wing Y=250 Taps Have Similar Behavior at 102 Seconds

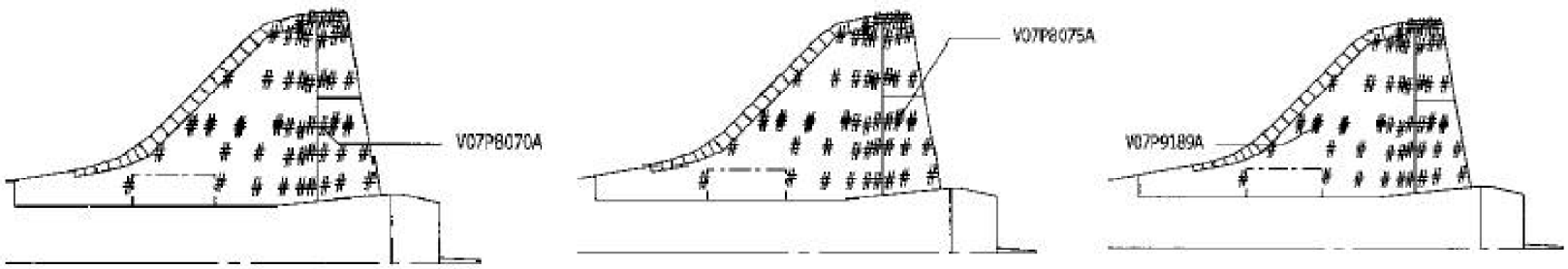

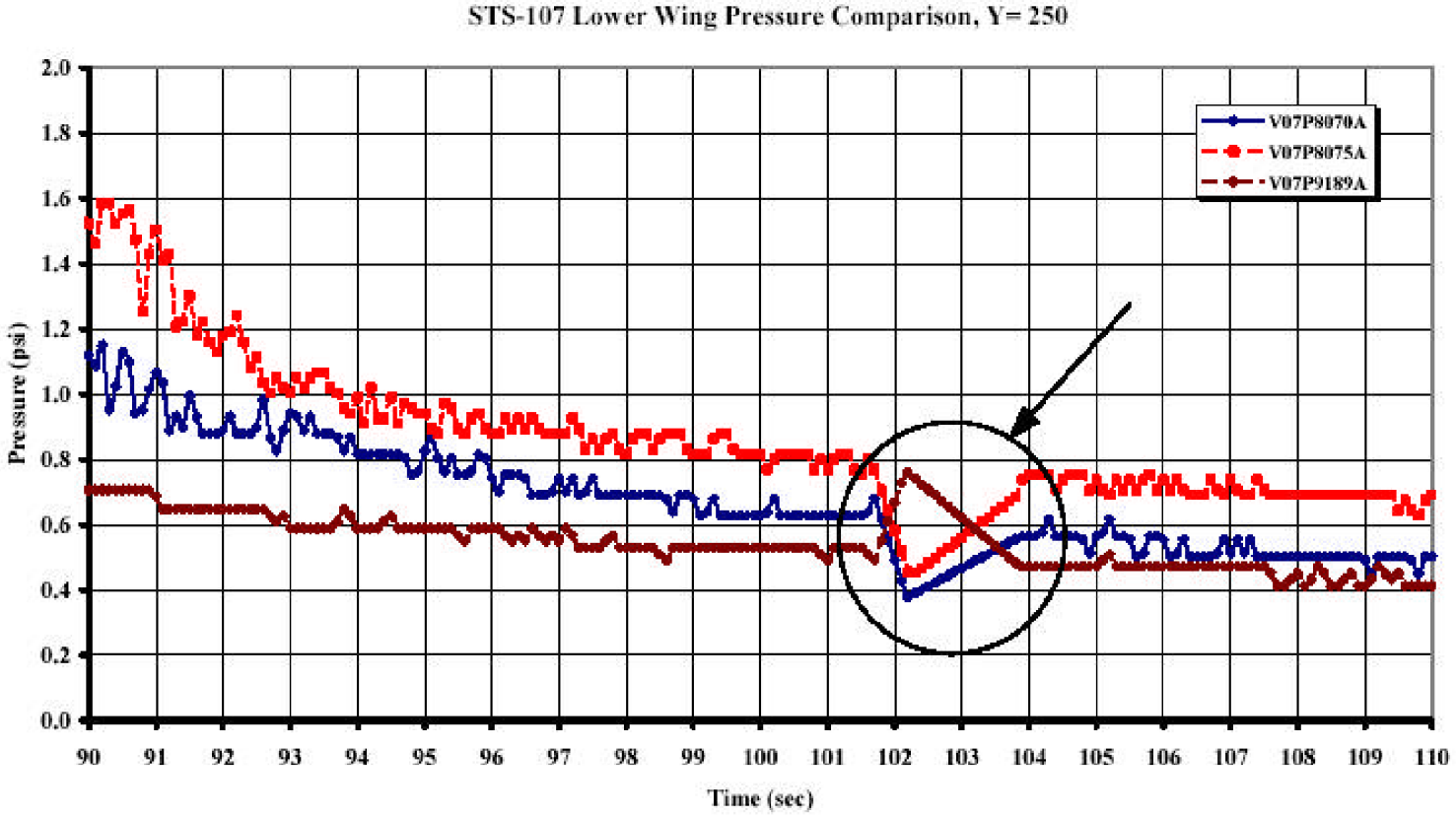

This material is PRELIMINARY information only. It is for limited distribution. DO NOT FORWARD.

Back-up Data

This material is PRELIMINARY information only. It is for limited distribution. DO NOT FORWARD.

Back-up Data, Temperature

This material is PRELIMINARY information only. It is for limited distribution. DO NOT FORWARD.

Comparison Left Side Surface - Entry

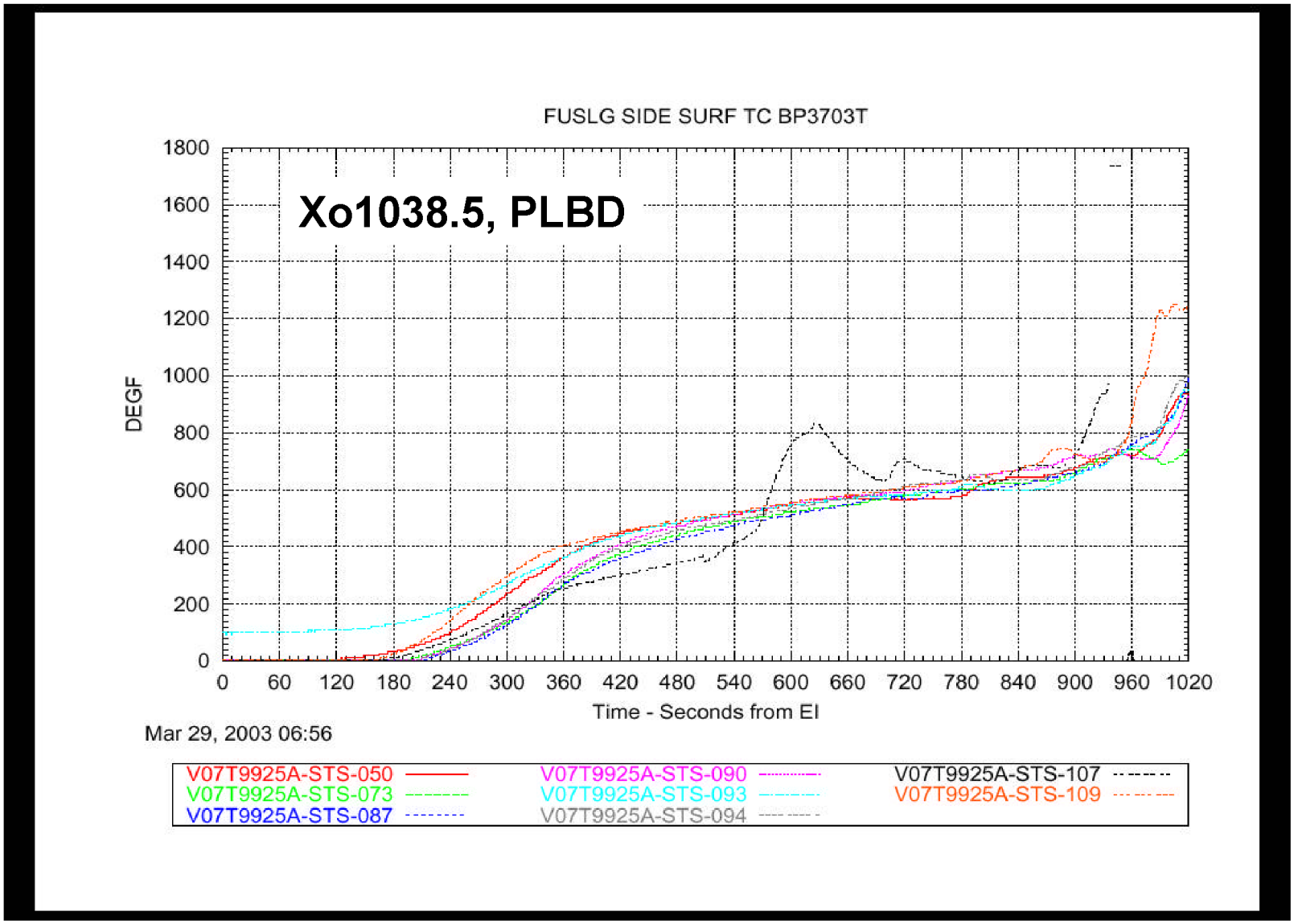

This material is PRELIMINARY information only. It is for limited distribution. DO NOT FORWARD.

Comparison Left Side Surface - Entry

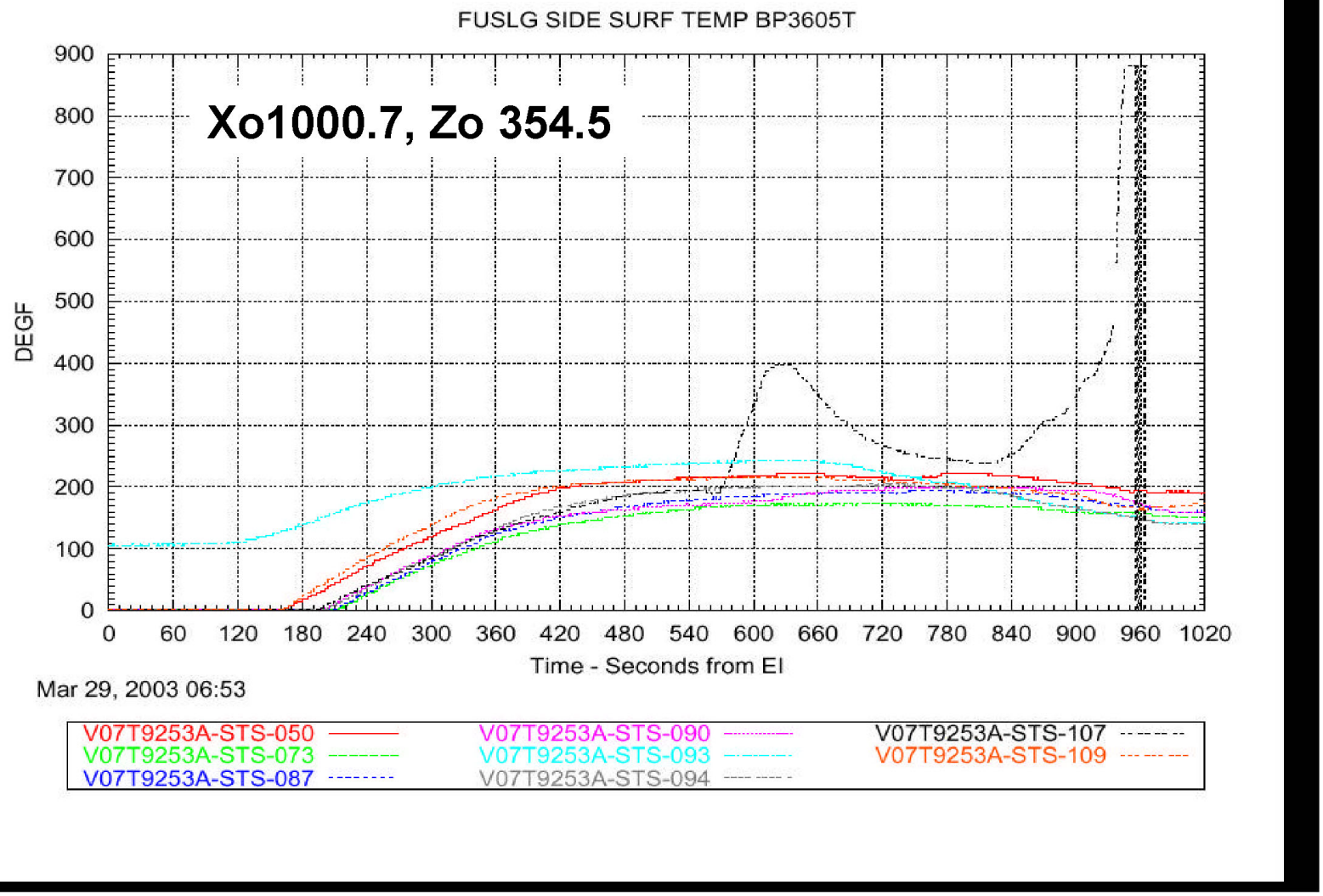

This material is PRELIMINARY information only. It is for limited distribution. DO NOT FORWARD.

Comparison Left Pod Surface Temp Response

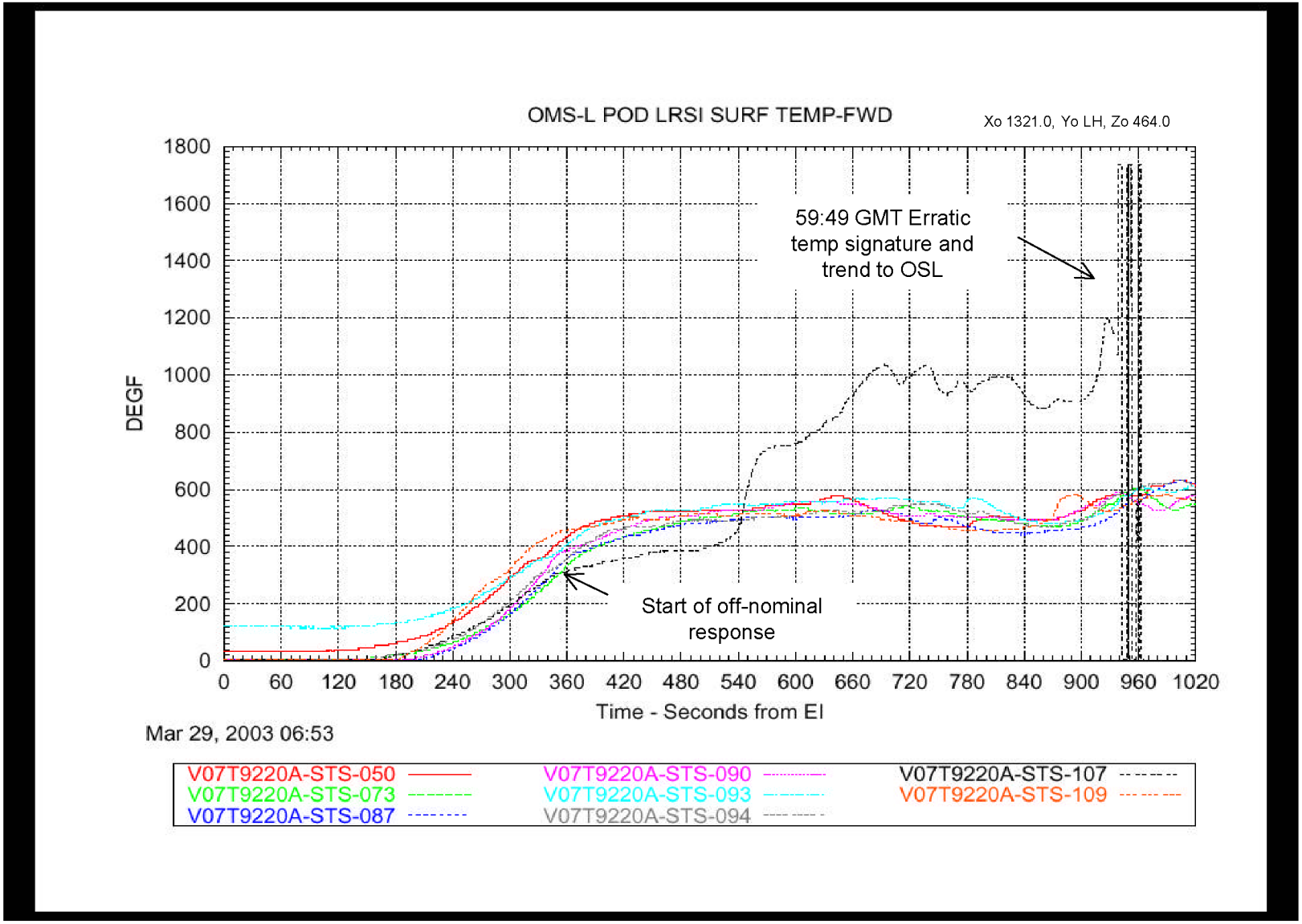

Back-up Data, Pressure

This material is PRELIMINARY information only. It is for limited distribution. DO NOT FORWARD.

Lower Left Wing Y=150 Taps

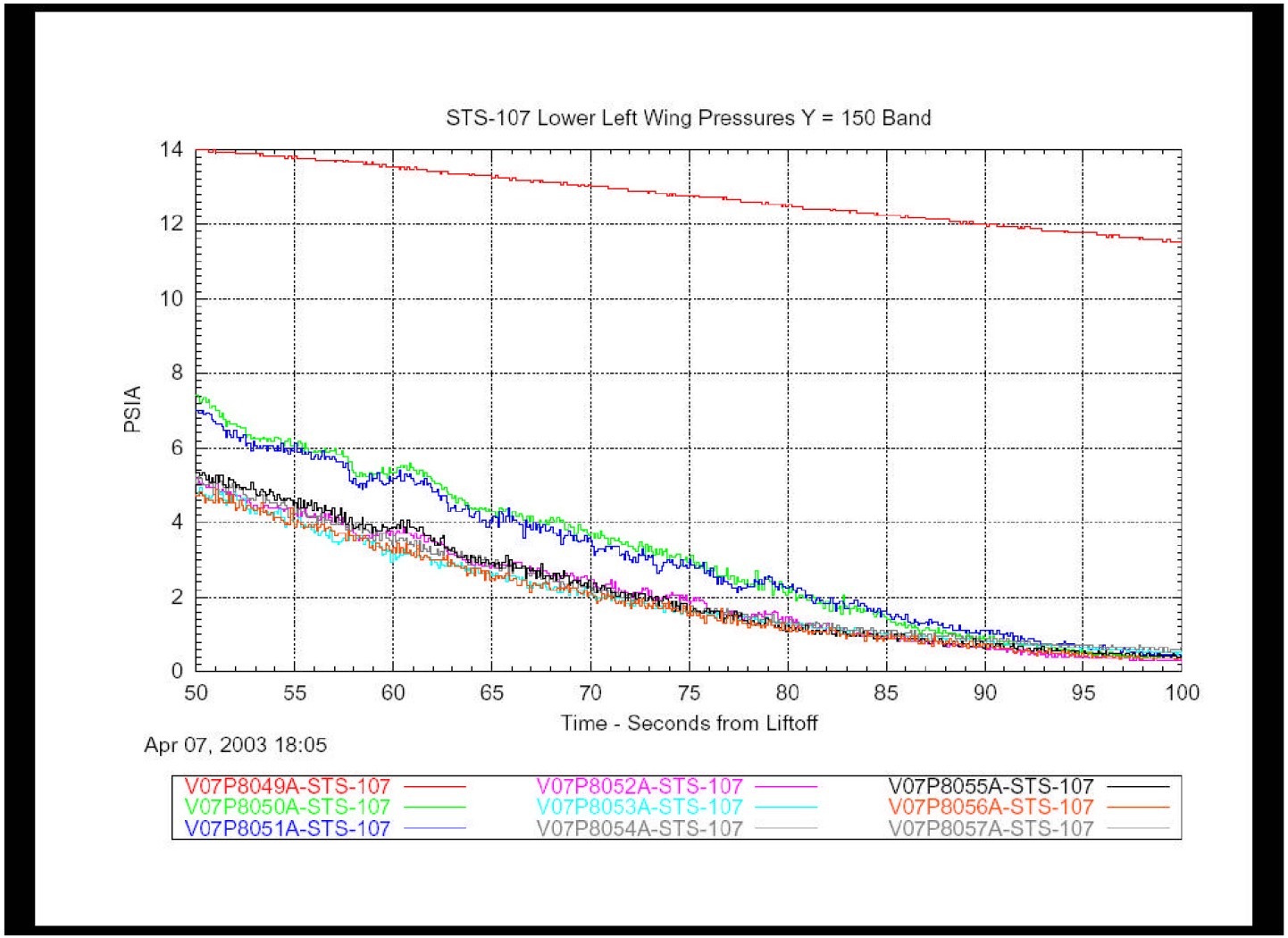

This material is PRELIMINARY information only. It is for limited distribution. DO NOT FORWARD.

Lower Left Wing Y=330 Taps

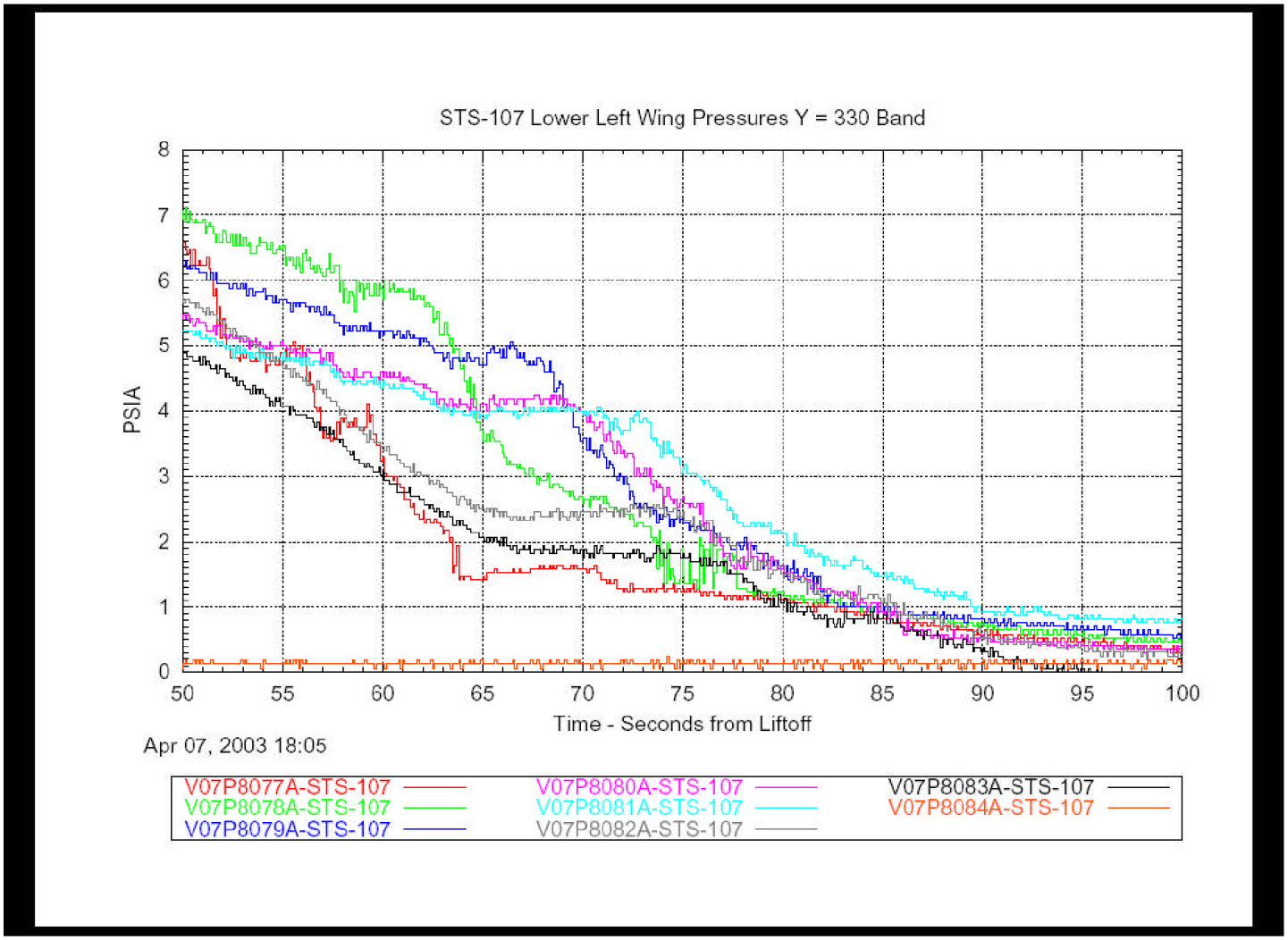

This material is PRELIMINARY information only. It is for limited distribution. DO NOT FORWARD.

Lower Left Wing Y=420 Taps

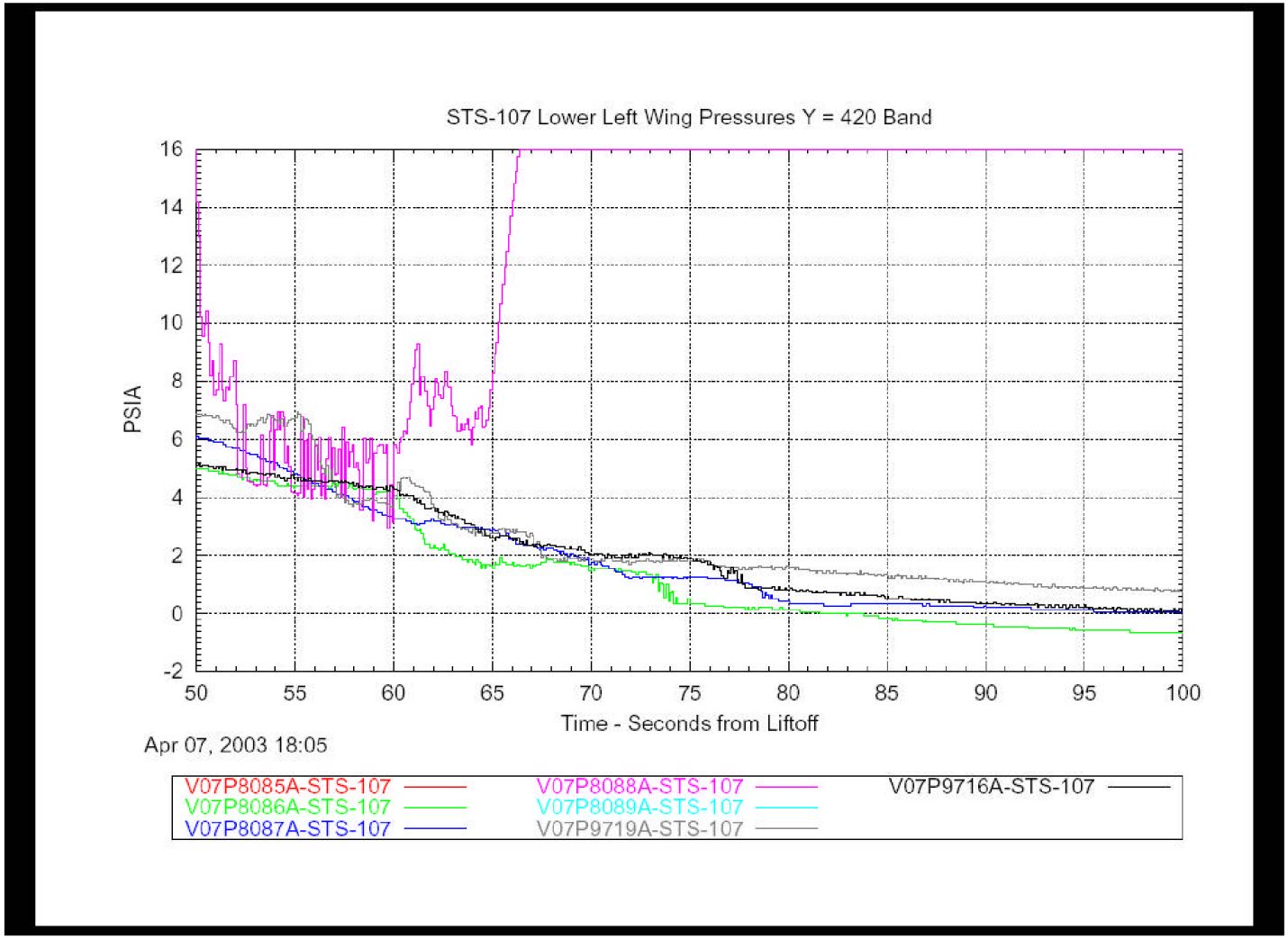

This material is PRELIMINARY information only. It is for limited distribution. DO NOT FORWARD.

Lower Left Wing Y=450 Taps

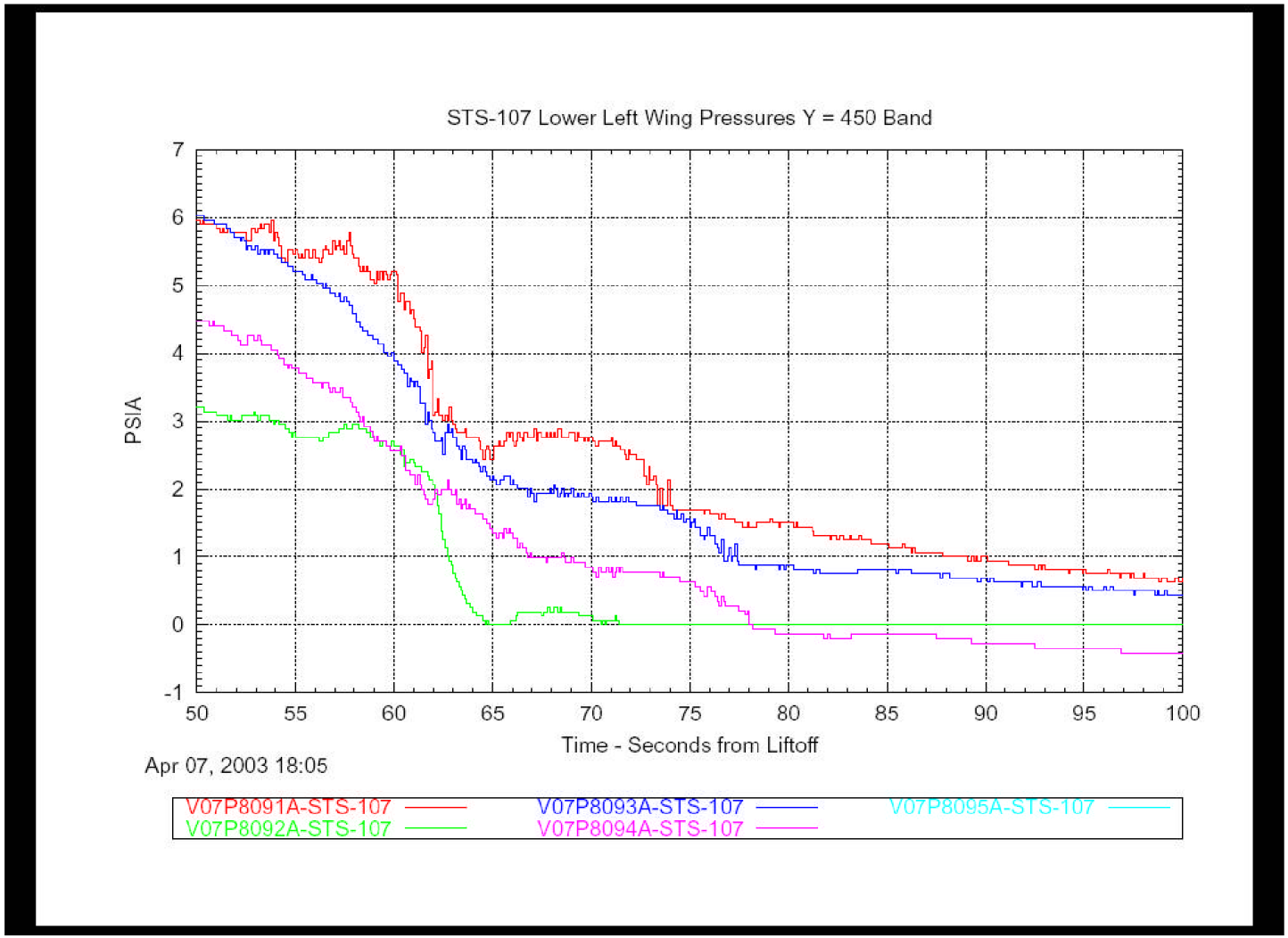

This material is PRELIMINARY information only. It is for limited distribution. DO NOT FORWARD.

Left Wing Leading Edge (Lower) Taps

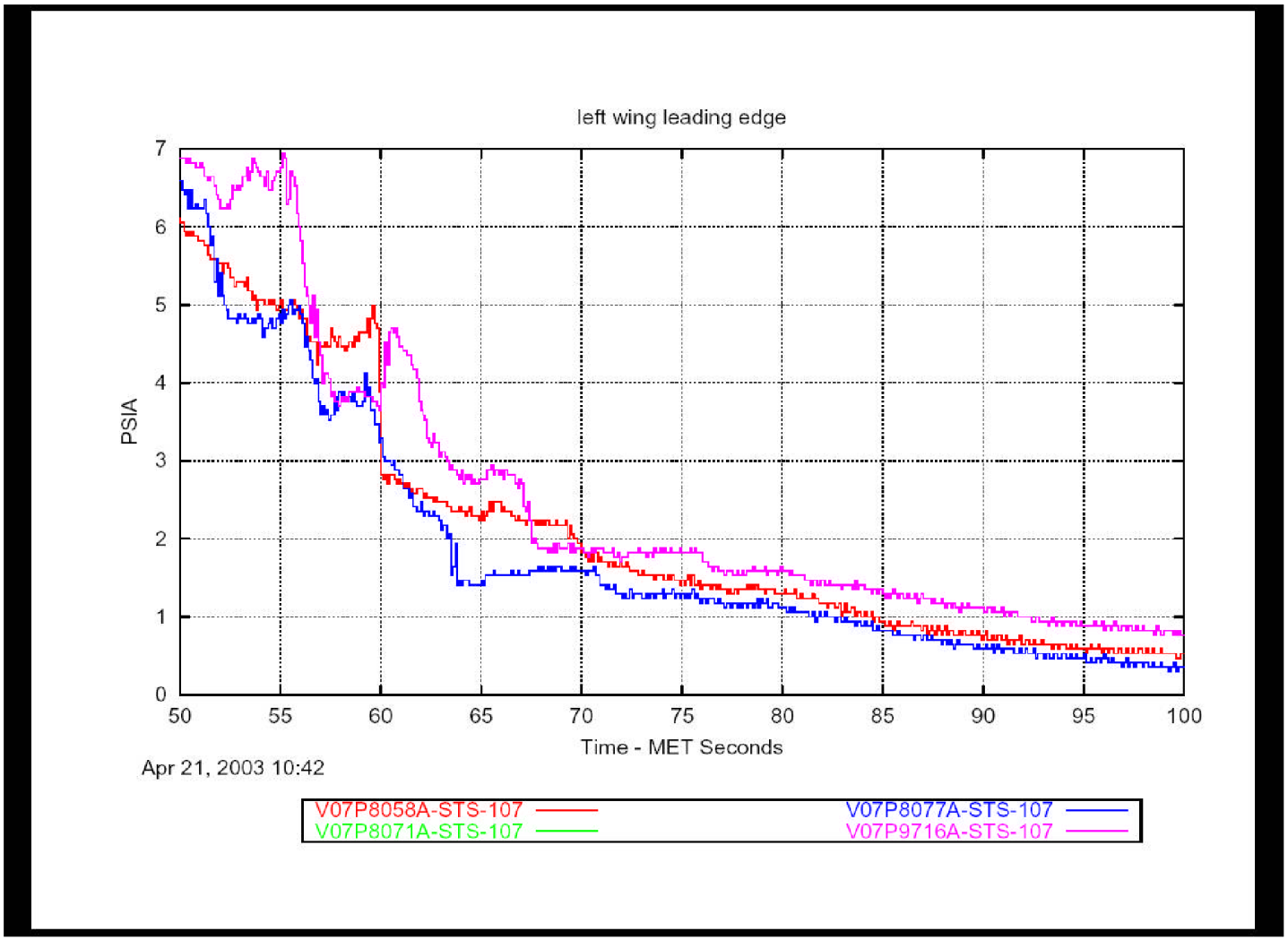

This material is PRELIMINARY information only. It is for limited distribution. DO NOT FORWARD.

Upper Left Wing Y=150 Taps

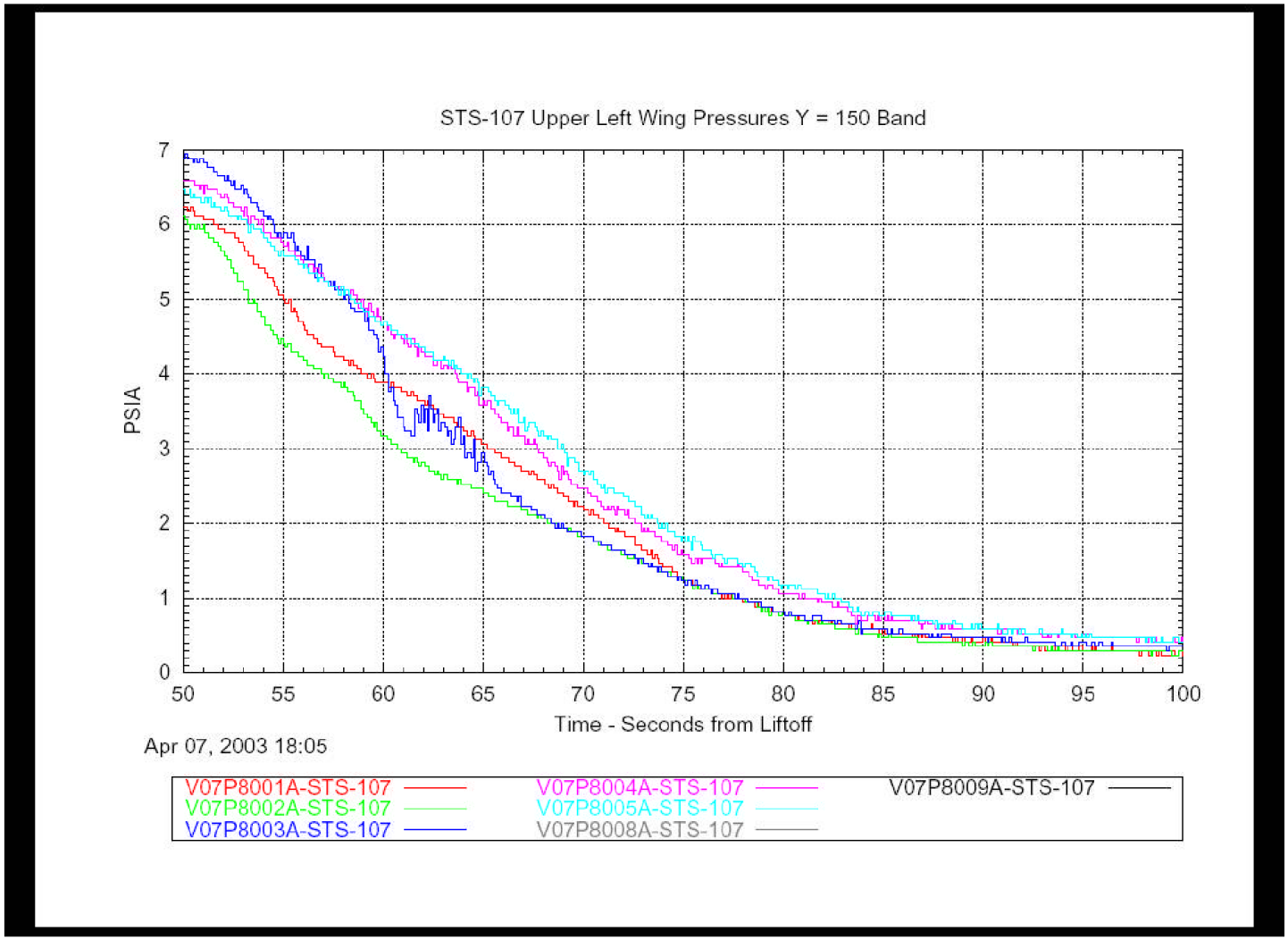

This material is PRELIMINARY information only. It is for limited distribution. DO NOT FORWARD.

Upper Left Wing Y=200 Taps

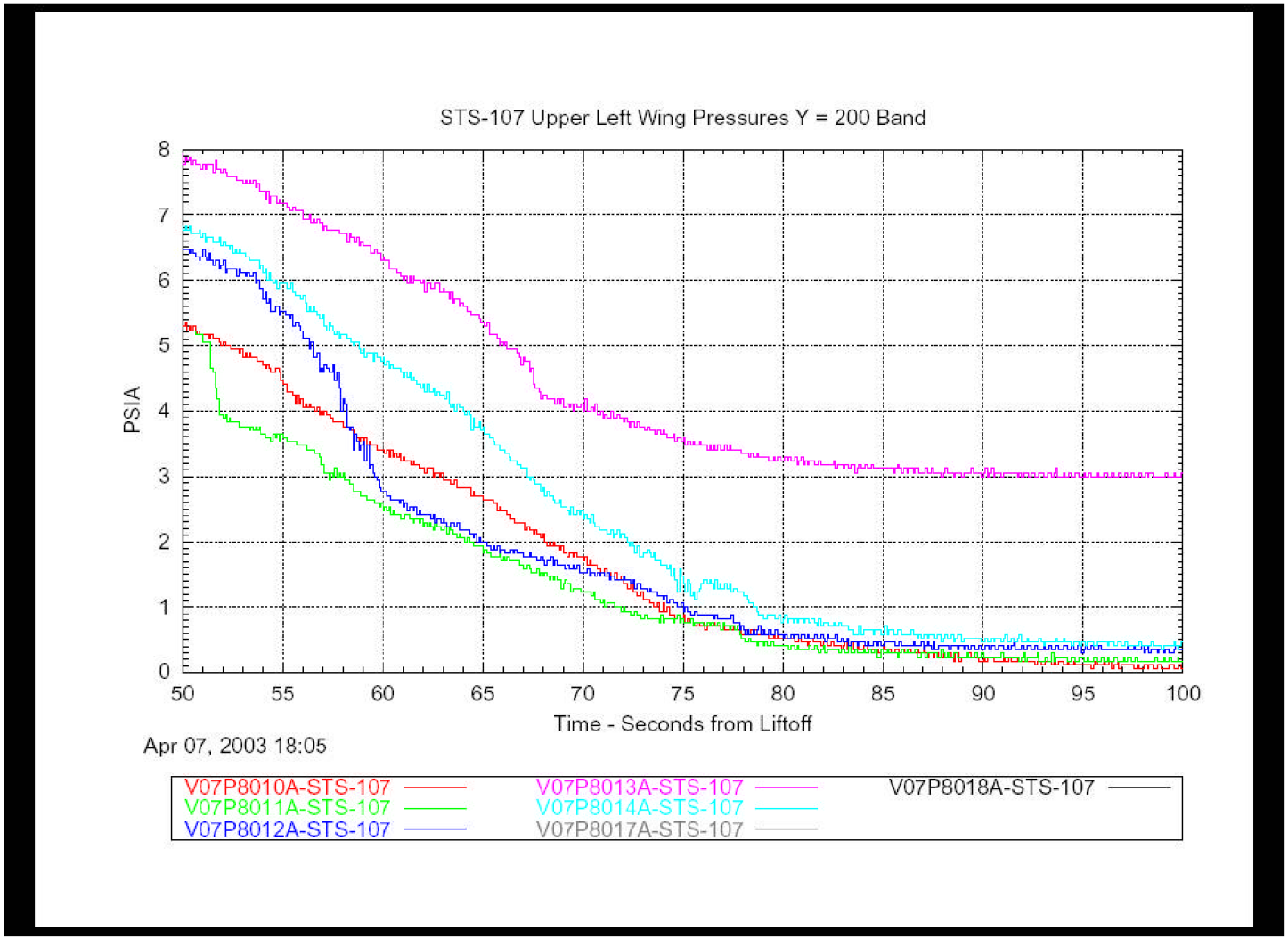

This material is PRELIMINARY information only. It is for limited distribution. DO NOT FORWARD.

Upper Left Wing Y=250 Taps (Fwd 8)

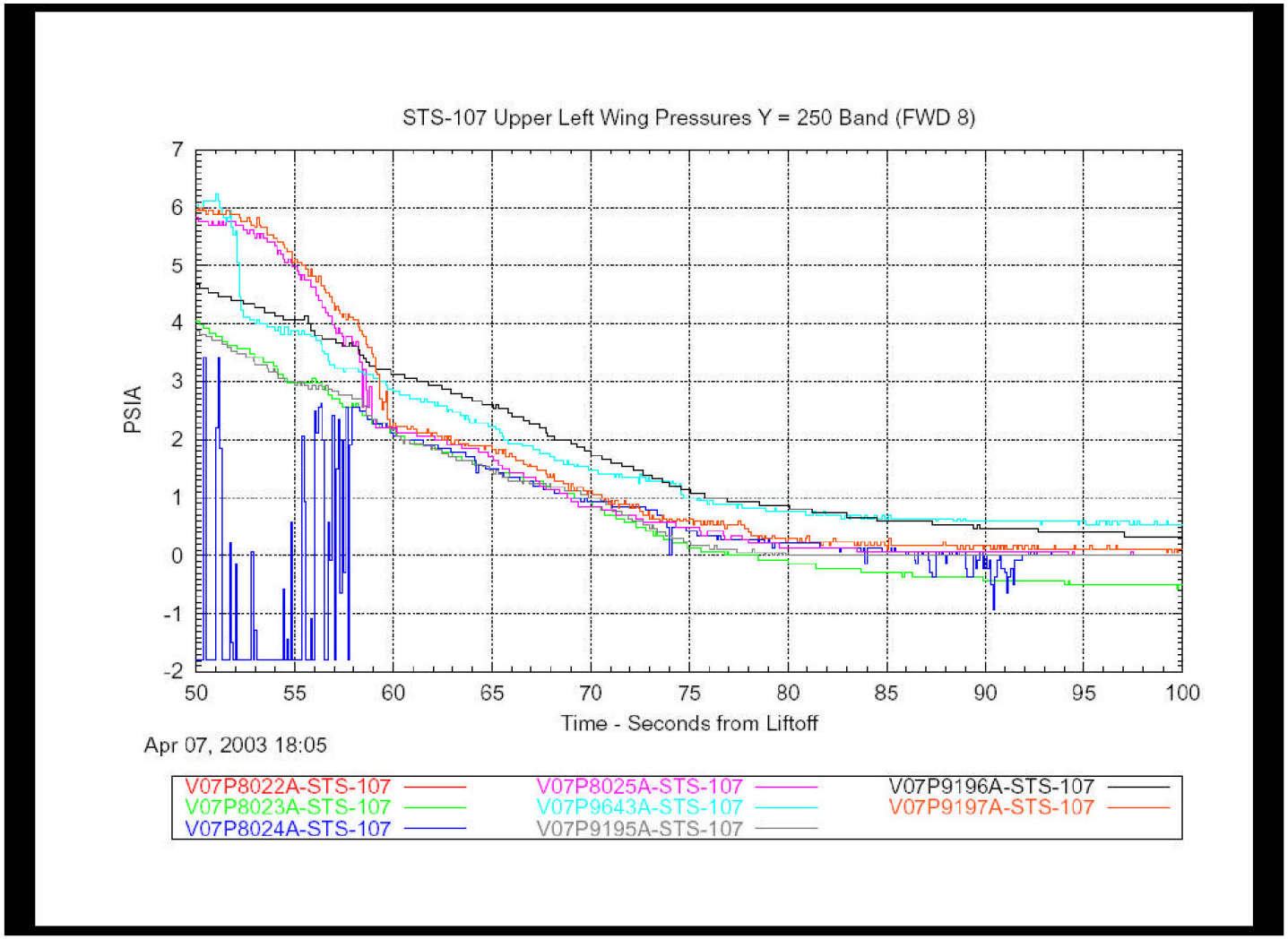

This material is PRELIMINARY information only. It is for limited distribution. DO NOT FORWARD.

Upper Left Wing Y=250 Taps (Aft 7)

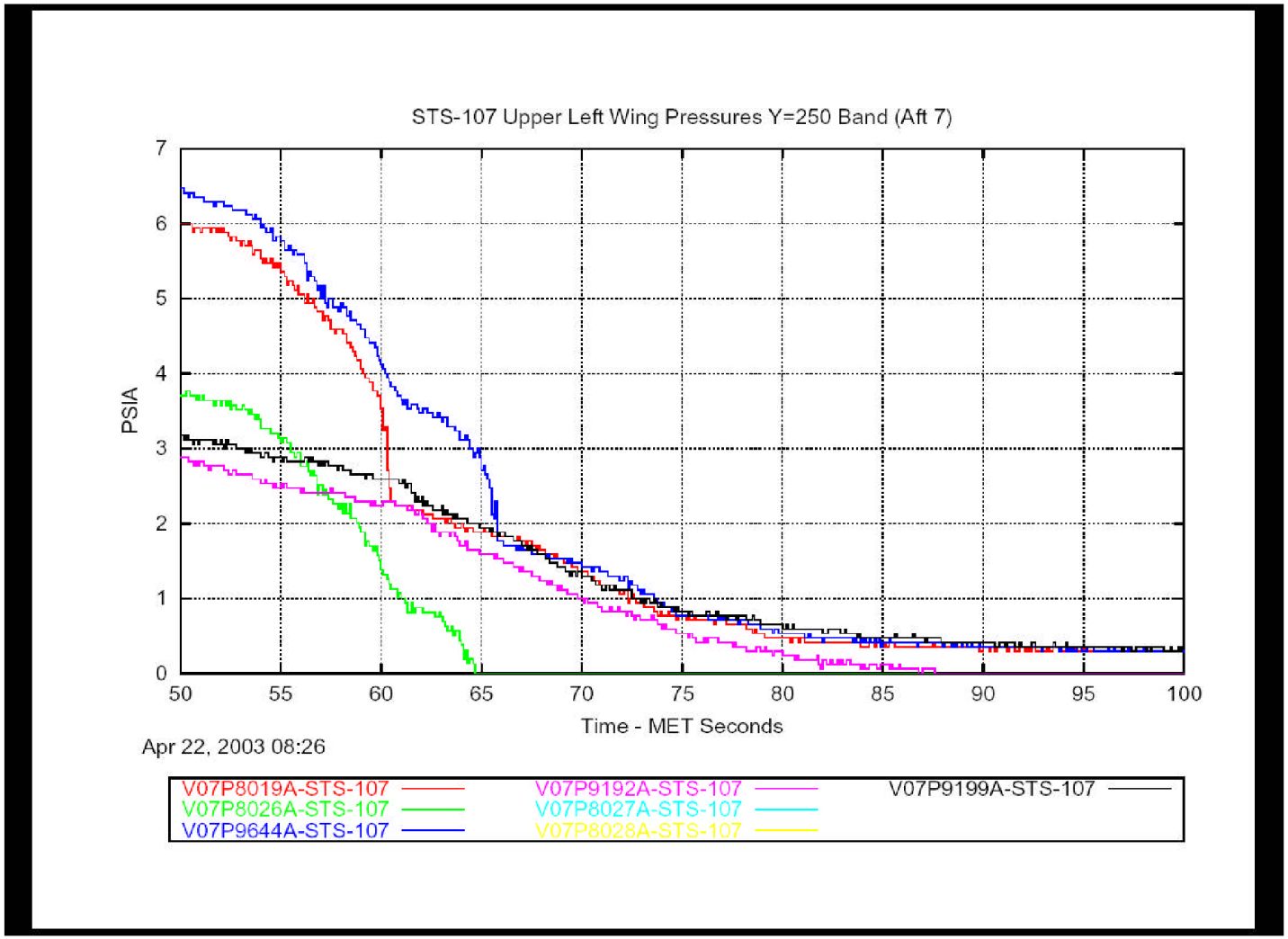

This material is PRELIMINARY information only. It is for limited distribution. DO NOT FORWARD.

Upper Left Wing Y=330 Taps

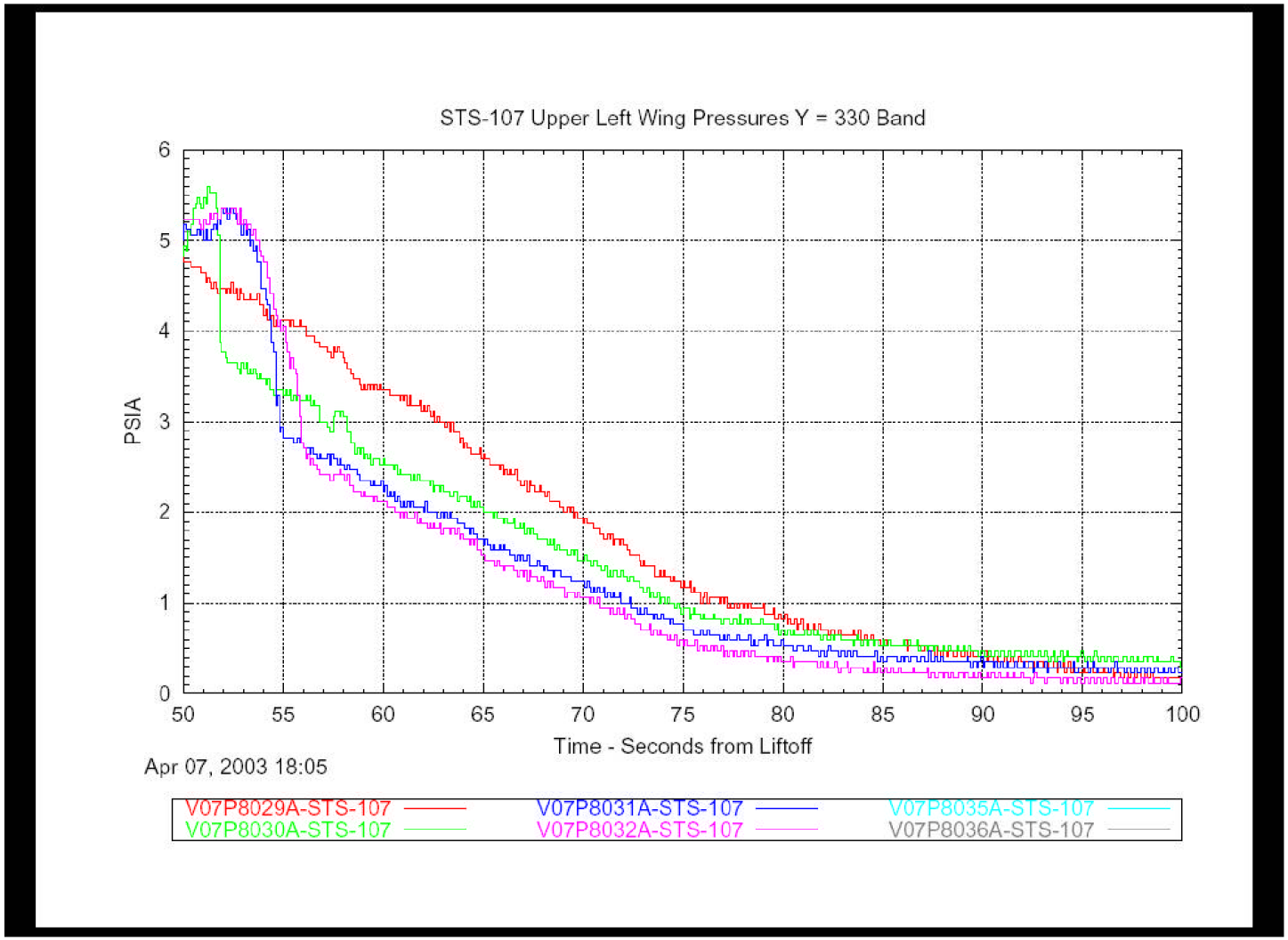

This material is PRELIMINARY information only. It is for limited distribution. DO NOT FORWARD.

Upper Left Wing Y=420 Taps

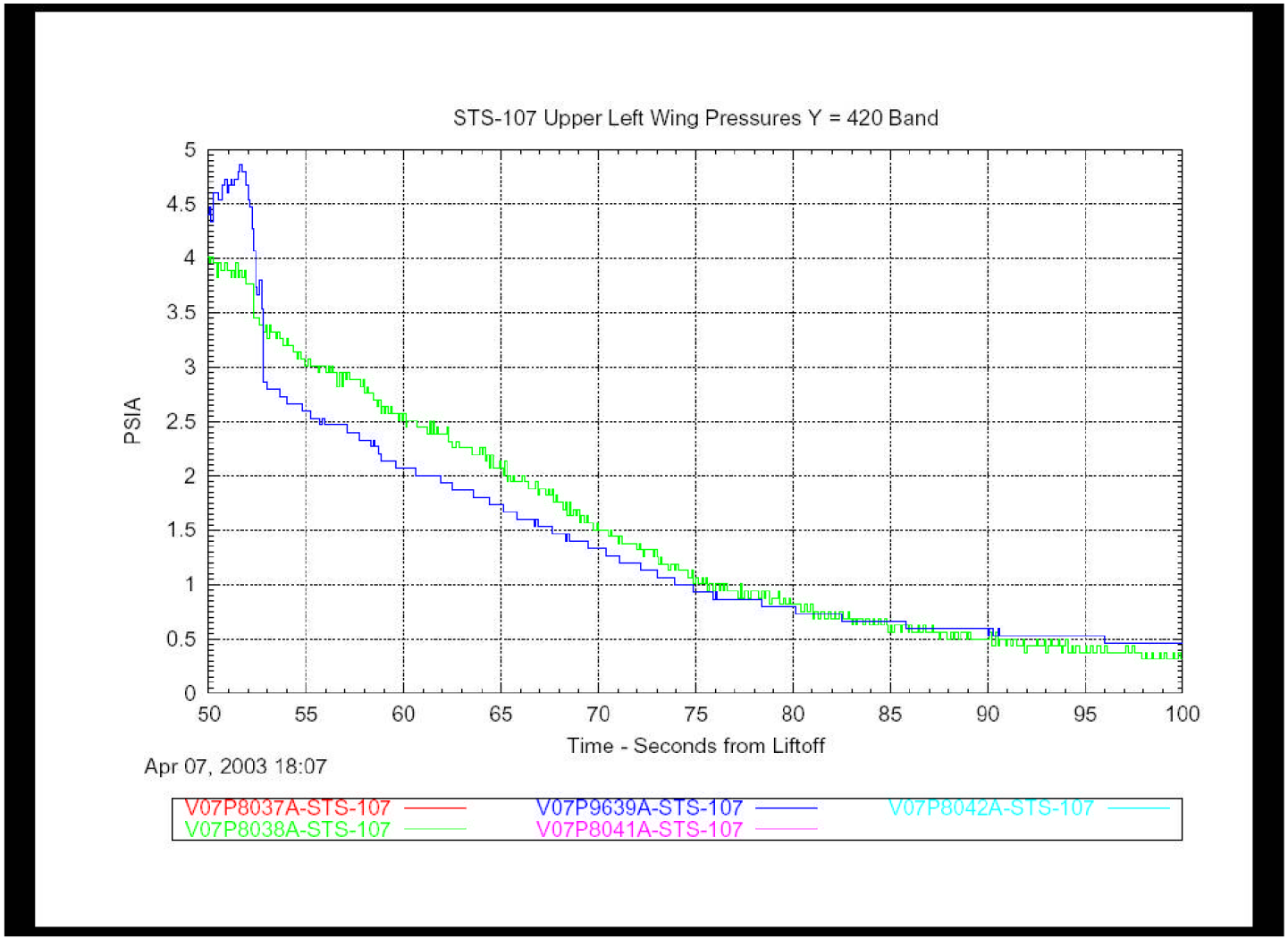

This material is PRELIMINARY information only. It is for limited distribution. DO NOT FORWARD.

Upper Left Wing Y=450 Taps

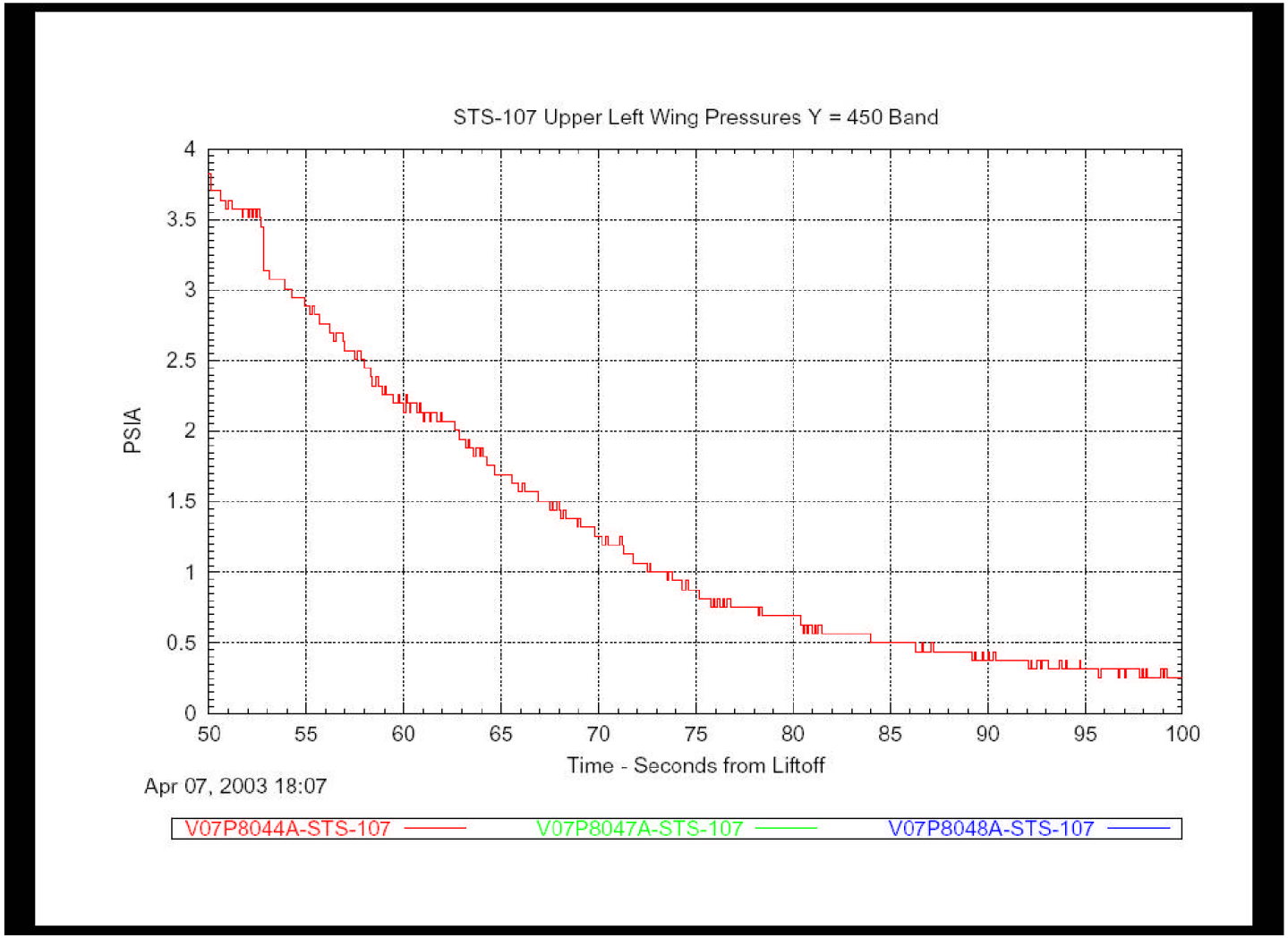

This material is PRELIMINARY information only. It is for limited distribution. DO NOT FORWARD.

Left Wing Leading Edge (Upper) Taps

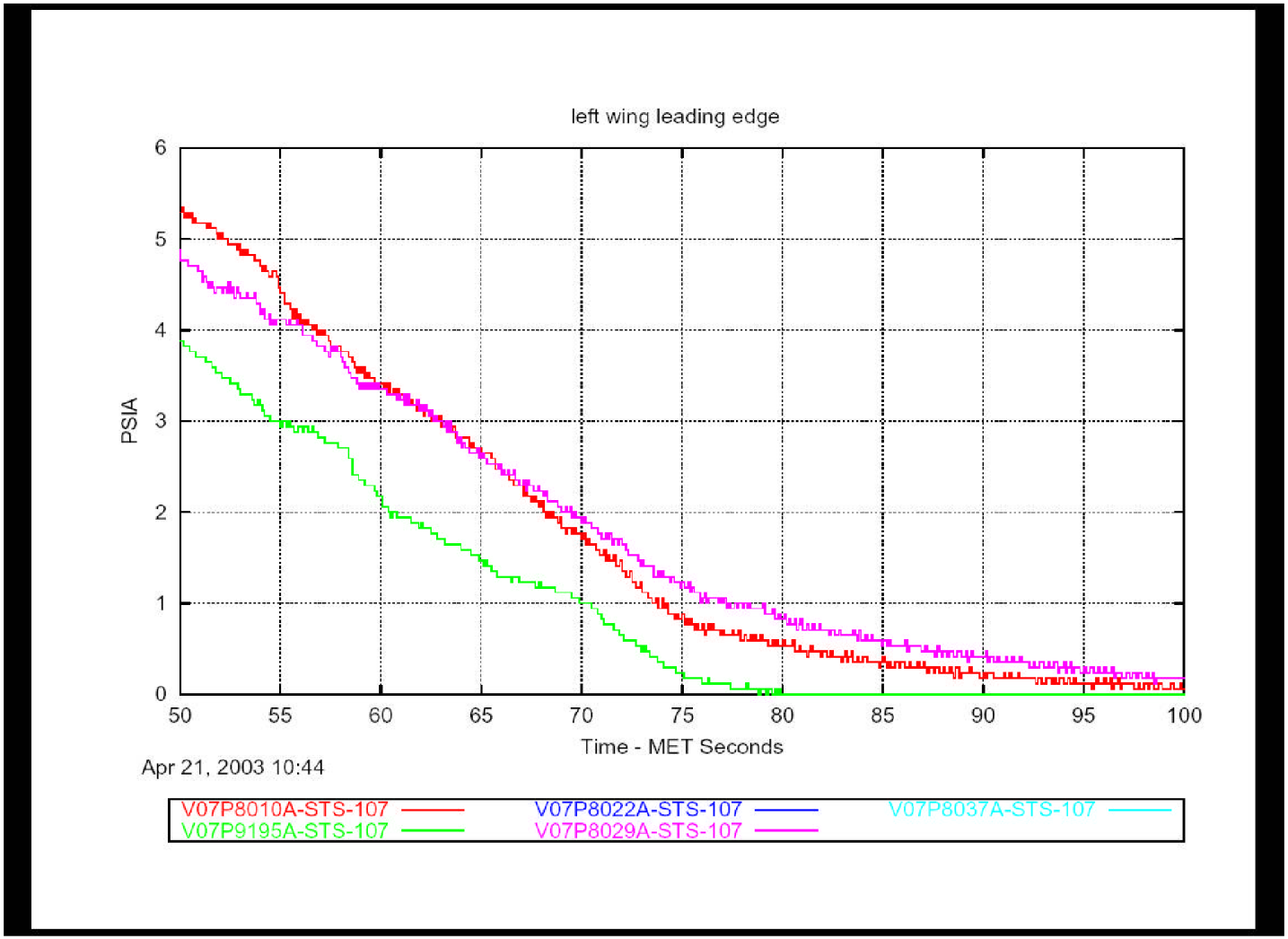

This material is PRELIMINARY information only. It is for limited distribution. DO NOT FORWARD.

Lower Left Wing Y=150 Taps (Fwd 4)

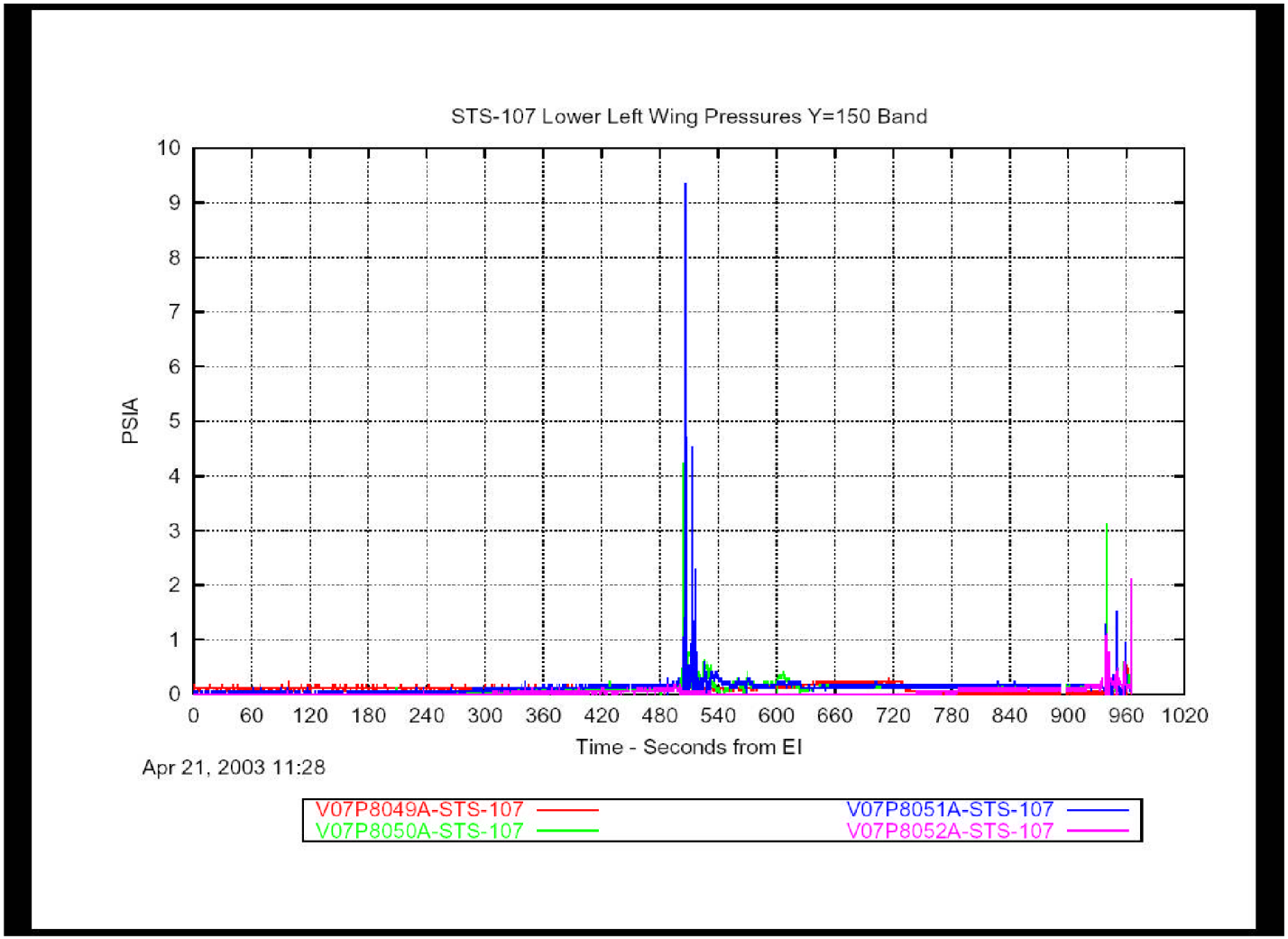

This material is PRELIMINARY information only. It is for limited distribution. DO NOT FORWARD.

Lower Left Wing Y=150 Taps (Aft 5)

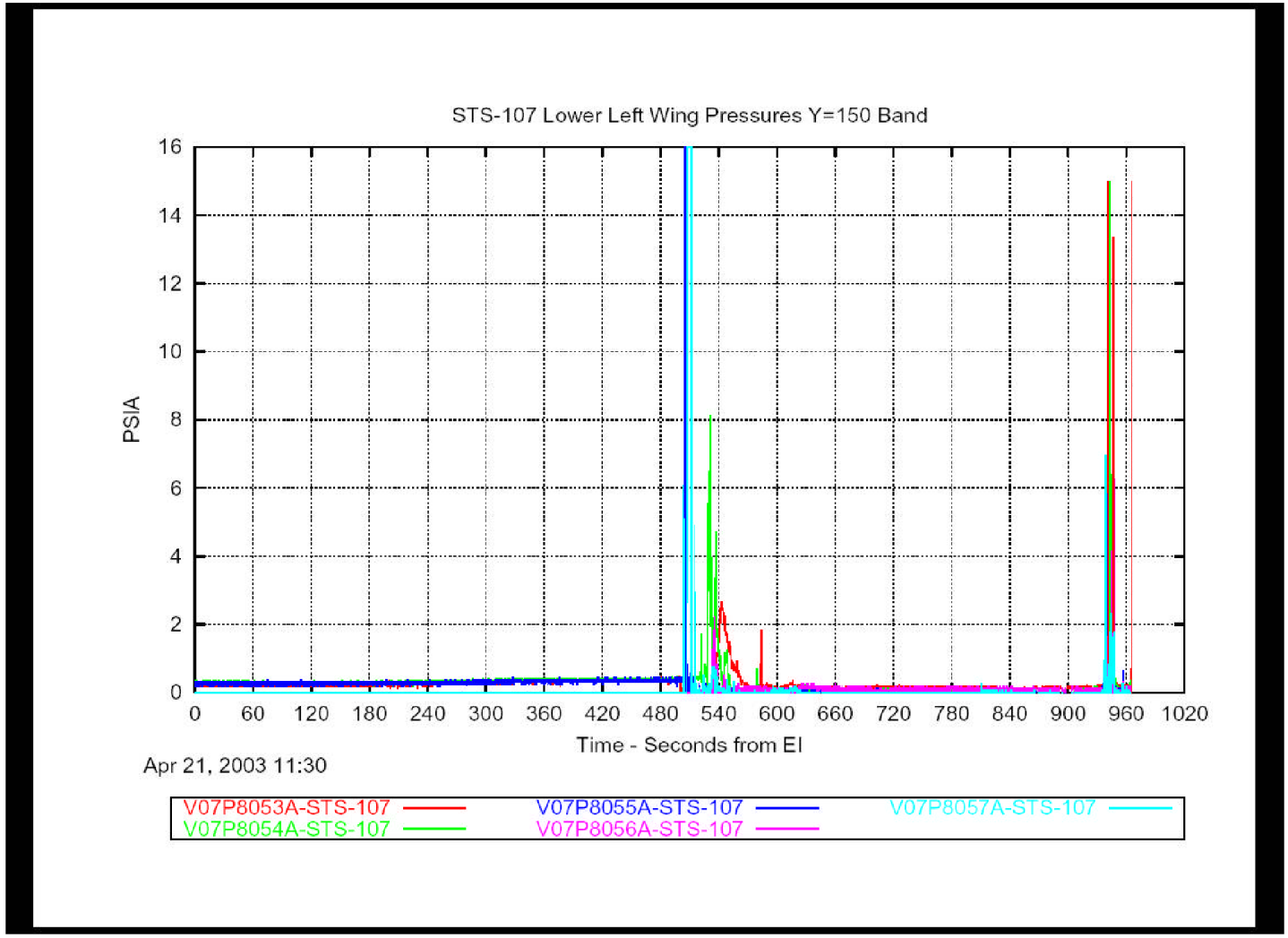

This material is PRELIMINARY information only. It is for limited distribution. DO NOT FORWARD.

Lower Left Wing Y=200 Taps (Fwd 4)

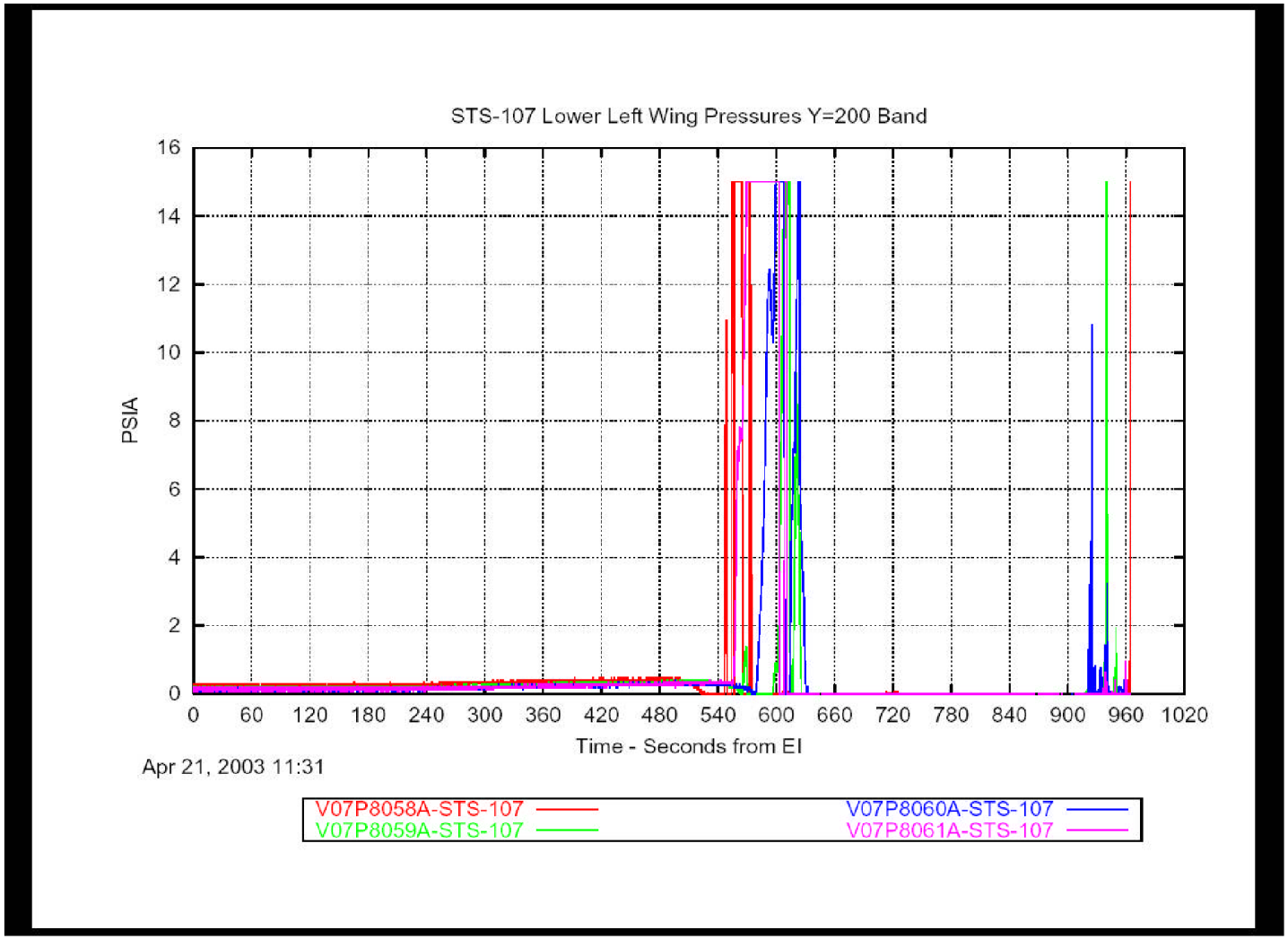

This material is PRELIMINARY information only. It is for limited distribution. DO NOT FORWARD.

Lower Left Wing Y=200 Taps (Aft 5)

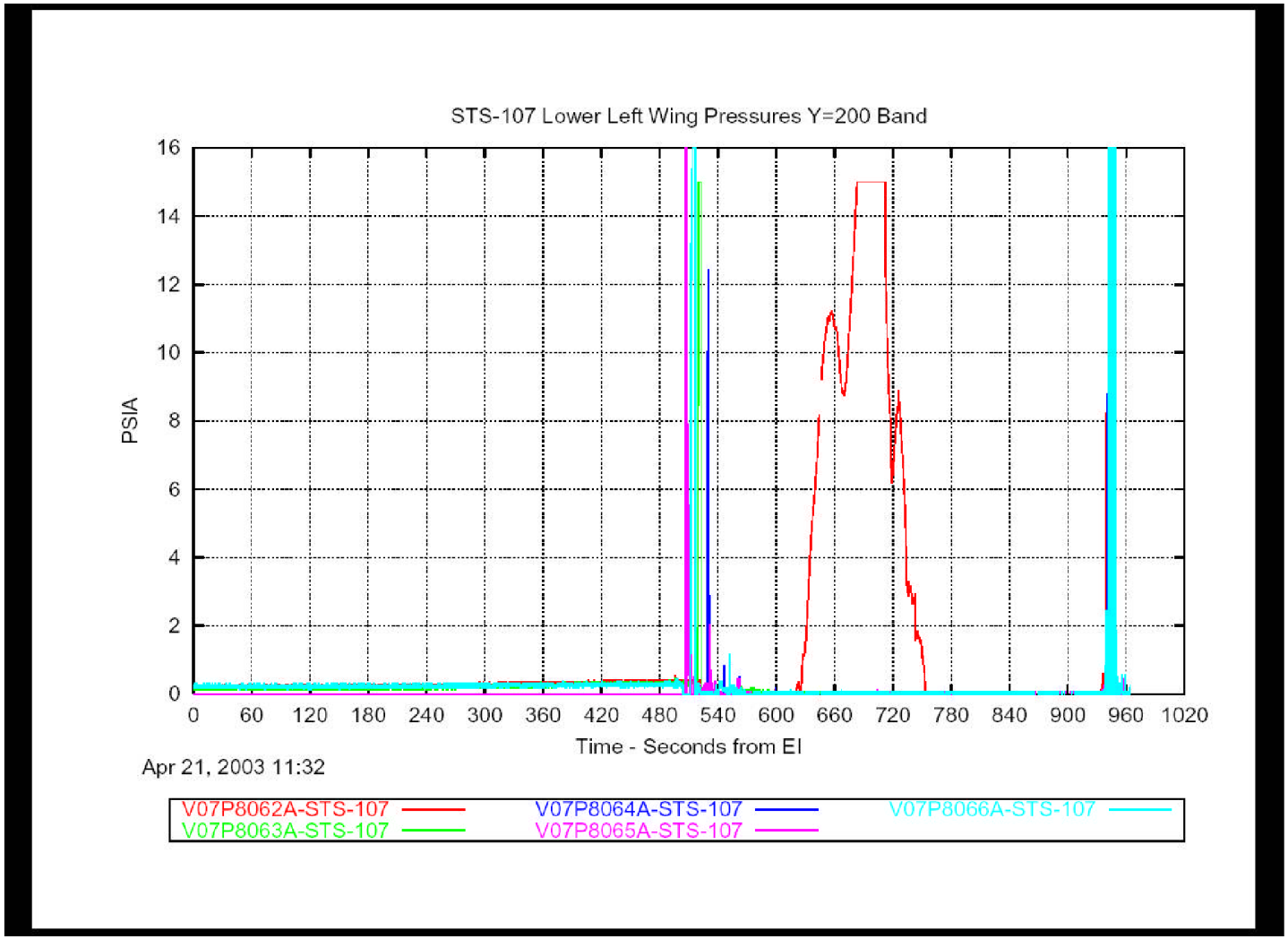

This material is PRELIMINARY information only. It is for limited distribution. DO NOT FORWARD.

Lower Left Wing Y=250 Taps (Fwd 8)

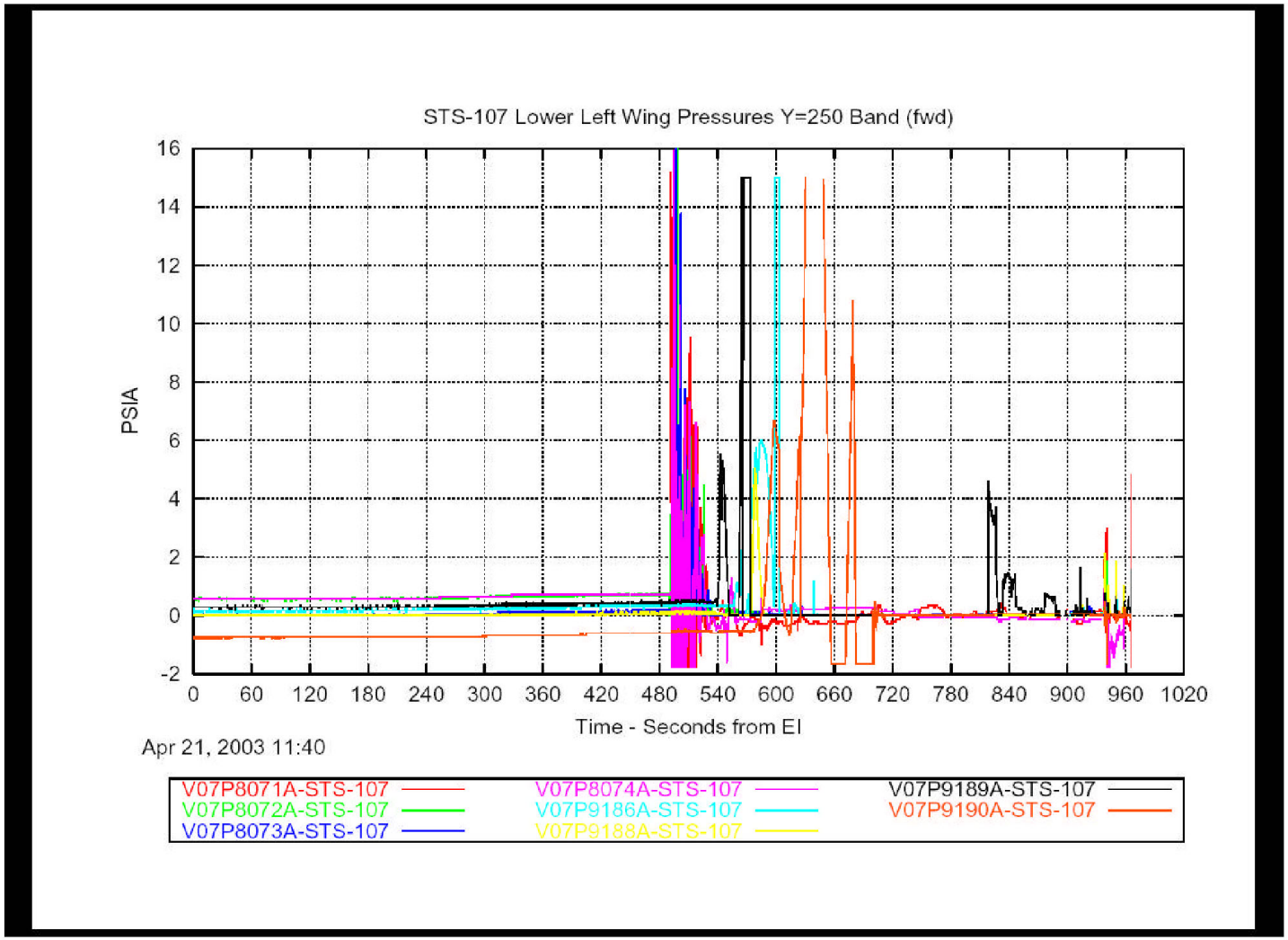

This material is PRELIMINARY information only. It is for limited distribution. DO NOT FORWARD.

Lower Left Wing Y=250 Taps (Aft 8)

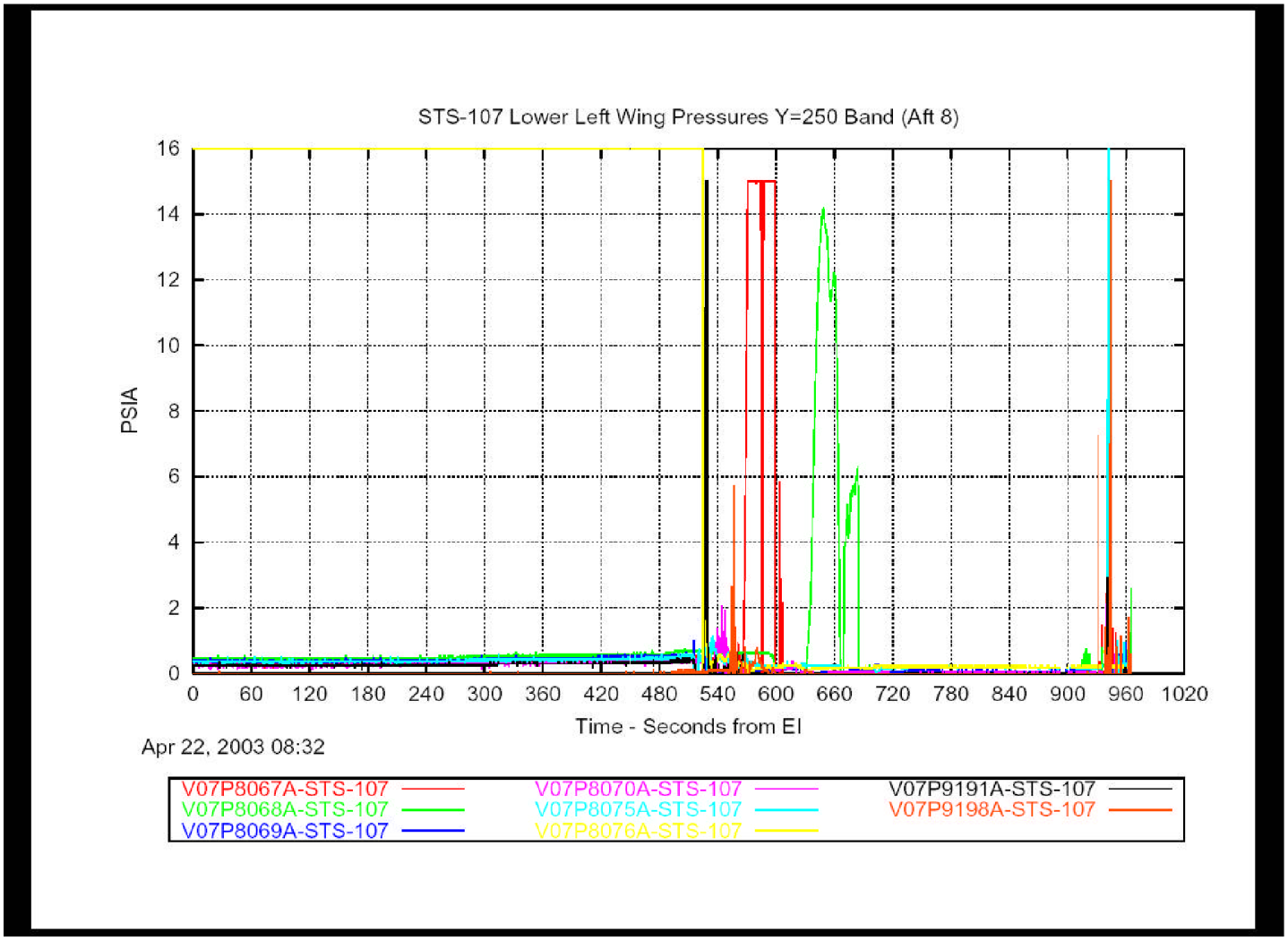

This material is PRELIMINARY information only. It is for limited distribution. DO NOT FORWARD.

Lower Left Wing Y=330 Taps

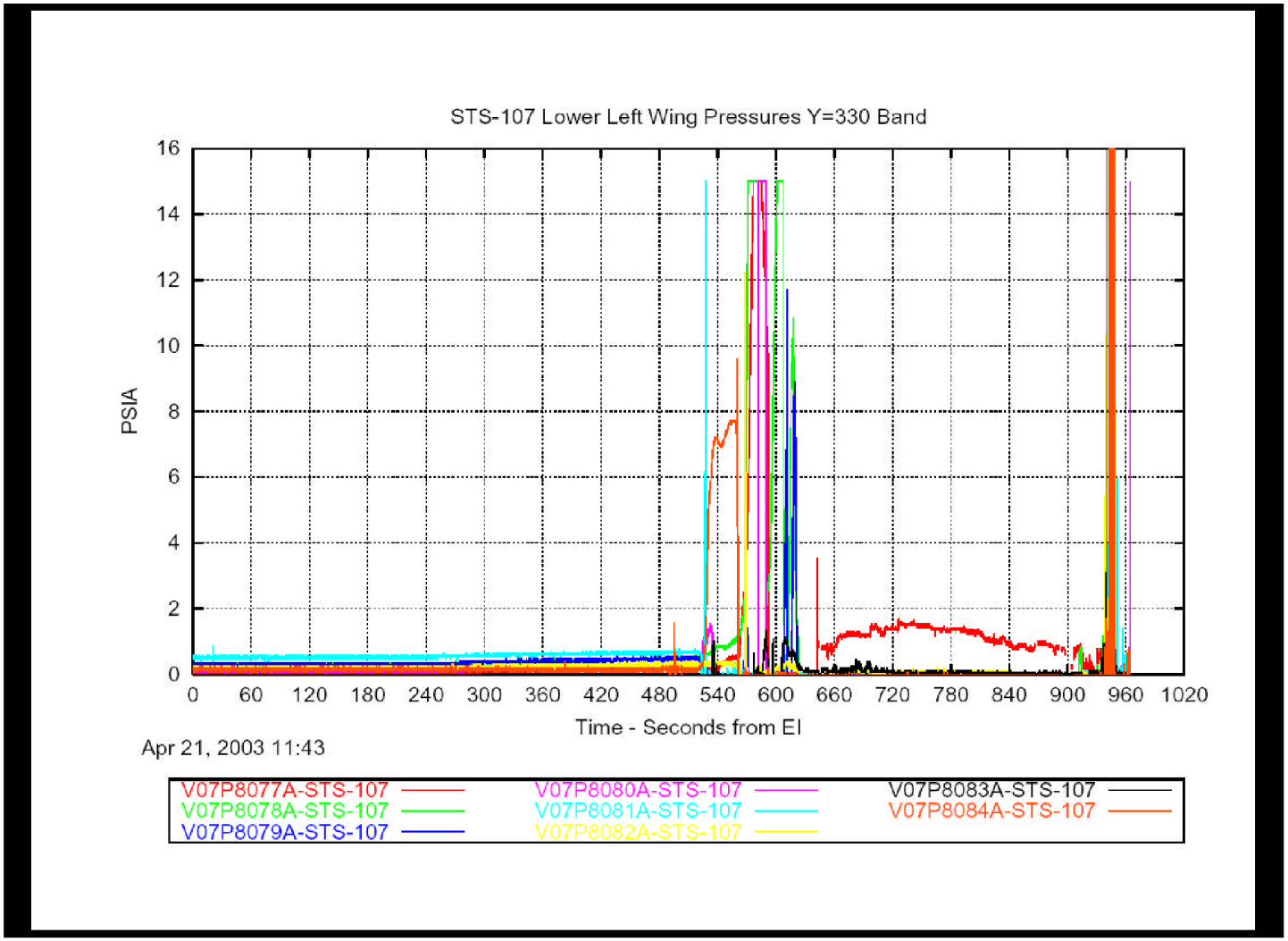

This material is PRELIMINARY information only. It is for limited distribution. DO NOT FORWARD.

Lower Left Wing Y=420 Taps

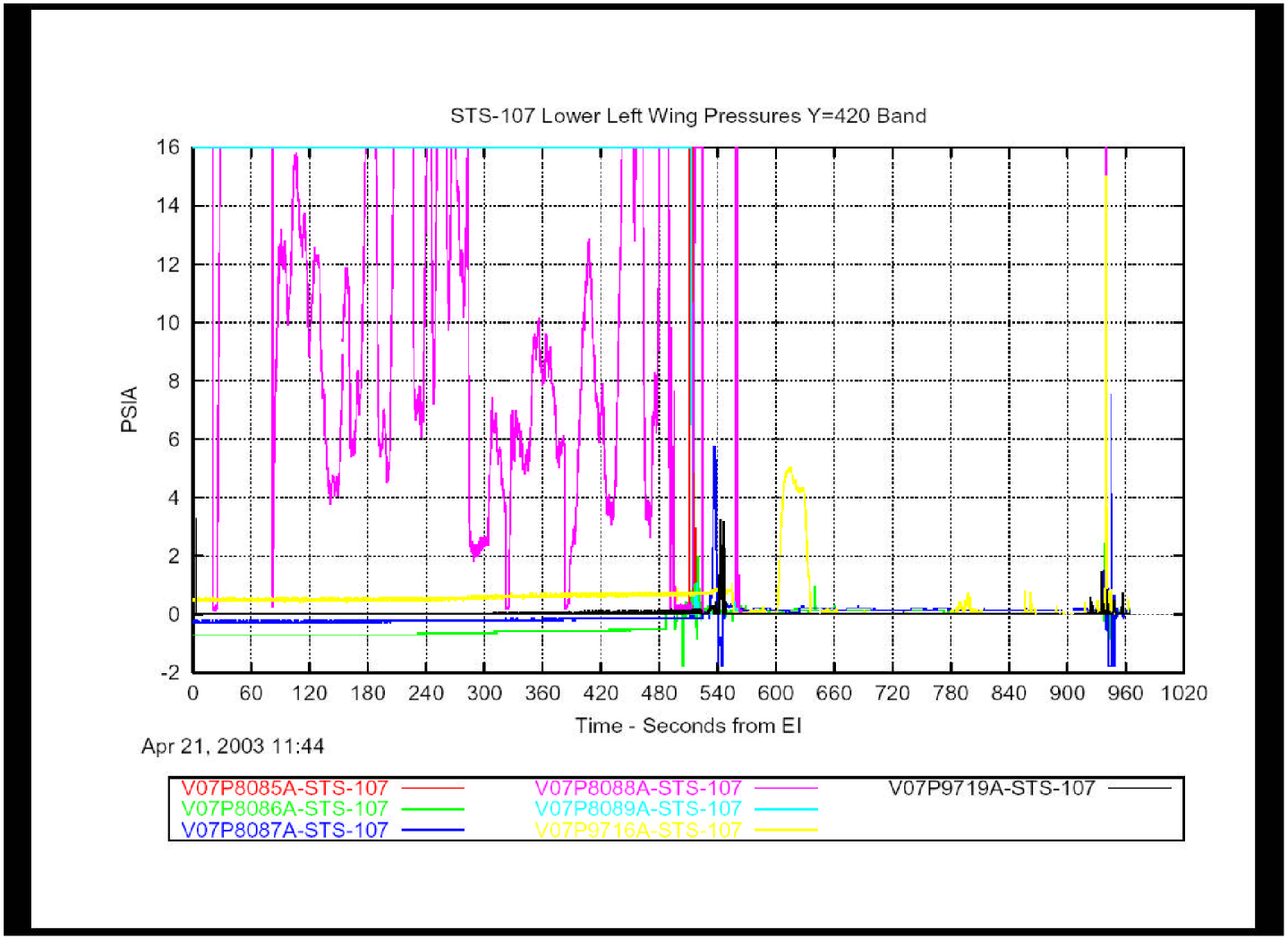

This material is PRELIMINARY information only. It is for limited distribution. DO NOT FORWARD.

Lower Left Wing Y=450 Taps

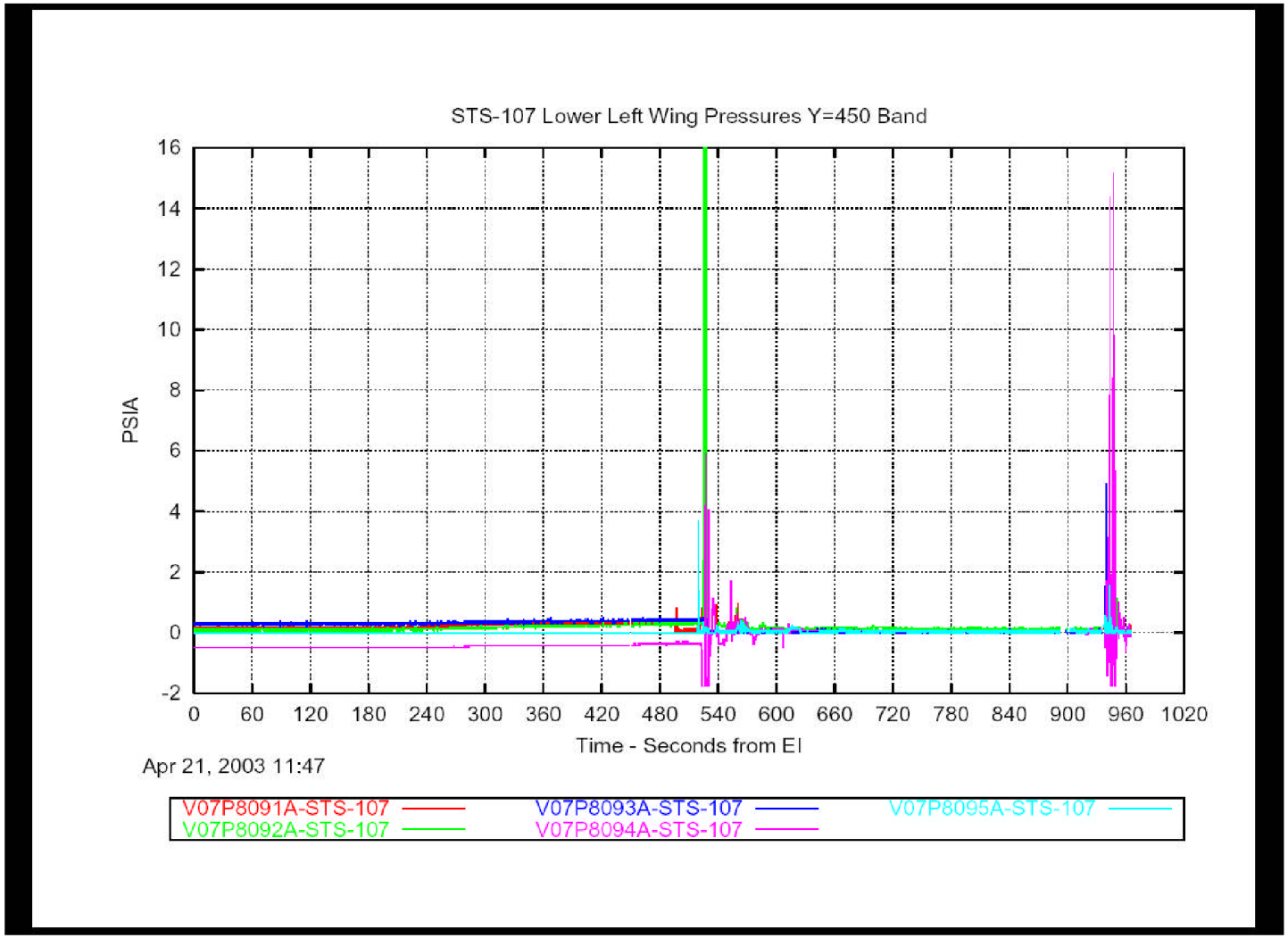

This material is PRELIMINARY information only. It is for limited distribution. DO NOT FORWARD.

Left Wing Leading Edge (Lower) Taps

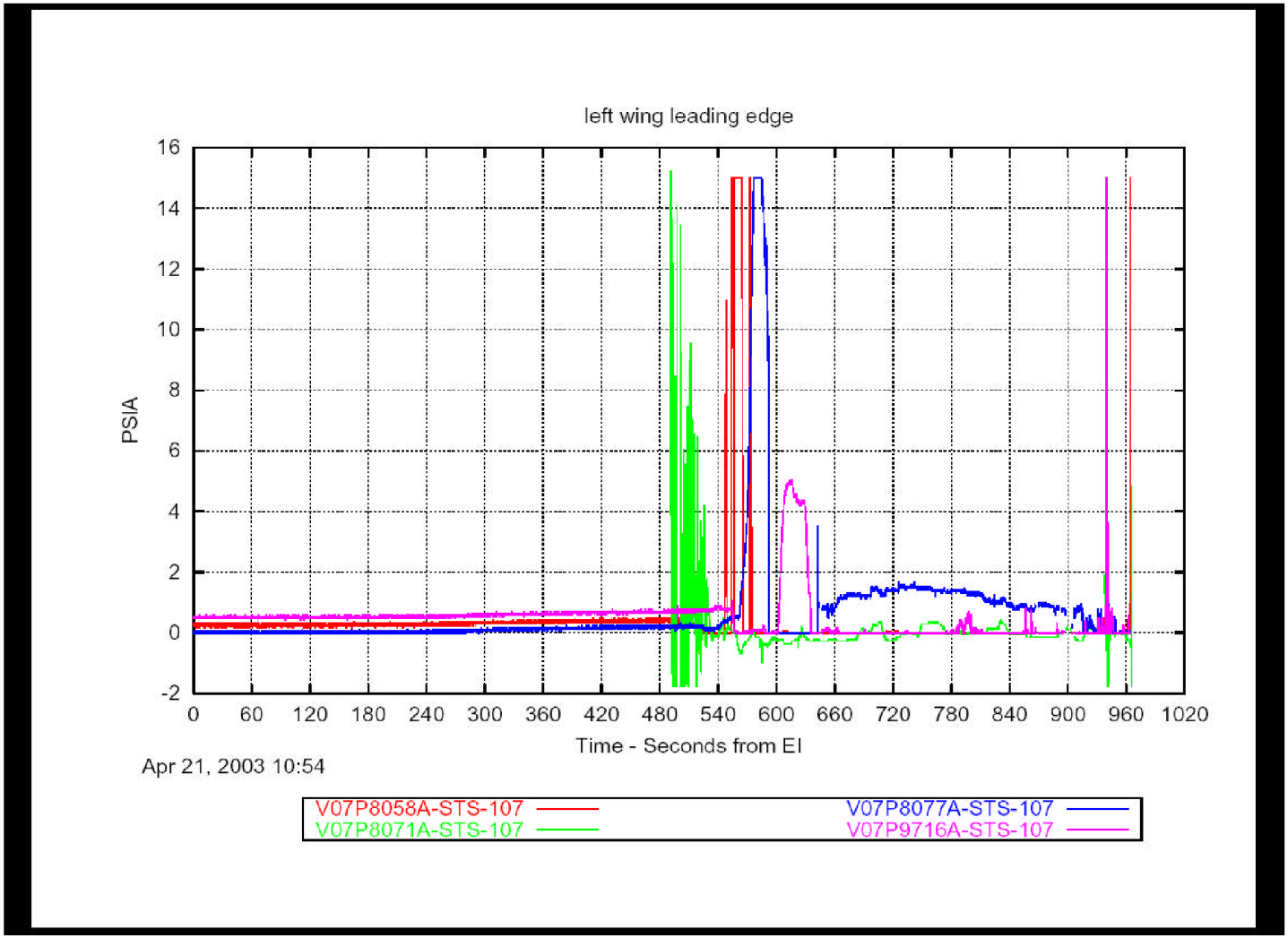

This material is PRELIMINARY information only. It is for limited distribution. DO NOT FORWARD.

Upper Left Wing Y=150 Taps

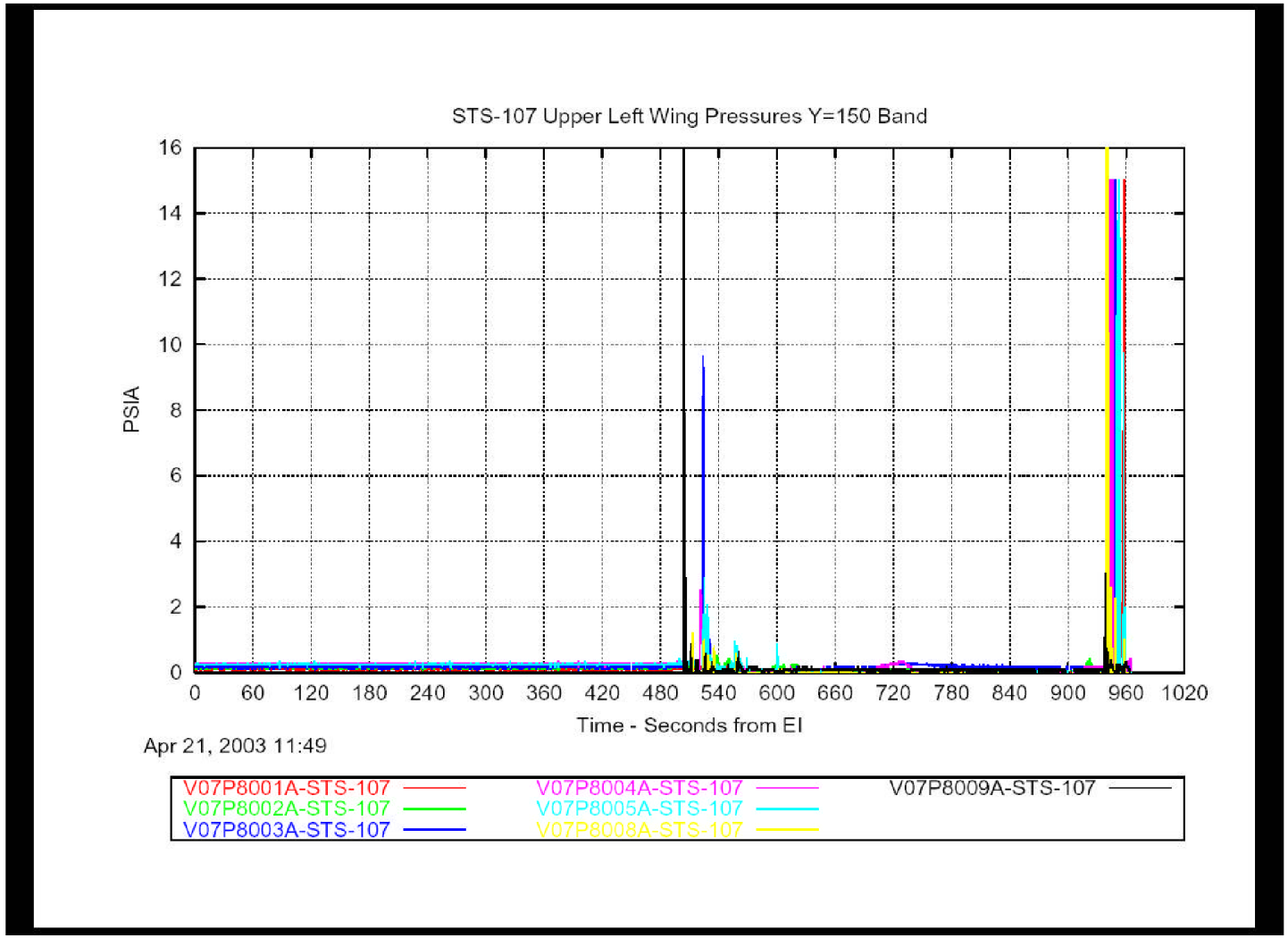

This material is PRELIMINARY information only. It is for limited distribution. DO NOT FORWARD.

Upper Left Wing Y=200 Taps

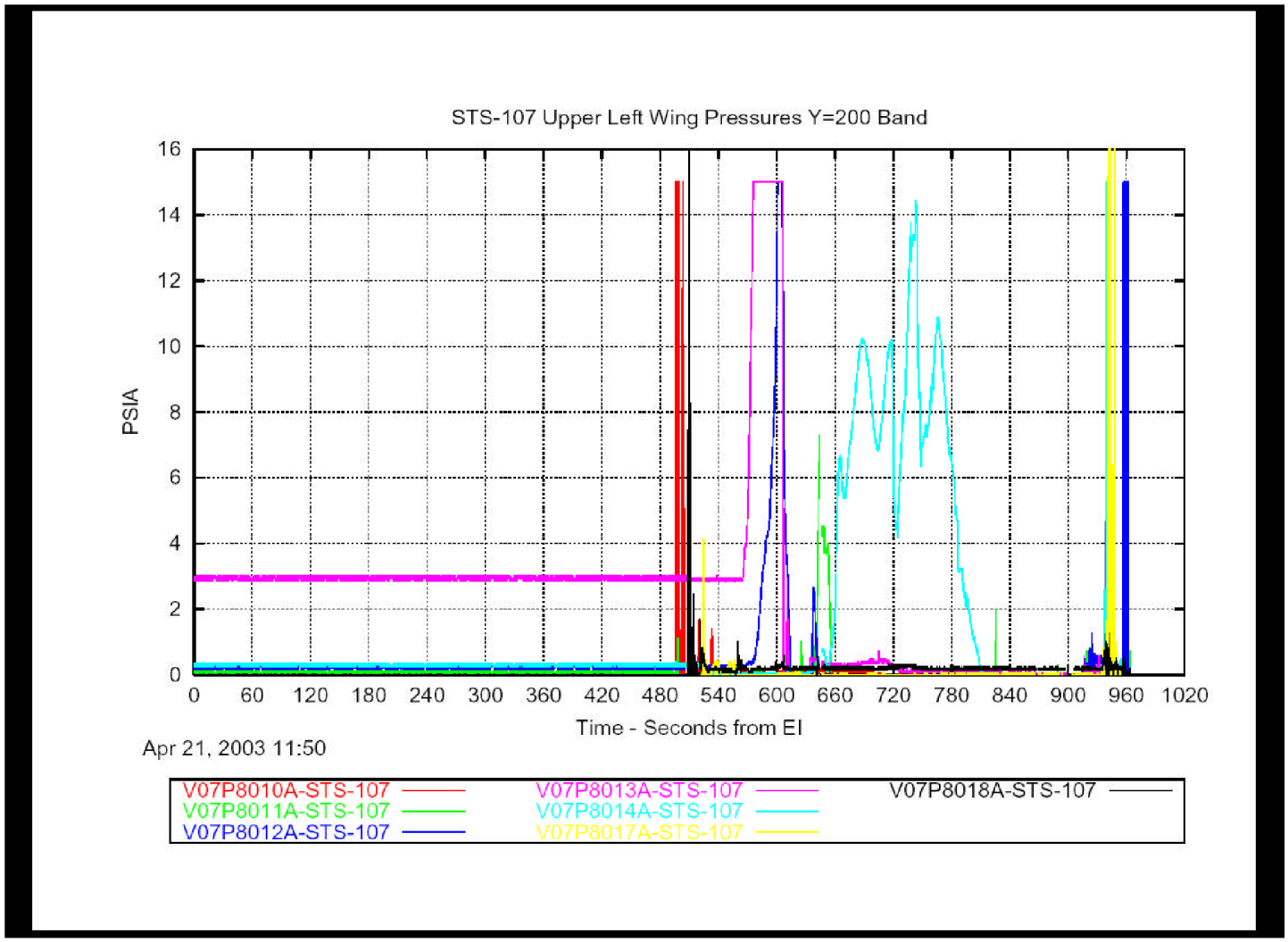

Upper Left Wing Y=250 (Fwd 8)

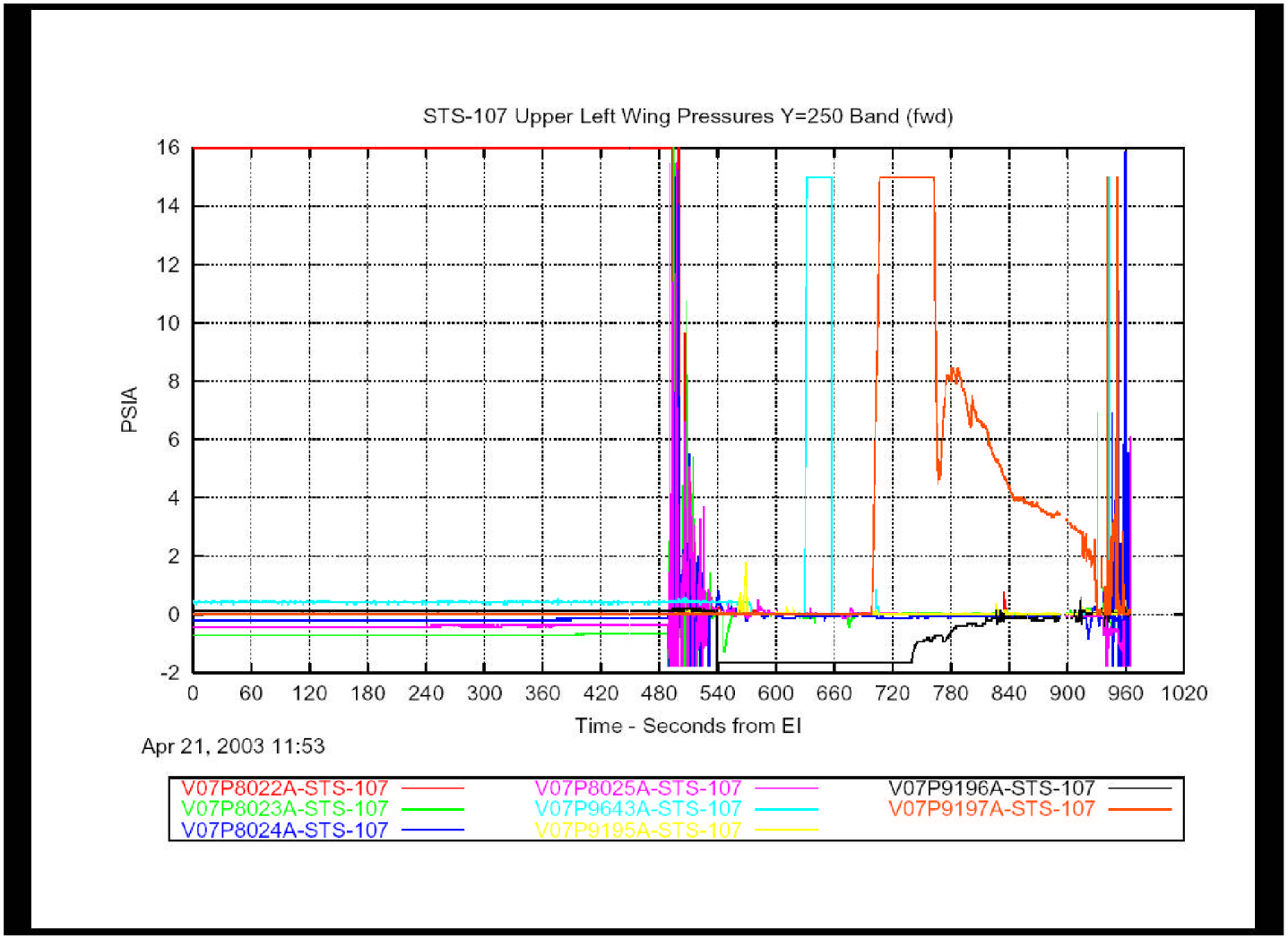

This material is PRELIMINARY information only. It is for limited distribution. DO NOT FORWARD.

Upper Left Wing Y=250 (Aft 7)

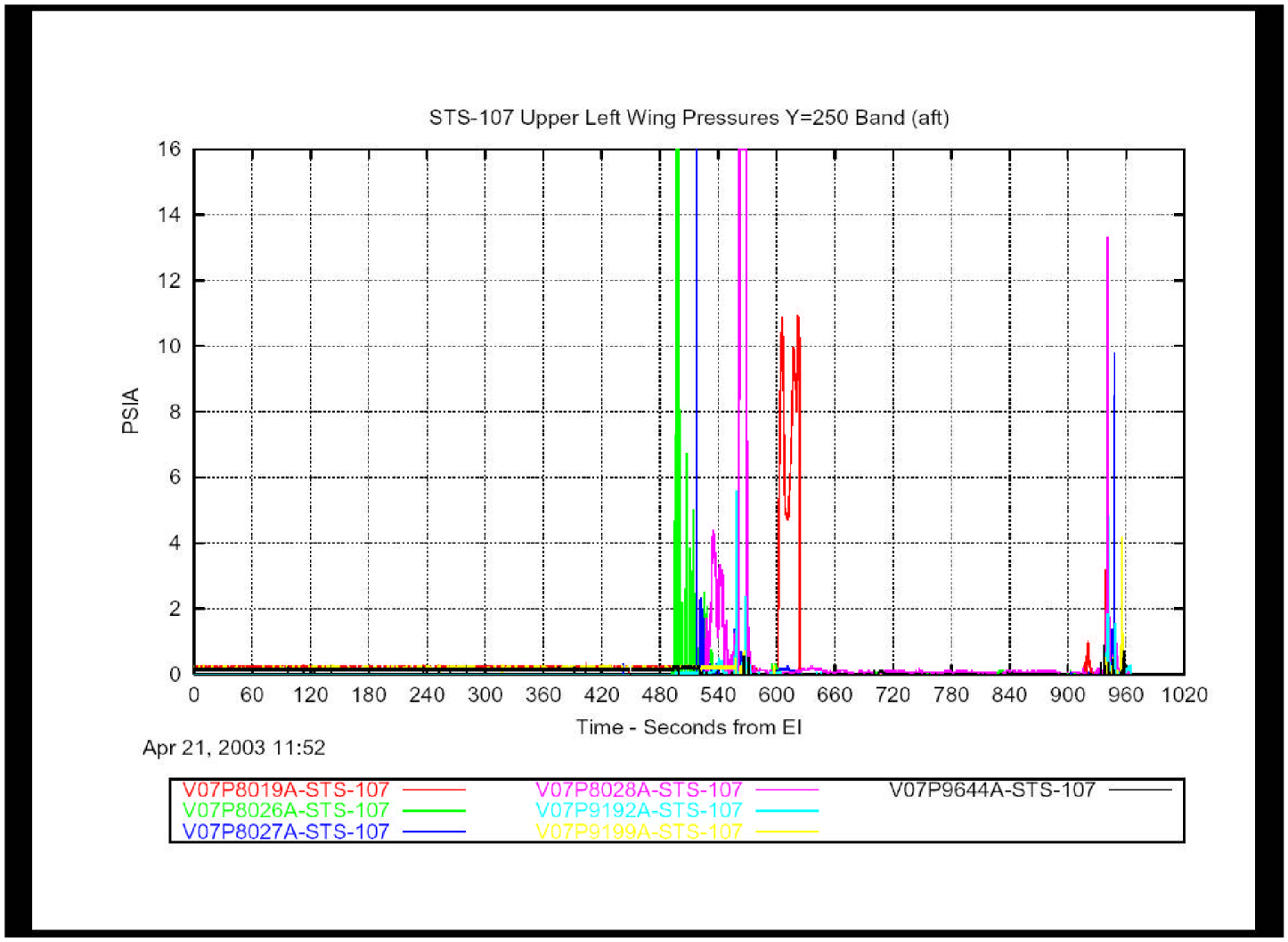

This material is PRELIMINARY information only. It is for limited distribution. DO NOT FORWARD.

Upper Left Wing Y=330

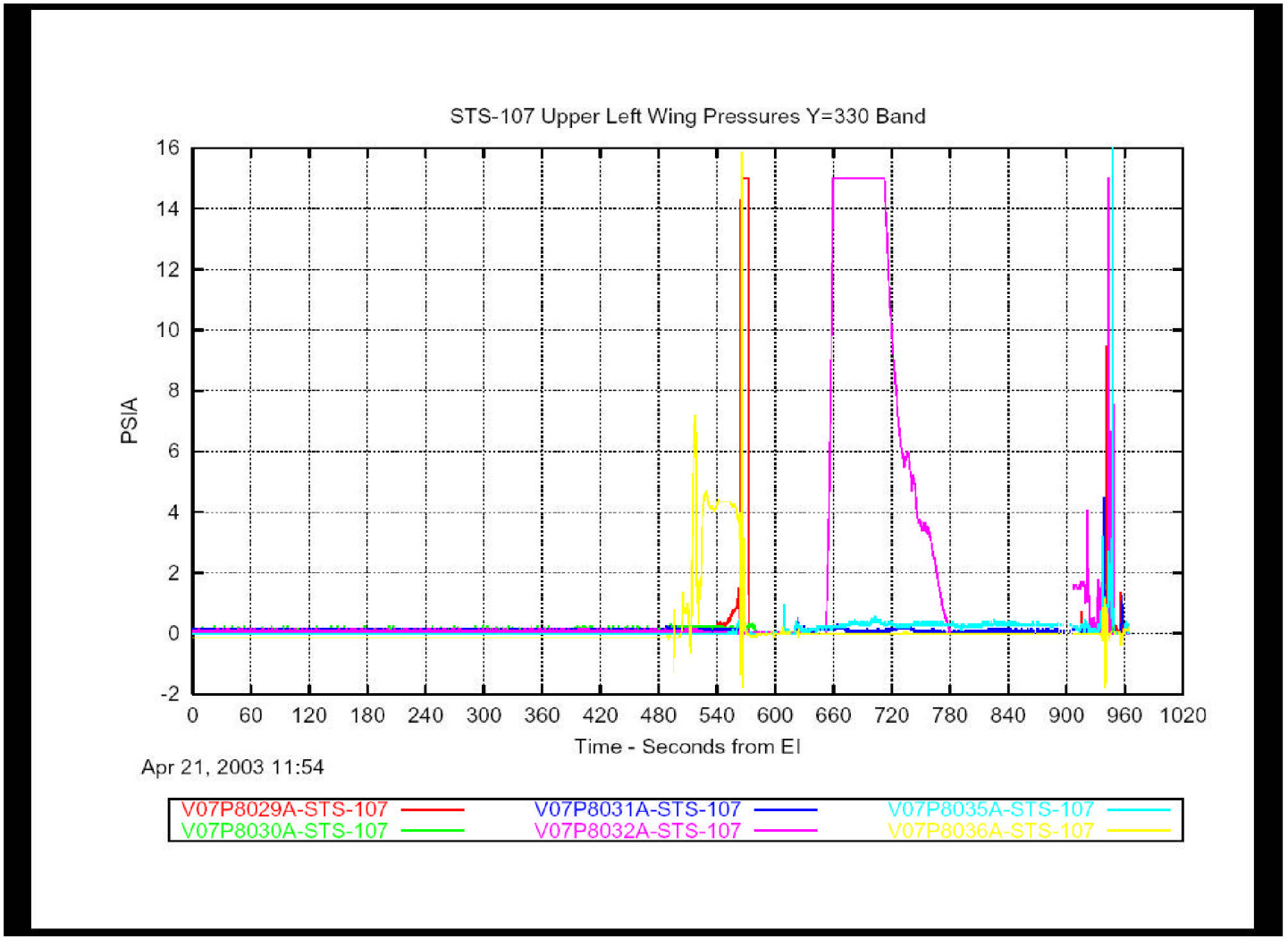

This material is PRELIMINARY information only. It is for limited distribution. DO NOT FORWARD.

Upper Left Wing Y=420

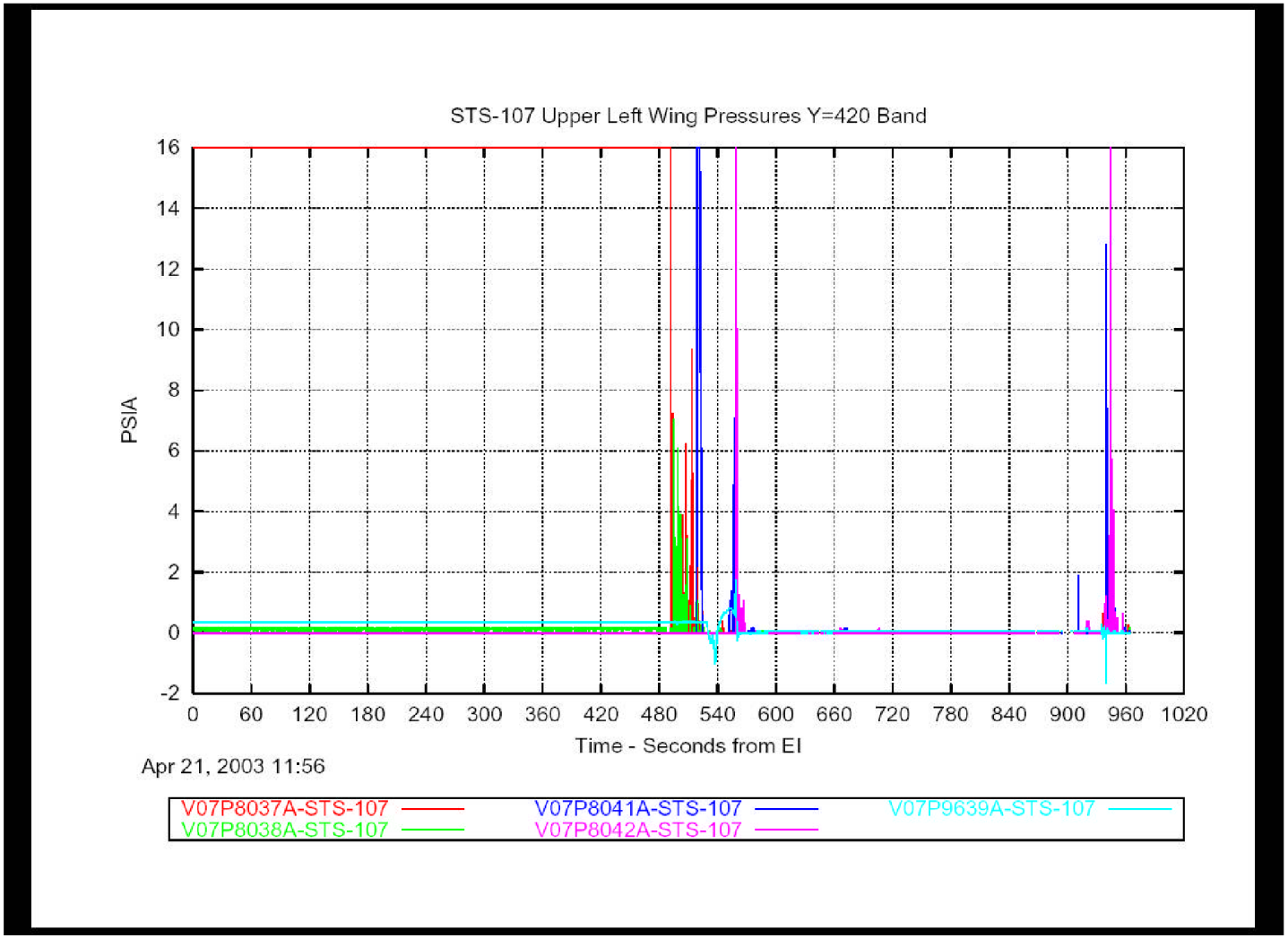

This material is PRELIMINARY information only. It is for limited distribution. DO NOT FORWARD.

Upper Left Wing Y=450

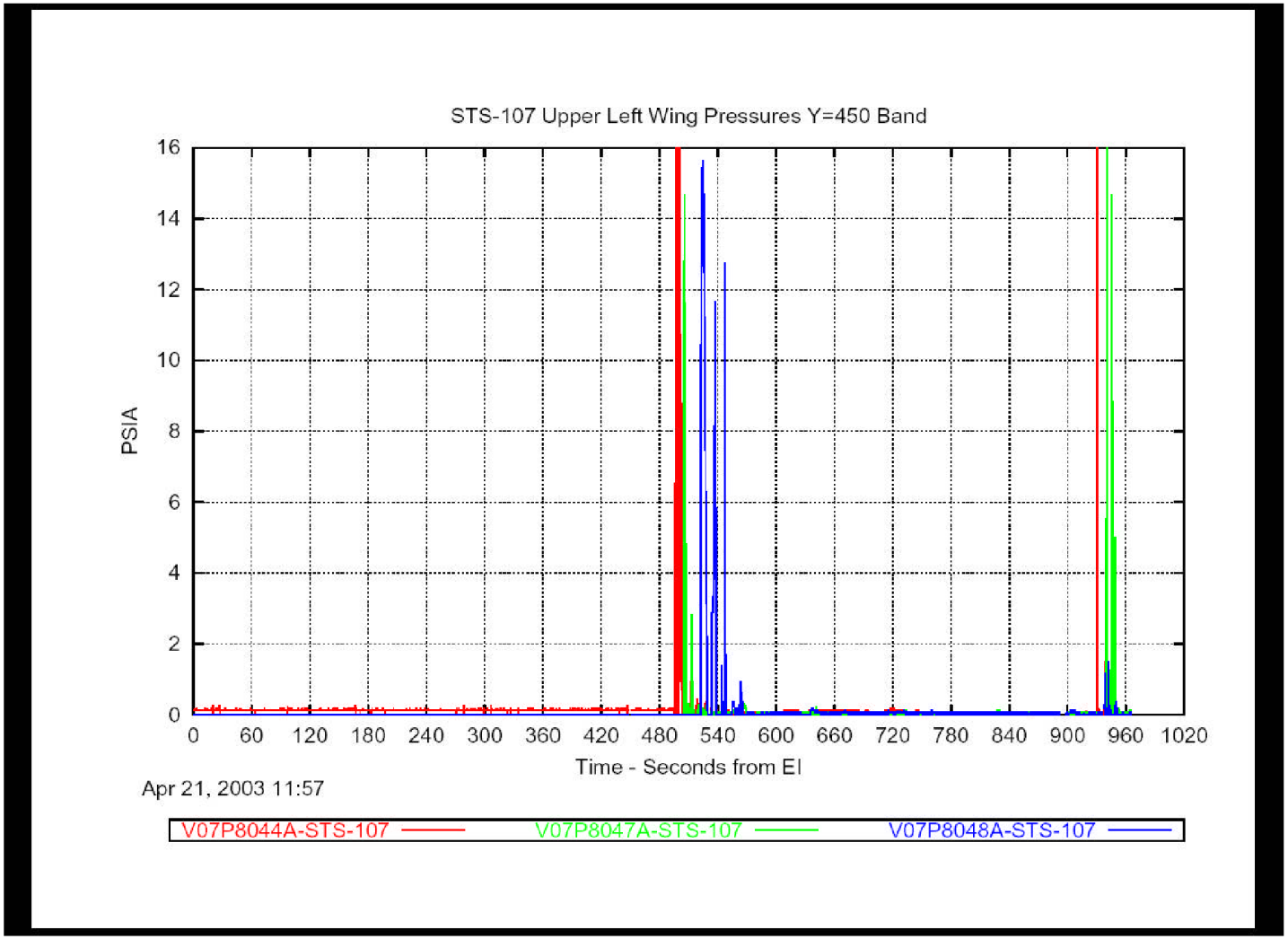

This material is PRELIMINARY information only. It is for limited distribution. DO NOT FORWARD.

Left Wing Leading Edge (Upper) Taps

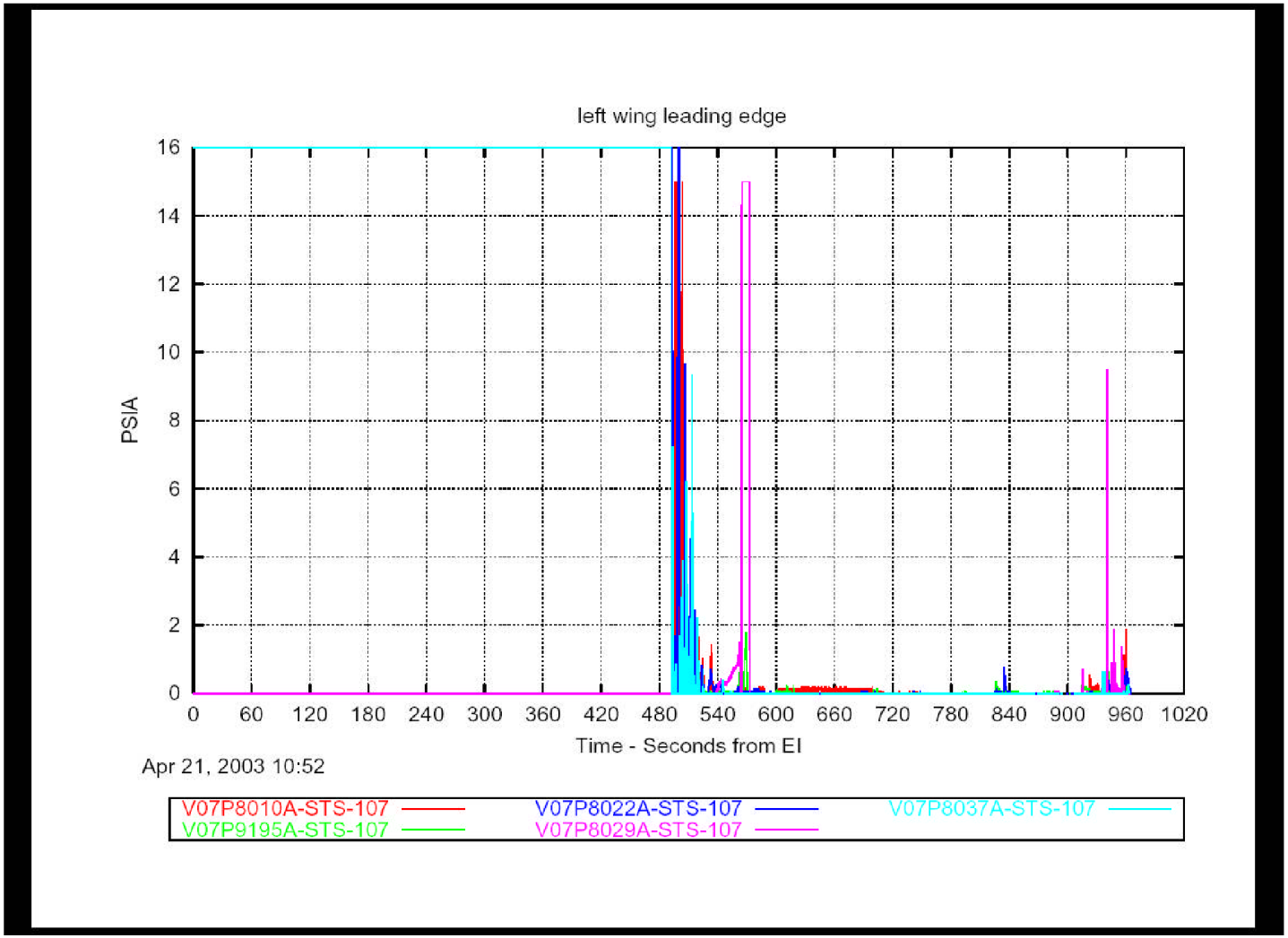

This material is PRELIMINARY information only. It is for limited distribution. DO NOT FORWARD.

STS-107 x1040 Spar Cap Strain Gage Assessment

S.C. Sorenson

Boeing Houston Orbiter Stress Analysis

13 June 2003

This material is PRELIMINARY information only. It is for limited distribution. DO NOT FORWARD.

Background

- **Anomalous strain gage signatures are presumed to result from instrumentation malfunction, thermally induced strain, load redistribution, or a combination.**
  - Thermal effects are a more reasonable explanation than load redistribution scenarios.
    - Lower spar cap shows a slope sign reversal.
    - No slope changes before or after sharp data changes.
- **The current analysis uses FEM methods to assess the feasibility of thermally induced strain as a mechanism to produce the observed signatures.**
  - Analysis does not attempt to model actual structural temperatures.
    - Objective is to determine the structural response to local temperature differentials.

This material is PRELIMINARY information only. It is for limited distribution. DO NOT FORWARD.

STS-107 Data Examination

- **STS-107 upper and lower spar cap strain data was examined and refined for analysis.**
  - Sharp data drop near EI+690 seconds is questionable data.
    - Drop occurs in one time step
      - No preceding slope change.
    - Current opinion of instrumentation is that the data is good up to the terminal phase (~EI+930 sec)
    - Also extremely unlikely as a real strain event
    - Data beyond EI+690 seconds will not be analyzed.
  - Nominal trend lines, based on STS-109 entry data, were superimposed for comparison.
- **Key data event times were annotated.**

This material is PRELIMINARY information only. It is for limited distribution. DO NOT FORWARD.

STS-107 Reconstructed Data

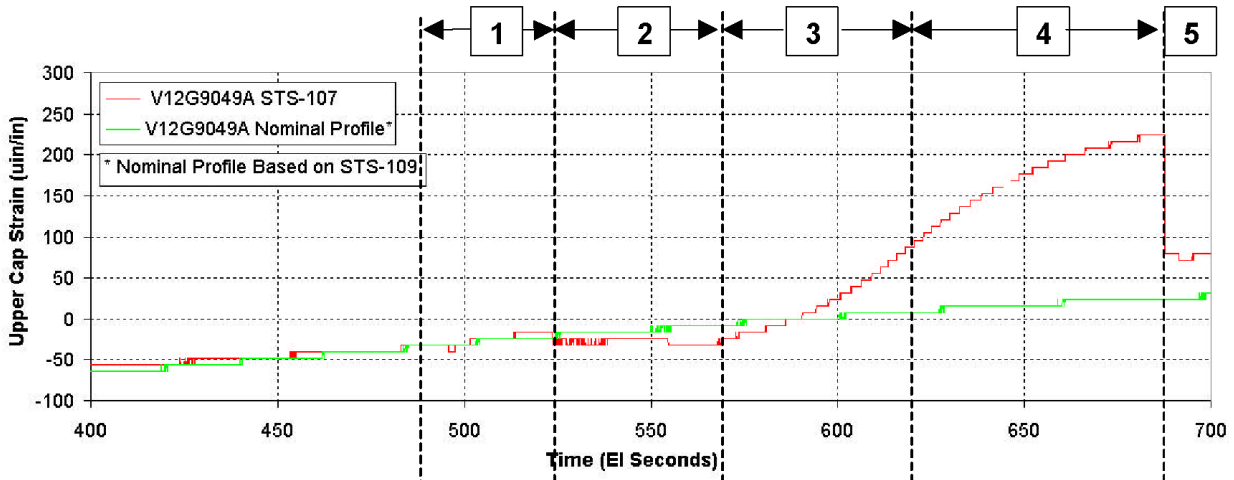

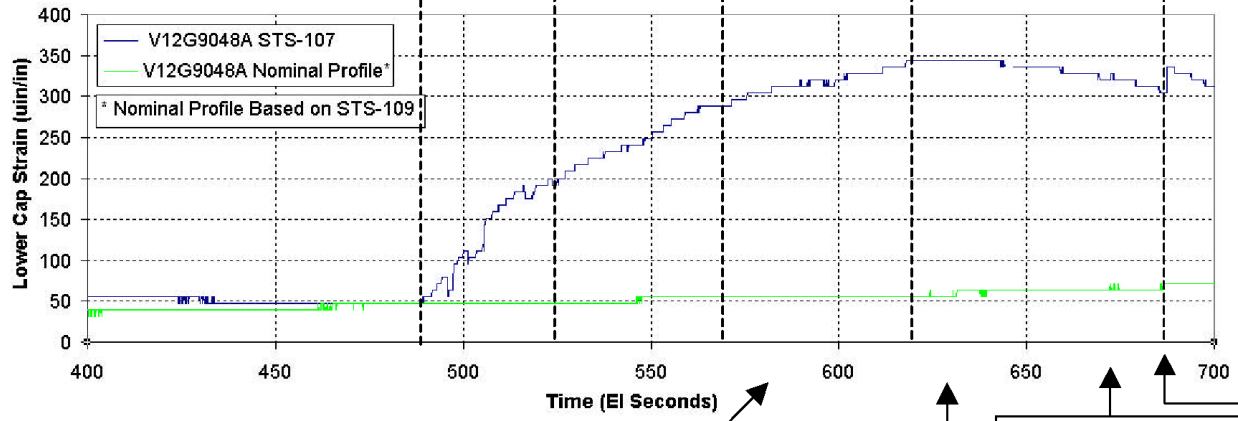

Debris #1-5 (576-602)

Debris #6 (626-628)

Debris #7-10 (655-680)

Debris #11 (686-690)

This material is PRELIMINARY information only. It is for limited distribution. DO NOT FORWARD.

FEM Results Summary

Qualitative summary of analyzed FEM cases & results:

Case	Description	Upper Cap Reaction	Lower Cap Reaction
4A	Calibration (all nodes @ 70°F)	None	None
4B	Equal heating of spar web, forward upper and lower skins	Significant tension (20% higher than lower cap)	Significant tension
4C	Heating of outboard, aft, upper skin only	Significant tension	Very low tension
4D	Combined 4B and 4C	Significant tension (effects additive)	Significant tension (effects additive)
4F	Heating forward lower skin only	Very low compression	Significant tension
4G	Heating of WLE nodes	Very low compression	Low compression (2x upper cap)
4H	Heating of outboard, aft, lower skin only	Very low compression	Very low tension
4I	Heating of spar web nodes only	Very low tension	Low tension (2x upper cap)
4J	Heating of Yo167 rib sections	Very low tension	Very low tension
4L	Heating of upper spar cap only	Significant compression	Very low compression
4M	Heating of aft upper skin only	Significant tension	Very low compression

This material is PRELIMINARY information only. It is for limited distribution. DO NOT FORWARD.

FEM Results Analysis

- **FEM temperature load cases may be combined in a number of ways to generate temperature profile sequences which produce the observed strains.**
  - Several profile sequences were developed, and screened versus corroborating scenario evidence to define the most likely profile that could have produced the observed strains.
- **The most rational temperature profile was selected.**
  - Combined heating of aft upper skin, spar web, upper and lower forward skins, and upper spar cap, with less heating to lower spar cap.

This material is PRELIMINARY information only. It is for limited distribution. DO NOT FORWARD.

FEM Scenario Temperature Profile

Case	Description	Upper Cap Reaction	Lower Cap Reaction	Scenario
A1	+40°F applied to spar web, forward upper & lower skins, and upper spar cap +75°F applied to outboard, aft, upper skin	13 µin/in **(8 µin/in) (Recorded strain)**	146 µin/in **(152)**	Heating in front of spar and aft upper skin.
A2	+75°F applied to spar web, forward upper & lower skins, and upper spar cap +120°F applied to aft, upper skin along y167 rib +5°F applied to lower spar cap	-11 µin/in **(-16)**	225 µin/in **(232)**	Continued heating in front of spar and aft upper skin. Some heating in lower spar cap.
A3	+105°F applied to spar web, forward upper & lower skins, and upper spar cap +145°F applied to aft, upper skin above MLG wheel well +10°F applied to lower spar cap	73 µin/in **(72)**	291 µin/in **(288)**	Continued heating in front of spar and aft upper skin. Continued heating in lower spar cap.
A4	+105°F applied to spar web, forward upper & lower skins, and upper spar cap +190°F applied to aft, upper skin above MLG wheel well +20°F applied to lower spar cap	200 µin/in **(200)**	237 µin/in **(232)**	Thermal EQ in spar web, forward skins, and upper cap. Continued heating in lower cap. Continued heating of aft upper skin.

This material is PRELIMINARY information only. It is for limited distribution. DO NOT FORWARD.

FEM Scenario Timeline Plot

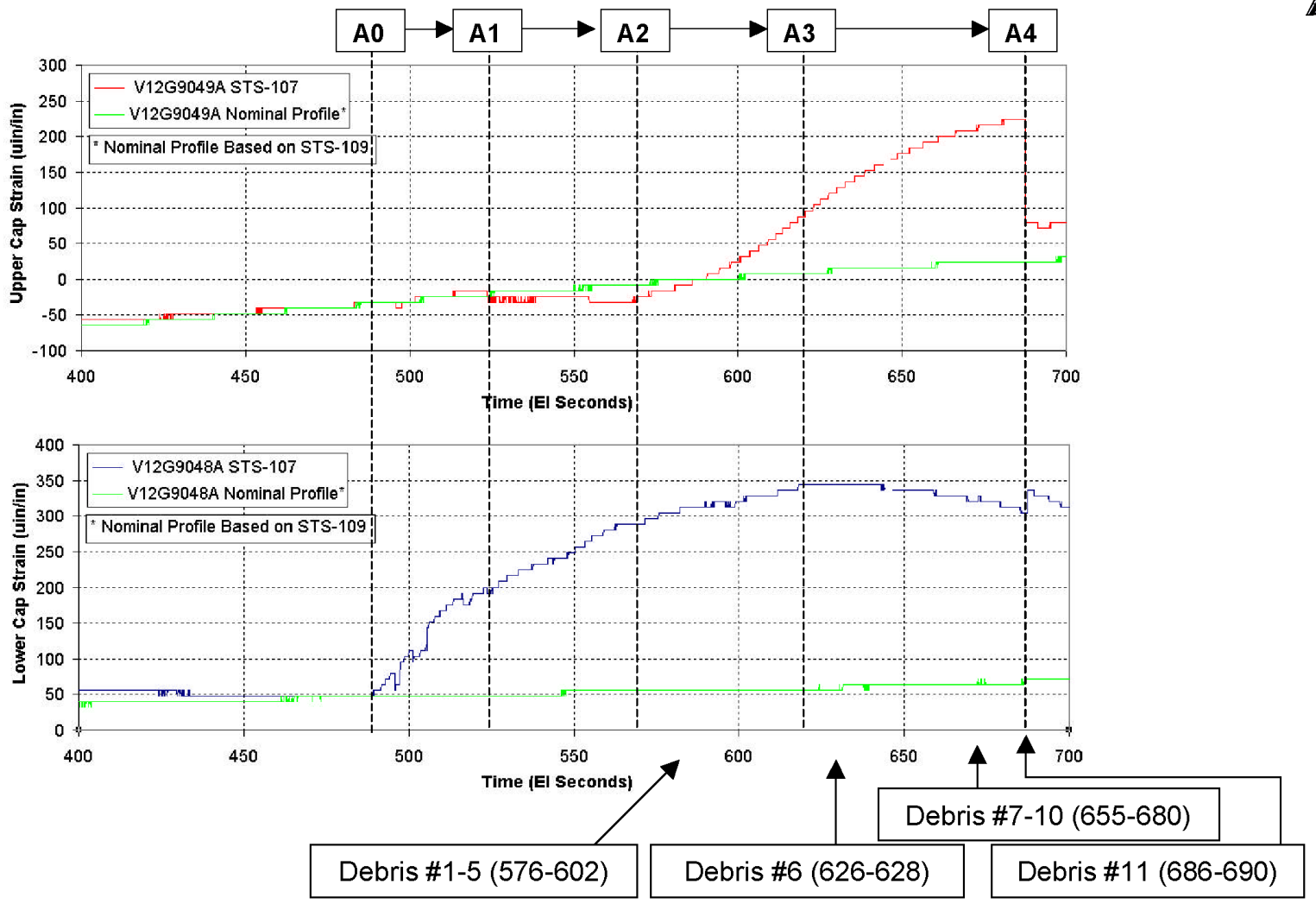

This material is PRELIMINARY information only. It is for limited distribution. DO NOT FORWARD.

Conclusions

- **Local temperature gradients could potentially explain the observed Xo1040 upper and lower spar cap strains.**
- **Strain gage evidence offers some support for failure scenarios involving hot gas intrusion from the wing cavity into the glove area and/or the MLG wheel well.**
  - Timing of strain gage events has reasonable correlation with breach times of WLE and MLG well.
- **Strain gage data does not, however, conclusively indicate this scenario.**
  - Results require the critical assumption that the lower spar cap is initially exposed to less heating than the upper cap, spar web, and nearby skins.

This material is PRELIMINARY information only. It is for limited distribution. DO NOT FORWARD.

Backup

- Wing Illustration
- Nominal entry strain plots
- STS-107 Full Data Reconstruction
- FEM Illustrations
- FEM Case Results Summary

This material is PRELIMINARY information only. It is for limited distribution. DO NOT FORWARD.

Wing Illustration

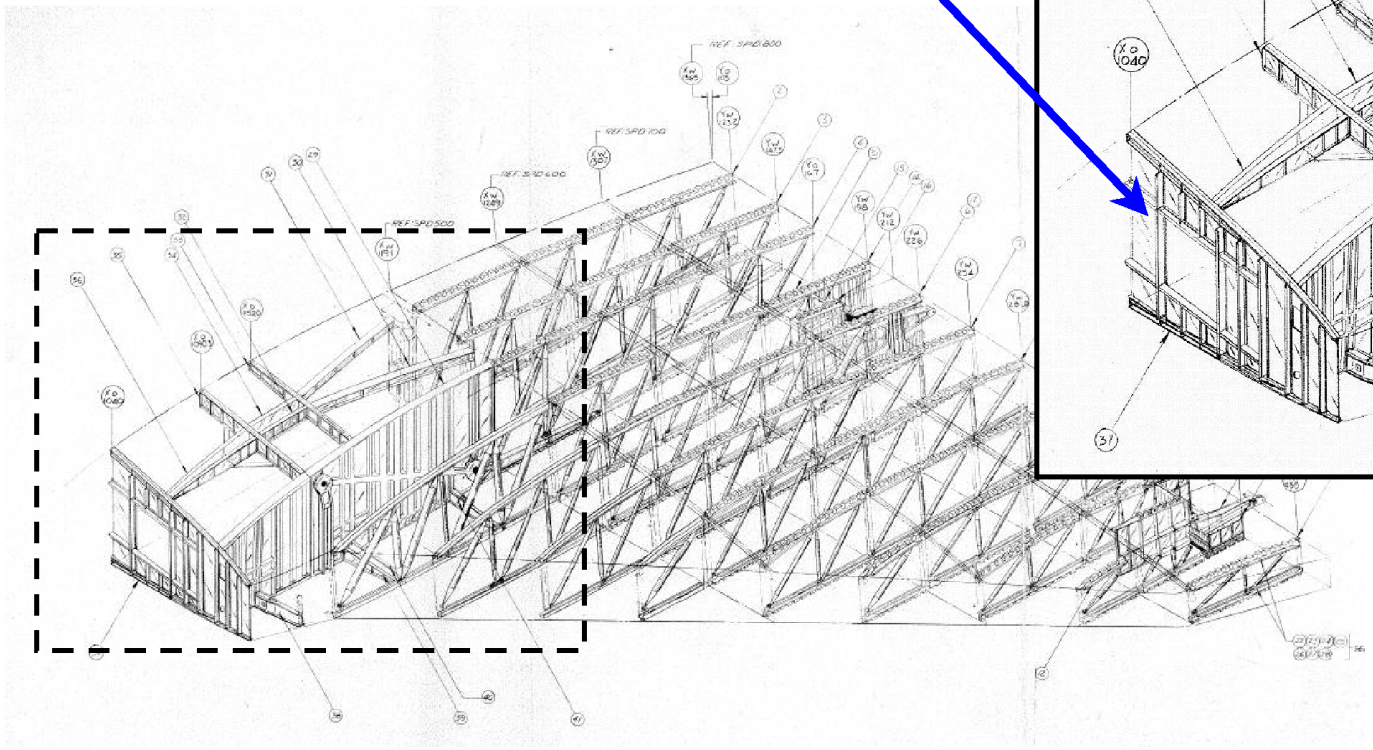

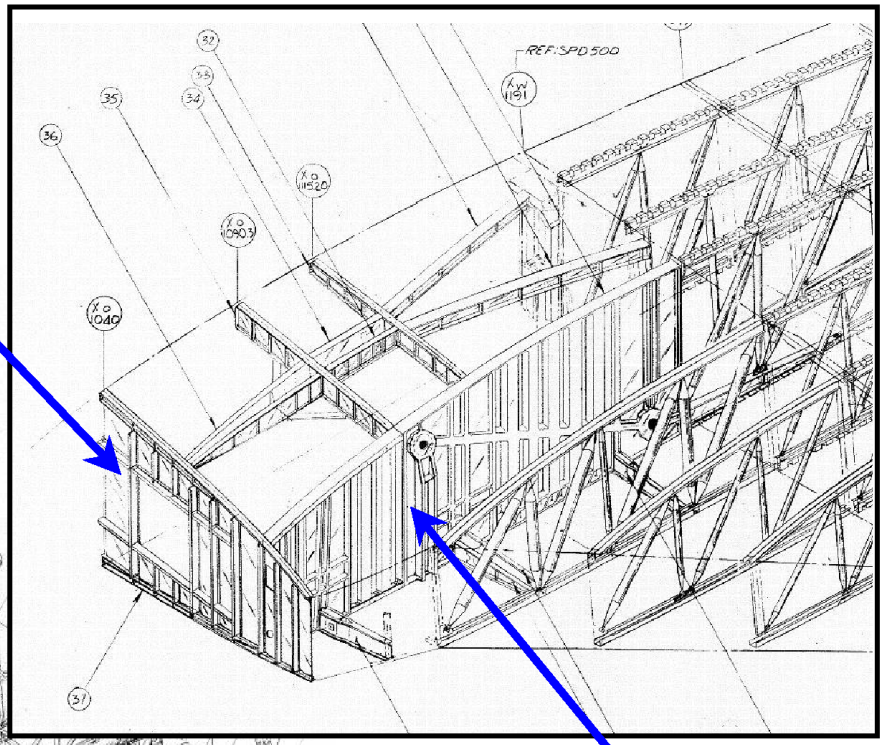

This material is PRELIMINARY information only. It is for limited distribution. DO NOT FORWARD.

Nominal Entry Strain Plots (STS-109)

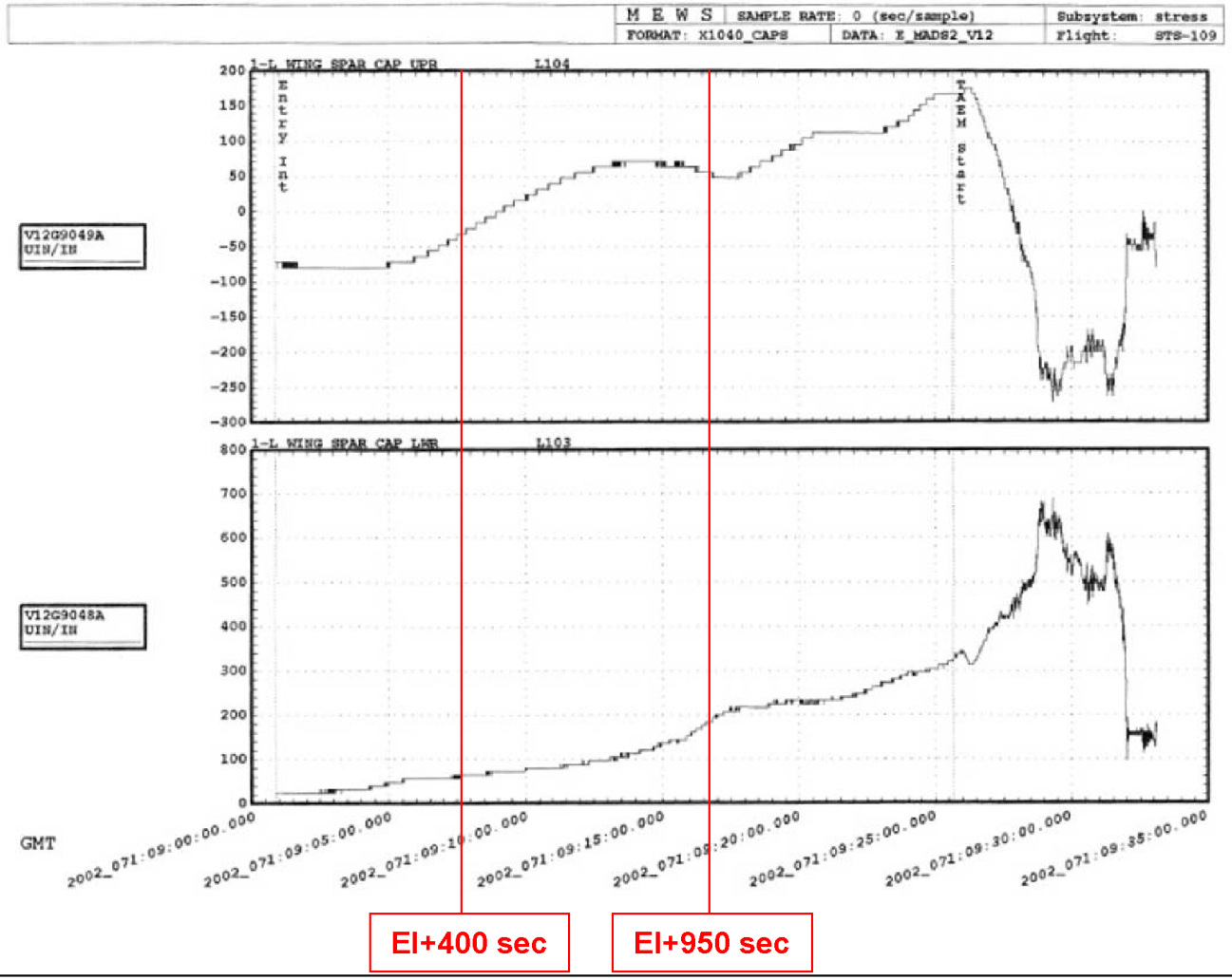

This material is PRELIMINARY information only. It is for limited distribution. DO NOT FORWARD.

STS-107 Full Data Reconstruction

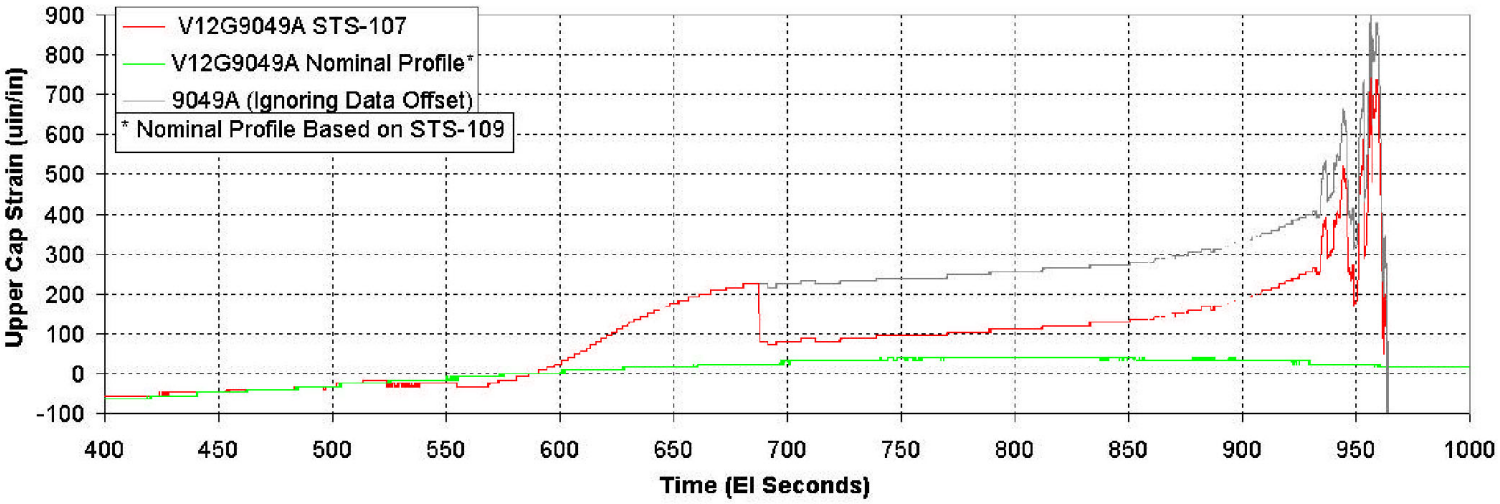

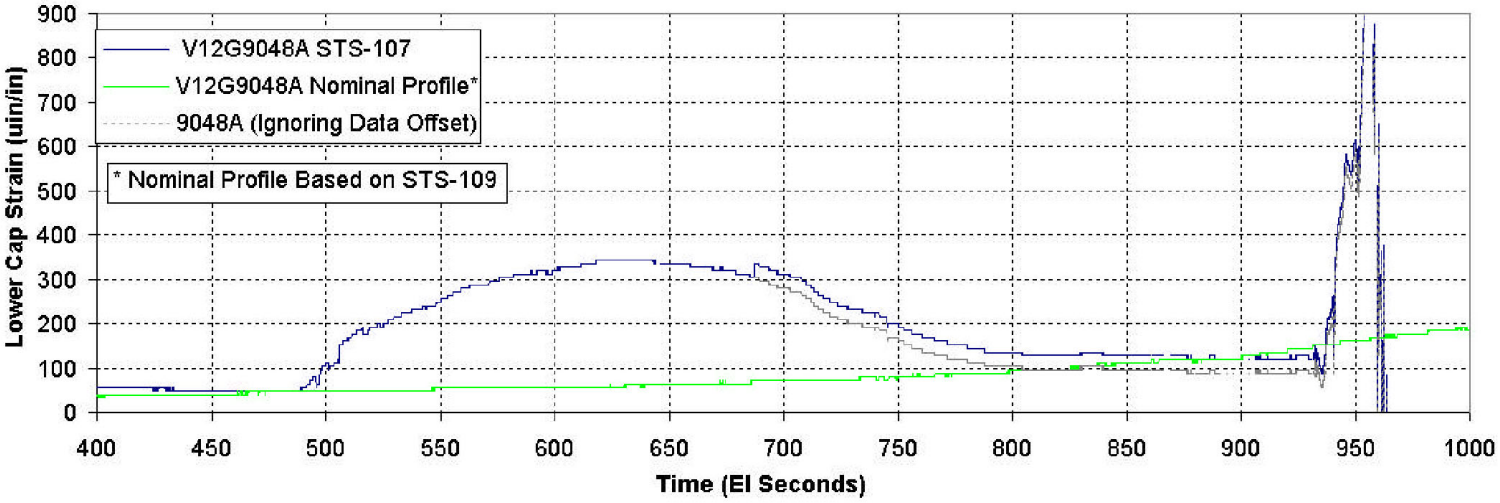

This material is PRELIMINARY information only. It is for limited distribution. DO NOT FORWARD.

FEM Illustration – x1040 Spar Nodes

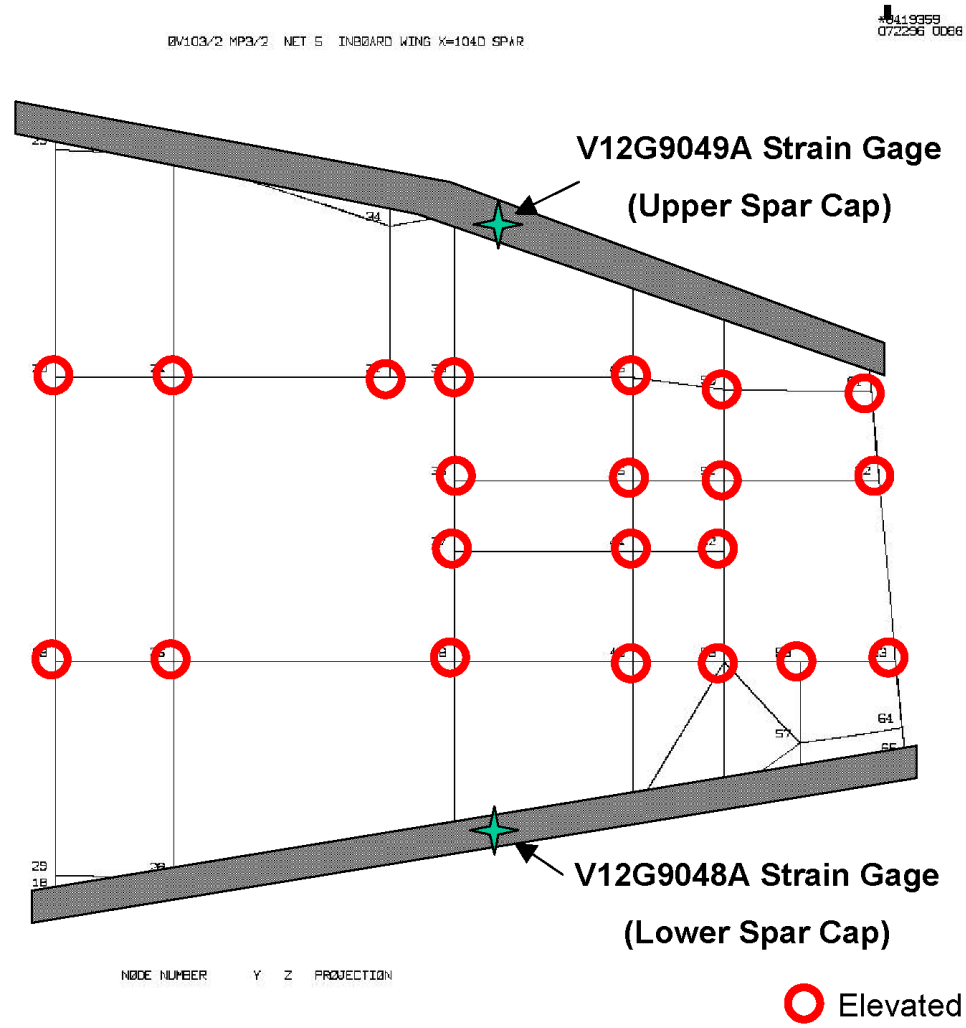

This material is PRELIMINARY information only. It is for limited distribution. DO NOT FORWARD.

FEM Illustration – Nearby Skin Nodes

UPPER SKIN

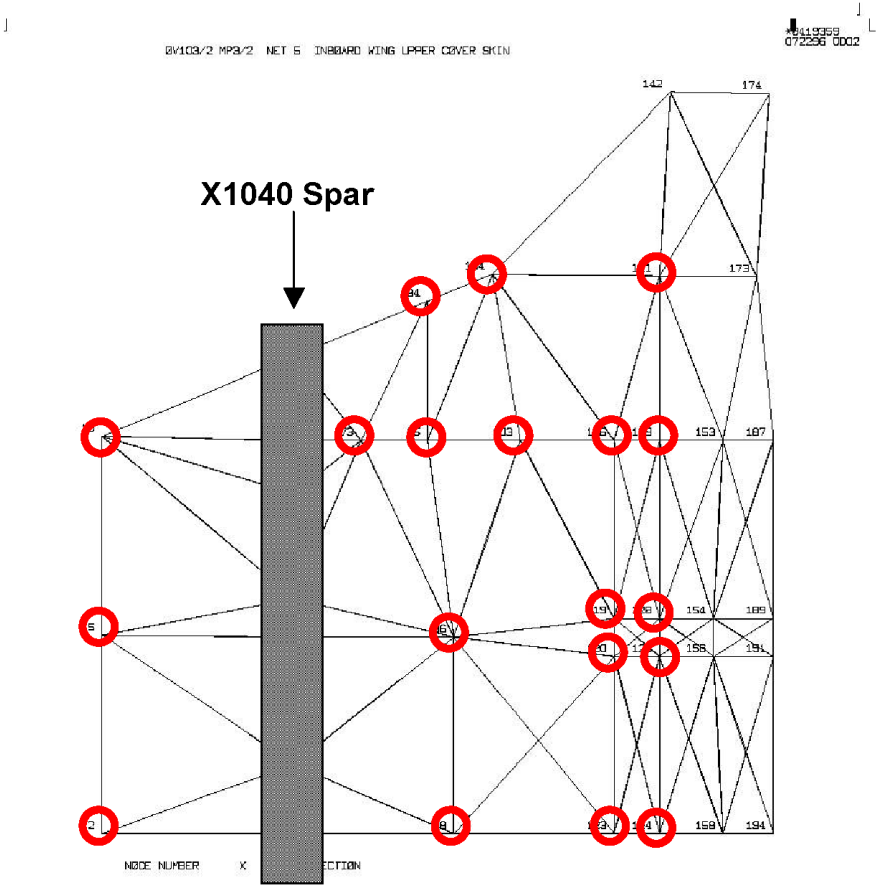

LOWER SKIN

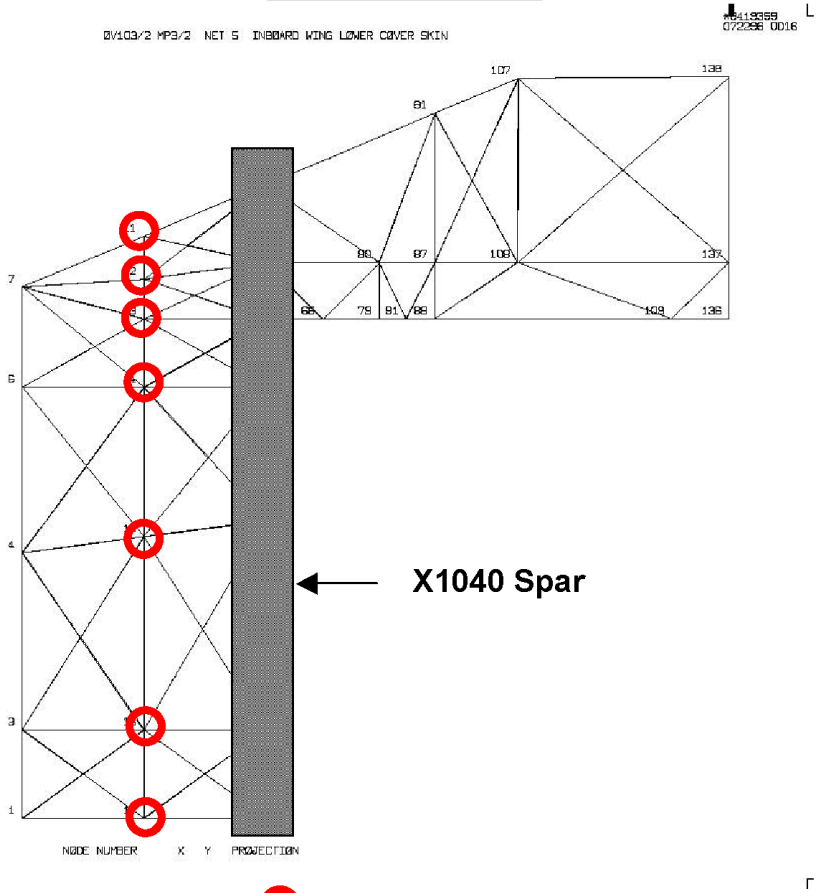

Elevated Temperature Node

This material is PRELIMINARY information only. It is for limited distribution. DO NOT FORWARD.

FEM Case Results Summary

Case	Description	Temperatures: Default	Spar Web	Upper Skin	Lower Skin	Upper Spar Cap	Lower Spar Cap	Obd/Aft Upper Skin	Other (see notes)		Results: Stress	Microstrain	Notes
4A	Calibration Case	70	70	70	70	70	70	70	-	Upper Cap (5073)	0	0	
										Lower Cap (5090)	0	0	
4B	Equal heating of spar web, upper and lower skins	70	180	180	180	70	70	70	-	Upper Cap (5073)	3749	354	
										Lower Cap (5090)	4445	419	
4C	Heating of only outboard, aft upper skin	70	70	70	70	70	70	400	-	Upper Cap (5073)	6668	629	
										Lower Cap (5090)	451	43	Nodes 73, 84, 95, 104, 103, 116, 141, 129
4D	Heat spar web, upper & lower skins, and outboard aft upper skin	70	180	180	180	70	70	400	-	Upper Cap (5073)	10416	983	
										Lower Cap (5090)	4896	462	
4F	Heat lower skin near spar only	70	70	70	180	70	70	70	-	Upper Cap (5073)	-171	-16	
										Lower Cap (5090)	2210	208	
4G	Heat WLE nodes near panels 8/9	70	70	70	70	70	70	70	400	Upper Cap (5073)	-276	-26	
										Lower Cap (5090)	-602	-57	Nodes at y226 to 400°F
4H	Heating of only outboard, aft lower skin	70	70	70	70	70	70	70	400	Upper Cap (5073)	-377	-36	
										Lower Cap (5090)	119	11	Outboard, aft lower skin
4I	Heat spar web nodes only	70	110	70	70	70	70	70	-	Upper Cap (5073)	413	39	
										Lower Cap (5090)	863	81	Compare to 4E
4J	Heat sections of y167 Rib	70	70	70	70	70	70	70	200	Upper Cap (5073)	1	0	
										Lower Cap (5090)	5	0	167 Rib Web Nodes to 200°F
4K	Heating of only outboard, aft upper skin (see 4C)	70	70	70	70	70	70	200	-	Upper Cap (5073)	2627	248	
										Lower Cap (5090)	178	17	Compare to 4C
4L	Heating of only upper spar cap nodes	70	70	70	70	150	70	70	-	Upper Cap (5073)	-5474	-516	
										Lower Cap (5090)	-343	-32	
4N	Heating of only aft upper skin (wheel well)	70	70	70	70	70	70	70	200	Upper Cap (5073)	3951	373	
										Lower Cap (5090)	-184	-17	4M plus nodes 73,95,103,116,129
M1	Mechanical load case TABR 2130 No Damage	-	-	-	-	-	-	-	-	Upper Cap (5073)	-1472	-139	
										Lower Cap (5090)	5868	554	
M2	Mechanical load case TABR 2130 Removed outboard aft upper skin	-	-	-	-	-	-	-	-	Upper Cap (5073)	-1432	-135	
										Lower Cap (5090)	5802	547	
A1	Combined heating	70	110	110	110	110	70	145	-	Upper Cap (5073)	141	13	
										Lower Cap (5090)	1549	146	
A2	Combined heating II	70	145	145	145	145	75	-	190	Upper Cap (5073)	-116	-11	Lose outboard aft upper skin (set to 70)
										Lower Cap (5090)	2388	225	Heat nodes 73,95,103,116,129 only
A3	Combined heating III	70	175	175	175	175	80	-	215	Upper Cap (5073)	777	73	
										Lower Cap (5090)	3082	291	Heat aft upper skin (wheel well) to 215
A4	Combined heating IV	70	175	175	175	175	90	-	260	Upper Cap (5073)	2122	200	
										Lower Cap (5090)	2513	237	Heat aft upper skin (wheel well) to 260

This material is PRELIMINARY information only. It is for limited distribution. DO NOT FORWARD.

Induced Thermal Strain Scenario

Presented by: Paul Parker

What is strain reaction both near and far from thermal event?

- How does strain react to distant thermal event?
- Thermal event occurs locally in structure
  - Maximum strain at thermal event boundary
  - Far field strains induced by thermal event
    - How far away, L, from thermal event does thermally induced strain field extend?
  - Strains reduce away from thermal event boundary
- Specifically focused on gage V12G9921A near panel 9 in middle of spar

This material is PRELIMINARY information only. It is for limited distribution. DO NOT FORWARD.

Temperature Readings Lag Strain Measurements

This chart represents a "snapshot" in time

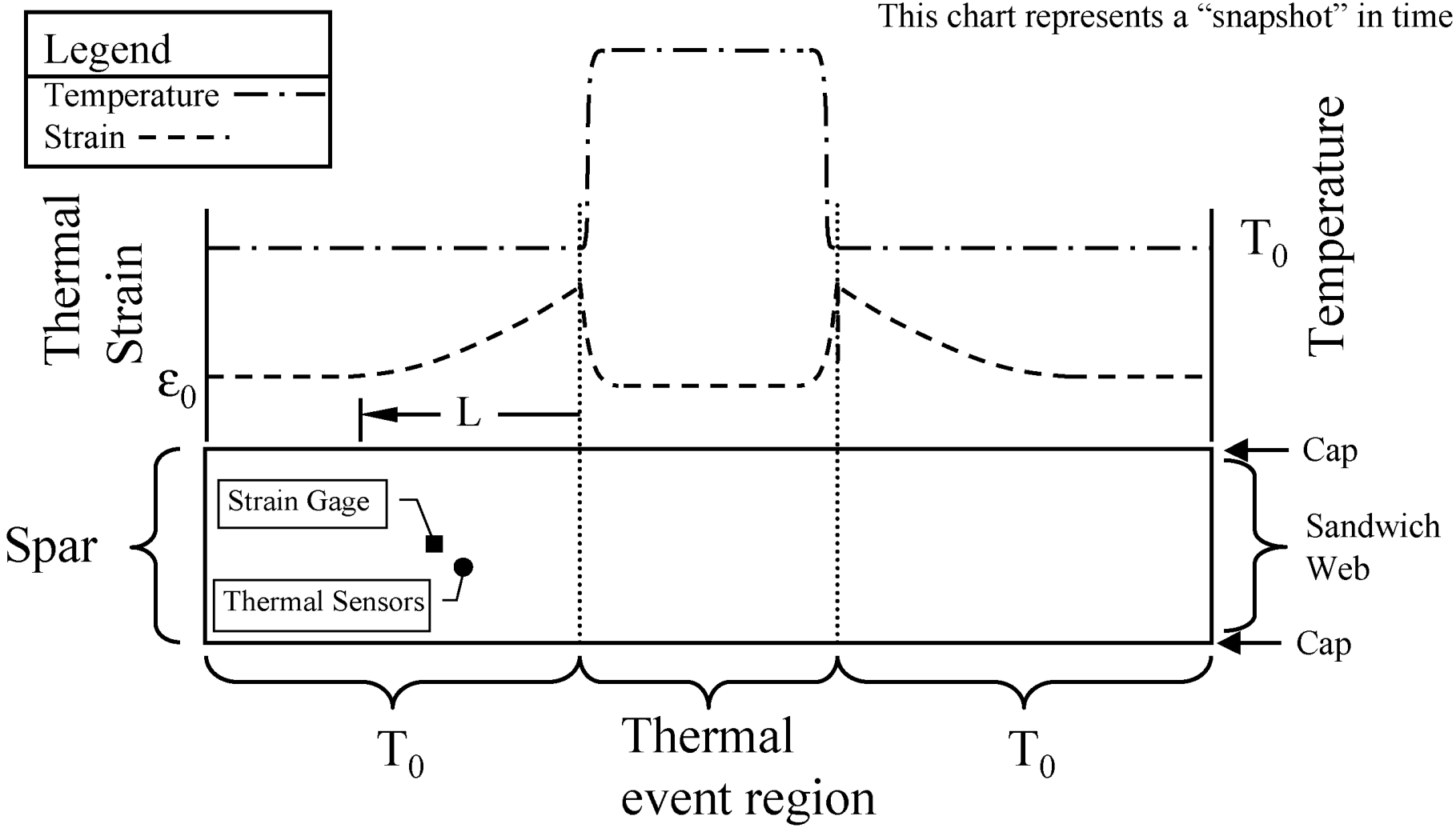

This material is PRELIMINARY information only. It is for limited distribution. DO NOT FORWARD.

Existing Model Refined for Local Region of Interest

- **Model Description**
  - **Spar model developed from existing loads model**
    - **Refined mesh on loads model in local region of interest**
    - **Incorporated temperature dependent CTE and Young's Modulus**

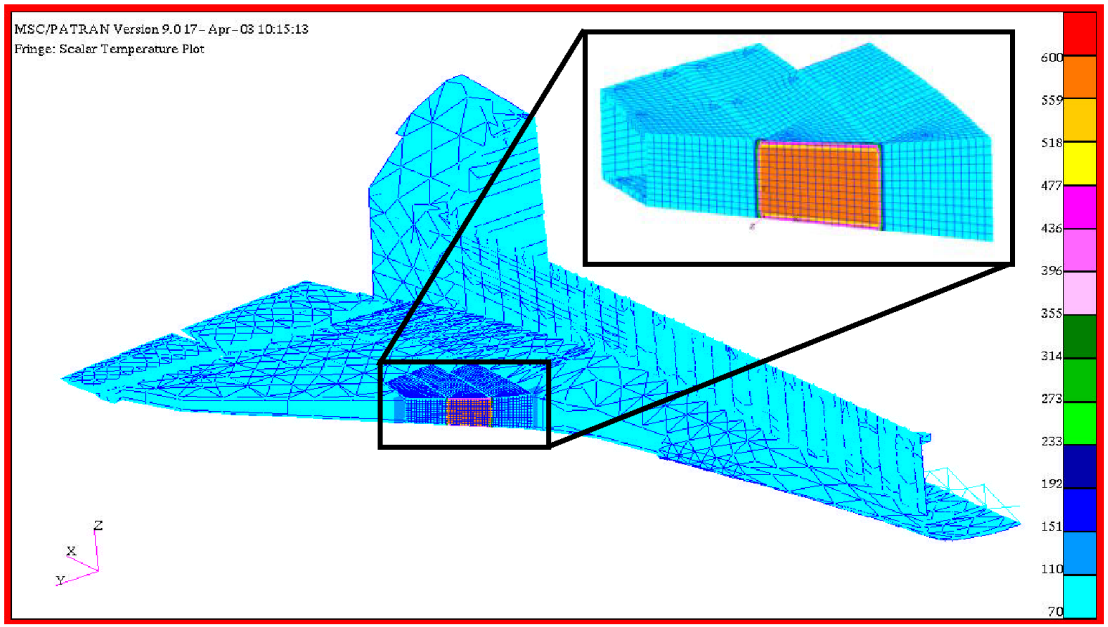

This material is PRELIMINARY information only. It is for limited distribution. DO NOT FORWARD.

Multiple Thermal Events Analyzed

- **Five thermal events analyzed**
  1. Assumed 600°F on WLE web, 400°F on spar caps, 70°F on rest of structure
  2. Assume upper half WLE sees primary heating
     - Assumed initial heating of 300°F on upper half of WLE spar web and cap
     - Assumed linear temperature distribution of 300°F to 70°F from middle of WLE web to bottom WLE cap
     - 70°F on rest of structure
  3. Continue heating upper half WLE sees primary heating
     - Assumed 600°F on upper half of WLE spar web and cap
     - Assumed linear temperature distribution of 600°F to 70°F from middle of WLE web to bottom WLE cap
     - 70°F on rest of structure

This material is PRELIMINARY information only. It is for limited distribution. DO NOT FORWARD.

Thermal Events Analyzed Continued…

- Thermal events analyzed continued…
  4. Assume burn through on upper half WLE spar web
     - Assumed 600°F on upper WLE cap, wing skin, and wing ribs up to 16 inches from WLE
     - Assumed linear temperature distribution of 600°F to 70°F from edge of burn through (middle of WLE web) to bottom WLE cap
     - 70°F on rest of structure
  5. Assume burn through on upper half WLE spar web and spar cap
     - Assumed 600°F on upper wing skin and wing ribs up to 16 inches from WLE
     - Assumed linear temperature distribution of 600°F to 70°F from edge of burn through (middle of WLE web) to bottom WLE cap
     - 70°F on rest of structure

This material is PRELIMINARY information only. It is for limited distribution. DO NOT FORWARD.

Thermal Event Temperature Distributions

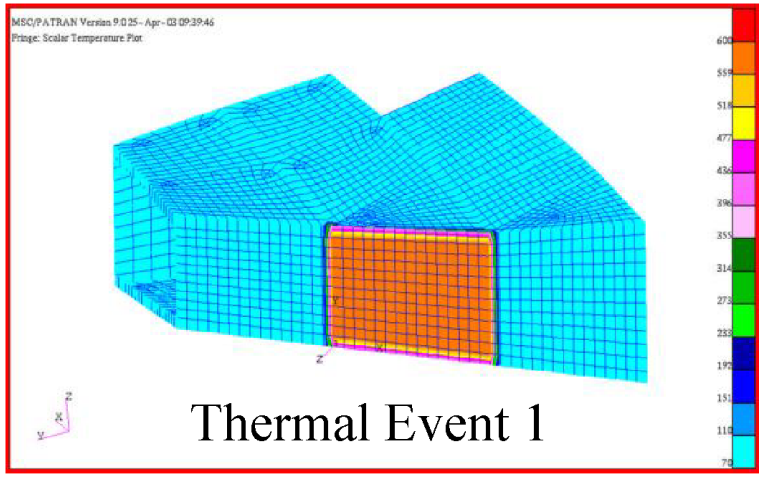

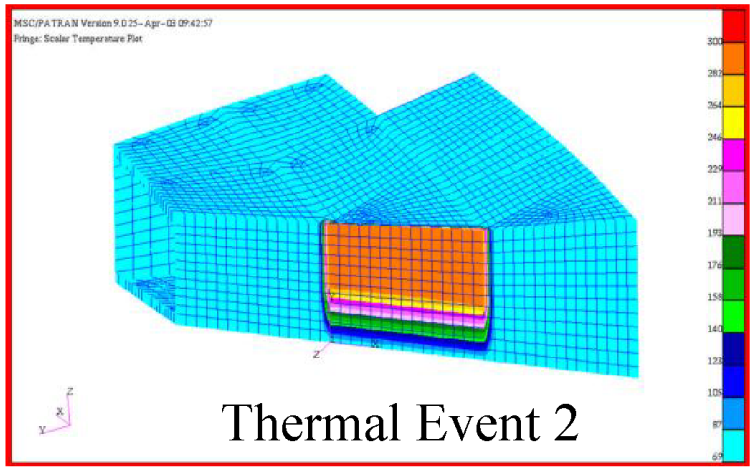

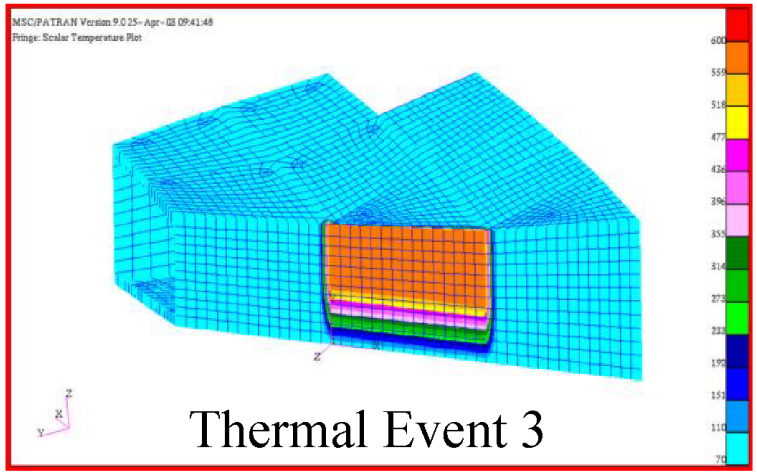

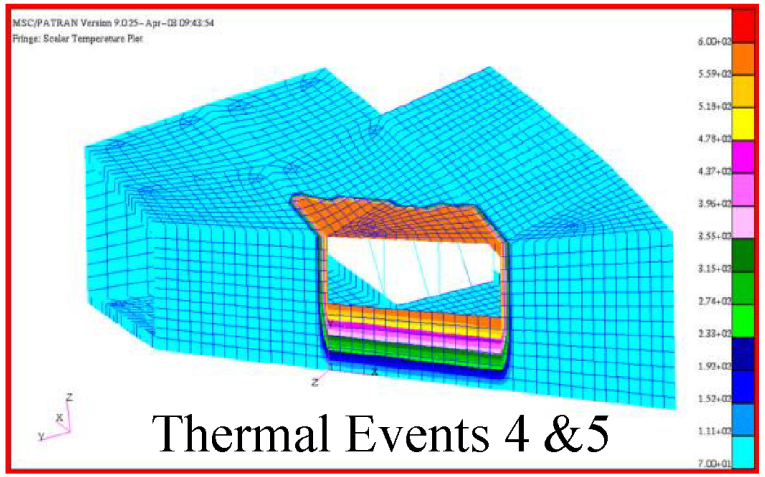

BOEING

6/4/2003
7

This material is PRELIMINARY information only. It is for limited distribution. DO NOT FORWARD.

Shear Strain Results Along Midspan of WLE Spar

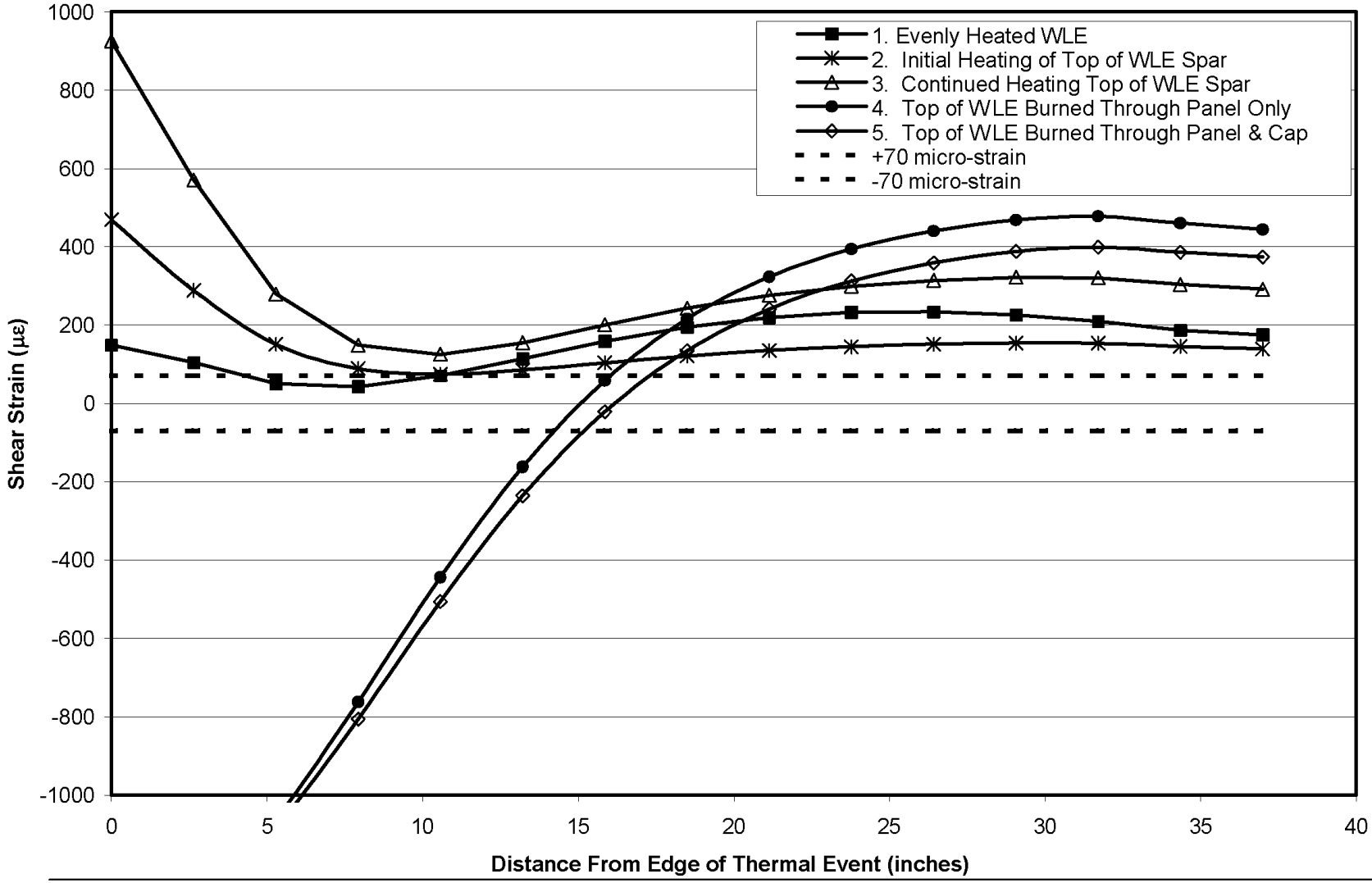

BOEING

6/4/2003

8

This material is PRELIMINARY information only. It is for limited distribution. DO NOT FORWARD.

Thermal Event Can Cause Increase in Shear Strain Magnitude

- **Results**
  - **Thermal event #1**
    - **Increase in shear strain magnitude along middle of WLE from edge of thermal event outward**
    - **Little change in strain magnitude in region outside of thermal event**
    - **No change in sign**

This material is PRELIMINARY information only. It is for limited distribution. DO NOT FORWARD.

Unsymmetric Thermal Event Creates Significant Shear Strain Magnitude Increase

- **Results Continued…**
  - **Thermal event #2**
    - **Significant Rise in shear strain magnitude near thermal event boundary**
    - **Reduction in shear strain magnitude with increased distance from thermal event boundary**
      - Shear strain magnitude changes little at distances ≥ 18 inches from thermal event boundary
    - **No change in sign**
  - **Thermal event #3**
    - **Significant rise in shear strain magnitude near thermal event boundary**
    - **Reduction in shear strain magnitude with increased distance from thermal event boundary**
      - Shear strain magnitude changes little at distances ≥ 18 inches from thermal event boundary
    - **Similar trend to initial heating, magnitude of strain increases**

This material is PRELIMINARY information only. It is for limited distribution. DO NOT FORWARD.

WLE Burn Through Can Cause Shear Strain Sign Reversal

- **Results Continued…**
  - **Thermal event #4**
    - **Reversal in sign of shear strain**
      - For distances ≤ 15 inches from thermal event boundary strain sign is negative
    - **Shear strain from 15 to 19 inches is less than undamaged structure**
    - **Significant rise in shear strain magnitude near thermal event boundary**
    - **Decrease in shear strain magnitude with increased distance from thermal event boundary**
      - Shear strain magnitude changes little at distances ≥ 26 inches from thermal event boundary

This material is PRELIMINARY information only. It is for limited distribution. DO NOT FORWARD.

Thermal Event #5 Results

- **Results Continued…**
  - **Thermal event #5**
    - **Further reduction of shear strain from thermal event #4**
    - **Reversal in sign of shear strain**
      - For distances ≤ 16 inches from thermal event boundary strain sign is negative
    - **Shear strain from 16 to 23 inches is less than undamaged structure**
    - **Significant rise in shear strain magnitude near thermal event boundary**
    - **Decrease in shear strain magnitude with increased distance from thermal event boundary**
      - Shear strain magnitude seems to be constant at distances ≥ 26 inches from thermal event boundary

This material is PRELIMINARY information only. It is for limited distribution. DO NOT FORWARD.

Burn Through Needed for Strain Sign Reversal

- **Possible scenario**
  - **Partial breech in WLE TPS allows plasma impingement on WLE spar**
    - **Causes general temperature increase on WLE panel and cap**
    - **Shear strain readings begin to increase**
  - **Upper WLE panel and spar subjected to primary heating**
    - **Creates temperature gradient on WLE spar from top to bottom**
    - **WLE shear strain gage readings continue to increase**
  - **Upper WLE spar panel burn through**
    - **Shear strains are reduced in region around thermal event causing a strain sign reversal**
      - Panel burn through relieves thermal stresses

This material is PRELIMINARY information only. It is for limited distribution. DO NOT FORWARD.

Scenario Description Overlay With Nominal Strain Gage Data

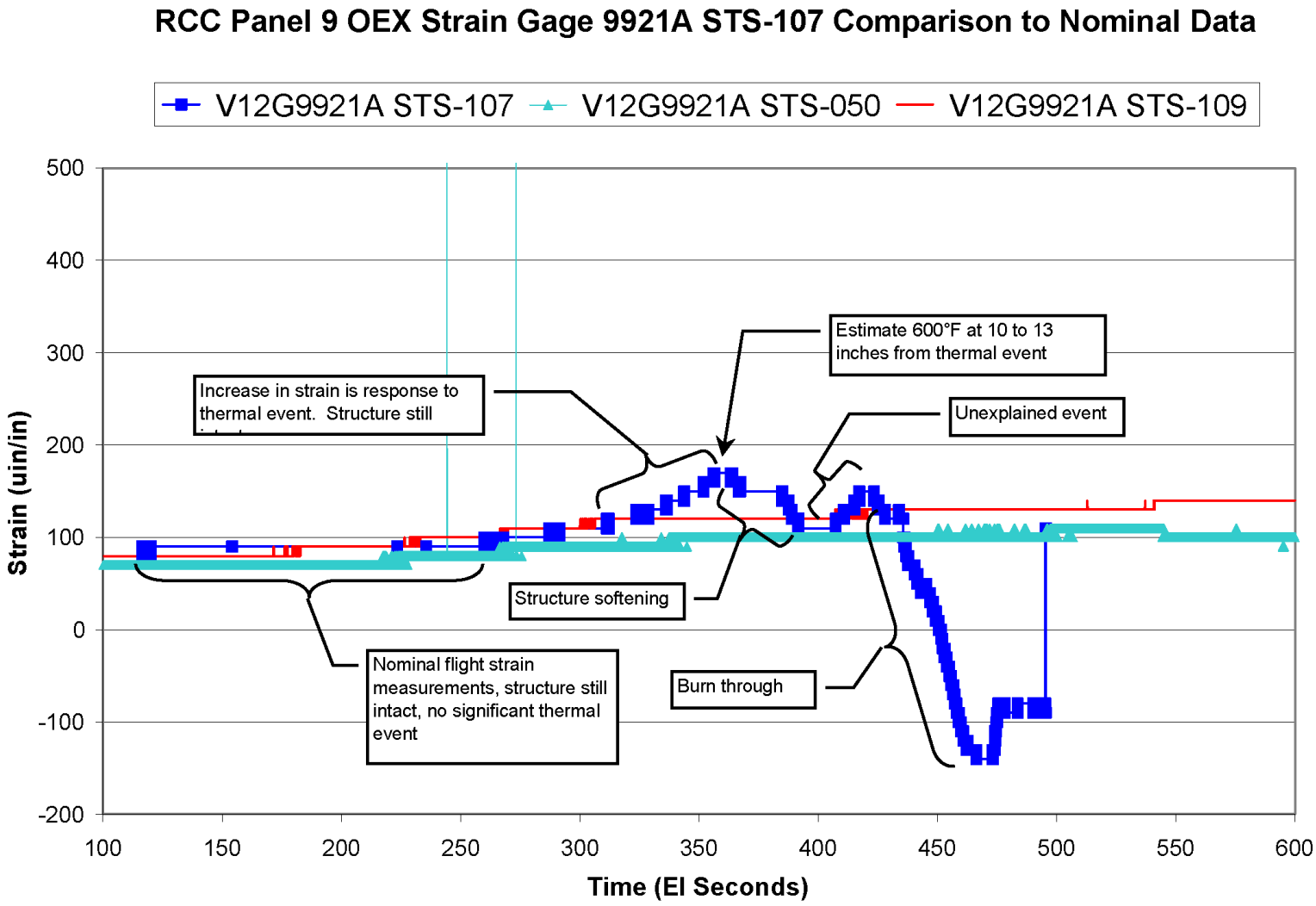

This material is PRELIMINARY information only. It is for limited distribution. DO NOT FORWARD.

Scenario Description Overlay With Thermal Flight Data

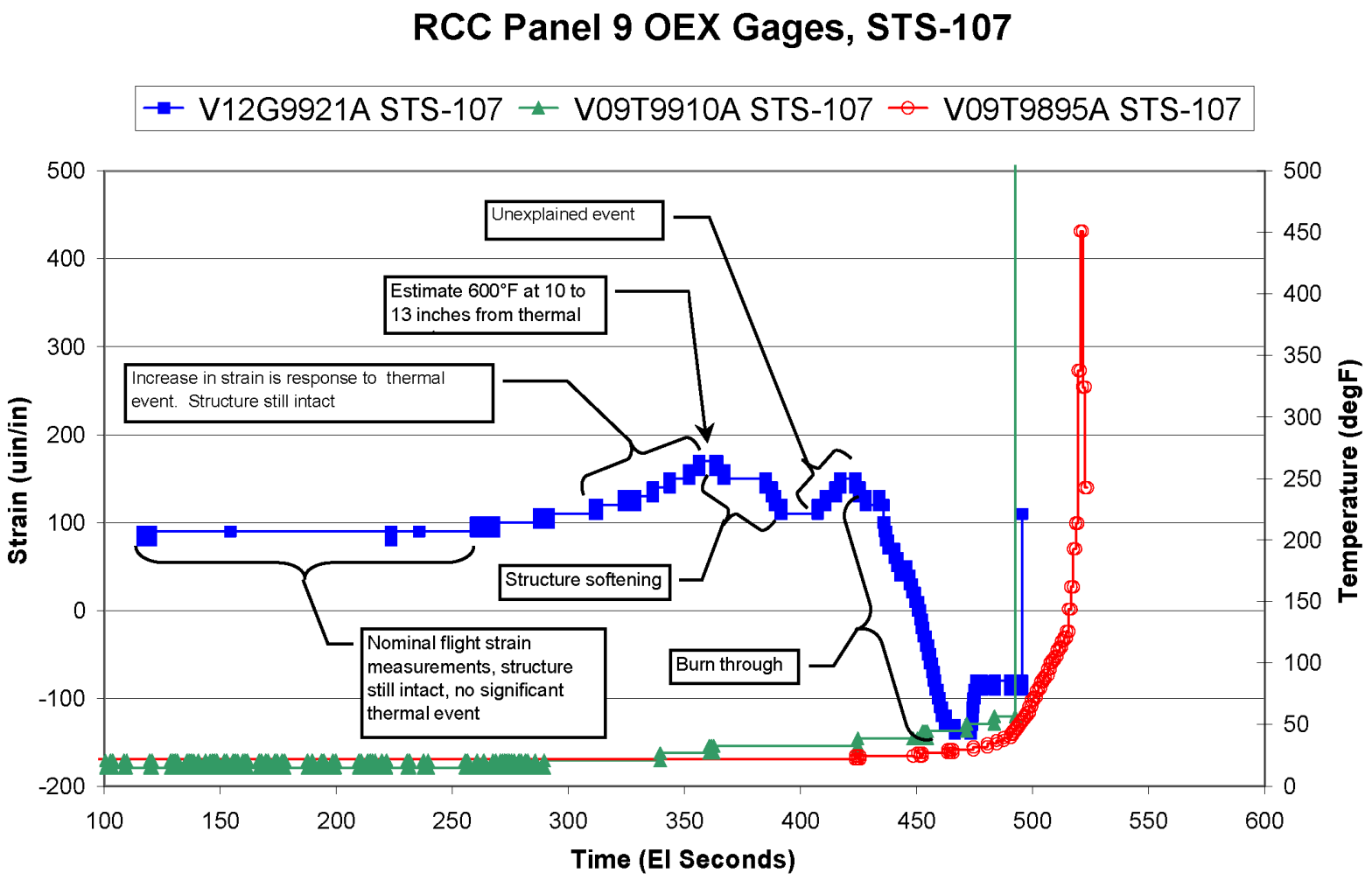

This material is PRELIMINARY information only. It is for limited distribution. DO NOT FORWARD.

Backup

This material is PRELIMINARY information only. It is for limited distribution. DO NOT FORWARD.

Shear Stress Results Along Midspan of WLE Spar

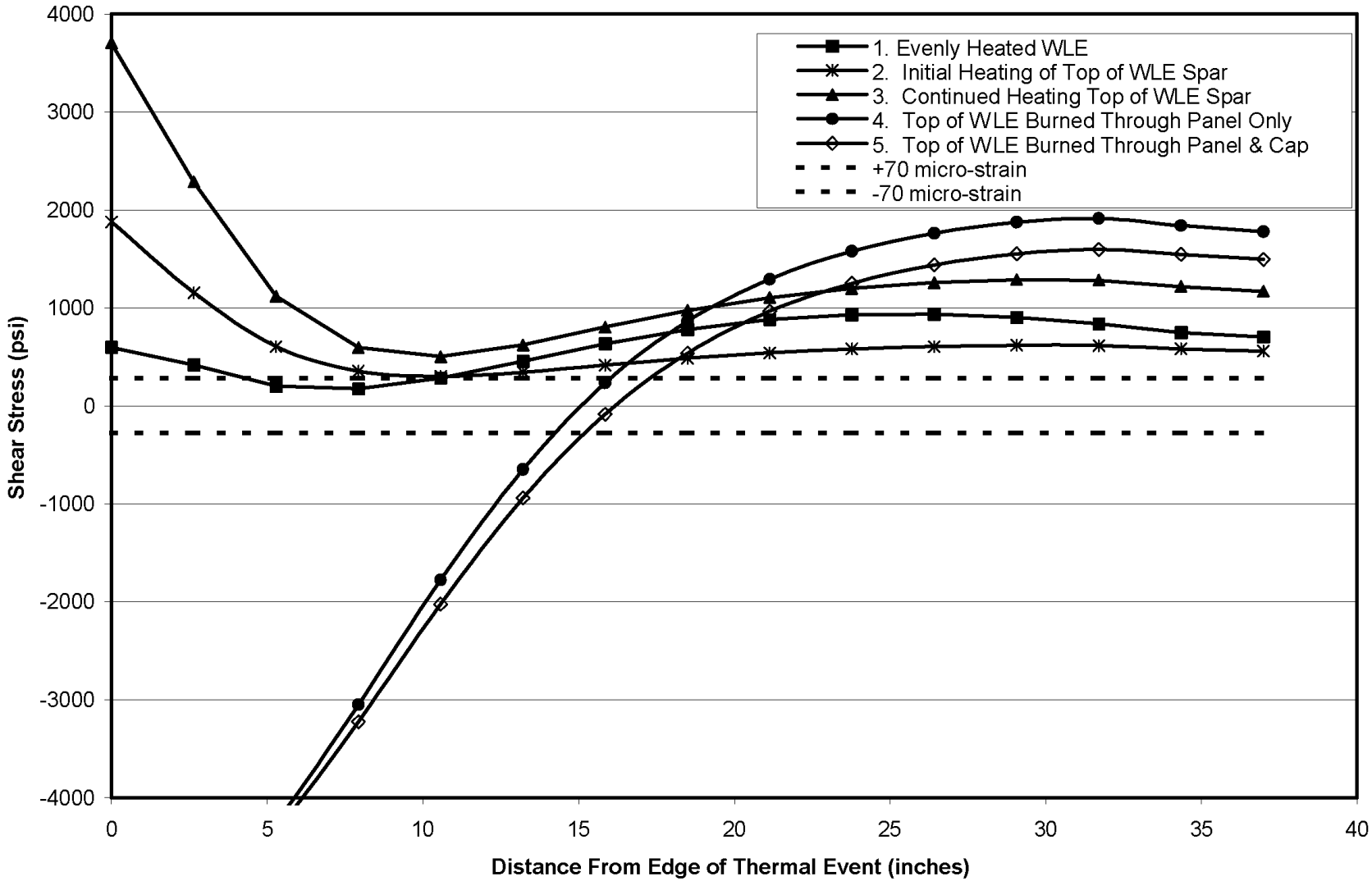

BOEING

6/4/2003

17

This material is PRELIMINARY information only. It is for limited distribution. DO NOT FORWARD.

THIS PAGE INTENTIONALLY LEFT BLANK

Volume IV
Appendix F.2
Follow the TPS

This Appendix presents an analysis to confirm or refute the following hypothesis put forth by the Columbia Accident Investigation Board during the launch of STS-107 Mission: A briefcase-sized piece of External Tank foam struck the RCC left wing leading edge system, compromising the RCC. During entry, the damage to the RCC led to structural failure of the wing, the tragic loss of Columbia, and the STS-107 crew.

THIS PAGE INTENTIONALLY LEFT BLANK

"Follow the TPS": An Analysis of What Occurred to the Thermal Protection System (TPS) During the Flight of Shuttle Columbia on STS 107

J. O. Arnold [†], H. E. Goldstein [‡], and D. J. Rigali [λ]

Executive Summary

This appendix presents an analysis to confirm or refute the following hypothesis put forth by the Columbia Accident Investigation Board (CAIB): During launch of the Space Transportation System (STS) 107 Mission, a briefcase-sized piece of External Tank (ET) foam struck the Reinforced Carbon-Carbon Left Wing Leading Edge Subsystem (RCC LW LESS), compromising the RCC. During entry, the damage to the RCC led to structural failure of the wing, the tragic loss of Columbia and the STS 107 crew.

The focus of this analysis was on what happened to the Thermal Protection System (TPS). The analysis supports the hypothesis and identifies the probable location of the breach. The analysis assumed that the ET foam strike was the initiating event. Other investigators have shown by test and analysis that the foam strike could have caused a breach in the RCC. Comparison of events following from the hypothesis to observations from flight data, debris forensics, ground test and analysis strongly suggests that the breach was in the lower part of RCC Panel 8, and that it existed at entry interface (EI).

Key information, in temporal order, from flight observations include: **Ascent, post foam strike**: Modular Auxiliary Data System/Orbiter Experiments (MADS/OEX) data from a thermocouple mounted behind the leading edge wing spar, behind Panel 9, recorded off-nominal temperature increases during ascent. **Entry**: MADS/OEX data from four sensors show the progression of damage is from the RCC toward the aft of the vehicle. Later, the thermocouple on the spar, behind Panel 9, recorded an abrupt temperature increase at Entry Interface + 487 seconds, interpreted to be caused by superheated air penetrating the leading edge wing spar. Analysis by NASA shows that these observations can be accounted for by the presence of a hole, 6 -> 10 inches in diameter, in the lower portion of RCC Panel 8. Greater than normal temperatures subsequently measured on the Orbital Maneuvering Systems (OMS) pod correlates with ground based observations of debris leaving Columbia. Later, a photograph was taken from the Starfire facility at Kirtland Air Force Base showing left wing damage consistent with the hypothesis.

Compelling evidence to support the hypothesis comes from the debris from Columbia. Study of the debris revealed significant damage in the LW RCC Panel 8/9 area. This included ablation, or "sharpening" of the very durable RCC and melting of high temperature metal fixtures and insulation, internal to the WLESS, believed to be caused by prolonged exposure to a superheated airflow. Arc jet simulations of RCC in such a superheated air stream support this conclusion. Flow out of a slot in the lower juncture between LW RCC Panels 8 and 9 caused severe erosion and flow patterning on the carrier panels below RCC Panel 9. Chemical analysis of "slag" on the debris shows "layering" that correlates with the hypothesis.

The authors believe it is quite likely that the breach caused by the foam strike was a hole of at least 6 –> 10 inches in diameter in the lower part of RCC Panel 8. Finally, it is noted that it is unreasonable to assign blame to the TPS for the tragic accident of Columbia. The total TPS for the shuttle has performed admirably during all of the STS flights (including STS 107) in the environments for which it was designed. Upgrades to the TPS being planned will make it better. The primary technical issue for the STS 107 accident is the integrity of the ET foam during launch.

[†] Senior Scientist, University of California, Santa Cruz and Retired Chief, Space Technology Division, NASA Ames Research Center and Fellow, AIAA.
[‡]Consultant, Valador, Consultant, Research Institute for Advanced Computer Science (RIACS), Retired Chief Scientist, Space Technology Division and Retired, Chief, Thermal Protection Systems Branch, NASA Ames Research Center and Fellow, AIAA.
[λ]Consultant, Valador, Retired Director of Aerospace Systems Development Center, Sandia National Laboratory.

Introduction

A hypothesis, presented by the Columbia Accident Investigation Board (CAIB) chair, Admiral H. Gehman, is that the tragic loss of the crew of STS 107 and the Space Shuttle Columbia was caused by a briefcase-sized piece of External Tank (ET) foam insulation striking the leading edge of Columbia's left wing (LW) about 82 seconds after the lift off of Space Transportation Systems (STS) 107 mission. The hypothesis assumes this strike compromised the thermo-structural wing leading edge made of reinforced carbon-carbon (RCC). During re-entry on February 1, 2003, superheated air entered a breach in the wing leading edge subsystem (WLESS), eventually leading to structural failure of the wing, break-up of the vehicle and loss of the crew.

Soon after the CAIB investigation began, board member G. Scott Hubbard assigned the authors of this appendix to "Follow the Thermal Protection System (TPS)" to develop supporting and/or refuting evidence for the aforementioned hypothesis (among others). Within the context of the charter of CAIB Group 3, the assignment was to look exclusively at "what happened to the TPS" during the flight, while those from other groups focused on issues such as aging or maintenance problems of the TPS that might have been the root cause of the problem.

Detailed analysis by NASA (References 1 and 2) of the launch imagery and comprehensive Computational Fluid Dynamics (CFD) simulations indicate that the area struck by the ET foam was on the LW LESS in the lower RCC Panel 5-8 areas. Tests (Reference 3) at Southwest Research Institute have been conducted where projectiles of ET foam (mass on the order of 1.7 pounds, sizes the order of a briefcase) were fired at speeds of around 770 ft/sec, impacting full-scale wing leading edge components to assess how much damage such a strike could inflict. These tests were designed with the help of newly developed physics-based codes, which were also used to interpret the results. These results show that such an impact does cause severe damage to the RCC. Observed damage included cracking and displacements of the panels and seals between them (T-Seals), as well as the formation of holes as large as 16 inches by 16 inches.

Furthermore, important data obtained during the flight of STS 107 from the Modular Auxiliary Data System (MADS)/Orbiter Experiments (OEX) were secured through the recovery of a magnetic tape in the Columbia debris. This information (Reference 4) has provided important facts regarding the sequence of events occurring during the STS 107 entry. Only the key MADS/OEX data establishing the temporal evolution of heating events is discussed herein.

Recovered debris from Columbia revealed significant damage in the RCC Panel 8/9 area. This included heavy ablation, or "sharpening" of the very durable RCC, and melting of metal fixtures and insulation, internal to the WLESS. Significant melting of LESS RCC mounting hardware is observed only in the Panel 8/9 area of the left wing. This debris evidence is believed to have occurred during exposure to a superheated flow environment, internal to the LW LESS, lasting for hundreds of seconds. Arc jet simulations (References 5, 6 and 7) of RCC in such a superheated air stream support this conclusion.

In the sections that follow, the timeline of events, analysis of key OEX data, aerothermodynamics/thermal analysis and debris forensics are compared to the hypothesis. The preponderance of evidence leads to the conclusion that the aforementioned hypothesis is what truly happened: An ET foam strike during launch created a breach in the LW LESS in the area of the lower RCC Panel 8. The breach was present at the Entry Interface (EI). Superheated air was ingested into the WLESS, melted through the leading edge spar, introduced hot gas into the wing box, weakened the structure and led to the loss of Columbia and the STS 107 crew.

Normal Entry Environment

In order to understand the function and need for the Shuttle's TPS, a brief review of the Shuttle reentry environment is discussed herein. Figure 1, supplied by NASA, shows two important aspects of the expected STS 107 entry profile: geodetic altitude versus Greenwich Mean Time (GMT) and normalized entry heating versus GMT. Entry was defined to begin at an altitude of 400,000 ft at GMT 13 hours, 44 minutes and 09 seconds (13:44:09). As can be seen from Figure 1(a), the time to descend from EI to 200,000 ft is approximately 15 minutes. During this period, Columbia passed over the coast of California, heading for an expected landing at the Kennedy Space Center (KSC), executing one roll to the right and one roll to the left during descent. Columbia entered as expected at a nominal angle of attack of 40 degrees, with its black underbelly facing into the wind. This maneuver and the rather blunt nose cap and wing leading edges of the Shuttle have the effect of reducing aeroconvective heating (blunt body concept, Reference 8).

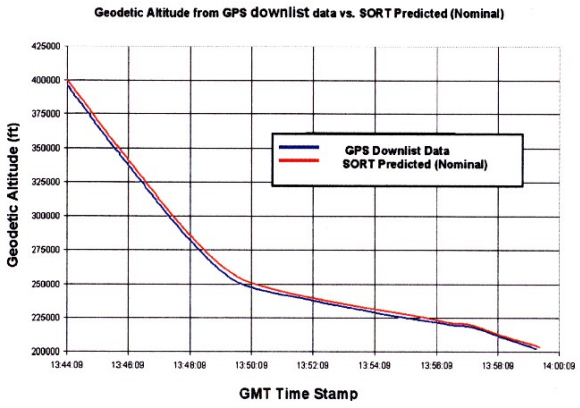

Figure 1(a): Normal Entry: Geodetic Altitude vs. GMT. Entry Interface (EI) at 400,000 ft. Angle of Attack: 40 Degrees.

Figure 1(b) shows a plot of expected heating rates, normalized to the stagnation point near the nose of the vehicle versus GMT. Here, one can see that the heating rate is nearly constant at a maximum for about 9 minutes. The heating rate on the landing gear door area in the wing is considerably lower than that at the nose of the vehicle. Color-coding on the figure shows TPS surface temperatures caused by these heating rates.

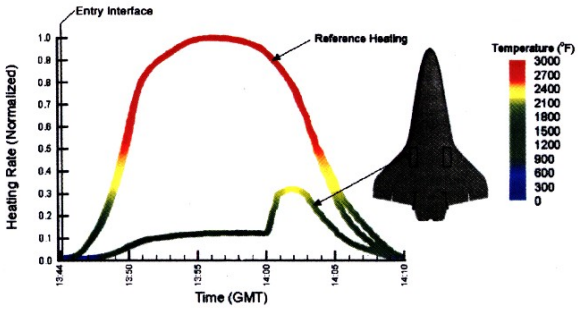

Figure 1(b): Normal Entry: Normalized Heating Rates vs. GMT. Entry Interface (EI) at Altitude: 400,000 ft, Angle of Attack: 40 Degrees.

Figure 2, based on Computational Fluid Dynamics (CFD) (Courtesy of NASA JSC J. Caram/NASA Ames J. Brown and D. Prabhu) gives one a feel for the vehicle environment experienced and flow field about the Space Shuttle during a "nominal entry", i.e., no damage to the vehicle. These results are state-of-the-art real-gas CFD, Reynolds Averaged Navier-Stokes solutions, assuming a laminar boundary layer. Real-gas effects include chemically reacting flows among the constituents; N_2, O_2, NO, N and O. At these conditions, there is nearly complete disassociation of diatomic oxygen (O_2) and formation of NO. A very slight amount of ionization occurs in reality. This is not accounted for in the solutions, but this has little effect on entry heating. TPS response is accounted for including realistic wall catalytic effects and surface emissivity. Shuttle surfaces tend to be non-catalytic, meaning that the atomic oxygen and nitrogen in the boundary layer do not recombine, reducing the sensible heat into the TPS. Full detail of the code used for this work and its validation against ground and flight (Shuttle) data can be found in Reference 9. The code used, GASP (commercially available by Aerosoft, Inc), is one of several codes used by NASA in the analysis of the Columbia accident. Results from other codes, including LAURA (Reference 10), developed by NASA Langley, will be discussed later.

Figure 2(a) shows temperature contours within the shock layer that forms about the Space Shuttle during entry. Flow is from lower left to upper right. A view in the pitch plane at the centerline of the vehicle is shown for conditions at 227,424 ft and an angle of attack of 39.59 degrees. The outer, blue envelope representing free stream or ambient air is outside of the shock front, within the computational grid. The rapid change in color represents the shock front. One can see that gas temperatures in the forebody, nose region of the shock layer, behind the shock front exceed 20,000 °F (red -> magenta). As the gases expand in the shock layer, cooling occurs, and the forebody gas temperatures drop into the area of 12, 000 -> 9000 °F (yellow -> green) along the windward side or underbelly of the vehicle. In the leeward portion of the flow, gas temperatures are much cooler (4,000 – 2,000 °F) as shown by the blue-green color.

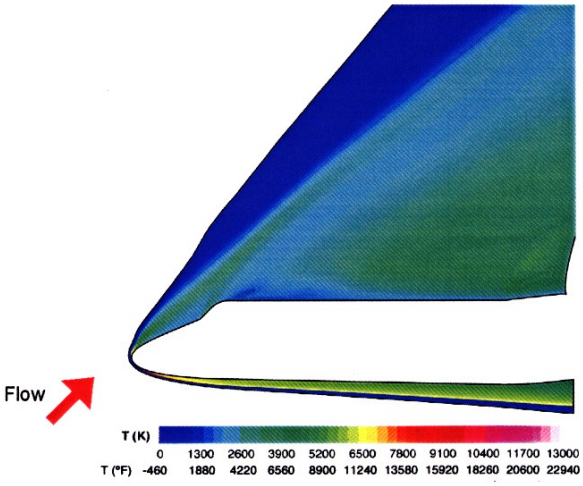

Figure 2 (a): Gas Temperatures from CFD Solution Pitch Plane, Near Peak Heating. Angle of Attack: 39.59 degrees, Altitude: 227,424 ft (69.319 km), Mach: 22.91, Velocity: 22,505 ft/sec (6.8595 km/sec) at 13:54:24. Reynolds Number based on length: 1.18 million.

Owing to cooling of the shock layer gases in the boundary layer formed over the Space Shuttle and the TPS material response, the surface of the vehicle operates at temperatures (denoted by T_w) considerably lower than those in the shock layer. These data are displayed in Figure 2 (b). These temperatures depend upon the response of the TPS and typically range from 3,000 - 2,900 °F on the nose and in the area of the shock-shock interaction on the wing leading edge. The shock-shock interaction arises from the merging of the body shock with the shock layer formed on the wing leading edge. This merging causes enhanced pressure and aeroconvective heating in this region.

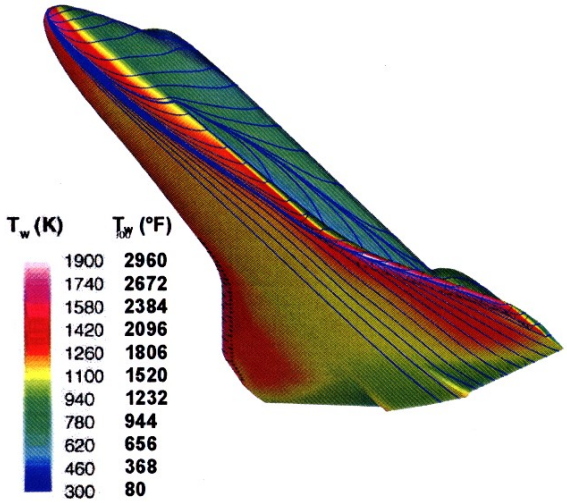

Figure 2 (b): CFD Solution for Surface Temperatures (T_w) with Streamtraces. Conditions as in Figure 2 (a).

From Figure 2 (c) displaying surface pressure, it is noted that the stagnation pressure near the vehicle's nose is 75 pounds per square foot (psf), dropping down to about 34 - 24 psf at the mid fuselage and aft fuselage locations, respectively. The shock-shock area, where the nose shock intersects the wing, runs at higher pressures (64 psf) than on the mid-belly region. Pressures on the top surfaces of the wings and fuselage sidewalls are near or below the free stream static pressure of 0.12 psf.

For comparison, Table 1 compares the gas and surface conditions for the Space Shuttle's entry environment at altitude to those on the surface of the Earth. Temperatures in the free stream are quite cold while those in the gas and on the vehicle's surface are extremely hot. Pressures are quite low, especially in the free stream at altitude as compared to near sea level (Palo Alto, California).

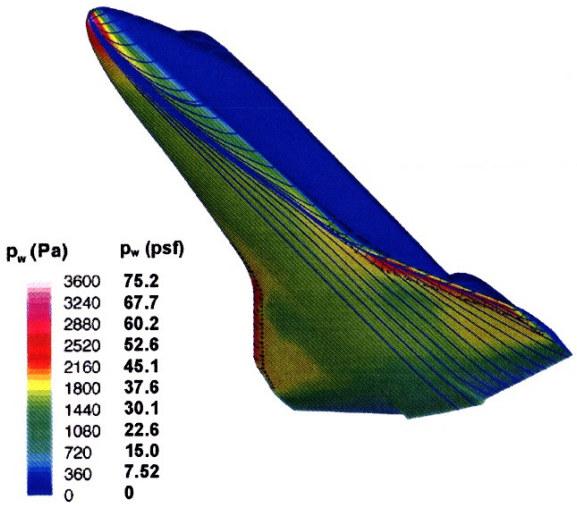

Figure 2 (c): Surface Pressure with Streamtraces. Conditions as in Figure 2 (a).

Location	Gas Pressure (psf)	Gas Temperature (°F)	TPS Temperature (°F)	Gas Speed (fps)	Number density (parts/cc)
Freestream	0.12	-61	-	22,400 (Mach 23)	$2x10^{15}$
Nose (stagnation)	75	22,000	2600	0	$1x10^{16}$
Mid-fuselage	34	12,500	1600	16,900 (Mach 3)	$1x10^{16}$
Aft fuselage	24	12,000	1350	16,600 (Mach 3)	$1x10^{16}$
Palo Alto, CA	2116	59 *Assuming no ionization*	- *Assuming adiabatic back wall*	-	$2.5x10^{19}$

*Local Mach number in flow

Table 1: Comparison of Vehicle Environmental Conditions at Peak Heating. Mach Number (Mach 23) to Ground Conditions.

Figure 3 is based on the CFD results from Figure 2. Here one sees zoom-in views of wall temperature and surface pressure distributions in the left wing leading edge area. Also shown are RCC panel locations. As can be seen, there is an attachment line along the wing leading edge where the flow divides, part going over the wing and part going below the wing. In both instances the flow is expanding into lower pressure locations. Along and near the attachment line, the principal direction of the flow at the surface is along the wing, in the outboard direction.

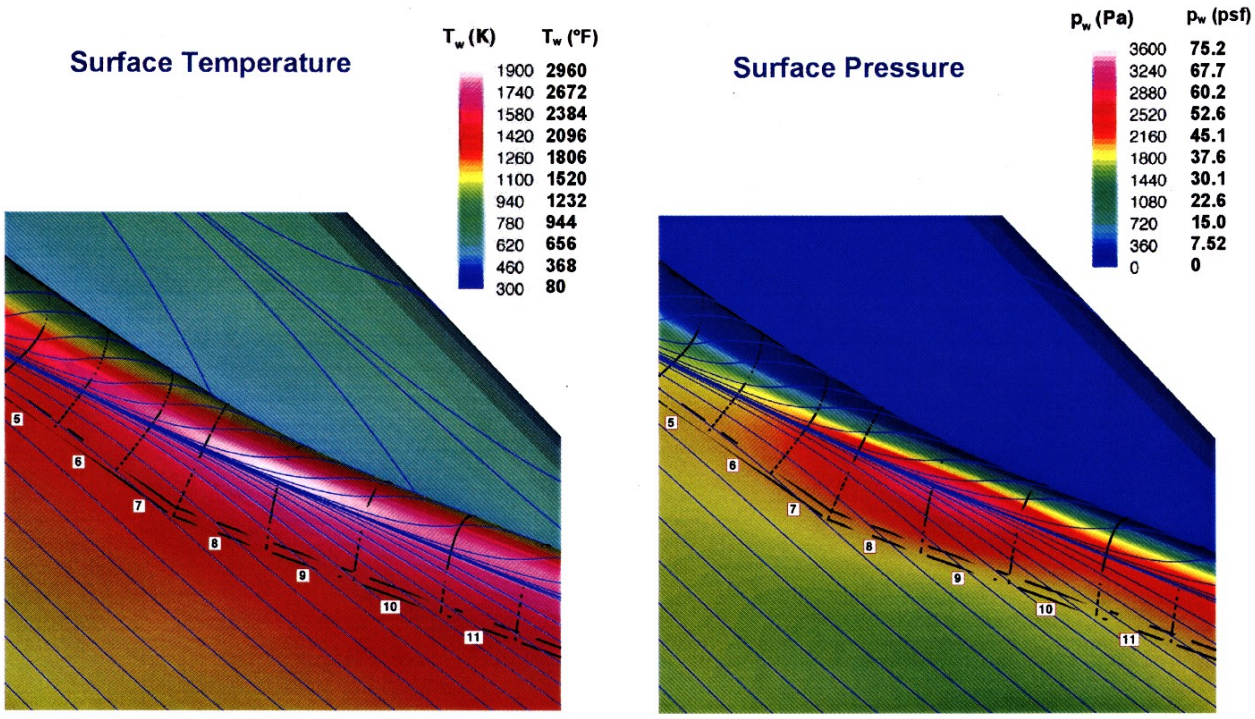

Figure 3: Zoom-in on CFD Solutions from Figure 2 in the Regions of RCC Panels 5-11.

Thermal Protection System TPS

From the previous section, one can understand the formidable problem facing designers of the Space Shuttle. A vehicle made of aluminum with its melting point of about 1000 °F would rapidly melt when exposed to the superheated air in the shock layer. Previous attempts to build a metal-skinned entry vehicle called Dynasoar using a hot structure approach had failed. The approach taken by the Shuttle Program in the late 1970's brilliantly solved this problem by dividing the problem into two parts that could be addressed independently:

(1) Build a cool aluminum structure based on existing aircraft technology.
(2) Solve the thermal problem with an external insulation tile system for acreage and a Carbon - Carbon hot structure approach for the nose cap and wing leading edges.

Figure 4 overviews the Shuttle TPS system with selected images from a comprehensive presentation (Reference 11) of the Shuttle Thermal Protection System TPS by NASA JSC TPS personnel, J. Kowal and D. Curry, delivered to the CAIB on February 10, 2003. As seen, the Shuttle's aluminum skin and structure are protected by a TPS configuration of RCC, a thermostructural material capable of reuse temperatures to 3,000 + °F on the wing leading edges and nose cap; lightweight ceramic tiles with multi–use capabilities to 2,300 °F; and two types of blankets, Advanced Flexible Reusable Surface Insulation (AFRSI) capable of reuse temperatures to 1200 °F and Flexible Reusable Surface Insulation (FRSI) capable of reuse temperatures to 800 °F.

RCC consists of a carbon substrate made of graphitized rayon fabric impregnated with phenolic resin and pyrolized to convert the phenolic into the carbon matrix. To protect the carbon substrate from hot oxygen, a silicon carbide (SiC) coating of 0.02 - 0.04 inches thick on all surfaces is provided. It is over coated with silica, formed from Tetraethylorthosilicate (TEOS) and a Type A sealant of sodium silicate glass.

The Reusable Surface Insulation (RSI) tiles are made primarily from very fine silica fibers sintered together in densities of 9 to 22 lbs/ft^3. Because of their low density and fibrous nature, they are extremely good insulators. RSI tiles are coated with a thin (0.012 inch) borosilicate glass coating called Reaction Cured Glass (RCG) which reradiates the incoming heat back into space. The design requirements for these tiles are that the bond line temperatures not exceed 350 °F at any time and that they are reusable for 100 flights.

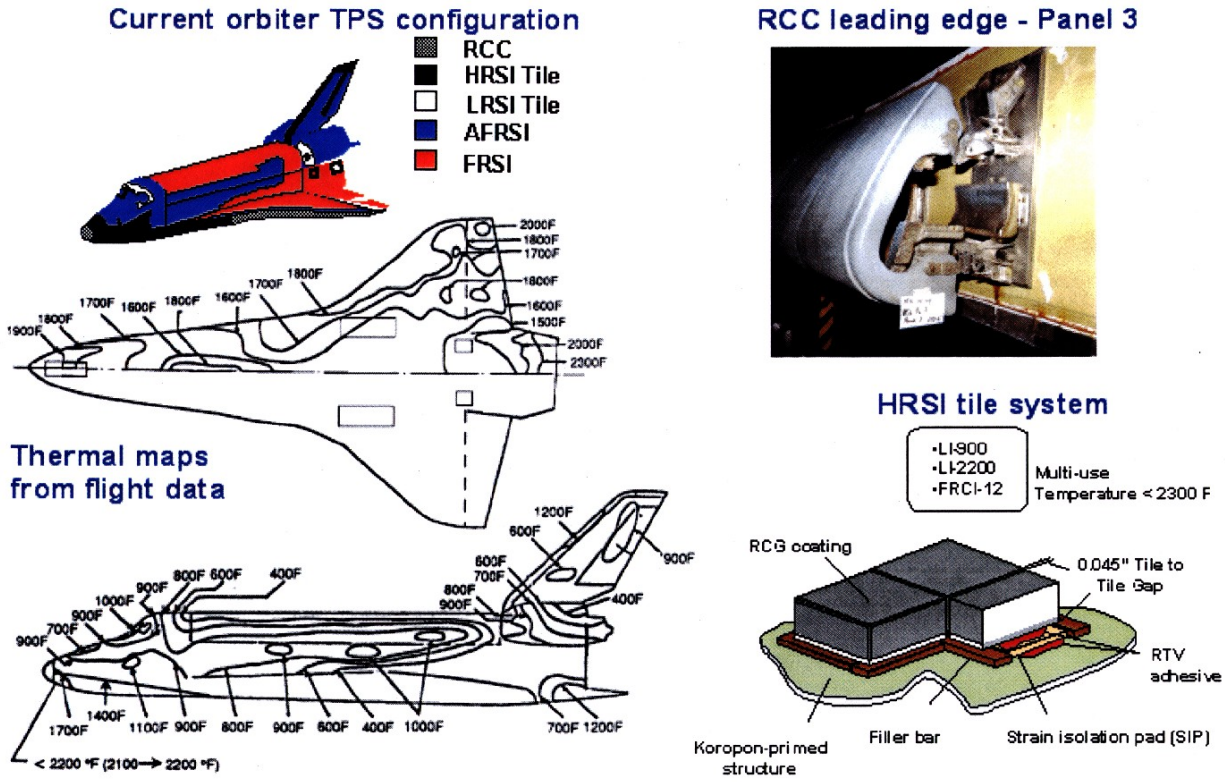

Figure 4: Overview of the Shuttle Thermal Protection System.

Thermal maps obtained from Orbiter Experiments (OEX) data early in the Shuttle Program, are shown in Figure 4. Also shown is a depiction of how the tiles are bonded to the Shuttle's aluminum skin. A photograph of a RCC wing panel (Panel 3) with the insulation, mounting attachments and the aluminum wing spar is also shown. Not used in the Panel 3 area are metal beams that span the open end of the RCC, from the top to bottom attachment points. These spanners are used in the Panel 8/9 area to provide additional strength. Note that there is a cavity behind the RCC and insulation between the RCC and the wing spar. This insulation protects the spar against radiation from the inside of the RCC. Not shown in this picture is the insulation that covers all internal metal surfaces ensuring that no structure is exposed to the radiation from the RCC. RCC has a very high thermal conductivity and therefore its inside surface is nearly as hot as the outer surface exposed to aeroconvective heating. During reentry, at an angle of attack of 40 degrees, the lower portion of the RCC panels receive most of the aeroconvective heating. The higher temperature lower panels are cooled by internal radiation through the cavity behind the RCC to the cooler top of the panels, which in turn radiates off to space. There are 22 RCC panels on each wing, and the gaps between them are covered with flush-mounted seals, called T-Seals, owing to the cross-sectional shape of the seal.

To understand the events that occurred on STS 107, to be discussed below, it is important to note that the RCC-LESS cavity is vented. The venting is accomplished by a gap, ranging in width from 0.065 to 0.164 inches between the upper back edge of the RCC panels and the upper wing tiles. This gap runs the entire length of all RCC panels, giving a total vent area of 47 to 74 square inches depending on the actual gap widths. The smaller area corresponds to using the minimum allowable, installed gap width requirements and the larger area corresponds to using the maximum allowable, installed gap width requirements. Details of the gap design and width specifications are shown in Figure 5. The location of the gap was chosen because of the low heating rates and pressures that exist there as listed in Table 2. As can be seen, the pressure ratio peaks at RCC Panel 10 and falls off gradually in both the inboard and outboard directions. The fluid physics of the wing flow provides an extremely large driver pressure differential for a breach through the wing leading edge as illustrated by these pressure ratios.

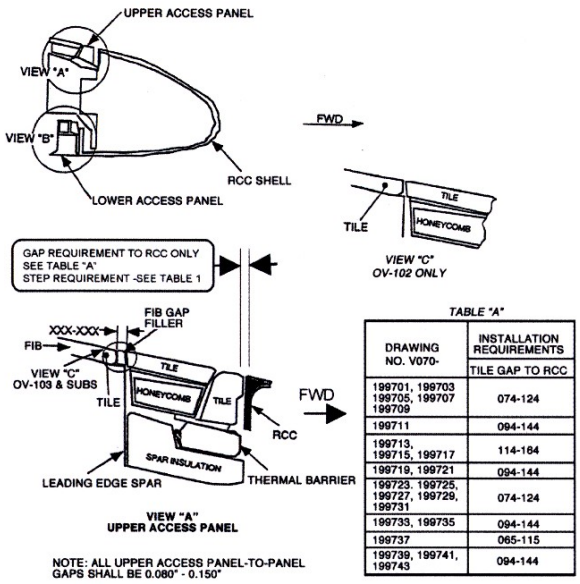

TABLE "A"

DRAWING NO. V070-	INSTALLATION REQUIREMENTS
	TILE GAP TO RCC
199701, 199703 199705, 199707 199709	074-124
199711	094-144
199713, 199715, 199717	114-164
199719, 199721	094-144
199723, 199725, 199727, 199729, 199731	074-124
199733, 199735	094-144
199737	065-115
199739, 199741, 199743	094-144

Figure 5: Details of Wing Leading Edge Subsystem Vent Design. Orbiter Vehicle (OV) 102 is named Columbia.

RCC Panel	Pvent/Panel 9 Peak	RCC Panel	Pvent/Panel 9 Peak
1	0.0048	12	0.0203
2	0.0052	13	0.0180
3	0.0053	14	0.0149
4	0.0053	15	0.0112
5	0.0063	16	0.0118
6	0.0082	17	0.0071
7	0.0083	18	0.0061
8	0.0115	19	0.0056
9	0.0210	20	0.0040
10	0.0255	21	0.0021
11	0.0228	22	0.0005

Table 2: Pressure Ratios for Leeside Surface Pressures at the WLESS Vents. Values at the Mid-point of the RCC Panel Trailing Edge. Ratios Normalized by the Peak Pressure on Panel 9 (3092.8 Pa or 64.6 psf). Results Based on NASA CFD Solutions for GMT 13:54:24, 227,424 ft, Mach 22.91 and Angle of Attack of 39.59 Degrees.

ENTRY INTERFACE (EI) GMT 13:44:09 –> 13:47:30: Early Heating of Wing and Initiation of Thermal Damage

According to the hypothesis, the ET foam strike, which occurred at 82 seconds after lift off, compromised the RCC leading edge. Analysis of launch imagery (Reference 1) and state-of-the-art CFD (Reference 2) computing the transport of the foam within the complex flow field about Columbia, and its launch elements (External Tank, Solid Rocket Boosters and attachments) have shown that the foam strike occurred in the RCC 5-8 panel area. Both studies show that the strike was below the wing apex. The strike also occurred in the region of the shock-shock interaction area where reentry heating is high, as previously noted.

Testing at Southwest Research Institute and associated analysis has shown (Reference 3) that a strike of debris on the RCC from the ET bipod (briefcase-sized, weighing about 1.7 lbs) striking the WLSS at speeds of 770 ft/sec can cause severe damage. Damage observed included RCC panel cracking, cracking of T-Seals, displacements of both panels and seals and the formation of holes as large as 16 inches by 16 inches.

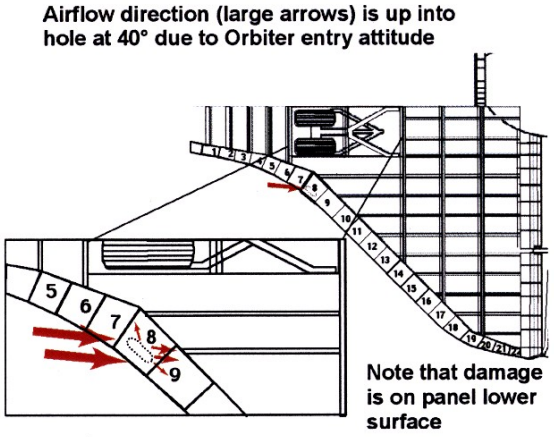

Figure 6: Hypothesized Entry Damage and Initial Entry Heating at Entry Interface.

Figure 6 depicts a breach (hole) in the lower RCC Panel 8. The view is down at the wing, looking through the top of the RCC panel. At entry interface, the flow is free molecular, and air molecules follow straight paths until they strike a solid surface. Assuming there was a hole in the lower part of Panel 8, the flow would be up into the hole, in the x-z plane of Columbia and at an angle of 40 degrees from the x-axis, corresponding to the angle of attack. The large red arrows show this flow direction in the plane of the paper (x-y) while the smaller red arrows show that there would be a "splash effect" when the air molecules strike the elements including insulation and metal mounting fittings inside the wing leading edge. Some of these elements are shown in the photograph in Figure 4.

As Columbia descended into the atmosphere, density increased and the free molecular flow transitioned to a continuum. As this happened, a shock wave formed over the vehicle giving rise to the flow field described above. In continuum flow, the flow vector is mainly along the wing surface instead of 40 degrees to the surface. For STS 107, superheated air from the shock layer entered the

breach and pressurized the cavity between the RCC and the insulated wing spar. Abnormal flow then exited out through the vents into the very low-pressure region at the top of the wing previously described.

Table 2, based on the CFD solutions discussed above for a normal condition corresponding to STS 107 at GMT 13:54:24, shows very large vent pressure ratios referenced to the lower side of Panel 9. Note that the ratios are large, ranging from 0.026 to .005 falling off from the Panel 9 - 11 area, both to the inboard and outboard direction. These ratios provide a very large driving potential to the internal flow.

One piece of evidence that corroborates that there was a breach in the wing at EI comes from the MADS/OEX thermocouple located behind the spar at the Panel 9 location. As discussed in References 4 and 12, there was "out-of-family" heating at this location during the STS 107 ascent. Figure 7 shows the time history of the measured thermocouple signal and the comparison of NASA's thermal analysis (Reference 12) of the ascent event. As indicated on the figure, the "stepped" curve is the flight data while the blue-colored, smooth curve is the result of the NASA analysis. Note that the temperature readings are not large, owing to the facts that ascent heating is small, relative to that for entry, and that the thermocouple is behind the spar and the spar insulation. Detail of thermocouple locations will be discussed later.

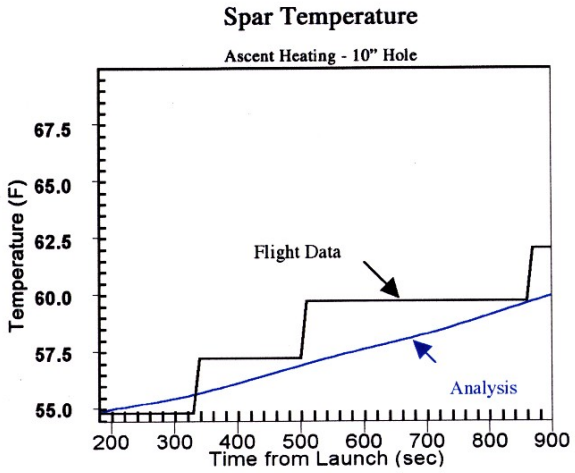

Figure 7: Data from OEX Thermocouple VO 9T9895 and Thermal Analysis by NASA (Reference 12).

NASA's thermal analysis of the signal between 200 -> 900 seconds after launch suggests that ascent heating due to a hole of 6 – 10 inches in diameter in the wing leading edge can account for this anomalous heating. While this is not conclusive evidence that a breach existed after the foam strike at 82 seconds into the launch, it is quite consistent with the hypothesis.

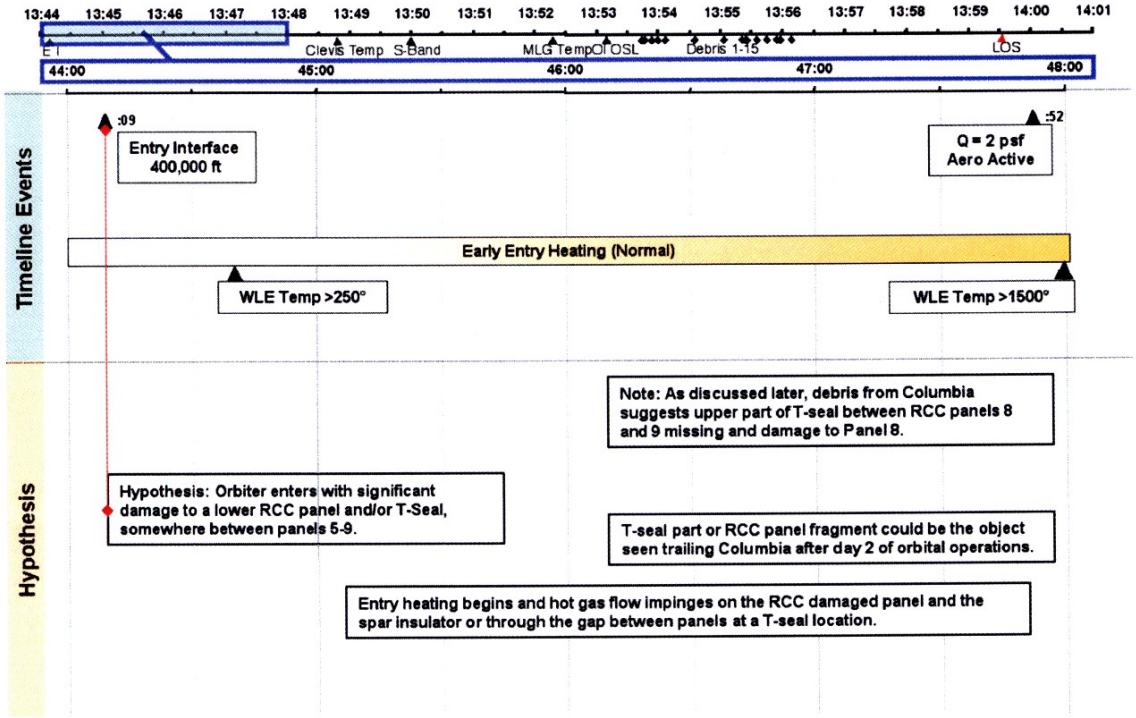

Figure 8: Timeline From EI 13:44:09 -> 13:47:30.

Figure 8 shows the comparison of timeline events from EI 13:44:09 to 13:47:30 to the hypothesis. This format, developed by NASA's Working Scenario Team (Reference 13), was adopted by the present authors. The format highlights portions of the entire sequence from EI through loss of signal (LOS) GMT 13:44:09 -> 13:59:32 shown at the top of the figure. The period being studied is highlighted with the blue rectangles, in this case 3 minutes and 21 seconds after EI.

Timeline events (tested and adopted as being "truth") appear on the upper half of the figure while those in the hypothesis (or scenario) are displayed in the lower portion of the figure. This figure shows the entry interface timing and wing leading edge heat-up for a normal wing during the expected STS 107 entry. In the lower part of the figure, the hypothesized damage to the lower RCC Panel 5-8 region as depicted in Figure 6 is noted, as is the beginning of the thermal attack on the wing leading edge subsystem. As discussed later, the debris recovered from Columbia strongly suggests the initial breach was in Panel 8, and the upper part of the T-seal between Panel 8 and 9 was missing or displaced.

ENTRY FROM 13:47:00 –> 13:50:00: MADS/OEX Data Show the Progression of Damage is From the RCC -> Aft

This section begins with a discussion of MADS/OEX sensor readings and then compares the interpretation of the data occurring between 13:47:09 until about three minutes later at 13:50:00 with the hypothesis.

Figures 9 and 10 depict the physical location of the MADS/OEX sensors in the Panel 9/10 area of Columbia's left wing. Figure 9 is a photograph of the backside of the wing spar, looking forward. The approximate locations of RCC Panels 9 and 10 are shown near the top of the photograph. Fortunately, this region of the wing on Columbia was instrumented for the Orbiter Experiments (OEX) activity early in the Shuttle Program, and the instruments were still operational and recording data during STS 107. Data from four sensors are extremely valuable in helping understand the temporal events leading up to the failure of the wing leading edge system: V12G9921, a strain gage mounted to the spar; V09T9895, a thermocouple mounted to the back of the spar at the Panel 9 location; V09T9910, a thermocouple mounted to the clevis which held RCC Panel 9 in place (under an "earmuff" which insulated the clevis); and VOT9666, a thermocouple mounted in a tile in the lower wing, near the tile surface, close behind the number 9 carrier panel tiles. VO9T9910 is imbedded in the RCC mounting hardware, which secures the panel to the spar.

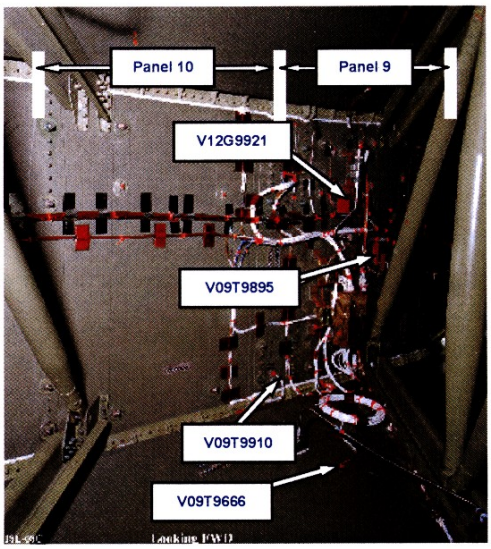

Figure 9: Photograph of Rearward Side of Columbia's Left Hand Wing Spar, Looking Forward. OEX Sensor Locations are Depicted.

To help visualize the geometric location of the sensors, Figure 10 shows portions of an engineering drawing from a document describing the OEX instrumentation. As can be seen, top and side views are shown along with a key identifying the type of sensor.

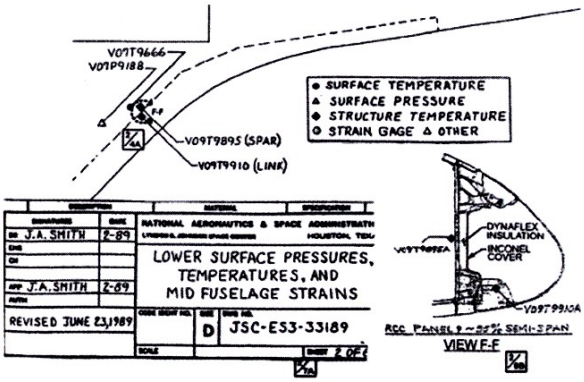

Figure 10: Portion of an Engineering Drawing Depicting the Location of OEX Sensors.

Figures 11 through 13 show data from the two sensors (one strain and one temperature) discussed in Figures 9 and 10. The information from these sensors is very significant in determining the progression of events as the thermal damage from the initial breach progressed to burn a hole through the wing spar. In addition to the data

obtained on STS 107, sensor traces taken on other flights, with similar entries are displayed with different color codes. Other investigators have made detailed analyses of these signals and data from many more sensors, but herein, only major events, appropriate to our "Follow the TPS" theme are discussed. In each plot, there is an indication of the first off-nominal or "out-of-family" event that will later be used in comparing flight data to the hypothesized events causing loss of vehicle and crew. The units in Figure 11, measured by the temperature compensated strain gage are micro inches/inch.

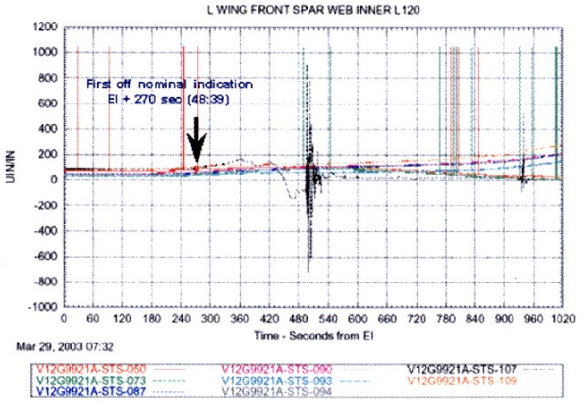

Figure 11: OEX/MADS STS-107 Flight Data.

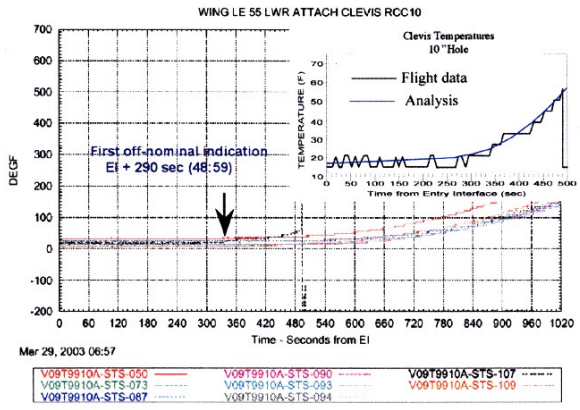

Figure 12: OEX/MADS STS-107 Flight Data and Thermal Analysis (Reference 12).

Figure 12, prepared in the same format as Figure 11 displays the time history of a thermocouple imbedded in the clevis fastener at the lower edge of the RCC located between Panels 9 and 10. The temperature changes recorded on the RCC clevis during STS 107 entry, appear to be quite small, but it is noted that this thermocouple is highly insulated and attached to a large thermal mass.

A thermal analysis by NASA (Reference 12) has shown that a hole of 6 -> 10 inches in diameter in the lower RCC Panel 8, could account for the early behavior of the thermocouple. The result of this analysis is shown in the inset in Figure 12. The "stepped" curve is the flight data while the blue, smooth curve is the result of the referenced analysis.

Figure 13 shows temperature histories from the left-hand Orbital Maneuvering Systems (OMS) Pod. Again, data from other, similar flights is shown. As can be seen, below nominal temperatures were recorded, starting at about 340 seconds after EI. The following figure explains that this is likely due to a modification to the normal flow field by damage in the wing leading edge. Note also from this figure that at about 540 seconds from EI, the temperature abruptly increases, to values well beyond that for a normal entry.

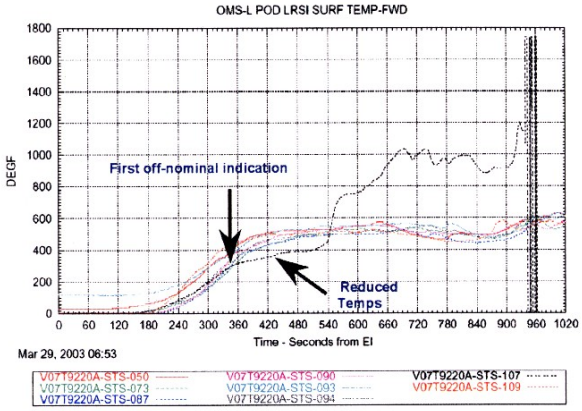

Figure 13: Off-nominal OMS Pod Temps.

Figure 14, prepared by NASA (Reference 14) shows the results of wind tunnel tests from Langley Research Center. Data were obtained in a Mach 6 air stream at the conditions specified on the figure. The three boxes on the right of the figure show the results of a thermally sensitive coating on a model of the Shuttle. As noted, for the results of RCC Panels 5 and 10 missing, there is a definite temperature decrease from the baseline on the left OMS pod location, noted by the absence (missing panel number 5) or dimming of the red dot on the forward location of the OMS pod. The conceptual sketch, also shown in Figure 14, suggests that the jet-like expansion directed from a damaged wing influences the leeside flow field, reducing OMS heating if there is a disturbance in the Panel 5-10 RCC area.

While this simulation does not duplicate flight conditions, the trends do help explain the below nominal

temperatures of the OMS pod seen in the OEX data. NASA Ames has also produced (Reference 7) CFD results supportive of the trends identified, in the wind tunnel testing, using the GASP CFD code previously described (Reference 9).

Figure 15 graphically depicts the timing of events recorded by the OEX sensors. The captions are self-explanatory. The MADS/OEX off-nominal data in the wing leading edge and spar are additional evidence that a breach existed in the RCC at the EI. The below nominal temperature on the OMS pod is consistent with the hypothesized damage in the wing leading edge in the RCC Panel 5 - 8 area.

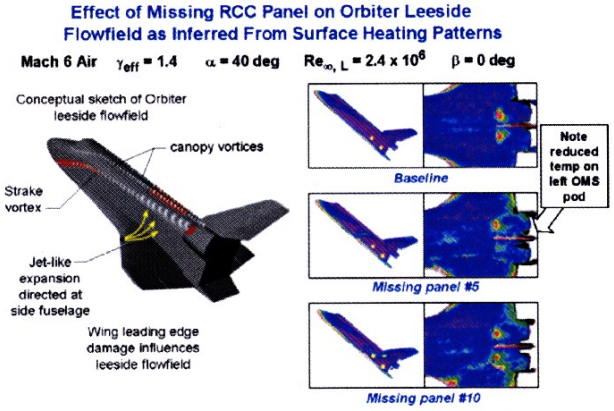

Figure 14: NASA Langley Wind Tunnel Test Data Help Explain Below Nominal Temperatures Recorded on the Left OMS Pod.

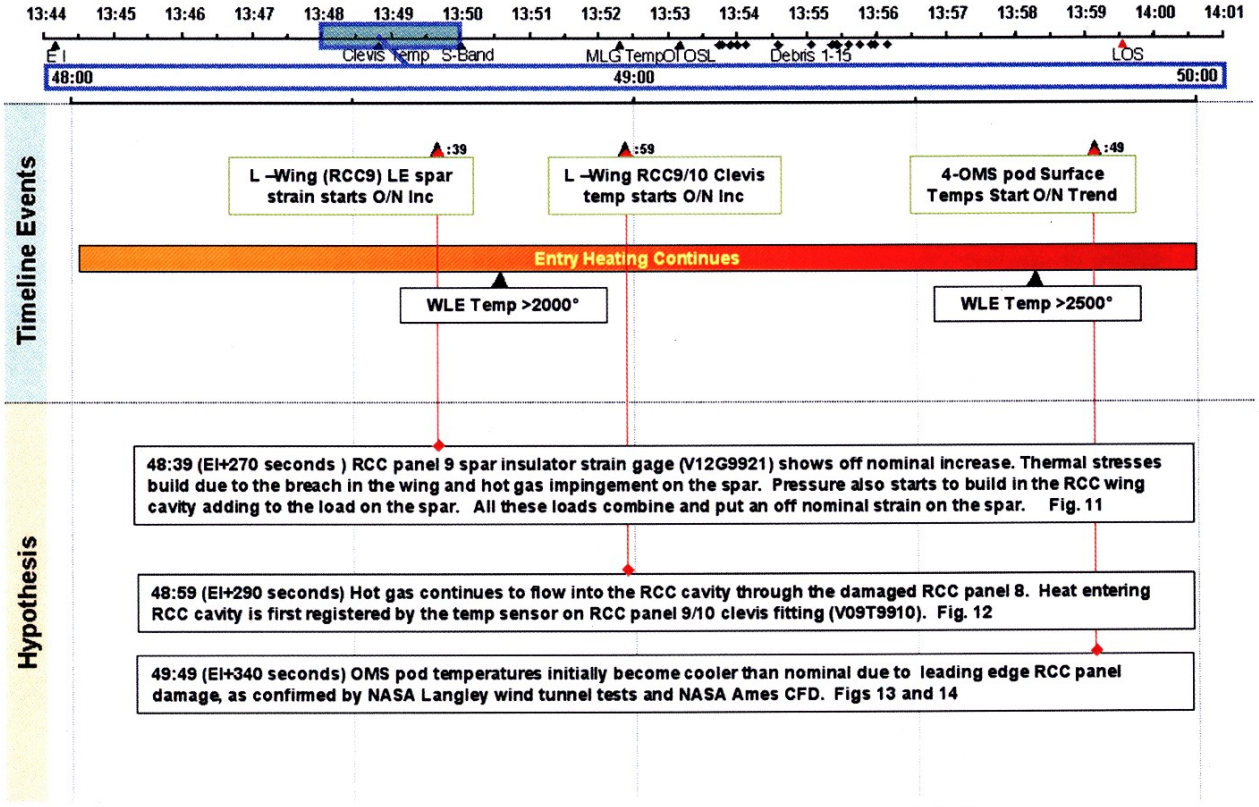

Figure 15: Timeline Versus Hypothesized Events 13:48:00 -> 13:50:00.

ENTRY FROM 13:50:00 –> 13:52:00: Entry Events Through Spar Burn - Through

Figure 16 depicts a possible explanation for some of the early (near 13:50:00) communication dropouts observed during Columbia's entry. As known from many years of experience with entry of vehicles, small amounts of charged species (electrons and ions) between an antenna and the receiver can cause communication signal attenuation and even its total loss. As shown in the figure, a possible explanation for some of the early signal attenuation could have been electrons and ions, along with molten materials from the wing hardware, being entrained in the flow and transported to locations between the antennae behind Columbia's cockpit and the receiving TDRS communications satellite.

At the request of the authors, D. Potter of Sandia National Lab performed a scoping study (Reference 15) which shows that melting aluminum would provide charged species concentrations in sufficiently large quantities for signal attenuation in the 13:50:00 –> 13:50:30 period. However, to date (July 2003) analysis by NASA has failed to provide an understanding of how the flow behind Columbia could have provided a pathway to place the charged species and/or molten metal between the antennae and the receiving satellite. Darling (Reference 4) has pointed out that the communications drop out occurred at times quite close to several major debris shedding events and to the breach of the LW spar. However, a definitive link between the two is still conjectural.

Figure 17 displays the left fuselage sidewall thermal profile for thermocouple VO7T9925A in the standard MADS/OEX format wherein the data for STS 107 are compared to those from other, similar entries of Columbia. As can be seen, there is an out-of-family lower temperature trend at EI + 360 seconds, correlating to GMT 13:50:09. This early below nominal, and later, above nominal temperature observation on the fuselage sidewall, for a number of thermocouples has been explained by the NASA team led by J. Caram (Reference 16) to arise from flow disturbances propagated from the wing leading edge. The study depends upon a combination of hypersonic wind tunnel data and CFD analysis. The reader interested in detail is referenced to this report and the Aerothermodynamics section of the CAIB report (Reference 17).

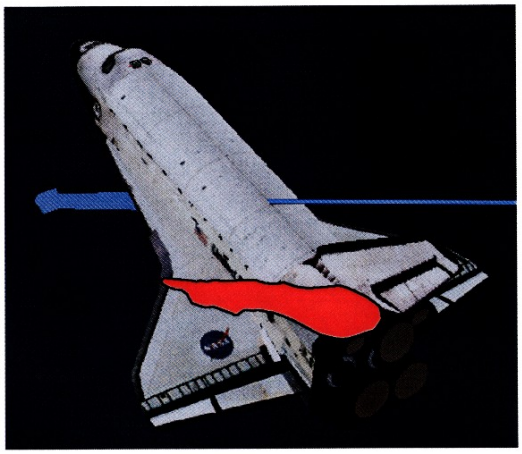

Figure 16: Entry Plume is Possibly Affected by Damaged Structure Accounting for Communications Dropout.

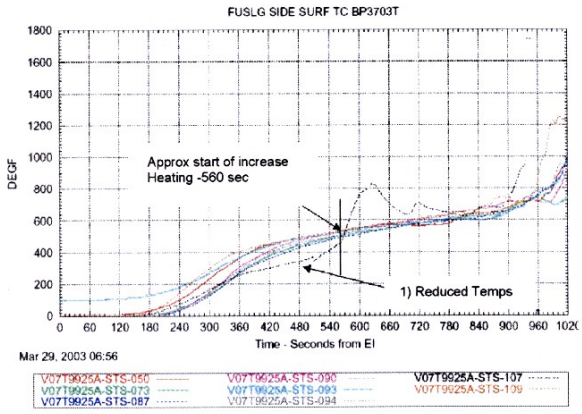

Figure 17: Representative Fusalage Sidewall Thermocouple Data.

Figure 18 displays the temperature recording from the thermocouple V07T9666A located in a lower wing tile, near the wing leading edge, behind Panel 9. This sensor location was shown above in Figures 9 and 10. As can be seen, there is an off-nominal heating trend in this thermocouple starting at EI + 370 seconds (GMT 13:50:19).

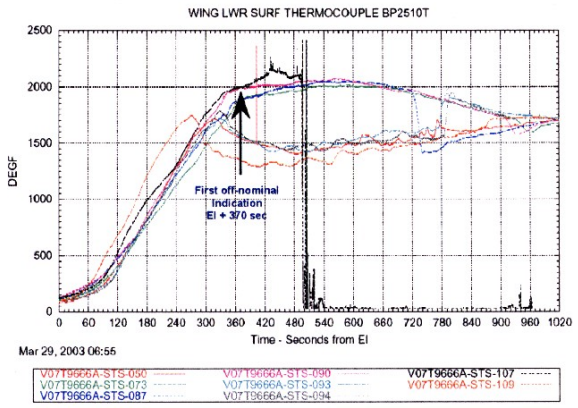

Figure 18: OEX/MADS STS-107 Flight Data.

As shown in Figure 19, thermocouple V07T9666A is in the flow area affected by Panel 8 (Reference 18). Specifically, as shown in the figure, the streamline, which passes over the junction of the lower Panel 8/9, also intersects the approximate location of this thermocouple. As will be discussed below, the forensic analysis shows compelling evidence that there was an outflow from the aforementioned 8/9 RCC lower panel junction that probably caused the above nominal readings of V07T9666A that started at EI + 370 seconds and continued till the spar breach occurred. This CFD solution by Gnoffo, Alter and Thompson (Reference 18), was the starting point of studies of flow into the breach, as will be discussed below.

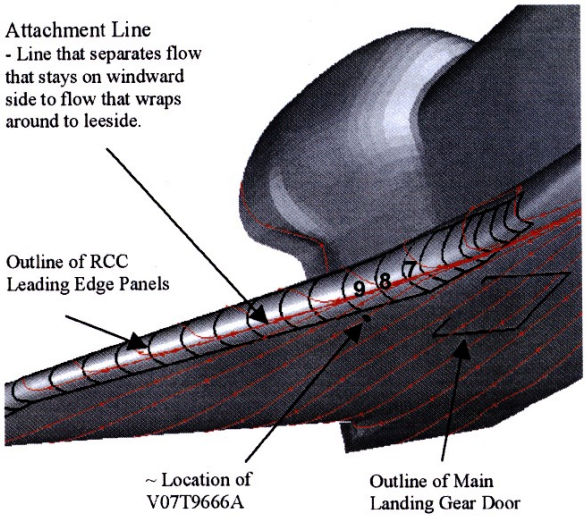

Figure 19: Orbiter Surface Streamlines. 13:50:53 (EI + 404), Mach: 24.9, Altitude: 243 k ft and Location of Thermocouple in Tile. CFD Solution from NASA (Reference 18).

Figure 20 displays the temperature recordings from thermocouple V0T9895A, located on the inside of the spar, behind Panel 9, as discussed in Figures 9 and 10 above. These data are quite valuable in understanding the progression of damage to the wing leading edge. As seen, the first off-nominal indication begins at 420 seconds after EI, GMT 13:51:09 with a very slight increase in temperature. Later discussion of this figure will focus on the burn through of the spar.

Figure 21 graphically depicts the timing of communication drop out and additional events recorded by the OEX sensors. The captions are self-explanatory. The MADS/OEX off-nominal data in the wing leading edge and spar are additional evidence that a breach existed in the RCC at the EI. The below nominal temperatures recorded on the fuselage sidewall is consistent with the hypothesized damage in the wing leading edge in the RCC Panel 5-8 area. The spatial correlation by the streamline analysis in Figure 19, showing how the outflow from the lower juncture of RCC Panel 8 and 9 can affect the lower tile thermocouple behind Panel 9 and the above nominal behavior of thermocouple V07T966, is additional and compelling evidence for the existence of a breach in the Panel 8/9 area. It is clear from this figure that the temporal evolution of the heat flow shows that the hot gas penetration began in the cavity in the wing leading edge prior to heating in the wing box behind the spar.

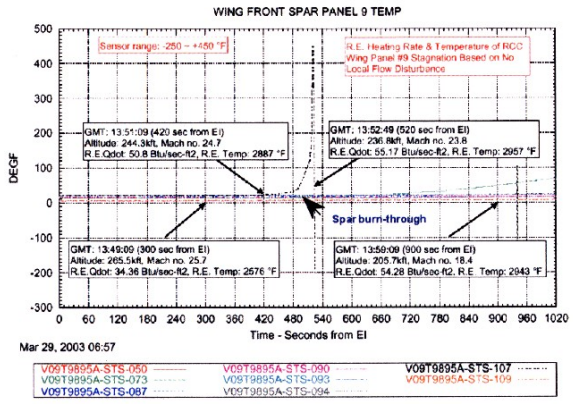

Figure 20: OEX/MADS STS-107 Flight Data.

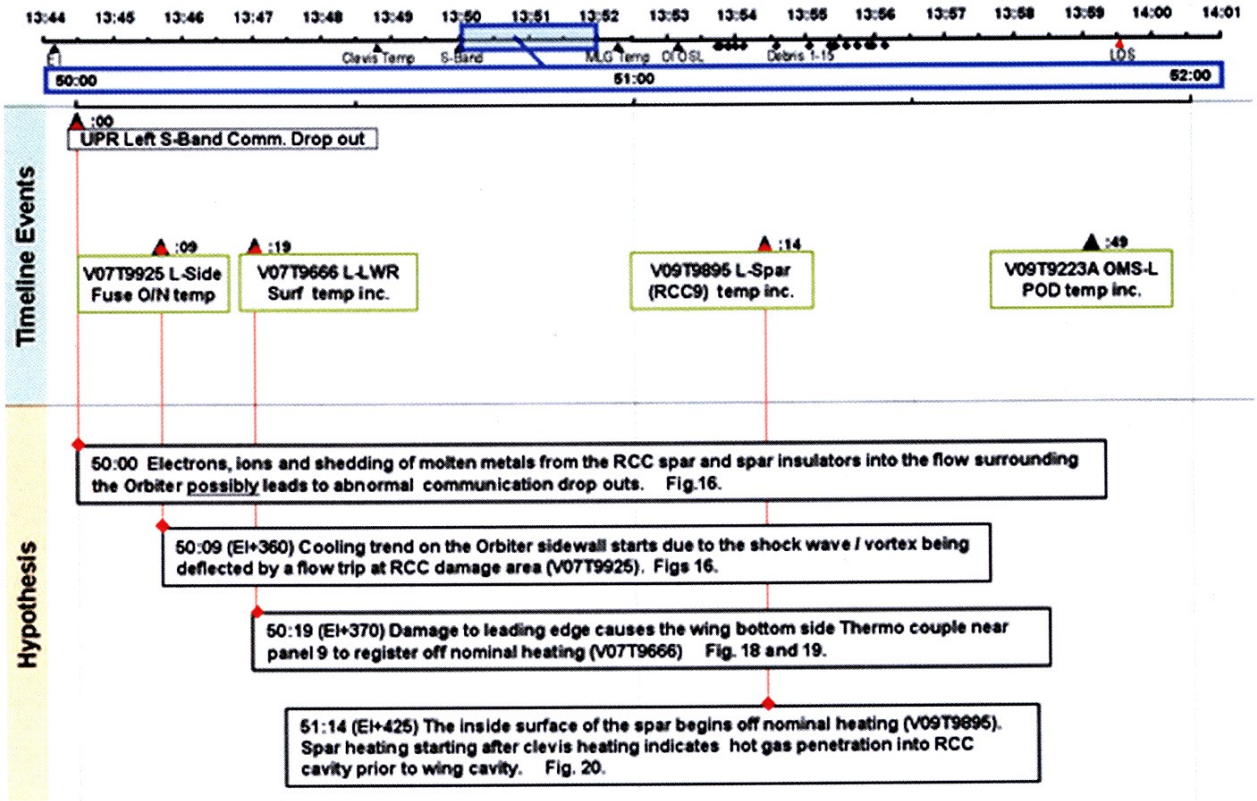

Figure 21: Timeline Versus Hypothesized Events – 13:50:00 to 13:52:00.

ENTRY FROM GMT 13:52:00 –> 14:00:00
(Includes Spar Burn-Through to Loss of Signal)

Figure 20 shows a rapid temperature increase at EI + 487 seconds as recorded by the thermocouple V0T9895A on the back of the spar behind Panel 9. This rapid increase at EI + 487 seconds strongly suggests an appearance of a plume of superheated air and that spar penetration had occurred. According to study (Reference 13 and 19) by NASA, this timing for spar burn-through is consistent

with a thermal analysis for a 6 -> 10 inch diameter hole in the RCC Panel 8, failure of the leading edge wire harnesses and bit flips observed in the wheel well.

Figure 22 and 23 are artist's concepts of the burn-through and hot gases filling the wing box.

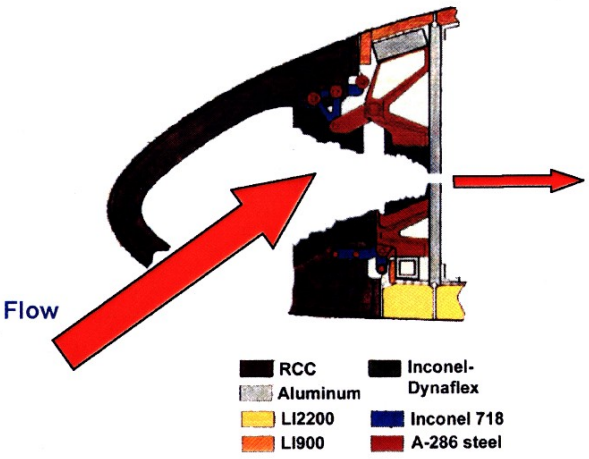

Figure 22: Spar Breach Occurs at EI + 487 Seconds.

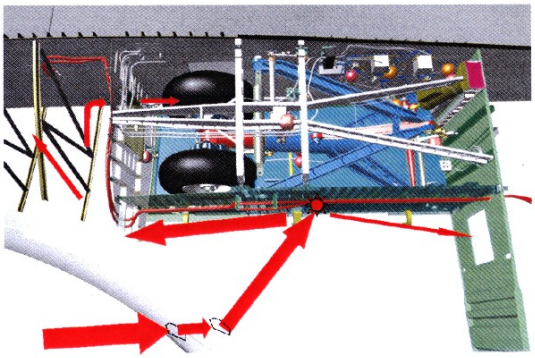

Figure 23: Hot Gas Begins to Fill Wing Box.

Figure 24 displays the time history of thermocouple V07T9220A located on the OMS Pod. The observation made by NASA (Reference 16) is that from 13:53:29 -> 13:55:29 (EI + 560 -> 680 seconds), there are continual off-nominal increases in OMS Pod temperatures that correlates with the timing of debris sightings 1-13 during the flight. This correlation clearly suggests increasing damage is occurring to the left wing, specifically to the TPS and its substructure.

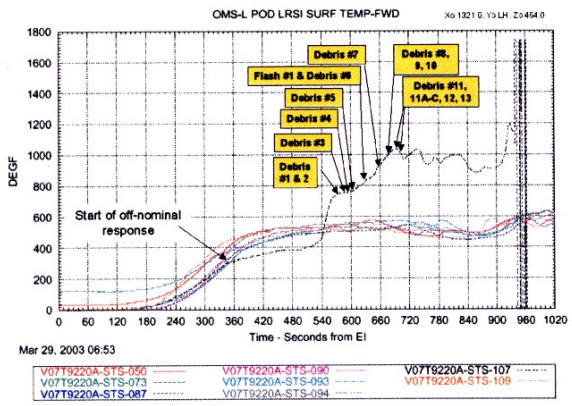

Figure 24: Left OMS Surface Temp Response Indicating the Progression of Damage.

Figure 25 is a photograph of Columbia, taken at GMT 13:57:14 from the Starfire Facility at Kirtland AFB in Albuquerque, NM. At this time, Columbia was about 50 miles NW of Starfire at an altitude of about 40 miles, it had an 80 degree left angle (with the left wing down) and a 40 degree angle of attack. Therefore, the view of the vehicle is from the forward, bottom, left side, so that any hot plumes spilling over the top of the left wing leading edge or out of the top of the wing near the leading edge are visible.

The image records the appearance of the shock layer around the vehicle. As is indicated by the model grid overlay, the left side of the fuselage would be visible if it were not for the shock layer brightness and the slight wrapping around of the flow over the lower part of the forward fuselage. The apparent enlarged portion of the nosetip area is also due to the shock layer expanding around the forward fuselage from the stagnation point at the lower part of the nosecap. The shock layer is also visible through the short (a few meters long) wake that persists behind the vehicle.

The left wing has two apparent "bulges" on the leading edge and two corresponding wakes behind the wing. The authors believe that these are due to the following: hot flow and burning material ejected upward over the wing leading edge from the Panel 8 area; and a large plume of hot gases and burning material and debris ejected upward from the breach in the top surface of the wing aft and outboard of the Panel 9/10 area.

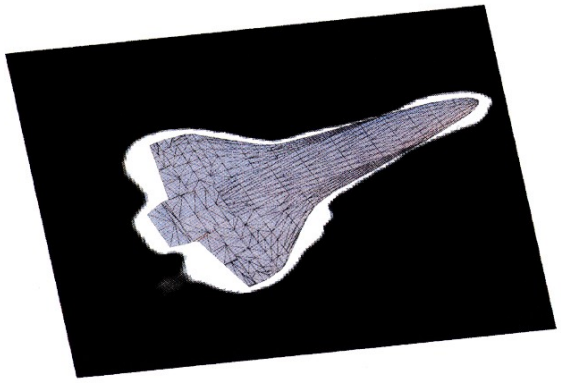

Figure 25: Starfire Photo from Kirtland AFB. GMT 13:57:14. Model Scaling and Orientation Based on Telemetry from NASA. The Columbia Model was Provided by NASA.

The captions within Figure 26 displaying the comparison to the hypothesis and the timeline between GMT 13:52:00 and 14:00:00 are self-explanatory. During this time, the breach through the spar and internal heating to the wing box and wheel well have rendered the loss of the vehicle inevitable. The temporal progression of damage to the TPS has been outlined herein with the exception of the shedding of tiles and RCC panels/parts. Geographic locations of the recovered TPS debris and ballistic analysis suggest that much of this occurred over Texas. Others have written in detail on the analysis of debris sightings, sensor readings, etc. and it is outside the scope of the "Follow the TPS" charter to dwell further on these topics.

In the following section one can see a detailed analysis of Columbia's TPS debris and what it infers.

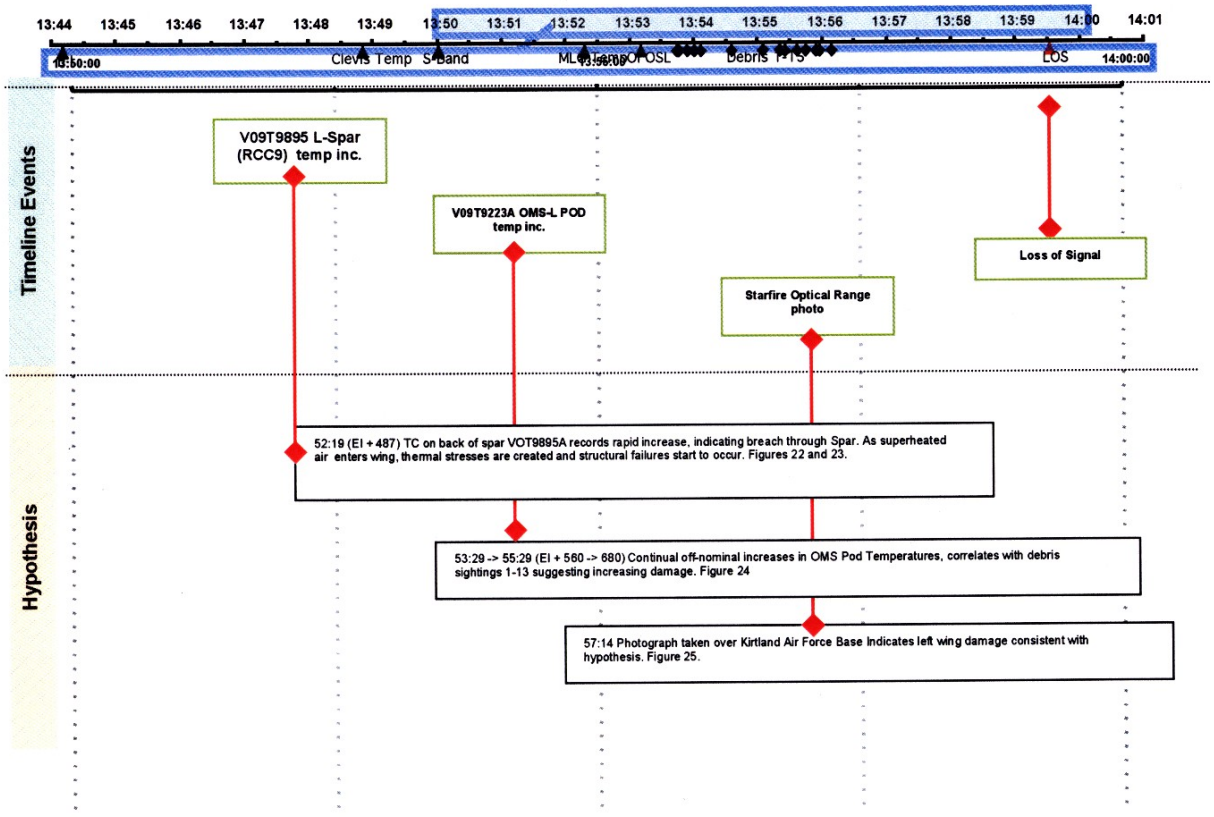

Figure 26: Timeline from 13:50:00 Through Loss of Signal 13:59:32 Versus Hypothesized Events.

TPS Debris and Forensic Analysis

In keeping with the "Follow the TPS" theme of this appendix, the focus herein is on the TPS debris and what story it tells about the demise of Columbia's RCC wing leading edge subsystem and tiles.

Figure 27, (Reference 20) provides a graphical description of debris recovered (as of April 30, 2003) from the left wing of Columbia in the RCC Panel 1 -> 11 region.

The following description provided to the authors by M. Ehret explains the symbols: Red means "Bad or Hot," Yellow is "So-So" and Green is "Good."

Note that one upper carrier panel tile from Panel 8, depicted by a "red" rectangle was slumped, showing evidence of prolonged heating. The paucity of upper carrier panel tiles in the 8/9/10 area may have been caused by hot gases exiting from the LW cavity volume through the vents between the upper rear portion of the RCC flanges and tiles. This hot flow, containing melted materials from the interior RCC, would have had a very aggressive erosion effect on the upper carrier panel tiles and their attachments.

For "Slag" the diamond symbol was used: Red (H) means heavy slag, Orange (M) means medium slag, Yellow (L) means light slag, Green (no letter) means none or very light slag. "Holes without fractures" refers to the unbroken holes in the RCC, interpreted as evidence that the Inconel fasteners melted out. Here, red circles indicate that prolonged heating occurred. Red triangles depict significant RCC erosion. Green triangles indicate no RCC erosion. "Fractures" indicate the possible evidence of hot-shortcracking of the A286 carrier panel attach bolts (as evidenced by intergranular fracture) as an indicator of prolonged high temperature exposure (Reference 20/Appendix, by L. Korb). The red square represents the only such finding among these debris.

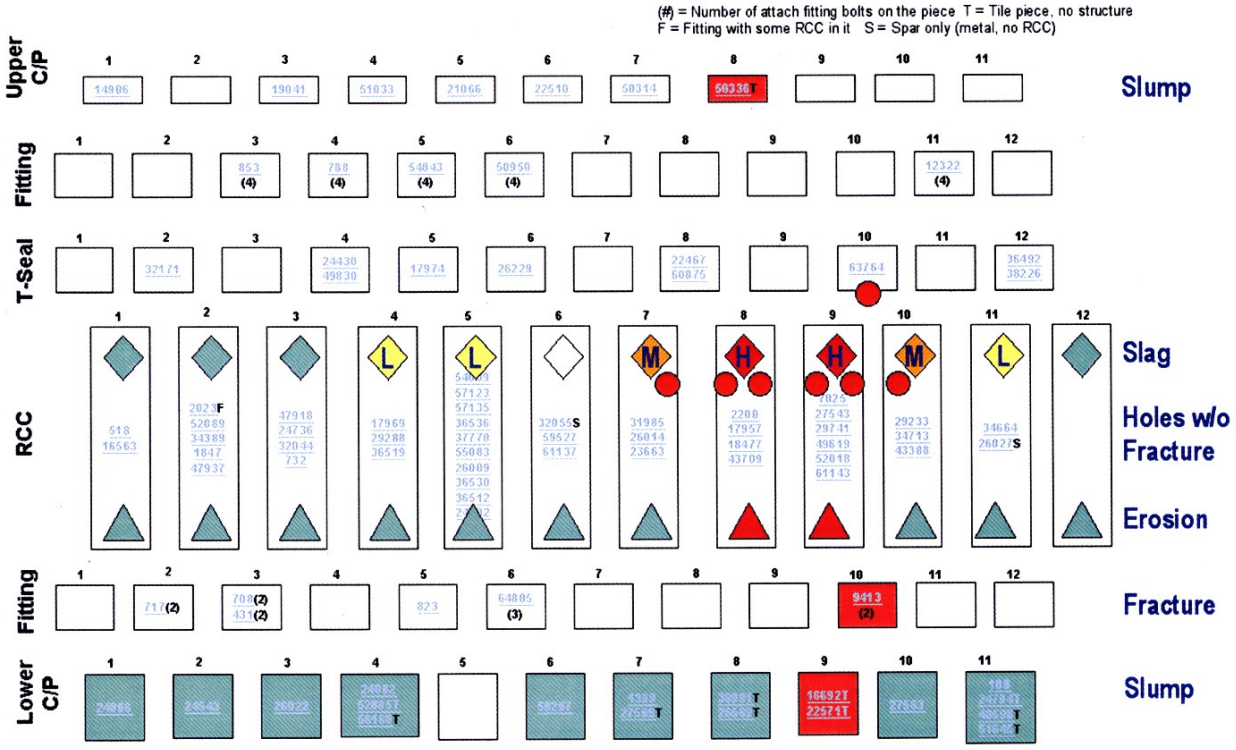

Figure 27: Left Hand Wing Debris Points to Breach in RCC Panel 8/9 Area (Reference 20).

Only lower carrier Panel 9 tiles showed the heavy slumping (red box). All other lower carrier panel tiles found as of 4/30/03 had no evidence of prolonged heating (Green).

In general, Figure 27 shows accumulated evidence that **only** the RCC Panel 8/9 region suffered PROLONGED heating. There is only one area on either wing where the attachment holes in the rear of the RCC panel flanges and ribs are intact (no fractures through the holes) and the attachment metal parts have been melted out. This is in the Panel 8/9 area of the left wing, indicating extreme heating conditions that completely melted out the Inconel fittings and in some cases even severely eroded the RCC mounting holes. All of the other recovered mounting holes in the RCC have either been fractured (the metal parts torn out) or the metal parts are still attached.

The photograph in Figure 28 is an outboard view of recovered parts of RCC ribs from Panels 8 and 9. For perspective, four recovered parts of the outboard rib of Panel 8 are shown sitting on white foam blocks: one upper part of rib 8, and three parts from the lower part of the rib 8 heel/lug bolt area. Two recovered parts from the inboard, upper rib of Panel 9 are shown laying on their full-scale drawing. A third part, placed on the drawing, not identifiable, is likely also from the inboard rib 9 in the location shown. Lack of positive identification of this part is indicated by the ? mark written on the yellow tag. These parts show heavy ablation, and the RCC LW LESS Panel 8/9 area is the only location found with this feature. Ablation features are labeled using yellow tags with the letter "A." The ablation patterns facing the camera on this side of the rib parts strongly suggests that superheated air had been flowing inside the wing, in a generally outboard direction. This indicates significant and prolonged flow from the Panel 8 area into the Panel 9 and outboard regions of the wing inside the RCC-LESS channel. Edges of the ribs are sharpened to a near "knife-edge" (0.05 inches compared to undamaged thickness of 0.365 inches), with a flat side away from the flow direction. Because of the durability of RCC and the extent of the ablation, this flow probably was sustained inside the RCC-LESS cavity area for hundreds of seconds. This type of damage is the result of oxidation (ablation) of the RCC carbon substrate. The following figure shows the same parts from an inboard view.

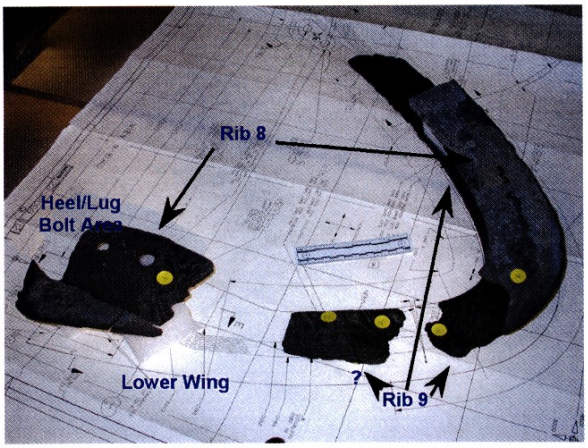

Figure 28: RCC Panel 8/9 Ribs (Outboard View).

Figure 29 is a photograph showing an inboard view of recovered parts of RCC ribs from Panel 8 and 9. Here, the two recovered and identified parts of the inboard rib of Panel 9 are sitting on white foam blocks. The recovered parts from the outboard rib of Panel 8 described in Figure 28 are now shown lying on their full-scale drawing. Note that the yellow tags here are labeled "NA," meaning not ablated and verifying the statements made in the discussion of Figure 28.

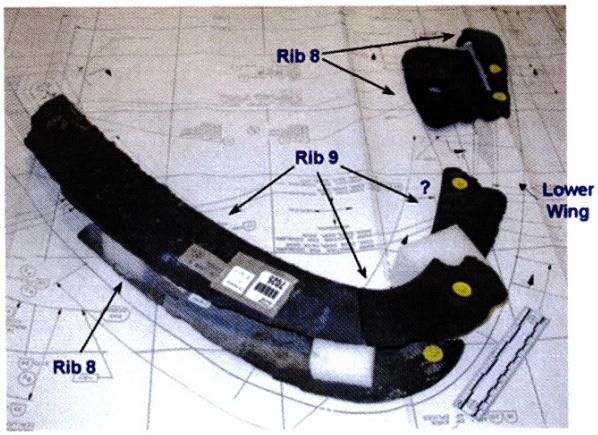

Figure 29: RCC Panels 8/90 Ribs (Inboard View).

Figure 30 is a photograph of the reconstructed left lower wing area of Panel 8/9. All parts shown are positively identified except for the "8/9" lower panels and the partial T-seal. Other left wing debris panels (16 and 17) were placed in the reconstruction to help visualize the original configuration. At the time the photograph was taken, the T-seal fragment was thought to be the T-seal which fits

between Panels 8 and 9, but later (4/26/03) thought to be from the 10/11 T-seal location. Definite identification of this T-Seal has been elusive and apparently is not possible (Reference 20/Appendix). Shown in the upper part of the photograph, in its approximate location, is the upper part of Panel 8. Note the slight flow patterning (possibly silica glass formed from the SiC coating) melt toward the upper part of the wing. This indicates that this was a late fracture, and that the exposed edge was in a super-heated air flow for a shorter time compared to the rib fragments shown in Figures 28 and 29. Note that the two LI 2200 carrier panel tiles below Panel 8 are in very good condition, while the three from the Panel 9 location show very heavy flow patterning, going in the inboard -> outboard direction. Close inspection of the heel area of outboard, lower Panel 8 shows a thumb-sized relief slot that was manufactured there to accept an inner panel thermal barrier. Hot flow exited out through this slot, causing the flow patterning on the three Panel 9 carrier panel tiles. The Panel 8 carrier panel tiles were not damaged, because they were protected by the lower Panel 8 and flow followed the direction of the external wing flow streamlines (Figures 2, 3 and 19). These findings are consistent with the erosion patterns observed in the internal flow patterns in the actual 8/9 ribs discussed above.

As discussed earlier in describing Figure 19, streamline patterns determined by CFD show that flow out of this lower RCC Panel 8/9 juncture area directly affect the thermocouple V07T9666A, located in the lower tile field, close behind RCC Panel 9. This flow relationship, strongly suggests the above nominal temperatures recorded by this thermocouple were caused by the flow out of the lower Panel 8/9 juncture, which also eroded the lower Panel 9 carrier panel tiles. The flow out of this slot, into a relatively high-pressure area (but below the pressure at the inlet breach) was probably the only outlet available to the large volume of ingested gases once the flow-through of the RCC vent slots was choked. The traces in Figure 18 suggest that this started at EI + 370 seconds and persisted until spar burn-through at approximately EI + 487 seconds.

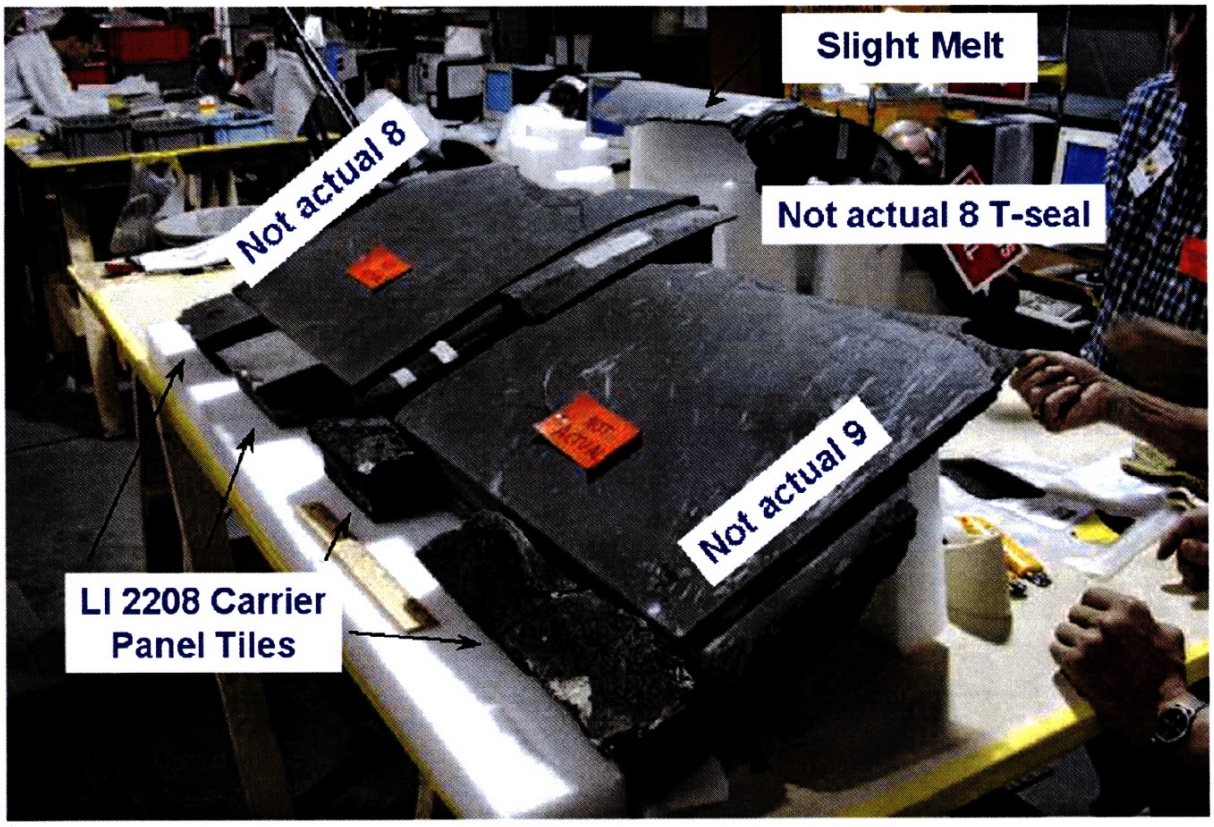

Figure 30: Reconstructed RCC Panel 8/9 Area.

The photograph in Figure 31 is a close-up of the slot in the heel of the outside, lower Panel 8 rib, manufactured there to accept an internal thermal barrier for the wing leading edge system. When hot flow existed inside the wing at the Panel 8 area, it created a "sneak" flow out of the wing causing the flow patterning on the Panel 9 lower carrier panel tiles previously described. There is also flow patterning on the side of the tiles facing the inner, lower part of RCC Panel 9 suggesting a channel flow there. This is not shown in this photograph.

Figure 32 is a close-up photograph of what was the RCC side of the vent gap on the upper Panel 8. See Figure 5 for an assembly drawing of the vent. As can be seen, there is a heavy accumulation of slag (up to 0.4 inches thick). This indicates that the gap at the top and outboard edge of Panel 8 and possibly Panel 9, were opened up from their normal configuration (0.114 to 0.164 inches) to at least 0.25 to 0.4 inches, and that melt from the interior fittings and insulation deposited there as the superheated air attacked the interior components of the WLESS and exited out of this vent location. The opening of the vent spacing could have happened at the time of the foam strike, or as the wing began to deform at the time of break-up; but most probably, it occurred during the long, high heating portion of the flight.

Figure 33 shows the probable initial breach location on the lower Panel 8 area. The size of the hole is difficult to determine, but could be bounded by the three dotted locations outlined by white tape. Analysis by NASA discussed above suggests the damage is consistent with a hole of 6 –> 10 inches in diameter. All of these are consistent with the flow patterning seen on the debris and the Computational Fluid Dynamics flow calculations to be discussed below. The authors note that areas this large would be consistent with the "piece" shown by DoD radar observations that "left" Columbia on day two of its orbital maneuvers. A part of a broken T-seal (possibly from Panel 8, located between Panels 8 and 9) could also account for the "piece" observed leaving the shuttle on day two of orbital operations. Note that on this photograph, the two recovered Panel 8 carrier panel tiles are not shown.

The authors believe that in addition to a breach in Panel 8, the upper part of the T-seal between Panels 8 and 9 must have been missing or severely misaligned for a major part of the entry. This is required to account for the severe erosion of the upper RCC Panel 8 outboard and Panel 9 inboard ribs shown in Figures 28 and 29 and discussed above. Flow patterns of the recovered upper Panel 8, suggest this happened as discussed in Reference 20.

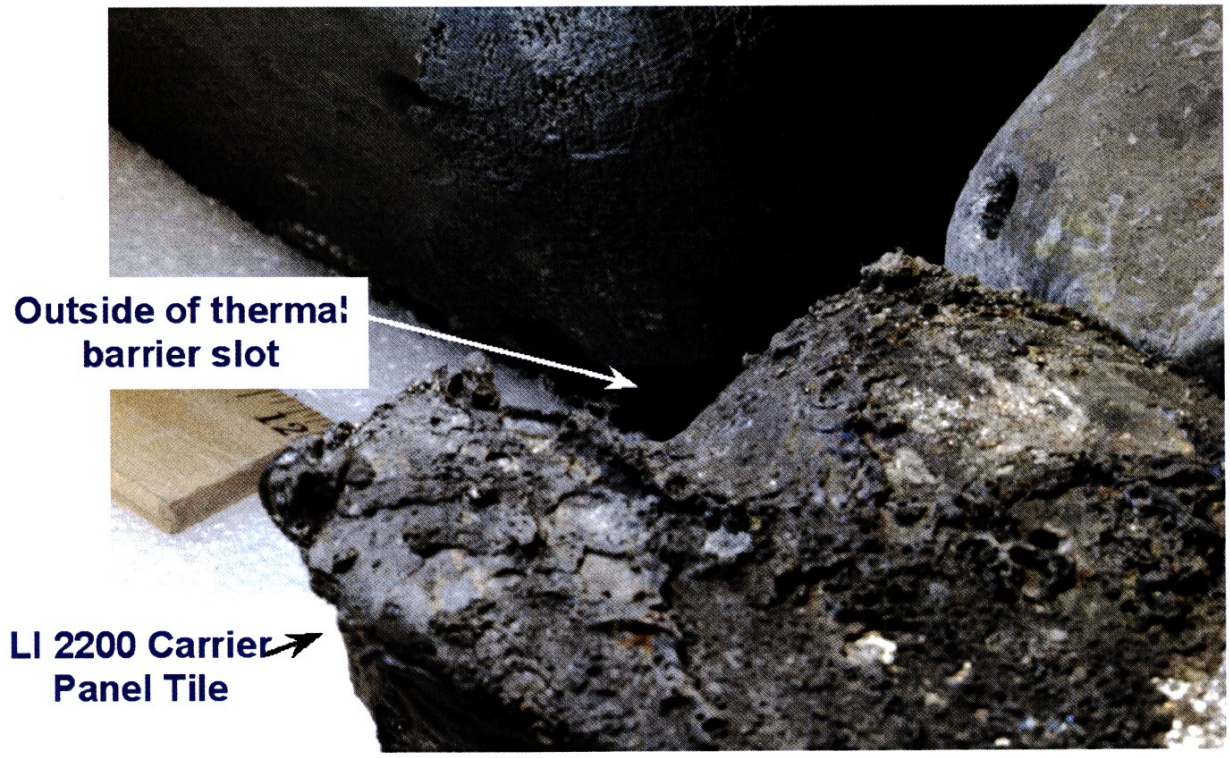

Figure 31: Close-up of Flow Location Affecting Panel 9 Carrier Panel Tiles

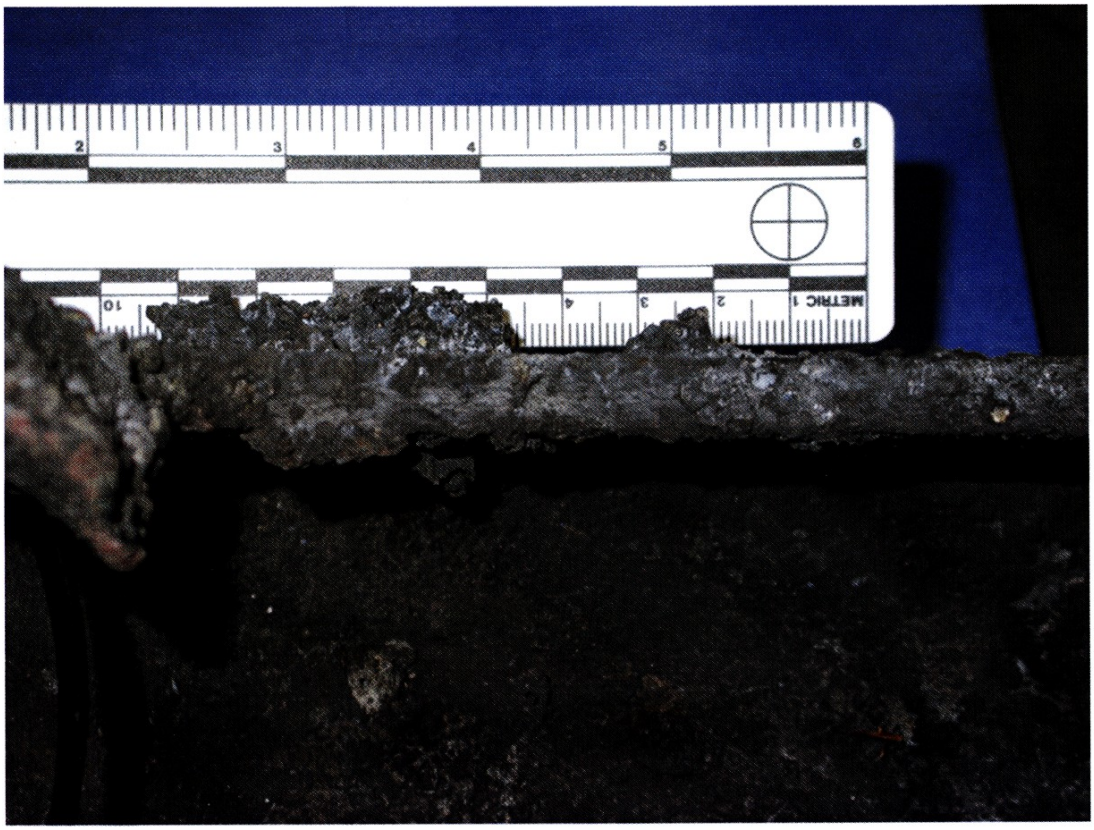

Figure 32: Slag Deposits on Upper Edge of Panel 8 on the RCC Side of the Vent.

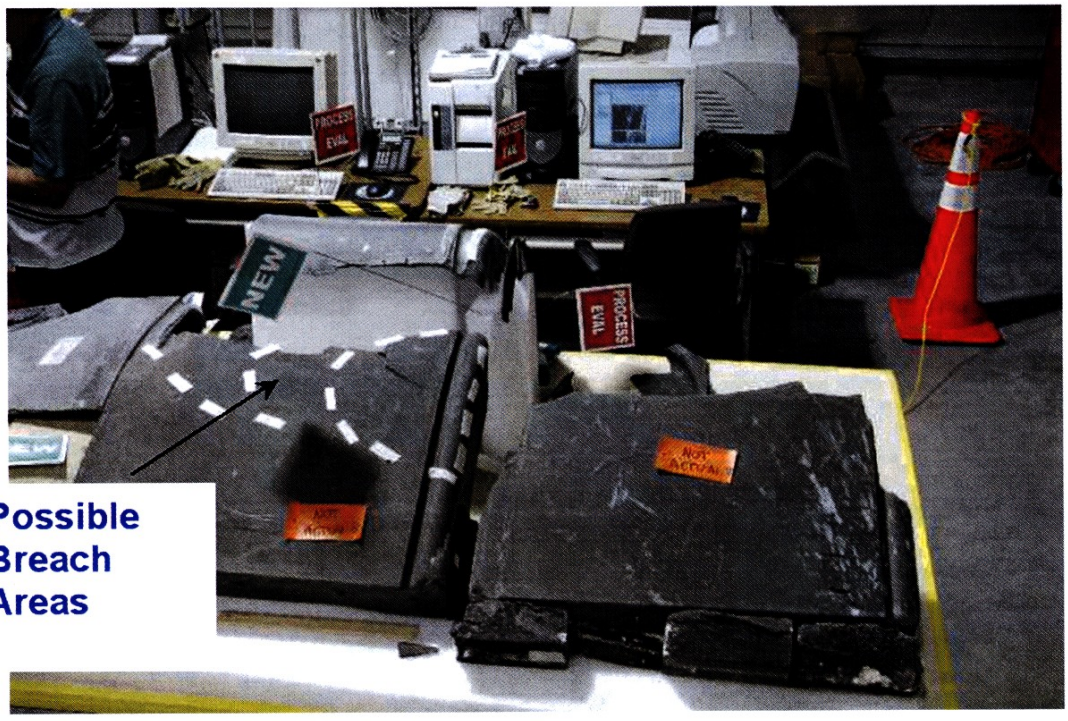

Figure 33: Probable Initial Breach in Panel 8.

Chemical and X-Ray Analysis of Debris from RCC Panels

Figure 34, adopted from Reference 20 summarizes work by the NASA Forensics Team. The analysis of the slag deposited on the inside of RCC Panel 8 shows that cerechrome and Inconel were deposited first in the slag layer. Deposition of aluminum occurred last. This is consistent with the sequence of thermal damage seen in the MADS/OEX data and is additional proof that the damage moved from the RCC -> aft. There were large amounts of melted cerachrome in the slag, consistent with prolonged presence of superheated air, since the melting point of cerachrome is in excess of 3200 °F. The presence of Inconel in the slag proves there was hot gas impingement on the RCC spanner bars, insulation foil and RCC panel fittings made of this material.

The absence of significant amounts of A286 stainless steel in the slag (Reference 20) suggests that the breach location was not close to these fittings. As shown by the figure, the deposition of Inconel spheroids and the cerachrome tears and globules suggests a "splashing" effect of the flow entering from a hole below the apex of the RCC Panel 8. As discussed above, some of the flow exited out of the vent at the top, rear of RCC Panel 8 and some came out in a "sneak flow" in the slot in RCC Panel 8 outboard and eroded the carrier panel tiles below RCC Panel 9. In addition, the slag on the vertical surfaces of the internal LESS hardware was generally on outboard surfaces of the hardware inboard of Panel 8 and on the inboard surfaces of the hardware outboard of Panel 8.

Finally, it is noted in Reference 13 that all other recovered RCC panels on both wings have a generally uniform and thin slag layer. All analyzed slag layers show a uniform mix of aluminum, Inconel and cerachrome suggesting short exposure to superheated air and uniform melting of WLESS components.

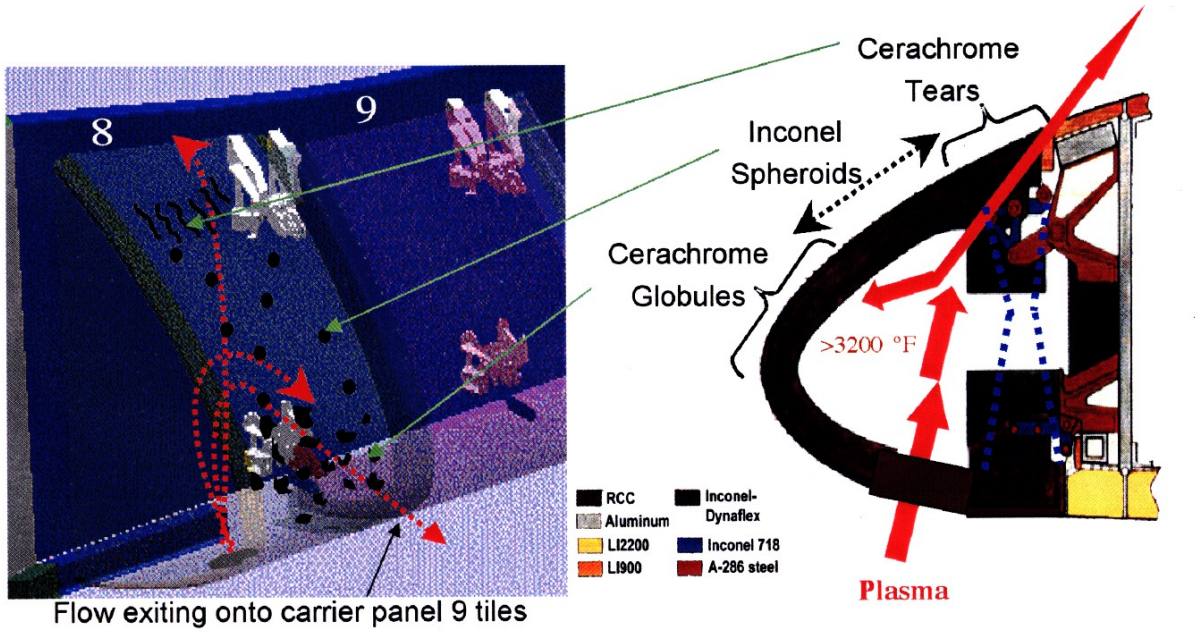

Figure 34: Wing Leading Edge Chemical Analysis of Panel 8 (Reference 20).

Recovered Tiles

Figures 35 and 36 show photographs of recovered tiles affixed to a 110 percent scale drawing of the left wing tile field. Here, a key of circular dots was used: Red means a tile is not in its final location, blue means a tile is in its final location and has been positively identified. Yellow means the tile failed at the densified layer, near the bond line and green means the tile failed owing to internal heating. In this case the Koropon/SIP failed or the Strain Insulation Pad (SIP) failed due to overheating. Koropon is the primer coating the aluminum skin.

There is a distinct pattern of RCG coated tiles, in the general X-direction downstream of Panels 8 and 9, outboard of the wheel well where the tiles appear to have little of the dark metal deposit (aluminum - rich) generally seen on the recovered tiles. These normal-appearing tiles all have been identified to have failure at the tile/Koropon bond line and departed from the wing surface prior to a major outflow of molten aluminum. This is indicative of extreme heat, inside the wing behind Panel 8. It then seems probable from this observation that the breach in the wing spar occurred at the Panel 8 location, and this is consistent with the observations discussed above. Ballistic analyses of the trajectories and the geographic location of the recovered tiles (both those detached owing to bond failure and those that did not) suggest they came off from about 100 nautical miles west of their recovery location in Texas.

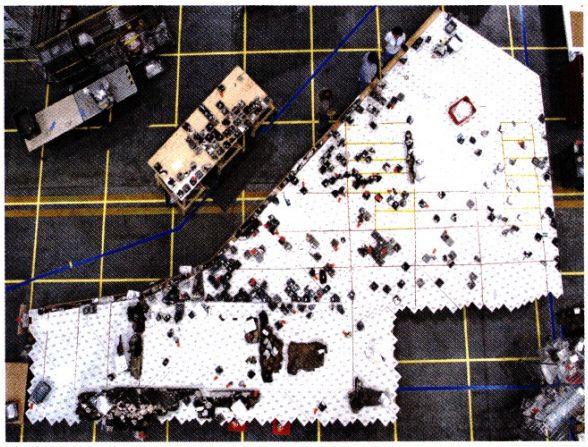

Figure 35: Overview of Tile Table. Left Wing, Lower Surface Tiles.

Figure 36: View of Tile Table from RCC Panel 8/9 Area.

CFD and Engineering Simulations of Flow into Breach Through the RCC

The Columbia accident stimulated an extra ordinary effort by a national team led by NASA JSC (J. Caram {overall lead}, S. Fitzgerald {internal flow} and C. Campbell {external, damaged edge flow}) to understand the flow into the breach in the Columbia's RCC WLESS. This is a very difficult undertaking owing to the complex geometry inside the wing cavity and the lack of knowledge of the damage location as well as its shape and size. Such a complex analysis has never been done, and thus the team was truly "cutting new ground."

Initial study by Fitzgerald and his colleagues assumed that the external shock layer would provide a "plenum" of hot gas and that a jet (similar to those for nozzle flows) would enter the WLESS cavity, essentially normal to the locale of the hole. Early studies of localized heating from the jets and the resultant damage to the wing interior insulation were conducted. This work was of great help in understanding plume properties and developing tools.

P. Gnoffo (NASA Langley) and his colleagues (Reference 18), were the first to study the flow through a hole in an RCC panel using real-gas CFD with the LAURA code. The beginning point for this study was the external flow depicted in Figure 19. Gridding for a two-inch diameter hole in an RCC panel was introduced and flow studied for a simplified case with a hollow LESS cavity at a constant, rarefied pressure. This seminal work showed that the momentum of the external flows drives the jet in an outboard direction, "hugging" along the inside of the RCC. Subsequent work using LAURA for larger holes, up to 10 inches in diameter, demonstrated that more of the high enthalpy gas from the external shock layer is ingested as the hole diameter is enlarged. Additionally,

this work also demonstrated that: (a) an imbedded shock forms on the windward lip of the hole where extremely high temperatures (3,000 °K or 4,850 °F) are generated, assuming a fully catalytic materials response and (b) that the local inviscid shock layer flow over the wing is essentially unchanged as a result of the presence of the hole.

Subsequently, Boeing Huntington Beach (BHB) personnel (Reference 21) carried out internal CFD coupled to the external flow solution by Gnoffo, et. al., for a 6 inch hole in RCC Panel 7 where the 7/8 spanner and its insulation ("earmuff") were not modeled. These results gave lip-heating rates similar to the LAURA solutions. Further, they showed that the plume strikes the outboard RCC Panel 7 rib at a near normal angle of incidence, creating very high local convective heating rates.

The external flow solution by Gnoffo discussed above (Figure 19) was used by the Boeing Rocket Propulsion and Power Group as a starting point for a CFD study (Reference 22) of the internal flow created by a 10 inch hole in RCC Panel 8. Their work utilized the ICAT CFD Code running equilibrium air and assumed fully laminar flow. The ICAT code was validated for this application through code-to-code (LAURA and a USA Code) comparison of predicted heat fluxes to a sphere in Mach 18 flow at an altitude of 165,000 ft. The calculation assumed constant boundary conditions into cavity dump regions of 0.087 psia (600 Pa).

Figure 37 depicts a view of the CFD results (Reference 22) from the front of the leading edge with the acreage of the panels rendered transparent. The hole in RCC Panel 8 is outlined on the lower left corner of the figure. Streamlines are color coded by Mach number and pressures on the earmuff and spar insulation "hot tub" are displayed by the color-coding shown in the figure. As can be seen, the subsonic flow is complex and the jet creates a significant high-pressure zone on the RCC 8/9 earmuff.

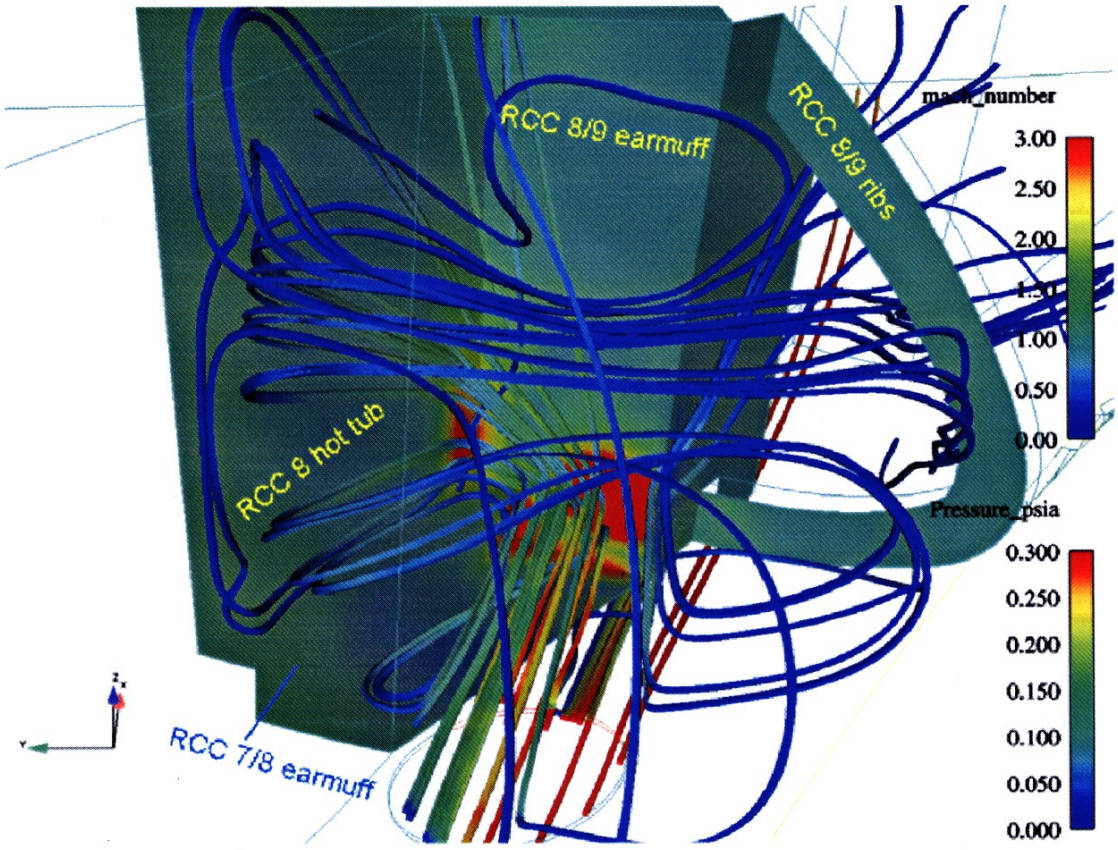

Figure 37: Results Adopted From Reference 22, Showing Streamlines From a 10" Diameter Hole in RCC Panel 8 (the Hole is Shown at the Lower Left). Acreage of RCC is Rendered Transparent. View is From Front of the RCC WLESS. Flight Conditions are Mach: 24.9, Altitude: 243 k ft, as in Figure 19. Pressure of 0.30 psia is Equal to 43.2 psf.

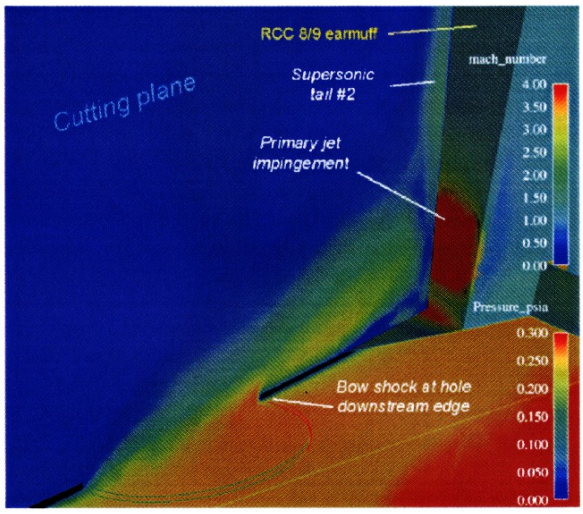

Figure 38 (a): CFD Predictions for Wall Static Pressure and Mach Number for a 10" Hole in RCC Panel 8, Corresponding to Solution in Figure 37. Static Pressure is Color Coded on Walls and Mach Number Distribution is Shown on the Cutting Plane.

Figure 38 (a) from the Boeing Propulsion and Power group depicts the static pressure on the WLESS internal walls and the Mach number on the cutting plane, which passes through the 10 inch diameter hole. The results indicate that all of the external boundary layer and some of the local inviscid (freestream) flow is ingested into the WLESS channel. The primary jet strikes the earmuff at a near-normal incidence (80°). Its stagnation pressure exceeds the freestream-shock pressure because of a precompression by the oblique vehicle shock.

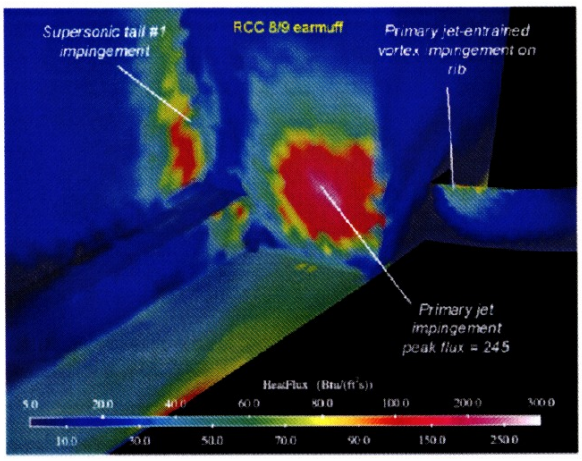

Figure 38 (b): CDF Predictions for Convective Heat Flux on Hot Tubs, Earmuff and Rib for a 10" Hole in RCC Panel 8, Corresponding to the Solution in Figure 37.

Figure 38 (b) shows CFD predictions for convective heat transfer to the spar insulation (hot tub), spanner insulation (earmuff) and the RCC outboard rib corresponding to the solutions shown in Figures 37 and 38 (a). The heat fluxes on the earmuff at the center of the jet impingement are significantly higher than that of an undamaged wing, immediately upstream of the breach in Panel 8 with a finite catalytic wall (Reference 18) (300 vs. 27.3 Btu/ft^{2}s).

In summary, this seminal work has shown that the flow in holes from 2 -> 10 inches in diameter allow superheated air jets to impinge on the inner surfaces of the WLESS creating complex internal flows with significant local heating rates significantly higher than those which occur on the exterior of an undamaged wing leading edge during the normal functioning of the Shuttle.

The results from the BHB study (Reference 21) were available when the CAIB requested arc jet simulations to demonstrate that super heated airflows inside the WLESS could cause sharpening of the RCC seen in the Columbia debris. They were used to define test conditions for arc jet simulations of RCC sharpening to be discussed below.

Arc Jet Simulations of Super Heated Flow Causing Ablation and "Sharpening" of RCC

Arc jet testing discussed by Curry, et. al., in 2000 (Reference 5) has shown that superheated air can cause "sharpening" of RCC when the SiC coating has been removed, the surface temperature of the undamaged SiC is at 2800 °F or greater and the pressure is 30 psf or greater. This testing was done on small circular holes in RCC samples, caused by simulated micrometeorite damage. Figure 39 shows the arc jet test set-up used in this testing.

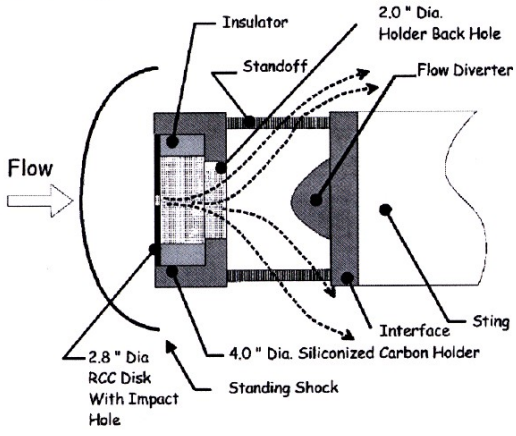

Figure 39: Arc Jet Test Set-up for Micrometeorite Testing of RCC (Reference 5).

Figure 40 displays photographs of the test article number 1159 pre and post arc jet test. Test conditions resulted in a surface temperature and pressure on test article number 1159 of 2500 °F and 50 psf, respectively, The exposure was for 450 seconds. Figures 40 c) -> 40 e) show that in this case, the hole growth grew by oxidation of the exposed carbon-carbon substrate. The oblique view in Figure 40 e) illustrates the "dishing out" of the carbon sandwiched between the SiC front and back coating. For these test conditions, Curry, et. al., did not expect hole growth owing to loss of the SiC coating because of its stability up to temperatures in the range of 2800-3000 ° F and this was confirmed by the tests.

Figure 41 displays photographs of test article number 1151, pre and post test. The temperature of exposed carbon at the SiC edge reached 3,250 °F +. For this test condition (2800 °F and 100 psf), there was significant front face SiC coating erosion as shown in Figures 41 c) and d). Curry, et. al., noted that in general, the front face of the damaged region grew faster than the backside of the specimen, resulting in a conical, or "sharpened shape," typical of all of their testing at a nominal temperature of 2800 °F.

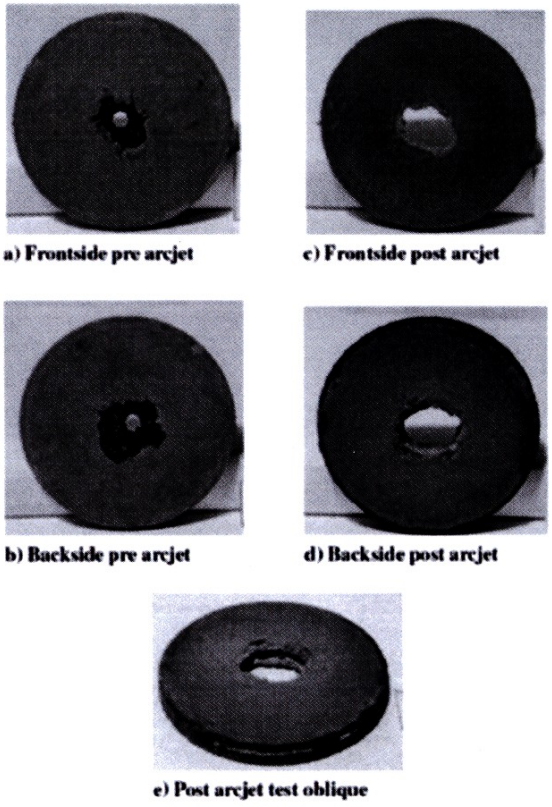

Figure 40: NASA/JSC Model Number 1159, Pre and Post Arc Jet Exposure at 2500 °F and 50 psf, 400 Second Exposure. (Reference 5).

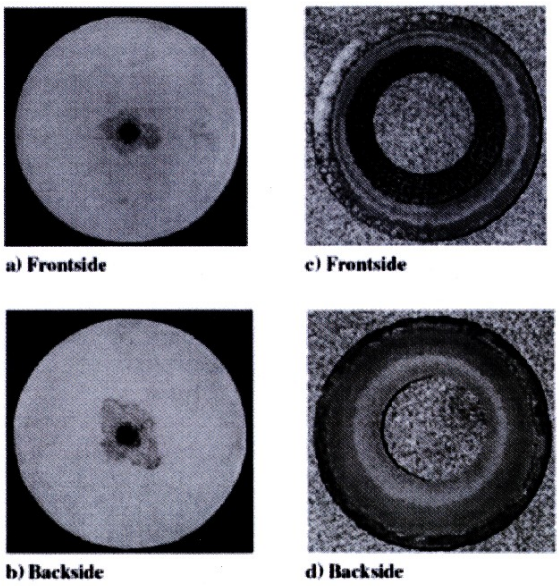

Figure 41: NASA/JSC Model Number1151, Pre and Post Arc Jet Exposure at 2800 °F and 100 psf, 450 Second Exposure. (Reference 5).

It can be concluded from these tests that the dominant mechanism for the ablation of RCC with the coating removed is diffusion-controlled oxidation. At the higher temperatures, SIC coating loss is expected. This result, which causes "knife edging" for a circular hole suggests that if RCC was damaged in a linear fashion, one would see formation of knife-edges in superheated air heating environments existing for hundreds of seconds in conditions like those in the arc jet tests discussed in Reference 5. This observation was the basis for the discussion of the "knife edging" seen in the RCC Panel 8/9 debris from Columbia.

In order to further determine if knife edging would occur on coated RCC due to flow inside the wing from a hole in Panel 8/9, additional arc jet tests (Reference 6) were performed in the JSC facility at the request of the CAIB. Two test articles were designed, built and tested. Test conditions were defined to simulate the flow into the wing based on the Boeing Huntington Beach CFD results previously discussed.

The first test, with two parallel plates shown in Figure 42 with flow impinging at 70 degrees to the flat face was intended to simulate the flow inside the wing impinging on RCC ribs. The results of the test on the parallel plates was inconclusive, because the surface temperatures attainable, without damaging the model holder, were not high enough to cause ablation of the SiC coating.

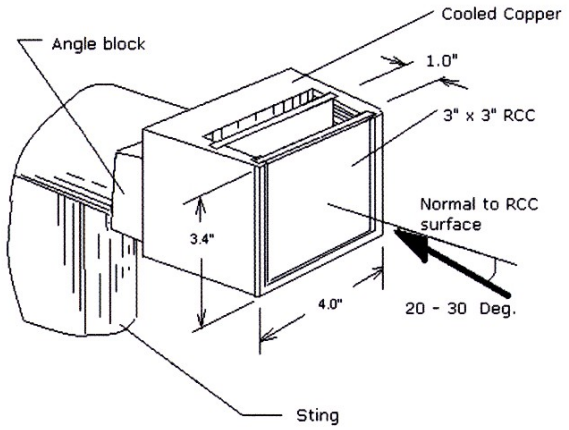

Figure 42: NASA/JSC Arc Jet Test Set-up for Linear Knife-edge Tests at Large Angle of Incidence (70°). Test to Simulate Flow Impingement on RCC Ribs.

The second test article, shown in Figure 43, was intended to simulate flow on the windward lip of a hole in Panel 8. This test, with a flow angle on the single plate at 20 degrees incidence showed that knife edging would occur when the temperature on the coated leading edge of the plate was above 3250 °F. Table 3 specifies the test conditions thought to simulate the enthalpy and impact pressure present in the damaged wing during Columbia's entry on STS 107.

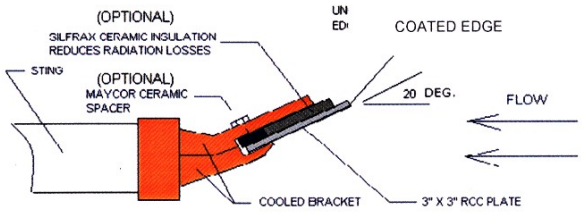

Figure 43: NASA/JSC Arc Jet Test Set-up for Simulation of RCC Knife-edge Erosion at Low Angle of Incidence (20°). Test Intended to Simulate Flow on Lip of Hole in RCC Panel.

Condition	Bulk Enthalpy (BTU/lbm)	Impact Pressure (psf)	Duration (sec)
1	11,200	75	350
2	10,800	129	173

Table 3: Operating Conditions for Tests Shown in Figure 44.

Figure 44 (a) is a pre-test photograph of the test article. Note that the coated edge of RCC is facing the flow for both the RCC sample and the RCC closeout pieces placed on either side.

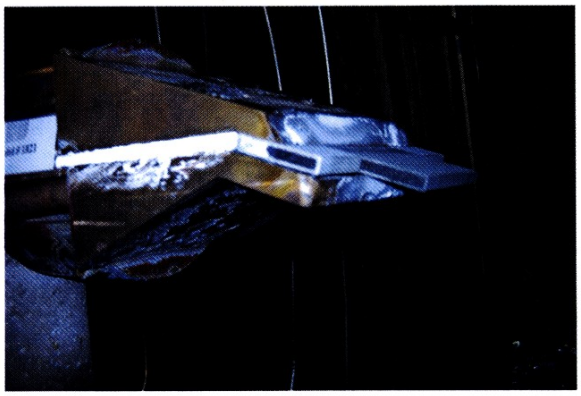

Figure 44 (a): Pre-test Photograph. Angle of Incidence: 20°, Coated Edge Facing Flow.

Figure 44 (b): Post-test Photograph Showing Knife-edges in Both RCC Test Article and Closeout.

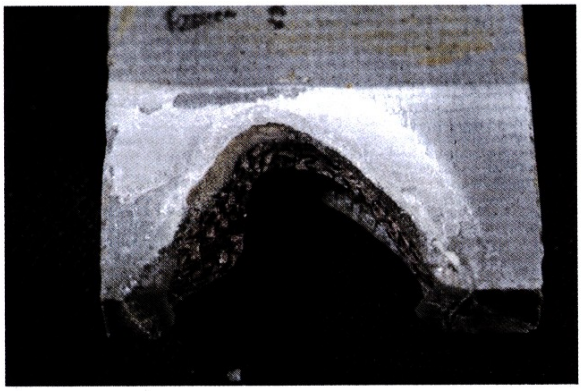

Figure 44 (c): Close Up, Post-test Photograph Showing Knife-edges in the RCC Closeout.

Figure 44 (b) is the corresponding post-test photograph of the test article. Here, erosion of the SiC coating is apparent, as is the formation of a knife-edge on the primary RCC sample, where the highest temperatures occurred. The edge temperature was in excess of 3200 °F or greater as shown by the failure of the SiC coating. Furthermore, as shown in Figure 44 (c) knife-edges also formed in the SiC coated RCC closeouts where flow from the primary RCC sample was impinging.

Tests like those just described were also performed using a test article with an uncoated RCC edge. Similar knife-edges were formed as a result of exposure to the superheated air stream, as expected.

The arc jet tests performed for the CAIB investigation and those previously performed by Curry, et. al. can be used to understand the process by which knife-edges were formed on the RCC components inside Columbia's damaged wing during entry.

If the heat transfer from the superheated airflows creates temperatures in excess of 3200 °F and impact pressures of greater than about 30 psf for extended times, the SiC coating will fail. The SiC coating on the RCC is stable to about 3200 °F, at which temperature it oxidizes, forming liquid silica glass, which either flows off the carbon surface or is evaporated as the temperature goes even higher. The same heating environment that heats the silicon carbide to 3200 °F will heat the exposed carbon to much higher temperatures because the exothermic oxidation of the carbon increases the energy at the surface. Once the carbon has been exposed by removal of the coating, the ablation process becomes more intense because the temperature at the interface between the coating and the carbon substrate gets higher and the SiC removal rate increases.

When the flow is at an angle to an edge (Figures 42 and 43), the heat transfer and mass transfer of oxygen will be higher on the windward side then the leeward side, so the SiC will be removed faster on the windward side. The heat transfer and diffusion of oxygen to the surface is the highest at the exposed sharp edge. As the gas flows downstream along the surface of the plate, the boundary layer becomes thicker and the heat flux and oxygen diffusion rate to the surface lowers. The amount of carbon that burns off decreases, because it is controlled by the rate of oxygen diffusion to the surface. As long as the temperature at the interface of the carbon and the silicon carbide coating is above the oxidation temperature of the silicon carbide this process will continue. When the temperature drops below that value the silicon carbide remains in place and protects the carbon. That is why, in the earlier tests by Curry, et. al., (Figure 41) and in the test results shown in Figure 44, the surface of the model facing the flow shows the knife edging and the back of the test article does not. The temperature on the back does not become high enough to oxidize the silicon carbide. At low heat flux the broken or penetrated edge of the RCC will experience ablation/recession of the carbon between the two silicon carbide coated surfaces causing a cavity. The silicon carbide will not recede because it never reaches its oxidation temperature (3200 °F).

It is probable that some broken edges of internal RCC were formed by the foam impact. In either case for RCC, coated or uncoated, knife-edges would be formed, provided that high temperatures and pressures of the type described above are present for extended periods. It is also possible that the SiC coating was damaged on relatively large, broad areas of the internal RCC surfaces due to the impact of fractured RCC and foam debris ejected from the back surface of the initial foam impact hole. This could have caused significant micro-cracking of the SiC coating on the surfaces facing the rear of the impact hole, i.e., the flow- facing, front side of the internal RCC pieces. In this case, surface recession would have occurred over relatively large areas of the damaged flow facing surfaces as the oxygen reached the carbon through the cracks in the SiC coating. This would produce very thin RCC panels with significant carbon removal on the front side and practically no damage to the rear side as is illustrated in Figures 28 and 29.

The exact configuration of the final knife-edge is highly dependent on the exposure time, heat flux, flow angle and initial condition of the edge. If the heat flux is high enough, the longer the exposure, the sharper the knife-edge is likely to get. If the edge is initially broken at an angle to the surface of the knife-edge, it is likely to be sharper. Inspection of the RCC ribs illustrated in Figures 28 and 29 show very sharp edges that indicate a long exposure to high heating rates. This indicates that this debris was exposed to high heating early during Columbia's final atmospheric entry lasting until break-up.

Summary

The authors have analyzed available information to confirm or refute Admiral Gehman's aforementioned hypothesis made in early February: During launch, an ET foam strike compromised the RCC left wing of Columbia. The breach was present at the Entry Interface (EI) and during entry severe internal heating occurred, the wing structure failed and this led to the tragic loss of Columbia and the STS 107 crew. As assigned, the focus of this analysis was on the TPS.

The vehicle re-entry environment of the Space Shuttle for a normal (undamaged vehicle) was reviewed in order to help the reader understand the need for TPS. A synopsis of the design and function of the Shuttle TPS was also

presented so the reader could understand how it performs during normal entry (successfully over one hundred missions).

Supporting evidence for the strike of ET foam and damage it may have inflicted is the subject of study by others. Analysis of launch films and video, together with CFD study of the transport of the foam trajectory, conclude that the area struck was in the area of the lower RCC panels from 5-8. Tests at Southwest Research Institute and physics-based models show that foam impacts can cause severe damage/cracking to RCC panels and T-Seals, physical displacement of parts and the formation of large holes (16 by 16 inches).

The analysis herein started with an assumption that the RCC compromise was in the areas of RCC Panels 5-8. Increasingly, the information developed strongly suggested that the breach was in the lower part of Panel 8, and that part of the upper T-seal between Panels 8 and 9 was missing or severely displaced at entry interface.

MADS/OEX data from a thermocouple mounted behind the leading edge wing spar, behind Panel 9 recorded out-of-family temperature increases during ascent, after the foam strike at 82 seconds into the launch. Analysis by NASA suggests that a hole in Panel 8, of 6 -> 10 inches in diameter could account for this temperature rise. Since the temperature rise is small, this information by itself is insufficient to confirm the hypothesis. However, with the preponderance of other information available, it does strongly suggest that the breach was in place at the entry interface, which occurred 16 days later.

MADS/OEX data from four sensors in the span of time from GMT 13:47:00 to 13:50:00 show the progression of damage is from the RCC toward the aft of the vehicle. The first indication is from a strain gage mounted on the spar, behind Panel 9. Its signal was interpreted to be caused by the RCC cavity being pressurized and building up thermal stress in the wing leading edge. Shortly thereafter, a thermocouple in the RCC mounting clevis, inside the wing leading edge at the Panel 9/10 area recorded a slight temperature increase. Then a thermocouple on the back of the spar behind RCC Panel 9 also displayed a temperature rise. Finally, in this span of time, the left OMS Pod thermocouple showed an initial below nominal trend. Wind tunnel data showed that this was likely caused by a flow field disturbance in the RCC Panel 5-10 region.

The interval from 13:52:00 -> 14:00:00 includes three key observations, which correlate with the hypothesis. First, the thermocouple on the back of the spar behind Panel 9 showed an abrupt increase at 13:52:19 (EI + 487 seconds) interpreted to be caused by superheated air penetrating the spar. Increasing heating on the OMS Pod correlates with debris leaving Columbia in events 1 - 13 occurring in the two minute time frame from 13:53:29 -- 13:55:29. At 13: 57:14, a photograph taken from the Starfire facility at Kirtland Air Force Base shows left wing damage that is consistent with the hypothesis. Compelling evidence to support the hypothesis comes from the debris from Columbia and its forensic analysis. Study of the recovered debris revealed significant damage in the RCC Panel 8/9 area. This included significant erosion, or "sharpening" of the very durable RCC and melting of metal fixtures and insulation, internal to the WLESS. Significant RCC erosion and melting of LESS RCC mounting hardware is observed only in the Panel 8/9 area of the left wing. This debris evidence is believed to have occurred during exposure to a superheated flow environment lasting for hundreds of seconds. Arc jet simulations of RCC in such a superheated air stream support this conclusion. Flow out of a slot in the juncture between RCC Panels 8 and 9 caused severe erosion and flow patterning on the carrier panels below RCC Panel 9. Streamlines from CFD solutions indicate that flow from this juncture washed over the thermocouple in the lower tile field, behind Panel 9. This thermocouple registered off-nominal heating during the STS 107 entry correlating well with the hypothesis.

Chemical analysis of "slag" on the debris showed that the composition of deposits closest (earliest) to the interior of the RCC upper Panel 8 correlates with the metal spanner bars and mounting hardware and cerechrome insulation. Outer (later) portions correspond to the aluminum deposition. This sequencing also correlates with the hypothesis.

Finally, analysis by NASA using both CFD and engineering analysis tools show a strong correlation of the observations (ascent heating, entry heating, timing for spar burn-through and OMS pod off-nominal high and low temperature) to those that would occur if a 6 –> 10 inch diameter hole existed in the lower section of RCC Panel 8 at entry interface.

Conclusion

Based on the information and analysis presented above as well as combined experience in the fields of aerothermodynamics, TPS, entry technology development and ballistic missile re-entry design and test, the authors believe that the hypothesis by the CAIB chair actually occurred.

Based on data and analysis, the general hypothesis that the accident was caused by a compromise to the Left Wing RCC from the ET foam strike has been narrowed considerably. The authors believe it is quite likely that the breach caused by the foam strike was equivalent to a hole

of at least 6 –> 10 inches in diameter in RCC Panel 8. Further, the upper part of the T-Seal between Panels 8 and 9 was missing or severely displaced. The damage existed at Entry Interface.

The authors assign a probability of 95 percent that the hypothesis above occurred, based on the preponderance of information available with 100 percent being absolute certainty.

Finally, the authors also point out that there has been an unwarranted tendency to "fault" the TPS for the Columbia accident. Clearly, the root cause of this accident is the ET foam strike. The design and implementation of the Shuttle TPS was and is a brilliant accomplishment, which for the first time enabled a reusable vehicle to undergo hypervelocity, atmospheric flight. Recommendations made by others for increasing the safety and reliability of the existing TPS may make the system even better for the Shuttle and future reusable vehicles. However, methods to decrease or eliminate impacts to the TPS by large or heavy objects, will be the most significant advances to the overall Shuttle safety and reliability.

Acknowledgements

We respectfully acknowledge the achievement of the thousands of NASA personnel and NASA contractors who developed the Space Shuttle during the late 1970 – 1981 time frame.

We acknowledge the tireless efforts by NASA and contractor personnel who have contributed to understanding what happened to cause the tragic loss of the STS 107 crew and Columbia. Much of the work herein is the result of their labor. Special acknowledgement is made for those who have worked so hard at KSC to reconstruct the debris. These include, Julie Kramer White, Mike Gordon, Tom Roberts, Lisa Huddleston, Janet Ruberto, Jim Meyers, Lyle Davis and Ann Micklos. We acknowledge the excellent support of Liz Fountain, Mike Conely and Tony Griffith of the JSC Columbia Task Force Team. Some of the charts, used herein, are adopted from NASA JSC/Boeing briefings by Phil Glynn/Mark Hasselbeck/Gene Grush/Steve Stitch, and we acknowledge excellent collaborations with them. We acknowledge the support by S. Bouslog, Lockheed Martin, in defining arc jet test conditions and the help of Jim Milhoan in the design of the arc jet tests. The technical support of J. Williams, J. Grinstead, Mark Tanner, Greg Kovacs and L. Chu-Thielbar is gratefully acknowledged. We appreciate Dr. J. Hallock's review of this appendix and Marla Arcadi's help in preparing the manuscript.

Finally, we acknowledge the very fruitful collaborations at the KSC debris site with the Boeing Debris Analysis Team of Larry Korb, Mike Ehret, and Don Hendrix. James Reuther's expertise in fluid flows in analyzing RCC Panel 8/9 debris at KSC was very helpful as well.

References

1. G. Burns, et. al., NASA Final Report, "Image Analysis" of ET foam Strike to Columbia/STS 107, Month 2003.

2. R. Gomez, et. al., NASA Final Report, "Transport CFD Analysis of Foam Strike on STS 107," Month 2003.

3. G. S. Hubbard and P. Wilde, "ET Impact Testing and Analysis," Appendix,_CAIB Final Report, Month 2003.

4. R. B. Darling, "Qualification and Interpretation of Sensor Data from STS 107," Appendix_CAIB Final Report, June 2003.

5. D. M. Curry, V.T. Pham, I. Norman, and D.C. Chao, "Oxidation of Hypervelocity Impacted Reinforced Carbon-Carbon," NASA/TP-2000-209760, March 2000.

6. A. Rodriguez, Section 6.10, Reference 7.

7. P.Madera, S. Labbe, J. Caram, C. Madden and M. Dunham (Principal Authors), et. al., "Aero/Aerothermal/Thermal/Structures Team Final Report in Support of the Columbia Accident Investigation," NSTS-37398, July 2003.

8. H. J. Allen and J. A. Eggers, "A Study of the Motion and Aerodynamic Heating of Missiles Entering the Earth's Atmosphere at High Supersonic Speeds," NACA RM-A53D28, August 1953.

9. D. Prabhu, M. Wright, J. Marvin, J. Brown, and E. Venkatapathy, "X-33 Aerothermal Design Environment Predictions: Verification and Validation," AIAA Paper 2000-2686, June 2000.

10. P. A. Gnoffo, K. J. Weilmuenster, S. J. Alter, "Multiblock Analysis for Shuttle Orbiter Re-entry Heating from Mach 24 to Mach 12," *Journal of Spacecraft and Rockets*, Vol. 31, No. 3, May-June 1994, pp 367 – 377.

11. T. J. Kowal and D. Curry, "Orbiter Thermal Protection System (TPS) Overview," 2/10/03.

12. A. Rodriguez and C. Madden, Section 6.1, Reference 7.

13. CAIB/NAIT, "Columbia Working Scenario Final Report," NSTS-60502, July 2003.

14. T. J. Horvath and N.R. Mirski, Section 5.2, Reference 7.

15. D. L. Potter, "Columbia Signal Attenuation Modeling PIRATE Scoping Study," Private Communication.

16. J. Caram, Section 5.2, Reference 7.

17. S. Widnall, CAIB Report Section on Aerothermodynamics, August 2003.

18. P. A. Gnoffo, S. J. Alter, and R. A. Thompson, Section 5.2, Reference 7.

19. C Madden, Section 6.2, Reference 7.

20. J. Kramer White, M. Eharet, L. Korb, D. Hendirx, et. al., "Hardware Forensics Team Final Report," NSTS-37385, June 12, 2003; and J. Kramer White, "Failure Analysis Final Report to OVWEG in Support of Columbia Accident Investigations," June 23, 2003.

21. K. Rajagopal, et. al. (Boeing Huntington Beach), Section 5.3, Reference 7.

22. S. Halloran and S. Barson, et. al. (Boeing Propulsion and Power), Section 5.3, Reference 7.

THIS PAGE INTENTIONALLY LEFT BLANK

Volume IV
Appendix F.5

Space Shuttle STS-107 *Columbia* Accident Investigation, External Tank Working Group Final Report – Volume 1

This report summarizes the results of the analysis, design, production, and performance of External Tank (ET-93), performed by the External Tank (ET) Working Group (ETWG), as part of the STS-107 *Columbia* Accident Investigation.

THIS PAGE INTENTIONALLY LEFT BLANK

Space Shuttle STS-107
Columbia Accident Investigation
External Tank Working Group
Final Report—Volume I

ETWG Final Report

Table of Contents

Volume I

List of Figures ..... **iv**
List of Tables ..... **vi**
Section 1 Purpose **1**
Section 2 Signature Page **1**
Section 3 List of Members, Advisors, Observers, and Others **2**
Section 4 Executive Summary **6**
Section 5 Method of Investigation, Board Organization, and/or Special Circumstances **8**
5.1 Method of Investigation 8
5.1.1 General 8
5.1.2 Scope of Assessments 10
5.1.3 Fault Tree Closure Database 11
5.2 Board Organization 11
5.3 Special Circumstances 12
5.3.1 ET-93 Performance until Notification of Mishap 12
5.3.1.1 ET-93 History 13
5.3.1.2 ET-93 Loading Summary 13
5.3.1.3 LH2 Tank Prepressurization 29
5.3.1.4 LO2 Tank Prepressurization 30
5.3.1.5 ET-93 Flight Summary 30
5.3.1.6 ET-93 Entry and Disposal 33
5.3.1.7 ET-93 Mass Properties 34
5.3.2 Foam Loss History 37
5.3.2.1 Methodology 37
5.3.2.2 TPS Loss from All Sources Excluding Bipod Ramps 37
5.3.3 Bipod Ramp TPS Loss 43
5.3.3.1 Bipod Area Description 43
5.3.3.2 Results 45
5.3.3.3 Analysis 47
5.3.3.4 Results 48
5.3.3.5 History of Significant Foam Loss 51
5.3.4 Summary 61
Section 6 ET-93 Unique Elements and Acceptance **63**
6.1 ET-93 Unique Elements 63
6.1.1 As-Designed Configuration 63
6.1.2 As-Built Configuration 63
6.1.3 Processing 64
6.1.4 Operational 64
6.2 ET-93 Acceptance 65
6.2.1 Overview 65
6.2.2 Assessment of Flight Hardware 66
6.2.3 ET Incremental Readiness Reviews 67
6.2.3.1 Hardware Element Acceptance Review (HEAR) 67
6.2.3.2 Contractor Pre-Flight Review (PFR) 68

6.2.3.3 S&MA Pre-Flight Assessment (PFA) 68
6.2.3.4 ET Project Pre-Flight Review 69
6.2.3.5 Shuttle Program ET/SRB Mate Milestone Review 69
6.2.3.6 Orbiter Rollout/ET Mate Readiness Review 69
6.2.3.7 SSP Flight Readiness Review 69
6.2.3.8 Pre-Launch Mission Management Team Review 70
Section 7 Data Analysis 71
7.1 Requirements 71
7.1.1 Generic Requirements 71
7.1.1.1 End Item Specification 71
7.1.1.2 Performance Requirements 71
7.1.1.3 Induced Environments 71
7.1.1.4 Interfaces 74
7.1.1.5 ET-Derived Requirements 75
7.1.1.6 ET Implementation of Requirements 76
7.1.2 Flight-Specific Assessments 77
7.1.2.1 Flight-Specific Assessments – Loads 77
7.1.2.2 Flight Specific Assessments – Pressurization 78
7.1.2.3 Flight-Specific Assessments – Thermal 78
7.1.2.4 Flight-Specific Assessments – ET Separation 78
7.2 Fault Tree Analysis 78
7.2.1 TPS Branch 81
7.2.1.1 Summary 81
7.2.1.2 Team Charter 82
7.2.1.3 Team Overview 83
7.2.1.4 Scope of Review 83
7.2.1.5 TPS Debris Branch Fault Tree Structure (Lower Branches and Sub-Branches) 88
7.2.1.6 Evaluation Criteria 91
7.2.1.7 Approach 91
7.2.1.8 Results 92
7.2.1.9 Summary of Tests 110
7.2.1.10 Recommendations 111
7.2.1.11 Conclusions 116
7.2.2 Non-TPS Debris Branch 117
7.2.2.1 Summary 117
7.2.2.2 Team Charter 118
7.2.2.3 Team Overview 118
7.2.2.4 Scope of Review 118
7.2.2.5 Non-TPS Debris Branch Fault Tree Structure 120
7.2.2.6 Evaluation Criteria 120
7.2.2.7 Approach 121
7.2.2.8 Results 123
7.2.2.9 Summary 125
7.2.2.10 Summary of Tests 126
7.2.2.11 Results of Tests 126

7.2.2.12 Recommendations 126
7.2.3 Interfaces Branch 128
7.2.3.1 Summary 128
7.2.3.2 Team Charter 128
7.2.3.3 Team Overview 128
7.2.3.4 Scope of Review 129
7.2.3.5 Interfaces Branch Fault Tree Structure 130
7.2.3.6 Evaluation Criteria 130
7.2.3.7 Approach 130
7.2.3.8 Results 131
7.2.3.9 Summary of Tests 138
7.2.3.10 Recommendations 138
Section 8 Contributing Root Causes, Significant Observations, and Recommendations 139
Section 9 Definition of Terms 145

List of Figures

Figure 5.1.1-1. Fault Tree Process Methodology 9
Figure 5.1.1-2. ET-93 Structure Reviewed during Fault Tree Investigation 10
Figure 5.2-1. ETWG Organization 12
Figure 5.3.1.2.2-1. ET LO2 Helium Inject Supply Pressure 15
Figure 5.3.1.2.2-2. ET LO2 Helium Inject Delta Pressure 16
Figure 5.3.1.2.3.1-1. Nose Cone Gas Temperature 17
Figure 5.3.1.2.3.1-2. Nose Cone Purge Heater Outlet Temperature 18
Figure 5.3.1.2.3.1-3. Nose Cone Flowrate 18
Figure 5.3.1.2.3.2-1. Intertank Gas Temperature 20
Figure 5.3.1.2.3.2-2. Intertank Purge Heater Outlet Temperature 21
Figure 5.3.1.2.3.2-3. Intertank Purge Flowrate 21
Figure 5.3.1.2.3.3-1. Anti-Icing Pressline Purge 22
Figure 5.3.1.2.3.5-1. Ambient Temperature 25
Figure 5.3.1.2.3.5-2. Relative Humidity 26
Figure 5.3.1.2.3.5-3. Wind Velocity 26
Figure 5.3.1.2.3.5-4. Wind Direction 27
Figure 5.3.1.6-1. ET-93 Nominal Impact Area 34
Figure 5.3.1.7-1. ET Post-MECO Reconstructed Weights 35
Figure 5.3.2.2-1. Areas of Observed Loss 37
Figure 5.3.2.2-2. Foam Loss Trend 38
Figure 5.3.2.2-3.a. Orbiter Tile Damage 39
Figure 5.3.2.2-3.b. Total Orbiter Damage and TPS Volume Loss 39
Figure 5.3.2.2-4. Correlation of Divot Weights to Orbiter Hits for All Missions 40
Figure 5.3.2.2-5. Correlation of Visible Foam Loss to Orbiter Damage 40
Figure 5.3.2.2-6. TPS Mass Loss (lb) 41
Figure 5.3.2-7. Schematic of Aggregate Foam Loss 42
Figure 5.3.3.3-1. ET/Orbiter Interfaces 43
Figure 5.3.3.1-2. Bipod TPS Configuration 44
Figure 5.3.3.1-3. Bipod Closeout Schematic 44

Figure 5.3.3.2-1. STS-7/ET-6 45
Figure 5.3.3.2-2. STS-50/ET-50 45
Figure 5.3.3.2-3. STS-52/ET-55 46
Figure 5.3.3.2-4. STS-62/ET-62 46
Figure 5.3.3.2-5. STS-112/ET-115 47
Figure 5.3.3.4-1. Altitude vs. Out-of-Plane Median Wind Speed for Bipod Foam Loss and No Bipod Foam Loss Flights 49
Figure 5.3.3.4-2. Q-Beta over Time for STS Flights with and without Bipod Foam Loss 49
Figure 5.3.3.4-3. Q-Beta over Time for OV-102 Flights with and without Bipod Foam Loss 50
Figure 5.3.3.4-4. Beta over Time for Flights with and without Bipod Foam Loss 50
Figure 3.5.3.4-5. CFD Model of Bipod Region 51
Figure 5.3.3.5-1. STS-32R/ET-32 Post-Separation Photograph 52
Figure 5.3.3.5-2. STS-35/ET-35 Post-Separation Photograph 53
Figure 5.3.3.5-3. STS-42/ET-52 Post-Separation Photograph 54
Figure 5.3.3.5-4. STS-50/ET-50 Post-Separation Photograph 55
Figure 5.3.3.5-5. Corrective Action Following STS-50 TPS Loss 55
Figure 5.3.3.5-6. STS-47/ET-45 Post-Separation Photograph 56
Figure 5.3.3.5-7. STS-56/ET-54 Post-Separation Photograph 57
Figure 5.3.3.5-8. Rollover/Crevicing Phenomenon 57
Figure 5.3.3.5-9. STS-58/ET-57 Post-Separation Photograph 58
Figure 5.3.3.5-10. STS-87/ET-89 Post-Separation Photograph 59
Figure 5.3.3.5-11. STS-95/ET-98 Post-SRB-Separation Photography 60
Figure 5.3.3.5-12. STS-112/ET-115 Post-Separation Photography 61
Figure 6.2.1-1. Milestone Review Process 65
Figure 7.1.1.6-1. Requirements Flowdown 77
Figure 7.2-1. Prioritized Hardware for the Fault Tree Investigation 80
Figure 7.2-2. ETWG Top Fault Tree Levels 81
Figure 7.2.1.4.1-1. Reviewed External Tank TPS Systems 85
Figure 7.2.1.5-1. TPS Debris Branch Top-Level Subheadings 88
Figure 7.2.1.8.1.1-1. NCFI Material Application 93
Figure 7.2.1.8.1.1-2. NCFI Scanning Electron Microscopy Photomicrograph (30X) 94
Figure 7.2.1.8.1.1-3. Foam Structure 95
Figure 7.2.1.8.4.1–1. SLA-561 106
Figure 7.2.2.4-1. Overview of General ET Hardware Investigated in the Non-TPS Debris Fault Tree Branch 119
Figure 7.2.2.5-1. Main Branches of the Non-TPS Debris Section of the ETWG STS-107 Fault Tree 120
Figure 7.2.2.7-1. Process for Auditing Hardware for Debris Potential 122
Figure 7.2.2.8.4-1. Example Non-TPS Debris Observation from the Lockheed Martin Product Assurance Non Fault Tree Database 127
Figure 7.2.3.4-1. ET Interface Orientation 129
Figure 7.2.3.5-1. Top-Level Interfaces Fault Tree 130
Figure 7.2.3.8.1.2-1. ET Strut Load Indicators 133

Figure 7.2.3.8.1.2-2. ET Interface Load Indicators 133

List of Tables

Table 5.3.1.2.1-1. LH2 Loading Cycle Durations 13
Table 5.3.1.2.2-1. LO2 Loading Cycle Durations 14
Table 5.3.1.2.3.4-1. Bipod Heater Standard Configuration HOSC Display 23
Table 5.3.1.2.3.5-1. Ambient Thermal Conditions after Earliest Fast Fill Time 25
Table 5.3.1.2.3.6-1. Camera Scan Results 27
Table 5.3.1.2.3.6-2. Pre-Loading TPS Surface Temperatures 28
Table 5.3.1.2.3.6-3. Fast Fill Surface Temperatures 28
Table 5.3.1.2.3.6-4. Replenish TPS Surface Temperatures 28
Table 5.3.1.2.3.6-5. Pre-Launch TPS Surface Temperatures 28
Table 5.3.1.6-1. ET Post-Flight Data 33
Table 5.3.1.7-1. Mass Properties Data 36
Table 7.2.1.4.1-1. TPS Materials Systems Properties Overview 85
Table 7.2.1.7-1. TPS Team Review Scope 92
Table 7.2.1.8.1.1-1. Spray Foam Acreage Development History 93
Table 7.2.1.8.1.1-2. Acceptance Tests 94
Table 7.2.1.8.1.2.3-1. Acceleration Forces (Table 12.30.2-1) 97
Table 7.2.1.8.1.2.6-1. Summary of Acreage Stress Analysis Parameters 99
Table 7.2.1.8.2.1-1. PDL-1034 Qualification Specimens 102
Table 7.2.1.8.2.1-2. PDL-1034 Analysis Inputs, Derived Requirements, and Verification 102
Table 7.2.1.8.3.3-1. BX-250 Analysis Inputs, Derived Requirements, and Verification 105
Table 7.2.1.8.4.2-1. Critical Analysis Cases 108
Table 7.2.1.8.4.2-2. SLA-561 Analysis Inputs, Derived Requirements, and Verification 108
Table 7.2.1.8.5.3-1. SS-1171 Qualification Specimens (Ref. MMC-ET-SE05-549) 110
Table 7.2.1.9-1. Test Summary 110
Table 7.2.3.8.1.2-1. Example of ET BET Load Indicators 134
Table 7.2.3.8.1.3-1. Structural Interface Investigation Findings 135
Table 8-1. Root Causes and Associated Observations and Recommendations .. 139

Volume II – Interactive CD of ETWG Fault Tree

Volume III – Appendices

Appendix A—Test Reports A-1
Appendix B—ET Working Group Independent S&MA Assessment Report B-1
Appendix C—External Tank Foam Technical Exchange Forum Participant Summaries C-1

Section 1 Purpose

This report summarizes the results of the analysis, design, production, and performance of External Tank (ET-93), performed by the External Tank (ET) Working Group (ETWG), as part of STS-107 *Columbia* Accident Investigation.

Section 2 Signature Page

We certify that the information contained herein is true to the best of our knowledge and represents the completion of the investigation and reporting process for the External Tank Working Group supporting the STS-107 *Columbia* Accident Investigation.

External Tank Working Group Final Report

Approved by

Paul M. Munafo, Chair National Aeronautics and Space Administration (NASA) ETWG	Wanda Sigur, Chair Lockheed Martin (LM) ETWG

Section 3 List of Members, Advisors, Observers, and Others

The following personnel were assigned to the ETWG of the STS-107 *Columbia* Accident Investigation:

Chair

Paul Munafo	Manager, Materials, Processes and Manufacturing Department, Marshall Space Flight Center (MSFC)

Alternate Chair

Neil Otte	Deputy Manager, External Tank Project (MSFC)

Contractor Chair

Wanda Sigur	Director, Engineering and Technology Laboratories

NASA ETWG Disciplines

Steven Gentz	Materials
Joanne Terek	Secretary
Lee Foster	Dynamics/Environments
Patrick Rogers	Structural
John Honeycutt	Propulsion Systems
Don Bryan	Thermal
Larry Nemecek	Safety and Mission Assurance (S&MA)
William Davis	Electrical
Tom Rieckhoff	Photographic Engineering Analysis
Steve Holmes	Induced Environments
Duane Carey	Astronaut Office
Chris Curtis	Orbiter
Ronald Clayton	Debris Analysis

ETWG Teams

James Feeley	Logistics/Administration, Lead (LM)
John Welborn	Data Collection/Control, Lead (LM)
Patrick Rogers	Failure Mode Assessment and Engineering Design, Lead (NASA)
Lynn Servay	Failure Mode Assessment, Lead (LM)
Scotty Sparks	Manufacturing Data Review and Michoud Assembly Facility (MAF) Processing, Lead (NASA)
Matt Wallo, James Moffett	Manufacturing Data Review, Lead (LM)
Steven Gentz, Norman Elfer	Material Properties/Testing, Lead (LM)

Paul Munafo, Wanda Sigur	Fault Tree, Lead (NASA/LM)
Fulvio Manto	Engineering Design, Lead (LM)
Warren Ussery	Nondestructive Evaluation (NDE) Assessment, Lead (LM)
John Key, Bob Atkins	Kennedy Space Center (KSC) Processing, Lead (NASA/LM)
Lee Foster	Performance Data Assessment Coordination, Lead (NASA)
Roy Steinbock	Performance Data Assessment
Lee Foster, Jon Sharpe	Testing Coordination, Lead (NASA/LM)
Eugene Sweet	MAF Processing, Lead (LM)

Personnel listed below provided data and/or expertise to the ETWG:

Astronaut Office Review Team
Duane Carey, Chair
Dominic Antonelli
Charlie Camarda
B. Alvin Drew
Nicholas Patrick

Emeritus Review Board
Arnold Aldridge
Richard Foll
James Odom

Fault Tree (FT) Review Teams

Thermal Protection System (TPS) Debris Team

NASA	**Lockheed Martin Space Systems Company (LMSSC)**
Scotty Sparks, Lead	Michael Quiggle, Lead
Patrick Rogers	Fulvio Manto
Stanley Oliver	Jeffrey Pilet
Sara Masterson	Jim Doll
Jay Samburmuthi	Kevin Montelepre
Christopher Reinecke	Christopher Bourgeois
Mike Prince	Norman Elfer
Elana Blevins	Faye Baillif
Darrel Deweese	Eugene Sweet
Jorge Rivera	John Bzik
John Key	Connie Johnson
	Preston Landry
	David Kirk
Defense Contract Management Agency (DCMA)	Michael Campbell

Cheryl Armand
Marilee Bourg

John DesForges
Roseann Augustine
Pamela Anderson-Behrens
Robert Atkins
David Scott Otto
Douglas Powell

Non-TPS Debris Team

NASA
Patrick Rogers, Lead
Robert Wingate, Deputy
Mark D'Agostino
Carl Foster
Phil Harrison
Kirby Lawless
Daryl Moore
Karen Oliver
Terry Prickett
Carolyn Russell
Frank Zimmerman
Chad Bryant
Kenneth Calandro
Steven Gentz
John Key
Larry Nemecek
Christopher Popp
Jorge Rivera

DCMA
John Carcamo
Velencia Ducre
Patrick Johnson
Tom Leslie

LMSSC
Ashok Prabhakar, Lead
Camille McConnell. Deputy
Robert Biggs
Elliott Brett
Norma Bute
John Carroll
Yeung Lee
Glenda Pates
Mark Pokrywka
Roger Reinmuller
Barney Roberts
Richard Smith
Riki Takeshita
Tom Thompson
Robert Atkins
Roseann Augustine
Daniel Callan
Rob Champagne
Herbert Claybrook
Michelle Guilliot
Paul Jordan
John Huggins
Joe Major
Juan Ramirez
Roy Steinbock

Interfaces Team

NASA
John Honeycutt, Lead
Rafiq Ahmed
Chad Bryant
Keith Layne
Tim White
Jorge Rivera
Terry Prickett
Christopher Popp
Terry Prickett

LMSSC
Daniel Callan, Lead
Shy Parikh
Joe Major
Frederick Williams
Diane Javery
Bernie Bilica
Mark Heinz
Dee Willick
John Welborn

Robin Flachbart
Kimberly Holt
Art Davis
Juan Ramirez

DCMA
Patrick Johnson
John Carcamo

Doug Webb
Jeffrey Pilet
Edward Newman
Jerry Roule
Barney Roberts
Michelle Guillot
Roger Reinmuller
Robert Champagne
Jimmy Hart
Graham Rashleigh
John Huggins
Mike Bankester
Juan Ramirez
Terry Clausing
Roy Steinbock
Charles Holding
Lyle Ferguson
Brian Piekarski
John Quintini
Mark Javery
Dave Brickner
Brian Knipfing
Lonnie Harness

Section 4 Executive Summary

The principal External Tank contributor to the loss of STS-107 is potentially detrimental debris, in the form of foam loss in the bipod area. The mechanism for bipod debris is the interaction (linking) of manufacturing defects, brought about by the complex launch environment, ultimately resulting in liberation of foam. Critical defects include: linear internal voids, attributable to foam curing mechanisms over complex contours ("rollovers"); weak knit lines between layers of foam; voids; and/or delaminations.

The ETWG process involved five complementary elements:

- A Fault Tree was developed to assure a systematic review of the entire ET.
  - 3470 Fault Tree blocks were dispositioned, assessing debris and interface issues on the entire vehicle.
  - Of the 3470 blocks, 142 were determined to be "possible events."
  - After thorough review of all critical portions of the tank, and in consideration of the findings documented by the other Shuttle Element Working Groups, the only significant anomaly was the event observed at approximately 82 sec after launch: foam loss in or near the left hand forward bipod ramp.
  - Six Fault Tree blocks were identified as likely contributors to release of major debris from the left hand forward bipod ramp area. The categories of contributing elements follow:

    Design verification and process validation did not account for all TPS material and processing variability or adequately address all failure modes.

    Quality Control (QC) verification of the manual spray application process did not preclude the existence of TPS defects that could cause release of debris.

    Available acceptance testing/inspection techniques were not capable of detecting adverse "as-built" features, which could compromise TPS integrity.

    Independent of the preceding elements, an undetected/unknown anomaly may have been present in the fabricated components.
- Consultation with outside experts was utilized to provide an independent assessment of postulated failure mechanisms and associated evaluation methods and to generate additional theories regarding possible failure modes and associated contributors.
- Coupon through full-scale component testing was performed to better understand foam systems and material interactions in the complex bipod region. This testing confirmed the defect interaction mechanism described above, and it demonstrated that other postulated foam release mechanisms, such as cryopumping, were unlikely to have led to major loss of TPS debris on STS-107.

- 13 major test programs and hundreds of tests were completed. Testing confirmed temperature distributions assumed in thermostructural analyses and revealed that significant foam loss could only occur as a result of the interaction of multiple, grossly out-of family manufacturing defects.
- Dissection of six bipods revealed manufacturing defects in all six ramps, in numbers sufficient to statistically support the preceding test observation.
- Testing of specimens containing simulated defects showed substantial loss of strength, confirming that defects could join and form debris surfaces.
- High-energy foam loss mechanisms (cryopumping, cryoingestion, *etc*.) could not be demonstrated in the laboratory, even when natural barriers to those mechanisms were artificially removed.
- Variability within the fleet was attributed to natural variations.

  Major variation: number and distribution (pattern) of defects
  Minor variations: loads, environments, *etc*.

- Analysis of critical areas was updated using state-of-the art analysis tools.
  - A detailed solid finite element model (FEM) was developed to replicate the geometry, materials, and environments at the bipod region.
  - All analyses confirmed assumed interactions of environments and supported definition of critical areas of the structure.
- Independent S&MA assessments were performed for systems in-place on the External Tank program (Non-Conformances, Failure Modes and Effects Analysis (FMEA), and Critical Items and Hazards).

Section 5 Method of Investigation, Board Organization, and/or Special Circumstances

5.1 Method of Investigation

5.1.1 General

The origin of the External Tank Working Group was the activation of the MSFC Space Shuttle Contingency Plan, MSFC-SSCP-5-77, specifically, para. 6.1.1, Contingency Working Groups: "…Working groups are activated by the SSPO Manager upon declaration of a contingency. The SSPO Manager works with the appropriate element project manager to coordinate working group activities..."

The primary focus of the ETWG was causes or issues that might have contributed to the *Columbia* accident and those associated with damage to the left wing of the Orbiter. The secondary focus was causes or issues that are generically similar to those that might have contributed to the *Columbia* accident or which otherwise merit consideration by the Space Shuttle Program (SSP).

A Fault Tree was the primary process driver. Two approaches were used:

- A top-down approach, which was used to develop logical fault paths in the classic FT format. The FT analyses and results are developed in great detail within this report.
- A "cross-cutting" approach, which involved the development of "scenarios," or possible chains of events that may or may not be "straight paths" on the FT. In the latter case, they were called "cut sets." Scenario development is a deductive or reverse logic tool where the consequence (top undesirable event) is developed into a number of root or base events. Partial scenarios/questions/observations/comments were identified during brain-storming sessions, interim FT reviews, and manufacturing process document examinations. These statements were collected in a variety of formats and transitioned into an archived database with linage to the originator, creation date, and FT. The identification of the Orbiter left wing debris zone limited the comments to those involving material release forward of the hydrogen to intertank flange. Review of these comments showed a combination of unique circumstances, linked events, and redundant ideas that were subsequently distilled into 54 separate or associated possible scenarios. Each of these possible scenarios had reference to specific FT blocks. These linkages are shown in Volume II, an interactive compact disk of the ETWG FT, and the scenarios also appear therein as a separate, linked database. The scenario analysis resulted in the systematic formulation of the causes of TPS debris loss in STS-107, shown in Section 7.2.1.11, "Conclusions."

Testing and analysis were used as required to augment the existing database. Ascent performance data, available through the ET, Orbiter, and Solid Rocket Booster (SRB), were available to support analyses of the interface branches. With the exception of the 82-sec foam loss event observed during ascent and Orbiter Vehicle Engineering (OVE) analyses, very little physical evidence existed

to support the Debris FT "branches." This necessitated a "probabilistic' treatment, using testing and analysis as required to evaluate the various possibilities for debris.

FT blocks were categorized as either "Possible" (Probable, Remote, Improbable) or "Impossible" contributors to damage to the Orbiter left wing. The FT process methodology is shown in Figure 5.1.1-1. Areas reviewed during the investigation area are shown in Figure 5.1.1-2.

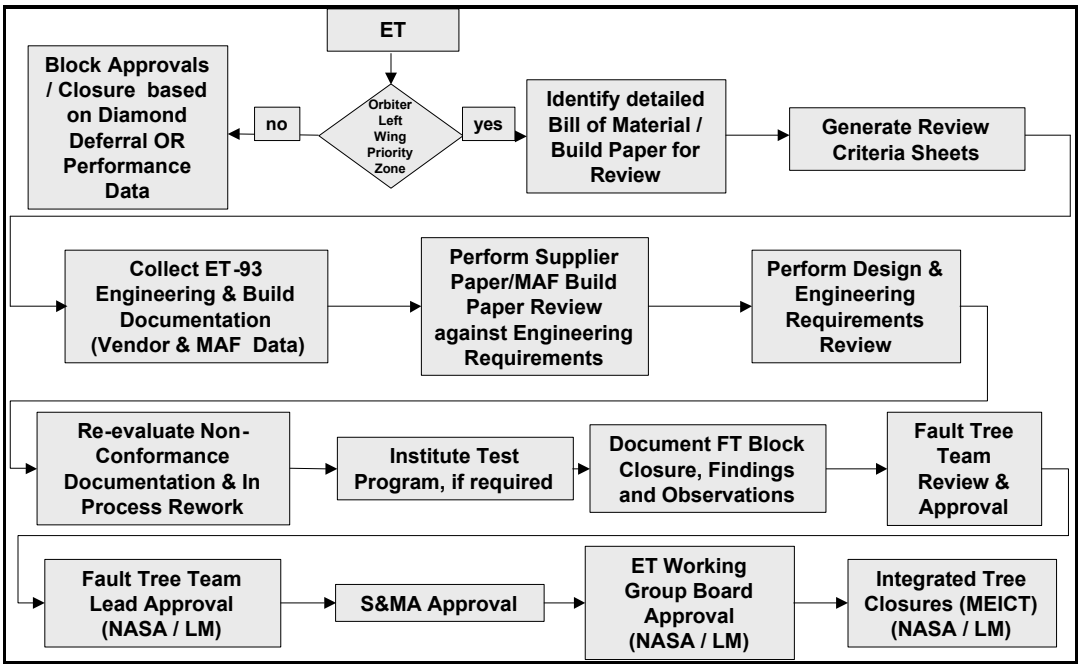

Figure 5.1.1-1. Fault Tree Process Methodology

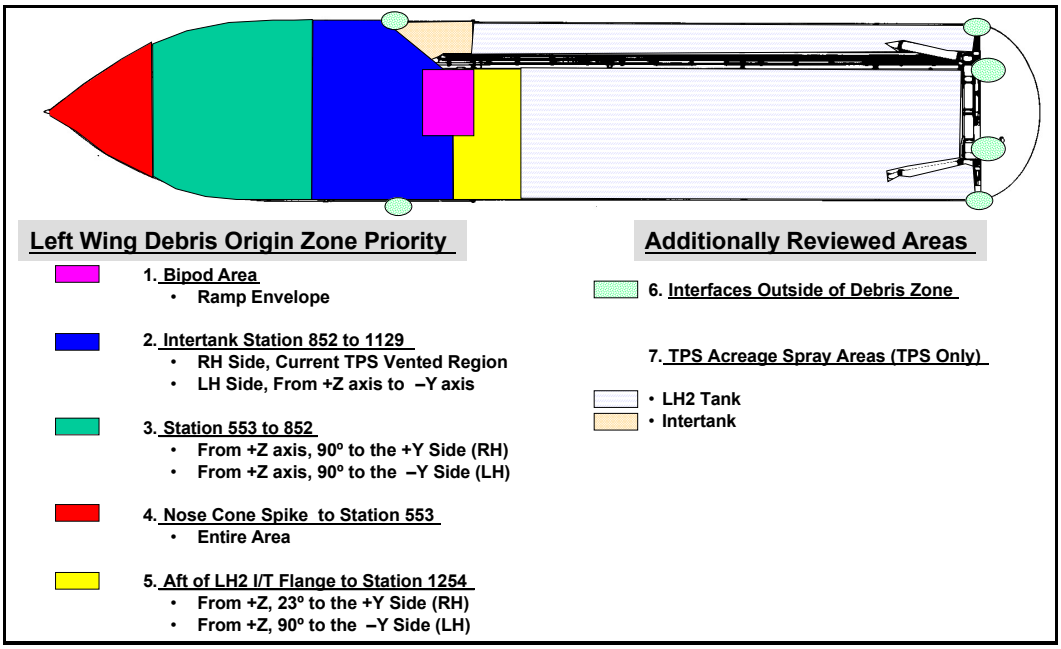

Figure 5.1.1-2. ET-93 Structure Reviewed during Fault Tree Investigation

5.1.2 Scope of Assessments

In general, data evaluated consisted of the following categories: (Note: Specific areas were adjusted to be consistent with appropriate data review for the FT branch assessed.)

- System requirements
- Design assessments
  - Structural materials
  - Analyses and verification
- STS-107 loads and environments
  - Best estimated trajectory (BET) loads
  - Flexible body loads
- ET-93 build records (supplier, MAF, and KSC processing records)
  - Standard Material Specifications (STMs)
  - Standard Process Specifications (STPs)
  - Manufacturing Process Plans (MPPs)
  - Acceptance testing records
  - Nonconformance Documents (NCDs)
  - In-Process Repair Authorizations (IPRAs)
  - KSC Problem Report and Corrective Action (PRACA)/Action Requests (ARs)

  - Practitioner Interviews
  - Previous ET Build histories
- Flight Performance Data
  - Film and Post Flight Inspections
  - All available electrical and propulsion measurements
  - Evidence of nominal performance or anomalies
  - Interface and structure functional performance
  - Any direct or indirect effects on TPS and Orbiter reentry system
  - Previous ET Flight histories
- STS flight experience, pre-flight predictions/expectations, and post-flight performance reconstructions
- Propulsion performance
- Electrical performance
- Additional Assessments
  - Personnel Training Records
  - Inspections and dissections of “sister” External Tanks

5.1.3 Fault Tree Closure Database

An electronic database was developed to manage the FT block closure process. A secure web site was established to allow access from local and remote locations. Electronic routing and approval provided an opportunity to reduce time significantly and provide an opportunity to share and correlate investigation results. The electronic investigation database is included as Volume II of this report.

Branch closures were performed at the lowest level and the system prompted approval through electronic notification. Each closed block required each of NASA, S&MA, and Lockheed Martin Corporation (LMC) approvals, both at the development level and at the FT management levels. A permanent record of approvals is recorded in the FT database.

5.2 Board Organization

The investigation effort was organized with multiple teams to allow effective simultaneous investigation efforts. Team structure is shown in Figure 5.2-1.

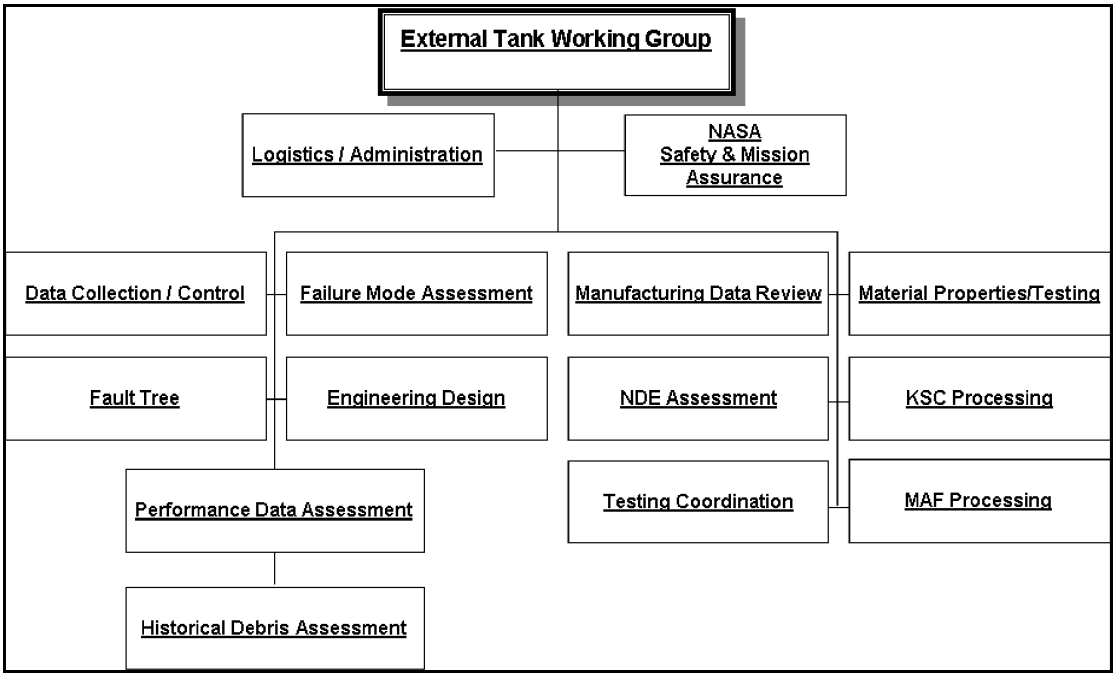

Figure 5.2-1. ETWG Organization

5.3 Special Circumstances

A Space Shuttle contingency was declared by Mission Control, Houston, as a result of the loss of communications with the Space Shuttle *Columbia* as it descended toward a landing at KSC, Florida, on February 1, 2003. Communication and tracking of the Shuttle were lost at 9:00 a.m. EST at an altitude of about 203,000 ft above north central Texas. It was later determined that the Space Shuttle *Columbia* and its crew of seven were lost.

At 9:29 a.m. EST, the NASA Headquarters Contingency Action Plan for Space Operations was activated. Data at all NASA sites and contractors was impounded at 10:00 a.m. EST, and the Headquarters Action Team was activated. Contingency plans were executed at ET contractors and suppliers.

5.3.1 ET-93 Performance until Notification of Mishap

Propellant loading was started at 2:07 a.m. CST on January 16, 2003. Launch occurred at 9:39 a.m. CST of the same day. All component and compartment pre-launch temperatures were maintained within acceptable limits. Loading and flight performance was satisfactory with the exception of TPS debris. Purges and the ET intertank heater operated properly. There were no ET-related Integration Control Document (ICD), Launch Commit Criteria (LCC), or Operations and Maintenance Requirements and Specifications Document (OMRSD) violations during loading. Liquid hydrogen (LH2) and liquid oxygen (LO2) tank ullage pressures were at predicted levels throughout loading and flight. All ET

measurement instruments performed satisfactorily. Main Engine Cut Off (MECO) occurred at approximately 502.6 sec after SRB ignition (T-0), with ET separation occurring at approximately T+523.8 sec. There was no unacceptable ice/frost formation reported by the Ice/Frost Team. In-flight video revealed that, at approximately T+81.7 sec, a piece of TPS debris from the left bipod ramp was shed and struck the left wing area of the Orbiter.

5.3.1.1 ET-93 History

The original launch of ET-93, STS-116, was delayed because of the discovery of cracks in Orbiter feedline flowliners. As a result, ET-93 was demated from the SRBs, and the mission was postponed until after *International Space Station* missions STS-112 and STS-113 were completed. The following dates provide the history of major milestones for ET-93:

DD-250	November 20, 2000
SRB Mate	May 8, 2002
SRB Demate	August 29, 2002
SRB Mate	November 4, 2002
Orbiter Mate	November 20, 2002
Rollout	December 9, 2002
Launch	January 16, 2003

5.3.1.2 ET-93 Loading Summary

Propellant loading was started at 2:07 a.m. CST on January 16, 2003. Two ground equipment problems delayed start of loading. All loading requirements were met. There were no ET-related ICD, LCC, or OMRSD violations.

5.3.1.2.1 LH2 Loading Summary

Loading of the LH2 tank was normal. All loading cycle durations were within previous experience. LH2 chilldown duration was 414.8 sec, near the maximum of 416 sec for the Light Weight Tank (LWT) since STS-40. Replenish duration was less than average because of a delay in the start of loading. The delay was related to two ground equipment problems. Table 5.3.1.2.1-1 summarizes the loading cycle durations as compared to LWT history since STS-40.

Table 5.3.1.2.1-1. LH2 Loading Cycle Durations

Cycle*	ET-93	Minimum	Average	Maximum
Chilldown	414.8	382	397	416
Slow Fill	2386	1437	2509	3524
Fast Fill	2926	2604	2779	3128
Fast Fill Reduced	1444	1127	1569	3412
Topping/Replenish	19,512	17,254	23,500	30,255
Total	**26,683**	**24,462**	**30,755**	**37,679**

* All cycle durations shown in seconds

The End of Replenish (EOR) absolute ullage pressure was 15.02 psia (versus 14.85 psia nominal). The EOR ET LH2 propellant load was 230,926 lbm (109 lbm

less than nominal), which is –0.05% and well within the requirement of +/-0.40%. This includes the effect of ET-93 specific LH2 tank volume.

5.3.1.2.2 LO2 Loading Summary

The LO2 replenish flow rate indication (MSID GLOQ2009A) was observed to be unusually high (approximately 200 gpm versus 130 gpm typical). IPR 107V-113 was taken as a result. If this measurement were inaccurate, it would have resulted in erroneously terminating Slow Fill up to 15 sec early (OMRSD S00FD0.073). The replenish flow rate was within historical limits throughout loading (in particular during Replenish) showing that such indications have occurred in the past. Slow Fill duration was 28 sec shorter than average for LWT since STS-40 but was 32 sec longer than the minimum LWT Slow Fill (STS-94). The concern is that initiating Fast Fill early may cause thermal shock to the LO2 tank vortex baffle. Examination of the original derivation of the 11-min timer for Slow Fill (MMC-3527-83-0018) showed that there is 54 sec of margin. It was concluded, therefore, that the Slow Fill duration was satisfactory and loading proceeded.

The LO2 tank vent valve actuation pressure (MSIDs GLOP4015A, GLOP4515A) exceeded the 800-psig maximum OMRSD limit (S00GEN.760) during replenish. The exceedence was related to a creeping of the 750-psig gaseous helium (GHe) regulator (S72-0697-01 facility GHe supply panel) that supplies the LO2 tank and LH2 tank vent valve actuation systems and the Ground Umbilical Carrier Plate (GUCP) cavity purge system. IPR 107V-115 was taken as a result. The regulator setting drifted because of ambient temperature changes and is not an uncommon occurrence. The maximum pressure observed was 816 psig. The concern is to maintain operation within the certified OMRSD valve timing limits. The ET Project approved a maximum pressure of 850 psig via waiver EK10320 based on the valve proof pressure of 1300 psig and minimal impact to leakage and valve timing during replenish. Both vent valves remain open throughout replenish, so valve timing issues are not an issue. Timing is also not an issue when the valves are closed before prepressurization.

Replenish duration was less than average because of a delay in the start of loading. The delay was related to two ground equipment problems.

Loading of the LO2 tank was otherwise normal. Geyser prevention procedures provided significant temperature margins throughout the vehicle LO2 feed system. The performance of the anti-geyser system is shown in Figures 5.3.1.2.2-1 and 5.3.1.2.2-2, which show the helium inject supply pressure and delta pressure data. Table 5.3.1.2.2-1 summarizes the loading cycle durations as compared to LWT history since STS-40.

Table 5.3.1.2.2-1. LO2 Loading Cycle Durations

Cycle*	ET-93	Minimum	Average	Maximum
Chilldown	1467	1439	1578	1706

Slow Fill	676	644	704	815
Fast Fill	7229	6928	7225	7805
Topping/Replenish	16,782	14,617	20,714	27,977
Total	26,154	23,972	30,272	37,225

* All cycle durations shown in seconds

The EOR absolute ullage pressure was 15.49 psia (versus 15.26 psia nominal). The EOR ET LO2 propellant load was 1,382,980 lbm (990 lbm less than nominal), which is –0.07% and well within the requirement of +/-0.29%. This includes the effect of ET-93 specific LO2 tank volume.

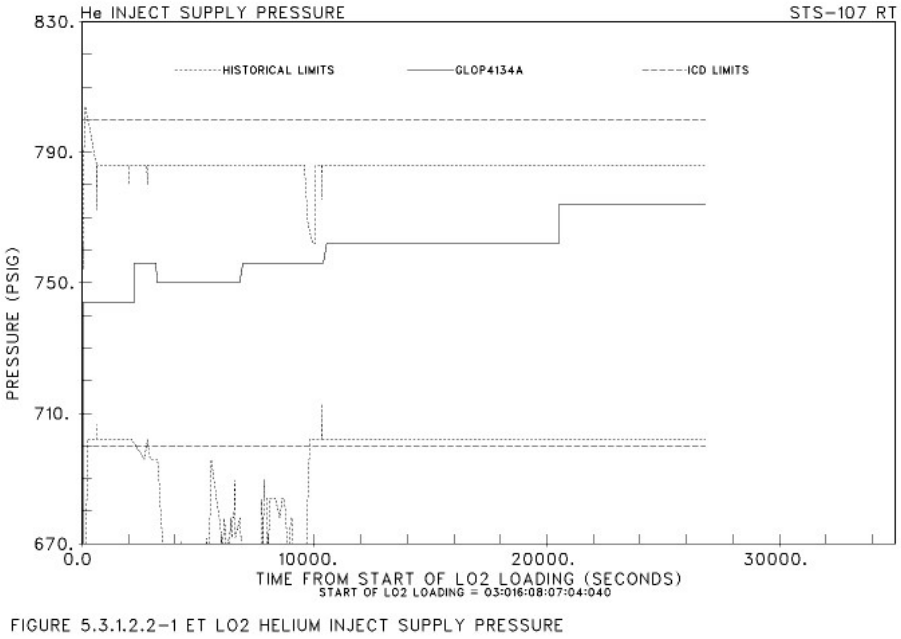

Figure 5.3.1.2.2-1. ET LO2 Helium Inject Supply Pressure

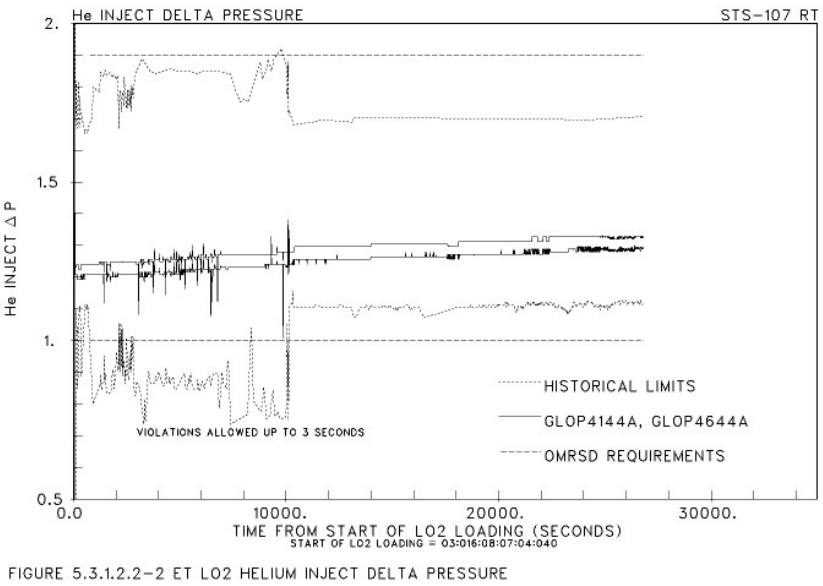

Figure 5.3.1.2.2-2. ET LO2 Helium Inject Delta Pressure

5.3.1.2.3 Thermal Assessment

There were no LCC violations on any of the ET thermal systems. Pre-launch compartment purge flow rate for the nose cone was within the ICD requirements. All electrical heater on/off timelines were met, as were power requirements for the forward bipod and facility purge heaters. All component and compartment pre-launch temperatures were satisfactorily maintained.

In discussions concerning compartment temperatures (Sections 5.3.1.2.3.1 and 5.3.1.2.3.2 below), there is a distinction made between basic redline limits in the text and measurement limits as denoted in the figures. Measurement limits allow for instrumentation and systems errors to protect against exceedance of the basic redline limits.

5.3.1.2.3.1 Nose Cone Compartment Purge

A heated gaseous nitrogen (GN2) purge is used to maintain a dry, thermally controlled environment inside the ET nose cone during pre-launch operations. This purge is initiated 30 minutes before chilldown and is terminated within the time period of T-3 min and T-70 sec. Temperatures inside the nose cone are controlled, using feedback from the primary or secondary temperature probe (MSID T41T1820H or T41T1821H) mounted inside the nose cone, by a controller that regulates power to the facility heater. Set point for the nose cone temperature control is 60°F throughout the entire operation.

Maximum and minimum basic redline limits for the nose cone gas temperatures are 140 °F and 0 °F. There is an allowance, per the LCC, for a minimum basic redline limit temperature down to 0 °F for low relative humidity conditions (protected by a 5-°F LCC redline limit). This allowance is in consideration of the low probability of ice/frost forming at the nose cone vent exit during low humidity conditions. There is also an OMRSD maximum temperature limit of 350 °F identified for the purge gas exiting the heater: MSID GLOT4104A (primary) or GLOT4604A (secondary).

Pre-launch measured nose cone gas temperatures are shown in Figure 5.3.1.2.3.1-1. Corresponding temperatures for the nose cone purge heater outlet are presented in Figure 5.3.1.2.3.1-2. Data in both figures are typical in that an increased demand on the nose cone purge heater is shown as the LO2 loading progressed. There were no LCC or OMRSD temperature violations for either the heater outlet or the nose cone compartment.

Figure 5.3.1.2.3.1-3 shows that the measured nose cone purge flow rate was within the ICD requirement of 9 to16 lbm/min, as it has been since KSC installed critical flow nozzles to limit flow rate (STS-55 on Pad A and STS-51 on Pad B).

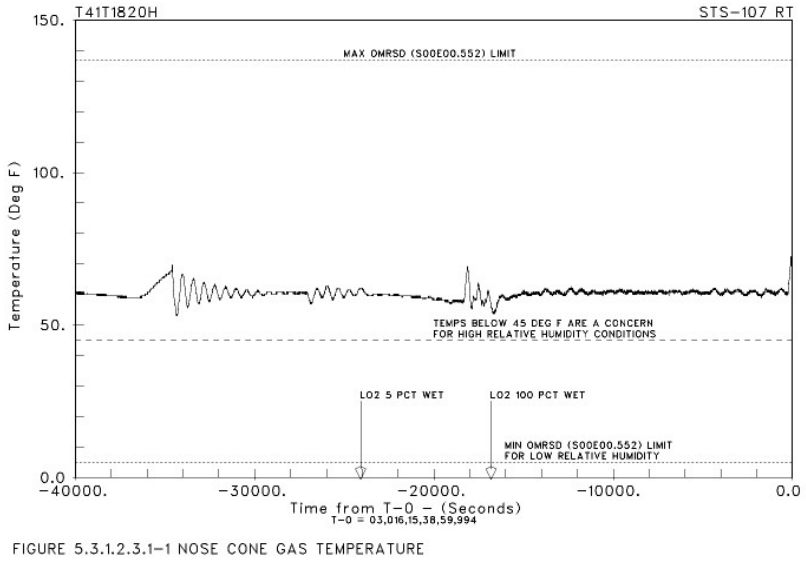

Figure 5.3.1.2.3.1-1. Nose Cone Gas Temperature

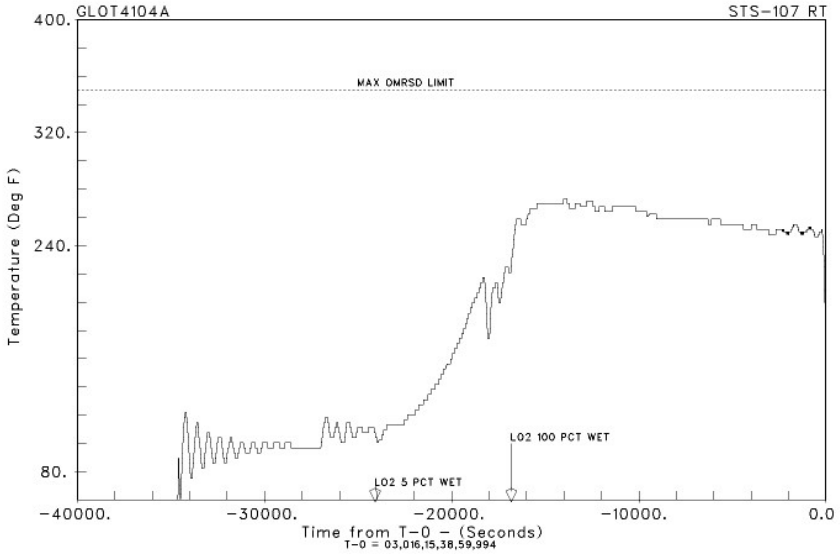

FIGURE 5.3.1.2.3.1-2 NOSE CONE PURGE HEATER OUTLET TEMPERATURE

Figure 5.3.1.2.3.1-2. Nose Cone Purge Heater Outlet Temperature

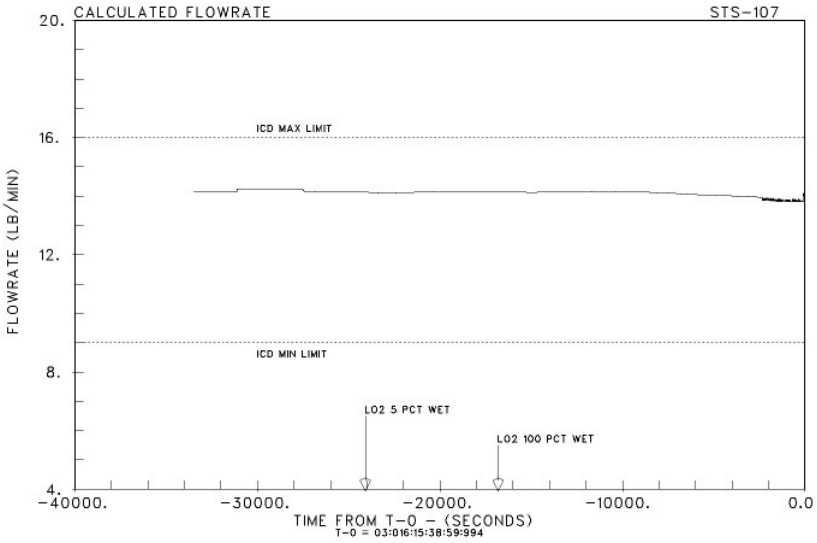

FIGURE 5.3.1.2.3.1-3 NOSE CONE PURGE FLOWRATE

Figure 5.3.1.2.3.1-3. Nose Cone Flowrate

5.3.1.2.3.2 Intertank Compartment Purge

A heated GN2 purge is used to maintain a dry, thermally controlled environment inside the ET intertank during pre-launch operations. This purge is initiated 30 min before chilldown and is terminated within the time period of T-3 min and T-70 sec. Temperatures inside the intertank are controlled by either using the feedback from the primary or secondary temperature probe (MSID T41T1810H or T41T1811H) or the feedback from the primary or secondary heater outlet temperature probe (MSID GLHT5736A or GLHT5737A), which regulates power to the facility heater. The first set of probes is mounted in the intertank, whereas the sec set of probes is located downstream of the heater. Normally, the intertank temperature is controlled based on the output from the intertank sensors with a set point of about 65 °F throughout the propellant loading operation. The set point is subsequently changed to about 56 °F before T-1 hr and is maintained there. During the chilldown and loading phase, the maximum and minimum OMRSD limits for the intertank gas temperatures are 103 °F and 37 °F, respectively. Between T-1 hr and T-3 min, the LCC defines the basic redline limits for the intertank gas temperature as 87 °F maximum and 32 °F minimum with an allowance for maximum and minimum redline exceedances of up to 5 min and 15 min, respectively. The ICD limit for the intertank purge is 350 °F. Measured temperatures of the purge gas exiting the heater, MSID GLHT5736A (primary) or GLHT5737A (secondary), and an analytically derived temperature drop of 6 to 8 °F between the heater outlet and the interface are used for ICD limit verification.

Typically, the gas in the intertank is cooled when either of the tanks is being loaded. The presence of LO2 in the aft dome of the LO2 tank and/or the presence of LH2 in the LH2 tank causes the thermostatically controlled heaters on the launch stand to increase the heater output. In practice, the heater set point is usually lowered when both tanks are in stable replenish, which is much earlier than the 1 hr before launch as required by the LCC.

Pre-launch measured intertank gas temperatures are shown in Figure 5.3.1.2.3.2-1. Corresponding temperatures for the intertank purge heater outlet are presented in Figure 5.3.1.2.3.2-2. The heater outlet temperatures were slightly lower than normal because of the lower demand on the heater that resulted from increased foam coverage on the aft dome of the LO2 tank. The intertank compartment temperatures were in the normal range. Both data traces are typical, showing increased demand on the purge heater as the loading progressed. These data show no LCC, OMRSD, or ICD temperature violations for either the intertank compartment or the heater outlet.

Figure 5.3.1.2.3.2-3 shows the GN2 mass flow rate versus time calculated from the intertank venturi pressure data, which indicated fluctuations in flow rate from approximately 133 lbm/min early in the countdown to an average of 119 lbm/min at the completion of loading. The minimum ICD purge flow limit of 103 lbm/min

was established to prevent air intrusion through the intertank vent areas for a worst-case wind scenario: 47 kts peak wind from 345 deg. Actual peak wind gust velocity during loading and launch was 10 kts from approximately 330 deg as indicated by looking at data from both camera sites 3 and 6. An ICD revision (Interface Revision Notice 0702), which was approved by Level II on September 17, 1992, changed the acceptable flow limits on the purge flow rate to 103 and 158 lbm/min based on an updated analysis. Additionally, effective on STS-73 the facility side of the intertank purge system was modified to provide a trickle purge to reduce the likelihood of intertank air intrusion problems in the event of a hold at T-31 sec.

All objectives of the intertank purge were met; temperatures inside the intertank compartment were maintained within accepted limits; all the components within the intertank performed satisfactorily; and pressure decay and separation pressures were as expected.

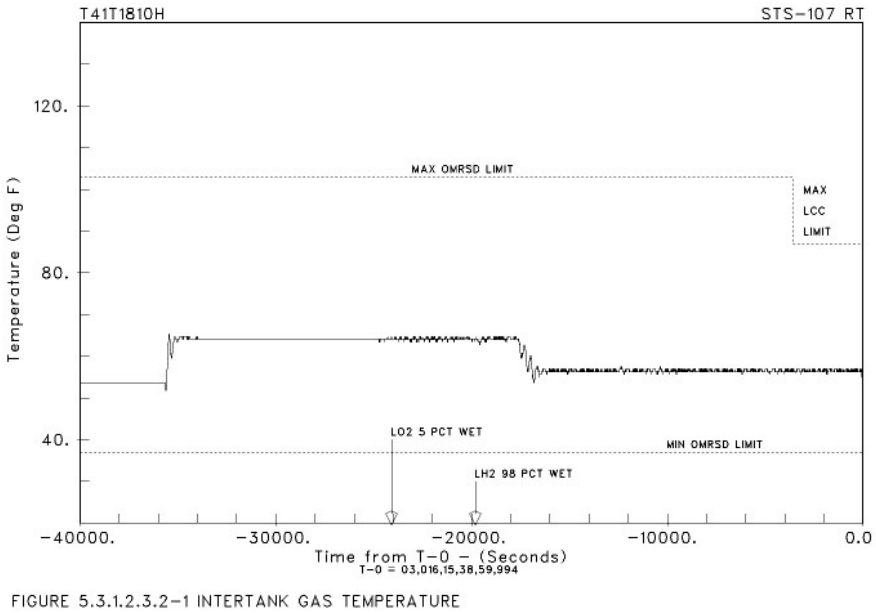

Figure 5.3.1.2.3.2-1. Intertank Gas Temperature

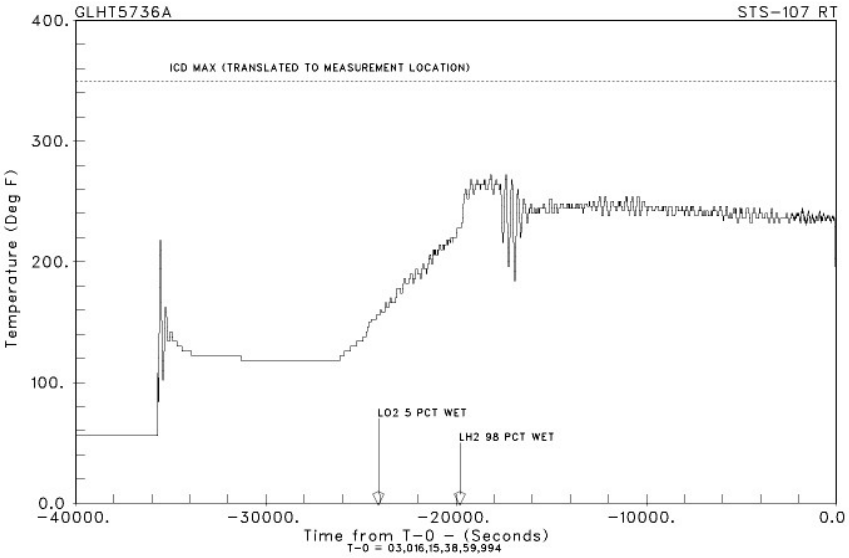

Figure 5.3.1.2.3.2-2. Intertank Purge Heater Outlet Temperature

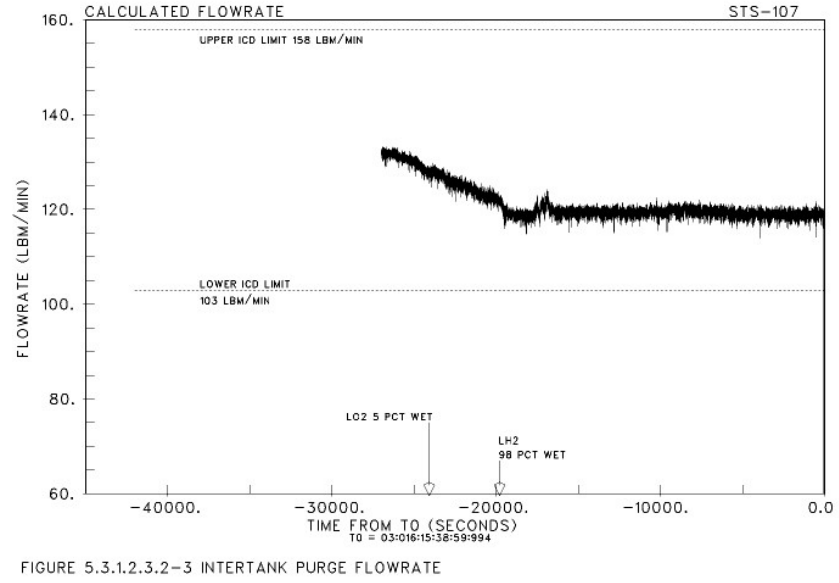

Figure 5.3.1.2.3.2-3. Intertank Purge Flowrate

5.3.1.2.3.3. Anti-Icing Pressline Purge

Heated helium is used to purge the gaseous hydrogen (GH2) and gaseous oxygen (GO2) pressurization lines until just before prepressurization. This requirement was implemented to eliminate the potential for ice/frost forming on the pressurization line at the slide mount bracket locations. Interface temperature of the helium supply is controlled within the acceptable OMRSD range of 245 ±15 °F; interface temperature data are monitored throughout the pre-launch operations (MSID GLHT4577A). Helium anti-icing purge flow rates through the GH2 and GO2 pressurization lines are controlled by the facility to comply with the ICD values of 0.30 ±0.06 lbm/min and 0.45 ±0.09 lbm/min, respectively.

Heater outlet temperature data for the anti-icing purge flow are presented in Figure 5.3.1.2.3.3-1. These data are shown in comparison with the OMRSD limits with select loading events identified on the time scale and indicate that, except for the shutdown transient, the anti-icing purge supply temperature was within specified OMRSD requirements throughout the pre-launch operations.

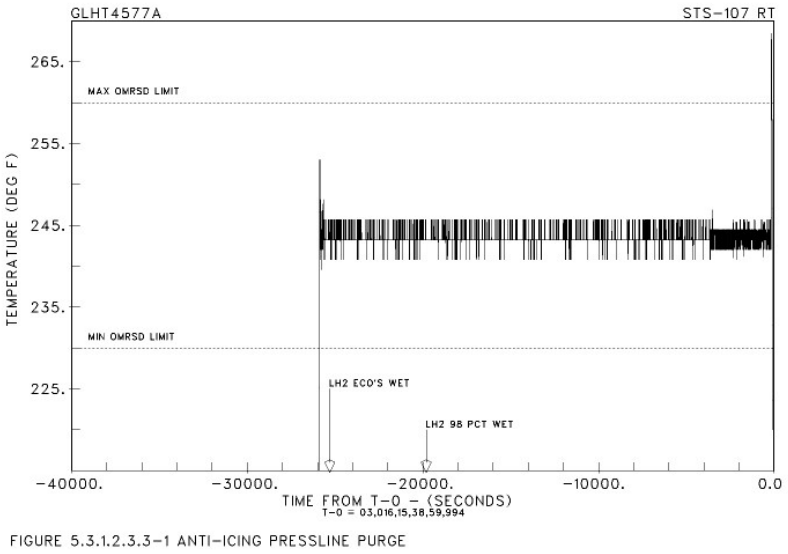

Figure 5.3.1.2.3.3-1. Anti-Icing Pressline Purge

5.3.1.2.3.4 Bipod Heaters

Calrod heaters are used in each of the bipod fittings to limit ice/frost formation on the bipod spindle to less than 6 sq. in. each. Control must be exercised to not turn the heaters on before the cryogen reaches the bipod location (to prevent overheating of the fitting and the surrounding TPS) and to turn them on in a timely manner after the cryogen has reached the bipod location (to prevent the formation of unacceptable ice). For this reason, the bipod heaters are to be turned on from 4 to 5 min after the 98% liquid level sensors are wet. This timeline

was developed from a series of bench tests at MAF and from the bipod spindle temperature data during LH2 loadings on ETs 14 through17; effective on ET-18 (flown on STS-51D), the bipod spindle temperature sensors were deleted.

The health of the bipod heater system is monitored during pre-launch operations using displays that record source voltage and current. Special programs are used to correct heater voltages based on cable/heater simulated tests and to display the wattage of each heater. Limits for each recorded and calculated data stream are unique to each launch pad. Details of the instrumentation and limits for the launch pad are presented in Table 5.3.1.2.3.4-1. All values were within the required limits and no anomalous conditions were reported. The bipod heaters were turned on within the time limits prescribed in the OMRSD, and they remained on until the umbilicals were dead-faced at T-31 sec.

Table 5.3.1.2.3.4-1. Bipod Heater Standard Configuration HOSC Display

PAD A -Left Bipod -3.5 Vac
Right Bipod -3.5 Vac

PAD A	LOW REDLINE	LOW WARNING	HIGH WARNIN
VOLTAGE			
G56V1115A (LFT)	86.0	87.0	90.00
M40Z1000S	82.5	83.5	86.50
M40Z1000S	86.0	87.0	90.00
M40Z1001S	82.5	83.5	86.50
CURRENT			
G56CO155A(LFT#1)	0.80	0.85	1.15
G56CO165A(LFT#2)	0.80	0.85	1.15
G56CO175A(RHT#1)	0.80	0.85	1.15
G56CO185A(RHT#2)	0.80	0.85	1.15
WATTAGE			
M40Z1002S(LFT#1)	66.0	70.98	99.48
M40Z1004S(LFT#2)	66.0	70.98	99.48
M40Z1003S(RHT#1)	66.0	70.98	99.48
M40Z1005S(RHT#2)	66.0	70.98	99.48

Voltage requirements for the bipod heaters are 85 ±0.85 Vac at the umbilical (GUCP). Voltage is established by tests using a cable/heater simulator with fixed resistors equivalent to the heater, ET cable, and pad cable resistance. When the correct current is measured through the heater simulator (1 ±0.2 amp), the voltage at the source is recorded.

Source voltages (MSIDs G56V1115A and G56V1125A) and currents (MSIDs G56CO155A, G56CO165A, G56CO175A, and G56CO185A) are monitored on all heaters during pre-launch. Huntsville Operations Support Center (HOSC) displays also provide corrected heater voltages (M40Z1000S and M40Z1001S) via a special computations program "Elect 1." These corrected voltages are based on the cable/heater-simulated test. Displays for the heater voltages are based on the worst-case drop from the source voltage (G56V1115A). Warning and redline limits for the heater voltages are 3.5 V lower than the source voltage limits. The HOSC also displays calculated wattages (M40Z1002S, M40Z1004S, M40Z1003S, and M40Z1005S

5.3.1.2.3.5 Thermal Environment

Ice/frost formation on an exposed surface is a function of surface temperature and the ambient conditions to which it is exposed. For the ET, a special thermal analyzer subroutine (SURFICE F) was developed to compute surface temperatures. The ambient conditions are recorded at a 60-ft high tower at camera site 3 and camera site 6. It is assumed that ambient data from camera site 3 or 6, which are approximately 1280 ft southeast and northwest of the launch pad, respectively, are valid for use as input for ambient conditions in the ET ice/frost calculations. The ambient data from camera site 6 was used in all the ice/frost and surface temperature calculations. Table 5.3.1.2.3.5-1 summarizes the ambient conditions encountered during pre-launch after the earliest Fast Fill time and the estimated TPS surface temperatures at lift-off, assuming nominal TPS thickness. Ambient conditions of temperature, relative humidity, wind velocity, and wind direction are plotted in Figures 5.3.1.2.3.5-1 to 5.3.1.2.3.5-4, respectively. Also shown on these figures are the significant loading timelines. These parameters are then used in the computer subroutine SURFICE F, which in addition to calculating the sprayed-on foam insulation (SOFI) surface temperature also calculates condensation rate and ice/frost rate in four regions of the ET.

The minimum surface temperatures for the LO2 tank and the LH2 tank were 21 °F and 17 °F, respectively. With these surface temperatures, ice/frost was predicted for the ET acreage during loading; only light frost was predicted for the upper region of the LH2 tank just before launch. Condensation was predicted for the four regions, given the humidity range of 67 to 97%. These predictions are consistent with the visual observations during pre-launch operations.

Table 5.3.1.2.3.5-1. Ambient Thermal Conditions after Earliest Fast Fill Time

	Range of Pre-launch Ambient Conditions		Acreage Temperature* Predictions at Lift-off (°F) Winds from 135°** at 3.2 kts
	Min	Max	
Temperature	48.8	64.8	LO2 Ogive 43.8
Humidity (%)	67.2	97.2	LO2 Barrel 33.6
Dew Point (°F)	47.4	58.0	LH2 Barrel (Fwd) 32.0
Wind Speed (kts)	0.0	9.6	LH2 Barrel (Aft) 42.0
Wind Direction (deg)**	62.6	393	(Predictions based on ET ambient conditions of 65°F and 68% relative humidity)
Surface Temp (°F)	16.8	44.7	

* Based on 5-minute average, ambient conditions
** Based on 360 deg north

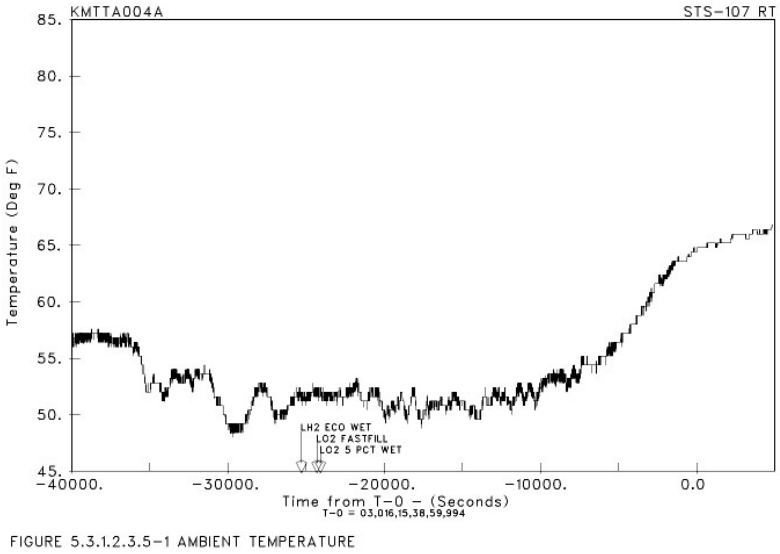

Figure 5.3.1.2.3.5-1. Ambient Temperature

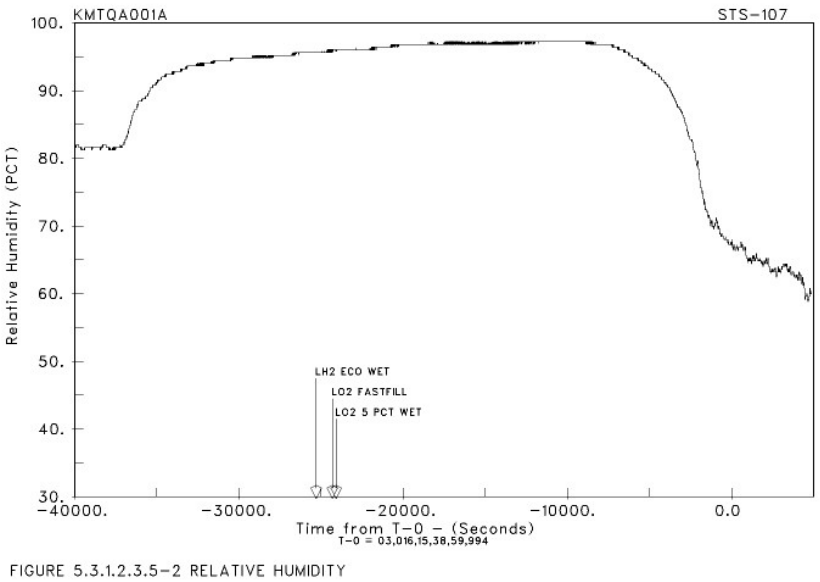

Figure 5.3.1.2.3.5-2. Relative Humidity

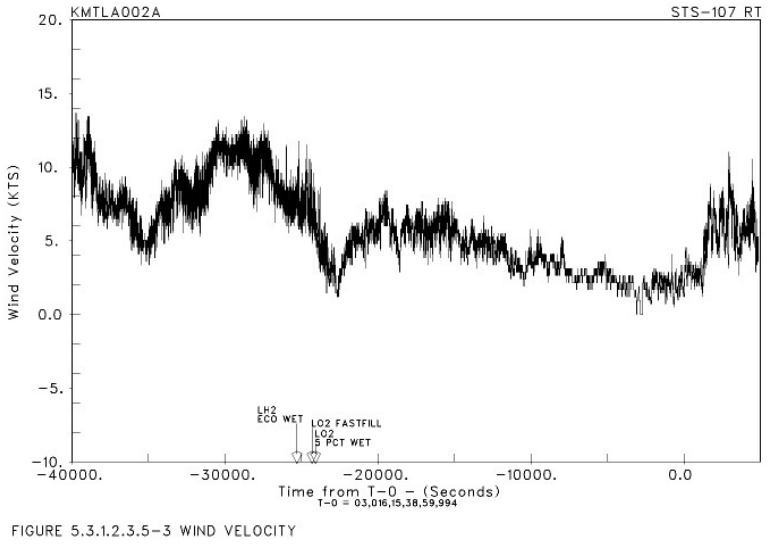

Figure 5.3.1.2.3.5-3. Wind Velocity

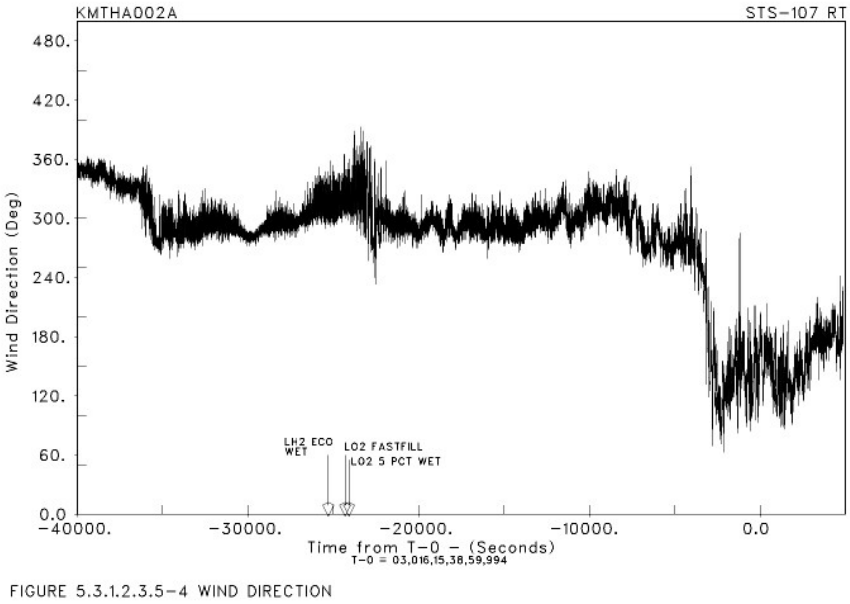

Figure 5.3.1.2.3.5-4. Wind Direction

5.3.1.2.3.6 TPS Assessment

Table 5.3.1.2.3.6-1 shows results of camera scans. Tables 5.3.1.2.3.6-2 through 5.3.1.2.3.6-5 show TPS surface conditions at selected times, with wind data based on 360 deg north.

Table 5.3.1.2.3.6-1. Camera Scan Results

Approx. CST Time	Scan/Results
2:30 a.m.	Initial scans completed/no anomalies
3:15 a.m.	LO2 feedline camera scan completed/no anomalies
4:15 a.m.	LO2 feedline camera scan completed/no anomalies
5:00 a.m.	Camera scan completed/no anomalies
6:00 a.m.	Camera scan completed/no anomalies
9:00 a.m.	Camera scan complete/no anomalies

Table 5.3.1.2.3.6-2. Pre-Loading TPS Surface Temperatures

TPS Conditions before Loading (~12:40 a.m.):		
Temperature: 49 °F Humidity: 94%	Wind Direction: 289 deg Wind Speed: 6 kts	
ET Section	Infrared (IR) Temperatures	
	RSS	CS2
LO2 Ogive	52 °F	52 °F
LO2 Barrel	47 °F	48 °F
Upper LH2	48 °F	49 °F
Lower LH2	50 °F	49 °F

Table 5.3.1.2.3.6-3. Fast Fill Surface Temperatures

Fast Fill TPS Conditions (~3:30 a.m.):			
Temperature: 51 °F Humidity: 96%	Wind Direction: 296 deg Wind Speed: 5 kts		
ET Section	Surface Temperatures	IR Temperatures	
		RSS	CS2
LO2 Ogive	40 °F	49 °F	47 °F
LO2 Barrel	30 °F	34 °F	44 °F
Upper LH2	25 °F	33 °F	45 °F
Lower LH2	37 °F	43 °F	39 °F

Table 5.3.1.2.3.6-4. Replenish TPS Surface Temperatures

Replenish TPS Conditions (~7:00 a.m.)		
Temperature: 50 °F Humidity: 97%	Wind Direction: 282 deg Wind Speed: 3 kts	
ET Section	Surface Temperatures	IR Temperatures RSS
LO2 Ogive	32 °F	36 °F
LO2 Barrel	20 °F	37 °F
Upper LH2	19 °F	38 °F
Lower LH2	30 °F	36 °F

Table 5.3.1.2.3.6-5. Pre-Launch TPS Surface Temperatures

Pre-Launch TPS Conditions (~8:48 a.m.):		
Temperature: 61 °F Humidity: 77%	Wind Direction: 166 deg Wind Speed: 0.5 kts	
ET Section	Surface Temperatures	IR Temperatures RSS
LO2 Ogive	39 °F	53-75 °F
LO2 Barrel	30 °F	43-60 °F
Upper LH2	39 °F	38-58 °F
Lower LH2	30 °F	44-60 °F

Final TPS inspections were conducted from approximately 5:15 to 6:45 a.m. Results from those inspections are listed below.

- Nose Cone: No condensation was noted. The seals were in good shape. No anomalies were observed.
- LO2 Tank: Handheld IR temperatures ranged from 30 to 34 °F. Firing room IR readings indicated temperatures of 35 to 40 °F (RSS). No condensation was noted. No anomalies were observed.
- Intertank: No cracks were observed in the stringer valleys. GH2 vent ice/frost was typical. No leaks or unusual vapors were observed.
- LH2 Tank: Handheld IR temperatures ranged from 20 to 36 °F. Firing room IR readings indicated temperatures of 35 to 41 °F (RSS). Light to moderate condensation was noted. No acreage anomalies were observed. Typical TPS crack on the –Y vertical strut cable tray forward face (12 in. x 0.375 in. with no off-set) was observed. Red tape was noted in the L-1 walk down and documented on IPR-107V-0105 and was observed to still be in place.

No facility or vehicle issues were noted. All observations were acceptable per 8303 criteria. There were no Interim Problem Report/Problem Report (IPR/PR) or LCC violations noted.

5.3.1.3 LH2 Tank Prepressurization

STS-107 was the fifth flight to use a cluster of three Block II Space Shuttle Main Engines (SSMEs). To accommodate the higher start pressure requirement of these engines, the LH2 tank prepressurization band was raised by 5.2 psi. Overall, LH2 tank prepressurization for ET-93 was satisfactory. Prepressurization was initiated at T–104.4 sec and the time to reach the control band was 16.3 sec. Three pairs of rapid GHe bursts were observed. The occurrence of rapid bursts has been observed before and is expected to continue to occur in the future. Rapid bursts are caused by a combination of variables: the set of pressure transducer biases, the short helium prepress burst duration (0.5 sec), signal conditioner and other electrical dispersions in the prepress control circuit, helium temperature, and slight variations in individual transducer construction (winding details, wiper hysteresis).

Ullage pressure transducer No. 1 was biased lower than the No. 2 and 3 transducers, as reported in the Pre-Flight Mission Report, and its indicated response is consistent with that of a low bias transducer. The bias was about 0.10 to 0.15 psi more than predicted, which is not too unusual.

The initial prepressurization of the LH2 tank into the control band indicated a slower rise rate for STS-107 than on the last LWT flight (STS-99, ET-92) but similar to the LWT ET-91 (STS-90). This suggests that the helium mass flow rate and/or helium temperature for STS-107 was not out of family but may have been on the low side. This is supported by the longer time to reach the prepressurization control band. Lower helium flow or colder helium can lead to a larger number of prepressurization cycles. LCC ET-04 limits the number of cycles

to a maximum of 13. This was not a problem as there was still a 30-sec margin to exceeding the maximum prepressurization cycle count. There were 10 prepressurization cycles during the LCC counting period. There were expected margins to LCC ET-05 pressure limits of 46.1 to 48.0 psia.

5.3.1.4 LO2 Tank Prepressurization

LO2 tank prepressurization was normal. Prepressurization was initiated at T–153.8 sec, and the time to reach the control band was 11.5 sec. There were expected margins to LCC ET-06 pressure limits of 19.3 to 22.5 psid. There were 21 prepressurization cycles before Engine Start Command, which is very common.

5.3.1.5 ET-93 Flight Summary

Launch occurred at 9:39 a.m. CST on January 16, 2003. Flight performance was satisfactory with the exception of TPS debris. LH2 and LO2 tank ullage pressures were at predicted levels throughout flight. All ET measurement instruments performed satisfactorily. MECO occurred approximately 502.6 sec after SRB ignition, with ET separation occurring at approximately T+523.8 sec. In-flight video revealed that at approximately T+81 sec, a piece of TPS debris from the left bipod ramp was shed and struck the left wing area of the Orbiter.

5.3.1.5.1 Propulsion Analysis

There were no propulsion system performance observations or anomalies noted.

5.3.1.5.1.1 LH2 Tank

In-flight pressurization of the LH2 tank was normal. The pressure decayed from the prepressurization control band (46.1 to 48.0 psia) to the in-flight control band of 32 to 34 psia in 7.2 sec and was maintained there through the end of powered flight. Approximately 959 lbm of GH2 were used to pressurize the tank from Engine Start Command. There were 13 GH2 Flow Control Valve cycles. These results constitute very nominal performance. Pressurant supply pressures and temperatures delivered by the SSMEs were within previous experience and very near predicted values. LH2 ET/Orbiter interface pressures and temperatures were within ICD limits. Uncover times for the 98% and 5% liquid level sensors were well within previous experience. The LH2 residual at MECO was 3320 lbm, very near predicted.

5.3.1.5.1.2 LO2 Tank

In-flight pressurization of the LO2 tank was normal. The maximum ullage pressure was 26.2 psid and occurred at T+149.5 sec. The minimum ullage pressure was 13.5 psid and occurred at T+12.5 sec. Approximately 2825 lbm of GO2 were used to pressurize the tank from Engine Start Command. These results constitute very nominal performance. Pressurant supply pressures and temperatures delivered by the SSMEs were within previous experience and comparable to predicted values. LO2 ET/Orbiter interface pressures and

temperatures were within ICD limits. Uncover times for the 98% and 5% liquid level sensors were within previous experience. The LO2 residual at MECO was 7354 lbm, very near predicted.

5.3.1.5.2 Structural Analysis

5.3.1.5.2.1 Loads Assessment

The LWT interface loads FTO1 through FTO9, FTB1 through FTB10, P1 through P13, and Zero Margin (α/β) constraints were predicted during the STS–107/ET–93 United Space Alliance (USA)/MOD reviews of the L–3.5 hr and L–2.0 hr Jimsphere balloon data on January 16, 2003. The interface loads provide a rapid validation of the ET interface predictions associated with the measured Day-of-Launch (DOL) conditions. For the data reported, using the L+15 min wind and L-30 min atmosphere, the FTB 5 and 6 interface loads were the highest at 92 and 93 %, respectively (at 76.9 sec into the flight). There were no issues with the ET protuberances. Data from the same balloon predicted the ET's Protuberance Zero Margin Q dispersed was 97% of limit at Mach 0.79. In accordance with Block Update 2002.01 (CR 052550MD), α - β are now reported as vector length margin. The minimum α - β margin was 1.88 at Mach 1.0.

Since the DOLILU II I-LOAD is now the only I-Load available, the ET interface loads provide a method to determine if the assessment made by Level II, and identified in BOEING letter 98MA0717 dated March 31, 1998, remains a valid selection criterion for the ET's DOL Active Indicator List. The interface loads protect the ET against exceedances of contractual design limits, and the Zero Margin squatcheloid provides the airload constraint for the protuberances during the USA/MOD operations for the as- measured pre-launch winds for each flight.

5.3.1.5.2.2 Compartment Venting Performance

Vent areas of the intertank and nosecap compartments that affect loads were:

COMPARTMENT	TOTAL VENT AREA (sq. in.)
Nosecap	19.9 ±2.7
Intertank (Generic)	60.1 ±4.4
Intertank (ET-93)	60.2 ±2.2

Intertank vent area for ET-93 is based on a measured area of 39.4 sq. in. at the base of the LO2 feedline fairing plus an additional 1.6 sq. in. related to LO2 feedline shrinkage from cryogenic temperatures. Planned pre-flight venting walkdowns and inspections verified the remaining intertank vent area of approximately 19.2 sq. in.. Similar planned venting walkdowns and inspections revealed no evidence of open issues associated with the nose cone vent area or with any of the other ET vented compartments, *e.g.,* cable trays, fairings, as defined in the ET leak/vent drawings.

Two normal mission trajectories are used for the pre-flight predictions: a ‘minimum’ throttle profile trajectory and a performance enhancement (PE) high

dynamic pressure trajectory. Minimal deviations in predicted pre-flight and post-flight pressure differentials were observed for the intertank compartment. For the nose cone compartment, there are some noticeable changes in the pressure differential for the initial 2 min of the flight. The differences in dynamic pressure and the angle of attack between the pre-flight predicted trajectories and the post-flight trajectory are the reason for the deviation. The dynamic pressure and attitude directly influence the pressure coefficient characteristics, which are much more sensitive to changes for the nose cone compartment vents than they are for the intertank vents. The deviations between the pre-flight and post-flight nose cone compartment pressures are not a flight concern.

Pre-flight predictions are based on two sets of criteria:

- LWT PE, Block 2A SSMEs, July, High Q, Low Energy, 104.5% Nominal Power Level, Narrow Throttle Bucket
- LWT PE, Block-2A SSMEs, February, Low Q, High Energy, 104.5% Nominal Power Level, Widest Throttle bucket.

Post-flight reconstructions are based on actual reconstructed BET induced environments.

5.3.1.5.3 ET Film Coverage

5.3.1.5.3.1 Ascent Video

Multiple pieces of ice debris were observed falling from the ET/Orbiter umbilicals during SSME ignition through lift-off. This is a typical observation. Ice debris was also observed falling near the LH2 recirculation line. No damage to the launch vehicle was noted.

At approximately 81 sec, a piece of debris was shed from an area near the ET/Orbiter forward attachment and is assumed to be a piece of the left bipod ramp TPS foam. Three separate cameras show the debris striking the left wing area of the Orbiter. The debris appeared to disintegrate upon contact with the wing. Comparison views of the strike area immediately before and after impact with the Orbiter were inspected for indications of surface damage. Although no damage was discernable from the videos, the resolution was insufficient to draw any conclusions.

5.2.1.5.3.2 On-Orbit Video and Film

Video taken by the crew of the ET after separation was downlinked and reviewed. The only view obtained was from the far side of the ET and provided no information on the source of the debris. All other video and photos were lost with *Columbia* on reentry.

5.3.1.6 ET-93 Entry and Disposal

STS-107/ET-93 entry data from a BET are presented in Table 5.3.1.6-1. Information relevant to the ET entry ground track and debris impact is depicted in Figure 5.3.1.6-1. The prediction for the ET impact point is based on state separation vectors and assumes the ET remains intact. As indicated in the figure, the post-flight predicted intact impact point is approximately 47 n.mi. uprange from the pre-flight prediction.

Table 5.3.1.6-1. ET Post-Flight Data

ET Telemetry Separation Time (from T-0)	507.2 sec
2ET Altitude @ ET/Orbiter Telemetry Separation	60.81 n.mi. 369,492 ft
Impact Point Latitude	2.283 deg N
Impact Point Longitude	139.420 deg W

For previous flights, NORAD provided observed ET entry data for assessment by Aerospace Corporation. These data supported the ground track prediction and allowed for assessment of the ET rupture altitude. Rupture altitude estimates for 63 extracted flights from STS-1 through STS-73 were statistically combined to produce ±3 sigma limits. This assessment of rupture altitudes was discontinued after STS-73 when the contract with Aerospace Corporation was canceled. The contract was reinstated to obtain additional rupture altitudes to encompass the Super Light Weight Tank (SLWT) design. The preliminary SLWT design database shown below consists of the current revised empirical rupture altitudes obtained from the Aerospace Corporation:

Flight	ET	Rupture Altitude (kft)
STS-91	96	238.8
STS-95	98	245.5
STS-88	97	235.8
STS-96	100	235.8
STS-93	99	221.8
STS-103	101	221.2
STS-99	92	236.4
STS-106	103	230.9
STS-92	104	233.9
STS-97	105	234.5

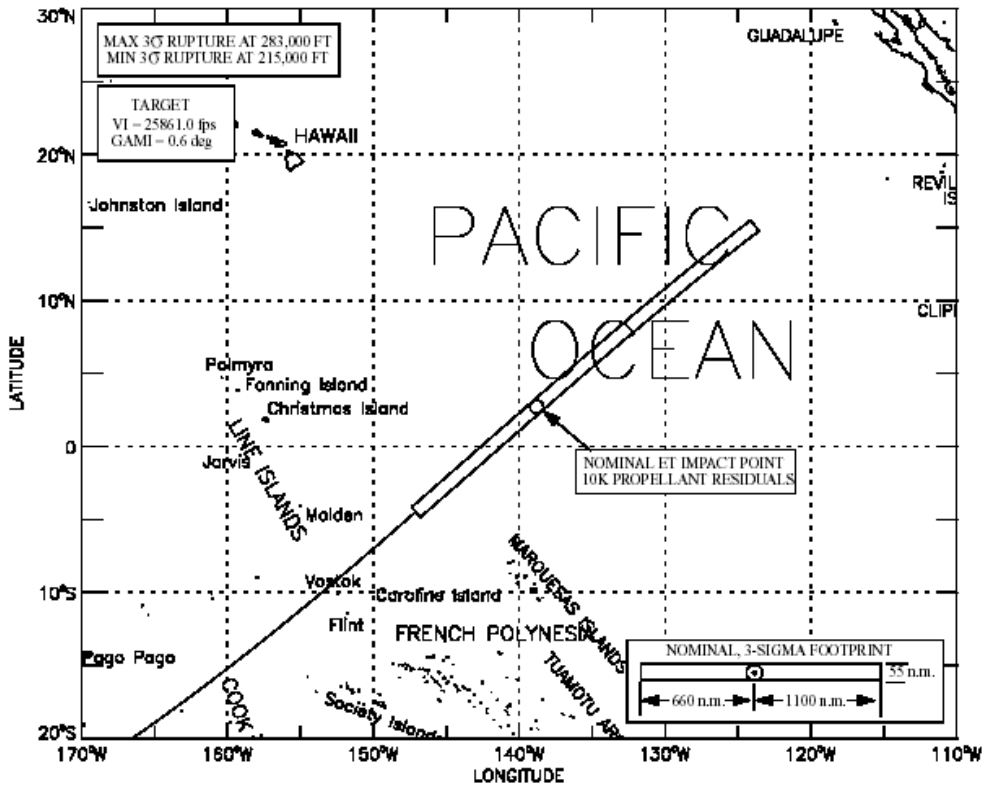

Figure 5.3.1.6-1. ET-93 Nominal Impact Area

5.3.1.7 ET-93 Mass Properties

The mass properties data provided are intended as a reference to compare flight-to-flight data and to assist with subsequent post-flight analyses. Figure 5.3.1.7-1 depicts ET post-MECO reconstructed weight history for missions since STS-40. Table 5.3.1.7-1 defines ET mass properties at lift-off (T-0) and post-MECO (after SSME shutdown transients). This information is based on the ET actual weight report (SE40) and Boeing reconstructed propellant data and is used to assist USA in generating entry trajectories for ET heating analyses.

Note: STS 79-84, 99, and 103 reconstructed data are generated using predicted dry weight. STS 85-98, 100-102, and 104-112 reconstructed data are generated using actual dry weight.

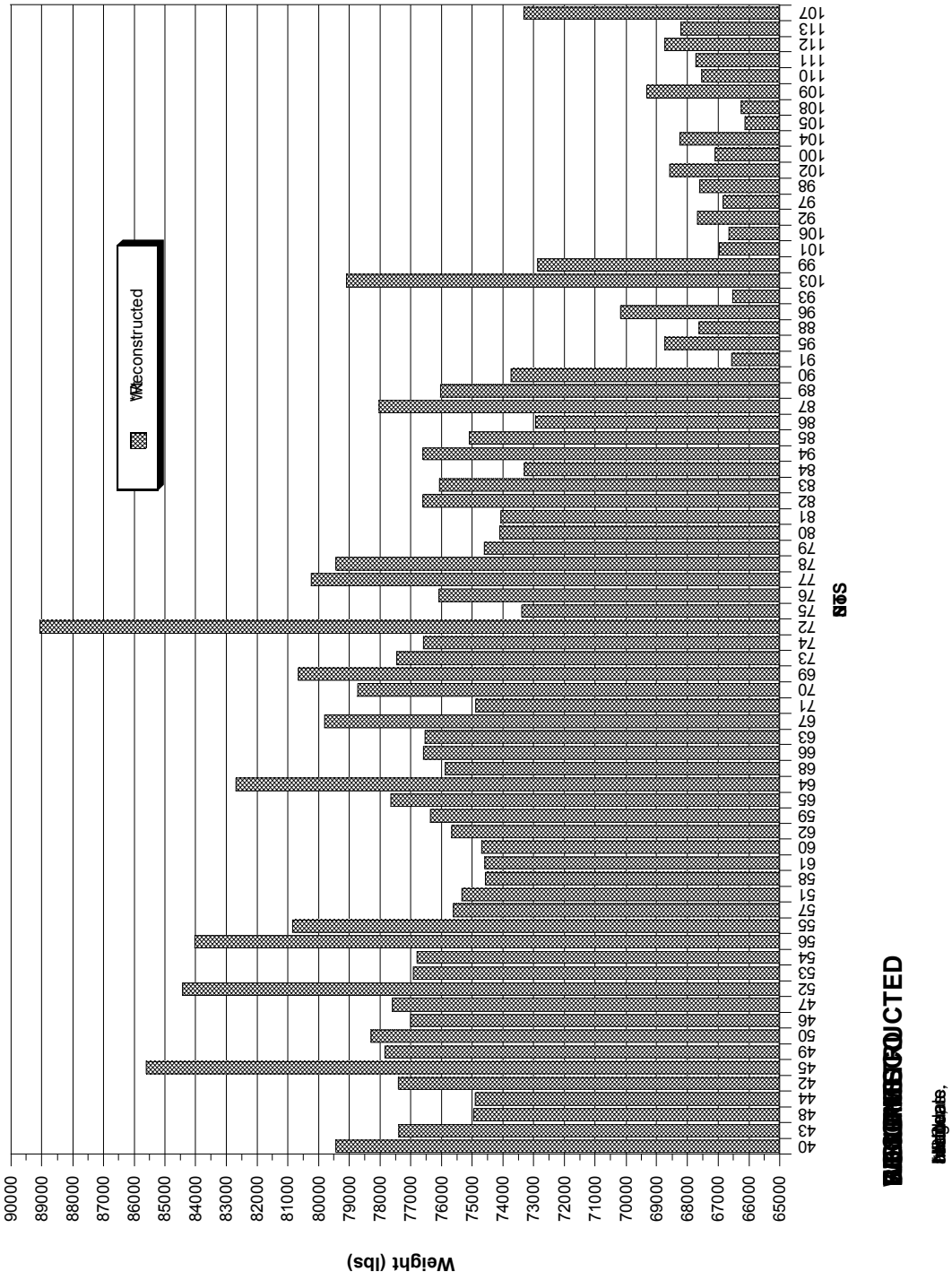

Figure 5.3.1.7-1. ET Post-MECO Reconstructed Weights

CAB109-0041
C2-000033
ETWG_FnlRpt_Volume_I.doc

DESCRIPTION	WEIGHT	CG			[illegible]	[illegible]	[illegible]	[illegible]	[illegible]	[illegible]	[illegible]	[illegible]	[illegible]
	LBS	X	Y	Z	KX	KY	KZ	IX	IY	IZ	PXY	PXZ	PYZ
		INCHES			INCHES			SLUG-FT2/1000			SLUG-FT2/1000		
[illegible]													
ET-93	65,115.0	1,355.18	2.70	424.70	158.33	519.63	519.86	352.32	3,794.91	3,798.27	2.73	154.65	6.45
[illegible]	1,366,913.0	732.40	0.56	401.35	15.74	165.31	164.79	73.09	8,062.53	8,011.89			
[illegible]	96.0	422.34	-0.30	399.20									
[illegible]	228,971.0	1,608.90	-0.02	400.06	3.23	313.69	313.67	0.52	4,863.11	4,862.49			
[illegible]	63.0	1,059.78	0.00	400.00									
NPC's	457.0	1,286.30	0.00	402.20	82.77	419.38	424.67	0.68	17.35	17.79			
[illegible]	893.0	1,954.00	0.00	429.60	178.61	317.68	351.62	6.15	19.45	23.83			
TOTAL	1,662,508.0	878.31	0.56	402.10	35.06	383.84	383.65	441.14	52,867.67	52,816.36	116.98	557.93	31.98
Post-MECO													
ET-93	64,970.0	1,354.60	2.71	424.71	158.50	518.89	519.13	352.30	3,775.73	3,779.11	2.73	154.65	6.45
[illegible]	1,179.0	2,035.40	70.00	570.59	12.67	35.88	34.09	0.04	0.33	0.30			
[illegible]	2,911.0	724.09	0.48	401.16									
[illegible]	2,270.0	2,149.60	-1.99	406.25	29.20	59.22	53.39	0.42	1.72	1.40			
[illegible]	1,063.0	1,589.16	0.00	400.00									
NPC's	47.0	1,360.62	-0.01	408.43	42.72	465.03	479.61	0.02	2.19	2.33			
[illegible]	888.0	1,954.00	0.00	429.60	178.61	317.68	351.62	6.15	19.45	23.83			
TOTAL	73,328.0	1,375.92	3.48	425.27	152.06	536.50	536.66	365.95	4,555.49	4,558.34	12.80	180.81	9.04

[illegible]

[illegible] PROPERTIES

Table 5.3.1.7-1. Mass Properties Data

C2-000033 ETWG_FnlRpt_Volume_I.doc CAB109-0042

5.3.2 Foam Loss History

5.3.2.1 Methodology

Evaluation of ET TPS performance is accomplished through an evaluation of the ground (ascent) and on-orbit imagery (most comprehensive). The +Z side of the ET (critical debris zone) is typically observed from the 16-mm or 35-mm cameras installed in the Orbiter umbilical wells. The -Z TPS performance is typically observed from crew handheld cameras; therefore, assessment of the -Z TPS performance is difficult because of the distance of the ET to the camera.

5.3.2.2 TPS Loss from All Sources Excluding Bipod Ramps

Of the 113 Space Shuttle flights, 79 flights had useable imagery of the +Z axis from these cameras. The data collected during the STS-107 accident investigation were aggregated into major areas of TPS loss (Volume III). TPS loss has been observed on 82% of the missions with useable imagery. Areas of observed loss are shown in Figure 5.3.2.2-1. Recent material changes and configuration changes were also reviewed in an attempt to further assess TPS loss. Foam loss over time is shown in Figure 5.3.2.2-2. The loss of acreage TPS is primarily related to an increase in intertank acreage TPS loss attributed to a recent material change (the blowing agent, HCFC 141b) in the intertank acreage TPS. The TPS loss phenomenon observed since this material change was subsequently mitigated through venting of the TPS to allow entrapped pressure to outgas. Although intertank TPS loss, through 'popcorn-type' divots, still occurs, the size and quantity of the divots has been greatly reduced.

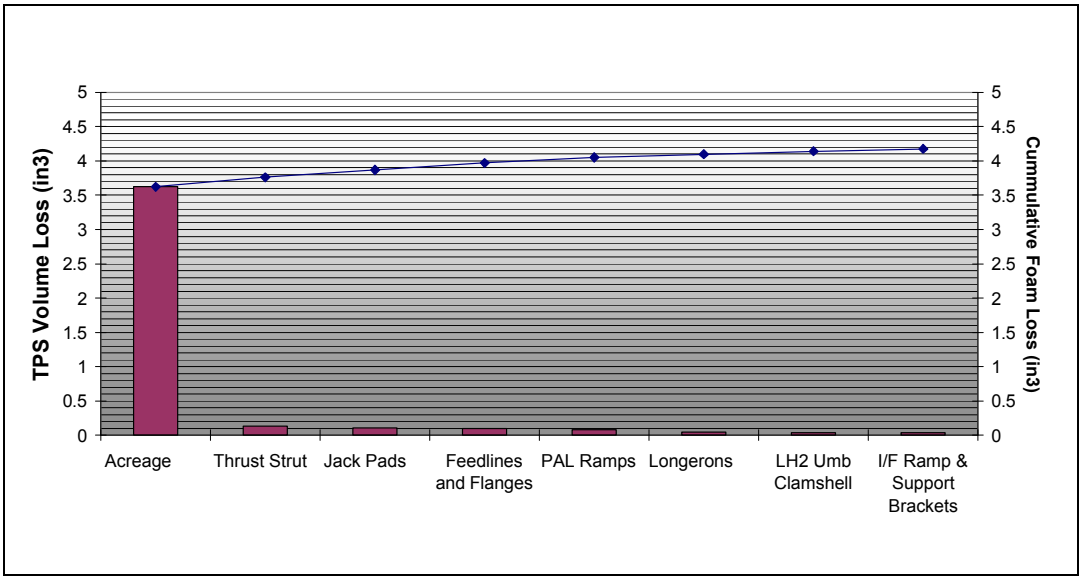

Figure 5.3.2.2-1. Areas of Observed Loss

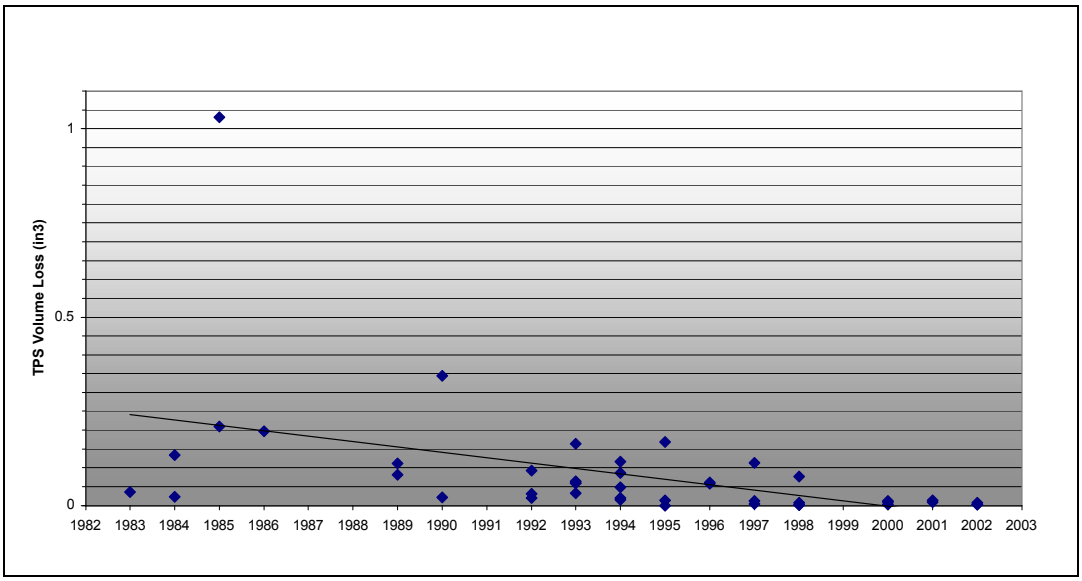

Figure 5.3.2.2-2. Foam Loss Trend

While on-orbit imagery is the only valid method for determining ET TPS performance, post-landing inspection of the Orbiter TPS is sometimes used as a measure of TPS performance. Figure 5.3.2.2-3 shows the number of Orbiter lower surface infects correlated to TPS damage. As shown below, there have been cases when Orbiter tile damage could not be correlated to significant ET TPS loss. Statistical analyses of data indicate that ET foam loss has a weak correlation to Orbiter damage. There are other significant sources of damage to the Orbiter tiles.

Foam loss data from the bipod ramp, flange, LO2 tank, Intertank, and LH2 tank were used in the analysis. Using all observed foam loss and Orbiter data correlated to this set of missions, there were no significant pair-wise correlations between foam loss and Orbiter hits. The regression chart of TPS loss weight versus tile damage is shown in Figure 5.3.2.2-4. Analyses of those missions that only assess missions with observable loss, however, indicate a slight correlation. None are statistically significant at the standard p = 0.05 level. Significance is approached at the p = 0.10 level for volume versus hits >1 in. (p = 0.102), volume versus lower surface hits (p = 0.095), weight versus hits >1 in. (p = 0.098), weight versus lower surface hits (p = 0.096), and weight versus lower surface hits >1 in. (p = 0.106). The associated regression chart for this case is shown in Figure 5.3.2.2-5.

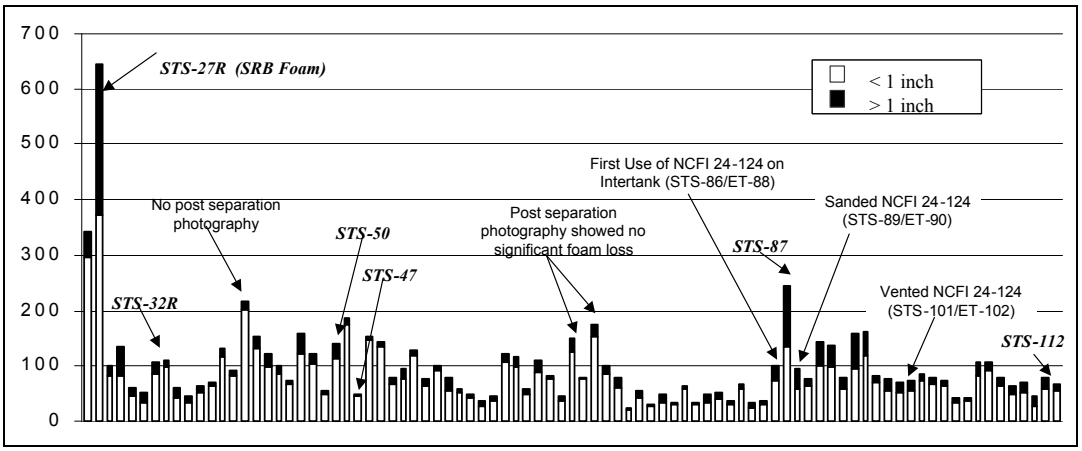

Figure 5.3.2.2-3.a. Orbiter Tile Damage

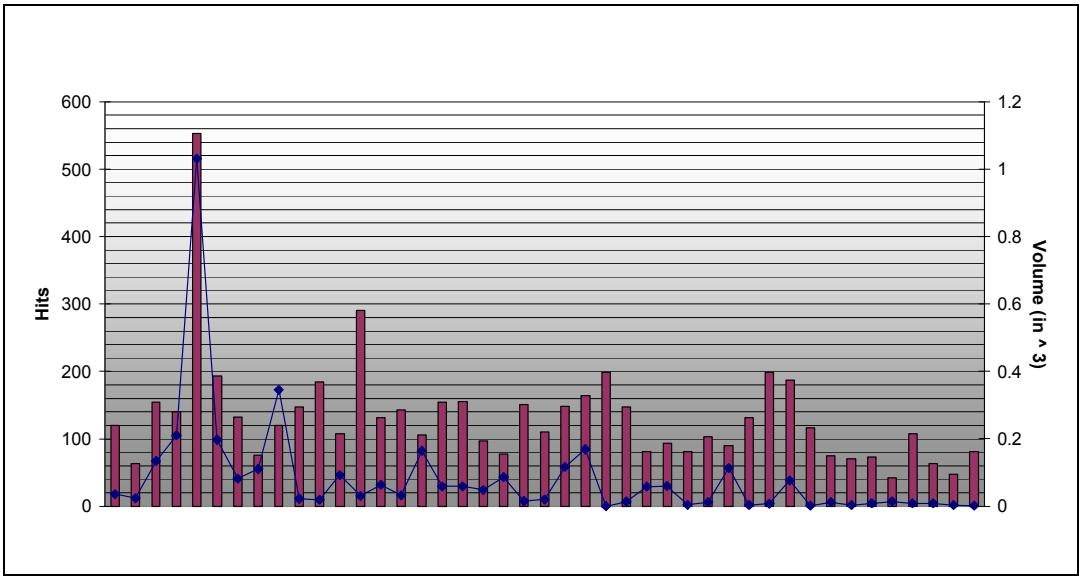

Figure 5.3.2.2-3.b. Total Orbiter Damage and TPS Volume Loss

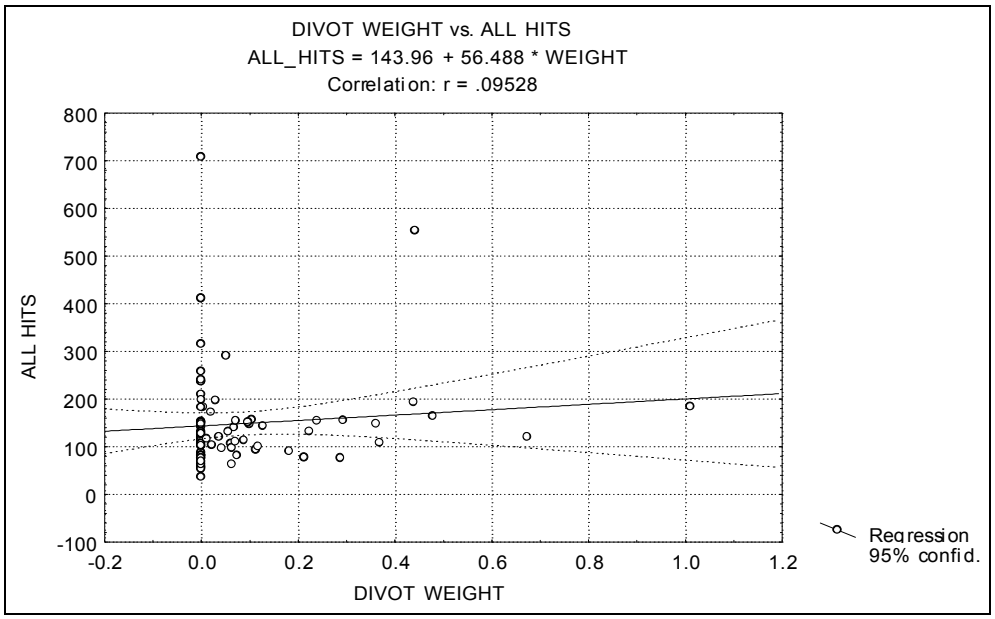

Figure 5.3.2.2-4. Correlation of Divot Weights to Orbiter Hits for All Missions

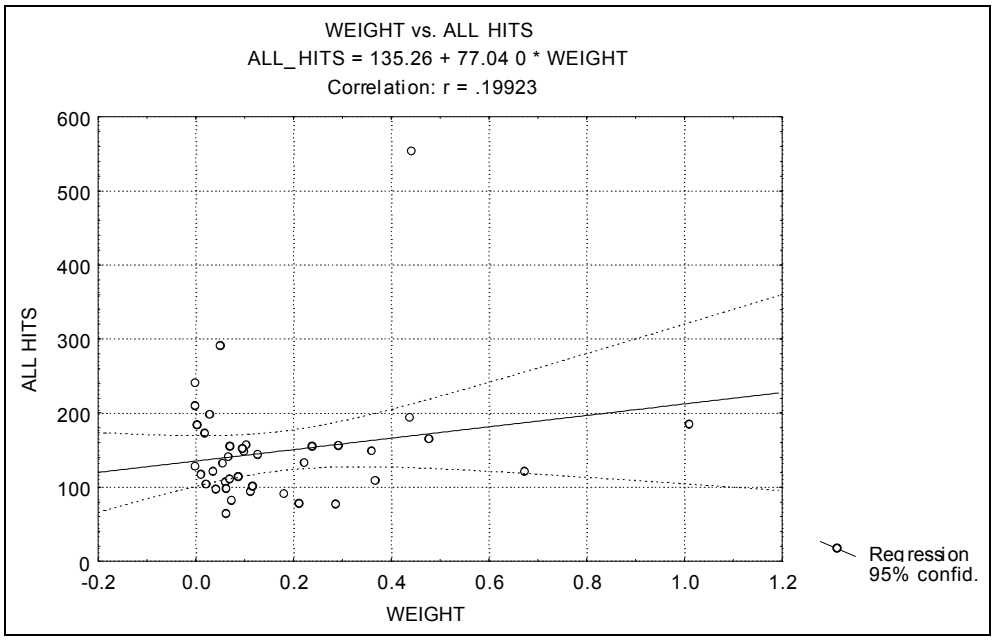

Figure 5.3.2.2-5. Correlation of Visible Foam Loss to Orbiter Damage

ET TPS loss is visible on each flight and can be categorized as either “typical” or “significant.” Typical” TPS loss is characterized as divots that are frequently observed with a mass of <0.1 lb. Divots of this mass are small shallow divots usually seen on the intertank-to-LH2-tank flange or tank acreage TPS. Smaller

divots (also known as “popcorning”) are commonly observed on the intertank thrust panels and LH2 aft dome. “Significant” TPS loss, as categorized by the SSP, is usually related to the size (>0.2 lb), location, or pattern of TPS loss that has occasionally correlated to an increased level of Orbiter TPS damage quantity or TPS damage size. Significant events through the program history are shown in Figure 5.3.2.2-6. Programmatic action was required for those events that were characterized by the Space Shuttle Program as ‘significant’ events, *i.e.,* determination of cause and identification of corrective action. As these TPS loss events were observed, flight rationale for the subsequent vehicles was presented to the SSP, and to the extent possible, probable causes were assessed, eliminated, or mitigated.

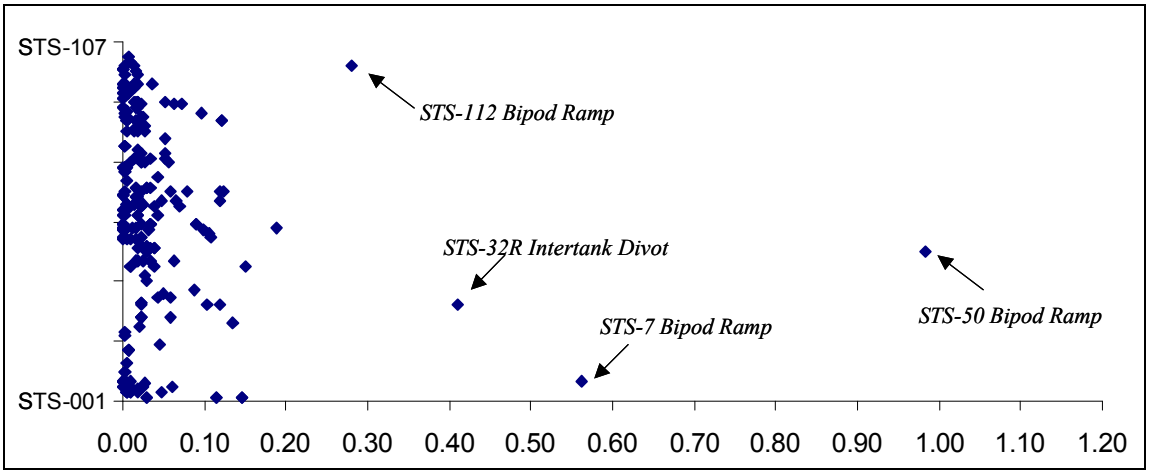

Figure 5.3.2.2-6. TPS Mass Loss (lb)

Historically, initiatives on the ET have gradually resulted in reduced foam loss over time. A progression of the aggregate of foam loss, as categorized by major TPS changes, is shown in Figure 5.3.2.2-7.

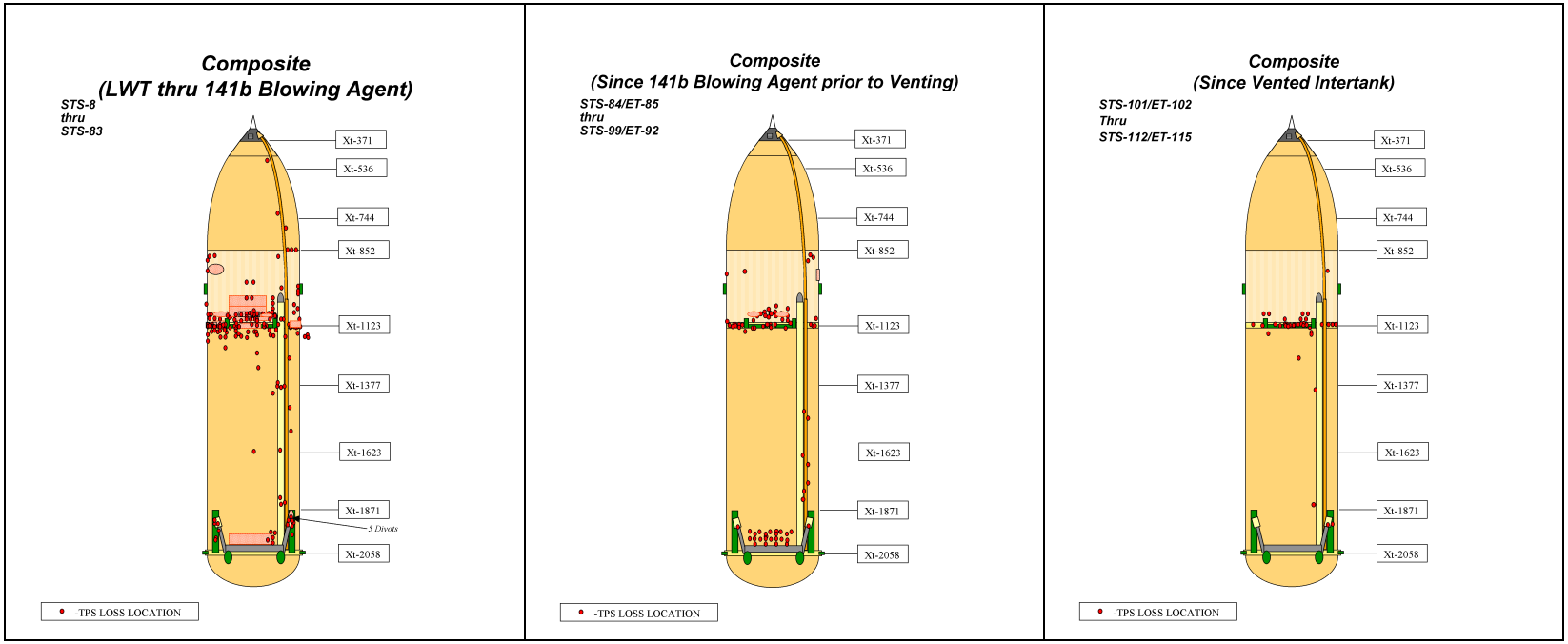

Figure 5.3.2-7. Schematic of Aggregate Foam Loss

5.3.3 Bipod Ramp TPS Loss

5.3.3.1 Bipod Area Description

The forward Orbiter attachment is a bipod. Interfaces between the ET and the Orbiter are shown in Figure 5.3.3.3-1. The bipod, weighing approximately 190 lb, has rotational freedom at its attachment to the forward LH2 tank ring frame and rotates about a Y-axis reference line so that changes in overall tank length resulting from thermal effects will not introduce loads into the Orbiter.

The forward bipod TPS configuration includes a complex combination of foams, ablator [Super-Light Ablator (SLA)] and underlying bipod structural substrate elements (Figure 5.3.3.1-2.) SLA is applied to the substrate, both using spray and manual hand-packed operations. Foam (BX-250 SOFI), is manually applied over the substrate and machined to final configuration. A schematic of the entire configuration and underlying details is shown in Figure 5.3.3.1-3.

The bipod ramp design has been stable since early in the ET program. There have been no changes in material and minimal changes to configuration, processing, and personnel certification/training. The BX-250 ramp angle, as described below, has been constant since ET-14:

- 30° maximum with a 5.0- ±1.0-in. radius at the forward edge (from 45° ±5.0, no radius). This was changed as a result of suspected foam debris (STS–7/ET-6).
- A 5.0- ±1.0 in. radius at the forward edge was eliminated at ET-76.

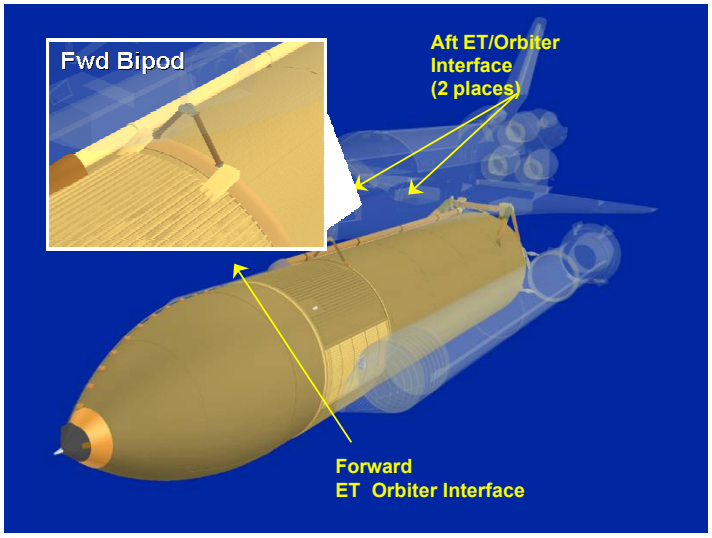

Figure 5.3.3.3-1. ET/Orbiter Interfaces

Bipod Housing
(Prior to Foam Application)

Bipod Ramp
(After Final Foam Trim)

Figure 5.3.3.1-2. Bipod TPS Configuration

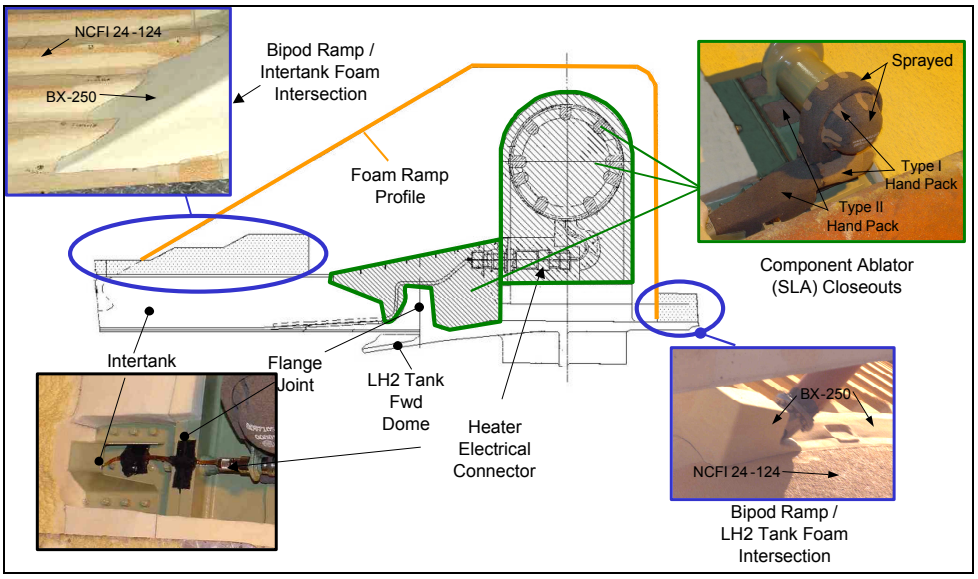

Figure 5.3.3.1-3. Bipod Closeout Schematic

5.3.3.2 Results

Assessment of post-flight imagery has shown five prior occurrences of bipod ramp TPS loss. All instances of ramp loss were isolated to the -Y (left hand) ramp. The first occurrence, STS-7/ET-6 (Figure 5.3.3.2-1), showed a large portion (18 in. x 12 in.) of the bipod ramp missing. The TPS area had an estimated weight of 0.6 lb. This TPS loss event was attributed to a repair in the forward edge of the ramp. Following this occurrence of TPS loss, the ramp repair criterion was limited to a maximum of 3 sq. in. on the forward face of the bipod ramp.

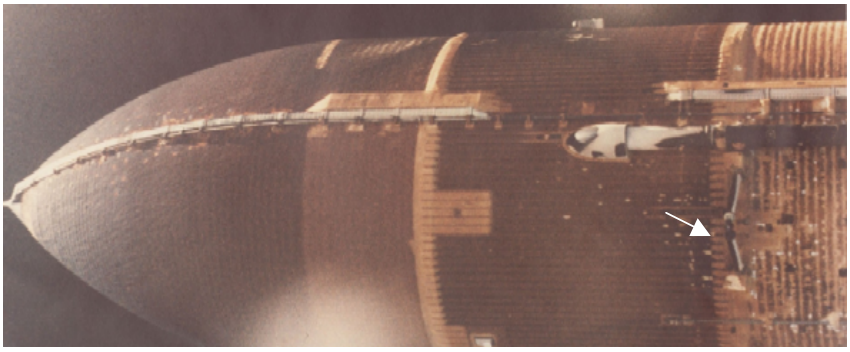

Figure 5.3.3.2-1. STS-7/ET-6

The TPS loss event on STS-50/ET-50 encompassed the majority of the bipod ramp, measuring 26 in. x 10 in. and weighing 0.98 lb (Figure 5.3.3.2-2). This loss was attributed to voids/debonds in the Isochem bond layer of the non-vented two-tone TPS area. ET-50 was the last ET built with this intertank TPS configuration.

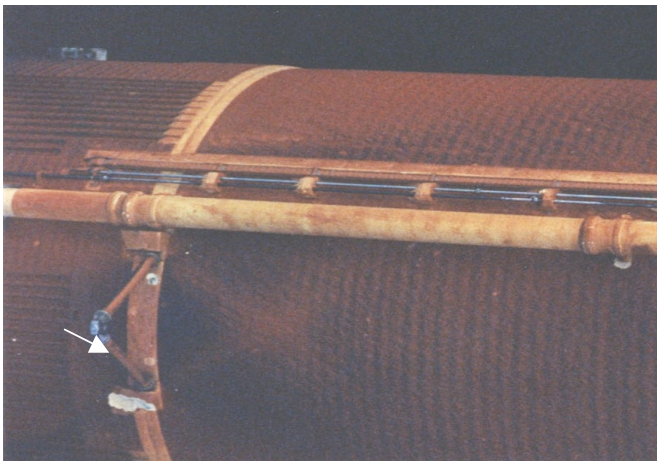

Figure 5.3.3.2-2. STS-50/ET-50

On STS-52/ET-55, the TPS loss was estimated to be 8 in. x 4 in., weighing 0.02 lb. (Figure 5.3.3.2-3)

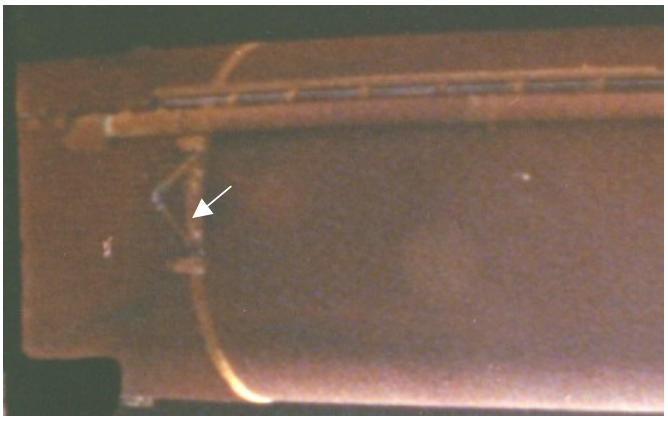

Figure 5.3.3.2-3. STS-52/ET-55

On STS-62/ET-62, there was a small divot in the aft face of the ramp measuring approximately 3 in. x 1 in. and weighing 0.001 lb. (Figure 5.3.3.2-4)

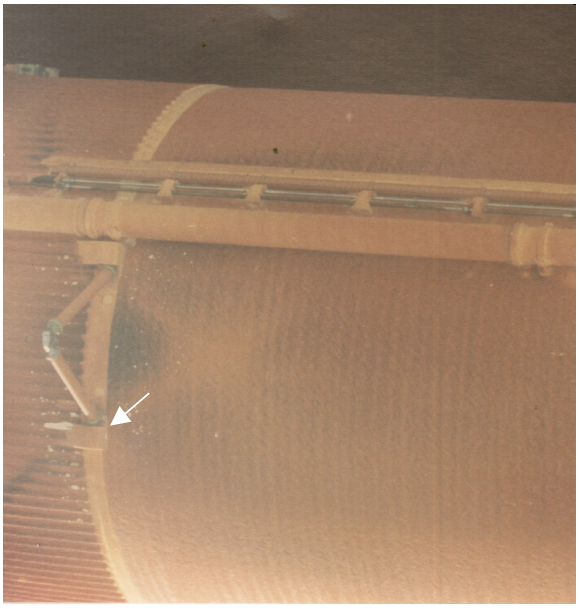

Figure 5.3.3.2-4. STS-62/ET-62

On STS-112/ET-11, the TPS loss location and shape was similar to that observed on STS-52 (Figure 5.3.3.2-5). The TPS loss on STS-112 was estimated to be 7 in. x 12 in. with a mass of 0.3 lb.

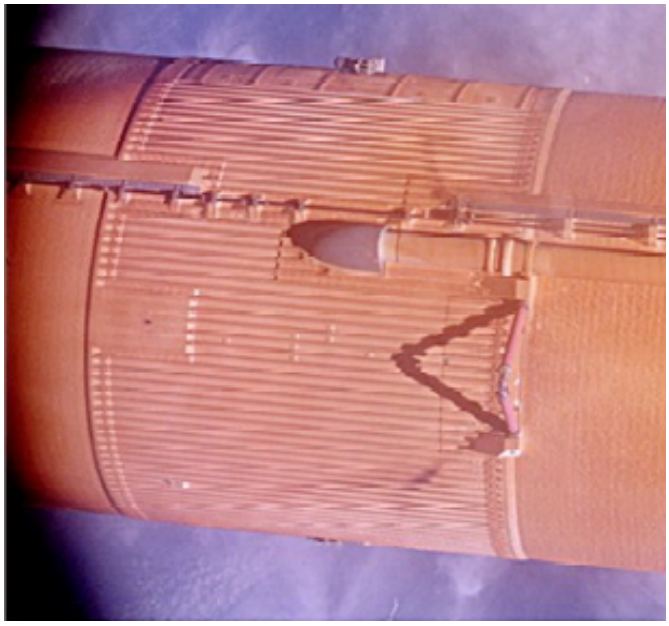

Figure 5.3.3.2-5. STS-112/ET-115

Following this occurrence of ramp loss, the ET Project initiated plans to evaluate the materials, design, and processes used for the ramps.

On STS-32R/ET-32, there was loss of foam very near the bipod ramps. The data for this event have been included in the following statistical analysis. The details of the event are described in Section 5.3.3.5.

5.3.3.3 Analysis

Statistical analyses of production, on-pad, and flight parameters were performed to characterize similarities in foam loss, both on the structure and with respect to direct loads to bipod foam. Assessed variables included:

- Production at MAF
  - Dates
  - Days in storage
  - Process variables
- Processing at KSC
  - Age at launch
  - Exposure
  - Tanking time
  - Thread count and offset at bipod area
  - On-pad environment
    - Rainfall
    - Temperature
    - Dew point

Relative humidity
Wind
Pressure

- Performance Data
  - Dynamic pressure (Q)
  - Angle of attack (α alpha)
  - Sideslip angle (β beta)
  - Q-alpha
  - Q-beta
  - In-plane wind velocity (V_{IP})
  - Out-of-plane wind velocity (V_{OP})
  - Vehicle weight and center of gravity
  - Flight regimes (Mach 0.6 – 2.2)
  - Bipod struts (P1, P2), load indicators ET4-1 through ET4-7
  - Tile damage
  - Foam loss

5.3.3.4 Results

No differences were found between any MAF production data or KSC processing data with the exception of on-pad rainfall. Comparison of distributions suggests most foam loss missions were wetter in total, as a maximum on a single day and on average. ET-112 data appear to be an outlier, however, even compared to all missions.

Sideslip angle, Q-beta and out-of-plane wind velocity showed a statistical correlation with regard to STS foam loss flights. Results are shown in Figures 5.3.3.4-1 through 5.3.3.4-4.

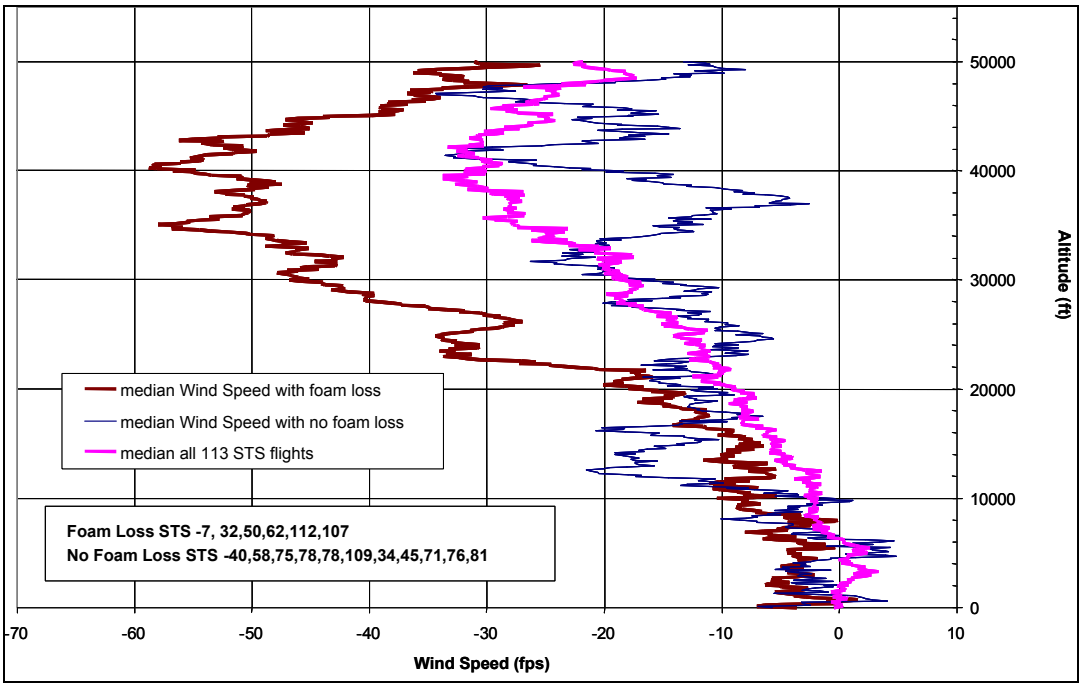

Figure 5.3.3.4-1. Altitude vs. Out-of-Plane Median Wind Speed for Bipod Foam Loss and No Bipod Foam Loss Flights

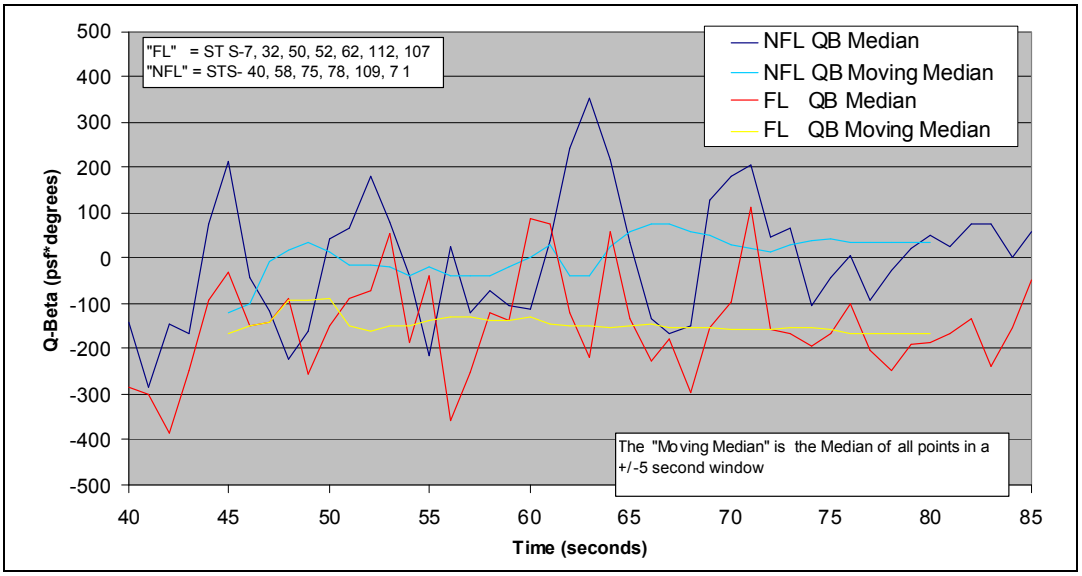

Figure 5.3.3.4-2. Q-Beta over Time for STS Flights with and without Bipod Foam Loss

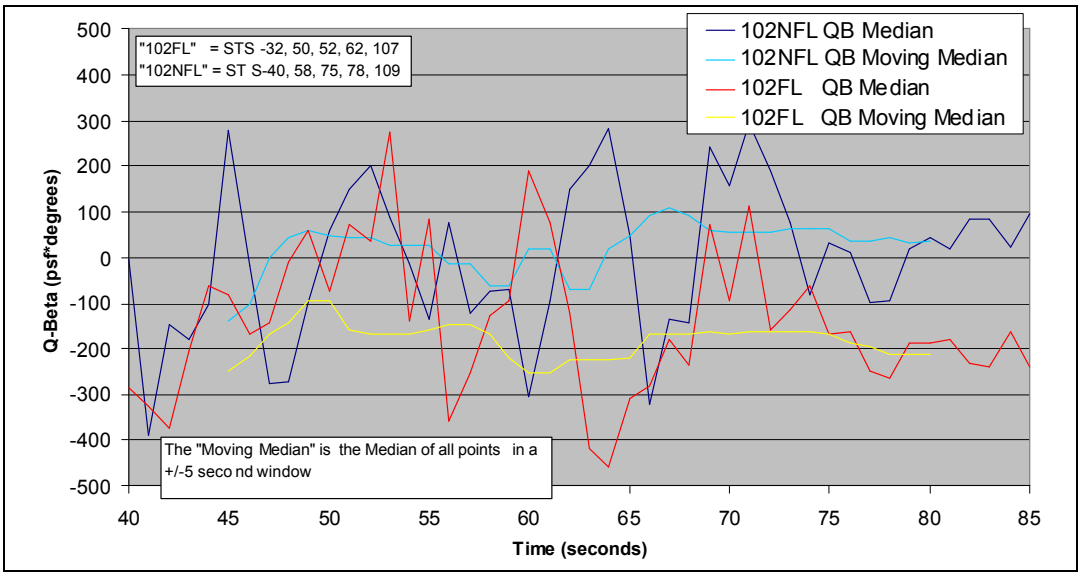

Figure 5.3.3.4-3. Q-Beta over Time for OV-102 Flights with and without Bipod Foam Loss

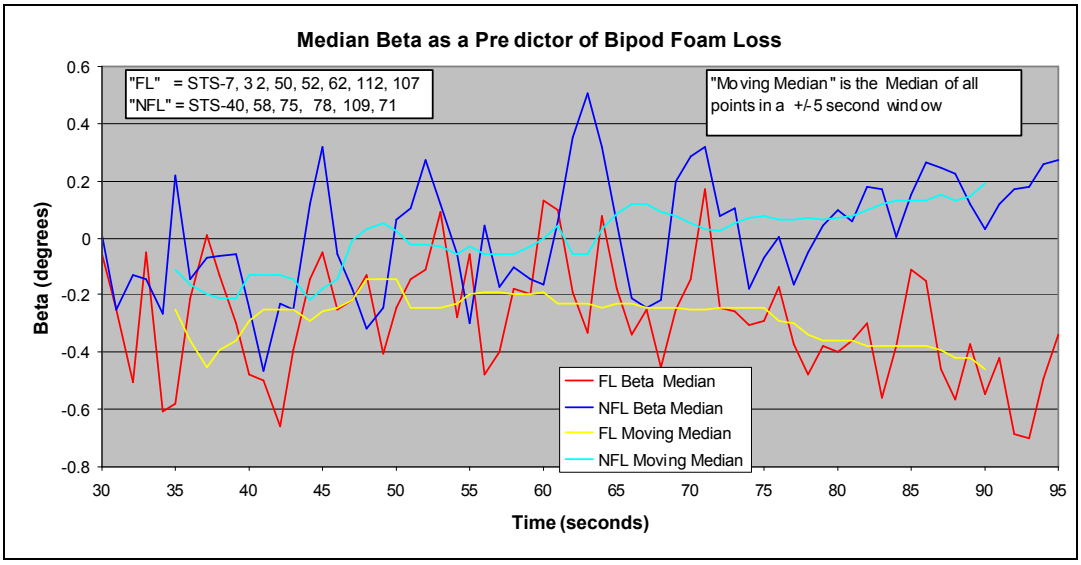

Figure 5.3.3.4-4. Beta over Time for Flights with and without Bipod Foam Loss

Bipod structural loads that were reviewed (P1, P2, FT01, FT02, *etc*.,) do not show a statistical difference with respect to STS flights with and without foam loss. These loads are more influenced by inertia and thrust effects. The analytical geometrical location of the integrated vehicle center-of-gravity and weight does not show a statistical difference with respect to STS flights with and without foam loss.

For altitudes of 25,000 to 45,000 ft (~Mach 1 to Mach 2), the STS flights with bipod foam loss had a statistically higher out-of-plane wind speed (20 to 40 fps) than those flights without bipod foam loss. During the high Q region of STS Flight (Mach 1 – 2), foam loss flights had a statistically higher negative Q-Beta as compared to flights with no foam loss. This statement is also true for *Columbia* flights with and without foam loss. The higher negative Q-Beta orients the vehicle's left hand (LH) side into the wind and, therefore, results in more wind exposure to the –Y bipod ramp.

Computational Fluid Dynamics (CFD) analysis of the LH bipod ramp shows that as Beta gets more negative (+2, 0, -1.56 deg), the axial, radial, and side forces on the Bipod Foam decrease for a constant alpha (-3.88 deg) and 1.4 Mach number. Shock loadings (impingements and movements) are extremely complex and very dependent on Mach Number, angle of attack (α), and angle of sideslip (β). Also, the LOX feedline produces asymmetric flow (Figure 5.3.3.4-5). A recent updated CFD geometry/grid system to include intertank stringers, detailed +Y bipod ramp and feedline geometries was developed. Results confirmed that there are a number of differences between air loads at the two ramp locations. The +Y ramp side force is much less sensitive to sideslip/β:

- At Mach 1.40, the –Y radial load is more than double +Y load.
- At Mach 2.46, the –Y radial load is smaller than the +Y load.

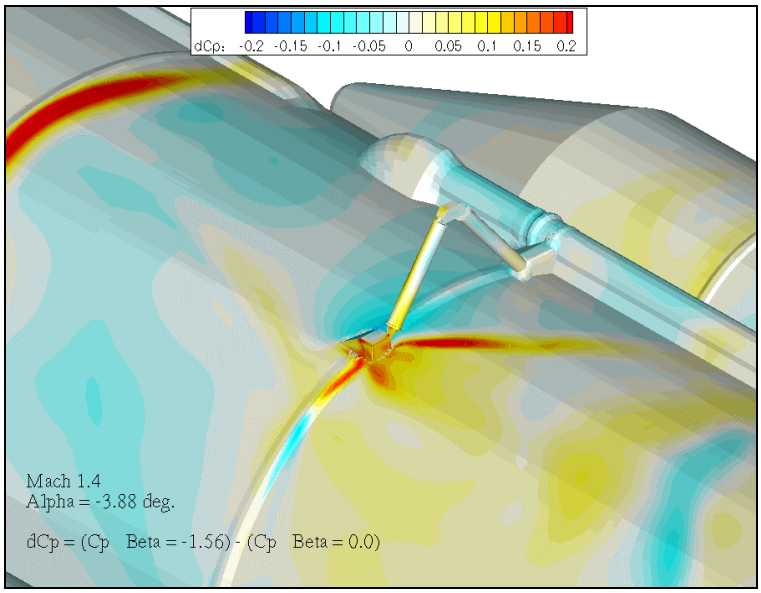

Figure 3.5.3.4-5. CFD Model of Bipod Region

5.3.3.5 History of Significant Foam Loss

A summary of the significant foam loss events experienced during the history of the ET program is presented below.

- STS-32R/ET-32 (launched January 9, 1990)

  Post-separation umbilical camera films showed several large divots in the area of the bipods. Two of the divots, measuring 12 to 14 in. in diameter, were located between the bipods just forward of the intertank-to-LH2-tank flange. A third divot, approximately 14 in. in diameter, was located between the bipod ramps and extended into the intertank-to-LH2-tank flange. The largest divot, measuring 28 in. wide, surrounded the forward part of the -Y (LH) bipod (Figure 5.3.3.5-1).

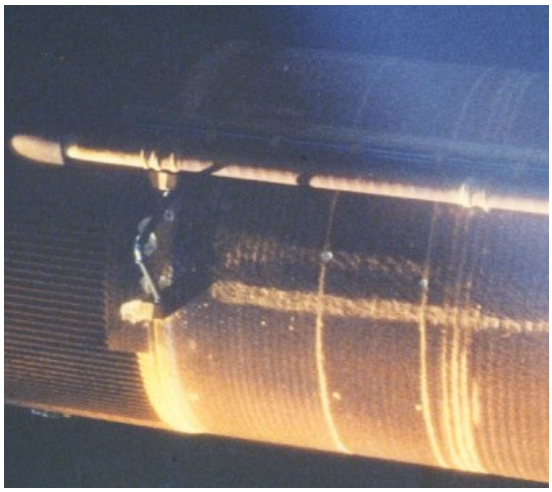

Figure 5.3.3.5-1. STS-32R/ET-32 Post-Separation Photograph

The most probable cause of this TPS loss was related to inadequate depth of drilled holes (venting) in this two-tone TPS location in conjunction with localized voids at the TPS CPR-488/Isochem bond layer. Following this occurrence of TPS loss, an inspection was added to the manufacturing process to verify vent hole depth. The most probable cause and corrective actions to preclude recurrence were presented/approved at the Level II Program Requirements Control Board (PRCB(PRCBD S044812A) on February 6, 1990.

Background on Isochem bond layer issues:

The two-tone TPS configuration on +Z side of Intertank was characterized by TPS (BX-250) applied in stringer valleys with a layer of Isochem adhesive over the top before final application of TPS (CPR-488).
Random divots had been experienced in the past for this configuration. The divots were caused by reaction between the Isochem resin and CPR-488 producing debonds/voids The Isochem problem surfaced because the supplier of the material switched sub-tier suppliers of the resin which later analysis showed was not as stable when heated (copper versus Silmar

resin). The supplier was subsequently required to use the original material. An interim corrective action was implemented earlier in the program (STS-27/ET-21) to reduce the potential for large size divots. The corrective action applied the use of holes drilled through the outer TPS layer to the Isochem interface to provide a vent path for the gasses in localized voids. The use of vent holes was only allowed in a non-cryogenic region so as to preclude the formation of ice/frost in the holes. The final corrective action was to implement an improved spray process, which eliminated the BX-250 and Isochem.

- STS-35/ET-35 (launched January 2, 1990)

  Post separation umbilical camera films showed five divots on the left side (-Y axis) of the intertank-to-LH2-tank flange closeout and five divots on the right side of the closeout (+Y axis). The largest divots ranged from 8 to 10 in. in diameter (Figure 5.3.3.5-2). Divots from this area (previously observed on other ETs) did not show a correlation with an increased level of Orbiter tile damage.

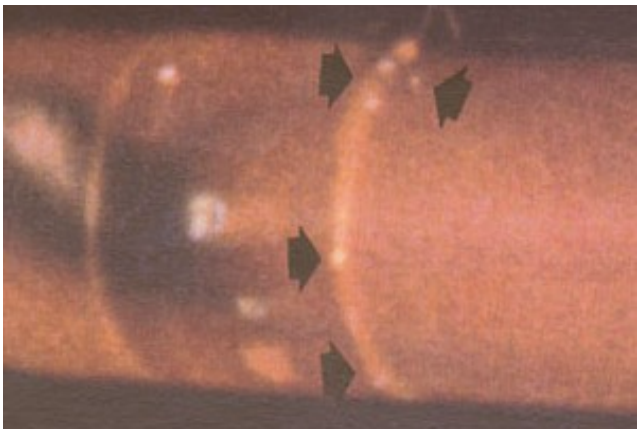

Figure 5.3.3.5-2. STS-35/ET-35 Post-Separation Photograph

The most probable cause of this TPS loss was localized voids behind the intertank-to-LH2-tank flange bolts. The closeout is a very complex manual two-step operation with TPS sprayed into a narrow/deep cavity and around the attach bolts. A review of the manual spray TPS technique showed that voids were a consequence of operator technique. Following this occurrence of TPS loss, an improved application technique was developed to reduce the potential for voids around the flange bolts. This process was validated and the operators were required to demonstrate their ability to perform the closeout successfully. Through the process enhancement, the number of divots was reduced but not completely eliminated.

The most probable cause and corrective actions to preclude recurrence were presented/approved at the Level II PRCB (PRCBD S044824C) on June 14, 1991.

- STS-42/ET-52 (launched January 22, 1992)

  Post-separation crew handheld camera films showed two divots on the intertank acreage. The divots were estimated to be approximately 8 to 14 in. in diameter (Figure 5.3.3.5-3).

Figure 5.3.3.5-3. STS-42/ET-52 Post-Separation Photograph

FT analysis was used to identify the possible causes of the divots. Major areas included excessive flight environments, mechanical damage, processing or assembly anomalies, and other causes, *i.e.,* material age, BSM impingement, fluid spill.

The most probable cause of this TPS loss could not be determined. ET–52 was the second tank to fly with the revised TPS configuration and application method (replaced two-tone configuration with two-gun spray application). No corrective actions were implemented.
Closure of this TPS loss occurrence was presented/approved at the Level II PRCB (PRCBD S044848H) on 09/01/92.

- STS-50/ET-50 (launched June 25, 1992)

  Post-separation umbilical camera films showed two areas of TPS damage near the forward bipod area. The first showed approximately 60% of the –

Y bipod ramp was missing with a 24 in. by 8 in. divot. The second location was the +Y jack pad closeout, measuring 4.5 in. sq., located just below the right bipod strut (Figure 5.3.3.5-4). The TPS surface under the bipod ramp was the intertank two-tone TPS configuration. The jack pad is a Polymer Development Laboratories (PDL) closeout of a tooling mount used to jack the Orbiter into place for mate at KSC.

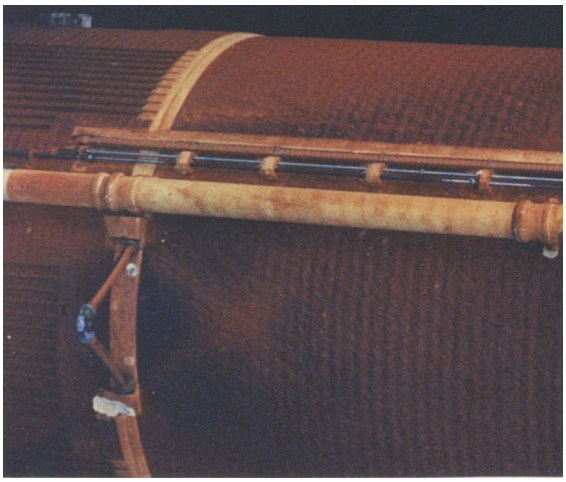

Figure 5.3.3.5-4. STS-50/ET-50 Post-Separation Photograph

The most probable cause of the bipod ramp TPS loss was related to debonds/voids in the Isochem bond layer of the two-tone TPS configuration. This area was not vented because of proximity to the cryogenic zone. Following this occurrence of TPS loss, the vented area on remaining ETs with Intertank two-tone TPS (ET-48/STS-46, ET-49/ST-53, and ET-45/STS-47) was revised to add vent holes just forward of the ramp to acreage interface (Figure 5.3.3.5-5).

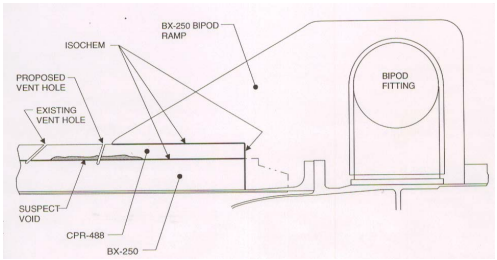

Figure 5.3.3.5-5. Corrective Action Following STS-50 TPS Loss

The most probable cause of the jack pad closeout was cryopumping of a subsurface void under the PDL pour TPS closeout. It was determined that loss of this TPS during ascent was not considered a flight or safety issue; therefore, it was recommended to fly the subsequent ETs with no

additional action. The only concern for the TPS loss was related to the potential to form ice during pre-launch. This concern was mitigated by the ability of the Final Inspection Team's ability to safeguard against this type of condition going undetected. This was the last of the tanks with the two-tone TPS application. Subsequent tanks incorporated the two-gun spray application, which eliminated the BX-250 and Isochem bond layer used on the two-tone configurations. The most probable cause and corrective actions to preclude recurrence were presented/approved at the Level II PRCB (PRCBD S044876C) on August 6, 1992.

- STS-47/ET-45 (launched September 12, 1992)

  Post-separation umbilical camera films showed a divot approximately 14 to 16 in. in diameter on the intertank between the left and right bipod fittings just forward of the intertank flange closeout in the two-tone TPS area (Figure 5.3.3.5-6).

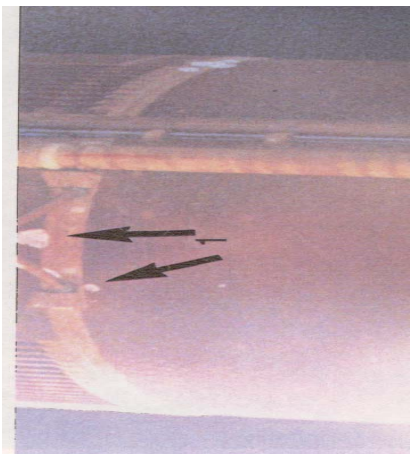

Figure 5.3.3.5-6. STS-47/ET-45 Post-Separation Photograph

Minimal Orbiter tile damage was observed post-flight on OV-105 (STS-47). TPS loss of this type was not considered a safety of flight concern but one of Orbiter tile maintenance.

Three possible causes were identified:
- Momentary spray anomaly coupled with compression during fabrication and flight environments,
- Freon contamination of Isochem, and/or
- Insufficient vent hole depth in the Isochem bond layer of the two-tone TPS configuration. No corrective actions were implemented, as ET-49 was the last of the two-tone TPS configuration tanks to fly.

The most probable cause was presented/approved at the Level II PRCB (PRCBD S044880A) on November 30, 1992.

- STS-56/ET-54 (launched April 4, 1993)

Post separation crew handheld camera films showed 10 large, shallow divots on the –Z side of the intertank acreage (Figure 5.3.3.3-7). The divots were in a unique pattern, with two lines with 3 and 4 divots each. The magnitude of the TPS loss experienced on STS-56 was within the STS experience base.

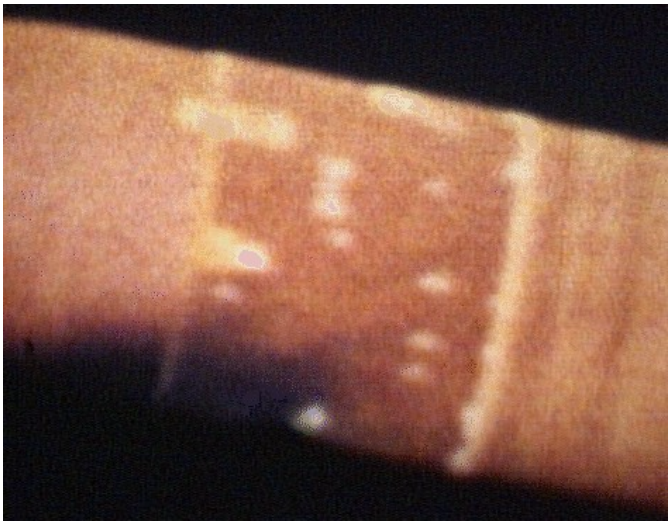

Figure 5.3.3.5-7. STS-56/ET-54 Post-Separation Photograph

The most probable cause of this TPS loss was not conclusively determined. The most likely scenario is rollover/crevicing anomalies in the TPS (Figure 5.3.3.5-8), and the effects in the flight environment. Differential pressure caused by aeroheating, flight loads, and panel flexure may have caused anomalies to propagate along the TPS knitlines (area between TPS spray passes), with shallow divots as the result.

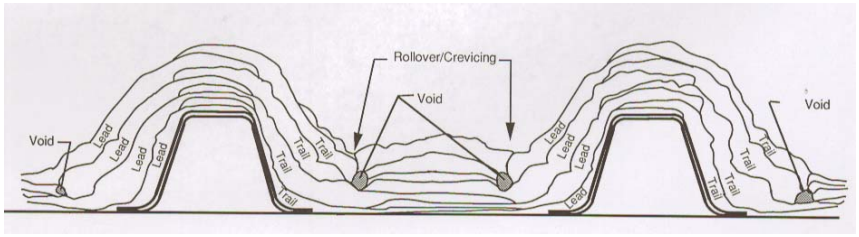

Figure 5.3.3.5-8. Rollover/Crevicing Phenomenon

No immediate corrective actions were implemented. An application process enhancement was implemented to minimize or eliminate the occurrence of rollover or crevicing. This enhancement would reduce the

variations in the spray process, such as spray angle, within the existing production operation.

The most probable cause and corrective action to preclude recurrence was presented/approved at the Level II PRCB (PRCBD S044895N) on July 29, 1993.

- STS-58/ET-57 (launched October 18, 1993)

  Post-separation umbilical camera films showed three areas of TPS loss on the intertank +Z side. One divot (approximately 28 in. L x 3 in. W) was in the acreage TPS, and the other two divots were identified as the TPS from the jack pad closeouts. Exposed primer was observed in both jack pad cavities (Figure 5.3.3.5-9), Divots of this magnitude and the Orbiter tile damage were within the STS experience base.

  The most probable cause of the intertank acreage divot on STS-58 is the same as suspected for the TPS loss on STS-56 – Anomalies in the TPS caused by rollover/crevicing phenomenon.

  The most probable cause of the jack pad closeout was cryopumping of a subsurface void under the PDL pour TPS closeout. Following this jack pad closeout TPS loss occurrence, a tool was developed to allow spray around the holes masking the jack pad tooling holes, leaving four 1-in. diameter holes on each side of the closeout to eliminate the large closeout/repair area (6 in. x 6 in. square). The jack pad itself is now closed out in conjunction with the flange closeout.
  The most probable cause and corrective actions to preclude recurrence were presented/approved at the Level II PRCB (PRCBD S044897L) on May 23, 1994.

Figure 5.3.3.5-9. STS-58/ET-57 Post-Separation Photograph

- STS-87/ET-89 (launched November 19, 1997)

  Post-separation crew handheld camera films showed areas of missing TPS on the +Y and -Y thrust panels (Figure 5.3.3.5-10). Post-landing inspection also showed a significant increase in Orbiter tile damage: 308 damage sites on the Orbiter lower surface, with 132 sites greater than 1 in. The total number of lower surface damage site and the number of damage sites greater than 1 in. were out of family when compared to previous missions.

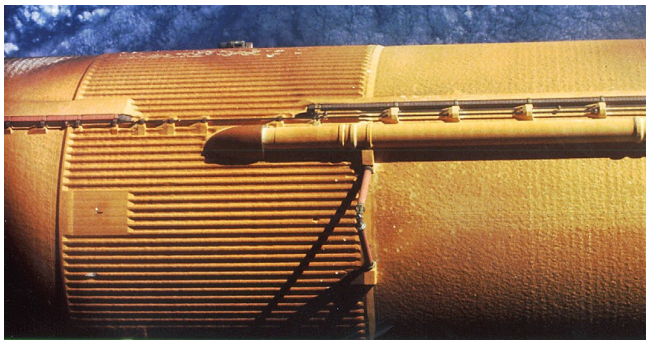

Figure 5.3.3.5-10. STS-87/ET-89 Post-Separation Photograph

The most probable cause of this TPS loss was a combination of the following factors:

- Reduced mechanical properties of the TPS and its trapped gases
- Environmentally induced cell gas pressure from heating, vacuum, and moisture in the cells
- Stress concentrating geometry, especially evident on the intertank thrust panels and to a lesser extent on the skin/stringer panels.

For the subsequent flights, incremental corrective actions were implemented to reduce TPS loss. An incremental approach was used to ensure that the corrective actions would 'do no harm'. The corrective actions included reduction in TPS thickness (STS-89/ET-90), reducing the amount of TPS that could be shed, and the placement of closely spaced, small diameter vent holes in the intertank TPS beginning with ET-101 (STS-103). SRB-mounted cameras showed the vent holes significantly reduced both the number and size of the "popcorning" debris from the intertank thrust panels. The vented area was expanded on each mission until the desired product was achieved.

The long-term corrective action plan was presented at the Level II PRCB (PRCBD S062127) on January 13, 2000. The plan incorporated the use of vent holes on the intertank thrust panels and the +Z stringer panel to

reduce the number and size of the TPS debris. The final corrective action was implemented for ET-102 (STS-101) and subsequent missions.

Background on intertank thrust panel TPS loss

Significant amounts of TPS loss and related Orbiter tile damage began occurring when CPR-488 was replaced with NCFI 24-124 TPS on the ET intertank. The change in TPS insulation materials was necessitated by the requirement to use environmentally compliant blowing agents (HCFC-141b) and the termination of production of one of the major constituents of CPR-488 by the supplier.

A study to gain an understanding of the TPS loss event ensued; the first data gathering exercise included the installation of a camera on one SRB of STS–95/ET-98. This camera imaged the ET intertank thrust panel during flight and provided the first opportunity to view TPS loss up close and in real time (Figure 5.3.3.5-11). The camera showed TPS loss initiating approximately 92 sec into the flight and continuing until SRB separation, at which time the view was lost.

Figure 5.3.3.5-11. STS-95/ET-98 Post-SRB-Separation Photography

TPS loss was seen to be most severe on the tops and sides of the thrust panel ribs but was not limited to these areas. Some material loss was also observed on the skin-stringer areas of the intertank. From a visual standpoint, the TPS loss closely resembled the phenomenon known as 'popcorning', which has been observed in thermal-vacuum testing at MSFC and MAF test facilities.

- STS-112/ET-115 (launched October 2, 2002)

  Post-separation crew handheld camera films showed an area of missing TPS (approximately 4 in. x 5 in. x 12 in.) on –Y bipod ramp exposing the bipod housing SLA closeout (Figure 5.3.3.5-12).

The ET Project was assigned an action at the SSP PRCB (S062151) on October 24, 2002 to analyze the ET bipod loss of TPS experience for root cause and corrective action.

The most probable cause of this TPS loss occurrence was suspect subsurface void(s) during bipod ramp closeout coupled with launch environments. The most probable cause was presented at the SSP PRCB (S062151, Action # MSFC-ET/1-1) on December 19, 2002 and at that time, the Project identified the corrective action that was under evaluation. The proposed corrective action was to enhance the closeout configuration by eliminating the SLA under the TPS, thereby eliminating the potential for air entrapment (subsurface voids). The final corrective action was to have been presented at the SSP PRCB on February 6, 2003.

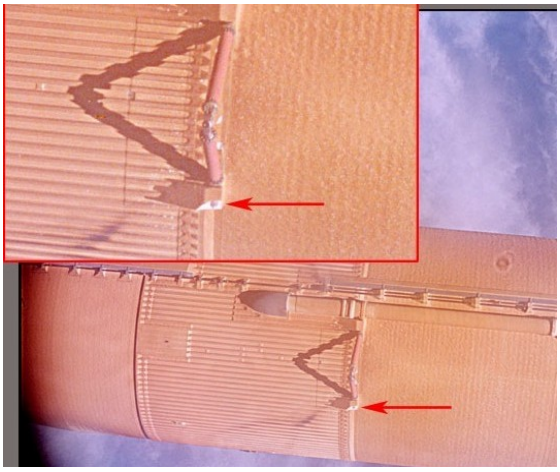

Figure 5.3.3.5-12. STS-112/ET-115 Post-Separation Photography

5.3.4 Summary

The ET has approximately 16,750 sq. ft. of external TPS. The overall ET TPS performance over the history of the program has consistently improved. Some areas have been problematic. As problems arose, evaluations were performed, and improvements were implemented.

The observed anomalies for the acreage TPS applications on the LH2 barrel and aft dome and LO2 tank have been few and minor in nature. These areas are applied to "smooth" structure by tightly controlled automated equipment and processes. In these areas, the very low-density TPS material is subjected to highly strained -423 °F substrate conditions, while the surface is subjected to ascent heating conditions that can raise the surface temperature to over 600 °F in approximately 1 in. of material thickness.

The TPS application to the intertank area has presented two major observed problems over the history of the program related to difficulties inherent to the

spray application of TPS over the external intertank stringers and thrust panel stiffeners. In both occurrences, extensive successful efforts to resolve the material loss observations resulted in venting of the intertank TPS (for two very different causes and for two very different venting configuration implementations) to eliminate or minimize the forces that caused the material loss. Resolution of the problems also included significant efforts to refine the processes and controls of applying the TPS to this complex structure.

Problems that have been observed on the myriad of small manual applications or parts over the history of the program (including LO2 feedline flange closeouts and pressurization line support TPS ramps) have been minimized or eliminated through significant efforts to improve mold tooling and processes as they were observed.
Some complex manual applications, especially the LH2-to-intertank splice application and to a much lesser extent the bipod ramp application, have presented a history of observed material loss which has been addressed with less than complete success in the past and should be the subject of an extensive re-evaluation in return to flight efforts.

Section 6 ET-93 Unique Elements and Acceptance

6.1 ET-93 Unique Elements

6.1.1 As-Designed Configuration

ET-93 was the second External Tank in the LWT Deferred Build Block. It was the first in-line production (MAF-processed) implementation of In-Flight Anomaly (IFA)/intertank TPS venting at the thrust panels and +Z stringer panels. It was the first LWT with machined foam on the intertank +Z stringers. ET-93 also represented the first use of BX-265 on the aft upper ET/SRB fairings.

This tank was also part of the continuing waterfall of improved extrusions on the External Tank. Grain sizes on Al 2219 extrusions were effectively screened for implementation to assure smaller grains and higher properties in welded hardware (Class II designation).

6.1.2 As-Built Configuration

ET-93 had no "out-of-family" nonconformances (NCs). All ET-93 processing anomalies were considered to be 'in-family' and the tank was generally low in overall NCs.

Typical repair work scope in critical areas included the following:

- Bipod Fitting Area: Two voids were observed in the SLA on the outboard side of the LH (-Y) bipod fitting. An area of crushed PDL foam was also identified on the aft side of the LH (-Y) Spindle Face. Two voids and two gouges were observed on the right hand (RH) (+Y) aft side.
- Flange Area: A small number of small voids were found on the upper flange.
- Closeout Processing Anomalies: SLA on the +Y bipod did not meet tensile strength requirements. The material was retested and passed minimum requirements. The area at the 10 o'clock position (facing the bipod looking outboard) approximately 0.4 in. L x 0.15in. W at the widest point did not meet the engineering drawing requirement. The area was assessed for risk of ice formation and established to be above minimum.
- Damage to Intertank –Z Stringer Foam: The foam on 37 consecutive stringers on intertank panels 6, 7, and 8 (-Z side of tank) was damaged by foam cutter head interference. The damage location was about 66 in. forward of the intertank-to-LH2-tank flange closeout. Twelve of the 37 damage locations were accepted 'use as is.' Loose foam was removed and red dye was also used to direct removal of cracks, cuts, crushed foam, and debonds/delaminations. The remaining foam exceeded that required for ascent and reentry. The remaining 25 damage locations were repaired in accordance with the approved repair procedures.
- Repair of LH2 recirculation burst disc

6.1.3 Processing

ET-93, a lightweight tank (LWT), was built as one of the "deferred LWT" builds, *i.e.,* it was built during the SLWT process flow. Weld schedules/parameters were adjusted for LWT materials to accommodate the materials change (Al 2219 for the LWT tanks versus Al 2195 for the SLWT vehicles), material thicknesses, and weld land thicknesses. One out-of-position event occurred during ET-93 processing. Weld repairs for the LO2 tank forward ogive weld, typically performed in a horizontal position, were performed in a vertical weld position to accommodate the existing production flow. (All repair processes were appropriately certified, performed, and validated.)

ET-93 was the first LWT to have the intertank access door closed out at MAF. ET-93 was mated and demated on STS-112 before mate with STS-107. During the course of processing, the ET/SRB attach fairing TPS was damaged and repaired.

No new tools were used on ET-93. The only tooling change identified for this effectivity was associated with modification of the air supply used for the TPS port bond tension tester. No new equipment or process or planning changes were associated with ET 93. There were neither new production vendors nor validations on hardware.

The following is a summary of new materials lots:
Hand Pack Type I Batch Number – 208080-101 Hand Pack Type II Batch Number – 208120-101DC-1200 Lot Number – 360747 (For Type I H/P)C-1200 Lot Number – 00G173 (For Type II H/P)GX-6300 Lot Number – 208080-102 (For Type I H/P); 208070-101Gx-6300 Lot Number – 208120-101 (For Type II H/P); 208100-101Conathane Lot Number – 00G114.

No new personnel were assigned to hardware fabrication. All sprayers and hardware mechanics had previous production experience.

6.1.4 Operational

ET-93 was the first tank to fly with three Block II engines. The LWT configuration was previously certified at ET-92 for the associated increased LH2 prepress pressures. ET-93 was the first LWT to use an Inconel 718 bellows probe on the Ground Umbilical Control Assembly (GUCA) quick disconnect (ground half of interface hardware). It also represented the first implementation of the nose cone heater outlet maximum temperature increase and the nose cone purge outlet maximum pressure increase. STS-107 was the first LWT to fly using the Haz Gas 2000 system. It was also the first tank incorporating the 2.0-sec delay in the ET separation sequence. (No impact was predicted for LWT.)

Paper/processing changes included:

- ET Sensor Requirements: Added/revised tables to clarify the functional requirements of the point level sensors.
- ET/Orbiter Visual Leak Monitoring: Relocated requirements from the OMRSD to LCC. There was no change in the requirement for visual monitoring.

6.2 ET-93 Acceptance

6.2.1 Overview

The SSP Flight Preparation Process (FPP) is defined in National Space Transportation System (NSTS) 08117, Requirements and Procedures for Certification of Flight Readiness. It defines the procedures for the Project Milestone Reviews, the Program Milestone Reviews, and the Flight Readiness Review (FRR). It also defines the endorsement documentation required at the completion of the FRR, which provides the Certification of Flight Readiness (CoFR) for a specific flight.

The FPP is incrementally implemented through milestone reviews, which ensure the readiness of all organizations for the operational phase following each review. Figure 6.2.1-1 illustrates the milestone review process for the Shuttle Projects. For the ET Project, the FPP requires a hardware element acceptance review and participation in the ET/SRB Mate Milestone Review and the FRR.

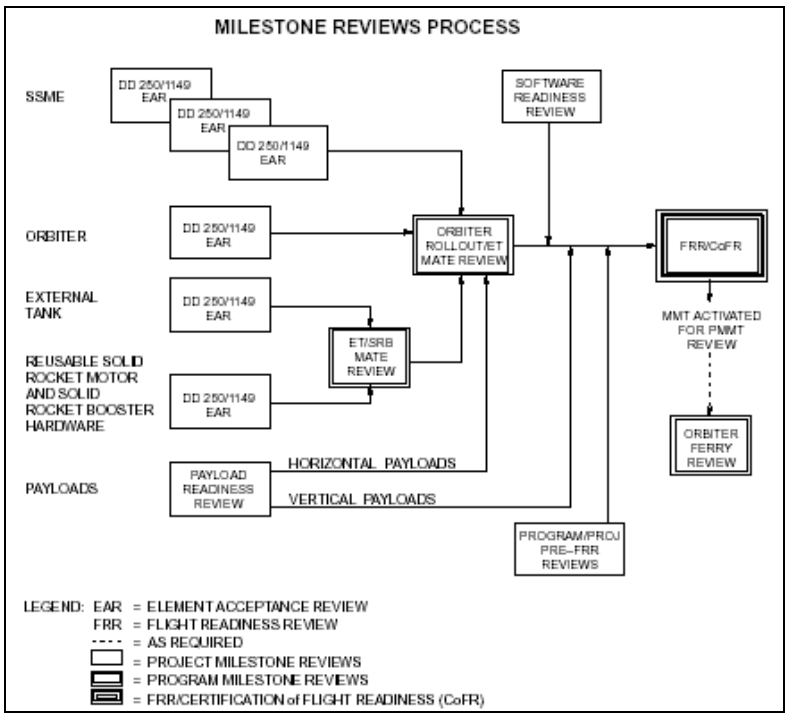

Figure 6.2.1-1. Milestone Review Process

6.2.2 Assessment of Flight Hardware

The External Tank Project builds and flies ETs under the provisions of contract NAS8–36200 for LWT articles and SLWT articles through ET-121. Subsequent articles are produced under the provisions of NAS8-00016. These contracts define the requirements for manufacturing, assembly, test, checkout, and delivery of operational flight articles.

In preparation of milestone reviews identified by the FPP, an assessment of the ET readiness for flight is conducted by the contractor and coordinated with the Project Office. Based on the results of the assessments, the ET Project Office and the contractor coordinate a list of candidate topics for the milestone reviews. At a minimum, the assessment of each ET includes:

- Baseline End Item Configuration: A comparison of the as–designed to the as–built end item configuration
- Acceptance Checkout: Completion of Acceptance Checkout Requirements, (MMC–ET–TM04k), including resolution of checkout discrepancies and any required associated retesting, will be documented and resolved by the appropriate NCD
- Ship–Loose Hardware: In preparation for shipment of the subject ET to the launch site, statusing of all shipping support hardware and uninstalled flight hardware.
- Planned Work/Mod Kits: Identification of all mission specific installations and/or assemblies and authorized modification kits scheduled for initiation/completion at the launch site
- Deferred Work: Identification of specific processing/manufacturing procedures normally performed/completed at MAF for which rationale is provided to justify performance and/or completion at the launch site for the subject effectivity
- Changes: All changes to the previous vehicle as–built/as–flown configuration or operating requirements for which the current mission is the first effectivity
- Processing Anomalies: Any out–of–family occurrence unique to or peculiar to the baselined methods of processing hardware
- Verification/Certification Status: As applied to this mission effectivity, a certification baseline status of program requirements revisions authorized since the previous mission.
- Exceptions/Waivers: Identification of any departures from specification and drawings and appropriate disposition of waivers, deviations or exceptions to program requirements, including project or program signature
- Prior Mission Performance: Review of available data from the previous mission in the following disciplines to assure current processes/procedures are adequate to support the current mission:
  - OMRSD/LCC
  - Instrumentation

  - Main Propulsion System (MPS)
  - Hazardous gas
  - Thermal Protection System
  - ET disposal
  - Orbiter tile damage
  - Post-separation photos
- KSC Processing: A status of launch site vehicle processing activity with application to the subject mission
- Discrepancy Report (DR)/PR/OMRSD Status: A status of discrepancy reports, problem reports, and OMRSD changes associated with this mission effectivity
- Mission Unique Assessment: Identification and assessment of mission profile unique integrated vehicle loads (flight and pre-flight), thermal environments, and other mission-specific data provided through analysis and/or instrumentation
- S&MA Assessment: Audit/monitor by the Office of Safety and Mission Assurance of applicable disciplines of ET Project/contractor operations and status findings to include the following:
  - ALERTs
  - DC&Rs
  - Material Review Boards (MRBs)
  - Hazards/Critical Items Lists (CILs)
  - Latent Defects/CAPs
  - Trending

6.2.3 ET Incremental Readiness Reviews

Incremental reviews are held to assess the readiness of the ET for continuing operations in support of specific mission objectives.

6.2.3.1 Hardware Element Acceptance Review (HEAR)

The delivery of each ET End Item to NASA (DD 250) is marked by this review. The NASA RMO holds this review for the ET Project Manager, and a NASA S&MA representative accepts the ET. At this time, the configuration and requirements for the article have been established. The current status of the ET as related to limited life, certification, planned work, and hardware acceptance testing and inspections is reviewed. The review also includes Deviation Approval Requests, non-compliance reports, Hazards, CAPS, DC&R, and MRB actions. A hardware readiness statement is signed at the conclusion of this review. This review is chaired by the ET Project Manager and is supported by the prime contractor, Shuttle Processing, Program Integration, and S&MA. At the conclusion of this review, a certification statement is signed to attest to readiness of the ET to be delivered to the launch site for flight processing.

6.2.3.2 Contractor Pre-Flight Review (PFR)

The emphasis of the Contractor PFR is on first–time, first effectivity (out–of–family) changes baselined since the last review. At a minimum, the following topics are presented at the review. Supporting information is included as an appendix to the presentation material.

- Modification Kits/Field Engineering Changes
- Significant Changes – Class I changes, Class II changes affecting
- Significant Processing Anomalies
- Verification/Certification Status
- Exceptions/Waivers
- Prior Mission Performance
- KSC Processing
- DR/PR/OMRSD Status
- Mission-Unique Assessment
- S&MA Assessment
- CAPS Status.

In addition, the review may include special topics related to the configuration or processing of the hardware or other events with possible impacts on ET readiness for flight.

Topics presented at this review are carried forward to the ET Project Pre-Flight Review.

6.2.3.3 S&MA Pre-Flight Assessment (PFA)

This review assesses all changes for readiness and acceptability before further presentation to the ET Project. Subjects include the following topics:

- Modification Kits/Field Engineering Changes
- Significant Changes – Class I changes, Class II changes affecting.
- Significant Processing Anomalies
- Verification/Certification Status
- Exceptions/Waivers
- Prior Mission Performance
- KSC Processing
- DR/PR/OMRSD Status
- Mission-Unique Assessment
- S&MA Assessment
- CAPS Status.

6.2.3.4 ET Project Pre-Flight Review

The ET Project Pre-Flight Review is conducted by the ET Project and is chaired by the ET Project Manager or designee. Review participants include: Contractor (LMSSC-Michoud), ET Project Office, Shuttle Processing, Space Shuttle Systems Integration, and S&MA. The review is typically held at MAF with MSFC/KSC/JSC participation by video or teleconference.

The emphasis of the ET Project Pre-Flight Review is on first–time, first effectivity (out–of–family) changes baselined since last review. At a minimum, the topics below are presented at the review. Supporting information is included as an appendix to the presentation material.

- Modification Kits/Field Engineering Changes
- Significant Changes – Class I changes, Class II changes affecting.
- Significant Processing Anomalies
- Verification/Certification Status
- Exceptions/Waivers
- Prior Mission Performance
- KSC Processing
- DR/PR/OMRSD Status
- Mission Unique Assessment
- S&MA Assessment
- CAPS Status

At the conclusion of the review, a board chaired by the ET Project Manager (or designee) decides if follow-up review is required before the FRR. At this time, topics to be carried forward to the FRR are identified.

6.2.3.5 Shuttle Program ET/SRB Mate Milestone Review

The ET Project presents significant changes, NCs, or issues as applicable to the milestone review and any out–of–family events occurring during processing following the delivery of the vehicle to the launch site.

6.2.3.6 Orbiter Rollout/ET Mate Readiness Review

The ET Project participates in this review if any out–of–family events occur during launch processing after the ET/SRB Mate Review and are considered to be a constraint to vehicle processing at the launch site.

6.2.3.7 SSP Flight Readiness Review

The ET Project presents significant changes, NCs, or issues as identified in the previous milestone reviews and any out–of–family events occurring during launch processing following the Orbiter Rollout/ET Mate Readiness Review. The CoFR is signed by the contractor and element Project Managers at the conclusion of this review.

6.2.3.8 Pre-Launch Mission Management Team Review

The ET Project participates in this review if any fleet issues are identified or out–of–family events occur during launch processing post SSP FRR.

Section 7 Data Analysis

7.1 Requirements

This section summarizes the top-level contractual environment requirements applicable to ET-93 verification. Only requirements imposed on the ET Project are included. Sub-tier requirements generated by in-house analysis are included in the assessment of the sub-tier hardware.

Requirements relevant to the following are included:

- Acoustics and random vibration
- Airloads
- Entry and breakup
- Gas temperatures, flow rates, and pressures
- Thermal
- Vehicle loads

There is a brief discussion on how the environments are implemented by stress analysis and verification testing.

The LWT was certified for generic environments, including the Performance Enhancement environments (NSTS 08209 Volume VII, Section 8.0). Additionally, mission-specific analyses were also performed for STS-107/ET-93.

7.1.1 Generic Requirements

7.1.1.1 End Item Specification

Top-level requirements for the LWT are defined in CPT01M09A, “External Tank Contract End Item (CEI) Specification – Part 1” End Item Specification (EIS).

7.1.1.2 Performance Requirements

Performance requirements for the LWT are specified in paragraph 3.2.1.5.2 of the EIS. These requirements include:

- 3.2.1.5.2.1 Fatigue
- 3.2.1.5.2.2 Design Factors of Safety
- 3.2.1.5.2.4 External Tank Entry Heating
- 3.2.1.5.2.5 ET/Orbiter Safe Separation Distance and ET Rupture Altitude

No source documents are referenced by these paragraphs.

7.1.1.3 Induced Environments

Requirements for induced environments are called out in paragraphs 3.2.7.2 (1) through (23) of the EIS.

.

- 3.2.7.2(1) Vibration, Shock, and Acoustics
- 3.2.7.2(17) ET/ORB Umbilical Interfaces and LO2 Feedline Loads
- 3.2.7.2(21) Vehicle Interface and Distributed Loads
- 3.2.7.2(22) Protuberance Airloads
- 3.2.7.2(23) Thermal Environments (including requirements for entry analysis)

Documents referenced by these paragraphs are identified in the paragraphs 3.3.1 through 3.3.6.

7.1.1.3.1 Induced Environments: Vibroacoustics

LWT components are designed and verified to the vibration, shock, and acoustics requirements specified in the EIS, paragraph 3.2.7.2(1). General environments are specified in NASA Reference Publication 1074, "Preliminary Vibration, Acoustic, and Shock Design and Test Criteria for Components on the Lightweight External Tank," February 1981

- Section VII: Vibration and Shock Specifications
- Section VIII: Acoustic Test Specifications

Specific exceptions are also called out:

- Vibration criteria for intertank Zone 3-3, forward of XT 980 are defined in SD74-SH-0082, "Revised Shuttle Acoustic and Shock Data Book," June 1987
- Vibration criteria for ET/Orbiter attach structure are defined in TMX-64868, November 1976, modified by letter ED-23-77-151, 5 July 1977
- Environments (random vibration and acoustic) for specific components are directly identified in the EIS, paragraph 3.2.7.2(1).

7.1.1.3.2 Induced Environments: Vehicle Loads

Paragraph 3.2.7.2(21) of the EIS specifies requirements for ET/Orbiter and ET/SRB interface loads and loads distributed over the ET structure. Loads shall be determined from the requirements of STS85-0169-3, "Structural Design Loads Data Book," Volume 3, "External Tank Structural Loads."

The LWT is certified to vehicle interface and distributed loads from load cases generated by Boeing and approved by Level II Integration and defined in the following sections of the Loads Data Book.

- Pre-launch Section 1.3
- Lift-off Section 1.4
- Maximum Dynamic Pressure Section 1.5
- Post High-Q Section 1.6
- Roll Maneuver Section 1.7

7.1.1.3.3 Induced Environments: Protuberance Airloads

LWT protuberances are designed and certified to the requirements of the following document, as required by the EIS, paragraph 3.2.7.2(22)

- "Structural Design Loads Data Book," STS85-0169 Volume 3, Book 1, September 2001

Airloads for major interface hardware are determined from an envelope of several databases called out in paragraph 3.2.7.2(22)(b), and airloads for SLWT Intertank Thrust Panel TPS (applicable to LWT) are in paragraph 3.2.7.2(22)(c). Other relevant contractual documents:

- "Operational Aerodynamic Design Data Book," STS85-0118, August 1996
- "Shuttle Vehicle Mold Lines and Protuberances," ICD-2-00001

7.1.1.3.4 Induced Environments: Venting

Venting of all critical void areas where pressure is not required is specified in paragraph 3.2.6.3.1(b) of the EIS. Venting Certification Cycle trajectories are called out in EIS paragraph 3.2.7.2(23)(I). Compartment venting requirements are covered by the following document:

- "External Tank/Solid Rocket Booster," ICD-2-24001

7.1.1.3.5 Induced Environments: Thermal

Thermal environment requirements for the LWT are detailed in paragraph 3.2.7.2(23) of the EIS, as follows.

- Para 23(A). Thermal interface requirements:
  - SSD97D0459, "Space Shuttle Program Thermal Interfaces Design Data Book Performance Enhancement Light Weight Tank," October 1997, replaces obsolete document SD74-SH-0144, "Space Shuttle Program Thermal Interface Design Data Book IVBC-3," July 1995 referenced in EIS. EIS update is pending.
- Para 23 (B). Ascent thermal environments:
  - Johnson Space Center (JSC) letter MS4-96-045, "Performance Enhancement (PE) Certification Thermal Environments for Lightweight Tank (LWT)," June 10, 1996
  - JSC letter MS4-97-092, "Performance Enhancements (PEs) for 109 Percent Intact Abort Certification External Tank Thermal Environments for Super Lightweight Tank (SLWT) and Lightweight Tank (LWT) Configurations," October 17, 1997
- Para 23(D). Ascent plume thermal environments:
  - SSD-90-D0016, "Space Shuttle Generic ETR Plume Heating Data Book External Tank," per PRCBD S052638", March 27, 1991

- Para 23(K).
  - JSC letter MS2-01-004, “Heating factors for ET intertank Hi-Lock Fastener TPS amps,” January 24, 2001

7.1.1.3.6 Induced Environments: Entry

Entry thermal environment and trajectory requirements for the LWT are detailed in paragraph 3.2.7.2(23) of the EIS.

- Para 23(E). Entry breakup thermal environments (Note, although SLWT, all documents were directed to be applicable to ET91 through 95):
  - JSC letter MS4-94-144, “Nominal No-Fail Heating for SLWT Breakup Analysis,” December 21, 1994
  - JSC letter MS4-96-046, “Transmittal of Mean SLWT Entry Trajectory,” June 5, 1996
  - JSC letter DM7-96-05, “Mean SLWT Entry Trajectory Delivery for -Z Side Heating Analysis,” June 19, 1996
- Para 23(F). Entry heating trajectories:
  - JSC 26025, “External Tank (ET) Entry Trajectory Data Book,” September 14, 1992
  - JSC letter MS4-97-003, “Trans-Atlantic Abort Landing (TAL) External Tank (ET) Entry Trajectories for Rupture Time Analysis,” January 9, 1997
- Para 23(G). Entry thermal environments:
  - MMC-ET-SE05-580, “Aero/Thermal Entry Heating Data Book for the External Tank – SLWT,” April 1997

7.1.1.3.7 Main Propulsion System Certification Trajectories

MPS certification trajectories for the LWT are specified in paragraph 3.2.7.2(23)(H) of the EIS.

7.1.1.4 Interfaces

Interface requirement documents controlling ET propulsion analysis are specified in the following paragraphs of the EIS:

- 3.6.2.2 Orbiter/ET Interfaces
- 3.6.2.3 ET/SRB Interfaces
- 3.6.2.4 ET/SS Launch Pad and MLP

Documents referenced by these paragraphs are identified below.

7.1.1.4.1 Design Requirements

LWT pressure and temperature design requirements are controlled by the following paragraphs of the EIS:

- Para 3.6.2.2. Orbiter/ET Interfaces
  - ICD-2-12001, “Orbiter Vehicle/External Tank,”

- Para 3.6.2.3. ET/SRB Interfaces
  - ICD-2-24001, "External Tank/Solid Rocket Booster,"
- Para 3.6.2.4. ET/SS Launch Pad and MLP
  - ICD-2-0A001, "Shuttle System Launch Platform Stacking & VAB Servicing."

7.1.1.4.2 Operational Requirements

Operational and procedural requirements are imposed by the following documents:

- Operations & Maintenance Requirements & Specifications Document (OMRSD), Files II and IV
- Launch Commit Criteria (LCC), ET 01-10, MPS 01-47(Partial), HazGas 01-12 (Partial)

7.1.1.5 ET-Derived Requirements

All ET internal loads resulting from the environments defined above are documented in the Loads Data Book (LDB), LM Drawing 80900200101. Models to produce these loads were derived using standard finite element techniques. The analysis to produce loads (from the models and prescribed environments) uses computer codes developed in-house, and maintained under configuration control; these programs are based on standard and accepted principles of mechanics. All the analysis models and results are stored on the AS4000 Jazz computer at Huntsville.

External Tank structural temperatures are documented in the Thermal Data Book (TDB), LM Drawing 80900200102, and reflect thermal analyses for design certification environments. The TDB thermal models use the requirements as documented in the End Item Spec as boundary conditions. The thermal math models are lumped parameter representations of the flight hardware based on the structural drawings. Materials data used in the models are test derived and referenced in the TDB. Systems Integrated Numerical Differencing Analyzer and Fluid Integrator (SINDA/FLUINT), which is widely used and accepted as an industry standard, is used in combination with in-house written subroutines, maintained under configuration control, to solve diffusion-type equations to generate temperatures. All models and results are archived on the AS4000 Blues computer in Huntsville.

The venting analysis data are documented in "Compartment Venting (Lightweight Model)," MMC-ET-SE05-95. The venting environments defined by Level II are referenced in MMC-ET-SE05-95. Venting analysis is carried out by computer codes [FD275 (One Compartment Venting,) MULTICOMP (Multiple Compartment Venting), and HAZGAS (Intertank Hazardous Gas Program)] maintained under configuration control. These programs use coefficients derived

from wind tunnel testing or flight measurements, or a combination of both. All models and results are archived on the AS4000 Blues computer in Huntsville.

MPS performance, including pressurization of the ET and propellant feed from the ET, is reviewed by Level II Propulsion Systems Integration Group (PSIG). The ET Project predicted ET performance is documented in Pre-Flight Prediction report; post-flight performance assessments are documented in the Quick Look, Flight Evaluation, and Engineering Evaluation reports. Design Criteria and Requirements are governed by the ICD, LCC, OMRSD, and the EIS. LWT LH2 pressure requirements were updated for PE trajectories by IRN IC-1432, which was approved by PRCBD S060604P signed 08-26-98. There were two subsequent updates:

- IRN IC-1657 approved by PRCBD S060604T signed December18, 2000
- IRN IC-1675 approved by PRCBD S06060V signed February 20, 2001

LWT LO2 requirements were updated by IRNs IC-1248, IC-1288, and again for PE trajectories by IC-1432. Approval of the IRN signifies acceptance by ET of the proposed revisions. In each instance, the ICD was updated by the specified IRN.

The two primary models used to assess ET performance are the Single Node Pressurization Program and the Propellant Loading Program. These models and results, maintained under configuration control, are archived on the AS4000 Blues computer in Huntsville.

7.1.1.6 ET Implementation of Requirements

To ensure ET hardware structural integrity and compliance with the EIS structural Factor of Safety requirements, a formal stress analysis is performed and documented in the ET Stress Report (826-2188). The stress report integrates all critical system- and element-level induced environments to produce a margin of safety for the as-designed ET hardware. The stress analysis is a key element in the overall design certification and verification of ET hardware. In addition to the stress analysis, a significant amount of ET hardware is verified by structural testing. Traceability to the appropriate certification/verification testing and analysis for a particular hardware element is documented and maintained by Systems Engineering.

In addition, LWT critical load indicators, documented in report 826-2363 “LWT Structural Load Indicators and Capabilities” are used for all flight assessments. Any violations of an indicator are flagged. Subsequent analysis then either clears the ET for the particular condition, or imposes a flight constraint.

Certification of the LWT design and hardware requirement compliance is documented in the Design Certification Sheets (DCSs), Certificates of Qualification (COQs), and Hardware Certification Sheets (HCSs) maintained by Systems Engineering. Table 4.2.2-1 of the EIS cross-references each design requirement to a DCS. EIS tables 4.3-1 and 4.3-3 list hardware and their

associated COQs and HCSs. The MMC-ET-TM09 document generated for each flight tracks the NSTS 07700, Vol. X, Book 1 requirements to EIS paragraph numbers, DCS, and ICD. Final certification of the ET is at Flight Readiness Review, where any deviation from baseline requirements is addressed. The specification flowdown and verification process is shown in Figure 7.1.1.6–1.

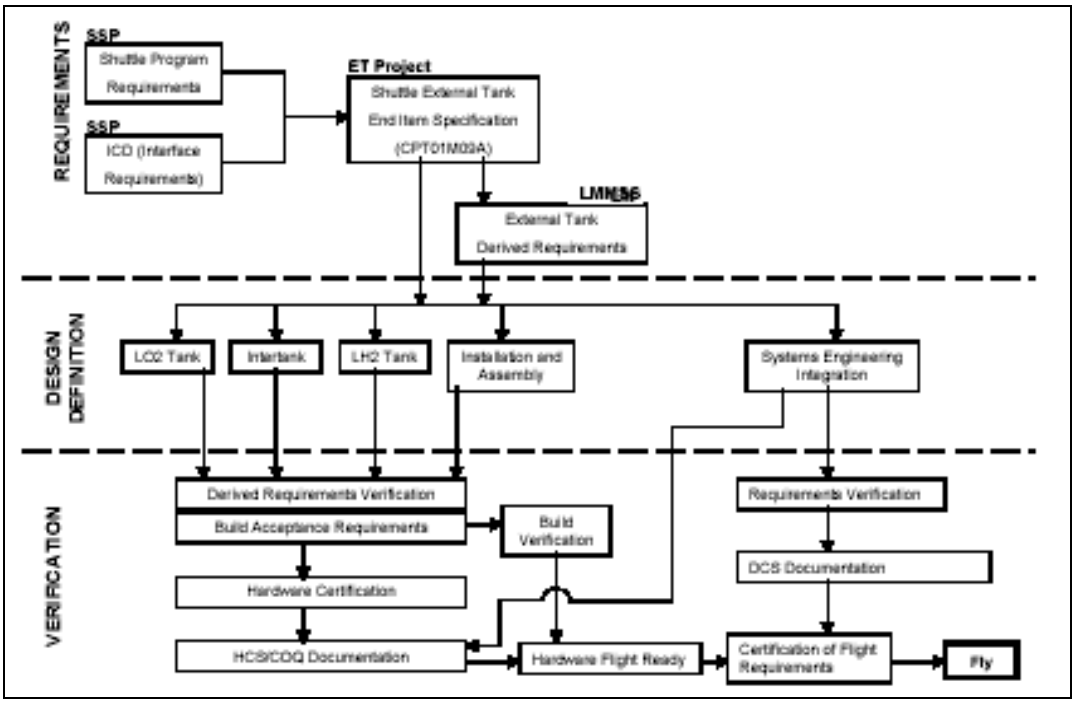

Figure 7.1.1.6-1. Requirements Flowdown

7.1.2 Flight-Specific Assessments

The following paragraphs address flight-specific assessments that were made for STS-107/ET-93. These assessments were performed using the same methods and tools described for the assessment of generic requirements.

7.1.2.1 Flight-Specific Assessments – Loads

7.1.2.1.1 Lift-off Loads Flight Margins Assessment (FMA) – Boeing

This study assessed lift-off loads using PE criteria, Block II SSME thrust and mass properties. The assessment was made against 826-2363, "LWT Structural Load Indicators and Capabilities," Rev R, January 2001.

One exceedance was identified and provided to the ET Project for evaluation (ref: Boeing letter 02MA0264, June 13, 2002). Lockheed Martin subsequently cleared this exceedance, reference contract letter 02MO-0540, July 23, 2002.

7.1.2.1.2 High-Q loads Launch Probability FMA – Boeing

This assessment was performed to certify operational high-Q design targets with LWT. Evaluation was made against 826-2363, “LWT Structural Load Indicators and Capabilities,” Rev R, January 2001.

No exceedances were identified, as documented in the Boeing presentation to the Level II Loads Panel, “STS 107 SI IVA Flight Readiness,” S. del Basso, November 18, 2002.

7.1.2.2 Flight Specific Assessments – Pressurization

7.1.2.2.1 Pressurization Performance Assessment – Boeing

This assessment evaluated GO2 and GH2 pressurization performance with Block II SSMEs. ICD violations were identified and provided to the ET project for assessment (Boeing letter 02MA0584, December 4, 2002)

ICD violations were cleared by Lockheed Martin. (Reference contract letter 03MO0025)

7.1.2.3 Flight-Specific Assessments – Thermal

7.1.2.3.1 Flight Margins Assessment for Late TAL Heating Analysis

This assessment included a 2-sec mated coast extension and Block II SSMEs. Exceedances were provided to the ET project for assessment (Boeing letter 02MA0161).

These exceedances were cleared by Lockheed Martin. (Reference Thermal Panel presentations on February 28, 2002, and a SSEIG presentation on December 9, 2002)

7.1.2.4 Flight-Specific Assessments – ET Separation

7.1.2.4.1 RTLS ET Separation and TAL Hit Evaluation

This evaluation included a 2-sec mated coast extension and Block II SSMEs. No issues were identified (reference Boeing presentation to Ascent GN&C Panel, “STS-107 RTLS ET-Sep and TAL Hit Evaluation,” G. Manich and S. Bingham, 11/13/01).

7.2 Fault Tree Analysis

There were four possible dispositions for each event in the FT:

- Not Possible
- Possible-Probable
- Possible-Remote
- Possible-Improbable.

Each basic event in the FT was assumed to be a cause or contributor to the shedding of debris or a contributing interface event if the event occurred. Details of the assessment of each FT branch are presented in the following sections. Each event was assessed for possibility of occurrence. If deemed possible, the event was assessed for the likelihood of occurrence. The assessment criteria were:

- Possible-Probable: The supporting data identified a high likelihood that the event occurred.
- Possible-Remote: The supporting data did not indicate a high likelihood of occurrence but did provide rationale that supported the potential for occurrence.
- Possible-Improbable: The supporting data did not indicate the event having a remote likelihood of occurrence but did not completely rule it out.
- Not Possible: The supporting data was sufficient to rule out the occurrence of the event.

The disposition of event blocks using these criteria was a subjective process. No probabilistic risk assessments or other numerical tools were used to reach conclusions. The ETWG established an arbitration board for cases in which the branch lead disagreed with the disposition selected by the initiator. NASA S&MA personnel were in the review/approval loop for every event disposition and rationale. The disposition of intermediate event blocks was selected to be the same as the most likely possible contributing event since, with the exception of cut sets (see Section 5.1.1), “or” gates were used to relate all events.

Early in the accident investigation, the scope of the investigation was prioritized to focus on debris that could strike the left wing of *Columbia*. With the support of the Shuttle Integration Group, the ETWG established a map of geographic zones (Figure 7.2-1) on the ET from which debris could originate and have credible aerodynamic transport to the left wing during lift-off and ascent. Only the hardware items within these zones were studied for debris potential. Investigation of items outside these zones was indefinitely deferred, and these items were identified in the FT as undeveloped events. (Deferred locations were to be reprioritized in the event of additional investigation results implicating the region in the accident, and additional locations were analyzed at the discretion of the major FT branch leads.)

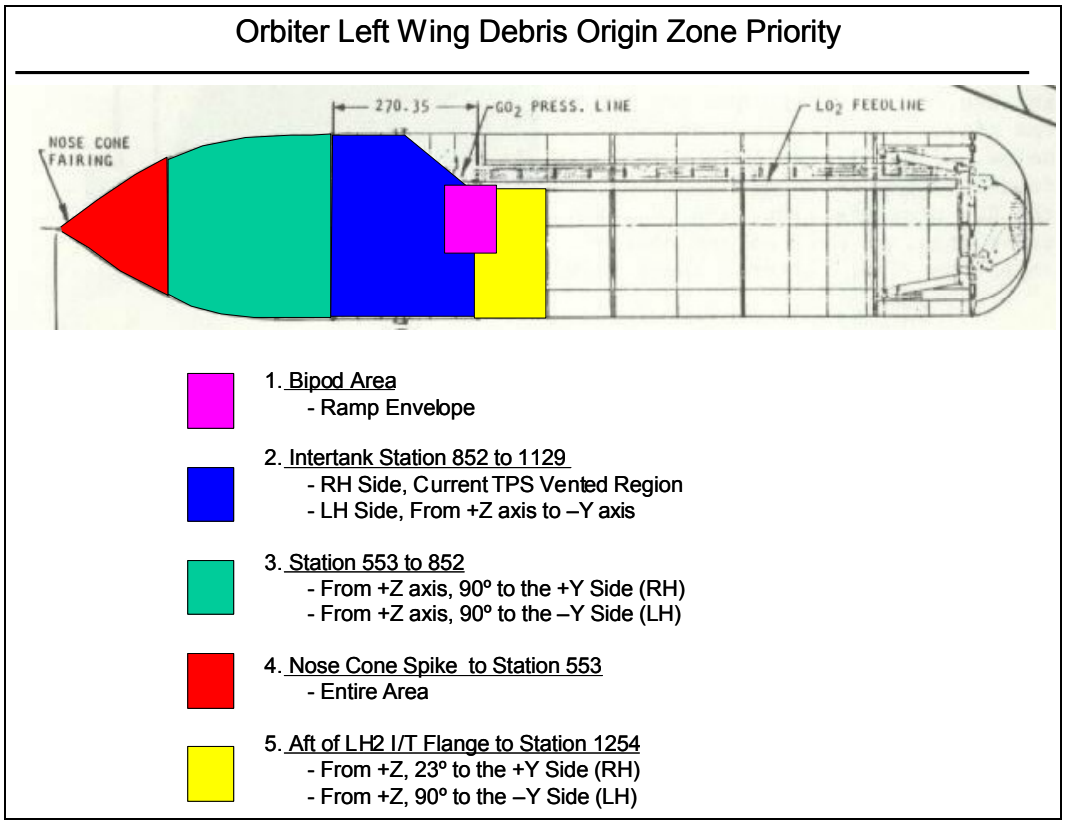

Figure 7.2-1. Prioritized Hardware for the Fault Tree Investigation

The top levels of the ETWG FT are shown in Figure 7.2-2. FT branches were developed to focus on the two possible causes associated with the External Tank following a successful ascent: debris damage to the Orbiter or contributions by the ET to an interfacial event. A demarcation of responsibility has been defined on the FT. The responsibility of the ETWG was established to be one of defining possible, likely credible debris or interface events. Disposition of those events with respect to the STS-107 accident was allocated to the OVE Working Group, as shown in Figure 7.2-2.

Results of the investigation of the 3470 blocks are included in Volume II, an electronic, interactive Fault Tree (CD) with attachments and query capability.

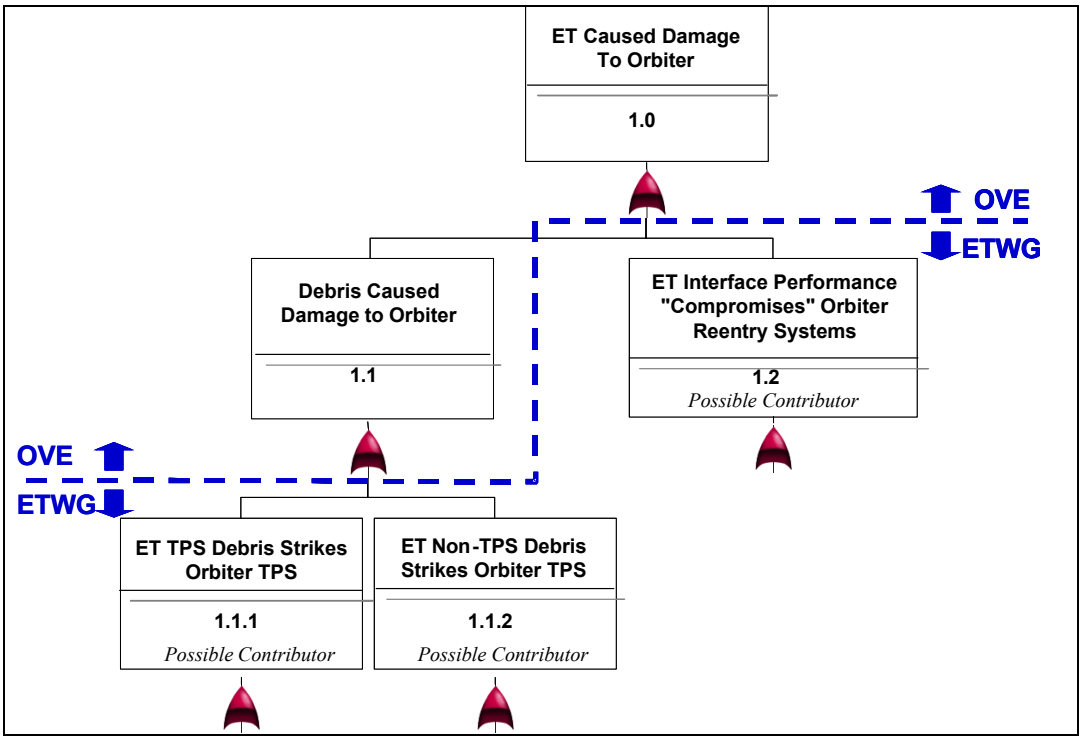

Figure 7.2-2. ETWG Top Fault Tree Levels

7.2.1 TPS Branch

7.2.1.1 Summary

The TPS Debris branch of the ETWG FT was one of two main branches investigating scenarios of debris originating from the External Tank and striking the Orbiter *Columbia* during lift-off and ascent on mission STS-107. In addition to assessing specific causes for the STS-107 accident, the TPS Debris Team was chartered with identification and assessment of additional debris-oriented issues. The Team mission and direction were two fold:

- First, identify any and all items that could have led to, or resulted in, the *Columbia* mishap.
- Second, and equally important, identify all items that must be addressed to enhance and improve the robustness of the ET TPS systems.

The assessment of TPS contributions to the STS-107 accident was systematically organized to assure complete coverage of all critical TPS systems, processes, practices, and implementation. The TPS tree branch was partitioned in tiers:

- The first level was organized by TPS materials (NCFI 24-124, NCFI 24-57, PDL 1034, BX-250, SLA-561, SS-1171, BX-265, and MA 25).
- The next level was organized by all components of the ET that use that material.

- The next level identified all lower level subcomponents.
- The next level identified the main thrust areas of the investigation:
  - Debris Due to Design
  - Debris Due to KSC Processing
  - Debris Due to Vendor
  - Debris Due to MAF Processing.

On conclusion of the assessment of the ET-93 TPS materials, processes, design, verification, validation, and operational performance, the following debris generation categories were identified:

- PDL Repairs
- Operator Input to Process
- External Impacts to ET TPS Produce Debris
- Inadequate Design and Verification Methodology
- Debris Due to Manufacturing Process Plan - (Manual spray overlap times not verified by QC)
- Improper Storage – shelf life discrepancies in STP
- Improper Application – additional operator verification steps needed
- Inadequately Defined Acceptance Testing
- Undetected Anomaly due to Processing at a Vendor, MAF or KSC

The following FT blocks were classified as “red,” or likely contributors to large foam loss on ET-93:

- BX-250 – “BX 250” (WBS 1.1.1.4)
- “Bipod” - (WBS 1.1.1.4.1)

The following FT blocks were classified as “yellow,” or possible contributors to TPS loss, either separately or in conjunction with other evets.

- BX-250 – “Bipod - Inadequate Design Methodology” - (WBS 1.1.1.4.1.1.1.1)
- BX-250 – “Bipod - Debris Due to Anomalous MAF Processing - Debris Due to Inadequate MPP” (WBS 1.1.1.4.1.1.3.2.1)
- BX-250 – “Bipod - Debris Due to Anomalous MAF Processing - Inadequately Defined Acceptance Testing” (WBS 1.1.1.4.1.1.3.3.6)
- SLA-561 – “Bipod Fitting - Inadequate Design Methodology” - (WBS 1.1.1.5.1.1.1.1)
- SLA-561 – “Bipod Plate Connector - Inadequate Design Methodology” - (WBS 1.1.1.5.1.2.1.1)

7.2.1.2 Team Charter

The ETWG directed the development and completion of a Fault Tree as the primary method or tool by which the ET potentially could have caused or

contributed to the loss of STS-107. One of the branches identified on the tree was "ET TPS Debris Strikes Orbiter TPS." The TPS Team charter was to review the engineering and build processing paper, beginning with the basic material vendors and ending with the launch at KSC. The first priority was to identify any abnormalities or concerns that could have resulted in the liberation of TPS within the Critical Debris Zone defined above. The secondary objective was to identify observations for assessments as possible enhancements following the Investigation.

7.2.1.3 Team Overview

The Team was composed of both NASA/MSFC and LMSSC personnel. The Team core members represented the senior TPS experts in the MSFC community.

The basic responsibility of the TPS Debris Team revolved around determining what happened, establishing corrective action, finding related issues, and determining additional appropriate corrective actions if required.

Scotty Sparks, NASA, and Mike Quiggle, Lockheed Martin, led the TPS Debris Investigation Team. The dedicated NASA S&MA Team Lead was Chris Reinecke.

7.2.1.4 Scope of Review

The scope of the TPS Debris Team review included all TPS materials and processes, from design and development through production and flight performance; all facets of the TPS process for configurations in the Critical Debris Zone; and, determination of probable cause for the liberation of TPS debris.

7.2.1.4.1 TPS Systems Overview

There are basically two types of TPS materials used on the ET: low density closed-cell foams, used for high insulation efficiency, and denser composite materials, used for high heat capability. Each type has variations that provide for application ease (spray, pour, pre-mold/bond installations) and specific mission requirements. Foams are used at low heating rates, and the composites are used where the foams are inadequate. The initial TPS thickness is determined by pre-launch requirements, and additional material (foam or ablator) is added as dictated by ascent and re-entry requirements.

The majority of the ET TPS is North Carolina Foam Insulation (NCFI) 24-124 SOFI and SLA-561 bonded ablator. NCFI 24-57 SOFI, a more dense and more heat-resistant foam, protects the aft LH2 tank dome. The SRB booster plume thermal environments require a more robust foam system than that applied to the acreage. The SOFI is applied over the SLA when both highly efficient insulation and high heating capability are required. In areas not exposed to ascent heating (LO2 tank aft dome and LH2 tank forward dome) and in various benign closeout

areas, urethane foams (BX-250, BX-265, SS-1171, and PDL-1034) are used because of their more liberal application constraints.

The pre-launch requirements basically define the foam installation thickness. Maintaining good quality/stable propellants and minimizing ice are the primary considerations. Protuberances and interface hardware utilize thermal isolators, heaters, and foam cover as required to provide an equivalent ice deterrent.

In summary, the TPS before launch serves the following functions:

- Maintains LO2 and LH2 boil-off rates below the vent valves capabilities
- Insures LO2 and LH2 specified temperatures at the Orbiter interface
- Controls air liquefaction on the LH2 tank
- Controls ice formation on the ET surface.

The ascent mission phase defines the requirement for an ablator. Maintaining the primary structure and subsystem components within the design temperature limits is the primary consideration. Heat input is derived from aero convective flow, the SSME and SRB plumes, the SRB separation motors, and autogenous tank pressurization gas.

Another function of the TPS occurs during ET re-entry when structural temperatures and tank pressures contribute to the ET fragmentation process and consequential debris size and impact area (footprint). The residual material must be adequate to provide the entry function and assure low altitude fragmentation to meet the 100- x 600-n. mi. footprint limits.

Figure 7.2.1.4.1-1 shows those TPS areas that were a part of the assessment for STS-107. Table 7.2.1.4.1-1 shows the various TPS systems and pertinent information about each.

7.2.1.4.2 TPS Materials and Application Analysis

The classical analytical methods used to analyze TPS consist of calculating stresses/strains using consistent equations/analytical methods. The analysis is used to correlate test conditions to flight conditions based on the most critical environments and failure modes. Since the flight stresses/strains and the test-demonstrated stresses/strains are calculated using the same methodology, the Test Demonstrated Factor of Safety (TDFS) adequately represents the relationship between the test conditions and flight conditions.

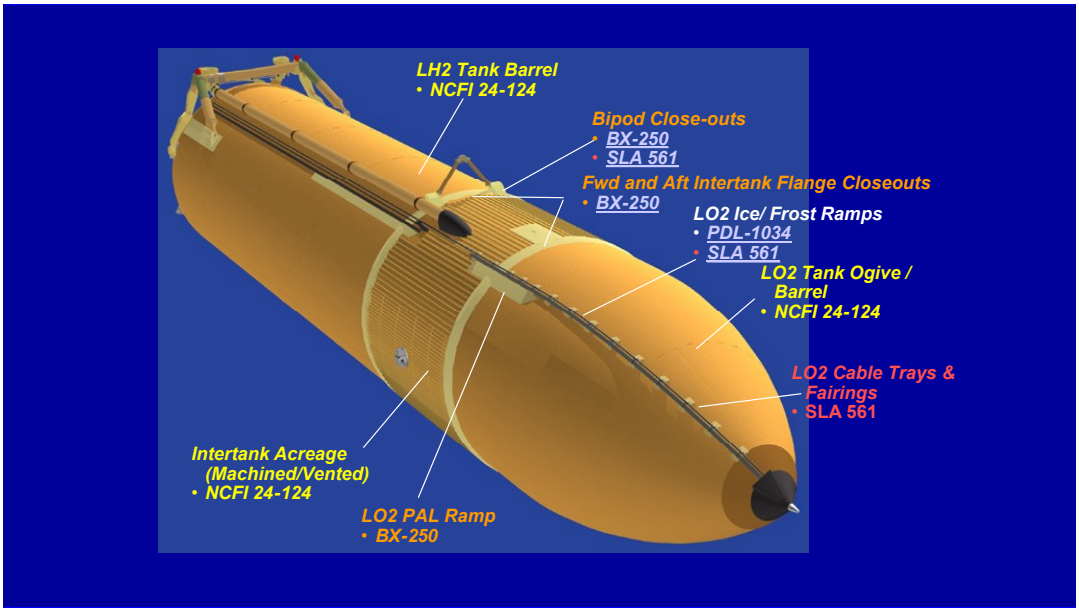

Figure 7.2.1.4.1-1. Reviewed External Tank TPS Systems

Table 7.2.1.4.1-1. TPS Materials Systems Properties Overview

Foam/Property	**NCFI 24-124**			**NCFI 24-57**			**PDL-1034**			**BX-250, BX-265 and SS-1171**		
• Application	LO2, LH2, Intertank sidewall			LH2 aft dome			Closeouts, repairs			LO2 aft dome, LH2 forward dome, closeouts		
• % of Total Foam	77%			7%			2%			14%		
• Process	Spray			Spray			Pour/Mold			Spray		
• Description	Isocyanurate			Isocyanurate			Urethane			Urethane		
Requirements	**Spec Reqmt**	**Typ Prop**	**Flt Reqmt**	**Spec Reqmt**	**Typ Prop**	**Flt Reqmt**	**Spec Reqmt**	**Typ Prop**	**Flt Reqmt**	**Spec Reqmt**	**Typ Prop**	**Flt Reqmt**
• Density (pcf)	2.0-2.5	2.2	N/A	2.6-3.1	2.97	N/A	2.3-3.1	2.6	N/A	1.8-2.6[3]	2.4	N/A
• Tensile, RT (psi)	30 min.	44	19	40 min.	66	19	60	113	19	35 min.	53	19
• Tensile, -423°F (psi)	N/A	34	19	N/A	49	19	N/A	50	19	N/A	62	19
• Tensile, +300°F (psi)	N/A	32	19	N/A	36	19	N/A	71 [1]	10	N/A	35 [1]	19
• Compression (psi)	25 min.	33	20	35 min.	49	20	30	61	20	24 min.	30	20
• Recession Rate @ 7 Btu/ft sq. sec.) (in./sec.)	N/A	.0094	N/A	N/A	.0099	N/A	N/A	.0303	N/A	N/A	.017 [2]	N/A
• Thermal Conductivity @ RT (Btu/hr ft°F)	.025	.017	N/A	.0225	.0180	N/A	.016	.015	N/A	.015	.013	N/A
• Cryostrain (ksi)	61 @ -423°F	65 @ -423°F	pass	58 @ -423°F	65 @ -423°F	pass	N/A	60 @ -423°F	pass	N/A	65 @ -423°F	pass

The critical failure modes for TPS on the ET are bond line delamination, outer fiber cracking, and bond adhesion. Detailed discussion of analysis methodology, inputs, and results are contained in section E of the SLWT External Tank Stress Report, EAS No. 3521-826-2188, Rev AA-S. A brief discussion of the critical TPS failure modes, along with the critical inputs to the analysis, is provided below.

Analysis of the bond line delamination failure mode requires substrate strain, substrate bending/flexure, material thickness, thermal gradient, thermal expansion/contraction, and modulus. Cryogenic thermal gradient, CTE mismatch between TPS and substrate, and the resulting differential thermal strain of the TPS and the aluminum substrate are primary drivers for bond line delamination. In essence, the TPS shrinks more than the aluminum, which produces a thermal stress distribution tangential to the tank surface. A free body diagram, in Figure E.1.6.2.2-2 pg. 3 Section E of the SLWT Stress Report (EAS No. 3521-826-2188 Rev. AA-S), shows the tangential thermal stress distribution, which is counteracted by a bond line stress distribution or “peel” stress. The aluminum substrate is considered infinitely rigid, and the “peel” stress is conservatively reacted on the TPS. This failure mode is most critical during pre-launch when the substrate is cryogenic. For non-cryogenic hardware, substrate strain is the primary driver for bond line delamination. Previous testing of TPS shows that bond line delamination failures are accompanied by a crack of the TPS, which progresses through the thickness of the TPS resulting in a ‘peeling’ of the TPS from the metallic substrate.

Analysis of the cracking caused by outer fiber strain failure mode requires substrate strain, substrate bending/flexure, material thickness, and the outer fiber strain capability. Substrate bending/flexure is the primary driver for outer fiber strain. This failure mode is critical for pre-launch and flight when the ET experiences thermal contraction caused by cryogenic temperatures and maximum tank internal pressure.

Analysis of the failure mode of bond adhesion requires cell burst pressure, substrate temperatures, local acceleration forces, and the TPS bond tension capability. The effect of cell pressure is the primary driver for bond adhesion of ET foam and vibroacoustic loading for ablator. As the Shuttle ascends, ambient pressure decreases, internal cell pressure increases because of increased substrate and TPS temperature, and acceleration loads produce forces on the TPS perpendicular to the tank surface. These forces are reacted through the TPS, producing stress in the TPS and on the TPS/substrate bond line. Bond adhesion stresses are critical at the end of ascent, when the TPS experiences maximum acceleration and thermal environments. The cell burst pressure adjacent to the cryogenic substrate will be significantly below the maximum possible of 14.7 psid as a result of reduced cell pressures due to cryogenic cooling. The analysis conservatively neglects relief related to cryogenic temperatures, however, and assumes pure vacuum so that the maximum

possible differential pressure is analyzed. For regions through the thickness of the TPS exposed to flow heating effects, testing has shown that the BX-250 material will recede before developing sufficient cell pressure to cause foam divots.

Protuberances are subjected to air loads during ascent. Direct tangential air loads are reacted as shear loads on the TPS material. The protuberance footprints provide adequate area and strength to accommodate the applied air loads. Crush pressure is an additional derived requirement because of aerodynamic load inputs normal to the ET tank membrane, which are analyzed and considered negligible. Other negligible environments are documented within pgs. 43-46, section E.2.5.6, of the SLWT Stress Report EAS No. 3521-826-2188 Rev. AA-S.

Cryogenic thermal gradient produces a moment or "peel" stress at the ET TPS/substrate bond line. Subsequent aerodynamic and substrate warming during ascent relieves thermal loading at the TPS to substrate bond line. During ascent, thermal analysis results predict significant outer surface temperature increases during ascent.

The ET NASTRAN model is used to derive the design (in-plane) substrate strain requirement. The ET NASTRAN model is the latest version of the model previously verified by correlation to STA test results (MMC-ET-TM03-0, Vol. I and III). The NASTRAN model loads are formatted and read into a FORTRAN program, which computes margins of safety for multiple load case assessments. Aerodynamic loads can be considered to be acting in normal and tangential directions to the ET membrane. Stress analysis uses 'zero margin' maximum air loads as provided in the Super Lightweight and Lightweight External Tanks Loads Data Book 80900200101 Rev. H, Table 12.31.3-1, to calculate shear stresses on TPS protuberances. The reconstructed loads for STS-107/ET-93 are lower in magnitude than the loads provided for the 'zero margin' analysis and result in increased factors of safety.

The basic ground rule used for the TPS analysis is to combine the most critical contributors for a given failure mode and to compare the resulting parameter, *e.g.,* maximum moment, stress, strain, cell pressure, radius, to test data using consistent analytical methods. The primary failure mode is bond line delamination. For this failure mode, the analysis considers thermal gradient, substrate strains (thermal and mechanical) and flexure. The LWT Delta Critical Design Review (CDR) established the methodology for determining factors of safety based on the internal moment, and RID T-1 initiated a minimum factor of safety requirement of 1.10 relative to strain compatibility.

7.2.1.5 TPS Debris Branch Fault Tree Structure (Lower Branches and Sub-Branches)

The TPS Debris Fault Tree section consisted of 2788 blocks, of which 2134 were "basic event" blocks. ("Basic event" blocks are those FT blocks that reflect the lowest level of analyzed event.) The tree was organized by the 8 different TPS material types (Figure 7.2.1.5-1.) and the tree was developed to a 9-digit level. TPS configurations that were not located in the Critical Debris Zone were "Diamond Deferred." There were 35 blocks that fit that definition (Example: TPS applied to the internal LO2 dome.) (The Diamond Blocks were not developed to the 9-digit level; had they been, the total number of blocks would have encompassed several thousand more.) Two FT branches, 1.1.1.2 "NCFI 24-57" (exclusively used for the LH2 aft dome acreage, outside the STS-107 debris zone) and 1.1.1.8 "BX-265" (exclusively used for the ET/SRB aft fairings, outside the STS-107 debris zone), were entirely "Diamond Deferred."

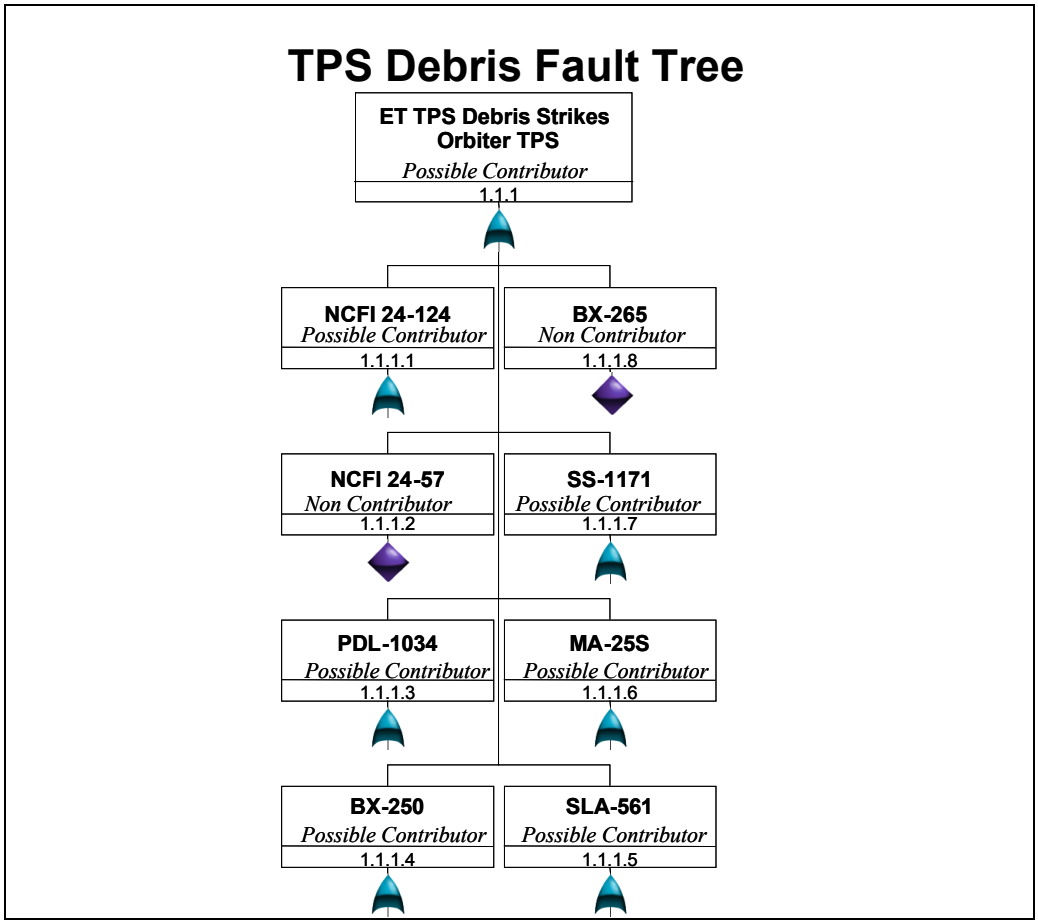

Figure 7.2.1.5-1. TPS Debris Branch Top-Level Subheadings

Each material was then populated with groupings of similar TPS configurations utilizing that material. Within each grouping, every different TPS configuration was identified by the applicable 8097XXXXXXX drawing number and its

corresponding FMEA code number and was transformed to a 1.1.1.X.X.X or a 6-digit code. Each TPS configuration 6-digit number was then expanded to include 7 digits to establish the four major areas that would be reviewed for each TPS component for each TPS material. For example, examination of the block number 1.1.1.4.1.1.1.1 reveals:

- The 1 in the 3rd column indicates that this is TPS
- The 4 in the 4th column indicates that this is BX-250
- The 1 in the 5th column indicates that this is a BX-250 Bipod TPS component
- The 1 in the 6th column indicates that this is the TPS Closeout Assembly, Forward Bipod Fittings Drawing 80971008434 and FMEA Code 5.8.35.1

A total of four possible numbers can be used in the 7th column. These represent the four primary areas of the TPS configurations that were potentially reviewed for inadequacies. Not every configuration required all areas to be assessed, as some areas were not applicable. The four major areas were:

- Debris Due to Design Resulting in a Cohesive, Shear, Delamination, or Crack Failure of TPS
- Debris Due to Vendor Manufacturing/Processing Resulting in a Cohesive, Shear Delamination, or Crack Failure of TPS
- Debris Due to MAF Processing Resulting in a Cohesive, Shear, Delamination, or Crack Failure of TPS
- Debris Due to KSC Processing Resulting in a Cohesive, Shear, Delamination, or Crack Failure of TPS

There are possibly 7 numbers that can be used in the 8th column, depending upon the major area identified in the 7th column:

- If the 7th column is Debris Due to Design Resulting in a Cohesive, Shear, Delamination, or Crack Failure of TPS, the following were underlying causes:
  - Inadequate Design Methodology
  - Inadequate Design Implementation
- If the 7th column is Debris Due to Vendor Manufacturing/Processing resulting in a Cohesive, Shear, Delamination, or Crack Failure of TPS, the following were underlying causes:
  - TPS Raw Material
  - Cleaning Raw Material (Acreage (NCFI) – Other parts provided cleaned/ready for TPS)
  - Primer Raw Material (Acreage (NCFI) – Other parts provided primed/ready for TPS)
  - Ducommun/MAF Material (Acreage (NCFI) – Other parts provided ready for TPS)
  - Adhesive Raw Material
  - Undetected Anomaly

- If the 7th column is Debris Due to MAF Processing Resulting in a Cohesive, Shear, Delamination, or Crack Failure of TPS, the following were underlying causes.
  - Debris Due to MAF Training
  - Debris Due to Manufacturing Process Plan
  - Debris Due to MAF TPS Material Processing
  - Debris Due to MAF Cleaning Material Processing (Acreage (NCFI))
  - Debris Due to MAF Priming Material Processing (Acreage (NCFI))
  - Debris Due to MAF Welding Processing (Pressure Vessels Acreage (NCFI))
  - Debris Due to MAF Adhesive Material Processing
  - Debris Due to External Events During MAF Processing
  - Debris Due to Mechanical Assembly Anomaly
  - Undetected Anomaly
- If the 7th column is Debris Due to KSC Processing Resulting in a Cohesive, Shear, Delamination, or Crack Failure of TPS, the following were underlying causes.
  - Debris Due to Nominal KSC Processing
  - Debris Due to Anomalous KSC Processing
  - Undetected Anomaly

There were possibly 8 numbers that could be used in the 9th column, depending upon the focus identified in the 8th column. Only three of the major areas were carried out to a 9th column. (KSC Processing was not expanded further.)

- The Debris Due to Design can expand to a 9th digit to capture the following basic events:
  - Inadequate Material Testing
  - Inadequate/Incorrect Analysis Methods
  - Inadequate Verification
  - Incorrect Materials Identified
  - Incorrect Processes Identified
  - Incorrect Configuration/Dimensions Identified
  - Incorrect ET Effectivity Identified
- The Debris Due to Vendor Manufacturing/Processing Raw Material blocks can expand to a 9th digit to capture the following basic events:
  - Incorrect Materials
  - Shelf Life Issue
  - Improper Storage
  - Contamination During Testing

  - Improper Shipping
  - Inadequate Resolution of Identified Anomaly
- The Debris Due to MAF Processing Training blocks can expand to a 9th digit to capture the following basic events:
  - Inadequately Trained Operator
  - Uncertified Operator
- The Debris Due to MAF Processing Manufacturing Process Plan blocks can expand to a 9th digit to capture the following basic events:
  - Debris Due to Inadequate Manufacturing Process Plan
  - Debris Due to Operator Not Following Manufacturing Process Plan
- The Debris Due to MAF Processing Material Process blocks can expand to a 9th digit to capture the following basic events:
  - Shelf Life Issue
  - Improper Storage
  - Contamination During Processing
  - Improper Surface Preparation
  - Improper Application Process
  - Inadequately Defined Acceptance Testing
  - Inadequately Performed Acceptance Testing
  - Inadequate Resolution of Identified Anomaly

7.2.1.6 Evaluation Criteria

A DCMA and/or NASA representative and a Lockheed Martin representative reviewed design, processing, acceptance, and build paper for each material system of each TPS configuration identified in the Critical Debris Zone.

The four possible dispositions for each event in the FT were used to categorize observations.

7.2.1.7 Approach

As a ground rule, all blocks were classified as a possible cause or contributor, until sufficient data were provided to reclassify them. The data included interviews, vendor and build paper review, testing, ascent photography, performance data, analysis, and engineering judgment.

The review scope for TPS is shown in Table 7.2.1.7-1. The Team reviewed each process step to verify compliance with the engineering requirements, *e.g.,* mix constituents, application time, certified operator, and acceptance test results, etc. Discrepancies were documented as issues or were resolved as either incorrectly entered data or that the anomaly was not a critical step and could not have been a cause or contributor to TPS debris.

Table 7.2.1.7-1. TPS Team Review Scope

Scope Item
Materials Specifications (STM) (26 ea)
Process Specifications (STPs) (22 ea)
Manufacturing Process Plans (159 ea)
Vendor data packages for the LO2 tank, LH2 tank, intertank structure
Vendor TPS materials data
TPS drawings (49)
NCDs (69) and IPRAs
Receiving acceptance data packages
Lab results
Interviews with practitioners associated with critical processes
Bipod TPS fabrication
Intertank to LH2 and LO2 tank interface closeout fabrications
Trend data for ET 93 TPS as compared to the 25 previous tanks were developed and compared

7.2.1.8 Results

Specific findings will be discussed in the categories of major TPS materials systems, consistent with the structure of this FT branch.

7.2.1.8.1 NCFI Fault Tree Blocks Summary (Fault Tree Branch 1.1.1.1)

7.2.1.8.1.1 Background

The primary foam material used on the ET is NCFI 24-124 spray-on foam insulation (Figure 7.2.1.8.1.1-1). It is a blown, closed cell rigid foam system with higher temperature stability than conventional urethane foams. (The NCFI 24-57 material is similar to NCFI 24-124 and provides improved temperature stability for the aft dome engine plume heat environment.) Locations are shown in Figure 7.2.1.8.1.1-1.

Table 7.2.1.8.1.1-1 provides a brief history of the evolution of the acreage spray foam.

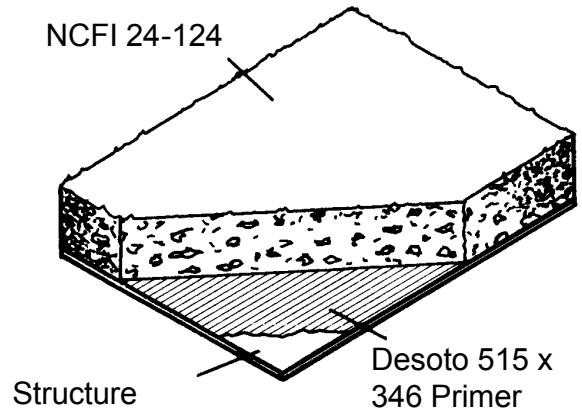

Figure 7.2.1.8.1.1-1. NCFI Material Application

Table 7.2.1.8.1.1-1. Spray Foam Acreage Development History

•	**1974**	**CPR 421 Selected for ET application**
•	**1975**	**Hooker Chemical (now Oxychem) polyol special arrangement for ET usage**
•	**1975**	**Toxicity issue identified with use of CPR 421 (Polyol with Flame Retardant)**
•	**1976**	**CPR 488 qualified to replace CPR 421 (Flame Retardant removed)**
•	**1982**	**NCFI 22-65 replaces CPR-488/SLA on LH2 Aft Dome**
•	**1984**	**UpJohn changes Isocyanate formulation used in CPR 488 (Iso 0414D)**
•	**1985**	**Dow acquisition of UpJohn and production location changed from Torrance to LaPorte**
•	**1986**	**1st production at LaPorte, Qualification of facility required**
•	**1988**	**UpJohn Isocyanate change #2 (PAPI Lite)**
•	**1993**	**CFC 11 blowing agent manufacture discontinued (accelerated EPA date of 1995)**
•	**1994**	**Oxychem phases out production of Polyol used in CPR 488, supplier refuses to continue making polyol due to expensive plant upgrades (CPR 488 lost)**
•	**1995**	**Qualified NCFI 24-124 to replace CPR 488, NCFI 24-57 to replace NCFI 22-65**
•	**1995**	**FR 1138 Flame Retardant discontinued used in both NCFI 24-124 and NCFI 24-57**
•	**1997**	**IFA issue identified with use of NCFI 24-124 on Intertank**
•	**1998**	**Bayer upgrades Texas plant to manufacture isocyanate vs. Spanish Iso used in NCFI foams**

Receiving and acceptance tests that are performed at MAF and at the vendor's are shown in Table 7.2.1.8.1.1-2.

Table 7.2.1.8.1.1-2. Acceptance Tests

Receiving Acceptance Required Test	Vendor Required Test
* Cream Time	Cream Time
* Rise Time	Rise Time
* Tack-Free Time	Tack-Free Time
* Density, Sprayed foam	Density, Free Foam
* Compressive Strength	HCFC 141b Content (percentage) added to material formulation
* Tensile Strength	
* Viscosity (Components A and B)	
* Specific Gravity (Components A and B)	
* Amine Equivalent (Component A)	
* Water Content (Component B)	
* Hydroxyl Number (Component B)	
* Acid Number (Component B)	
* HCFC 141b Content (Components A and B)	
Workmanship (Components A and B)	
Finger Printing (Component B)	
* Test performed on Shelf -life lots	

The internal cell structure of the NCFI material is a closed-cell foam, as shown in Figure 7.2.1.8.1.1-2.

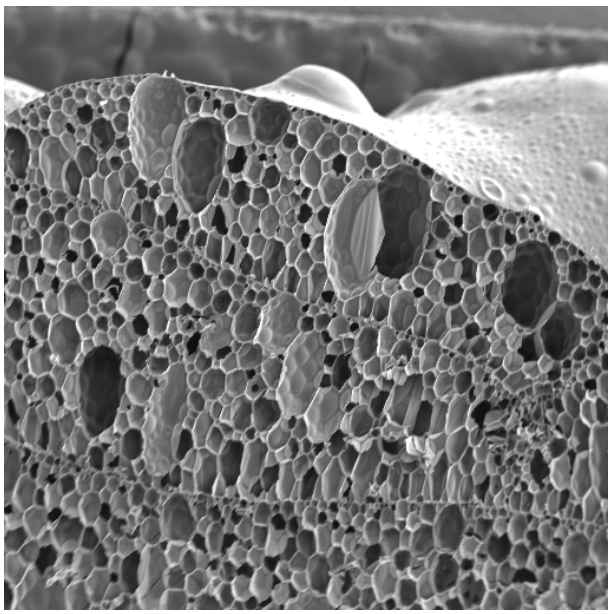

Figure 7.2.1.8.1.1-2. NCFI Scanning Electron Microscopy Photomicrograph (30X)

The foam acreage materials are low viscosity, two-component liquid systems, which are applied to the acreage structure by automated spray equipment. The

application is controlled to provide an "as-sprayed" finish within the required ET thickness, roughness, and waviness constraints without machining. During the SLWT design process, however, a decision was made, which is being revisited as the acreage foam transitions to NCFI 27-68, to machine the intertank TPS surface in acreage regions outside of the LO2 and LH2 ice/frost regions for weight savings. Figure 7.2.1.8.1.1-3 shows a section through the intertank thrust panel foam.

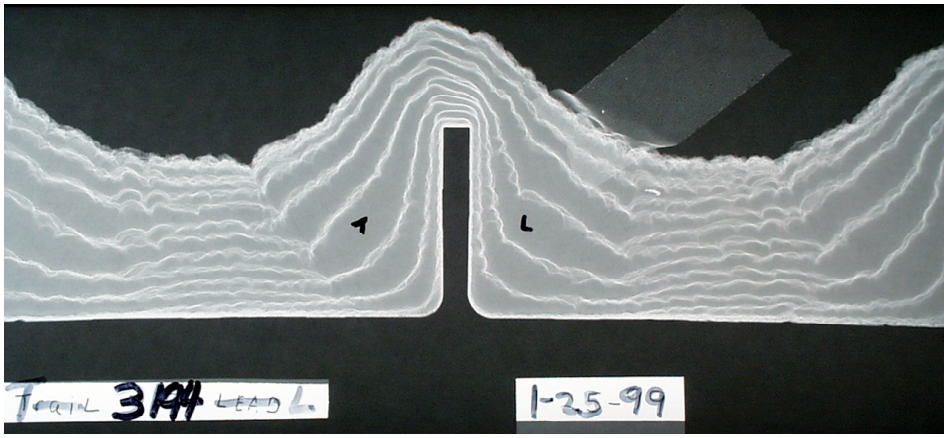

Figure 7.2.1.8.1.1-3. Foam Structure

7.2.1.8.1.2 Analysis Methodology

7.2.1.8.1.2.1 Stress

The stress analysis performed for the NCFI 24-124 TPS applied to the acreage External Tank membrane (LMMSS Drawings 80971118408-529 LO2 Tank Foam Application, LMMSS 80971118413-509 Intertank Foam Application, and 80974018411-510 LH2 Tank Foam Application) utilized classical stress analysis methods that take into account the substrate strain, substrate bending/flexure, cell burst pressure, local acceleration forces, aerodynamic loads, and thermal effects as individual environments. The primary failure modes for TPS include bond line delamination, bond adhesion, and outer fiber cracking. Detailed discussion of analysis methodology, inputs, and results are contained in section E of the SLWT External Tank Stress Report EAS No. 3521-826-2188, Rev AA-S.

As summarized above, the classical analytical methods used to analyze TPS consist of calculating stresses/strains using established equations/relations. These equations/relations are used to correlate test data to flight data, based on the most critical environments and failure modes. Since the flight and the test demonstrated stresses/strains are calculated using the same methodology, the TPS Factor of Safety adequately represents the relationship between the test data and flight data.

Based upon the above rationale, the analysis for individual environments was correctly validated and adequately represented the relationship between flight and test. Methodology, analyses, and conclusions were reviewed for the acreage foam. Outer fiber cracking and bond line delaminaton failure modes were assessed against stresses and material strengths.

For the failure mode of bond adhesion, stresses are critical at the end of ascent, when the TPS experiences maximum acceleration and thermal environments. To ensure a more robust design for NCFI 24-124 acreage TPS, the minimum bond tension allowable (35 psi per process specification LMMSS Drawing STP-1535) exceeds the bond adhesion requirement, which is provided in the cell pressure section.

The acreage TPS material specification, geometry, and thickness LWT TPS and substrate configurations are similar to SLWT; however, LWT substrate thickness is more robust and results in reduced substrate strain levels.

7.2.1.8.1.2.2 Thermal Gradient

The stress analysis uses the critical thermal gradient experienced during pre-launch, which is –297 °F (LO2)/-423 °F (LH2) at substrate and ambient at the outer surface. Thermal gradient produces a moment or “peel” stress at the ET TPS/substrate bond line. Subsequent aerodynamic and substrate warming during ascent relieves the thermal moment at the TPS to substrate bond line.

Substrate temperature effects are considered for bond line integrity. Aerodynamic heating and back face heating contribute to bond line temperatures, which increase the TPS cell pressures. The critical bond line temperatures are provided in the External Tank TDB 80900200102, Rev G. Upon assessment of the data, the design temperature requirements are adequate and correct.

7.2.1.8.1.3.3 Acceleration Forces

Stress analysis uses “G” loads as provided in the Super Lightweight and Lightweight External Tanks LDB 80900200101, Table 12.30.2-1 for the bond adhesion requirement. Table 12.30.2-1 is provided as Table 7.2.1.8.1.2.3-1.

Table 7.2.1.8.1.2.3-1. Acceleration Forces (Table 12.30.2-1)

Zone	Location	Station (Xt)	LWT (G's) (1)	SLWT (G's) (3)
1	Nose Cap	322 to 371	550	550
	(2) Nose Cone/Ogive I/F	371	157	157
2	Fwd Ogive	371 to 536	425	425
3	Aft Ogive	536 to 744	150	150
	LOX Barrel	744 to 852	150	150
4	Intertank - Includes LOX Dome LH2 Fwd Dome	852 to 1130	275	275
5	LH2 Fwd Cylinder	1130 to 1624	250	325
6	LH2 Aft Cylinder	1624 to 2058	225	230
7	Aft LH2 Bulkhead	2058 to cap	350	350

Based upon the above information, the design acceleration requirement was adequate and correct.

7.2.1.8.1.2.4. Cell Pressure

The TPS cell pressure is the primary driver for the limit bond adhesion requirement for acreage TPS. The bond adhesion requirement is derived from an adjusted cell pressure for a maximum substrate temperature of 300 °F under pure vacuum. The maximum temperature and pure vacuum inputs account for 21.1 psi of the requirement, whereas the dynamic load and mass inputs account for 2.5 psi. The maximum bond adhesion design requirement for LO2 acreage NCFI 24-124 TPS is 23.6. At 80 sec, the temperature is conservatively assumed to be 70 °F, which results in a 17.2-psi bond adhesion requirement. To ensure a more robust TPS bond, the minimum allowable bond adhesion requirement for NCFI 24-124 is 35 psi in accordance with STP-1535.

Based on the above information, the cell pressure and derived bond adhesion requirements are adequate and correct.

7.2.1.8.1.2.5. Substrate Strain

The TPS critical case for substrate strain (in plane) is driven by the lift-off flight regime in the LO2 tank barrel. As mentioned previously, the delamination failure mode is critical at pre-launch in the presence of the maximum thermal gradient and internal ullage pressure. The lift-off regime introduces an additional environment as the Shuttle system accelerates and produces mechanical strain on the substrate, in addition to the ullage pressure and cryogenic effects. The ET NASTRAN model is used to derive the design (in plane) substrate strain requirement. The ET NASTRAN model is the latest version of the model previously verified by correlation to STA (MMC-ET-TM03-0, Vol. I and III). The NASTRAN model loads are formatted and read into a FORTRAN program, which

computes margins of safety for multiple load case assessments. The maximum design (in plane) substrate strain requirement for all flight regimes is 0.0036 in./in. for the LWT LO2 tank barrel and 0.0048 in./in. for SLWT LO2 barrel. LWT is a more robust design and is enveloped by SLWT LO2 tank barrel strain.

Based upon the above information, the design (in-plane) substrate strain actual and derived requirements are adequate and correct.

7.2.1.8.1.2.6. Substrate Bending/Flexure

Substrate bending of the acreage TPS is caused by the combined effects of internal pressure and cryogenic shrinkage of the LO2 tank. The relative stiffness of the ring frame to the surrounding tank membrane creates a transition in radial deflection. Additionally, the LO2 Protuberance Air Load (PAL) ramp flanks the outboard side of the cable tray system at 31° 31' from the +Z and spans across the LO2-to-intertank flange. The LO2 PAL ramp is 7 in. in height, is sprayed over existing NCFI 24-124, and acts as additional insulation for the NCFI; therefore, more of the underlying NCFI is cryogenic through the thickness, which results in increased thermal moments on the NCFI. The ramp also induces mechanical moment on the underlying NCFI because of the significant height of the ramp relative to acreage NCFI. The LO2 PAL ramp test verifies the NCFI 24-124 configuration as well as the BX-250 ramp configuration for substrate bending and thermal effects.

BOSOR analysis is utilized to determine radii of curvature as a function of tank station for acreage TPS and PAL ramp requirements. The I/T-to-LO2-tank splice joint is divided into regions. This methodology was verified by correlation to the "Intertank Formed Skin/Stringer Panel Compression Test" for the SLWT program. The BOSOR analysis has also been correlated to the LH2 STA and ISTA verification tests (MMC-ET-TM03-0, Vol. I and III).

Based on the BOSOR analysis results, the LO2 acreage TPS radius of curvature requirement is 200 in. and 160 in. for limit and ultimate design loads, respectively. The most critical requirement on the LWT LO2 tank occurs on the barrel membrane where the substrate strain is 0.0036 in./in. Radius cryoflex testing combines substrate strain with maximum cryogenic thermal gradient.

Based upon the above information, the design substrate bending actual requirements and derived requirements are adequate and correct. Critical analysis results are summarized in Table 7.2.1.8.1.2.6-1.

Table 7.2.1.8.1.2.6-1. Summary of Acreage Stress Analysis Parameters

Primary Failure Modes			Delamination			O/F Cracking		Bond Adhesion				Factor of Safety is based on: (1)	Minimum Test Demonstrated / Analytical Factor of Safety	Test Report Reference, Stress Report Reference, or Test Data
Analysis Inputs		TPS t	Gradient ΔT	Shrinkage αΔT	Modulus E	Strain ε	Substrate Bending	O/F ε	Substrate Temp.	Press. ΔP	Vac.	Accel. "G"s			
Derived Requirements		(Thick/Thin) (in.)	Total Moment (in.-lbs.)			Strain (in./in.)	Radius (in.)	Strain (in./in.)	Cell Pressure (psi)						
LO2 Fwd Ogive	Flight Requirement	3.50	49.0			<0.0036	Infinite	N/A	23.6 (17.2 @ 80 secs)						826-2188
	Wide Panel Test	3.50	54.8		(3)	N/A	Infinite						Mom	1.12	826-3000-07
	Radius Cryoflex Test	3.50	100.2			0.0054	500						Sub ε	1.50	TPS-0466-96
	Bond Tension Test								30.0				ΔP	1.27	STP-1535
LO2 Aft Ogive	Flight Requirement	2.40/1.05	29.2 / 5.9			0.0036	>200	0.0125	19.2 (15.2 @ 80 secs)						826-2188
	C/E "1a"	1.80	(3) N/A			0.0064	Infinite						Sub ε	1.77	826-3000-10
	Wide Panel Test	3.50	54.8		(3)	N/A	Infinite						Mom	1.88	826-3000-07
	Radius Cryoflex Test	1.82	40.8			0.0066	100						Mom	1.40	TPS-2112-96
	Flexstrain Test	1.87						0.0240					O/F ε	1.92	TPS-0001-98
	Bond Tension Test								30.0				ΔP	1.56	STP-1535
LO2 Barrel	Flight Requirement	1.15/1.05	7.6 / 5.9			0.0036	200	0.0067	15.9						826-2188
	C/E "1a"	1.80	23.6			0.0064	Infinite						Sub ε	1.77	826-3000-10
	Radius Cryoflex Test	1.90	40.8			0.0066	100						Sub ε	1.84	TPS-2112-96
	Radius Cryoflex Test	1.32	26.1			0.0066	50						Sub ε	1.84	TPS-2112-96
	Flexstrain Test	1.87						0.0240					O/F ε	3.57	TPS-0001-98
	Bond Tension Test								30.0				ΔP	1.89	STP-1535
Intertank	Flight Requirement	1.80	12.0			0.0022	1976	0.0010	19.7 (15.4 (@ 80 secs)						826-2188
	C/E "1a"	1.80	23.6			0.0064	Infinite						Mom	1.97	826-3000-10
	Flexstrain Test	1.87						0.0240					O/F ε (2)	24.96	TPS-0001-98
	Bond Tension Test								30.0				ΔP	1.52	STP-1535
LH2 Tank Barrel	Flight Requirement	1.77/1.01	20.9 / 6.0			0.0033	600	0.0030	16.3 (15.5 (@ 80 secs)						826-2188
	C/E "1a"	1.80	23.6			0.0064	Infinite						Mom	1.13	826-3000-10
	Radius Cryoflex Test	1.90	40.8			0.0066	100						Mom	1.95	TPS-2112-96
	Radius Cryoflex Test	1.32	26.1			0.0066	50						Mom	1.24	TPS-2112-96
	Flexstrain Test	1.87						0.0240					O/F ε	7.99	TPS-0001-98
	Bond Tension Test								30.0				ΔP	1.84	STP-1535
LO2 Splice Joint	Flight Requirement	1.15					200								826-2188
	LO2 PAL Ramp Test	1.25					160						Rad	1.25	MMC-ET-SE05-549
LH2 Splice Joint	Flight Requirement	1.35					600								826-2188
	LH2 PAL Ramp Test	1.25					480						Rad	1.25	MMC-ET-SE05-549

Notes:
(1) **The minimum factor of safety is based on the allowable divided by the flight requirement for the following derived requirement:**
Total Moment = Mom
Substrate Strain = Sub ε
Radius of Curvature = Rad
O/F strain = O/F ε
Cell pressure = ΔP
(2) **The FS is based on longitudinal bending. Hoop bending produces O/F cracking, is covered in 1.1.1.1.2.1.1.1.2, and is acceptable per "8303" picture book (MMC-ET-SE05-404 Appendix A)**
(3) **N/A = Not Applicable. The test was not meant to cover all derived requirements for the TPS for the hardware.**

7.2.1.8.1.2.7 Adequacy of Stress Analysis Methodology

The basic ground rule used for the TPS analysis was to combine the most critical contributors for a given failure mode and to compare the resulting maximum stress, strain, or cell pressure to test data using consistent analytical methods. The primary failure mode for the acreage TPS is bond line delamination. For this failure mode, the analysis does consider the critical environments consisting of thermal gradient, substrate strains (thermal and mechanical), and flexure.

Based on the rationale above, the NCFI 24-124 acreage TPS analysis methodology is adequate for the combination of critical 'design' environments.

7.2.1.8.1.2.8 Findings

The conclusion reached through analysis of the NCFI branch of the FT was that this TPS material, and specifically the acreage ET structures, could not have been a cause or contributor to the TPS Debris associated with STS-107. The design, vendor, MAF, and KSC blocks were all "green".

7.2.1.8.2 PDL-1034 Fault Tree Blocks Summary (Fault Tree Branch 1.1.1.3)

7.2.1.8.2.1 Background

Urethane closed cell rigid foams are used for applications that do not require high temperature materials. As with NCFI, these are two-part liquid systems. BX-250, BX-265, and SS-1171 are materials that have a short work time and are suitable for spray-pour operations with automatic mix equipment. PDL-1034 is a material that has a longer work time (40 sec.) and is suitable for hand pour operations or for filling complex shaped cavities. Both have overall properties similar to NCFI, except that they have limited thermal substrate conditions and have limited ablation capability. The closed-cell foams resist moisture absorption and the elements without significant performance degradation. Basic material properties are shown in Table 7.2.1.4-1, above.

PDL-4034 was the original pour foam selected for the ET. PDL is useful for mold-in-place applications for closeouts, for TPS repairs, and for filling areas that are difficult to which to apply spray foam. The integrity of all ET PDL-4034 pour foam insulation (POFI) applications was questioned upon finding debonds during LO2 feedline flange closeout repair on LWT-27 during May 1986 (CAPS T-055C). A preliminary assessment of all PDL-4034 POFI applications was made by the resulting debris Team, which used flight separation photographs to conclude that the LO2 feedline flange and thrust strut flange closeouts were the only problem applications. A new mold process was developed and during retrofit of ETs, NASA again raised the question of acceptability of all other PDL applications. A Tiger Team was created to perform that assessment.

The Tiger Team was composed of members of Materials Engineering, Design Engineering, Manufacturing Engineering, Quality Engineering, and Advanced Manufacturing Technology (AMT). Their task was to assess the quality of every PDL-4034 closeout in terms of adequacy of process control, process instructions, MPP validation results, and bond adhesion to the appropriate substrates; the objective was to assure that the process was sufficient to meet the void criteria and bond adhesion requirements of the design. Report No. 826-2060-02 details the methodology used to make this assessment, the findings, resulting conclusions, and recommendations. In addition, it will serve as documentation of the validation of all PDL-4034 scheduled closeouts. PDL-1034 was subsequently chosen to replace PDL-4034. The following is a brief chronicle of PDL history:

- Original ET material, PDL 4034, manufactured by PDL
- 1994-Urethane Technologies purchased Polymer Development Laboratories.
- 1995-First lot of UTI PDL-1034 (HCFC 141b) intended for production.
- 1996-Re-certification plan for UTI PDL-1034 created involving NASA and LMMSS
- 1997-Atlanta Facility and PDL-1034 formulation rights awarded to Hess

- 2000-BASF Procures Hess Polyurethane's, Inc.
- 2001-BASF moves production of PDL 1034 to Carrolton, Texas
- 2002-BASF Carrolton Facility conditionally certified pending evaluation of 3 lots.

7.2.1.8.2.1 Receiving Inspection / Shelf Life Storage

Upon receiving shipments from the vendor, the following receiving inspection testing is done per STP-1532:

- Viscosity (A&B)
- Specific Gravity (A&B)
- Amine Equivalent (A)
- Tack-Free Time
- Workmanship (A&B)
- Cream Time
- Water Content (B)
- Hydroxyl Number (B)
- Density
- Hydrochlorofluorocarbon (HCFC) Content (B)
- Tensile Strength
- Compressive Strength
- Rise Time
- Thermal Conductivity
- Flammability
- Hydrolytic Stability
- Coefficient of Expansion.

A review of each item was performed. Results were documented in FT block closures. Table 7.2.1.8.2.1-1 provides a matrix of the specimens tested in the qualification of PDL-1034. Table 7.2.1.8.2.1-2 summarizes the PDL-1034 analysis inputs, derived requirements, and verification results.

Table 7.2.1.8.2.1-1. PDL-1034 Qualification Specimens

Test Description:	-423°F	-320°F	RT	+200°F	Total
Bond Tension	60	60	60	60	240
Flatwise Tension	24	29	49	24	126
Density/Compression			4		4
Plug Pull			17		17
Cryoflex @ 1.5"	4	48			52
Monostrain	12		12	20	44
Torsion Shear	6		6	6	18
Poisson's Ratio	6		6	6	18
Wide Panels	1 repair				1 repair
Combined Environments	1 repair				1 repair
Hot Gas	25				25
Wind Tunnel	9				9

Table 7.2.1.8.2.1-2. PDL-1034 Analysis Inputs, Derived Requirements, and Verification

Primary Failure Modes		All	Delamination	Bond Adhesion			Factor of	Minimum Test	Test Report
Analysis Inputs		TPS t	Strain e	Substrate Temperature	Pressure ΔP	Vacuum Acceleration "G"s	Safety is	Demonstrated Factor	Number / LMMSS
Derived Requirements			Strain	min/max	psi	psi	based on:	of Safety	Dwg. Number
		in.	in./in.				1		
Bipod Fitting	Flight Requirement	0.50	0.0043		19.1				826-2188
Spindle INC718	Monostrain Test	0.38	0.0069				Sub ε	1.60	826-2188
	Bond Tension Test	2.00					ΔP	1.42	826-2188
LH2 & LO2	Flight Requirement	2.50	0.0006		23.1				826-2188
Intertank Flanges	Monostrain Test	0.38	0.0069				Sub ε	11.50	826-2188
Closeout	Radius Cryoflex Test	2.00	0.00542				Sub ε	9.03	TPS-3038-95
	Bond Tension Test	2.00			27.2		ΔP	1.18	826-2188
Bipod Fitting	Flight Requirement	0.54	0.00135		18.7				826-2188
Base Plate	C/E "1a"	1.80	0.0059				Sub ε	4.37	826-3000-10
	Monostrain Test	0.38	0.0069				Sub ε	5.11	826-2188
	Bond Tension Test	2.00			27.2		ΔP	1.45	826-2188
LO2 Tank /	Flight Requirement	7.00			23.2				826-2188
I/T Pal Ramp	Bond Tension Test	2.00			27.2		ΔP	1.17	826-2188
Closeout									
LO2 Ogive &	Flight Requirement	1.90	0.0048		19.7				826-2188
Barrel	C/E "1a"	1.80	0.00587				Sub ε	1.22	826-3000-10
Closeout	Monostrain Test	0.38	0.0069				Sub ε	1.44	826-2188
	Bond Tension Test	2.00			27.2		ΔP	1.38	826-2188
	Radius Cryoflex Test	1.54	0.0075				Sub ε	1.56	TPS-3260-95
P/L & C/T	Flight Requirement	0.50	0.00496		18.7				826-2188
Support Bracket	Monostrain Test	0.38	0.0069				Sub ε	1.39	826-2188
	Bond Tension Test	2.00			27.2		ΔP	1.45	826-2188
Ice Frost Ramps	Flight Requirement	5.50			30.97				826-2188
	Bond Tension Test	2.00			35		ΔP	1.13	STP 1532

Notes:

1 **The minimum factor of safety is based on the following derived requirement:**
Substrate Strain = Sub ε
Cell pressure = ΔP
Shear stress= τ

7.2.1.8.2.2 Findings

The current TPS material testing, analysis methodology, and verification adequately addresses the combination of critical design environments for PDL–1034.

7.2.1.8.3 BX-250 Fault Tree Blocks Summary (Fault Tree Branch 1.1.1.4)

7.2.1.8.3.1 Background

BX-250 was the primary SOFI material identified for the ET during the proposal activities. It was essentially supplied by MSFC as a flight-verified material, with proven processing capability from the Saturn program. Early in the ET program, some testing was conducted to expand the database supplied by MSFC for ablation/erosion characteristics in aero-thermal ascent environments, so that analysis techniques could be developed to predict thickness requirements in the relatively severe (compared to Saturn) Shuttle environments. Tests revealed that BX-250 was not appropriate for the majority of the acreage areas of the ET, and alternate, more erosion resistant materials were identified and developed (CPR-421, CPR-488, and NCFI 24-124).

During the development/verification activities for the CPR material, BX-250 was included on most major test articles for closeouts and repairs. These test articles included the mini-tank test series (LH2), a heated 10-ft diameter tank (LH2), and the combined environments panel test series (liquid helium). In most cases, these test configurations for the BX-250 closeouts were not designed to simulate the ET configurations but were representative of the BX-250 applications on the ET. In addition, a wind tunnel test series was conducted in Arnold Engineering Development Center (AEDC) Tunnel A at maximum dynamic pressure to verify that the PDL in the ramp configuration used around cable trays and pressurization line attachments and BX in a ramp configuration representative of the aft SRB cable tray (and by similarity to the bipod ramp) could withstand the aero-loading environments. Combined environments test panels included a panel that represented the BX over SLA closeout on the LH2 tank aft dome apex. Additionally, a combined environments facility calibration panel completely coated with BX was tested to assess the stress distributions on the panels at cryogenic temperatures and loads above yield. Another test developed and implemented for verification of BX applications was the PAL ramp test. This test employs a “plank” coated with the acreage SOFI material (CPR or NCFI) with a full-scale section of a PAL ramp applied (LO2, LH2, and SRB cable tray). The test article is chilled to the appropriate temperature and then “bent” to the appropriate radius in a test fixture to simulate the vehicle design cases.

7.2.1.8.3.2 Receiving Inspection

Upon receiving shipments from the vendor, the following receiving inspection testing is performed per STP-1536:

- Viscosity (A&B)
- Specific Gravity (A&B)
- Amine Equivalent (A)

- Water Content (B)
- Hydroxyl Number (B)
- Acid Number (B)
- Density (Free Foam)
- HCFC Content (B)
- Tensile Strength
- Density (Sprayed Foam) Compressive Strength
- Tack-Free Time
- Workmanship (A&B)
- Cream Time
- Rise Time
- Thermal Conductivity
- Flammability
- Hydrolytic Stability.

7.2.1.8.3.3 Acceptance Testing

Each BX-250 spray application must meet acceptance criteria per STP-1536, which provides processing parameters for BX-250, density criteria, and a minimum room temperature acceptance value of 35 psi for tensile strength. For each application, plug pulls, core holes where applicable, and densities are evaluated against the acceptance criteria. These physical and mechanical properties link the spray application for each tank back to the material property database.

Table 7.2.1.8.3.3-1 summarizes the BX-250 analysis inputs, derived requirements and verification results. The detailed review of the bipod area is included in Volume III.

Table 7.2.1.8.3.3-1. BX-250 Analysis Inputs, Derived Requirements, and Verification

LMMSS Drawing Number (* = 809)	W.B.S Fault Tree Block	Primary Failure Modes / Analysis Inputs / Derived Requirements		TPS t (in.)	Delamination: Gradient ΔT; Shrinkage αΔT; Modulus E; Strain ε; Total Moment (in.-lbs.); Strain (in./in.)	O/F Cracking: Substrate Bending; Radius (in.)	Shear: Airload σ; Stress (psi)	Bond Adhesion: Substrate Temp.; Press. ΔP; Vac.; Accel. "G"s; Cell Pressure (psi)	Factor of Safety is based on: [2]	Minimum Test Demonstrated / Analytical Factor of Safety	Test Report Reference, Stress Report Reference, or Test Data
*71008434-090	1.1.1.4.1	Bipod Ramp [1]	Flight Requirement	11.70	461.6	Negligible	13.2	< 23.1 (21.3 @ 80 seconds)	Mom	2.75	826-2188
		LO2 PAL Ramp	LO2 PAL Ramp Test	8.25	1269.0	160			τ	1.32	MMC-ET-SE05-549
			Shear Test				17.5				826-2188
			Bond Tension Test					35	ΔP	1.52	826-2188
*71008422-509	1.1.1.4.6	LO2 PAL Ramp	Flight Requirement	8.25		200	7.2	< 23.1 (21.3 @ 80 seconds)	Rad	1.25	826-2188
			LO2 PAL Ramp Test	8.25		160			τ	2.43	MMC-ET-SE05-549
			Shear Test				17.5				826-2188
			Bond Tension Test					35	ΔP	1.52	826-2188
*71118414-509	1.1.1.4.3	LO2 Flange C/O	Flight Requirement	4.00	37.5	<0.0006	Negligible	< 23.1 (21.3 @ 80 seconds)			826-2188
			Cryoflex Test	2.70	202.5	0.0074	50		Mom	5.40	TPS-0260-97
			Bond Tension Test					35	ΔP	1.52	826-2188
*71018424-519	1.1.1.4.2	LH2 Flange C/O	Flight Requirement	3.25	39.7	0.0006	Negligible	< 23.1 (21.3 @ 80 seconds)			826-2188
			Cryoflex Test	2.70	202.5	0.0074	50		Mom	5.10	TPS-0260-97
			Bond Tension Test					35	ΔP	1.52	826-2188
*71008428-019	1.1.1.4.5	LO2 Feedline Supports	Flight Requirement	1.25		0.0048		< 23.1 (21.3 @ 80 seconds)			826-2188
			Widepanel "2"	2.10		0.0064			Sub ε	1.33	826-3000-07
			Bond Tension Test					35	ΔP	1.52	826-2188
*73018416-509	1.1.1.4.4	I/T TPS Wedges	Flight Requirement	1.88		0.0022		< 23.1 (21.3 @ 80 seconds)			826-2188
			Widepanel "2"	2.10		0.0064			Sub ε	2.90	826-3000-07
			Bond Tension Test					35	ΔP	1.52	826-2188

Notes: [1] Addressed in detail in Appendix 1

[2] The minimum factor of safety is based on the allowable divided by the flight requirement for the following derived requirement:
Total Moment = Mom
Substrate Strain = Sub ε
Radius of Curvature = Rad
O/F strain = O/F ε
Cell pressure = ΔP
Shear stress= t

7.2.1.8.4 SLA-561 Fault Tree Blocks Summary (Fault Tree Branch 1.1.1.5)

7.2.1.8.4.1 Background

The primary ablator material is molded or sprayed SLA-561 (Figure 7.2.1.8.4.1–1). It is a composite mixture of silicone resins highly filled with cork particles, silica glass eccospheres, silica fibers, and phenolic microballoons that, after fabrication, is bonded onto the prepared structure. Ambient and heat cures, during fabrication, are required to achieve strength. Similar formulations are used to accomplish sprayed parts and to accomplish "hand pack" ambient cure applications. The materials are compatible with cryogenic stressed structure (within design constraints).

The SLA strength requirements were established during ablator qualification on ET-1. The strength and density requirements are documented in STPs 1506, 1508, 1509, 1510 and 1522, which control SLA processing. All SLA raw materials must meet receiving inspection material property test requirements to ensure that SLA finished product strength and density are achieved. Each and every completed SLA batch is tested to verify strength and density via testing on the production part and/or its associated process witness panel.

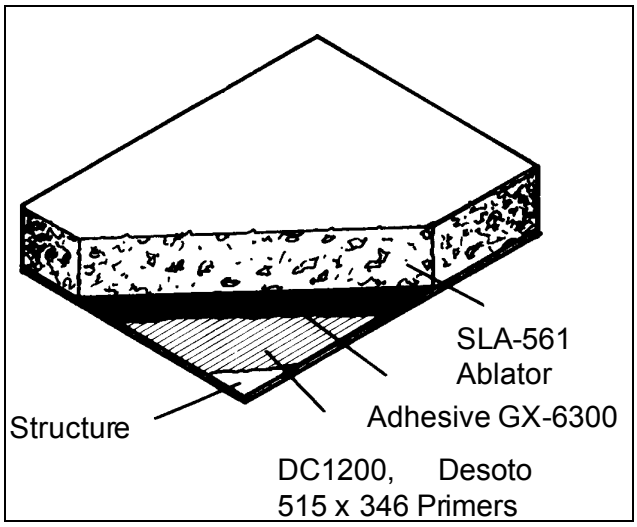

Figure 7.2.1.8.4.1–1. SLA-561

The rest of the SLA material properties, which were established during ablator qualification and/or requalification for the resin change in 1995, are linked to SLA finished product requirements via the SLA qualification material properties database. All SLA is formulated per the process established during the qualification of SLA. This SLA application process, which was established during the qualification programs, is documented in each STP for lot-to-lot and acceptance testing. This process indirectly verifies the established properties. The process is documented in STP specifications, which controls all SLA processing parameters. The requirements that must be met on each production part and/or its associated process witness panel are summarized below for receiving inspection and ablator testing to verify required homogeneity, tensile strength, and density. [Note: (A) refers to the SLA base mix and (B) refers to the curing agent.]

- Receiving Inspection and Shelf Life Requirements
- Processed Ablator Testing (3 lots of material)
- Color (A & B)
- Bond Tension
- Tensile Strength
- Flatwise Tension
- Elongation
- Monostrain
- Viscosity (A)
- Cryoflex
- Index of Refraction
- Cryogenic Lap Shear
- Gel Time or Mixed

- Torsion Shear
- Viscosity
- Plug Pull
- Haze (A & B)
- Density
- Specific Gravity
- Specific Heat
- Density
- Pot Life
- Shelf Life
- Minimum Cure Temp
- Minimum Cure Time
- Flammability
- SOFI Adhesion
- Poisson's Ratio
- Thermogravimetric Analysis (TGA) and Differential Thermal Analysis (DTA).

7.2.1.8.4.2 Analysis

The TPS critical cases for substrate strain (in plane) for the subsequent parts are listed in Table 7.2.1.8.4.2-1.

The maximum strain exhibited by this group of parts is 0.00496 at 120 °F on the LO2 P/L and C/T brackets. Substrate bending/flexure is minimal and its effects are included in the substrate strain requirement. As previously stated, direct aerodynamic loads are analyzed and considered negligible. Air loads, however, can act in normal and tangential directions, and they are incorporated into the component hardware derived substrate strain requirement.

TDFSs for the most critical SLA-561 parts met the EIS Factor of Safety and are provided in Table 7.2.1.8.4.2-2. The LO2 Pressline/Cable Tray Support experiences the highest substrate strain of all SLA-561 parts.

Table 7.2.1.8.4.2-1. Critical Analysis Cases

Part	Stress Report Section	TPS Thickness	Temperature @max load	Flight Strain
Bipod Fitting	C.4.2.6	0.35	-272	0.0015
Connector Plate	C.4.2.6	0.35	-272	0.0015
Bipod Strut	E.2.5.6	0.52	100	0.0036
GO2 P/L Barry Mounts on LO2 Tank	D.7.15 / E.2.5.7.2	0.64	35	0.00231
CO-cell M, LO2 P/L Brackets Sta 464.34	D.7.1 / E.2.5.7.2	0.34	120	0.00496
LO2 Cable Tray Segment	D.2.1 / E.2.5.7.2	0.6	130	0.00371
LO2 Tank P/L & C/T Support, Sta 371	D.7.1 / E.2.5.7.2	0.5	120	0.00496
Cover Cable Tray	D.2.1 / E.2.5.7.2	0.35	130	0.00367
LO2 Tank C/T Covers & LO2 C/T Tray Fairing	D.2.1 / D.8.2 / E.2.5.7.2	0.63	130	0.00367
Gap Closures - LO2 Tank C/T	D.2.1 / E.2.5.7.2	0.63	130	0.00371
LO2 Tank P/L & C/T Support Bracket	D.7.1 / E.2.5.7.2	0.5	120	0.00496
Composite Nose Cone Foam Seal & Blend	D.8.1	2	100	0.00201
GO2 & GH2 P/L Barry Mount Slide Cap	D.7.15 / E.2.5.7.2	0.57	35	0.00231
Fairing - LH2 C/T Fairing - LO2 Feedline	D.8.5 / E.2.5.7.2	0.62	120	0.00396
Fairing - LO2 Tank Cable Tray	D.8.2 / E.2.5.7.2	0.6	120	0.00396
Yoke LO2 Feedline	C.4.2.6.7	0.4	100	0.00228

Table 7.2.1.8.4.2-2. SLA-561 Analysis Inputs, Derived Requirements, and Verification

Primary Failure Modes		All	Delamination				Bond Adhesion			Factor of Safety is based on:	Minimum Test Demonstrated Factor of Safety	Test Report Number / LMMSS Dwg. Number
Analysis Inputs		TPS t	Gradient ΔT	Shrinkage αΔT	Modulus E	Strain ε	Substrate Temperature	Pressure ΔP	Vacuum	Acceleration "G"s		
Derived Requirements		in.	Total Moment in lbs			Strain in./in.	min/max	psi		psi	2	
Bipod Fitting & Connector Plate 1	Flight Requirement	0.35	3 2742.0			0.0015	-423 / 188		1.95			826-2188
	Monostrain Test	0.38				0.0068	-320				Sub ε	4.54	826-2188
	Cryoflex Test	0.60	89.6			0.0047	-320				Sub ε	3.14	3077-B
	Bond Tension Test	2.00					200		46		ΔP	23.59	826-2188
	Plug Pull Test	0.52					70		15		ΔP	7.69	STP 1522
	C.E."1a"	0.20	48.9			0.0051	-423				Sub ε	3.41	826-2188
Bipod Strut	Flight Requirement	0.52				0.00357	70 / 380		2.78				826-2188
	Monostrain Test	0.38				0.0264	70				Sub ε	7.39	826-2188
	Cryoflex Test	0.60				0.0047	-320				Sub ε	1.32	3077-B
	Bond Tension Test	2.00					300		34		ΔP	12.23	826-2188
	Plug Pull Test	0.52					70		15		ΔP	5.40	STP 1509
LO2 Pressline & Cable Tray Support	Flight Requirement	0.50				0.0050	120		1.95				826-2188
	Monostrain Test	0.38				0.0264	70				Sub ε	5.32	826-2188
	Bond Tension Test	2.00					200		46		ΔP	23.59	826-2188
	Plug Pull Test	0.52					70		15		ΔP	7.69	STP 1506
GO2 Pressline Barry Mounts	Flight Requirement	0.50	3 25.3			0.0023	35		1.95				826-2188
	Monostrain Test	0.38				0.0264	70				Sub ε	11.43	826-2188
	Bond Tension Test	2.00					200		46		ΔP	23.59	826-2188
	Cryoflex Test	0.60	89.6			0.0047	-320				Sub ε	2.03	3077-B
	Plug Pull Test	0.52					70		15		ΔP	7.69	STP 1506

Notes:

1 **Addressed in detail in Appendix 1**

2 **The minimum factor of safety is based on the following derived requirement:**
Total Moment = Mom
Substrate Strain = Sub e
Radius of Curvature = Rad
O/F strain = O/F e
Cell pressure = DP
Shear stress= t

3 **Not Applicable. This is for engineering information only. The bond line delamination analysis methodology is used for acreage TPS applications. The handpack SLA 561 application on the bipod fitting heater wire and barry mounts is assessed for substrate strain and bond adhesion. The bond line delamination failure mode is not applicable for this local application. In addition, this SLA application is serrated and encapsulated in BX-250 foam.**

7.2.1.8.4.3 Findings

SLA-561 TPS testing, analysis, and verification adequately address the combination of critical design environments with exception to the bipod fitting application.

7.2.1.8.5 SS-1171 Fault Tree Blocks Summary (Fault Tree Branch 1.1.1.7)

7.2.1.8.5.1 Background

SS-1171 was initially tested and selected for potential replacement of BX-250. The chemical, physical, and mechanical properties are similar between SS and BX, and the materials are considered interchangeable on the ET. SS-1171/141b Phase III requalification was accelerated in March 1994. This acceleration was related to the fact that BX-250 with 141b in the formulation yielded inconsistent data and could not perform per the engineering requirements. Data obtained in Phase II formulation optimization supported the preliminary conclusion that SS-1171 / 141b was a viable foam replacement for BX-250. Phase III requalification initiated in mid Fiscal Year (FY) 1994 and FY 1995 continued to yield promising data. Five lots of material were sprayed in the TPS Engineering Spray Booth at various room temperatures, substrate temperatures, and percent relative humidity. Results were analyzed, and it was concluded that SS–1171/141b chemical, physical, and mechanical properties are comparable to that of BX–250/CFC-11. In 1995, various flight qualification tests, such as thermal acoustic panels, combined environment panels, plasma arc, wind tunnel test, LO2, LH2, and SRB PAL ramp test, were performed. All flight simulation testing and analysis were acceptable and comparable to BX-250.

7.2.1.8.5.2 Receiving Inspection/Shelf Life Storage

Upon receiving shipments from the vendor, the following receiving inspection testing is performed per STP-1536.

- Viscosity (A&B)
- Specific Gravity (A&B)
- Amine Equivalent (A)
- Water Content (B)
- Hydroxyl Number (B)
- Acid Number (B)
- Density (Free Foam)
- HCFC Content (B)
- Tensile Strength
- Density (Sprayed Foam)
- Compressive Strength
- Tack-Free Time

- Workmanship (A&B)
- Cream Time
- Rise Time
- Thermal Conductivity
- Flammability
- Hydrolytic Stability

7.2.1.8.5.3 Acceptance Testing

Each SS-1171 spray application must meet acceptance criteria per STP-1536 (shown in Table 7.2.1.8.5.3-1), which provides processing parameters for SS-1171, density criteria, and a minimum room temperature acceptance value of 35 psi for tensile strength. For each application, plug pulls, core holes where applicable, and densities are evaluated against the acceptance criteria. These physical and mechanical properties link the spray application for each tank back to the material property database.

Table 7.2.1.8.5.3-1. SS-1171 Qualification Specimens (Ref. MMC-ET-SE05-549)

Test Description:	-423°F	-320°F	RT	+200°F	TOTAL (Each Lot1to2) (All Nominal Spray Conditions)	TOTAL (EachLot 3to5) (All Nominal Spray Conditions)	TOTAL (EachLot 6to7) (All Nominal Spray Conditions)	TOTAL (All Lots) (All Nominal Spray Conditions)
Bond Tension	1000	1000	1000	1000	4,000	1,536	1,920	16,448
Flatwise Tension	1000	1000	1000	1000	4,000	1,056	1,920	15,008
Density/Compression			300		300	264	288	1,968
Plug Pull			124					124
Cryoflex @ 1.5"	150				150	150	150	1,050
Monostrain	64	14	36	32	146	146	146	1,022
Torsion Shear								50
Wide Panels	1							1
Combined Environments	2							2
PAL Ramp	3							3
Hot Gas	25							25
Plasma Arc	19							19
Wind Tunnel	36							36

7.2.1.9 Summary of Tests

Tests that were performed in support of this investigation are summarized in Table 7.2.1.9-1. Test reports are included in Volume III.

Table 7.2.1.9-1. Test Summary

		Test Objectives	Conclusions
Tile Damage Test Support (including BX 250 Impact Characterization)		Provide ongoing ET interface and credible ET debris size inputs to Orbiter tile impact testing. Determine crush characteristics of BX 250 under cryo and vacuum.	Preferred BX 250 Failure Mode is internal cell crushing over spalling or divoting. Vacuum does not change impact failure modes. Colder specimens fail in more brittle manner.
Bipod Thermal/ Vacuum/ Cryogenic Test	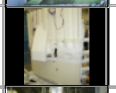	Simulated bipod configuration with cryogenic backface, simulated ascent skin temperatures, and ascent pressure profile to characterize TPS debris generation.	Simulated environments on nominal configuration hardware produced no effects.
Foam Loss Secondary Effects Assessment		Static and dynamic coupon tests of BX 250/SLA lay-ups in tension and shear	Tests showed BX-250 failures <= -100 deg F. No failures in SLA for dynamic tests.
Bipod Foam Dissection Test	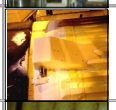	Perform dissection of ET 120 and ET 94 bipod areas to characterize the subsurface configuration of the as-processed hardware.	Substrate complexity produces characteristic roll-over. Analysis of roll-over voids and at weak knitlines indicate potential for foam loss near machined surfaces.
I/T to LH2 Tank Splice Dissection Test		Perform dissection of ET 120 and ET 94 Intertank to LH2 splice to characterize the subsurface configuration of the as-processed hardware.	Substrate complexity produces characteristic roll-over. Analysis of roll-over voids and at weak knitlines indicate potential for foam loss near machined surfaces.
SLA Data Augmentation Test		Augment existing SLA basic materials database to expand knowledge of cryogenic behavior (LN2 absorption, etc.) to support fault tree closure and engineering analysis.	Additional data consistent with historic database and analytical projections
SLA Data Base		Designed experiments of type I and II SLA to characterize effects of mixing, packing, lay-up, moisture and conditioning and interaction with BX 250	SLA processing is sensitive. Multiple complex contributors to cracking exist.
Cryopumping / Cryoingestion Fundamental Data Test		Perform test series for collection of fundamental cryopumping and cryoingestion data to support fault tree closure and engineering analysis	Cryoingestion not accomplishable due to SLA back-pressure. Forced LN2 in SLA produced cracking (not divots) in 100% of tests (consistent with hardware observations).
Thermal/ Mechanical/ Vacuum Bipod Configuration Test		Perform test of simulated bipod configuration to include structural loads, cryogenic conditioning, and ascent skin temperatures	Data will be used to confirm scenario hypothesis and provide data and test bed for return-to-flight.
Thermal/Bending/ Vacuum Bipod & Flange Tests (incl. Simulated Defects)		Perform thermal and mechanical tests of bipod configuration using bending to simulate structural loads. Cryogenic conditioning and ascent temperature profiles.	Data will be used to confirm scenario hypothesis and provide data and test bed for return-to-flight.
Defect/Pressurization Tests	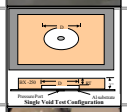	Evaluate BX-250 SOFI sensitivity to the presence of subsurface voids under internal pressure loading and cryogenic environments	Interval void/delamination depth is inversely proportional to likelihood of divot formation.
Moisture Tests		Determine water absorption characteristics of BX 250	Foam does not absorb moisture. Optimized freezing conditions for water may produce a layer of ice 0.004 in thick at exactly 32 deg F at the liquid/solid interface.
Crush Test	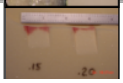	Determine depth of crushed BX 250 below visible damage due to compression loading.	Foam crushes to 30-40% max below visible deformation.

7.2.1.10 Recommendations

Observations have been organized into three general categories: Manufacturing, Design, and Material. Within each category, several issues or concerns have been identified and should be assessed as a follow-on activity to the investigation.

First and foremost of the observations noted was the need for a thorough review of procedures for training and certification. In particular, the manual spray applications appear to be without the formalized attention inherently required for these processes, and they are in need of training requirements that extend beyond normal TPS processing.

1. Special certifications need to be assessed for those manual spray configurations that are in the ET Critical Debris Zone or for which the size/location is such that liberation of TPS debris could lead to a potentially catastrophic event. The configurations for which special certifications need to be closely assessed are, as a minimum, the LO2 and LH2 PAL ramps, the intertank/LH2 tank flange closeout, the intertank/LO2 tank flange closeout, the longerons, and the aft dome apex closeout.
2. Enhancements to training are required, *i.e.,* mock-up sprays and dissections, length of certification before renewal, and on-the-job training. The use of mock-ups and dissections should be assessed for all TPS applications and instituted as appropriate. No sprays on flight hardware should be allowed without acceptable passing results on mock-ups. The logic for length of time that a certification is valid needs to be re-evaluated; for example, a renewal for a plug pull certification occurs on a 1-year basis, while the TPS spray certification is good for 2 years. Certification retention needs to be tied to performing a TPS spray on flight hardware on a regulated time interval and said spray passing inspection. An individual's service in an OJT capacity needs to be monitored and potentially revoked if certification is not achieved within a specified period of time. A mechanism for transferring best practices from production back to the classroom must be initiated. Finally, TPS material or equipment changes must be introduced into the classroom and an assessment must be performed to determine whether the changes are significant enough to necessitate the recertification of affected individuals.
3. The project should assess implementation of a more active system to document training status for those people requiring certification. Notification of lapsed certifications should be more proactive and visible, *i.e.,* Compliance Training, with notification to the employee, employee's supervisor, the Director of ET Production, and the Director of Safety and Quality Assurance. This visibility must exist as a minimum for TPS and, incidentally, welding, and other areas should be assessed for applicability.

Attention must also be focused on MPP steps requiring documentation, stamps, stamp warranty, and acceptance testing. Specific issues with these topics need to be assessed, reviewed, and addressed. The manual spray applications appear to be without the formalized attention inherently required for these processes. The manual applications are certainly more process related and complicated and in need of training requirements that extend beyond normal TPS activities.

1. Engineering should reassess those steps in an STP (PPD) that must be stamped by Engineering and/or Quality as critical steps within a MPP. Such

steps include, but are not limited to, spray overlap times and not initiating the spray on the part.

2. Engineering should also review the STPs and add those steps that need to be recorded within the MPPs, *i.e.,* separate lines for the stamp of the individual(s) actually performing the spray operation and the individual operating the equipment, the identification number of the formulator used for a spray operation, and the ratio of the A and B components before and after the spray.
3. Quality should reassess the proper use of stamps to buy off MPP steps. In particular, the practice must be reassessed by which a supervisor, who has not undergone the same level of training as a subordinate, stamps off the associated work. Stamps represent the acceptance of flight-quality workmanship, and their use must reflect the importance that they carry.
4. Quality should consider the revocation of stamps for those individuals with lapsed certifications or other options that guarantee that only currently certified individuals perform tasks requiring certification.
5. Production and Quality have responded in a very positive manner with respect to contamination control. This topic should be monitored on a continuing basis and significant issues reported to the Program Manager.
6. Engineering should reassess all aspects of acceptance tests. This review should include as a minimum the procedures for curing and testing TPS and witness panels. TPS that is part of the acceptance testing must not only be from the same material lot as the flight article but must be sprayed and cured under the same conditions as the flight article and have configuration characteristics, *i.e.,* thickness, similar to that of the flight part. The rationale and continued applicability of performing early testing, *i.e.,* 24 hr versus 48 hr for SLA, needs to be re-evaluated. Engineering should also continue assessment of NDE systems to locate internal voids and defects based on the recommendations of the TPS Verification Team.
7. The practice of IPRAs should be reviewed. There should be consistency across the production flow with respect to the use of Standard Repair Instructions. Engineering should review those repairs that can be performed as an IPRA, the logic flow that defines if they remain appropriate, and the sequence for transitioning to an NCD. Finally, a mechanism must be established that requires Engineering to participate in the solution for recurring IPRAs.
8. Production should develop a mechanism to enhance the data recorded within the MPPs and adherence to the statements within the MPPs. Several issues were documented, *i.e.,* incorrect times recorded, incorrect material lot codes. Several instances were also identified, particularly for SLA, where one or more constituents were outside the allowance tolerances. There also appeared to be instances where batch sizes not approved by STP were

prepared. Although this might prevent waste for small applications, it is a violation and must be avoided.

TPS design should also be reassessed. Issues identified within the FT with respect to design included inadequate verification. This was related, in large part, to the fact that verification/validation sprays did not identify the potential issues associated with the bipod ramp. These issues included the voids, rollovers, and thermal cracks that could exist and that were identified during the dissections of this area that were part of the Investigation. Another inadequacy that was identified was the insufficient testing to address possible failure mechanisms, such as the defects identified during the dissections. Finally, the fact that the design did not preclude the possibility of cryopumping is another issue.

1. Engineering should reassess the TPS verification. Initial focus should be directed toward those higher risk items, specifically manual spray operations located within the Critical Debris Zone. This task will verify that every failure mode is addressed by sufficient rationale for each TPS configuration.
2. One specific and important deliverable that should be produced by the TPS Verification Team is a matrix of additional testing that is required to preclude the failure modes identified for each TPS configuration. This will include any basic material property, subcomponent, or full-scale verification/validation testing required. Acceptance testing should also be reassessed for potential improvements. Any tasks required to provide “Added Confidence” for existing configurations, such as PAL ramps, should also be recommended. Finally, Engineering should continue assessment of NDE systems to locate internal voids and defects.
3. The intertank/LH2 flange closeout should be assessed for Return to Flight, including a longer term redesign to a ”smooth intertank,” which would encompass the flange closeout and a smooth LO2 tank. The smooth LO2 tank should be the first area of focus.

Finally, attention must also focus on the TPS material. Specific issues should be addressed. The manual spray applications appear to lack the special attention inherently required for these processes. The manual applications are certainly more process related and complicated and, as stated above, are in need of training requirements that extend beyond normal TPS activities.

1. Engineering should reassess several issues. First, there is the definition and criteria for shelf life. Current requirements allow for the vendor to manufacture the TPS products 90 days before shipment. Once received at LM, the vendor guarantees the product for 6 months and typically two extensions of 3 months each are allowed with the completion of designated testing. A reassessment is needed to consider changes, such as the vendor’s simply guaranteeing the products for 9 months from the date of manufacture and eliminating allowance of extensions.

2. Receiving and acceptance testing needs to be reviewed from several perspectives. With respect to the laboratory equipment, the equipment should be calibrated against standards, and the tolerances for each measurement should be documented. An understanding of each component in a given material should be developed, including the upper and lower compositional limits. Material Data Analysis Team (MDAT) review times should be assessed so that trending data can be assessed and actions can be initiated in a timely manner. An assessment should be performed with respect to the leadership of the MDAT; it appears that Material Sciences should guide the task, and the membership should include the cognizant engineers associated with the systems. One objective of this group should be to make the "technicians" aware of the material trends and to gain their participation in the trending analysis.
3. The end users of material property test data, such as recession and thermal conductivity, should have access to the raw data. The Material Sciences group should verify the test setup and the subsequent testing procedures, but the cognizant engineers for the material system and the properties that are being evaluated should have access to the raw data and the data reduction process.
4. Engineering should continue to work closely with the vendors to understand all changes that could potentially alter the performance of TPS materials, with the objective of keeping current the receiving and acceptance testing protocols. Although the date of manufacture is known, blending at the vendor's should be assessed, including the time of manufacture for the base constituents. Since the TPS materials are not a large part of any vendor's business base, NASA must explore all avenues that could result in any enhancements to the material capabilities.
5. Engineering should resolve discrepancies that exist within the shop paperwork. While the STM calls for controlling the temperature of the TPS materials to 50 °F to 70 °F, the STP allows production to store the material at high as 85 °F upon release to the floor. The documentation should be made consistent and should incorporate reasonable and realistic exposure times and temperatures. This situation appears to exist for all foam systems, although the potential exposure times vary greatly for each.
6. Engineering should also complete an assessment of the additional testing or verification that is required to support a change in the Safety Factor requirement for TPS. The EIS currently calls out a requirement of 1.10. The testing that is currently performed has substantiated the use of higher safety factors. An assessment assuming a required Safety Factor of 1.40 should be performed and the issues identified. The use of a Safety Factor of 1.25 may be acceptable for acreage foam, since it is a more controlled process, but the goal for all TPS should be a Safety Factor of 1.40.

7.2.1.11 Conclusions

An unconservative TPS design and a process that did not account for BX-250 and SLA-561 processing variations in the bipod most probably caused the liberation of major TPS debris from STS-107/ET-93. These findings were limited to the bipod region, based upon ascent photographic coverage of STS-107, which indicated an anomalous condition in the bipod region, coupled with historical foam loss records. With respect to STS-107/ET-93, all other TPS materials were without significant findings. In particular, PDL-1034 used in the bipod region was found to be a non-credible initiator or source of debris, based on volume used and its proven performance in combined environment and aerodynamics testing.

As-built data for each of the TPS materials indicated that the final product was built in accordance with engineering specifications. All nonconformances were either returned to engineering configuration or otherwise properly dispositioned by the Engineering organization. Extensive analysis and testing, including full-scale testing of flight configuration bipod hardware, revealed that nominally built hardware should perform nominally, even in the case of out-of-family induced environments. That testing and analysis also provided, however, sufficient insight to conclude that the release of debris from STS-107/ET-93 was caused by a combination of worst-case effects, attributable to the following root causes.

7.2.1.11.1 BX-250

- Design Methodology: The potential for cryopumping and/or cryoingestion, the presence of subsurface defects, and the fact that these phenomena are not addressed by verification and validation testing resulted in identifying "Inadequate Design Methodology" as a possible/remote cause or contributor to the release of debris from STS-107/ET-93.
- MAF Processing Plan: The manufacturing paperwork and the associated checks and controls on the material and processing parameters were not sufficient to provide assurance that the as-built configuration would satisfy nominal engineering requirements. This included Quality Control buy-off stamps of critical operations, which were not required, and possibly not practical, which made it impossible to confirm the absence of subsurface defects, as revealed by dissection of flight assets. An optimized manual spray technique with enhanced operator training might have controlled the number and size of these features, but the Processing Plan required neither. These factors led to identifying "Inadequate MAF Processing Plan" as a possible/remote contributor.
- Acceptance Testing: The acceptance testing was not sufficient to determine whether the as-built material properties and/or the internal configuration were sufficient to satisfy flight requirements. Verification of material properties is performed on a "witness" specimen, utilizing material that will subsequently be machined away and discarded; the flight ramp material is not tested. Dissection and subsequent testing of ET-94 bipod ramp material revealed

the possibility of out-of-family mechanical properties, as well as internal features such as voids and "rollovers." Although the actual number, size, or location of such features on ET–93/STS-107 can not be determined, testing of specimens containing defects showed clearly that identifying and properly dispositioning them, utilizing a suitable NDE technique, would have improved the performance of the foam closeout. These factors led to identifying "Inadequate Acceptance Testing" as a possible/remote contributor.

- Undetected Anomaly: Notwithstanding the preceding findings, material properties and non-destructive testing are inherently probabilistic in nature. For that reason, the possibility of an "Undetected Anomaly" had to be identified as a possible/remote contributor.

7.2.1.11.2 SLA-561

- Design Methodology: There existed a potential for a high-energy release of debris related to cryopumping and cryoingestion, with SLA-561 serving as a reservoir or a path, respectively. There was also a possibility of SLA-561 being entrained with foam debris if the temperature at the interface exceeded –100 °F. These factors led to the identification of "Design Methodology" as a possible/remote contributor.
- Undetected Anomaly: In the absence of the high-energy release mechanisms or the temperature-related entrainment of SLA-561 within foam debris, there still existed the possibility of a (secondary) loss of debris because of undetected cracks or low-strength material within the SLA-561. For that reason, the possibility of an "Undetected Anomaly" had to be identified as a possible/remote contributor.

7.2.2 Non-TPS Debris Branch

7.2.2.1 Summary

The Non-TPS Debris branch generally investigated all possible debris sources other than those directly attributable to the TPS. In executing this investigation, there was some overlap with the activities of the team managing the other FT debris branch, TPS Debris, and with the team managing the Interfaces branch. This overlap will be described as appropriate in the following sections.

Upon conclusion of a detailed review, the Non-TPS Debris Team identified two items as possible debris sources:

- Ice: which has been historically observed during launch. (Acceptable ice conditions were noted on STS-107, however.) (WBS 1.1.2.13.2)
- Non-TPS debris from interface hardware (WBS 1.1.2.13.5)

Each item was dispositioned by the ETWG and identified as a non-contributor to the *Columbia* accident.

7.2.2.2 Team Charter

The charter of the Non-TPS Debris Team was to support the *Columbia* accident investigation by assessing the likelihood that the External Tank shed any debris other than TPS on STS-107. The team was responsible for ensuring that the Non-TPS Debris branch of the FT was sufficiently developed to adequately investigate all potential debris within this charter.

7.2.2.3 Team Overview

A joint NASA and Lockheed Martin team was assembled to investigate the events of the Non-TPS Debris FT branch. The backgrounds of the members provided the team with necessary expertise in appropriate engineering disciplines, as well as in production, quality assurance, and safety.

Pat Rogers, NASA, and Ashok Prabhakar, Lockheed Martin, led the Non-TPS Debris Investigation Team. Deputy Team Leads were Rob Wingate (NASA) and Camille McConnell (LM). The dedicated NASA S&MA Team lead was Darol Moore.

7.2.2.4 Scope of Review

The Non-TPS Debris branch of the FT investigated all possible sources of debris to the Space Shuttle *Columbia* (OV-102) from the ET (ET-93) other than those directly attributable to the TPS during lift-off and ascent of STS-107. This section of the FT was developed primarily as a component-by-component audit, rather than as a logic-based study of failure events. Components were identified for review based on the CIL Aerodynamically Sensitive Items (ASI)[1], augmented by a separate review of potential non-TPS debris items conducted by the ET Contingency Team during the first week of February 2003. (ASI are those hardware items exposed to the air stream that could be a debris source to the Orbiter should they fail structurally.) Each component or assembly was investigated for debris potential related to design deficiencies, inadequate manufacturing and processing, or mission problems. Other non-TPS debris concerns, such as ice and foreign object debris (FOD), were also included in this FT branch for completeness.

Consistent with the methodology used on all teams, the scope of the investigation into non-TPS ET debris was limited to focus only on debris that could strike the left wing of *Columbia*. The major hardware assemblies that were reviewed are illustrated in Figure 7.2.2.4-1.

[1] MMC-ET-RA04b-K, Volume IV, Space Shuttle External Tank Critical Items List (CIL) Aerodynamically Sensitive Items (ASI), June 29, 2001 including Change Notice DCN-003, October 18, 2002.

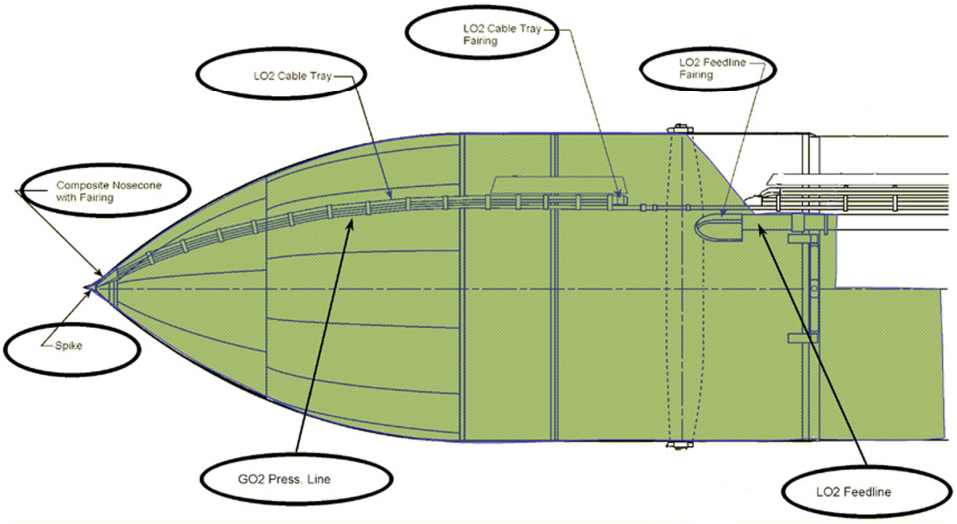

Figure 7.2.2.4-1. Overview of General ET Hardware Investigated in the Non-TPS Debris Fault Tree Branch

The scope of the Non-TPS Debris investigation into substrate structure was limited to address substrate structure not identified on other branches of the ETWG FT.

For hardware within the scope of the Non-TPS Debris branch and which also was covered by TPS, *e.g.,* the feedline fairing, all aspects were considered for the structural design and fabrication, up to and including primer application, but excluding TPS selection, application, or performance. Debris issues directly attributable to the TPS remained under the scope of the TPS Debris branch.

The interface hardware, *e.g.,* the bipod fittings and struts, was included within the scope of the Non-TPS branch; however, the investigation into this hardware for debris potential was conducted by the team working the FT branch dealing with the performance of the ET interfaces. The Interfaces Team documented all findings with respect to debris from interface hardware as part of their disposition of all events in the interfaces branch of the FT. These findings were then cross-referenced to the appropriate event in the Non-TPS Debris branch of the FT.

The possibility of debris caused by the installation of counterfeit or substandard fasteners was investigated as part of a separate review of quality records for all fasteners on ET-93 that, should they have failed, would have created debris to the Orbiter left wing. Information regarding the fastener review, as related to the various ET assemblies, is presented in section 7.2.2.8.1.

7.2.2.5 Non-TPS Debris Branch Fault Tree Structure

Main branches of the Non-TPS Debris section of the FT are shown in Figure 7.2.2.5-1. The fully indentured breakout of the Non-TPS Debris Branch is included in Volume II. The Non-TPS Debris FT section had 498 blocks, of which 343 were "basic event" blocks. This section was developed primarily as a component-by-component audit rather than as a logic-based study of failure events. As such, main branches within this FT section appear more typical of a drawing tree than a traditional FT. Organization of the main branches was heavily influenced by the layout of the ET stress report and a drawing tree 'mind set.'

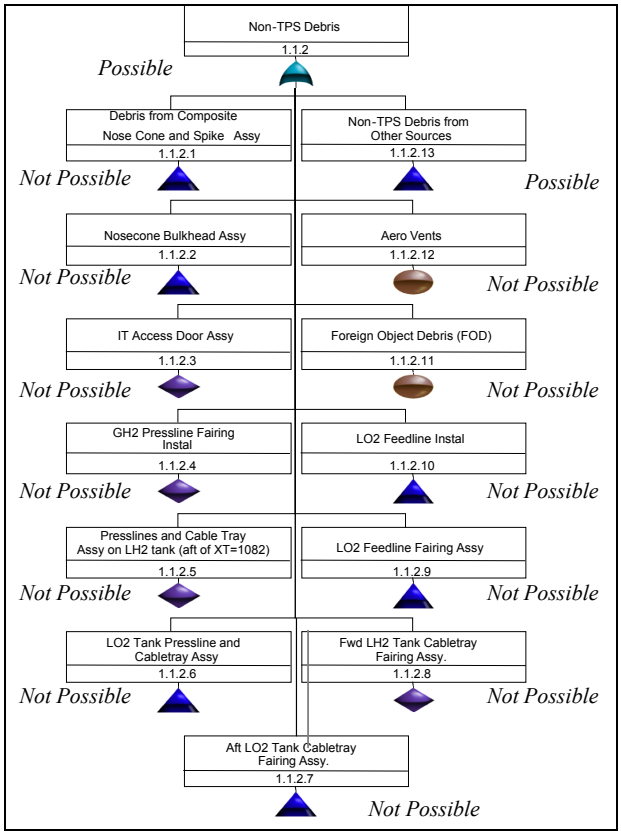

Figure 7.2.2.5-1. Main Branches of the Non-TPS Debris Section of the ETWG STS-107 Fault Tree

7.2.2.6 Evaluation Criteria

As with each other FT branches, there were four possible dispositions for each event in the FT: Possible-Probable, Possible-Remote, Possible-Improbable, or Not Possible. Each basic event in the Non-TPS Debris branch of the FT was assumed to be a cause or contributor to the shedding of debris if the event occurred. Each event was assessed to see if it could have happened, and if so, the event was assessed for the likelihood that it did happen.

The disposition of event blocks was a subjective process. No probabilistic risk assessments or other numerical tools were used to arrive at conclusions. The ETWG established an arbitration board for cases where the branch lead disagreed with the disposition selected by the initiator. The Non-TPS Debris team never had a need to use the arbitration board. It is also important to note that NASA S&MA personnel were in the review/approval cycle for every event disposition and rationale.

The disposition of intermediate event blocks was selected to be the same as the most likely possible contributing event since "or" gates were used to relate all events.

7.2.2.7 Approach

The general process for auditing components for debris potential is illustrated in Figure 7.2.2.7-1. The components identified for investigation in the Non-TPS Debris FT branch are actually hardware assemblies composed of several individual parts. All MAF and vendor build paper, *i.e.,* fabrication records, was reviewed for each part under investigation. For non-serialized parts, multiple data packages for each part from relevant manufacturing dates and production uses were reviewed to assess the hardware installed on ET-93. The build paper review verified that parts were manufactured per drawing requirements using the correct materials, processes, and procedures. Review of all build paper was conducted in accordance with the ground rule that each record be reviewed by both a Lockheed Martin representative and a U.S. Government representative (DCMA and/or NASA S&MA). A review of some fabrication records was not performed if it was the engineering judgment of both Lockheed Martin and NASA that debris potential was not possible because of containment of the parts. Approximately 253 drawings and 228 packages of build paper (MAF and vendor) were reviewed.

Criteria checklists were used to assess the fabrication of each part or assembly. Sufficient evidence of proper manufacture was typically considered to consist of:

- Certification that the correct materials were used (type, grade, and heat treatment), *e.g.,* material certification
- Certificates of Conformance
- Document Accountability Sheets (DASs)
- Acceptance Test Data
- Reference in the build paperwork that the correct steps/instructions were used, including STPs or supplier PIs for forming, heat treat, cleaning, NDE, necessary to meet all drawing requirements.

All NCDs pertinent to ET-93 hardware under investigation were audited for proper disposition. For those hardware items where assessment of primer was required, a separate criteria checklist was used to audit such things as primer type, lot code, shelf life, pot life, cure time, etc.; however, evidence of a

successful wet tape test was considered to be the only necessary criterion. All primer checklists were delivered to the TPS Debris Team for review.

The possibility of debris caused by the installation of counterfeit or substandard fasteners was investigated as part of a separate review of quality records for all fasteners on ET-93 that, should they have failed, would have created debris to the orbiter left wing. Information regarding the fastener review is presented in section 5.4.2.2.8.1. Fasteners are an example of non-serialized parts that required the review of multiple fabrication/receiving records to assess the quality of hardware that could have been installed on ET-93. In four cases, the Non-TPS Debris Team had to expand on the initial fastener review and examine purchasing records to determine if fasteners installed on ET-93 were drawn from purchase lots that the fastener review had identified as having questionable quality.

The SLWT Stress Report was reviewed as necessary to audit the stress analysis. In reviewing the applicable requirements, data and requirements from Level II were considered outside the scope of this investigation. Review of the Lockheed Martin ET Loads Data Book and Thermal Data Book was also considered to be out of the scope of the investigation; however, correct use of this data in the stress report was verified.

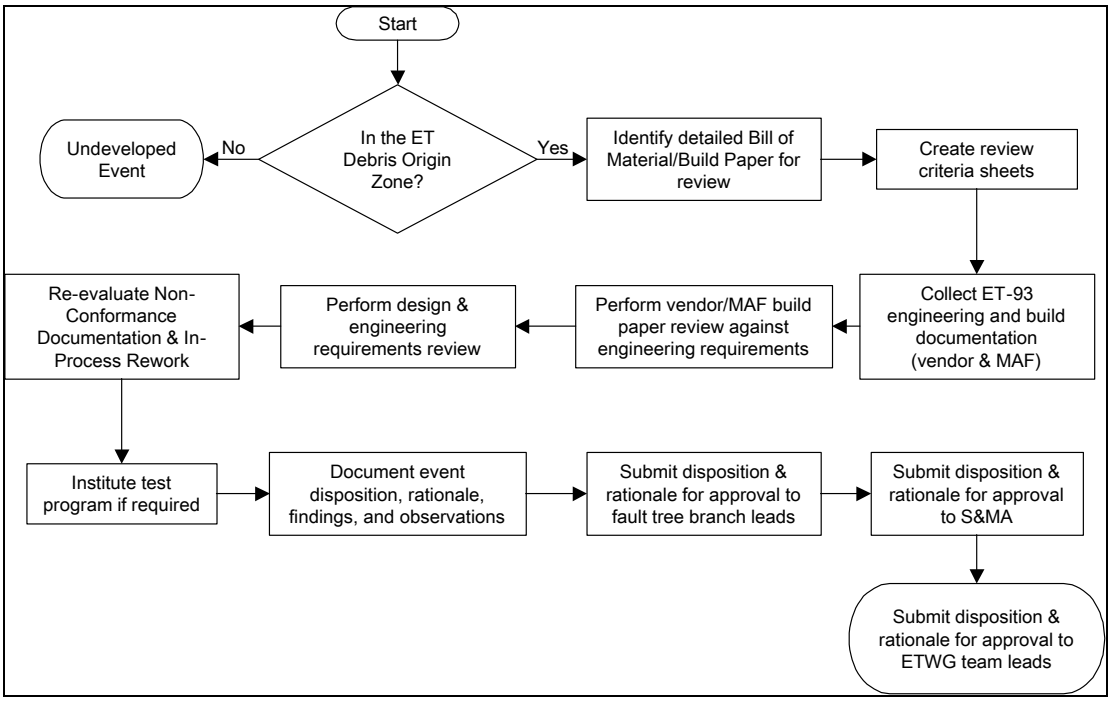

Figure 7.2.2.7-1. Process for Auditing Hardware for Debris Potential

7.2.2.8 Results

7.2.2.8.1 Summary of Findings

It is possible, but improbable, that ET-93 shed non-TPS debris capable of striking the left wing of the Space Shuttle *Columbia* during the lift-off and ascent of STS-107. It is possible, but improbable, that ice or interface hardware was the source of this debris.

No findings pertinent to the *Columbia* accident investigation were found for any other Non-TPS Debris basic events. There were no findings of debris potential for any of the other Non-TPS hardware items audited, including the composite nose cone and spike assembly, the nose cone bulkhead assembly, the LO2 cable tray and pressurization line assembly, the aft LO2 tank cable tray fairing assembly, the LO2 feedline fairing assembly, the LO2 feedline installation, or the aerovents. The disposition and rationale for every event in the FT are documented in the ETWG STS-107 Fault Tree Block Closure database. There were some observations, *i.e.,* audit items, that should be corrected but that were not considered either a debris issue or pertinent to the *Columbia* accident investigation. The audit items are discussed below.

The initial fastener review conducted outside of the Non-TPS Debris Team found two lots of 25L3-6-6 bolts and one lot of 33L1-3 nuts of questionable quality and of potential concern to the Non-TPS Debris Team. Further review of manufacturing lot traceability to purchase orders ruled out the use of both of the suspect bolt lots in any of the Non-TPS Debris hardware on ET-93 in the debris origin priority zone (see the rationale for event blocks 1.1.2.9.2, 1.1.2.6.1, and 1.1.2.10.3.) Use of under-strength nuts from the suspect lot was found to only be a potential investigation concern for the intertank cable tray and pressurization line supports; however, revised stress analysis with reduced nut strength allowables was used to conclude this discrepancy was not a debris concern. (See the rationale for event block 1.1.2.6.3.)

7.2.2.8.2 Pertinent Findings and Rationale

The following findings with regard to Non-TPS ET debris on STS-107 were provided to the NASA Accident Investigation Team (NAIT) and the *Columbia* Accident Investigation Board (CAIB).

7.2.2.8.2.1 Ice

Sequence of events:
Ice→Non-TPS Debris From Other Sources→Non-TPS Debris

Basic event block 1.1.2.13.2 “Ice” documents the investigation of external ice as a possible debris hazard to the Orbiter. There is also reference to external ice in basic event block 1.1.2.11 “FOD.” Ice debris could not be completely ruled out

because historically external ice has been observed, and acceptable ice conditions were noted on STS-107 as described below.

All observations noted by the KSC STS-107 Ice/Frost Team were deemed acceptable in accordance with the Ice/Debris Inspection Criteria, NSTS-08303, and no anomalies were noted in the as-run OMI 6444-J04-R01, "Space Shuttle Vehicle Ice and Debris Assessment." The observations (ice formation on the aft ET/Orbiter umbilicals and the LO2 feedline bellows, a crack in the vertical strut forward surface TPS, light frost on the ET TPS acreage) were consistent and "in-family" to previously documented occurrences and dispositioned with regard to the STS-107 mission. There were no Interim Problem Report (IPR)/PR or LCC violations nor facilities or vehicle issues. The limited ice/frost conditions noted were judged to be typical. In addition, the KSC Integrated Film Review Team completed an extensive post-launch review of all pad-based and long-range tracking launch films. (Long-range tracking films provide a view of the ET up to SRB separation, at which time the view of the ET is greatly diminished and no discernable details can be obtained.) Typical ice/frost was noted falling aft from the ET/Orbiter umbilicals at SSME startup and T-0. Ice/frost from the LH2 umbilical was noted contacting the LH2 Orbiter umbilical doorsill during SSME start-up, with no damage observed. Ice from the ET umbilicals or LO2 feedline was not observed contacting any other portion of the ET.
Since the presence of any ice whatsoever could not be completely ruled out, the possibility of ice sufficient to be a threat to the Orbiter was considered improbable based on the following:

- No anomalous icing conditions were noted in the STS-107 Final (Pre-Launch) Inspection results. This inspection, conducted on January 16, 2003 (day of launch) between 0615 and 0745 hours, documents the ambient conditions and analytical "SURFICE" predictions.
- Just minutes before launch, certain areas of the tank, including the bipod, were scanned using infrared (IR) spectroscopy to assess the surface temperature. The bipod was recorded to be 64-68 deg F and the LH2 acreage was recorded at 48 deg F. These temperatures are not sufficient to form ice.
- The ambient temperature at the time of launch was 65 °F.

It should be noted that the possibility of ice recontacting the External Tank and causing the generation of TPS debris was also investigated in the TPS Debris event block 1.1.1.1.4 "External Impacts to ET TPS Produce Debris."

7.2.2.8.2.2 Non-TPS Debris From Interface Hardware

Sequence of events:
Non-TPS Debris From Interface Hardware→Non-TPS Debris From Other Sources→Non-TPS Debris

The basic event block 1.1.2.13.5 "Non-TPS Debris From Interface Hardware" highlights findings related to potential sources of debris. These findings are

traceable to basic event findings from the ET Interface Performance branch of the FT. The ET team responsible for FT branch 1.2, "ET Interface Performance 'Compromises' Orbiter Reentry Systems," conducted the investigation of the debris potential of the interface hardware while they investigated interface performance. Details of the debris potential findings are documented in this report and the basic event FT blocks as shown in Volume II. Each finding is categorized as a possible, but improbable, contributor to the *Columbia* accident.

7.2.2.8.3 Interaction of Findings

The FT logic in the Non-TPS Debris branch assumes "or" gates between all events. No interaction of any findings is necessary to progress from a basic event to the top event of the branch. Of the two findings in the Non-TPS Debris branch, the events of ice and debris related to interface hardware was judged to be unrelated, and interaction of these findings to create a more likely or worst-case event was judged to be not possible.

7.2.2.8.4 Observations

During the audit of hardware for debris potential on STS-107, several observations were noted that were not considered a debris issue, but that should be corrected. The observations, *i.e.,* audit items, were logged by Lockheed Martin Product Assurance into the ET-93 Non Fault Tree Database and will require NASA S&MA concurrence with the resolution. Fifty-eight observations resulting from the investigation by the Non-TPS Debris team were input to the database. One example of an observation is shown in Figure 7.2.2.8.4-1.

7.2.2.9 Summary

It is possible, but improbable, that ET-93 shed non-TPS debris capable of striking the left wing of the Space Shuttle *Columbia* during lift-off and ascent of STS-107. Specifically, it is possible, but improbable, that ice or interface hardware was the source of this debris.

A Fault Tree branch was developed as part of the overall ETWG STS-107 Fault Tree to conduct the investigation into any debris originating from the External Tank other than that directly attributable to the TPS. This FT branch was developed primarily as a component-by-component audit rather than as a logic-based sequence of failure events. Debris potential related to design deficiencies, inadequate processing, or mission problems was investigated. The investigation included review of supporting analyses and manufacturing and launch processing paperwork, as required. All appropriate ET-93 fabrication records and manufacturing NCDs were reviewed in detail in accordance with the ground rule that each record be reviewed by both a Lockheed Martin representative and a U.S. Government representative (DCMA and/or NASA S&MA).

The FT basic event blocks 1.1.2.13.2 "Ice" and 1.1.2.13.5 "Non-TPS Debris From Interface Hardware" highlight findings related to potential, but improbable, sources of debris. These were the only discrepancies noted during the

investigation into ET-93 non-TPS debris that were considered findings pertinent to the *Columbia* accident investigation.

7.2.2.10 Summary of Tests

No tests were conducted to support the disposition of events in the Non-TPS Debris branch of the ETWG Fault Tree.

7.2.2.11 Results of Tests

No tests were conducted to support the disposition of events in the Non-TPS Debris branch of the ETWG Fault Tree.

7.2.2.12 Recommendations

It is recommended that corrective action be taken as necessary to address the observations (or the root cause of the observations).

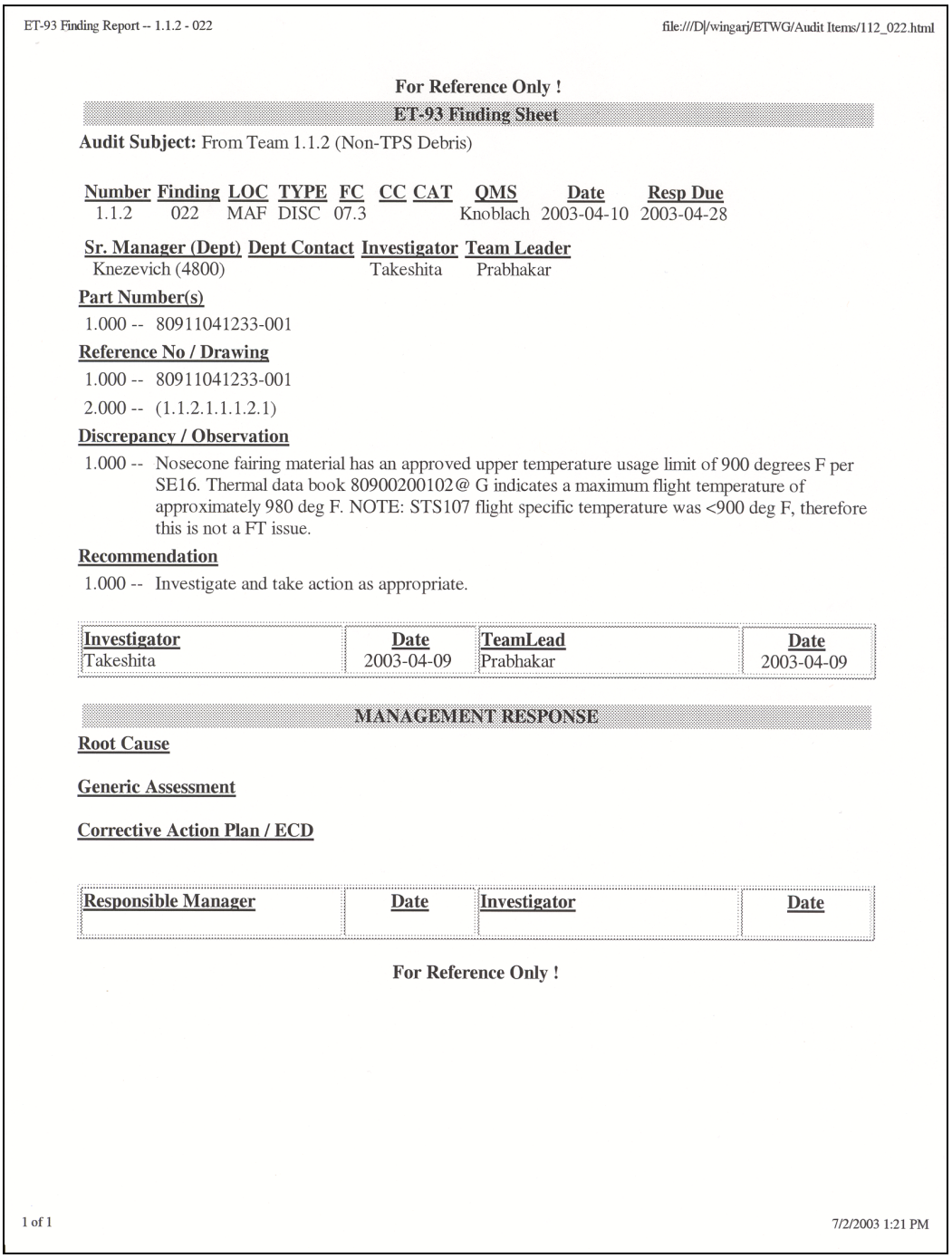

ET-93 Finding Report -- 1.1.2 - 022 file:///D|/wingarj/ETWG/Audit Items/112_022.html

For Reference Only !

ET-93 Finding Sheet

Audit Subject: From Team 1.1.2 (Non-TPS Debris)

Number	Finding	LOC	TYPE	FC	CC	CAT	QMS	Date	Resp Due
1.1.2	022	MAF	DISC	07.3			Knoblach	2003-04-10	2003-04-28

Sr. Manager (Dept)	Dept Contact	Investigator	Team Leader
Knezevich (4800)		Takeshita	Prabhakar

Part Number(s)

1.000 -- 80911041233-001

Reference No / Drawing

1.000 -- 80911041233-001

2.000 -- (1.1.2.1.1.1.2.1)

Discrepancy / Observation

1.000 -- Nosecone fairing material has an approved upper temperature usage limit of 900 degrees F per SE16. Thermal data book 80900200102@ G indicates a maximum flight temperature of approximately 980 deg F. NOTE: STS107 flight specific temperature was <900 deg F, therefore this is not a FT issue.

Recommendation

1.000 -- Investigate and take action as appropriate.

Investigator	Date	TeamLead	Date
Takeshita	2003-04-09	Prabhakar	2003-04-09

MANAGEMENT RESPONSE

Root Cause

Generic Assessment

Corrective Action Plan / ECD

Responsible Manager	Date	Investigator	Date

For Reference Only !

1 of 1 7/2/2003 1:21 PM

Figure 7.2.2.8.4-1. Example Non-TPS Debris Observation from the Lockheed Martin Product Assurance Non Fault Tree Database

One additional recommendation is made based on the *Columbia* accident investigation of External Tank non-TPS debris: the requirement for length of time for record retention by vendors should be reviewed for consistency with the actual time between receipt of hardware at MAF and launch of an External Tank

based on the current and projected flight rate of the Space Shuttle system. It was noted that by the time ET-93 flew, the record retention requirement had been exceeded in some cases, and some vendors had destroyed fabrication records.

7.2.3 Interfaces Branch

7.2.3.1 Summary

The Interfaces branch of the ETWG FT was to determine if ET interface (I/F) performance was a possible cause of the *Columbia* Incident. The emphasis of the ET interface investigation was on evaluating interface structural, propulsion, and electrical functional performance, identifying any evidence of performance anomalies, and determining if the ET interfaces had any direct and indirect effects on ET TPS or Orbiter reentry systems. Additionally, shipping and handling interfaces related to the ET complete activities were evaluated both at MAF, during barge transport, and at KSC.

Five items were identified by the Interfaces Team as "possible/Improbable" contributors to the STS-107 mishap based on detailed paper / design review:

- MPP did not call out torque sequencing for bipod strut assembly (WBS 1.2.1.1.3.6)
- MPP did not call out Loctite® shelf life verification for SRB fitting fasteners (WBS 1.2.1.7.3.1)
- Torque sequence not called out in MPP for bipod installation on tank (WBS 1.2.1.1.3.5)
- Omission of break-away torque verification in Operations and Maintenance Instruction (OMI) that installs RSS fairing (WBS 1.2.1.7.4.1.1.4)
- Operational anomaly related to bipod foam loss exposing underlying Bipod interface hardware leading to connector/connector plate becoming debris (WBS 1.2.1.1.5.4)

Each item was dispositioned by the ETWG and identified as a non-contributor to the *Columbia* accident.

7.2.3.2 Team Charter

The objective of the ETWG Interface Team was to determine if ET interface performance was a possible cause of the *Columbia* Incident. The charter of the Interfaces team was to support the *Columbia* accident investigation by assessing the likelihood that the ET performance during ascent and upon separation introduced any opportunities for atypical Orbiter separation or subsequent detrimental performance.

7.2.3.3 Team Overview

A joint NASA and Lockheed Martin (LM) team was assembled to investigate the ET Interfaces FT branch. The backgrounds of the members provided the team

with necessary expertise in appropriate engineering disciplines as well as production, quality assurance, and safety.

John Honeycutt, NASA, and Dan Callan, Lockheed Martin, led the Interface Investigation Team. The dedicated NASA S&MA Team lead was Keith Layne.

7.2.3.4 Scope of Review

The interface investigation evaluated interface structural, propulsion, and electrical functional performance. A functional summary of the ET interfaces includes structural interconnections with the two SRBs and the Orbiter, fluid and electrical interfaces with the Orbiter, fluid and electrical interfaces with the launch facility, the Orbiter to SRB interface cabling, and provisions that facilitate the attachment of transportation and handling support equipment. Figure 7.2.3.4–1 provides an orientation of the ET interfaces.

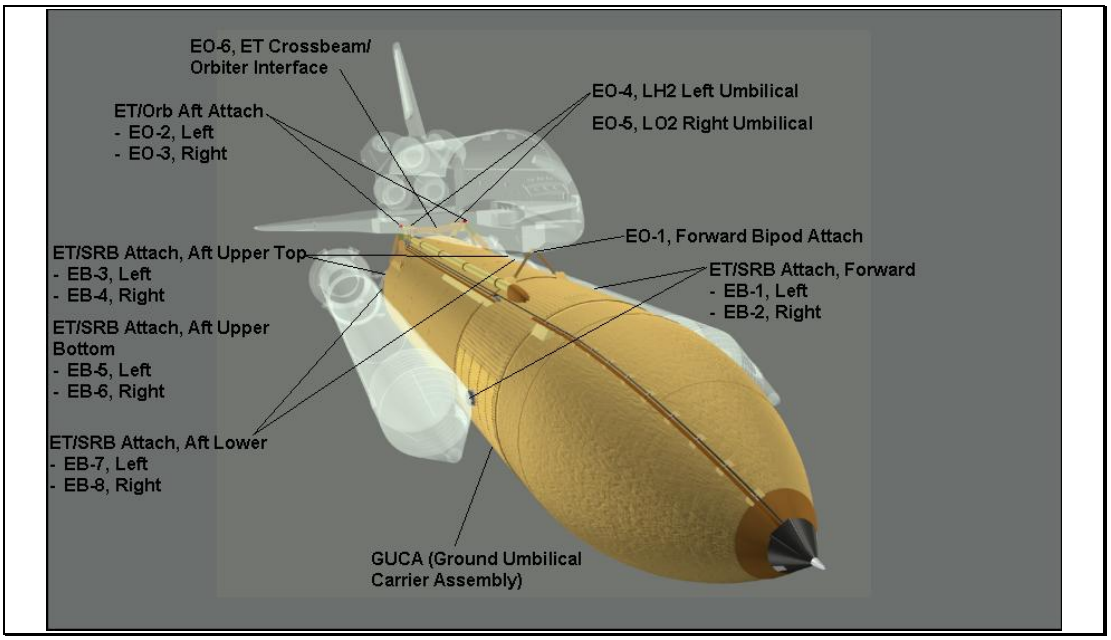

Figure 7.2.3.4-1. ET Interface Orientation

The applicable ICDs include:

- ICD-2-00001, Shuttle Vehicle Mold Lines and Protuberances
- ICD-2-12001, Orbiter Vehicle/External Tank
- ICD-2-24001, External Tank/Solid Rocket Booster
- ICD-2-0A001, Shuttle System Launch Platform Stacking & VAB Servicing
- ICD-2-0A002, Space Shuttle Launch Pad & Platform
- ICD-2-2A001, External Tank/Receiving, Storage & Checkout Station

7.2.3.5 Interfaces Branch Fault Tree Structure

The ET Interface Team FT consisted of four major branches:

- Structural Interfaces (1.2.1)
- Propulsion Interfaces (1.2.2)
- Electrical Interfaces (1.2.3)
- Transportation & Handling (T&H) Interfaces (1.2.4)

There were a total of 184 FT blocks; of these blocks, 143 were basic events.

The top level of the FT is shown in Figure 7.2.3.5-1. Decomposition of the tree was consistent with methods used by the other teams. Supplier contributions, materials, processes, verification, assembly, and processing were each considered. The fully indentured breakout of the Interfaces Branch is included in Volume II.

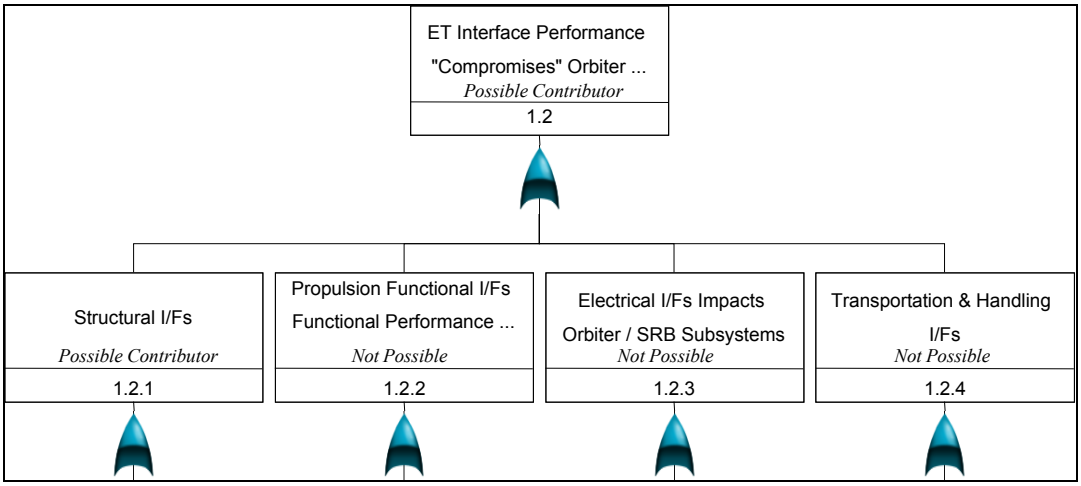

Figure 7.2.3.5-1. Top-Level Interfaces Fault Tree

7.2.3.6 Evaluation Criteria

The interface investigation Team used the same ground rules as the ETWG ground rules identified in Section 7.2 with the following exceptions:

- No ET interfaces were “Diamond Deferred” based on the ETWG “out of left wing debris zone” ground rule.
- Performance analysis was used to support closure of structural, electrical, and propulsion I/Fs outside of the ETWG debris zone.

7.2.3.7 Approach

Because each area of interface investigation required differing evaluation methods, both approaches and findings will be summarized by section.

7.2.3.8 Results

7.2.3.8.1 Structural Interfaces Fault Tree Blocks Summary (Fault Tree Branch 1.2.1)

7.2.3.8.1.1 Approach

The objective of the ET structural I/F investigation was to re-evaluate ET structural I/F requirements and to verify whether ET structural performance could have contributed to the *Columbia* incident. This included both performance anomalies that could have impacted other ET or vehicle systems or the potential for any of the interfaces to be a source of debris.

Two basic approaches were used in the investigation of the ET structural interfaces: a performance-based approach to interfaces outside the ETWG Debris Zone, including post-flight reconstructions of structural or mechanical performance and film review; and detailed analysis and build/processing paper reviews combined with performance analysis and film reviews for the interfaces within the ETWG Debris Zone. The forward bipod and forward ET/SRB interfaces used the later approach (reference Figure 7.2.3.4-1, EO-1, EB-1 and EB-2), and all other interfaces used the former approach.

The performance-based assessment of STS-107 structural I/Fs included either load reconstructions, propulsion-based performance analysis, or post-flight operational reconstructions. Ascent and post-separation film was used wherever possible. The following is a list of the affected interfaces:

1.2.1.2 EO-2 Aft Attach, -Y (Loads based)
1.2.1.3 EO-3 Aft Attach, +Y (Loads based)
1.2.1.4 EO-4 LH2 Umbilical Plate (Mechanical) (propulsion performance)
1.2.1.5 EO-5 LO2 Umbilical Plate (Mechanical) (propulsion performance)
1.2.1.8 Canceled (EB-2 Fwd SRB Attach +Y is addressed in 1.2.1.7)
1.2.1.9 Aft SRB Attach -Y (EB-3, EB-5, EB-7) (Loads)
1.2.1.10 Aft SRB Attach +Y (EB-4, EB-6, EB-8) (Loads)
1.2.1.11 GUCA (Mechanical) (propulsion performance, film review, post- flight inspections)
1.2.1.6 EO-6 LO2 Cross Beam/Orbiter (Aerodynamic) (acceptance inspections, film review)
1.2.1.12 LO2 Vent Hood (film review)
1.2.1.13 Post-Separation ET/Orbiter Contact or at ET Breakup (post-flight analysis, post-separation film)

The second structural interface investigation approach included performance-based loads reconstructions, similar to the first approach, but also included detailed review of the interface requirements; design, supplier and MAF fabrication paper; KSC processing paper; and special investigations of

operational anomalies. These interfaces were within the ETWG left-wing debris zone. This approach was used on the following interfaces:
1.2.1.1 EO-1 Fwd Bipod Attach Interface
1.2.1.7 EB-1 Fwd SRB Attach -Y & EB-2 Fwd SRB Attach +Y

The following discussion will address the detailed approach, data, and investigation results of each of these groups of structural interfaces.

7.2.3.8.1.2 Performance-Based Approach: Loads Evaluation

For structural I/Fs outside of the ETWG left-wing debris zone, two approaches to structural performance were applied to determine if these interfaces had any indirect relationship to the *Columbia* incident: structural loads reconstruction of primary interfaces and an evaluation of STS-107 propulsion system performance data, for mechanical interfaces.

The evaluation of load reconstructions of STS-107 was performed by comparing flight specific load indicators from STS-107 load reconstructions against design limits. Three different sets of load indicators were reviewed, including pre-launch, lift-off, and ascent load (BET) indicators. The interfaces affected included the following branches of the Fault Tree:
1.2.1.2 EO-2 Aft Attach, -Y (Loads based)
1.2.1.3 EO-3 Aft Attach, +Y (Loads based)
1.2.1.9 Aft SRB Attach -Y (EB-3, EB-5, EB-7) (Loads)
1.2.1.10 Aft SRB Attach +Y (EB-4, EB-6, EB-8) (Loads)

As noted previously, three I/Fs within the ETWG left-wing debris zone were also included in this performance-based evaluation and will be discussed at this time.
1.2.1.1 EO-1 Fwd Bipod Attach Interface
1.2.1.7 EB-1 Fwd SRB Attach -Y & EB-2 Fwd SRB Attach +Y

Figures 7.2.3.8.1.2-1 and 7.2.3.8.1.2-2 show the location of the load indicators evaluated with respect to the ET interfaces: truss members and interface load indicators. The Boeing analysis group, through the SSP loads board, provided the reconstructions to the Interface Team. The BET loads reconstruction was based on a rigid body analysis. In addition to the BET loads indicator sets, an additional flexible body reconstruction was provided.

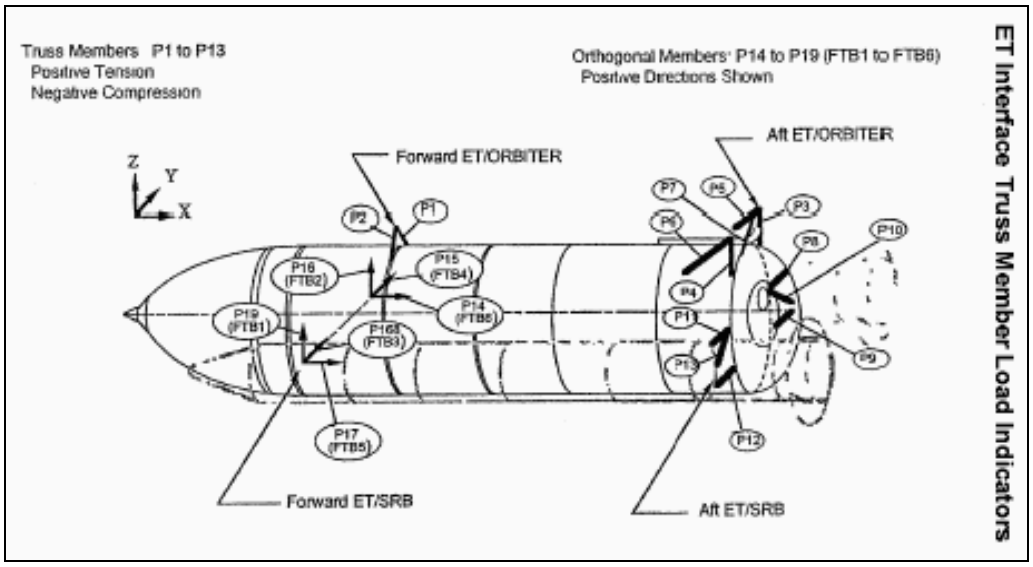

Figure 7.2.3.8.1.2-1. ET Strut Load Indicators

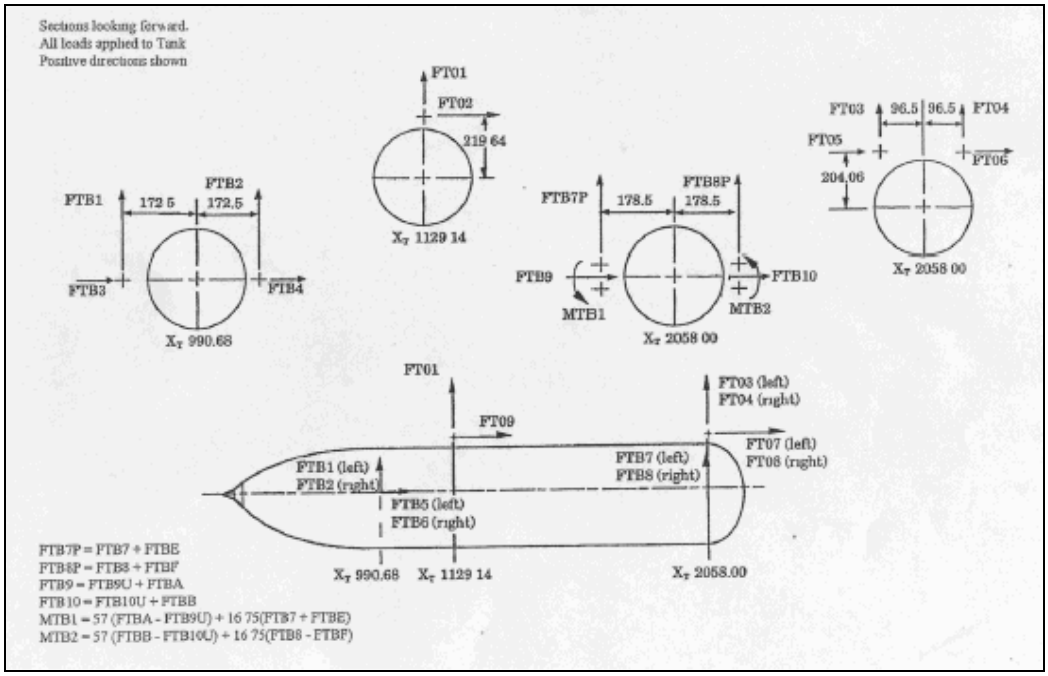

Figure 7.2.3.8.1.2-2. ET Interface Load Indicators

No loads issues were found with any phase of operations. All indicators were well within design limits. The flex body loads reconstruction was actually less than the BET reconstruction, so they did not affect the evaluation. All of the analysis to date shows no evidence of excessive or anomalous loading.

Table 7.2.3.8.1.2-1 is an example of the loads comparisons done for each of these interfaces. The ETWG Fault Tree database contains a complete set of all load indicators that were reviewed.

Table 7.2.3.8.1.2-1. Example of ET BET Load Indicators

- **Loads Shown: Forward Bipod**

Load Indicator	Max Positive (% of limit load)	Max Negative (% of limit load)
FTO1	15	31
FTO2	26	20
FTO9	24	11
P1	19	34
P2	15	27

Structural loads reconstructions were not available for propulsion related, mechanical interfaces, which included the following:
1.2.1.4 EO-4 LH2 Umbilical Plate (Mechanical)
1.2.1.5 EO-5 LO2 Umbilical Plate (Mechanical)
1.2.1.11 GUCA (Mechanical)

The performance of these I/Fs was evaluated, based on the propulsion and electrical functional performance of the interfaces, which provided a strong indicator of nominal performance. No anomalous performance or unusual conditions were evident during STS-107 operations. In addition, film review and post flight inspection reports of the GUCA provided high confidence that there were no issues related to the mechanical performance of this interface. No off-nominal conditions or anomalous conditions were evident.

The investigation found no evidence of anomalous operations of these structural I/Fs, and it was concluded that these I/Fs performed nominally and in no way contributed to the *Columbia* incident.

7.2.3.8.1.3 Findings

There were four findings identified as a result of the structural interfaces investigation effort. The findings were limited to the forward bipod and the forward SRB interfaces within the ETWG debris zone, and all were judged

"possible but improbable." A summary of the findings and the probability rationale/corrective actions are listed in Table 7.2.3.8.1.3-1.

Table 7.2.3.8.1.3-1. Structural Interface Investigation Findings

Finding	Fault Tree Block	Probability Rationale/ Corrective Action
Use of proper torque sequence was not called out in MPP for bipod strut flange fasteners. This could lead to debris.	1.2.1.1.3.5 Incorrect Parts Assembly *Parents* 1.2.1.1 EO-1 Fwd Bipod Attach Interfaces 1.2.1.1.3 Incorrect/Inadequate MAF Processing	Probability Rationale: Potential debris source determined improbable due to final torque verification and separation analysis showing high margin of Safety. Corrective Action: Modify MPP to include proper torque sequence requirements and verification
The Loctite® fastener locking compound for the intertank-to-SRB fitting fasteners (2 per each SRB fitting) did not have lot traceability recorded on the MPPs. This could potentially be a source of debris.	1.2.1.7.3.1 Incorrect Parts Material Usage *Parents* 1.2.1.7 EB-1 Fwd SRB Attach -Y & EB-2 Fwd SRB Attach +Y 1.2.1.7.3 Incorrect/Inadequate MAF Processing	Probability Rationale: Potential debris source determined improbable due to final Torque verification and separation analysis showing high margin of Safety. Corrective Action: Modify affected MPPs to verify shelf life
Use of proper torque sequence was not called out in MPP for bipod fitting installation on tank. This could lead to debris.	1.2.1.1.3.5 Incorrect Parts Installation *Parents* 1.2.1.1 EO-1 Fwd Bipod Attach Interfaces 1.2.1.1.3 Incorrect/Inadequate MAF Processing	Probability Rationale: Potential debris source determined improbable due to final torque verification and separation analysis showing high margin of safety. Corrective Action: Modify MPP to include proper torque sequence requirements and verification
Omission of breakaway torque verification in OMI that installs RSS fairing.	.2.1.7.4.1.1.4 Incorrect Parts Installation *Parents* 1.2.1.7 EB-1 Fwd SRB Attach -Y & EB-2 Fwd SRB Attach +Y 1.2.1.7.4.1.1 Incorrect/ Anomalous ET/SRB Mate	Probability Rationale: Potential debris source determined improbable due to final torque verification and separation analysis showing high margin of safety. Corrective Action: Update OMI to include verification of break-away torque

Finding	Fault Tree Block	Probability Rationale/ Corrective Action
Operational anomaly related to Bipod foam loss exposing underlying bipod interface hardware leading to connector/connector plate becoming debris	1.2.1.1.5.4 Bipod hardware/ components under foam are exposed during ascent and become debris *Parents* 1.2.1.1 EO-1 Fwd Bipod Attach Interfaces 1.2.1.1.5 Operational Anomalies (Pre-launch, Ascent, Separation)	Probability Rationale: Analysis and test demonstrated loss of underlying hardware highly unlikely. Corrective Action: Redesign effort will eliminate bipod heater connector/connector plate

7.2.3.8.2 Propulsion Interfaces Fault Tree Blocks Summary (Fault Tree Branch 1.2.2)

7.2.3.8.2.1 Approach

The objectives of the ET propulsion interface investigation was to re-evaluate ET propulsion interface requirements, to reverify the ET propulsion analysis process, and to determine whether there were any STS-107/ET-93 propulsion system performance anomalies that could have contributed to the *Columbia* incident. These objectives were met by performing a thorough evaluation of STS-107/ET-93 fluid interface data versus pre-flight predications and against historical experience. The historical evaluation included the development of historical limits for measurements near the fluid interfaces for different survey groups of past flights including LWTs (67), SLWTs (21), and Block II cluster flights (5).

The propulsion interfaces FT branch was broken down into five functional performance groups, as shown in Volume II.

For each of these functional performance groups, extensive STS-107 performance data comparisons were made against the I/F requirements as well as the historical performance groups identified above and documented as part of the FT closure rationale. Review of recorded STS-107/ET-93 ET loading and flight propulsion data, including post-flight performance reconstruction and interface data, indicated no data outside of requirements, STS program experience, or pre-flight predictions and expectations. The data examined encompassed the loading, prepressurization, and ascent (through ET separation) operations.

7.2.3.8.2.2 Findings

No indications of any unusual propulsion conditions were found in the functional or interface data. There were no findings related to the STS-107 ET propulsion interface performance. ET propulsion system performance was determined not to be a contributor to the *Columbia* incident.

7.2.3.8.3 ET Electrical Interfaces Fault Tree Blocks Summary (Fault Tree Branch 1.2.3)

7.2.3.8.3.1 Approach

The objective of the ET electrical interface investigation was to re-evaluate ET electrical I/F requirements, to reverify the ET electrical acceptance testing and inspections, and to determine whether there were any STS-107/ET-93 electrical system performance anomalies that could have contributed to the *Columbia* incident. These objectives were met by performing a thorough evaluation of STS-107/ET-93 electrical acceptance testing at MAF and at KSC and by verifying all available pre-launch and ascent electrical measurements and film and available post-flight inspections of the GUCP and SRB interfaces.

The electrical interfaces FT branch was broken down into seven functional performance groups, as shown in Volume II. For each these major branches, electrical design, MAF and KSC acceptance data, and operational electrical performance data were evaluated for adequacy and/or anomalies.

7.2.3.8.3.2 Findings

All ET-93 acceptance and inspection test paper and electrical related NCs/PRs were evaluated against the requirements, and no issues were identified. No indications of any unusual conditions were recognized in the functional or I/F data. There were no findings related to the STS-107/ET-93 electrical I/F performance. ET electrical system performance was determined not to be a contributor to the *Columbia* incident.

7.2.3.8.4 ET Transportation & Handling Interfaces Summary (Fault Tree Branch 1.2.4)

7.2.3.8.4.1 Approach

The objective of the ET T&H interfaces investigation was to re-evaluate ET T&H interface requirements, plans, and ET-93 specific events for any anomalies or incidents that could be related to the *Columbia* incident. This branch captured all T&H-related activities beginning with initial transport to the barge at MAF and including transport to the barge, barge transport, KSC stand-alone processing, and Mobile Launch Platform (MLP) and pad integration before pre-launch. Orbiter and SRB mating operations were evaluated as part of FT branches 1.2.1.1 (Bipod Structural Interface) and 1.2.1.7 (-Y and +Y SRB Structural Interfaces). These objectives were met by performing a thorough evaluation of STS-107/ET-93 related to T&H and mating, including MPPs and Manufacturing Handling Plans (MHPs) at MAF and T&H-related OMIs at KSC. Special attention was given to verification of planned inspection steps and results of these inspections that may have been documented during T&H operations.

7.2.3.8.4.2 Findings

All ET-93 T&H-related requirements, MPPs, and MHPs were reviewed and no anomalies or incidents were found. In addition, the NC system was searched, and no ET-93 T&H NCs were found. No issues were found in the review of ET-93 KSC interface-related processing paper. A review of the KSC PRACA systems identified no ET-93 T&H-related problem reports. There were no findings related to the STS-107/ ET-93 T&H interface processing. ET-93 T&H-related processing was determined not to be a contributor to the *Columbia* incident.

7.2.3.9 Summary of Tests

No tests were conducted to support the disposition of events in the Interfaces branch of the ETWG Fault Tree.

7.2.3.10 Recommendations

The Interfaces Team recommends corrective action to address the low-risk items uncovered during the investigation:

- Implement corrective action to modify affected MPPs to verify shelf life of Loctite® material
- Update all appropriate MPPs to include torque sequence requirements and verification.

Section 8 Contributing Root Causes, Significant Observations, and Recommendations

Root causes and associated observations and recommendations are summarized in Table 8-1.

Table 8-1. Root Causes and Associated Observations and Recommendations

No.	Root Cause	Observation	Recommendations
E-1	Debris	• TPS debris loss observed at 81.7 sec during STS-107 ascent most probably originated from left-hand bipod ramp • Other areas on ET have histories of debris shedding	• Review verification and validation of complex closeout configurations for performance risks • Redesign (and reverify/revalidate) high risk configurations • Incorporate inspectability of as-built configuration in assessment of acceptable hardware design
E-2	Defect formation in TPS	Dissections have shown various types of defects in the as-applied TPS.	• Develop a characterization/test program to determine gun types, fan pattern settings, overlap time requirements, spray techniques, etc., that will enable TPS applications without defects for both current and any “improved” systems. • Incorporate periodic dissections of production parts in QC plans
E-3	Material Properties and Validation	Compression tests of BX 250 SOFI identified significant difference in properties in rise direction vs. perpendicular to rise direction.	• Develop a characterization/test program to determine material strength/debris potential vs. thickness, vs. density, vs. spray pattern, vs. rise direction, vs. etc., for all TPS systems and application methods.
E-4	Stress Models	The stress model for modeling TPS materials is not adequate to predict failure.	Consult with other and outside entities to develop 2-D or 3-D models that can accurately predict failure.
E-5	General TPS Environment	Changes in precursors, materials, requirements, and vendors create a turbulent environment, making control of TPS materials, systems and processes difficult	• Form a TPS Materials Working Group (Civil Service and contractor team) to address the following topics. Consider implementation of rigor associated with structural materials • Training and Certification • Raw Material Acceptance • MPP Process Control • MPP Acceptance Testing

			• Traceability • Contamination Effects and Control • Production Parts Dissection Recommendations
E-6	MPP Process Control and Acceptance Testing	Difficult application techniques and operations are left to the discretion of the operator during hardware processing	• Develop more detailed technique sheets for difficult manual SOFI sprays and ablator hand pack operations. Include Engineering (Material Sciences) oversight and approval
E-7	Acceptance Testing / Inspection Technique Limitations	Available acceptance testing/inspection techniques are not capable of rejecting ramps with diverse "as-built" features that would threaten the TPS integrity	• Assess nondestructive evaluation methods for evaluation of critical defects
E-8	MPP Process Control and Acceptance Testing	Due to ease of logistics, witness specimens are maintained in a separate area from the hardware during the cure cycle	• Review the adequacy (number, location and size of specimens) of witness coupon process. For example when spraying multiple parts, make coupons from an extra part rather than a separate witness panel. • Maintain witness specimens in the same area and environment in which the parts are cured
E-9	Spray Process Control & Equipment Traceability	• The engineering requirement for verification of ratio and other processing parameters is not adequate. Ratio could be checked as infrequently as 2 years. • No traceability of actual foam spray equipment used (including proportioner) to the ET component being insulated.	• Implement a 100% recording of spray equipment operational data. • Check ratios from SOFI spray proportioner on a more frequent basis (two cup method or extended spray to check output.) • Record serial number of proportioner in the event an error is found in the unit.
E-10	Spray Overlap Time Verification	Determination that overlap time requirements have been met are subjective at best.	• Develop and implement QC methods for overlap time verification on difficult configurations
E-11	Training and Certification of Manual Spray Practitioners	• Current foam spray certification of operators is permanent, providing certain "on-the-job training" is performed and a person performs one successful spray close-out every two years. • Tooling and mockups for training need to be improved and kept current with changes in	• Review time period for recertification • Reduce Manual Spray certifications from 2 years to 1 year • Assess reducing the time to revoke certifications for non-use • Include spray operations on test panels during training prior to

		production materials and application methods.	spraying on hardware by OJT. • Implement test panels more representative of actual part geometries and techniques (24”x 24” instead of 6” panels when required, specific guns, total thickness, knitline thickness, orientation, and part complexity) • Increase number of specific certifications, if required • Evaluate continuous improvement of the process. Any best practices (material and/or equipment changes) should be certified and incorporated into the training and recertification program. • Establish pass/fail criteria based on design-critical attributes, e.g., mechanical properties, critical void locations • Improve the process of involving Training personnel in process and tooling changes that affect training courses.
E-12	Stamp Warranty Implementation	• One person observed as stamping for multiple operations • Stamps not fully legible • Shop supervisors do not hold individual certifications; however, some are authorized to stamp off build process operations, and do in fact stamp operations off.	• Review stamp warranty practices and training • Review practices for stamp replacement • Review training and cert requirements for Supervisors • Review the description of supervisors approval of processes
E-13	Raw Material Acceptance and Control	• Specification for a particular material stated that material shall meet requirements when stored in original sealed containers at one temperature range for 6 months. Implementing documentation (process specification) allowed relocation in the preparation/using area at a larger temperature range with no reduction in shelf life. • Trending data is based on original acceptance test data only	• Reassess storage requirements and update documentation for consistency • Fingerprinting and Acceptance data trends need increased tracking when trends are observed within statistical or STP acceptance limits. • Incorporate NCD test results in trend databases
E-14	Traceability Issues	Improperly recorded numbers identified	• Improperly recorded numbers should be emphasized in training. • Correct lost logs • Consider more clocks with military time and date to minimize

			errors. • Review paperless manufacturing system requirements to verify minimized potential for errors • Proper recording practices and correction of current faults should be implemented (Munafo verbal interpretation)
E-15	General Traceability and Data Retrieval	Reduced staffing levels have resulted in increased reliance on supplier quality and related documentation, sometimes making access difficult	• Assess overall levels vendor quality control and recommend additional controls, as needed
E-16	Contamination Effects and Control	Potential SOFI contaminants identified in walk-down of factory	• Establish a Contamination Control Team • Incorporate contamination control requirements and selected verification methods into STPs. • Conduct contamination walk-downs on a regular basis
E-17	Torque Sequence Call-out in Build Paper	A specified torquing sequence was not identified in the bipod strut MPP. (However, training methods mandate the star-pattern sequence and the final torque of the fasteners was verified in the MPP.)	• Modify build paper to reflect star-pattern torque sequence • Review running torque and break-away torque verification requirements
E-18	Loctite® Shelf Life Traceability Call-out Requirement	• Loctite® fastener locking compound used at the Forward ET/SRB fittings did not have any lot traceability recorded on the MPP. Loctite® is used to retain fasteners as a secondary locking feature when other locking features are not applicable. • There is a shelf life associated with Loctite®. The material is verified in Receiving/Labs prior to being issued to Production. The MPP only requires recording the grade and not the shelf life	• Modify build paper to reflect shelf-life recording requirement
E-19	ICD Responsibilities	ICD Responsibilities for bolt catcher were unclear between elements	• Reassess all interfaces to assure clear responsibility delineation between elements and updated ICDs • Implement a full requirements/verification

			traceability tool on critical implementations
E-20	Post-Flight Performance Assessment	Post-flight assessment of TPS performance was difficult at best.	• Implement downlinked digital video coverage of the external tank. • Improve the Orbiter umbilical well imaging and launch imaging capability.
E-21	Debris	100% guarantee of no foam debris is impossible	• Develop a viable and quantitative definition of debris • Develop a better understanding of the effect of ET foam debris particle impacts on Orbiter TPS.
E-22	TPS	Changes in precursors, materials, requirements and vendors create a turbulent environment, making control of TPS materials, systems and processes difficult for all elements of the Shuttle Program.	• Form a TPS senior expert advisory board to be made available to all Shuttle Program elements as a resource for assessment of future changes, and to provide continuity and assess credibility of verification.
E-23	Staffing Levels	External Tank Civil Service & Contractor workforce levels have declined for the past several years	• Assess technical and other critical staffing levels to assure adequate capability for Return-to-Flight activities and for follow-on sustaining engineering. • Sponsor the TPS Materials Working Group
E-24	Chief Engineer function	The current Shuttle Project Management scheme at MSFC has the Chief Engineer reporting to the Project Manager; this tends to inhibit proper checks and balances on technical issues.	• Work to re-institute at MSFC an organizational separation of the Project Manager and Chief Engineer functions.
E-25	Contract Award Fee Criteria	Incentivization to reduce NCDs greatly reduced the number of NCDs but did not result in a corresponding improvement in TPS performance.	• Contract incentive methodology should be changed to base performance onuses on more representative technical performance metrics.
E-26	Influence of Technical Operations	Product Assurance and Production Operation organizations control the fabrication, repair methods, and training requirements for ET manufacturing.	• The team for implementing the preceding functions should consist of Product assurance, Production Operations, AND Technical Operations personnel.
E-27	Contingency Teams	The MSFC Contingency Plan document should be updated to reflect lessons learned regarding the team make up, technical expertise required (depending on the problem), and chain of	• The MSFC SSPO should work with the STS-107 Working Groups to update the Contingency Plan.

		command.	
E-28	Contingency Teams	While initial completion schedules for the investigation were aggressive and did ensure no less than "full throttle" effort by the Working Groups, these schedules caused compromises to be made in testing and analysis options.	• Initial schedules should be reassessed and revised at the earliest opportunity during an investigation based on assessments of the magnitude of technical efforts that will be required during the investigation. This will ensure that severe "short cuts" will not be required to meet schedule that could possibly adversely affect the quality of the investigation.
E-29	Contingency Teams	The urgencies of flight schedule and budget too often force the Agency into a reactive mode when dealing with contingencies. There seems to be neither time nor resources available to proactively seek out and solve problems before they occur.	• Create and fund a function, either within the Shuttle Program or accountable to it, that would proactively seek out, define preemptive actions against, and advocate resources to correct the so-called "Unknown Unknowns" that threaten mission success.
E-30	Contingency Teams	There was a certain amount of confusion over the focus of the Fault Tree. Strictly speaking, it should have been directed specifically toward events that could have led to the loss of STS-107; however, good engineering judgment dictated that the scope should be broader, and that the Shuttle Program could gain a large benefit with a small additional expenditure of resources by expanding the Fault Tree investigation to identify other events that could cause a similar result in the future.	• As a minimum, state in the documentation guiding incident investigations that the working groups should determine factors that could have been causal to the incident, and also any other events that might be generically similar but for one reason or another did not cause this particular incident.
E-31	S&MA	S&MA is expected to take a leadership role in incident investigations; however, S&MA investigative procedures and required forms are not in place. Furthermore, S&MA does not have its own funding for investigations, having to rely on the Project Manager, for example, to provide travel funding.	• S&MA should develop an Operational Instruction (OI) for incident investigations. Early in the process, discretionary funding should be provided to S&MA.

Section 9 Definition of Terms

α, alpha	Angle of Attack
AEDC	Arnold Engineering Development Center
ALERTS	Acute Launch Emergency Reliability Tips
AR	Action Report
ASI	Aerodynamically Sensitive Items
β, Beta	Sideslip Angle
BET	Best Estimated Trajectory
CAIB	*Columbia* Accident Investigation Board
CDR	Critical Design Review
CEI	Contract End Item
CFD	Computational Fluid Dynamics
CIL	Critical Items List
CM	Configuration Management
CoFR	Certificate of Flight Readiness
COQ	Certification of Qualification
CTP	Controlled Test Plan
D&V	Development and Verification
DAS	Document Accountability Sheet
DC&R	Design Criteria and Requirements
DCMA	Defense Contract Management Agency
DCS	Design Certification Sheet
DFI	Development Flight Instrumentation
DoD	Department of Defense
DOL	Day of Launch
DR	Discrepancy Report
DTA	Differential Thermal Analysis
EIS	End Item Specification
EOR	End of Replenish
ET	External Tank
ETA	External Tank Attach
ETM	Engineering Test Motor
ETP	Engineering Test Plan
ETWG	External Tank Working Group
FEM	Finite Element Model
FMEA	Failure Modes and Effects Analysis
FMA	Flight Margin Assessment
FOD	Foreign Object Debris
FPP	Flight Preparation Process
FRR	Flight Readiness Review

FSS	Fixed Service Structure
FT	Fault Tree
FTA	Fault Tree Analysis
FY	Fiscal Year
GHe	Gaseous Helium
GN&C	Guidance, Navigation, and Control
GN2	Gaseous Nitrogen
GO2	Gaseous Oxygen
GUCP	Ground Umbilical Cable Panel
GUCA	Ground Umbilical Cable Assembly
HCFC	Hydrochlorofluorocarbon
HCS	Hardware Certification Sheet
HEAR	Hardware Element Acceptance Review
HOSC	Huntsville Operations Support Center
HPM	High Performance Motor
HR	Hazards Report
ICD	Integration Control Document
I/F	Interface
IFA	In-Flight Anomaly
IOP	Ignition Over Pressure
IPR	Interim Problem Report
IPRA	In-Process Repair Authorization
IR	Infrared
JSC	Johnson Space Center
KSC	Kennedy Space Center
LCC	Launch Commit Criteria
LDB	Loads Data Base
LH	Left Hand
LH2	Liquid Hydrogen
LM	Lockheed Martin
LMC	Lockheed Martin Company
LMSSC	Lockheed Martin Space Systems Company
LOCV	Loss of Crew and Vehicle
LO2	Liquid Oxygen
LOX	Liquid Oxygen
LWT	Lightweight Tank
MAF	Michoud Assembly Facility
MDAT	Material Data Analysis Team
MECO	Main Engine Cut Off

MEICT	Multi-Element Integrated Closure Team
MET	Mission Elapsed Time
MHP	Manufacturing Handling Plan
MLP	Mobile Launch Platform
MPP	Manufacturing Process Plan
MPS	Main Propulsion System
MRB	Material Review Board
MRT	Mishap Response Team
MSFC	Marshall Space Flight Center
NAIT	NASA Accident Investigation Team
NASA	National Aeronautics and Space Administration
NC	Nonconformance
NCD	Nonconformance Document
NCFI	North Carolina Foam Insulation
NEQA	NASA Engineering and Quality Audit
NPC	Nonpropulsive Consumables
NSTS	National Space Transportation System
OFI	Operational Flight Instrumentation
OI	Operational Instruction
OIS	Operational Intercommunication System
OMI	Operations and Maintenance Instruction
OMRSD	Operations and Maintenance Requirements and Specifications Document
OPT	Operational Pressure Transducer
OVE	Orbiter Vehicle Engineering
PAL	Protuberance Air Load
PAS	Problem Assessment System
PASR	Problem Assessment System Report
PCA	Process Control Alert
PD	Process Departure
PDL	Polymer Development Laboratories
PE	Performance Enhancement
PFA	Pre-Flight Assessment
PFOR	Post-Flight Observation Record
PFR	Pre-Flight Review
POFI	Pour on Foam Insulation
PR	Problem Report
PRACA	Problem Report and Corrective Action
PRCB	Program Requirements Control Board
PRD	Program Requirements Documents
PRR	Program Requirements Review
PSIG	Propulsion Systems Integration Group

Q	Dynamic Pressure
QAR	Quality Assurance Representative
QC	Quality Control
QTP	Qualification Test Plan
RH	Right Hand
RMS	Root-Mean-Square
RSRM	Reusable Solid Rocket Motor
RSS	Rotating Support Structure
S&A	Safe and Arm Device
S&MA	Safety and Mission Assurance
SCN	Specification Change Notice
SINDA/FLUINT	Systems Integrated Numerical Differencing Analyzer and Fluid Integrator
SLA	Super Light Ablator
SLWT	Super Light Weight Tank
SOFI	Spray-On Foam Insulation
SPC	Statistical Process Control
SRB	Solid Rocket Booster
SRM	Solid Rocket Motor
SSEIG	80? 82?
SSME	Space Shuttle Main Engine
SSP	Space Shuttle Program
SSV	Space Shuttle Vehicle
STM	Standard Material Specification
STP	Standard Process Specification
STS	Space Transportation System
T&H	Transportation and Handling
TAL	Trans-Atlantic Abort
TD	Technical Directive
TDB	Thermal Data Book
TDFS	Test Demonstrated Factor of Safety
TGA	Thermogravimetric Analysis
T_o	Lift-Off
TPS	Thermal Protection System
TR	Technical Report
USA	United Space Alliance
UUEC	Unexpected, Unexplained Event or Condition
VAB	Vehicle Assembly Building
V_{IP}	In-Plane Wind Velocity
V_{OP}	Out-of-Plane Wind Velocity
VV&A	Verification, Validation & Accreditation

WBS	Work Breakdown Structure